LEABHARLANN CHOLÁISTE NA TRÍONÓIDE, BAILE ÁTHA CLIATH | TRINITY COLLEGE LIBRARY DUBLIN
Ollscoil Átha Cliath | The University of Dublin

Terms and Conditions of Use of Digitised Theses from Trinity College Library Dublin

Copyright statement

All material supplied by Trinity College Library is protected by copyright (under the Copyright and Related Rights Act, 2000 as amended) and other relevant Intellectual Property Rights. By accessing and using a Digitised Thesis from Trinity College Library you acknowledge that all Intellectual Property Rights in any Works supplied are the sole and exclusive property of the copyright and/or other IPR holder. Specific copyright holders may not be explicitly identified. Use of materials from other sources within a thesis should not be construed as a claim over them.

A non-exclusive, non-transferable licence is hereby granted to those using or reproducing, in whole or in part, the material for valid purposes, providing the copyright owners are acknowledged using the normal conventions. Where specific permission to use material is required, this is identified and such permission must be sought from the copyright holder or agency cited.

Liability statement

By using a Digitised Thesis, I accept that Trinity College Dublin bears no legal responsibility for the accuracy, legality or comprehensiveness of materials contained within the thesis, and that Trinity College Dublin accepts no liability for indirect, consequential, or incidental, damages or losses arising from use of the thesis for whatever reason. Information located in a thesis may be subject to specific use constraints, details of which may not be explicitly described. It is the responsibility of potential and actual users to be aware of such constraints and to abide by them. By making use of material from a digitised thesis, you accept these copyright and disclaimer provisions. Where it is brought to the attention of Trinity College Library that there may be a breach of copyright or other restraint, it is the policy to withdraw or take down access to a thesis while the issue is being resolved.

Access Agreement

By using a Digitised Thesis from Trinity College Library you are bound by the following Terms & Conditions. Please read them carefully.

I have read and I understand the following statement: All material supplied via a Digitised Thesis from Trinity College Library is protected by copyright and other intellectual property rights, and duplication or sale of all or part of any of a thesis is not permitted, except that material may be duplicated by you for your research use or for educational purposes in electronic or print form providing the copyright owners are acknowledged using the normal conventions. You must obtain permission for any other use. Electronic or print copies may not be offered, whether for sale or otherwise to anyone. This copy has been supplied on the understanding that it is copyright material and that no quotation from the thesis may be published without proper acknowledgement.

Modelling of Hydrological Pathways in Irish Catchments

Ronan O'Brien

A thesis submitted for the Degree of Doctor of Philosophy

to the University of Dublin, Trinity College

March 2013

Department of Civil, Structural and Environmental Engineering

University of Dublin

Trinity College

Dublin

TRINITY COLLEGE
2 4 MAY 2013
LIBRARY DUBLIN

Thesis 9878

Declaration

I declare that this thesis has not been submitted as an exercise for a degree at this or any other University and is entirely my own work.

I agree that the Library may lend or copy the thesis upon request. This permission covers only single copies made for study purposes, subject to normal conditions of acknowledgement.

Signed

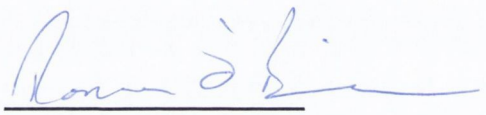

Ronan O'Brien

Summary

Conceptually, the main hydrological pathways contributing to river discharge are overland flow, interflow, shallow groundwater and deep groundwater. The percentage of the river hydrograph derived from each of these pathways is an important aspect of any hydrological study and is the focus of this research. Data collected from four study catchments as part of this research (rainfall, river discharge and temperature data from the river and boreholes) and available data from supplementary catchments, were analysed to determine the contribution of the pathways to river discharge through the application of various analytical techniques. Physical separation methods (recharge coefficients, master recession curve analysis, digital filtering algorithms and temperature tracer analysis) were employed to provide realistic ranges for the percentage of the river discharge derived from each of the pathways utilising measured discharge in the river, the geological setting of the catchment and temperature measurements in the river and the subsurface into account.

These physical separation methods were modified as necessary for use with the conceptual model of this research. The recharge coefficient approach was altered to account for point recharge (particularly in karst catchments); the master recession curve was applied in a novel manner, allowing the characteristic response of the pathways to be identified; the Lyne and Hollick 'one-parameter' algorithm was significantly modified to remove subjectivity and enable its use as an investigative tool for identifying the four pathways of the conceptual model; while the novel application of time series analysis in conjunction with a simple temperature mixing model provided further insight into the contribution of the pathways to the river. The lumped and conceptual rainfall-runoff model NAM provided temporal variation of the contributions of each of the pathways to the river hydrograph, applying the ranges of each of pathways, determined from the physical separations, as constraints when calibrating the model output.

The groundwater pathways contributions to river discharge were further investigated, implementing the fully distributed MODFLOW groundwater model. This finite difference model provided a hydrograph of the contribution of the groundwater

pathways for the same time period as the NAM simulation in one of the study catchments. The comparison of the two hydrological models highlighted the large demand for high spatial resolution data from such a model as MODFLOW, with the results implying that the data available was not sufficient for achieving a good fit between simulated and observed discharge in the river, even in a catchment that would be considered well instrumented by Irish standards.

Following this, the parameters implemented in NAM to obtain the pathway separations were related to the different catchment characteristics, i.e. soil, subsoil, catchment area, slope etc., using multiple linear regression. This provided a means of implementing the hydrograph separation methodology of this thesis in ungauged catchments of similar type to the study catchments and supplementary catchments of this thesis. Utilising the uncertainty associated with the multiple linear regressions, a sensitivity analysis of the NAM parameters was carried out. This identified the parameters that are of most importance, with regards to the pathway separations obtained and the comparison of the simulated and observed river discharges, when implementing the NAM in Irish catchments. While this framework for quantifying the contribution of the pathways was developed for Irish catchments, the methodology is applicable internationally, provided the necessary data are available and the conceptual model is consistent with that of the catchment being assessed.

This research was carried out as part of the *Pathways Project*, which is investigating the fate of diffuse contaminants, along the hydrological pathways transporting them and their subsequent impact on aquatic ecosystems in Irish catchments. This is of fundamental importance to the Environmental Protection Agency and River Basin Managers during decision making towards achieving the aims of the EU Water Framework Directive. The *Pathways Project* aims to develop a Catchment Management Tool (CMT) that will meet the needs of these decision makers. The contaminants investigated by the CMT will include phosphorus, nitrogen, sediments, pesticides and pathogens. An important aspect of the development of this CMT is the quantification of the pathways' contributions to the river hydrograph.

Acknowledgements

To sum up all the thanks and gratitude I have for everyone over the last three and a bit years in one page is not possible, this could never do justice to all the support I have received and great times I have had with everyone during my time as a postgrad, but sure here we go anyway...

Firstly to my supervisors Bruce Misstear and Laurence Gill, you have both been constant voices of reason during my time here, offering encouragement when needed and guidance when necessary (lots!). I sincerely thank both of you for all your time you have given to me.

For all those people who have offered me guidance during my research, your help has been much appreciated. I would like to thank all those involved with the *Pathways Project,* especially Marie Archbold, Jenny Deakin, Bjoern Elsaesser, Taly Hunter-Williams and the EPA hydrometric teams based in Monaghan and Kilkenny, particularly John Agnew for his time and expertise. The help from the lab technicians in Trinity has also been great, Pat, Kev, Martin, Mick, Eoin and Dave you have always been on hand to help out. To all the undergrad and MSc. guys that have helped me on site (particularly Ro), thanks a mill guys for help and entertainment in the field.

To everyone in the department, you have really made these last few years special, our adventuring days, our snow days, our nights out (our days out!), our weekends away, our holidays, football, tag, tennis, golf, races...it's all been a great experience and one I will always look back on with a smile.

To my office (Enviro for life!), where do I begin, Andy 'Rugbydump' Lochaden, Avril 'Sam is going Weist I say' Challoner, Clare '£$"%$$£%' O'Farrell and Paddy 'maybe it's just me but...' Morrissey, it's been amazing. Lunches, breakfasts, photoshoots (I can explain...actually no I can't), quizzes, baked goods, Simpsons, Father Ted, Rugby, Football and just generally having the craic, a great bunch.

Mam, dad and the rest of the O'Brien clan (too many to name) thanks for all the support, the minding and providing somewhere to escape to at weekends and during holidays. As always, you've been great to me.

To Tara, you've made this all a lot easier than it could have been, thanks for keeping a smile on my face during 2012. Here's to 'Cultural Thurdays' (Cosmo you also get an honourable mention here!) and to having free time again.

To the lads, Badge and Johnny, it's been some three years and the rest. To plenty more to come, you've been great during this PhD, providing plenty of opportunity for distraction, ridiculousness and good times. YOTL!

And last and by no means least thanks to everyone else that I didn't get a chance to name, you have all been so good to me over the last few years and I can only say you have my heartfelt thanks. (Stevo, my good buddy and print machine provider, this actually wouldn't have happened without you!)

Table of Contents

Declaration *iii*
Summary *v*
Acknowledgements *vii*
Abbreviations and Symbols *xv*

Table of Contents

1 Introduction *1*

1.1 Background and Overview of Thesis **1**

1.2 Research Aims and Objectives **4**

1.3 Scope and Layout of Thesis **5**

2 Literature Review: Physical Hydrograph Separation Techniques *7*

2.1 Introduction **7**

2.2 Graphical **9**
2.2.1 No Bank Storage 9
2.2.2 Bank Storage 11

2.3 Recession Analysis **12**
2.3.1 Master Recession Curve (MRC) 13
2.3.1.1 Correlation Method 14
2.3.2 Matching Strip Method 14
2.3.3 Tabulation Method 15

2.4 Frequency Analysis **16**
2.4.1 Flow Duration Curves 16
2.4.2 Fixed interval, sliding interval and smoothed local minima turning point methods 17
2.4.3 Recursive Digital Filters 19

2.5 Geochemical Analysis **24**
2.5.1 Natural Tracers 26
2.5.2 End Member Mixing Analysis (EMMA) 27

2.6 Recharge Coefficients **28**

2.7 Discussion **30**
2.7.1 Ability to identify multiple pathways 31
2.7.2 Objectivity of separation methods 31
2.7.3 Length of flow records required 32
2.7.4 Independence and suitability of methods 33

3 Literature review: Hydrological Models *34*

3.1 Introduction **34**

3.2 Lumped/Semi-Distributed Models **35**

3.2.1 HBV 35

3.2.2 HSPF 37

3.2.3 NAM 41

3.2.4 SWAT 43

3.2.5 TOPMODEL 46

3.3 Distributed Models **49**

3.3.1 Finite Difference 49

3.3.1.1 MODFLOW 50

3.3.1.2 SHETRAN 52

3.3.2 Finite Element 55

3.3.2.1 FEFLOW 55

3.4 Selection of models **58**

3.4.1 Ability to simulate all pathways 58

3.4.2 Lump and distributed models 59

3.4.3 Data requirements 59

3.4.4 Overland flow generation mechanisms 59

3.4.5 Application to the Irish Setting 60

3.4.6 Over-parameterisation 60

3.4.7 NAM and MODFLOW 61

4 Study Catchments *62*

4.1 Introduction **62**

4.2 Carrigan's Catchment, Gortinlieve **63**

4.2.1 Instrumentation 64

4.2.2 Land-use and Geology 65

4.2.3 Hydrology 68

4.2.4 Hydrogeology 69

4.3 Glen Burn (Mount Stewart) Catchment **71**

4.3.1 Instrumentation 72

4.3.2 Land-use and Geology 73

4.3.3 Hydrology 75

4.3.4 Hydrogeology 76

4.4 Mattock catchment, Co. Louth/Meath **78**

4.4.1 Instrumentation 78

4.4.2 Land-use and Geology 79

4.4.3 Hydrology 83

4.4.4 Hydrogeology 85

4.5 Nuenna catchment, Co. Kilkenny 86

4.5.1 Instrumentation 87

4.5.2 Land-use and Geology 88

4.5.3 Hydrology 92

4.5.4 Hydrogeology 93

5 Research Methodology 96

5.1 Introduction – Research Strategy 96

5.2 River stage monitoring 99

5.3 Borehole level monitoring 102

5.4 Rainfall 105

5.5 River gauging 106

5.5.1 Measurement of discharge 107

5.6 Electric conductivity 109

5.7 Temperature 110

5.8 Evapotranspiration 111

5.9 Riverbed Surveying 111

5.10 Visual Surveying 112

5.11 Raw data Analysis 114

5.11.1 Rainfall 115

5.11.1.1 Gortinlieve 115

5.11.1.2 Glen Burn 117

5.11.1.3 Mattock 117

5.11.1.4 Nuenna 118

5.11.2 Evapotranspiration 119

5.11.2.1 Mattock 121

5.11.2.2 Nuenna 122

5.11.3 River Discharge Rating Curves 123

5.11.3.1 Gortinlieve 124

5.11.3.2 Glen Burn 124

5.11.3.3 Mattock 126

5.11.3.4 Nuenna 128

5.11.4 Water Balance 130

5.11.5 Discussion of Data Analysis 133

6 Physical River Hydrograph Separation 135

6.1 Introduction 135

6.2 Recharge Coefficients **136**
6.2.1 Implementation 136
6.2.2 Modification of standard recharge coefficient approach 137
6.2.3 Results of recharge coefficient approach 138
6.2.3.1 Gortinlieve 139
6.2.3.2 Glen Burn 140
6.2.3.3 Mattock 141
6.2.3.4 Nuenna 142

6.3 Recession Analysis **144**
6.3.1 Implementation 144
6.3.1.1 Tabulation method 145
6.3.1.2 Matching strip method 146
6.3.2 Calculation of relative storages 146
6.3.3 Results of recession analysis 147
6.3.3.1 Gortinlieve 147
6.3.3.2 Glen Burn (Mount Stewart) 149
6.3.3.3 Mattock 151
6.3.3.4 Nuenna 155

6.4 Digital Filtering Algorithm **157**
6.4.1 Adapted Lyne and Hollick filtering algorithm 158
6.4.2 Results of recursive digital filter algorithm 161
6.4.2.1 Gortinlieve 161
6.4.2.2 Glen Burn 162
6.4.2.3 Mattock 163
6.4.2.4 Nuenna 166

6.5 Hydrograph Separation using Temperature Data **167**
6.5.1 Fourier analysis 168
6.5.2 Temperature mixing model 168
6.5.3 Signal Identification 169
6.5.4 Results of hydrograph separation using temperature data 175

6.6 Discussion **177**
6.6.1 Recharge coefficient approach 177
6.6.2 Master recession curve analysis 179
6.6.3 Modified Lyne and Hollick algorithm 179
6.6.4 Temperature separation 180
6.6.5 Conclusion of physical hydrograph separations 181

7 Lumped Hydrological Modelling ***182***

7.1 Introduction **182**

7.2 NAM **184**

7.3 Preprocessing Data **187**

7.3.1 Rainfall 187

7.3.2 Potential Evapotranspiration 190

7.3.3 River discharge 191

7.3.4 Catchment Area 192

7.4 Model Execution **194**

7.4.1 Parameters 194

7.4.2 Preliminary modelling 194

7.5 Calibration **197**

7.5.1 Calibration Results 198

7.5.1.1 Gortinlieve 198

7.5.2 Glen Burn 200

7.5.3 Mattock 203

7.5.4 Nuenna 207

7.6 Validation **211**

7.7 Discussion **212**

7.7.1 Preliminary modelling 212

7.7.2 Calibration 215

7.7.3 Validation 220

8 Catchment Modelling: Finite Difference Modelling ***224***

8.1 Introduction **224**

8.2 MODFLOW **225**

8.3 Conceptual model and model design **227**

8.3.1 Modelling the continuous surface 230

8.3.2 Layer elevations 231

8.3.3 Hydraulic conductivity 232

8.3.4 Storage characteristics 234

8.3.5 Boundary conditions 236

8.3.6 Recharge 237

8.3.7 Target heads 237

8.4 Model Design **238**

8.4.1 Model set-up 1 238

8.4.2 Model set-up 2 239

8.4.3 Model set-up 3 241

8.5 Results **241**

8.5.1 Model set-up 1 241

8.5.2 Model set-up 2 243
8.5.3 Model set-up 3 245

8.6 Sensitivity analysis of transient simulation 252

8.7 Discussion 256
8.7.1 Model set-up 1 256
8.7.2 Model set-up 2 257
8.7.3 Model set-up 3 258
8.7.4 Sensitivity Analysis 260
8.7.5 Limitations of distributed modelling 261
8.7.5.1 Bedrock topography 262
8.7.5.2 Hydraulic conductivity 262
8.7.5.3 Storage 262
8.7.5.4 River heads 263
8.7.5.5 Recharge 263

9 Generalisation of NAM Parameters 265

9.1 Introduction 265

9.2 NAM Modelling 265
9.2.1 NAM parameters 266

9.3 Catchment Characteristics 270
9.3.1 GIS database 270

9.4 Multiple Linear Regression 273
9.4.1 Statistical model 274
9.4.2 Assessing the regression analysis 275
9.4.2.1 Analysis of Variance 276
9.4.2.2 Objective functions 277
9.4.3 Residual Analysis 278

9.5 Catchment descriptor and NAM parameter relationships 280
9.5.1 Relationships 280

9.6 Discussion 293
9.6.1 Limitations of regression 295
9.6.2 Framework for determining pathway contributions to Irish rivers. 296

10 Uncertainty Analysis 299

10.1 Introduction 299

10.2 Regression Equation Error 300

10.3 Sensitivity Analysis 301
10.3.1 One at a time sensitivity analysis 301

10.3.2 Evaluation of sensitivity 302
10.3.3 Parameter prediction distributions 302
10.3.4 MATLAB/NAM syncing 303

10.4 Results 303

10.5 Discussion 316
10.5.1 Performance of predictors equations 316
10.5.2 Sensitivity of discharges to NAM parameters 317
10.5.2.1 Nash-Sutcliffe Coefficient (R^2) 318
10.5.2.2 Square-root Nash-Sutcliffe coefficient 318
10.5.2.3 Bias 318
10.5.2.4 Deep and Shallow Groundwater 319
10.5.2.5 Interflow 319
10.5.2.6 Overland flow 320
10.5.3 Identifying upper and lower bounds to pathway contributions 320

11 Conclusions 323

11.1 Introduction 323

11.2 Physical Separation Methods 324
11.2.1 Recharge coefficient approach 324
11.2.2 Master recession curve analysis 325
11.2.3 Modified Lyne and Hollick algorithm 325
11.2.4 Temperature separation 326

11.3 Lumped Hydrological Modelling 326

11.4 Distributed Modelling 328

11.5 Generalisation of NAM Parameters 329

11.6 Uncertainty Analysis 329

11.7 Further Research Recommendations 330

References 332

Appendix A Supplementary Catchments

Appendix B Supplementary Physical Separations

Appendix C Supplementary NAM Modelling

Appendix D Supplementary Catchments' Regression Performance

Abbreviations and Symbols

Δ – Slope of the vapour pressure curve

A, Alluv – Alluvium

AE – Actual evapotranspiration

ANOVA – Analysis of Variance

b – River channel width

BFI – Baseflow Index

BFI_{max} – Eckhardt coefficient

BktPt – Blanket Peat

C – Boughton coefficient

CK – Overland flow time constant

CKBF – Shallow groundwater time constant

CKIF – Interflow time constant

CKLow – Deep groundwater time constant

CQOF – Overland flow runoff coefficient

d – River channel depth

DEM – Digital Elevation Model

Dr – Soil moisture deficit

e_a – Actual vapour pressure

EMMA – End Member Mixing Analysis

EPA – Environmental Protection Agency

e_s – Saturation vapour pressure

f – Frequency

FAO – Food and Agricultural Organisation

FEFLOW – Finite Element Flow

G – Soil heat flux density

G, GLPSSss, GLs – Gravel

GIS – Geographic Information System

GSI – Geological Survey of Ireland

GUI – Graphical User Interface

h – Head

HBV – Hydrologiska Byrons Vattenbalans-avdelning

HSPF – Hydrological Simulation Program-Fortran

K – Hydraulic conductivity

k – Recession coefficient

Ks – Water stress coefficient

L – Lower storage

MLR – Multiple Linear Regression

mOD – Metres above Ordinance Datum

MODFLOW – Modular Flow

MRC – Master Recession Curve

NAM – Nedsbor Afstromings Model

OAT – One at a time

PE – Potential evapotranspiration

Pl, Pu, Ll – Poorly productive aquifer

Q – Discharge

R – Rainfall

r^2 – Coefficient of determination

R^2 – Nash-Sutcliffe coefficient

r^2_{adj} – Adjusted coefficient of determination

RAW – Readily Available Water

Rck – Rock

Rkd – Regionally important karst aquifer

RMS – Root Mean Squared

Rn – Net radiation

S – Storage

SHE – Systeme Hydrologique Europeen

Ss – Specific storage

SWAT – Soil and Water Assessment Tool

SWG – Surface Water Gley

Sy – Specific yield

T – Temperature

TAW – Total Available Water

TG – Recharge threshold

TI – Interflow threshold

TMp, TLp – Till

TO – Overland flow threshold

U – Upper storage

v – Velocity

WFD – Water Framework Directive

γ – Psychrometric constant

θ – Soil water content

ρ – Density

τ – Reservoir time constant

1 Introduction

1.1 Background and Overview of Thesis

An understanding of the hydrological processes involved in a catchment is vital to predicting the impacts of human actions on river ecology and requires the identification of the important pathways transporting diffuse contaminants to rivers and aquatic ecosystems. Conceptually, the main flow pathways contributing to rivers in Ireland are: overland flow, interflow, shallow and deep groundwater flow (Figure 1-1). The aims of a major current research project (*Pathways Project*) are to achieve a better understanding of these pathways, the fate and transport of waterborne contaminants, and their subsequent impact on aquatic ecosystems in Irish catchments. The contaminants being investigated include phosphorus, nitrogen, sediments, pesticides and pathogens. The project is to develop a Catchment Management Tool (CMT) to assist the Irish Environmental Protection Agency and River Basin District managers in achieving the objectives of the European Water Framework Directive (WFD, 2000), in improving the management and protection of the country's water resources. This project is being carried out by a consortium of Queen's University Belfast, Trinity College Dublin and University College Dublin.

An important element of research within this broad project was to quantify the proportion of the river hydrograph that is derived from each of the main pathways. The research described in this thesis has utilised river discharge, rainfall and temperature measurements in four study catchments. These study catchments are: Gortinlieve in Co. Donegal, Glen Burn in Co. Down, Mattock on the Co. Louth/Meath border and Nuenna in Co. Kilkenny; these reflect a range of catchment characteristics, typical of the Irish setting, ensuring that this research will provide a methodology that can be applied throughout Ireland and will have international applications. The data from these study catchments are used throughout the thesis to determine the contribution of these pathways to river discharge.

The initial conceptual model applied in this thesis supposes that water flows along hydrological pathways before becoming part of total runoff in the stream. The conceptual model identifies four pathways: overland flow, interflow, shallow groundwater flow and deep groundwater flow (Archbold et al., 2010). Overland flow is considered to be the flow that occurs close to the surface of the land when the soil has reached saturation, or when rainfall is of sufficient intensity, that the rainfall cannot infiltrate into the soil. Interflow is lateral flow that occurs in soils and subsoils. It may be saturated or unsaturated. Shallow groundwater flow is that which occurs in the upper few metres of the fractured bedrock aquifer that often has higher permeability than the deeper parts of the aquifer in which deep groundwater flow occurs. Figure 1-1 illustrates four of the four pathways.

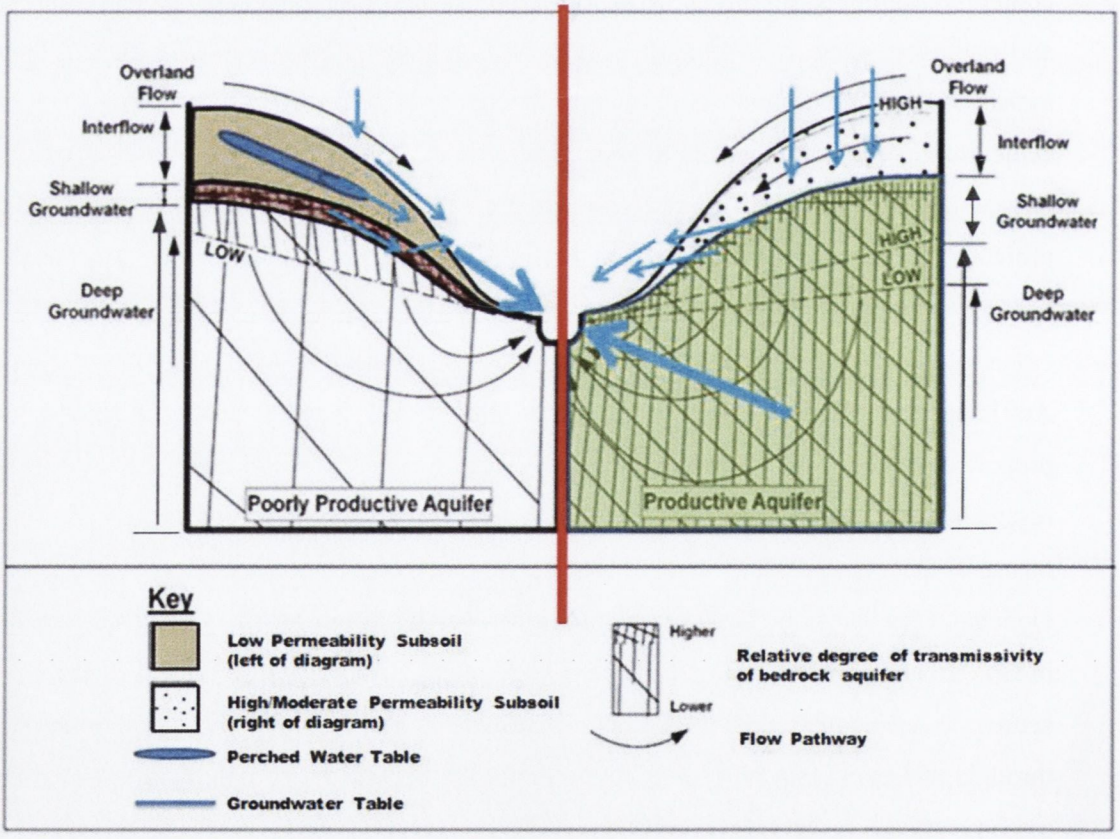

Figure 1-1 Pathways present in poorly productive and productive aquifers on the left and right respectively (J. Deakin: after N. Hunter-Williams and D. Daly).

A combination of physical separations evaluating the responses of the river to rainfall, a recharge coefficient approach assessing the soils, subsoils and aquifers of a catchment and temperature time series analysis were employed to provide realistic ranges for the contribution of each of these pathways. Therefore, these ranges, based on knowledge of the measured discharge in the river, the geological setting of a catchment and temperature measurements in the river and the subsurface, provided a robust means of constraining the lumped hydrological model that was applied to the study catchments. This model represented catchments as a series of linked reservoirs with discharges from the reservoirs corresponding to the different pathways. It was possible to calibrate this model applying the range of separations obtained from the separation methods outlined and the observed discharge of the river.

An important function of the CMT would be its application to ungauged catchments within Ireland. As the lumped model would be one of the main influences on the hydrological modelling development of this tool, it was important to generalise the modelling approach described in this thesis and ensure that the model could be employed in these ungauged catchments. Therefore, utilising multiple linear regression, equations were developed to relate the model parameters to physical catchment characteristics in the catchment that could be identified from geographical information systems (GIS). The errors associated with these regressions were then utilised to determine the sensitivity of the model parameters, this provided an assessment of the importance of each parameter with regards to each pathway's contribution and the overall match with simulated and observed discharge in the river. To the author's knowledge, this rigorous evaluation of the sensitivity of the rainfall-runoff model NAM's parameters has not been conducted before.

The integrated approach of this thesis to determining the contribution of each of the pathways to the river, employing hydrograph separation methods and hydrological, will be vital for the development of attenuation modelling of contaminants along the pathways, also undertaken within the *Pathways Project* but outside the scope of this thesis, and for informing the hydrological modelling aspect of the CMT.

1.2 Research Aims and Objectives

The primary aim of the research was to develop a methodology for separating the river hydrograph into its four contributing pathways using catchment characteristic data available in GIS databases. Towards this end, four study catchments together with supplementary catchments, for which data were available, were investigated in detail. The objectives of this research are:

- Application of a variety of physically based hydrograph separation techniques (including necessary modifications) in order to provide model calibration constraints.
- Implementation of lumped and fully distributed hydrological models to quantify pathway contributions.
- Original approach towards the development of regression equations linking lumped model parameters to GIS datasets.
- Assessment of sensitivity of model parameters for future applications of lumped model.

These objectives have been achieved through the following activities:

- The monitoring of rainfall and river flow, through the siting of rain gauges and the establishment of hydrometric stations (including the rating curves) to measure river stage in two catchments (the Mattock and Nuenna) for which the author was primarily responsible for hydrometric data collection.
- Application of physical river hydrograph separation methods to the study catchments and supplementary catchments to assess contributions of the hydrological pathways to rivers and provide constraints for calibration of hydrological modelling.
- Application of a lumped model to simulate the temporal variation throughout the year of the pathways in the study catchments and in supplementary catchments.

- Investigation of the correlation between the response time of the fastest pathways and the temporal resolution of inputted rainfall required to achieve accurate simulations of peaks in the hydrograph.
- Application of a distributed finite-difference model in one of the study catchments to further investigate the groundwater interactions with the surface water and to evaluate the feasibility of using such an approach at a catchment scale in data-scarce environments.
- Development of relationships between catchment descriptors, such as soils, subsoils, catchment area etc., and the parameters of the lumped model for application in ungauged catchments in Ireland.
- Implementation of a Monte-Carlo simulation of the lumped model varying the parameters to assess their sensitivity and further assess the importance of each parameter during simulations.

1.3 Scope and Layout of Thesis

The overall scope of this thesis is laid out as follows:

- Review of the available literature regarding previous research in physical hydrograph separation techniques (Chapter 2).
- Review of the available literature in relation to hydrological models and their application to catchment scale studies (Chapter 3).
- Description of study catchments, their land-use, hydrological characteristics and hydrogeological settings (Chapter 4).
- Outline of research methodology regarding the collection of data from study catchments and assessment of data quality (Chapter 5).
- Application of physical hydrograph separation techniques, modified as required, to study catchments with discussion of results (Chapter 6).
- Application of lumped and conceptual rainfall-runoff model NAM to study catchments with additional discussion of results (Chapter 7).
- Application of fully distributed groundwater model MODFLOW to Mattock catchment with further discussion of results (Chapter 8).

- Regionalisation of NAM parameters using multiple linear regression and available GIS data (Chapter 9).
- Assessment of uncertainty associated with each of the NAM parameters (Chapter 10).
- Conclusions and recommendations (Chapter 11).

2 Literature Review: Physical Hydrograph Separation Techniques

2.1 Introduction

The literature review is being carried out in two chapters, one chapter for hydrograph separation techniques and the other focusing on hydrological models. This chapter views the current methods available to hydrological modellers for partitioning the effective rainfall that falls within a catchment into the principal components of the hydrograph. The initial conceptual model used in this thesis supposes that these principal components are the hydrological pathways that water flows along before becoming part of total runoff in the stream. As outlined in Chapter 1, the conceptual model identifies four pathways; overland flow, interflow, shallow groundwater flow and deep groundwater flow. The approaches reviewed in this chapter are drawn together from journal papers, government documents and best practice standards. The approaches perused relate to the following methods of investigating the processes of the hydrological cycle: hydrograph separation techniques, lumped, semi-distributed and fully distributed hydrological models and numerical modelling approaches. This research ensures that decisions concerning data collection and the iterative nature of model development and testing were better informed.

In general, the objectives of hydrograph separation were to determine the deep groundwater flow contribution to stream flow in order to calculate base flow index (BFI), generally defined as the ratio of baseflow to total river flow (Institute of Hydrology, 1980) and which has been subsequently applied in most studies involving hydrograph separations: Nathan and MacMahon (1990), Boughton (1993), Chapman and Maxwell (1996), Mugo and Sharma (1999), Eckhardt (Eckhardt, 2008), etc. In this thesis BFI is defined to be the ratio of deep and shallow groundwater flow to total stream flow. Few studies separate the hydrograph further than into quick flow and baseflow. These techniques and their implementation are reviewed with those capable of separating the hydrograph into more than two pathways further discussed in Section

2.7. Along with these, the approaches that have the potential to separate the hydrograph into more than two pathways, with modification where necessary, are also discussed.

When separating baseflow from the observed discharge, certain qualitative rules have been applied to assist in assessing separations. These rules of thumb allow one to ascertain if the results of techniques applied are realistic or act as a guidance in graphical separations carried out by hand on available hydrographs. The Australian Rainfall and Runoff report on Baseflow for Catchment Simulation (Merz et al., 2009) summarises five such rules concisely as:

1. Low flow conditions prior to the commencement of a flood event consist entirely of baseflow.
2. The rapid increase in river level relative to the surrounding groundwater level results in an increase in bank storage. The delayed return of this storage to the river causes the baseflow recession to continue after the peak of the total hydrograph.
3. Baseflow will peak after the hydrograph due to the storage-routing effect of the sub-surface stores.
4. The baseflow recession will most likely follow an exponential decay function.
5. The baseflow hydrograph will rejoin the total hydrograph as quickflow ceases.

These five objectives of baseflow separation are utilised when assessing the techniques employed in the study catchments (see Chapter 5).

In this literature review of separation techniques, methods that separate hydrographs into the standard quick responding flow and baseflow, and those separation methods that can identify more than two pathways. Separation techniques can be divided into five main approaches: graphical separation, recession analysis, frequency analysis, geochemical separation and recharge coefficient approach. None of these techniques are completely reliable (Nathan and McMahon, 1990; Brodie and Hostetler, 2005; Scanlon et al., 2005). To address this issue, a number of these approaches may be implemented in conjunction with one another to estimate the separation of the river into its flow components.

2.2 Graphical

Graphical methods for hydrograph separation can be arbitrary in nature. They rely on the experience of the user rather than on the physical properties of the catchments. They separate a hydrograph into quick and slow response flow. Due to their arbitrary nature, it is difficult to relate each response to a physical process as the hydrograph is typically comprised of more than two components (Hewlett and Hibbert, 1967; Anderson and Burt, 1980). For the conceptual understanding of flow pathways in this thesis, it can be considered that overland flow and interflow are responsible for the quick response and that shallow and deep groundwater flows are responsible for the slow response. Though the rate at which each individual pathway will respond will vary from pathway to pathway. This provides one way of identifying pathways. This may not hold true in all cases, particularly for interflow and overland flow, which will be discussed later in Chapter 6.

There are two main types of graphical separation: those that assume the slow response responds concurrently with the runoff and those that include the effects of bank storage in the separation of the hydrograph.

2.2.1 No Bank Storage

Four graphical methods are displayed in Figure 2-1. The simplest method is of the form of joining point A directly to point B. This is known as the constant slope method. Point A is the beginning of surface water runoff for the event recorded. Point B can be identified using many different approaches, both graphical and analytical. One graphical method (Linsley, 1958) uses Equation 2-I:

$$N = 0.83A^{0.2} \qquad 2\text{-I}$$

where A is the catchment area [km^2] and N is the time interval [days] from peak of the hydrograph to the end of quick response flow. In Linsley's method the recession line before rising limb begins is continued from A to under the peak. This point is then joined to point B, as is shown in Figure 2-1. An analytical approach (Horton, 1933) can

be applied to locate *B* as the point that runoff becomes linear in a plot of the natural logarithm of flow versus time.

Applying Gray's method (Gray, 1973), a line is drawn backwards from the recession limb from *B*, the point at which quick response flow is said to have ended, to under the peak of the hydrograph. The slope of this line is that of the linear recession plot used to locate *B*. This line is then connected to point *A*.

Also displayed in Figure 2-1, is Subramanya's method (Subramanya, 1994) which is applied in a similar manner to Gray's method, except the line drawn backwards from end of quick response flow stops under the point of inflexion of the recession limb of the hydrograph rather than under its peak. This reflects the delay of the groundwater flow peak due to the time taken for rainfall to infiltrate into the aquifer. Therefore, this point occurs after the total runoff peak.

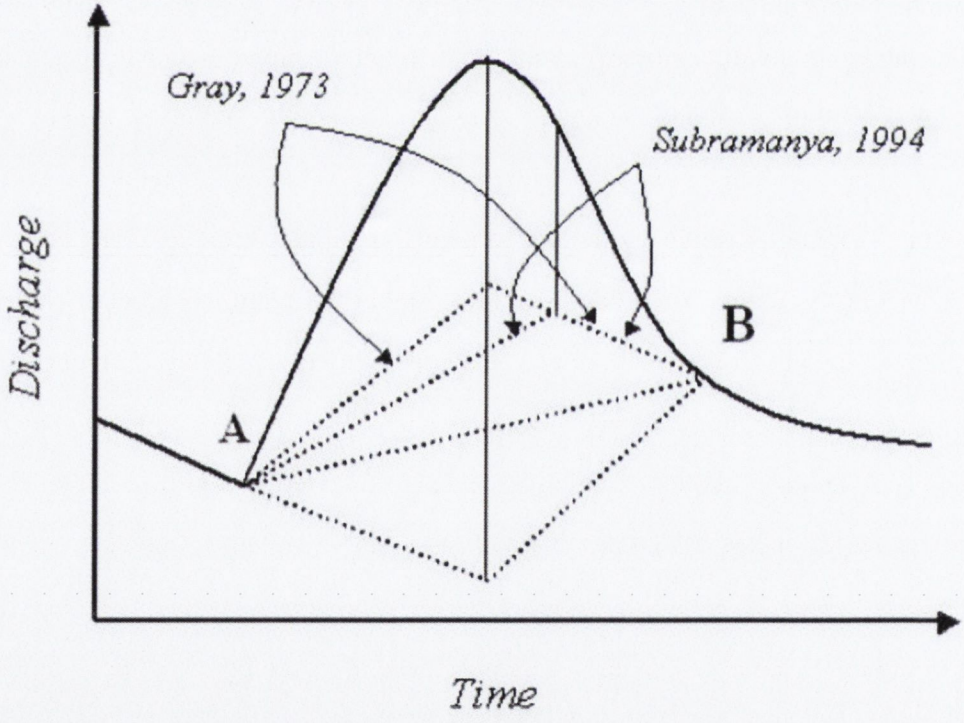

Figure 2-1. Graphical separation approaches (RPS, 2008).

2.2.2 Bank Storage

The final graphical separation method in Figure 2-1 is the bottom line from *A* to *B*. In this approach, water flowing from the river into unsaturated soils in the banks surrounding the river is accounted for. In Figure 2-2, line *a-b-c* shows hydrograph separation ignoring the effects of bank storage, while line *a-d-e-c* is hydrograph separation taking the initial flow into river banks and subsequent flow out of them into account (Nathan and McMahon, 1990; Chen et al., 2006). During a rainfall event overland flow and interflow arrive at the river first as these are the quickest response flow. The river stage increases due to this flow and until the slower response flows have increased sufficiently, a reversal in the direction of the local hydraulic gradient occurs. This then causes the water to flow into the surrounding banks from the river and hence decrease the slow response flow as this is considered negative flow against the hydraulic gradient. Once the slow response flow from the event reaches the river, the hydraulic head starts to return to its original state and water starts to flow into the river from the banks. In Figure 2-2, the period over which this happens is *d-e*. Slow response flow reaches a peak at e and then starts to recede as in the case where no bank storage is taken into account. Barnes (1939) suggests that e is located under the point of inflection of the recession limb.

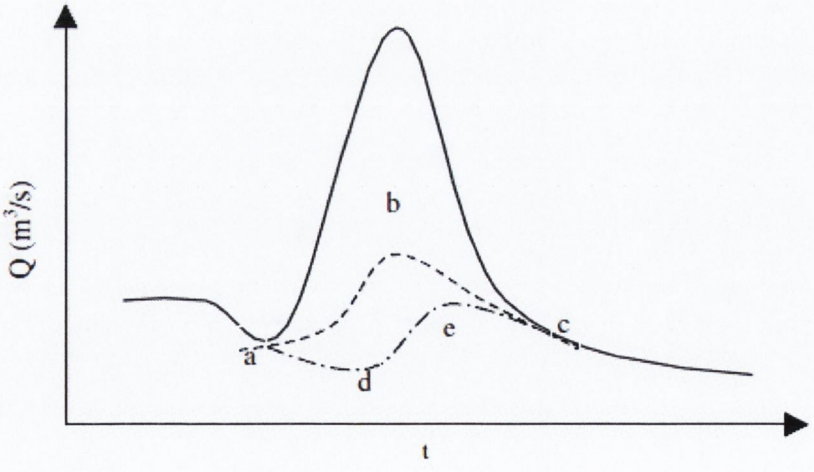

Figure 2-2. Streamflow and baseflow hydrographs (Chen et al., 2006).

2.3 Recession Analysis

The characteristics of catchments, more particularly the aquifers that contribute groundwater flow to stream flow, are best observed during periods of drought. An absolute drought period in Ireland is considered to be 15 consecutive days, or more, without 0.2 mm or more rainfall on each day, while a partial drought is defined as at least 29 consecutive days when the mean daily rainfall does not exceed 0.2 mm (Rohan, 1975). Any discharge to streamflow during a drought period is thought to be composed entirely from deep and shallow groundwater flow. The shape of a hydrograph can also indicate the type of catchment the river is located in. If heavy rainfall is recorded in the catchment and a sharp rise in the hydrograph is recorded, this indicates that there is a large proportion of quickly responding flow, suggesting the catchment may be dominated by steep slopes and/or low permeability soils, subsoils or poorly productive bedrock, resulting in a low BFI value.

Research has shown (Maillet, 1905; Barnes, 1939) that the recession limb of the hydrograph can be approximated by Equation 2-II:

$$Q_t = Q_0 e^{-t/\tau} = Q_0 K^t \qquad \text{2-II}$$

where Q_t and Q_0 are the discharge at times t and start of the recession, time 0, and τ is the response or time constant of the reservoir. The term $e^{-(1/\tau)}$ is usually termed the recession constant k and can be used to inform the automated signal filtering techniques (Chapman and Maxwell, 1996). Equation 2-II is obtained from the solution to the water continuity equation:

$$Q = -\frac{dS}{dt} \qquad \textbf{2-III}$$

where S is the storage of the reservoir (m^3), using the linear relationship of discharge to storage:

$$Q_t = \frac{S_t}{\tau} \qquad \textbf{2-IV}$$

The general suitability of the assumption of the groundwater storage being a linear reservoir has been questioned as many recessions do not always form a straight line on

a semi-logarithm plot, e.g. (Barnes, 1939; Chapman, 1999; Fenicia et al., 2006). It has been shown that although simplistic in its approach to groundwater discharges, the linear reservoir assumption, subject to incorporating recharge into the analysis, can suitably model the groundwater behaviour in catchments (Chapman, 1999). Where the groundwater behaviour cannot be adequately modelled applying the linear reservoir assumption, a non-linear model should be used. Equation 2-II is shown to be the special case solution of the generalised non-linear reservoir (Coutagne, 1948), Equation 2-V:

$$Q_t = Q_0[1 + (n-1)t/\tau_0]^{-n/(n-1)} \qquad \textbf{2-V}$$

where $\tau_0 = S_0/Q_0$ is the turnover time at time zero and n is the measure of the non-linearity of the reservoir.

Another approach for approximating this situation would be to split the non-linear reservoir into smaller reservoirs that could each be modelled as being linear (Tallaksen, 1995). This was the approach taken in this thesis for calculating the τ related to each of the reservoirs representing the subsurface pathways. In this case the hydrograph recession was modelled using the superposition of the recession of three individual reservoirs, one for each subsurface pathway:

$$Q_t = Q_0 e^{-t/\tau^*} + Q_{0I} e^{-t/\tau_I} + Q_{0S} e^{-t/\tau_S} + Q_{0D} e^{-t/\tau_D} \qquad \textbf{2-VI}$$

where *, $_I$, $_S$, and $_D$ refer to combined, interflow, shallow and deep groundwater storages respectively.

2.3.1 Master Recession Curve (MRC)

A master recession curve (MRC) involves the construction of an average recession curve from multiple individual recession curves. The objective is to identify the most frequent recession discharge response and therefore reduce the influence that antecedent recharge events have on the individual recessions. In a MRC that is non-linear on a semi-log plot, it is suggested that overland flow, interflow and groundwater flow can be identified from the slopes of the different straight line segments (Barnes, 1939).

2.3.1.1 Correlation Method

Discharge at one time is plotted against discharge at another arbitrary interval N days later during the recession periods. All periods during the N day period are utilised and points from the same recession are joined. Equation 2-II is rearranged to:

$$k = e^{-\alpha} = \left(\frac{Q_t}{Q_0}\right)^{1/t} \qquad \text{2-VII}$$

where t is N days after the initial time. An enveloping line can be drawn along the perimeter of the region where the curves run most densely together. The slope of this enveloping line is used in Equation 2-VII to give the recession constant (k), as shown in Figure 2-3.

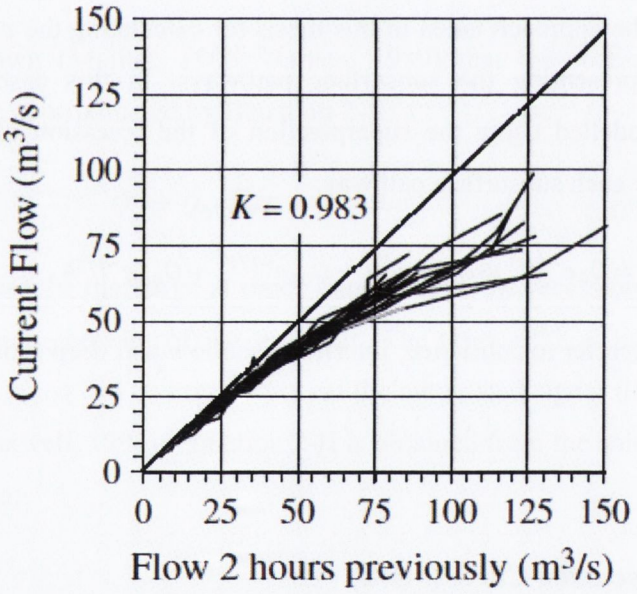

Figure 2-3. Correlation method with the recession constant equal to 0.983 (Sujono et al., 2004).

2.3.2 Matching Strip Method

This method is based on Equation 2-II. The form of the equation implies that logarithm of flow against time will plot as a straight line. Each recession is plotted and then adjusted horizontally until the recessions overlap to form the MRC. The procedure of

adjusting the individual recessions can be semi-automated on a computer. Each recession is plotted in order of decreasing minimum discharge (Toebes and Strang, 1964). An initial MRC is drawn, after which the individual recessions can be manually adjusted along with the slope of the MRC until an acceptable fit is achieved. A MRC can be constructed from as few as two recessions (Lamb and Beven, 1997) in order to obtain a k value (Figure 2-4).

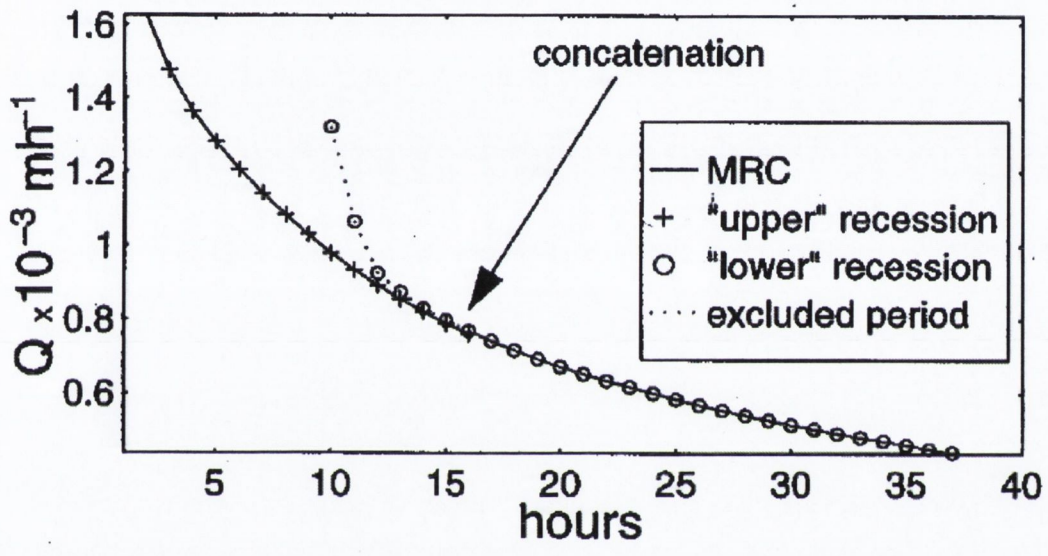

Figure 2-4. Plot of recession segments (Lamb and Beven, 1997).

2.3.3 Tabulation Method

Plotting many recessions side by side, as per the tabulation method (Johnson et al., 1956), the characteristic response of a catchment at different discharge levels can be inferred from the rate of recession of the discharges. This approach emphasises the quicker responding pathways as it is the upper section of the recession that is matched and not the lower section as is the case applying the matching strip method. Figure 2-5 shows an example of the tabulation method applied to a catchment.

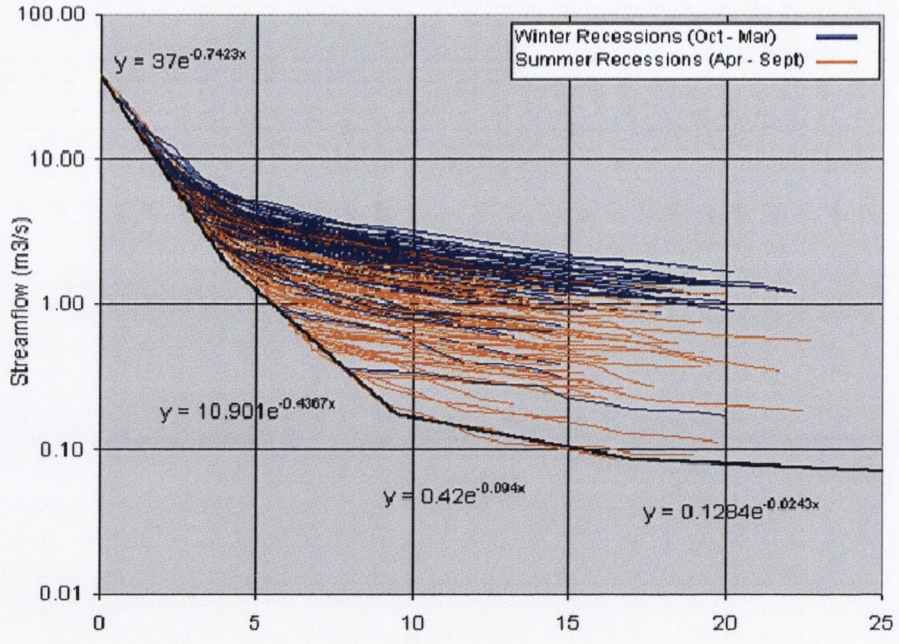

Figure 2-5. MRC Tabulation method analysis (RPS, 2008).

2.4 Frequency Analysis

2.4.1 Flow Duration Curves

Flow duration curves provide another measure of groundwater contribution to streamflow through the application of a dimensionless ratio. This ratio is obtained by dividing Q_{90}, the flow that is exceeded 90% of the time, by Q_{50}, the flow that is exceeded 50% of the time. Q_{90} is notionally considered to be a representative measure of the groundwater contribution to streamflow (Nathan and McMahon, 1990).

The shape of the flow duration curve across all percentiles gives an insight into the type of response a catchment has to rainfall. If the flow duration curve below the Q_{50} has a shallow slope, this indicates a large groundwater contribution to the river, whereas a steep curve indicates comparatively smaller contributions from groundwater storage and thus indicates a flashier catchment response to rainfall (Brodie and Hostetler, 2005). If there is a steady decrease in the slope below the Q_{50}, as depicted in Figure 2-6, this indicates a sustained groundwater input to the catchment.

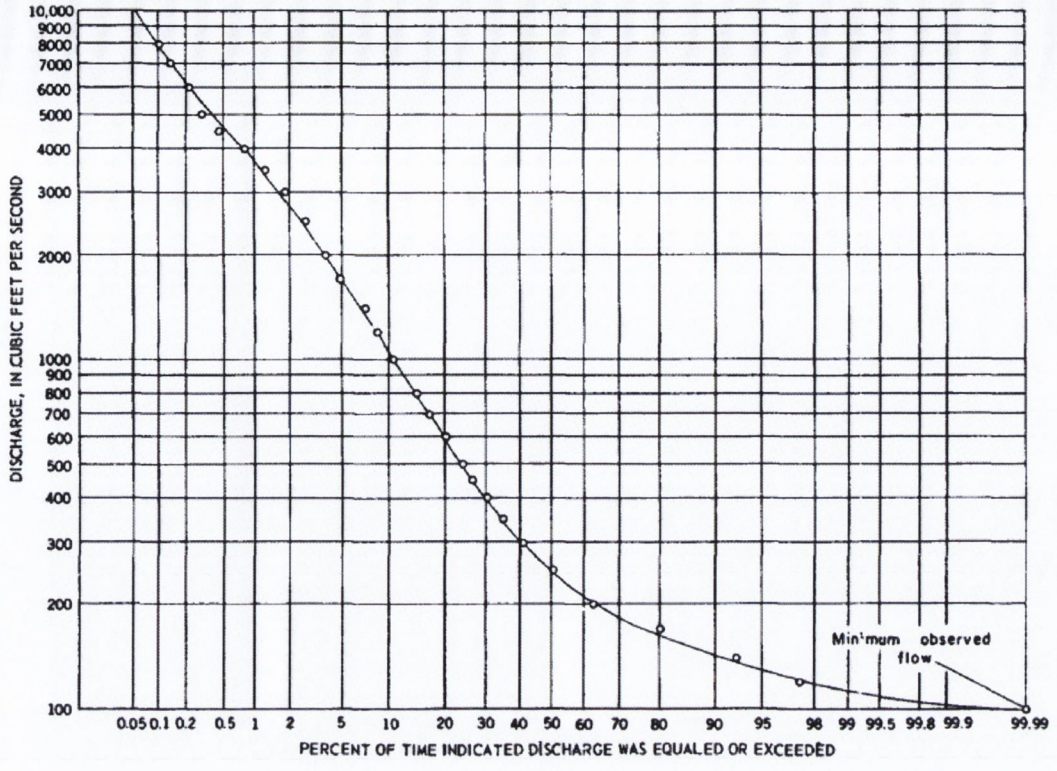

Figure 2-6. Example of a flow duration curve (Searcy, 1959).

2.4.2 Fixed interval, sliding interval and smoothed local minima turning point methods

Three methods, two of which are available in the HYSEP model (Sloto and Crouse, 1996), while the third is a modified version of a third method available in HYSEP, are commonly applied for calculating BFI from discharge data. These methods provide a consistent and automated technique that could be applied to separate the hydrograph into quick and slow response flow. The time step $2N$, used in each of these methods, is calculated with Equation 2-I.

The fixed interval method involves identifying the minimum discharge within an interval and setting it as the baseflow for that interval. The sliding interval method is analogous to the fixed interval method, but the interval moves forward in the discharge series by one time step each time, with the minimum value of the interval being set as the value of baseflow at the median of the interval (Pettyjohn and Henning, 1979). Examples of these methods are provided in Figure 2-7.

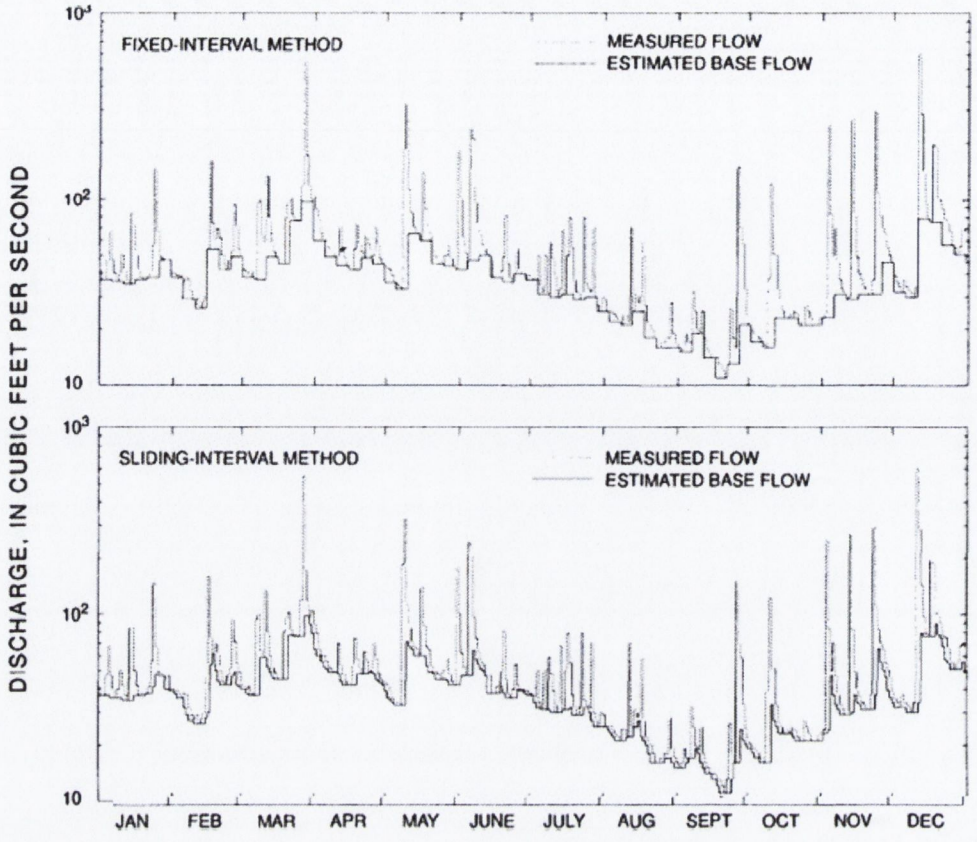

Figure 2-7 . Fixed interval and sliding interval methods (Sloto and Crouse, 1996).

The Smoothed Minima technique (Institute of Hydrology, 1980) was developed to provide a consistent and automated technique that could be utilised to separate the hydrograph into quick and slow response flow. The procedure involves dividing the recorded flows into non-overlapping blocks using a time base of five days. The minima of each of these blocks would then be compared to the minima of the block before and the block after it. If the minima were less than 90% of the outer values, it would be termed a turning point. The choice of the time base has a large effect on the BFI calculated, as the minima values chosen from each block are sensitive to the time base value (Misstear and Fitzsimons, 2007).

At the end of the process all the turning points are connected to construct the separation line between quick and slow response. This method provides a crude but repeatable means of separating a hydrograph.

2.4.3 Recursive Digital Filters

This technique is based upon a recursive digital filter commonly implemented in signal analysis and processing. The basis of this method is that filtering out high-frequency signals is analogous to the separation of 'low-frequency' slow response flow from 'high-frequency' quick response flow. The main drawback of this type of method is that the selection of parameters can be subjective (though not always) and physically unrealistic. It is however repeatable and easily automated (Nathan and McMahon, 1990).

In Chapman (1999), three types of recursive digital filters are compared to each other. These are the 'one-', 'two-' and 'three-parameter' algorithms. It was found that the BFIs obtained using these algorithms varied widely. There was a similarity between the 'one-' and 'two-parameter' algorithms, but no comparison could be made between the 'three-parameter' algorithm and the others.

- **One-parameter algorithm**

  The first 'one-parameter' algorithm (Lyne and Hollick, 1979) was shown to maintain baseflow at a constant value once overland flow had ceased. This was updated (Chapman and Maxwell, 1996) to a form that has the groundwater flow being a weighted average of the quick response flow and the slow response flow from the previous time interval:

$$Q_s(i) = \frac{k}{2-k} Q_s(i-1) + \frac{1-k}{2-k} Q(i) \qquad \text{2-VIII}$$

  subject to the condition that:

$$Q_s(i) \leq Q(i) \qquad \text{2-IX}$$

  where Q_s is slow response flow [L^3/t], Q is stream flow [L^3/t], k is the recession constant and i is the time step.

- **Boughton two-parameter algorithm**

  Implementation of the 'one-parameter' algorithm in practice tends to estimate baseflow as close to fifty percent of the total hydrograph, since quick flow

maintains the same percentage of itself in time step t as baseflow does. The 'two-parameter' algorithm (Boughton, 1993) was developed from the 'one-parameter' algorithm in order to overcome this constraint. It replaces $1 - k$ with C to add another degree of flexibility to the algorithm. Equation 2-VIII becomes:

$$Q_s(i) = \frac{k}{1+C} Q_s(i-1) + \frac{C}{1+C} Q(i) \qquad \text{2-X}$$

subject to Equation 2-IX.

The addition of parameter C, although making the algorithm more flexible, reduces objectivity as C must be chosen by the user of the filter. If an optimisation programme is implemented to select a value for C, C will be increased until the entire streamflow that is observed becomes groundwater flow. Therefore, C should be selected with a focus on achieving the correct point for quick response flow to end on the hydrograph and obtain a more intuitively realistic shape to the separation time series.

Eckhardt (2005) developed a 'two-parameter' filter (Equation 2-XI)to remove the subjectivity of the C parameter from Boughton's algorithm (Equation 2-XI). This algorithm assumes there is *a priori* knowledge of the catchment or at least a surrogate catchment that would provide an estimate of the maximum baseflow index (BFI_{max}), the maximum value of the ratio of baseflow (slow response pathways) to total streamflow.

$$Q_{St} = \frac{1 - BFI_{max}}{1 - kBFI_{max}} kQ_{St-1} + \frac{1-k}{1-kBFI_{max}} BFI_{max} Q_t \qquad \text{2-XI}$$

subject to Equation 2-IX.

This algorithm again involves a subjective parameter in that BFI_{max} cannot be measured *a priori*. Therefore, there will be an element of calibration involved using the filter that will require the updating of the BFI_{max} applied until a satisfactory separation is acquired.

- **Three-parameter algorithm**

In the linear form of the IHACRES model (Jakeman and Hornberger, 1993) the excess rainfall u, is partitioned in slow and quick components using the following equations:

$$Q_s(i) = \beta_s u(i) - \alpha_s Q_s(i-1) \qquad \text{2-XII}$$

$$Q_q(i) = \beta_q u(i) - \alpha_q Q_q(i-1) \qquad \text{2-XIII}$$

where α and β are parameters and the suffixes s and q refer to slow and quick response flow. The u can be eliminated by combining Equation 2-XII and Equation 2-XIII to give Equation 2-XIV:

$$Q_s(i) = \frac{k}{1+C} Q_s(i-i) + \frac{C}{1+C}\left[Q(i) + \alpha_q Q(i-1)\right] \qquad \text{2-XIV}$$

where $C = \beta_s/\beta_q$ and $k = -\alpha_s - \alpha_q\beta_s/\beta_q$. This can be seen as an extension of Equation 2-XI and implies that the slow response flow is positively linked to change in total streamflow, given that $\alpha_q < 0$.

For the same reasons as with Boughton's 'two-parameter' algorithm, an optimisation program cannot be applied to obtain all the parameters in Equation 2-XIV and therefore it can be difficult to fit to observed data.

Although the k values can be informed from MRC analysis, the remaining C parameter in the Boughton algorithm and the BFI_{max} parameter in the Eckhardt algorithm are free variables which are very sensitive in relation to the BFI value calculated. In a comparison of the algortihms, the 'two-parameter' Boughton algorithm appears to be the most satisfactory overall, although as stated it suffers from the disadvantage that the parameter selection is subjective. However, the variations from one operator to another seem likely to have less effect on the BFI than use of the objectively fitted 'one-' and 'three-parameter' algorithms, both of which can result in implausible separations on some catchments, with consequently high or low BFI values (Chapman, 1999).

- **Wavelet analysis**

Wavelet transform analysis (Morlet et al., 1982; Grossmann and Morlet, 2006) is a mathematical method similar to Fourier analysis that represents a signal with the summation of functions bounded in frequency. Unlike Fourier analysis, wavelet transform analysis functions are also bound in time. This provides a means to break down signals into their different components (Newland, 1996). This has been used for the analysis of a flood hydrograph recession (Sujono et al., 2001) and demonstrates that wavelet transform analysis can be a powerful tool for hydrological time-series analyses.

Arbitrary signals like flood events are transformed into infinite summation of wavelets at different levels according to Equation 2-XV (Newland, 1996):

$$f(x) = \sum_{j=-\infty}^{\infty} \sum_{l=-\infty}^{\infty} c_{j,k} W(2^j x - l) \qquad \text{2-XV}$$

where $c_{j,k}$ are wavelet coefficients, $W(2^j x - l)$ represents wavelet functions and l is an integer. The integer j describes different levels of wavelets, l represents the number of wavelets in each level covering an interval $0 < l < (2^j - 1)$, x is an independent variable commonly defined for $0 < x < 1$. Assuming $f(x) = 0$ outside the interval $0 < x < 1$, Equation 2-XV can be rewritten as Equation 2-XVI (Newland, 1996):

$$f(x) = a_0 + \sum_{j} \sum_{k} a_{2^j+k} W(2^j x - k) \qquad \text{2-XVI}$$

where a_o is a wrapped scaling function that is equal to the average of signal $f(x)$, a_{2^j+k} is the coefficient of the wavelet expansion and $W(2^j x - k)$ represents the wrapped wavelet functions.

In order to analyse the signal behaviour in frequency-time domain, the mean square values of the signal $f(x)$ are required. This is calculated by squaring both sides of Equation 2-XVI and integrating between $0 < x < 1$. The result can be expressed as Equation 2-XVII (Newland, 1996):

$$\int_0^1 f^2(x)dx = a_0^2 + \sum_j \sum_l a_{2^j+l}^2 \left(\frac{1}{2^j}\right) \quad \text{2-XVII}$$

This provides values that can be illustrated graphically by a three-dimensional plot called mean-square wavelet maps that can be interpreted as a plot of frequency against time (Sujono et al., 2004). By examining these maps, changes in signal behaviour can be identified easily, as the signal behaviour affects the mean-square values.

The recession constant, *k*, can be determined by analysing the recession applying Equation 2-XVII or wavelet maps. Slow response flow would be the lowest frequency component of the recession. The lowest frequency can be regarded as a cut-off frequency (f_c). Its value and location can be found using Equation 2-XVII or the wavelet maps by identifying when the mean-square value reaches maximum. Instead of utilising wavelet levels to draw the wavelet map, the level's frequency allows easier analysis of flood recession behaviour. The centred frequency of each level is computed by using Equation 2-XVIII:

$$f = \frac{2^j f_s}{N} \quad \text{2-XVIII}$$

where f is the centred frequency, j is wavelet level, f_s is $1/\Delta t$ and $N = 2^n$ is the length of the dyadic discrete wavelet transform in which $n = j-1$. Figure 2-8 shows how a wavelet map can be used to calculate *k*.

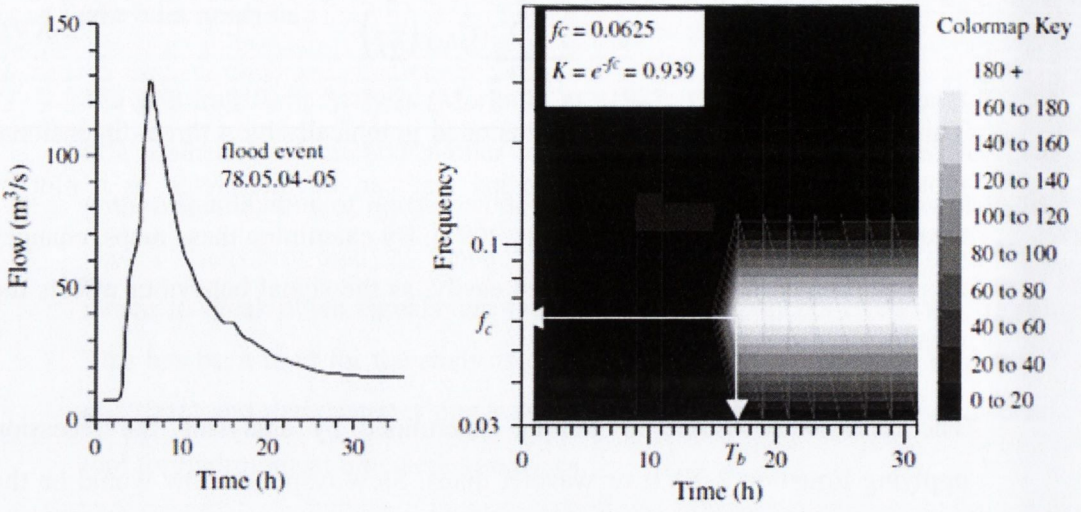

Figure 2-8 Example of a wavelet map at Bojongloa (Sujono et al., 2004)

The wavelet maps show that the highest mean-square value indicating the starting point or location of the slow response component T_b can be recognized easily. While identifying this point easily, the method does have the weakness that f_c is a function of $2^j/N$ in Equation 2-XVIII. As a result k for a number of events may occur at the same frequency values. This is a result of the fact that in the dyadic discrete wavelet transform, the length of data must be a power of two. Despite this, it has been shown (Sujono et al., 2004) to produce useful results.

2.5 Geochemical Analysis

The application of geochemical analysis for hydrograph separation is based on techniques that relate the concentration of solutes in streams and the different components of flow with residence time in the soil and contact with geological materials (Pinder and Jones, 1969). Although not a direct part of the data collection and analysis of this thesis, some of these principals will be applied in Chapter 6 for pathway separation utilising temperature data in the Mattock catchment. Therefore, a brief account of these principles is included here.

As precipitation infiltrates through the soils and subsoils, solute concentration increases with residence time and contact with the different geological materials. The variation in solute concentration between the stream and the different flowpaths may then be utilised to estimate the contribution each flowpath makes to the streamflow.

The principle of hydrograph separation, using water chemistry and natural tracers, is based on the mass flow equation:

$$Q_T c_T = Q_1 c_1 + Q_2 c_2 \dots Q_n c_n \qquad \text{2-XIX}$$

where Q_T is the discharge in the stream (m^3/s), c_T is the concentration of the tracer being measured (mg/L) and subscripts 1 to n refer to the components of flow that contribute to the stream. The separation of a stream into n components, requires *(n-1)* tracers.

Statistical methods are then applied to the data to estimate the contribution of each of the pathways to the flow and to estimate the degree of uncertainty in the results. Many methods rely on Monte-Carlo analyses using generated data or direct comparison to field data and other statistical approaches. One approach that has the potential to separate hydrographs and validate the choice of pathways is End Member Mixing Analyses (EMMA) (Hooper et al., 1990). This application has been implemented widely since its development in the early 1990s.

There are a number of assumptions that must be satisfied when carrying out hydrological mixing analysis. These include:

- The tracer being used is conservative and is not impacted to a significant degree by chemical or biological processes spatially or temporally. Reactive tracers may be used if their variations can be accounted for (Hoeg et al., 2000).
- There is no significant storage in the system that could influence the tracer concentrations (Hooper and Shoemaker, 1986).
- There is a significant difference between tracer concentrations of each component of flow so that they are distinguishable (Hoeg et al., 2000).

- Where the number of stream flow components are small, the difference between tracer concentrations of combined components is small (Sklash and Farvolden, 1979).
- Temporal and/or spatial variations in stream flow compositions are negligible or variations are accounted for in the model (Hoeg et al., 2000).

Several of these assumptions are likely to be difficult to satisfy in a heterogeneous catchment with a range of land-uses, such as those studied in this thesis, as will be outlined in Chapter 4. Some may be reasonably assumed to be met in some catchments, but are not appropriate in others. Nitrate, ammonium and potassium for example, would usually not be considered conservative due to nitrification, in the case of nitrate and ammonium, while potassium is influenced by biological activity. Many authors conclude that the technique still may be applied once the uncertainties encountered due to assumptions not being satisfied are taken into account (Hooper et al., 1990; Hoeg et al., 2000; Uhlenbrook and Hoeg, 2003).

2.5.1 Natural Tracers

The selection of a tracer to be used for the analysis of a catchment being studied depends on the catchment's hydrological characteristics and also the land use within it. Silica has been widely utilised as it is a weathering product of a range of common geological materials, e.g. granite, clay. It is usually conservative and its concentration is proportional to its residence time in the soil, i.e. the contact time it has had with the geological material. $\delta^{18}O$, D (deuterium) and ^{3}H (tritium) are widely used as stable isotopes (Sklash and Farvolden, 1979; Hoeg et al., 2000). These stable isotopes have been used to distinguish event water from pre-event water in a stream as precipitation event water concentrations are significantly different to groundwater, pre-event water. Other tracers that have been used, particularly in End Member Mixing Analysis, are alkalinity, pH, sulphate, sodium, calcium, magnesium, chloride, potassium and nitrate. Temperature also provides a useful means of investigating the interactions between the different pathways. Locations of groundwater discharging to the stream may be identified by changes in longitudinal temperature profiles of the stream (Stonestrom and Constantz, 2003; Anderson, 2005). Temperature also can be utilised to separate

pathways provided it can be monitored in those pathways (Shanley and Peters, 1988; Birkinshaw and Webb, 2010). There are advantages and disadvantages to each of these tracers, but ultimately their selection will depend on the catchment characteristics.

2.5.2 End Member Mixing Analysis (EMMA)

EMMA (Hooper et al., 1990) is a technique that links pathway chemistry (end members) to stream water chemistry. It assumes that the stream water is a mixture of end members which, to a first approximation, are considered to be invariant spatially and temporally. The key advantage of EMMA is that while it can be applied to calculate the flow in each pathway identified, it can also be utilised to validate the conceptual model of the catchment. This means that it can recognise if the correct pathways have been identified and if the end member concentrations used are suitable throughout the catchment.

The choice of end members and tracers is an important process. The end members should be identified in the conceptual model, while the choice of tracers should aim to satisfy as many of the assumptions for tracers as possible. The end members are selected to be at a point where water last had sufficient interaction with soil to acquire its chemical signature. End member concentrations of solutes 'bound' the stream water concentrations for all pair combinations of solutes in a two-dimensional plot of one solute against the other. The stream water concentrations lie in the interior of such a plot, as shown in Figure 2-9.

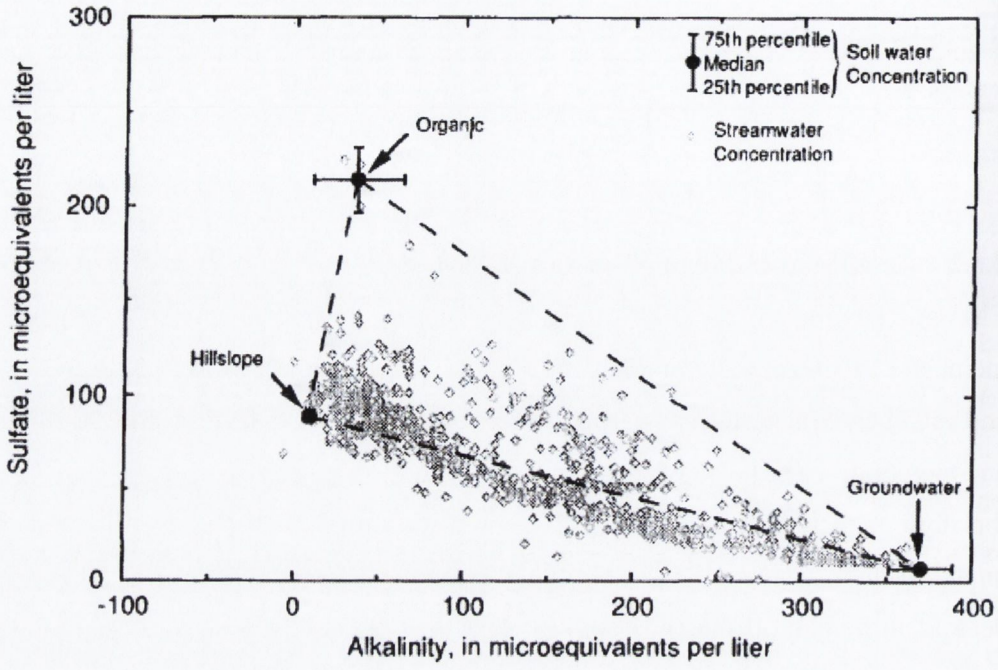

Figure 2-9 . EMMA of sulfate plotted against alkalinity (Hooper et al., 1990).

When there are n end members, n-1 tracers are needed to test the validity of the conceptual model and perform the hydrograph separation. When more than n-1 tracers are considered, the validation of the predicted stream water concentrations can be tested against observed concentrations. Two-dimensional mixing plots are one way of doing this, but sometimes an acceptable fit is not apparent. A further test is to evaluate the hydrograph predicted by EMMA against the observed hydrograph. Discrepancies in either method of validation would then indicate further fieldwork would be required to refine the conceptual model of the catchment (Burns et al., 2001).

2.6 Recharge Coefficients

Recharge to aquifers can be estimated by calculating effective rainfall, applying a soil moisture budget technique, and then multiplying by recharge coefficients to indicate the proportion of effective rainfall contributing to groundwater recharge (Misstear et al., 2009a) describes the hydrological setting relating to each recharge coefficient and the

range over which these coefficients tend to vary. These recharge coefficients are identified from soil and subsoil GIS data for the catchment in conjunction with a recharge coefficient table (Working Group on Groundwater, 2005), shown in Table 2-1.

Table 2-1 Recharge coefficients for different hydrogeological settings adapted from (Hunter Williams et al., (In Press)).

Recharge coefficients for different hydrogeological settings				
Vulnerability category	Hydrogeological setting	Recharge coefficient		
		Min (%)	Inner range	Max (%)
Extreme	Areas where rock is at ground surface	30	80-90	100
	Sand/gravel overlain by well drained soil	50	80-90	100
	Sand/gravel overlain by poorly drained (gley) soil	15	35-50	70
	Till overlain by well drained soil	45	50-70	80
	Till overlain by poorly drained (gley) soil	5	15-30	50
	Sand/ gravel aquifer where the water table is ≤3 m below surface	50	80-90	100
	Peat	1	15-30	50
High	Sand/gravel aquifer, overlain by well drained soil	50	80-90	100
	High permeability subsoil (sand/gravel) overlain by well drained soil	50	80-90	100
	High permeability subsoil (sand/gravel) overlain by poorly drained soil	15	35-50	70
	Moderate permeability subsoil overlain by well drained soil	35	50-70	80
	Moderate permeability subsoil overlain by poorly drained (gley) soil	10	15-30	50
	Low permeability subsoil	1	20-30	40
	Peat	1	5-15	20
Moderate	Moderate permeability subsoil and overlain by well drained soil	35	50-70	80
	Moderate permeability subsoil and overlain by poorly drained (gley) soil	10	15-30	50
	Low permeability subsoil	1	10-20	30
	Basin peat	1	3-5	10
Low	Low permeability subsoil	1	5-10	20
	Basin peat	1	3-5	10
	High to low High permeability subsoil (sand and gravel)	30	80-90	100
	Moderate permeability subsoil overlain by well drained soils	35	50-70	80
	Moderate permeability subsoil overlain by poorly drained soils	10	15-30	50
	Low permeability subsoil	1	5-10	20
	Peat	1	5	20
Note: Areas of 'made ground' are assigned a recharge coefficient of 20 %.				

Effective rainfall is calculated as rainfall less actual evapotranspiration. Actual evapotranspiration is estimated with recorded values of potential evapotranspiration and a soil moisture budgeting approach such as FAO Penman-Monteith method (Allen et al., 1998). Due to the low storage properties of some aquifer types, there is a limit to the amount of recharge that can be accepted by the aquifer. Therefore, a cap on the amount of recharge is defined for locally important and poorly productive aquifers: 200 mm/yr for locally important aquifers and 100 mm/yr in poorly productive aquifers (Working Group on Groundwater, 2005). GIS data, freely available from the Geological Survey of Ireland, and rainfall and evapotranspiration data, collected from the study site, are applied to calculate the recharge coefficients. The layers of most relevance are the subsoil, soil and aquifer mapping. The soil and subsoil data indicate the permeability of the overburden above the aquifer, while the aquifer data define the productivity of the aquifer and thus if it is limited in the recharge it may receive. The vulnerability mapping carried out in Ireland to rate the risk of contaminants entering the aquifer's groundwater system is also informative, as the approach was used to develop these maps is analogous to the method required for calculating the recharge coefficients. The recharge coefficient approach therefore provides a basis for separating the quicker response pathways from the slower response pathways.

2.7 Discussion

After reviewing the different approaches currently available for separating the hydrograph into its constituent pathways, assessments of the methods that show most potential in their current form and with modification for identifying the pathways of the conceptual model are implemented in Chapter 6. The different techniques are thus appraised under the following headings:

- Ability to identify multiple pathways
- Objectivity of separation methods
- Length of flow records required
- Independence of methods when applied in conjunction with other methods

2.7.1 Ability to identify multiple pathways

The ability of an approach to identify more than the usual two pathways – the quick and slow responding flows – is vital for this work to be capable of modelling the catchments using the four-pathway conceptual model. The approaches that display the most potential to meet this objective, in their current form, would be the master recession curve and the geochemical tracer approach. There is a caveat involved when comparing the output of these two methods. The MRC approach will tend to identify the recessions with different response times, that is, it will fail to separate pathways that respond at the same rate which may actually mean a combination of two pathways such as initially fast responding interflow and equally fast responding overland flow. The geochemical tracers, on the other hand, will help identify the sources of the water from which hydrograph is derived. This will result in the pathway separations supported by geochemical principals if the end members have been sampled correctly, but there is a lot of uncertainty involved in obtaining these samples due to the generally unobservable nature of subsurface flow. As part of the *Pathways Project*, a fellow PhD researcher is carrying out geochemical tracer studies in the study catchments. This work complements the research described in this thesis by providing a more holistic approach to hydrograph separation.

2.7.2 Objectivity of separation methods

The repeatable nature of separation methods is important for the transferral of results from one study catchment to another. A method needs to be robust enough to allow different users to obtain comparative results when the method is employed in a catchment. Therefore, to ensure a method's successful implementation, it must be as free as possible from subjectivity. The separation approaches best suited for this purpose are the flow duration curve, the fixed interval, sliding interval and minimum turning point approaches, the one parameter recursive digital filter and the MRC, geochemical tracers as well recharge coefficient approaches to an extent given that there are upper and lower limits for each coefficient provided in Table 2-1. The flow duration curve, fixed interval, sliding interval and minimum turning point methods are easily repeatable and thus easily automated for objective use. The one-parameter recursive digital filter is also easily automated and objective once the k value has been

specified. Generally accepted values may be utilised or else the k value can be interpreted from MRC analysis. MRC analysis itself is generally objective in terms of identifying k values. The different methods described for constructing the MRC and the actually overlapping of recessions to create the MRC does involve some subjective decisions. These decisions won't affect the k values, but will have an impact on relative storages calculated from integrating the area under the MRC. The geochemical tracer approach is subjective in that the ability of a user to correctly identify and sample end members will vary from one application of the method to another. The recharge coefficients approach is an easily automated approach, but as each coefficient applied for calculating recharge has a range, a decision has to be made in each case for what value the coefficient will take on. If this is decided *a priori* for each situation, a consistent and objective automated approach may be employed.

2.7.3 Length of flow records required

Due to time constraints of the *Pathways Project*, time series of flow and other hydrology data will not be much longer than a couple of years. This provides a constraint on which separation methods to implement, as some perform better than others with relatively short data sets. The only approaches that are restricted by the quantity of data that they require in order to get the best reflection of the dominant characteristics of the catchment are the flow duration curve and the MRC analysis. While the time series that this thesis will be dealing with will be adequate for these methods, longer time series will always improve these methods' performance due to more varied weather conditions that are likely to be encountered. The length of recessions required by the MRC analysis can be relaxed in order to be able to construct approximate MRCs that will allow the general characteristics of the catchment to be identified. Recharge coefficients will only require an estimation of the total effective rainfall for the year in order to estimate the cap on the recharge coefficients in poorly productive aquifers.

2.7.4 Independence and suitability of methods

In order to obtain separations with the most value when assessing the output of the different approaches, it is important that the approaches are as independent of one another as possible to avoid bias of certain methods over others. These methods must also be suitable for the geological setting of the catchment. Some methods perform better than others in certain environments; for example, karst catchments with point recharge are not suitable for the recharge coefficient approach as this only takes account of direct (diffuse) recharge. With this in mind, the approaches that work well together and are sufficiently independent of one another to provide insights into the system of hydrological pathways at work are: MRC, geochemical tracers, flow duration curves and the recharge coefficient approach. As chemical analysis is outside the scope of this thesis, the only natural tracer time series that will be analysed will be temperature. Also while the MRC and the recursive digital filters provide useful means of separating the quick and slow responding flows, these methods will be modified as part of this research in order to provide more useful tools for the environments being studied. This will be further discussed in Chapter 6.

3 Literature review: Hydrological Models

3.1 Introduction

Hydrological models are utilised to investigate the hydrological pathways present in catchments and to predict responses that are not measurable in the field for research purposes and to inform decisions makers (Anderson and Woessner, 1992; Beven, 2001). On the other hand, they are not purely decision making tools themselves, although some models do include modules that suggest solutions to issues raised by model output. Hydrological models can be categorised as numerical or non-numerical. This thesis investigates the use of numerical models in catchments, and as such, non-numerical models are not discussed further. Numerical models can be further subdivided into deterministic and stochastic models. A deterministic model is one that attempts to represent, simplistically but realistically, the physical processes of the hydrological cycle. A stochastic model conversely uses a 'black box' approach, where no attempt is made to understand the processes involved (Clarke, 1973). A set of empirical equations are derived from statistically analysing data inputs and outputs until a solution approaching observed outputs is obtained. While a set of equations modelling the data can be calculated, no understanding of the system is obtained. It is for this reason that the deterministic approach is taken in modelling in this thesis. There are a range of models that have a physical basis but rely on such techniques as Monte-Carlo simulations for ranges of input parameters. These models would fall in between the two classifications, deterministic and stochastic. Due to the statistical nature of the selection of parameters, though not all, they would be deemed stochastic (Chow, 1964).

Deterministic numerical models can be further subdivided again into: lumped, semi-distributed and distributed models. Lumped models do not account for spatial and temporal variations of certain parameters within a catchment. Instead a characteristic value is said to apply in every situation across the entire catchment, for example, rainfall varies across the catchment but a single averaged value is inputted in a lumped model. In a semi-distributed model the catchment is divided into several subcatchments. Within each subcatchment parameters are lumped. The streamflow of the entire catchment is then

the sum of routed outputs of the subcatchments. Most models that were originally developed as lumped models, now contain river routing modules in order to allow them to be considered semi-distributed. In distributed models, catchments are divided into gridded meshes with each block of the grid having its own set of parameters that describe the characteristics of that block. In the following pages examples of each will be presented along with the workings of each model and its advantages and disadvantages. Snow applications will not be reviewed, as these are not applicable to the temperate climatic conditions in the research catchments and those of Ireland in general, while quality modelling is outside the scope of this thesis and so water quality features of models are also not discussed.

Models were chosen for review based on applicability to the objectives of the thesis, their use internationally and prior instances of their application in the Irish setting. How models are applied spatially within a catchment is also important as this will affect the input data required for the models. Therefore a selection of well known models was chosen within each of the spatial distribution categories for models: lumped, semi-distributed and fully distributed. Additionally, lesser known models with the potential to meet the requirements of this were also reviewed.

3.2 Lumped/Semi-Distributed Models

3.2.1 HBV

The Swedish Hydrologiska Byrans Vattenbalans-avdelning (HBV) (Hydrological Bureau Waterbalance-section) model was developed by the Swedish Meteorological and Hydrological Institute (SMHI) in the early 70's to provide hydrological forecasts to assist in hydropower operations (Bergstrom, 1976). It is a deterministic, conceptual rainfall-runoff model that can be used as a semi-distributed model by dividing the catchment being modelled into sub-basins. This is followed by further subdivision of the sub-basin into zones according to altitude. Within each altitude zone, further subdivision into vegetation zones can be made (forested or non-forested areas), as depicted in Figure 3-1.

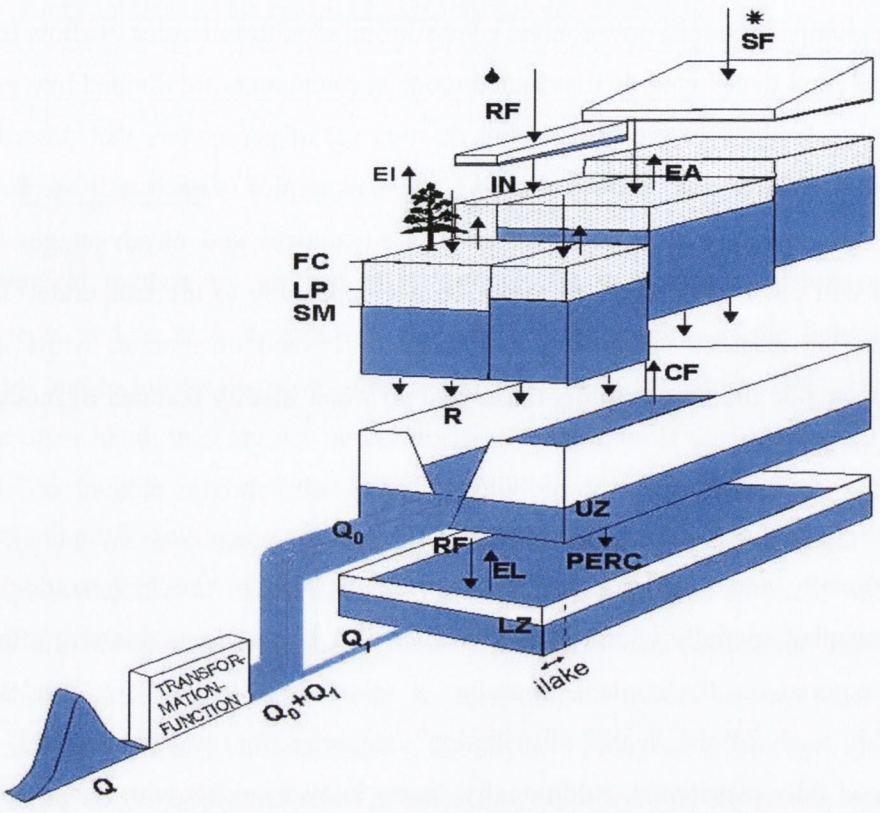

Figure 3-1. HBV model structure (SMHI, 2008).

The model contains subroutines that calculate inflow of water from both snowmelt and rainfall. The soil routine uses this inflow to calculate quick response flow from excess soil moisture and also calculates the infiltration of water into groundwater storage, a linear reservoir. Evapotranspiration is a function of the soil moisture stored in soil storage zone. Quick response flow is routed through a non linear reservoir, while slow response flow is the output of the groundwater storage, which is then routed through a linear reservoir. Water can move between the lower and upper zone storages and also between the upper and soil zone storages by means of capillary rise. This is calculated as being a function of the soil moisture content in each of the storages.

HBV requires rainfall and potential evapotranspiration data as input to the model. The model will then weight data to give lumped mean area values of precipitation and potential evapotranspiration in a catchment. Air temperature, wind speed and vapour

pressure are only required if snowmelt runoff applies to the catchment being modelled. Discharge observations are used for calibration and validation. Groundwater abstraction values are subtracted from local runoff and inflow.

HBV has been applied internationally as a rainfall-runoff model both in gauged (Lindström et al., 1997; Zhang and Lindström, 1997) and ungauged (Engeland and Hisdal, 2009) catchments. These applications of HBV only include quick flow and baseflow in the simulations due to the model structure.

3.2.2 HSPF

The Hydrological Simulation Program – Fortran (HSPF) model was developed by the United States Environmental Protection Agency (US EPA) in the late 1970's (Johanson and Davis, 1980). The model is a semi-distributed, quasi-physically based conceptual model that can simulate the hydrologic processes, as well as the associated water quality processes in a catchment. The model simulates the quantity and quality values of these processes on a continuous basis. The model was designed using a top-down approach placing emphasis on systematic management of data and the use of uniform programming standards and conventions to facilitate increased compatibility with other models. The focus of this overview of HSPF will be on the primary module, Water Budget Pervious (PWATER), which simulates the hydrological processes in the catchment being modelled. It is this aspect of HSPF that is relevant to the research objectives of this thesis.

The PWATER module is composed of six storages: interception storage, surface detention storage, interflow storage, upper zone storage, lower zone storage and active groundwater storage. Evapotranspiration can reduce the water content in four of the six storages, the exceptions being the surface detention storage and the interflow storage. The module also provides four outflows: surface runoff, interflow, groundwater flow and deep percolation which is modelled as being lost completely from the system. The interconnections between, storage, evapotranspiration and outflows are displayed in Figure 3-2 and Figure 3-3.

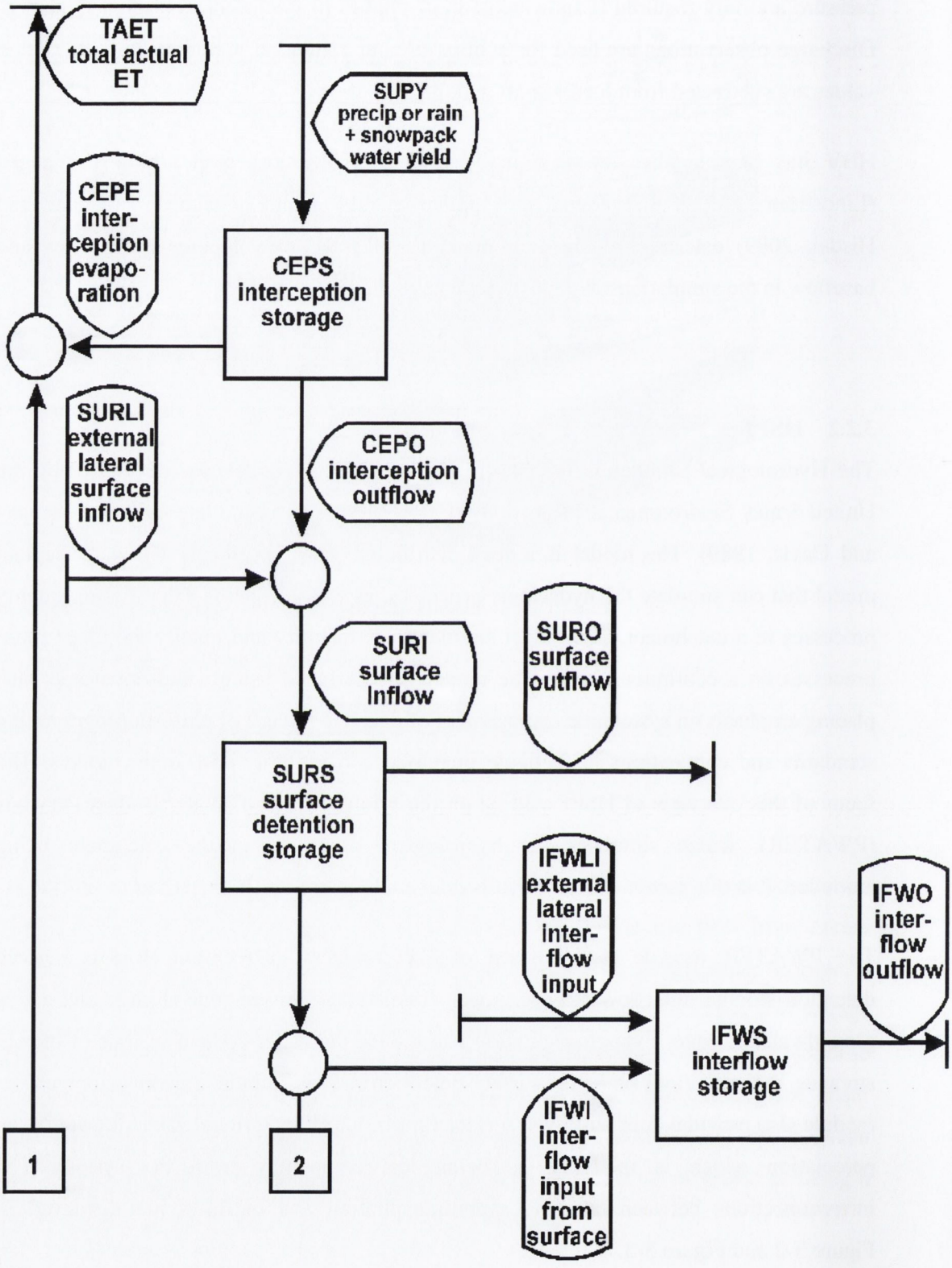

Figure 3-2. HSPF model structure for upper storages and discharges (Bicknell et al., 2001).

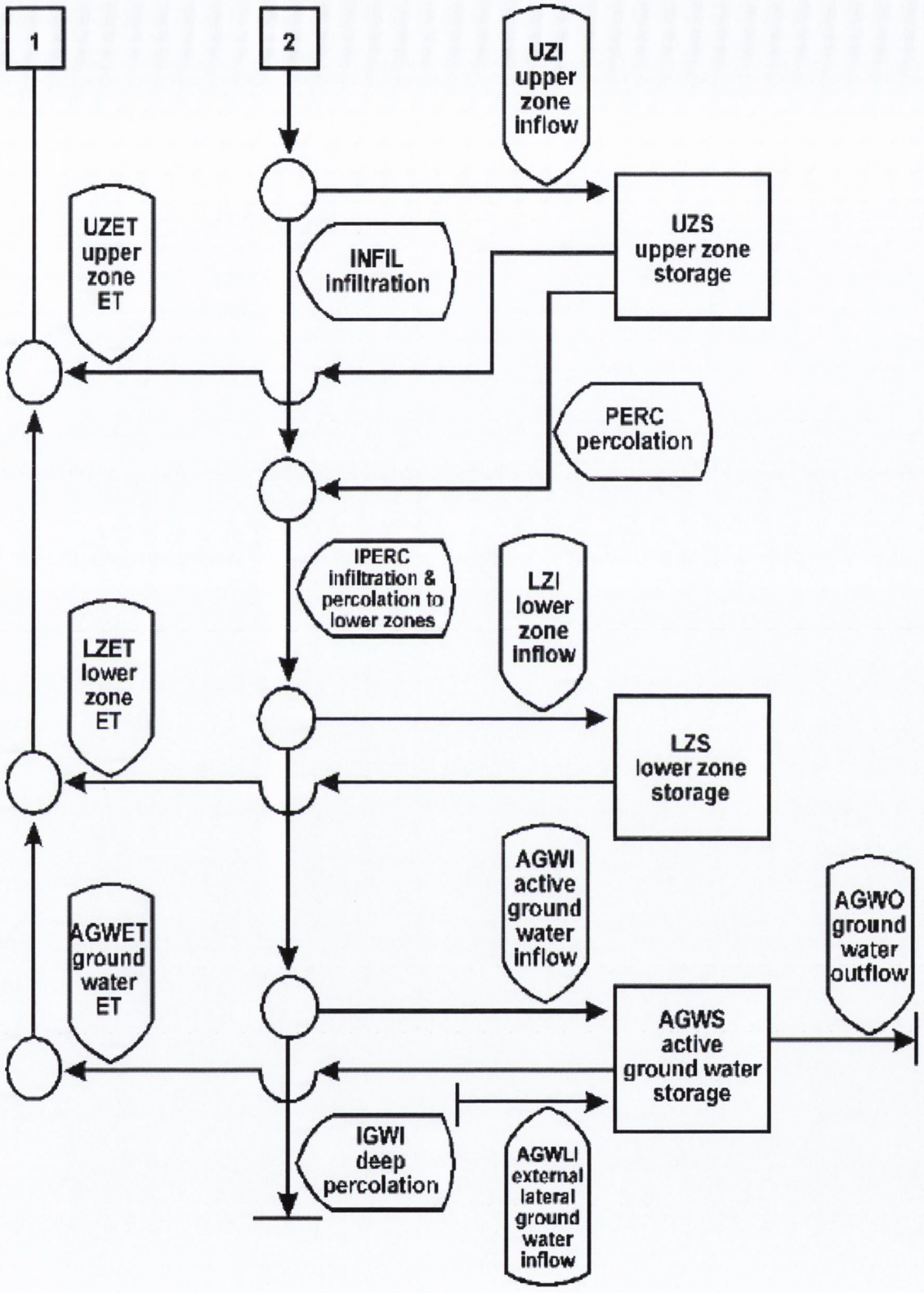

Figure 3-3. HSPF model structure for lower storages and discharges (Bicknell et al., 2001).

Water enters the interception storage from precipitation and irrigation applied to the catchment. The water is intercepted by vegetation and other ground cover. The capacity of this storage is set by the user based on the type of land cover. Once the capacity is exceeded, the excess water is available as infiltration or overland flow. The partitioning of water between the two is dependent on infiltration capacity of the soil and the amount of interflow currently being generated. Overland flow is calculated using the Chezy-Manning equation (Chezy, 1769; Manning, 1889) and is considered to be generated as infiltration excess flow. Water that is held in storage is removed by evapotranspiration.

The water that infiltrates down, either enters infiltration storage and is then released as interflow, or enters the upper zone storage, where evapotranspiration can take place. The partitioning depends on the soil moisture content of the upper zone storage. Interflow is calculated as being the discharge from linear reservoir storage. Further infiltration occurs in the upper zone storage and water percolates down into the lower zone storage. The water that enters into the lower zone storage is dependent on its remaining capacity. The water remaining from the infiltration process then enters the groundwater storages below. The evapotranspiration in the lower zone is dependent on soil moisture content in its storage. The water entering the active groundwater storage is equal to the water infiltrating from the upper and lower zone storages, less the water lost from the hydrological cycle through deep percolation. The groundwater flow is then calculated analogous to Darcy's Law.

As with the HBV model, the inputs of the model for the PWATER module are precipitation and potential evapotranspiration for the catchment. The catchment can be divided into subbasins. The output from each of the storages in the subbasins can then be directly inputted to the storages in the larger subbasin to describe catchments that are heterogeneous. These direct inputs are displayed in Figure 3-2 and Figure 3-3 for surface detention, interflow and active groundwater storage.

HSPF has been applied internationally in a range of different catchment settings (Johnson et al., 2003; Albek et al., 2004; Singh et al., 2005). The HSPF can only simulate three pathways (overland flow, interflow and groundwater flow) and as such, these studies are limited to these pathways.

3.2.3 NAM

The Danish "Nedbør-Afstrømnings-Model" was developed in 1973 by the Department of Hydrodynamics and Water Resources at the Technical University of Denmark (Nielsen and Hansen, 1973). It is a deterministic, lumped, conceptual rainfall–runoff model used to simulate the hydrological cycle. Its basic structure is presented in Figure 3-4.

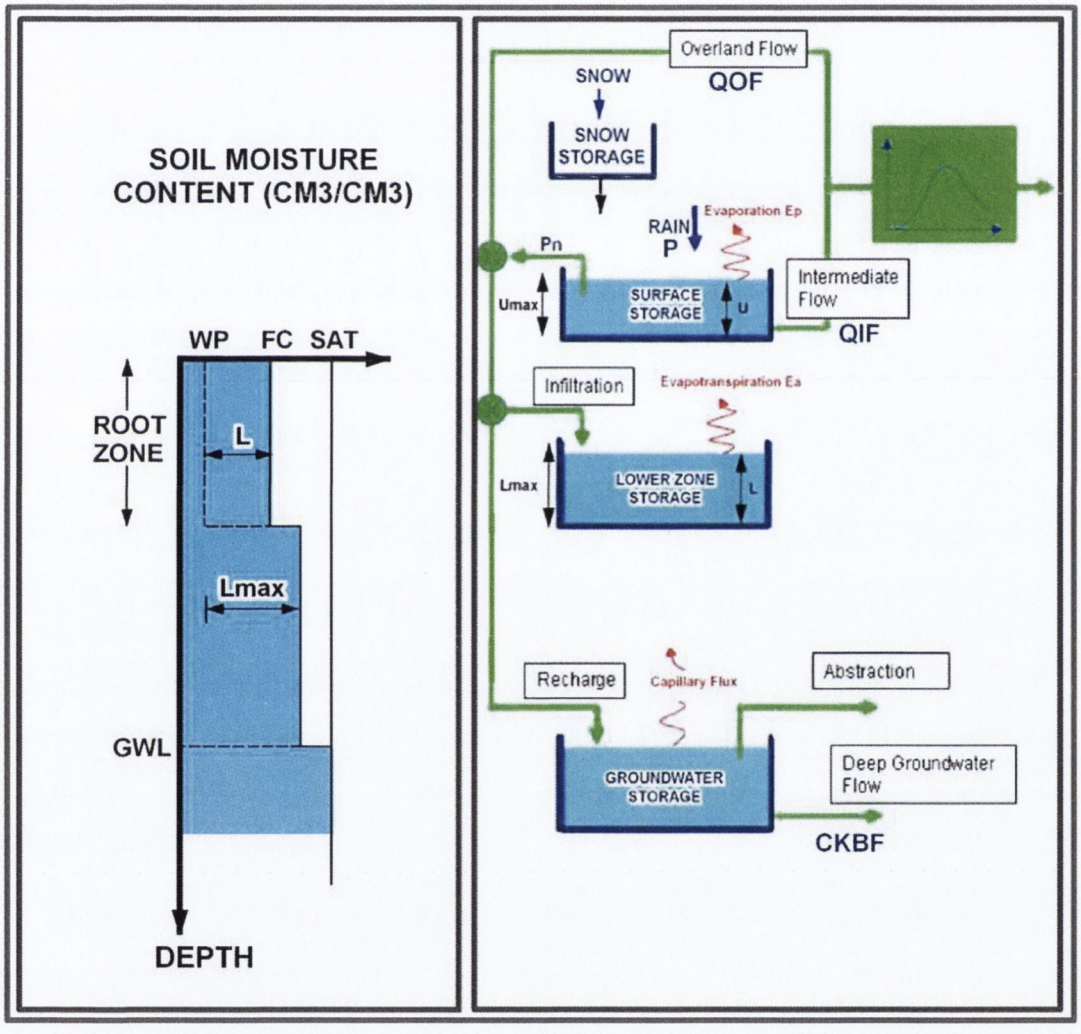

Figure 3-4. NAM structure (Madsen, 2000).

It is composed of four different storage zones: snow storage, surface storage, root storage and groundwater storage. It is possible to extend the groundwater storage to two storages,

an upper zone that simulates shallow groundwater flow and a lower zone that simulates deep groundwater flow.

NAM can be applied to an entire catchment or the catchment can be divided into multiple contributing catchments. The discharge from each contributing catchment is a portion of the final discharge at the outlet of the entire catchment. The discharge from each catchment can then be simply routed to achieve the best fit to the observed hydrograph at the outlet of the catchment. The basic structure of the model uses meteorological inputs to produce catchment runoff as well as information on the hydrological cycle. The runoff produced is composed of overland flow from excess soil moisture in surface storage, interflow produced from soil moisture contained in surface storage and groundwater flow from groundwater storage. Groundwater flow can be divided into shallow and deep groundwater flow by providing an extra groundwater storage zone. The hydrological cycle processes that can be modelled within the different storages include temporal variation in soil moisture content, evapotranspiration, groundwater recharge and capillary rise.

Meteorological data required for the model are rainfall and potential evapotranspiration values which are usually sufficient for daily time steps. Smaller time steps of rainfall and potential evaporation may be required if catchment sizes are particularly small or 'flashy'. NAM will then combine data to give lumped mean area values of precipitation and potential evapotranspiration in a catchment. Air temperature and radiation are only required if snowmelt runoff applies to the catchment being modelled. Hydrological data required are discharge values at the outlet of the catchment for calibration and validation. Groundwater abstraction values are only required if they are judged to have a significant impact on the catchments water balance.

NAM has been implemented internationally as a rainfall-runoff model (Refsgaard and Knudsen, 1996; Tingsanchali and Gautam, 2000) and for real time forecasting of discharges (WMO, 1992; Srikanthan et al., 1994). The approach taken with these studies only includes the three pathways (in the same manner as HSPF) that is the default structure of NAM.

3.2.4 SWAT

The Soil and Water Assessment Tool (SWAT) can be traced to previously developed United States Department of Agriculture – Agricultural Research Services (USDA-ARS) models, including the Chemicals, Runoff and Erosion from Agricultural Management Systems (CREAMS) model. The current SWAT model is a direct descendant of the Simulator for Water Resources in Rural Basins (SWRRB) model, designed to simulate management impacts on water and sediment movements for ungauged rural basins in the U.S. (Gassman et al., 2007). SWAT has undergone continued review and expansion since it was created in the early 1990s (Arnold et al., 1998).

SWAT is a catchment scale, semi-distributed deterministic, conceptual rainfall-runoff model with added capabilities to model attenuation processes of nutrients, pesticides, pathogens and also has a module to assist in the decision making process relative to water land management practices. The focus of this overview of SWAT will be on the hydrological capabilities of the model. The relevant major model components are the weather and hydrology modules.

The catchments in SWAT are divided into multiple subcatchments, which are then further subdivided into hydrologic response units (HRUs) that consist of homogeneous land use, management and soil characteristics. Alternatively HRUs can consist of the dominant land use, management and soil characteristics, to avoid HRUs that cannot be recognised spatially in the subcatchments. The discharges from each of these HRUs are then routed through the streams and rivers to produce the final streamflow of the catchment. An overview of the composition of an HRU is presented in Figure 3-5.

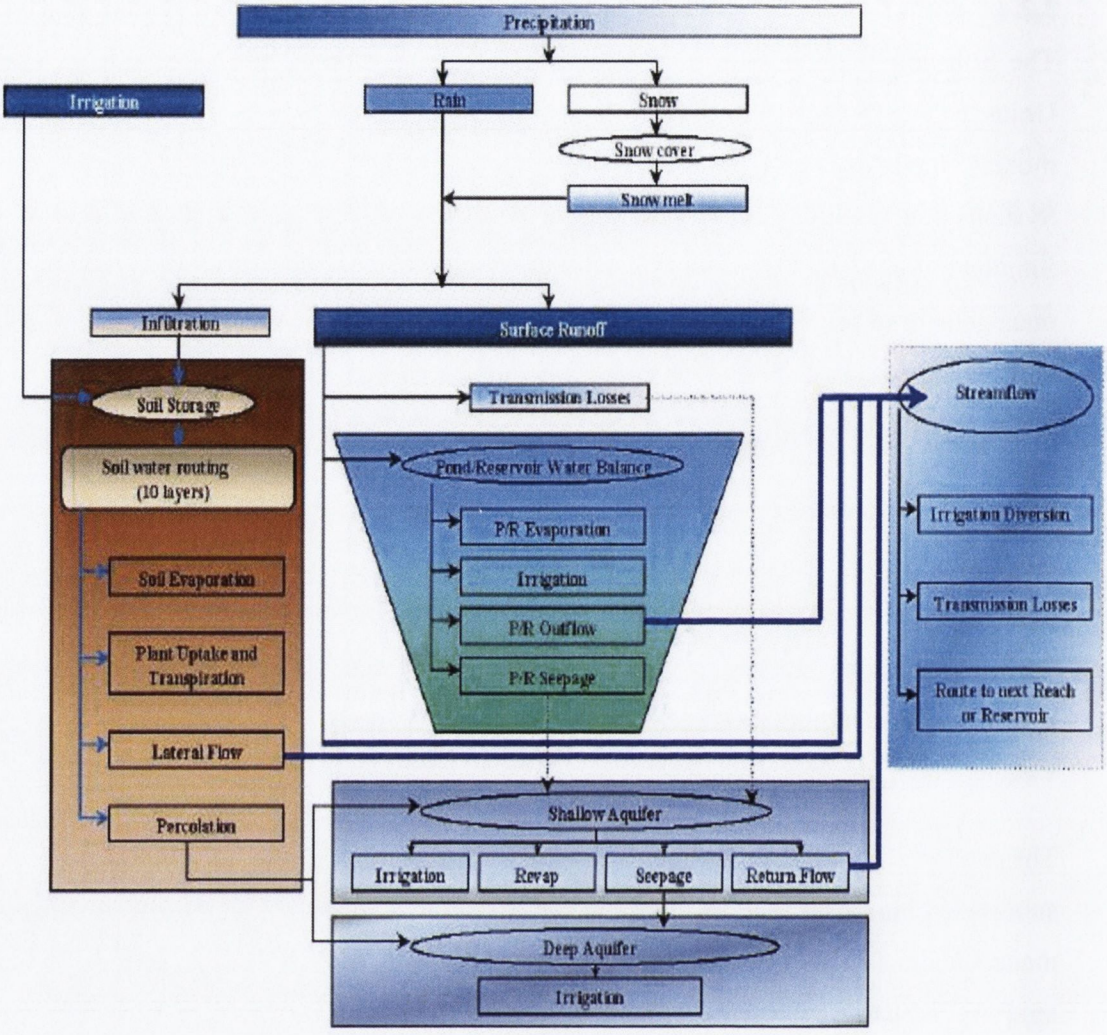

Figure 3-5. SWAT model structure (Neitsch et al., 2005).

Similar to NAM and HBV rainfall-runoff models, SWAT's HRU are based and a series of interconnected reservoirs or zones, the majority of which produce outflows to form the HRU's hydrograph. Like NAM and HBV the snow melt function is not applicable to the catchments in this research and is discussed no further. Rainfall is partitioned between infiltration into soil storage and surface runoff, once interception and surface storage effects have been taken into account. Surface runoff is modelled as infiltration excess runoff, therefore when rainfall intensity (once interception has been accounted for) is greater than the rate of infiltration of the soil and all surface storage has been filled, surface runoff occurs. This type of runoff is more suited to drier climates rather than

Ireland's temperate climate. Transmission losses occur when surface runoff exceeds a threshold value set by the user. The surface runoff is then extracted by channels that significantly reduce the runoff volume. The water is then assumed to percolate into the shallow aquifer.

Rainfall less surface runoff infiltrates into the soil storage zone. Once there water is removed by four processes: by evaporation from the upper layers of the soil; by plant transpiration; by percolation through the unsaturated soil zone and into the aquifer below or by lateral movement in the soil profile and contribution to streamflow as interflow. Evaporation and transpiration processes depend on the potential evapotranspiration calculated using the FAO Penman-Monteith method (Allen et al., 1998) or directly input values of evapotranspiration. Percolation occurs once the soil moisture, resulting from infiltration, exceeds the soil's field capacity. Interflow is modelled as occurring in the soil layers of the vadose zone that are underlain by impermeable or semi-impermeable soil layers that restrict the percolation of soil moisture into the aquifer below. The discharge due to interflow is calculated using the principle of mass continuity, with the soil layer in which it is produced in being considered a controlled volume.

Water percolating into the shallow aquifer from either the soil zone or the pond/reservoir water balance is removed by four processes: further percolation into the deep aquifer below, abstraction (marked as *irrigation* in Figure 3-5), capillary rise (marked as *revap* in Figure 3-5) or it can be removed by contributing to streamflow as groundwater flow. Water entering the aquifers is immediately partitioned between the shallow and deep aquifers by means of a partitioning coefficient. The water percolating into the deep aquifer is considered lost to the hydrological cycle as it may only be removed by means of abstraction. The remaining water after partitioning to the deep aquifer is the shallow aquifer recharge. Losses by abstraction are again user-defined input values. Capillary rise occurs when the overlying unsaturated soil layer experiences evapotranspiration and the water removed in that layer is replaced by water from the shallow aquifer zone. This can only occur if water stored in the shallow aquifer zone is above a threshold value. Once above this value capillary rise depends on evapotranspiration on that day. The groundwater flow is then calculated as a simple approximation of Darcy's Law.

Rainfall, surface runoff, interflow and groundwater flow are also routed through ponds and reservoirs present in the catchment. The quantity of rainfall entering these storage areas is a function of rainfall and surface area of the storage. The inflows into the storage are calculated using the fraction of the subcatchment draining into the area of storage and multiplying this by the sum of surface runoff, interflow and groundwater flow in the subcatchment. Water is removed from this zone by means of evapotranspiration, abstractions for irrigation, outflow from the storage to the stream and percolation into the aquifer below. Evapotranspiration is dependent on surface area of storage and a coefficient calculated using Penman-Monteith (Monteith, 1965) formula or directly input values of evaporation. Abstractions are defined by user input values. Percolation into the shallow aquifer is a function of the surface area of storage and permeability value of the underlying soil. The outflow is dependent on the stage of the storage.

To create the final streamflow hydrograph that is recorded at the subcatchment's discharge point, each of the flows – overland flow, interflow and shallow groundwater – have a lag constant applied to them after they have been calculated as the discharge from each zone.

SWAT while developed in the U.S.A. has been applied internationally in countries as China, South Africa, Tanzania and Austrailia (Xiuwan, 2004; Govender and Everson, 2005; Ndomba et al., 2008; Githui and Thayalakumaran, 2011), but these studies only included overland flow, lateral flow and groundwater as simulated pathways

3.2.5 TOPMODEL

The TOPMODEL rainfall-runoff model was first developed by Beven in 1975 (Beven, 1977). TOPMODEL is a set of programs that can model the response of a single or multiple catchments. It is a physically based, semi-distributed conceptual model that uses gridded elevation data for the catchments being simulated. It is applicable to catchments with shallow soils and moderate topography, which do not suffer from excessively long dry periods (Parsons et al., 1998).

The main factors affecting the model are the topography and soil hydraulic conductivity of the catchment. The model assumes that the local surface slope is equivalent to the local

hydraulic gradient within soil. Thus an index, the topographic index (*a/tanB*), is defined for each sub-catchment. The topographic index is obtained manually from analysis of contours maps or from digital analysis of GIS digital elevation model (DEM) files by dividing the drained area of the contributing area of the sub-catchment in question per contour length *a* by the slope of the contour *tanB*. The soil profile in each sub-catchment is then defined by a set of storages.

The storages are divided into three stores: root zone, unsaturated zone and saturated zone. An interception zone may be added also to represent forest canopy and other vegetation interception of precipitation, while a surface storage zone could be used to represent storage of water in depressions in the land that must be exceeded before overland flow can occur. The storages in the soil profile are displayed in Figure 3-6.

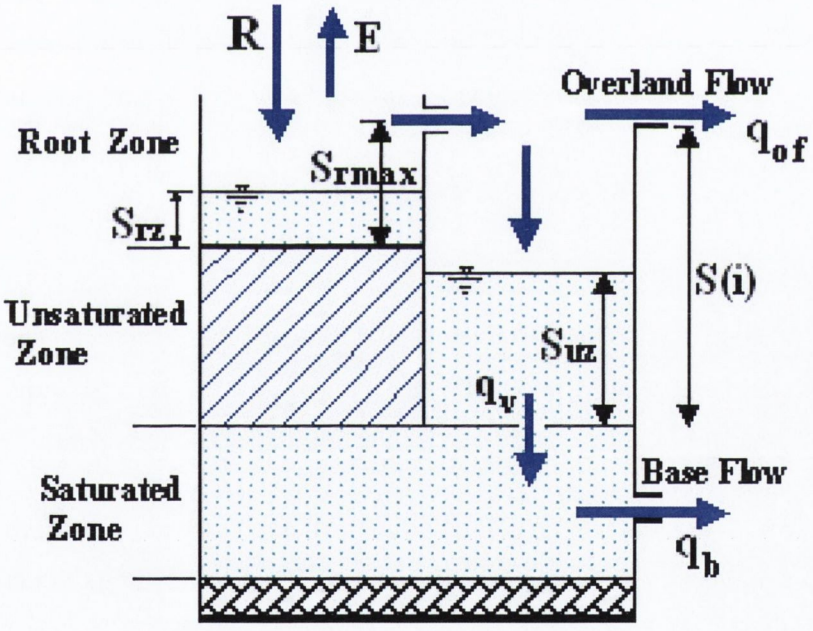

Figure 3-6. TOPMODEL model structure (Nawarathna et al., 2001).

Rainfall infiltrates into the root zone until the field capacity of the zone is exceeded. Once this occurs further infiltration of the soil moisture into the unsaturated zone will occur. The unsaturated zone is then linked to the saturated zone via a gravity drainage store that

calculates percolation into the saturated zone using a time delayed linear function. A Darcian flux based approach at the base of the unsaturated zone may also be used.

Excess saturation overland flow occurs when the deficit of the unsaturated zone is zero, i.e. become saturated as the water table depth would now be zero. The storage deficit of the zone is calculated using the local value of a function of the topographic index. The hydraulic conductivity of the saturated subsurface (subsoil and aquifer, though not specifically defined) is assumed to decay following a negative exponential law that provides the local storage deficit in terms of $ln(a/tanB)$. The groundwater flow component of the overall discharge is calculated as being the discharge from a linear reservoir. The saturated zone acts as this linear reservoir. The discharges from the sub-catchments are then routed linearly to produce the final catchment discharge.

TOPMODEL also provides the option of computing overland flow as being the result of infiltration-excess flow. This is calculated using the Green-Ampt model (Green and Ampt, 1911), but would not usually be appropriate for Ireland's temperate climate as saturation-excess of the soil profile in the riparian zone is the source of overland flow in the catchments being studied in this thesis.

TOPMODEL requires DEM files to calculate the topographic index for the each of the sub-catchments. The subsurface hydraulic conductivity is also required to predict the Darcian fluxes within the storages of the soil profile of each sub-catchment. The meteorological requirements for the sub-catchments are rainfall and potential evapotranspiration data at the temporal resolution at which the model is to output data.

TOPMODEL has been used internationally for a variety of applications: validation studies (Franchini et al., 1996; Güntner et al., 1999), impacts of climate modelling (Niu et al., 2005), flood frequency prediction (Blazkov and Beven, 1997), etc., with each application of TOPMODEL limited to simulating two pathways (overland flow and saturated subsurface flow).

3.3 Distributed Models

In a distributed model the catchment area is discretised into blocks and layers. The shape, type and size of the blocks and layers depend on the type of model being implemented. Finite difference and finite element approaches are the models utilised to solve the differential equations applied to describe the flow within the catchment.

3.3.1 Finite Difference

In a finite difference model, differential equations are solved by means of discretising the catchment into a block-centred grid or a mesh-centred grid. Block-centred grid approach locates the flux boundaries at the edge of the block, while mesh-centred grid locates boundaries coinciding with grid nodal points (Figure 3-7).

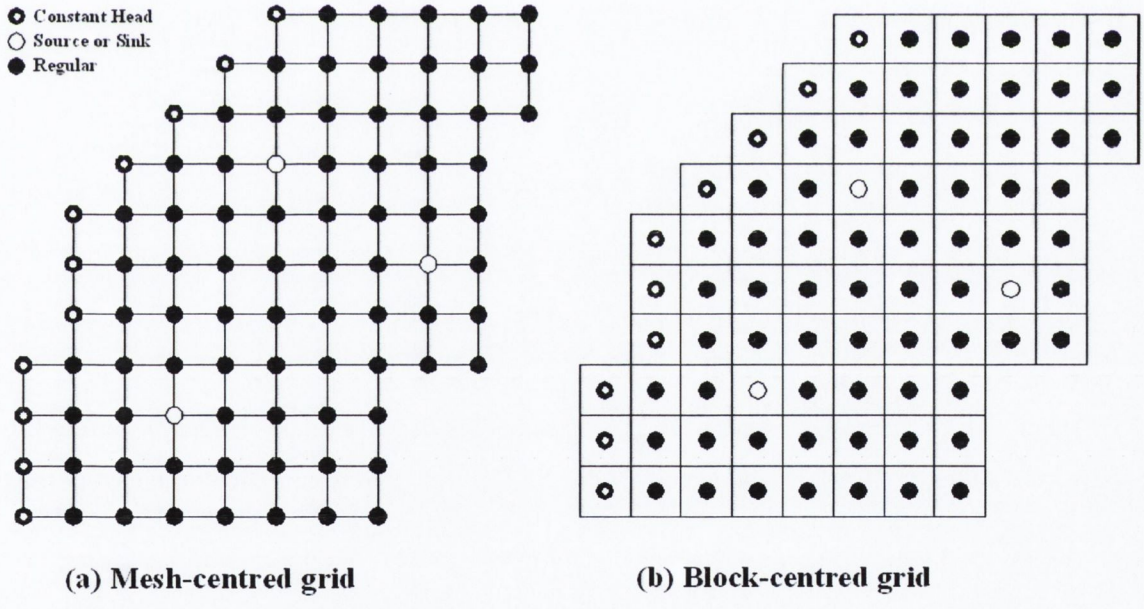

Figure 3-7. Mesh-centred and block-centred grid.

The mathematics related to block centred approach are more easily incorporated into computer code. It is for this reason most codes use this approach when using finite

difference solutions. Grids can be spaced regularly or irregularly. Irregular spacing may be used to obtain more detail in areas where hydraulic head varies over short distances. The trade-off is that finite difference equations solved with irregular spacing are less accurate than those that apply regular spacing. It is a rule of thumb to expand grid spacing by no more than 1.5 times the previous nodal spacing to minimise the associated error with irregular spacing (Anderson and Woessner, 1992).

3.3.1.1 MODFLOW

MODFLOW was developed by the United States Geological Survey (USGS) between 1981 and 1983 using FORTRAN computer language (McDonald and Harbaugh, 1984). It was developed as a result of a need to consolidate all the USGS's commonly used groundwater simulation capabilities into one package that was easy to use, understand and modify. MODFLOW can be used for either two or three-dimensional modelling. It implements a modular structure in which similar program functions are grouped together and constructed to be independent of other function groups. This enables new function groups to be added without the necessity of changing existing function groups.

Three-dimensional groundwater flow through porous material is described in MODFLOW by the following partial-differential equation:

$$\frac{\delta}{\delta x}\left(K_{xx}\frac{\delta h}{\delta x}\right)+\frac{\delta}{\delta y}\left(K_{yy}\frac{\delta h}{\delta y}\right)+\frac{\delta}{\delta z}\left(K_{zz}\frac{\delta h}{\delta z}\right)+W=S_s\frac{\delta h}{\delta t} \qquad \text{3-I}$$

where water has constant density, K is hydraulic conductivity in axis direction [m/day], h is hydraulic head [m], W is change in water flux [days^{-1}], S_s is specific storage of porous material [m^{-1}], t is time [days].

Equation 3-I can be solved using finite difference techniques to calculate the head h at a point in the aquifer being modelled. Groundwater flow described by Equation 3-I can be confined, semi-confined or unconfined flow. The initial conditions input into the model will define this aspect. The aquifer is divided into blocks called cells. Flow occurs horizontally along the x and y axis or vertically along the z axis. Each cell is neighboured by six cells. The finite difference solution to the partial-difference equation has seven

unknowns. Each cell has its own finite difference solution, therefore, in an aquifer there n equations with n unknowns allowing a solution for the heads in each cell to be calculated. The edge boundaries of the catchment can be defined as no-flow, prescribed varying head or prescribed varying flow. The bottom boundary can be defined varying flux, a free draining out of the catchment or a no flow boundary. The upper boundary can be defined as a prescribed varying head boundary; with surface water present or a mixed type boundary with evaporation and rainfall at the surface. Initial estimates of h are made to enhance the rate of convergence towards a solution. Once this initial estimate is made, Equation 3-I is solved iteratively to a desired degree of accuracy set by the user.

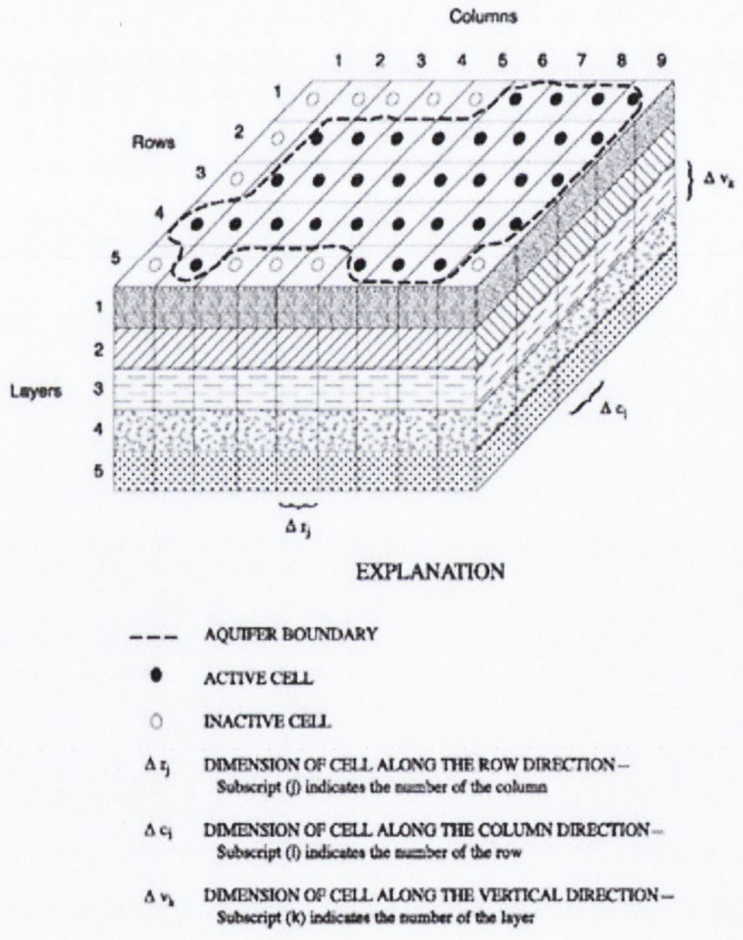

Figure 3-8. Spatial representation in MODFLOW (Harbaugh, 2005).

W in Equation 3-I represents external influences on the aquifer such as inflows from infiltration, abstractions, etc. Add-on packages describing more complex hydrological

situations such as wells and groundwater and river interactions can be modelled using these packages. Data requirements for the model depend on what packages are being implemented. Typical data requirements are large to simulate the catchment successfully. In each vertical cell column continuous temporal data is needed for rainfall, evapotranspiration rates, river stage and abstraction rates. Also required in each cell are values for the aquifer's hydraulic conductivity in the three principal directions and specific storage of the aquifer.

MODFLOW is an international standard groundwater model that has been applied in numerous studies across the world (Restrepo et al., 1998; Osman and Bruen, 2002; Lautz and Siegel, 2006; Black et al., 2012; Taylor et al., 2012). MODFLOW only simulates saturated flow (typically taken to be groundwater flow) and does not differentiate between deep and shallow groundwater. However, this would be implicit from the differences in hydraulic conductivity, with higher conductivities being equivalent to shallow groundwater and lower conductivities equivalent to deep groundwater.

3.3.1.2 SHETRAN

The SHE-Transport (SHETRAN) model is based on the Système Hydrologique Européen (SHE) model developed by a consortium of three European organizations: the Institute of Hydrology (IOH) of the United Kingdom, Société Grenobloise d'études et d'applications hydrauliques (SOGREAH), Grenoble hydraulics studies and applications company, of France and the Danish Hydraulic Institute (DHI) of Denmark in 1986 (Abbott et al., 1986a; Abbott et al., 1986b). This was expanded upon by the Water Resource Systems Research Laboratory, School of Civil Engineering and Geosciences, University of Newcastle upon Tyne in the early 1990s (Wicks et al., 1992). SHETRAN is a physically based, distributed, finite difference integrated hydrological, sediment transport and contaminant transport model. This focus of this review will be on the hydrological modelling capabilities of the model. Figure 3-9 presents the different processes simulated in SHETRAN.

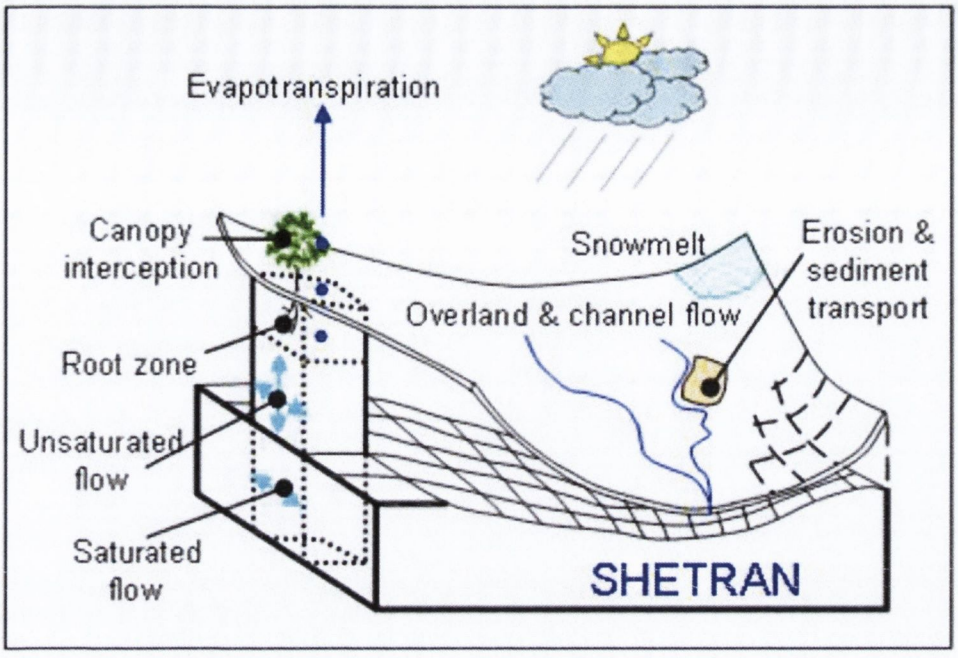

Figure 3-9. SHETRAN conceptual model (Parkin, 1995).

SHETRAN has a modular design, composed of five main components. The water flow component (WAT) is responsible for the hydrological modelling. WAT is composed of four modules that simulate the different aspects of the hydrological cycle. These are evapotranspiration/interception (ET), overland/channel (OC), variably saturated subsurface (VSS) and snowmelt (SM). This review will not focus on SM as it is not applicable to the catchments being modelled in this thesis and generally not applicable to Ireland's climate.

The ET module is responsible for calculating the evapotranspiration from the vegetation, soil and free surface water in the catchment. The interception, storage and subsequent drainage from canopies intercepting rainfall is also calculated using this module and therefore provides the net rainfall input to the ground surface of the model. Evaporation from surfaces is estimated using the Penman combined energy/turbulent transfer equation (Penman, 1948) or can be directly input if the value is known. Evapotranspiration is estimated applying the Penman-Monteith method (Monteith, 1965) or can be estimated by setting moisture content as the controlling parameter, providing a coefficient that the

Penman-Monteith value is multiplied by or, as is the case of evaporation, direct values of evapotranspiration can be entered.

The interception of rainfall is also calculated by the ET module. The quantity of rainfall that is intercepted is dependent upon the storage capacity of the vegetation covering the ground surface. This storage is emptied by evaporation and drainage from the vegetation. Evaporation occurs over the area covered by leaves, including those lying below other leaves, with the maximum aerial coverage equal to that of the catchment area due to limitations in the volume of water the air can retain. Drainage from the vegetation is simulated as discharge from a reservoir and depends on the volume of water held in the storage of the vegetation.

The OC module is responsible for calculating the depth of surface water above the ground level during floods. It is also responsible for calculating the stage of water in channels and the flow of water across the ground surface, in channels and between ground surface and channels and vice versa. The overland and channel flows are based on the diffusive wave approximation of the Saintt-Venant equations (Saint-Venant, 1843). Water can flow between ground surface cells, between ground surface and bank cells if used, between ground surface and channel cells or between channel and bank cells if used. OC also simulates the overbank flow that occurs when the stage of a stream is higher than the adjacent banks during a flooding event. When this occurs flow between cells is modelled as water flowing over a broad crested weir.

The VSS module is responsible for simulating three-dimensional flow in the saturated and unsaturated permeable, porous material. The flow can be confined, semi-confined or unconfined. Wells and transpiration are considered sinks within the system. The boundary conditions and initial conditions are input in a similar manner to MODFLOW with wells and transpiration considered as sinks within the system.

A similar partial differential-equation as MODFLOW, Equation 3-II is used to describe the three-dimensional flow in a porous material with the added term k_r to describe the saturation of the cell in question and the +1 term in the z direction is to take evaporation into account in the model. The W also includes the extraction of soil moisture by transpiration.

$$\frac{\delta}{\delta x}\left(k_{xx}k_r\frac{\delta h}{\delta x}\right)+\frac{\delta}{\delta y}\left(k_{yy}k_r\frac{\delta h}{\delta y}\right)+\frac{\delta}{\delta z}\left(k_{zz}k_r\left[\frac{\delta h}{\delta z}+1\right]\right)+W=S_s\frac{\delta h}{\delta t} \qquad \text{3-II}$$

Like MODFLOW, SHETRAN requires a lot of data to simulate the catchment successfully. In each vertical cell column: the precipitation and evapotranspiration meteorological inputs are required, the vegetation type and cover, the aquifer hydraulic conductivity in the three principal directions, the specific storage, well abstractions as well as all the initial and boundary conditions. This model therefore requires high-resolution data gathering before it can be effectively run for simulations.

SHETRAN has been applied internationally as a rainfall-runoff model in gauged catchments investigations and real time forecasting analysis (Bathurst et al., 1996; Lukey et al., 2000; Mellor et al., 2000; Nasr et al., 2007). SHETRAN, much like MODFLOW, does not label the saturated flow in the model but implicitly simulates all the pathways of the conceptual model in Chapter 1.

3.3.2 Finite Element

When using finite element models, the grid is implemented in a variety of element types; tetrahedron and prism shaped elements would be the most common element types employed by most methods (Allik and Hughes, 1970; Anderson and Woessner, 1992; Beven, 1997). The hydraulic head is defined at each of the nodal points. Equations relate to the hydraulic head at each nodal point similar to finite difference. The main distinguishing feature is the use of interpolation functions to define the hydraulic head throughout the catchment area. Finite element models approximate differential equations with an integration approach to produce the algebraic equations to be solved, whereas finite difference models approximate differential equations with a differential approach (Faust and Mercer, 1980).

3.3.2.1 FEFLOW

The Finite Element Flow model (FEFLOW) was developed in 1979 by the Institute for Water Resources Planning and Systems Research Inc. (WASY GmbH) of Berlin,

Germany (Diersch, 1980). FEFLOW is a physically based, fully-distributed, deterministic hydrogeological model. It has extensive functionality in simulating groundwater flow, heat transport and multi species reaction transport, with particular proficiency in variable saturated flow and variable fluid density mass (Trefry and Muffels, 2007). Again the heat and contaminant transport functionality will not be discussed further as it is outside the scope of this thesis. The model has increased flexibility thought its support of both triangular and square finite elements. An example of a mesh of triangular finite elements in FEFLOW is presented in Figure 3-10.

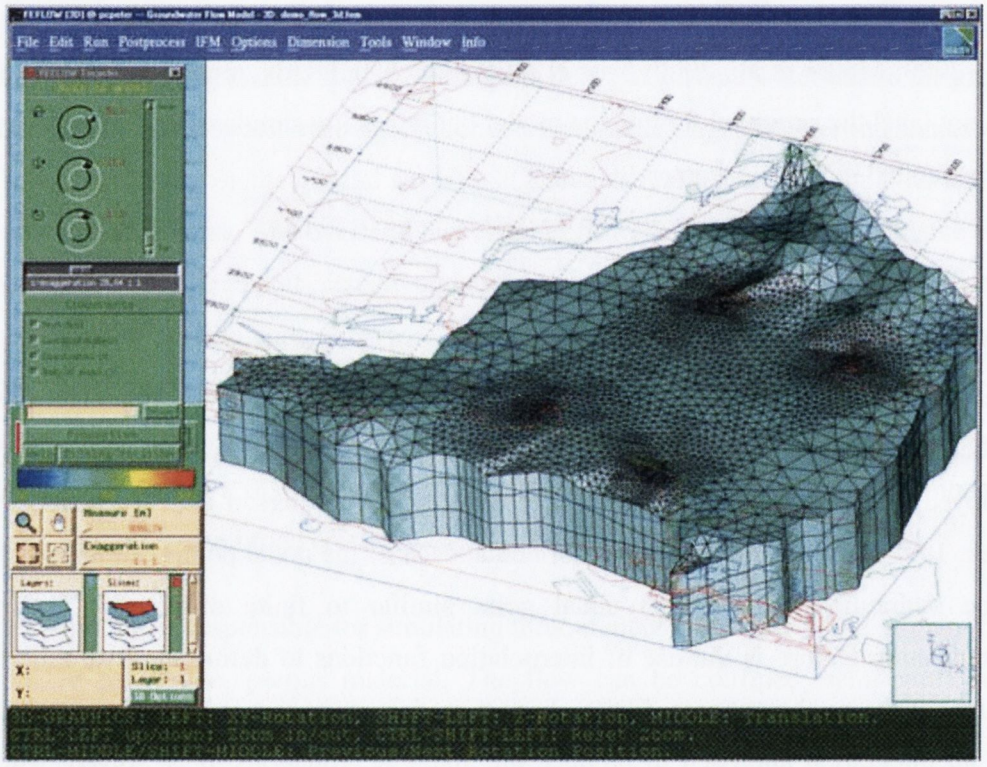

Figure 3-10. FEFLOW output (Diersch, 2002).

A finite element approach can be used for simulating the physical processes in heterogeneous and anisotropic catchments, especially with sloping geological layers, more consistently with the actual field conditions, provided the necessary input data are

available. This approach also provides high resolution spatial representation of the layer to improve modelling of well locations, rivers, fractures and tunnels.

The core of the mathematical hydrological modelling in FEFLOW is based upon three fundamental physical principles: the mass conservation of fluid and solid continua, the momentum conservation of fluid and solid continua and the first law of thermodynamics. The principles are then used to construct the partial differential Equation 3-III to describe the three-dimensional flow in a porous material:

$$S_o \frac{\delta_h}{\delta_t} + \frac{\delta_{q_i}}{\delta_{x_i}} = Q_p \qquad \text{3-III}$$

where S_o is the specific storage coefficient [m^{-1}], h the hydraulic head [m], t is the time [days], q_i the Darcy velocity vector of the fluid in the i direction [m/day], the i variable covers horizontal (x,y) and vertical (z) axes, x_i is the direction of the flow, Q_p is a source or sink volume flux per unit time [$days^{-1}$] being added or extracted from the cell, e.g. a well or irrigation. The value of q_i is calculated using Equation 3-IV:

$$q_i = -K_i f_\mu \left(\frac{\delta_h}{\delta_{x_i}} + \frac{p - p_o}{p_o} e_i \right) \qquad \text{3-IV}$$

where K_i is the hydraulic conductivity tensor in the i direction [$days^{-2}$], f_μ is the viscosity relation reference function [m.days], ρ, and ρ_o are the fluid and reference fluid density, respectively [g/m^3] and equal to zero if water is the only fluid and there is no saline intrusion, and e_i is the gravitational unit vector.

Through the iterative solution of Equation 3-IV, the heads in each of the finite elements can be calculated and the flow through the elements can be obtained. The finite element approach also provides FEFLOW with the means to manipulate the gridded mesh of elements simulating the surface of flows in unconfined aquifers. Therefore, as the free surface shape changes with fluctuating hydraulic head values, the three-dimensional moving meshes can accurately model its shape.

FEFLOW has also been applied to catchments internationally (Schöniger et al., 1997; Youhao et al., 2004; Ashraf and Ahmad, 2008; Monninkhoff and Li, 2009). Like

SHETRAN, FEFLOW can model all of the pathways of the conceptual model in Chapter 1.

3.4 Selection of models

The review of models provides a basis for the selection of the model that will meet the aims of the research project; specifically, the model will need to have the capability of simulating the different pathways of the conceptual model, providing output in the form of time series of discharge that will be used for attenuation modelling calibration. This work will then be utilised to inform the hydrological modelling engine of the CMT in order to provide generic approaches to modelling these pathways in ungauged catchments in Ireland. The model selection process involved the appraisal of the following aspects of the models:

- Ability to simulate all pathways
- Lumped and distributed models
- Data requirements
- Over parameterisation

3.4.1 Ability to simulate all pathways

In order to investigate the appropriateness of the conceptual model, the model applied must be able to simulate all of the pathways. Of the models reviewed NAM, SHETRAN, FEFLOW and HSPF are able to model the four pathways. In general, it is the simplistic approach of the other models to the two groundwater pathways that prevent their use with the project's conceptual model. Most models tend to look at the groundwater pathway as one pathway with a free variable of leakage employed to achieve a good water balance by having water lost out of or gained into the catchment. While this disqualifies a lot of the models when implemented on their own, should they be linked with a model like MODFLOW, that is weaker in simulating the quicker responding pathways, but an industry standard for modelling groundwater, these models would still be beneficial to the project.

3.4.2 Lump and distributed models

The lumped model provides a simplistic approach to modelling; generally more focused on achieving a desired output rather than adhering to strict physical representation of the hydrological pathway processes. This tends to be most useful for catchment scale and river basin scale modelling as the information available is generally not of a high enough spatial resolution to inform a more detailed distributed model. Therefore, a distributed model simulates target output through detailed physically realistic modelling of the different heterogeneous conditions of the catchment. Typically this will require significantly more computational capability and detailed input data, that may not be available, in order to obtain meaningful results.

3.4.3 Data requirements

Typically, the minimum data requirements for every hydrological model are rainfall, potential evapotranspiration and then a time series to calibrate the output of the model against, whether this is a discharge or water level time series. The more complex a model is, the more data it will require simulate a catchments hydrology. Therefore, it is important that the model chosen and its requirements are consistent with the data that are available nationwide in order to run the model on ungauged catchments. The CMT will be required to operate on ungauged catchments and therefore should be informed by a model of similar structure to it. It is important that the modelling that is carried out in this research takes into account the datasets available to it nationwide and that it can function adequately with these datasets.

3.4.4 Overland flow generation mechanisms

In arid regions where rainfall can occur from intense storms over short durations, the ground's ability to allow the incoming rainfall to infiltrate into the soil is limited. As the infiltration rate of the incoming rainfall reaches capacity any excess rainfall is rejected from infiltrating and runs off as overland flow. This is infiltration excess overland flow. The contrasting case to this situation is saturation-excess flow. In this scenario water will infiltrate into the soil until the soil becomes saturated. Any further rainfall will be unable to enter the soil and so runs off as overland flow. In Ireland's humid climate and

geological setting, saturation excess is a better approximation of the type of overland flow being generated, though infiltration excess will occur during large intense rainfall events.

3.4.5 Application to the Irish Setting

Though not necessary, prior application of a hydrological model to catchments in Ireland will help indicate the applicability of the model structure to Irish conditions. With Ireland's widespread till cover (predominantly consisting of clay and silt, as sands and gravels are classified separately in mapping data available from Teagasc), fractured aquifers and a general lack of high spatial resolution data for implementing distributed models, it is very useful to assess prior applications of the hydrological models to catchments of these types. NAM has been applied to a multitude of catchments in Ireland in the Groundwater-Surface water report (RPS, 2008). While a different conceptual model was used for the modelling – only three pathways were identified – NAM performed well. SWAT and HSPF been applied to Ireland also in many catchments, with comparisons of each model's performances carried out (Coffey et al., 2010) and once including a comparison of the HSPF model (Nasr et al., 2003) and a variant of the SHETRAN model (Nasr et al., 2007). MODFLOW has been applied with varying degrees of success in Ireland (Doherty et al., 2002; Osman and Bruen, 2002; Misstear et al., 2009b) but as referred to in Section 3.3.1.1, this has been with the focus of the investigations on the groundwater pathways. The FEFLOW has also implemented in Ireland with success, but generally in relatively small areas due to the demand for high spatial resolution data (Yang et al., 2003; Banks, 2009).

3.4.6 Over-parameterisation

Over-parameterisation is the problem of too many variables being used to achieve a desired output from a model to match observed data. If there is a lot of parameters in a model a situation arises where a multitude of different sets of values for these parameters will give output data that matches observed data 'nearly' as well as each other. Due to the wide range of values for each parameter, it is very hard to identify relationships between the parameters and data in the field. This problem is known as equifinality as discussed by Beven (1993).

In order to avoid this being a major issue the parameters of the model will need to be linked back to catchment descriptors or characteristics of the pathways that can be identified from the hydrograph separation methods. Sensitivity analysis of the different parameters will also assist in identifying the parameters that have a large effect on the output simulated.

3.4.7 NAM and MODFLOW

After considering the different structures and functionality associated with the different models, NAM was selected as the model of choice to simulate the pathways in the study catchments. NAM provides a lumped framework that can be applied in a semi-distributed form, much like the proposed CMT. It has the capability to simulate the four pathways of the conceptual model in Chapter 1 and has overland flow being generated as saturation excess flow. The groundwater pathways are modelled analogously to the linear reservoirs of the master recession curve (MRC) analyses (Chapter 2) which should allow the groundwater parameter to be associated with the MRC's τ values. NAM requires catchment area, rainfall and potential evapotranspiration to run the model, with observed discharge being utilised to calibrate the parameters. This will ensure that data collected from the catchments for this model will be available nationwide, though most likely not at the same temporal or spatial resolution.

As well as NAM, which was chosen as the main model for investigation and simulation of the pathways, it was decided to implement MODFLOW in one of the research catchments (the Mattock) in order to further investigate the groundwater-surface water interactions occurring in this catchment. MODFLOW is a distributed model that has its main focus on groundwater pathways. This will be applied to further compare with the separations in this catchment obtained from NAM and to also inform the CMT. MODFLOW will require a lot of input data in order to allow it run effectively. All this data will not be available nationwide and it is for this reason that it is being implemented as an investigative tool in only one of the study catchments.

4 Study Catchments

4.1 Introduction

The study catchments of this research were investigated as part of the *Pathways Project*, as outlined in Chapter 1. In order to be able to transfer knowledge from these study catchments to catchments more widely in Ireland, the individual study catchments were chosen so as to reflect a range of catchment characteristics. The generalisation of results is an important output of this work as it will facilitate the separation of flow pathways in ungauged catchments in Ireland utilising catchment characteristics as predictors (see Chapter 9). Evaluating aquifer classification GIS data, approximately 73.5% of Ireland is underlain by poorly productive aquifers and to reflect this, three catchments (Gortinlieve, Glen Burn and Mattock) underlain by poorly productive aquifers were chosen. In addition, it is important that this project should consider the effects of diffuse contaminants in a catchment underlain by a regionally important aquifer and to address this, the Nuenna catchment was selected. These catchments were determined from a short list of potential catchments using a range of criteria to rank them. This ranking process is described in detail in the *Pathways Project* Inception Report (Archbold et al., 2010) with catchment size, land-use, rainfall and geology along with other characteristics being important indicators of a catchment's suitability for selection. Each catchment characteristic was weighted and from the shortlist of potential catchments in the report the four study catchments were chosen. The location of each catchment, Gortinlieve (Donegal), Glen Burn (Down), Mattock (located on the Louth/Meath border) and Nuenna (Kilkenny), can be seen in Figure 4-1.

During the course of the *Pathways Project* an interim conceptual model report (Archbold and Deakin, 2011) was produced, this chapter will focus on the outcomes of this report. New data, available since this report was compiled, was used to update the hydrological aspect of the conceptual model. This new data in conjunction with the conceptual model report was combined to describe the study catchments in this chapter. The author was responsible for collecting the rainfall and river stage data in the Mattock and Nuenna, as well as for checking the data from Gortinlieve and Glen Burn.

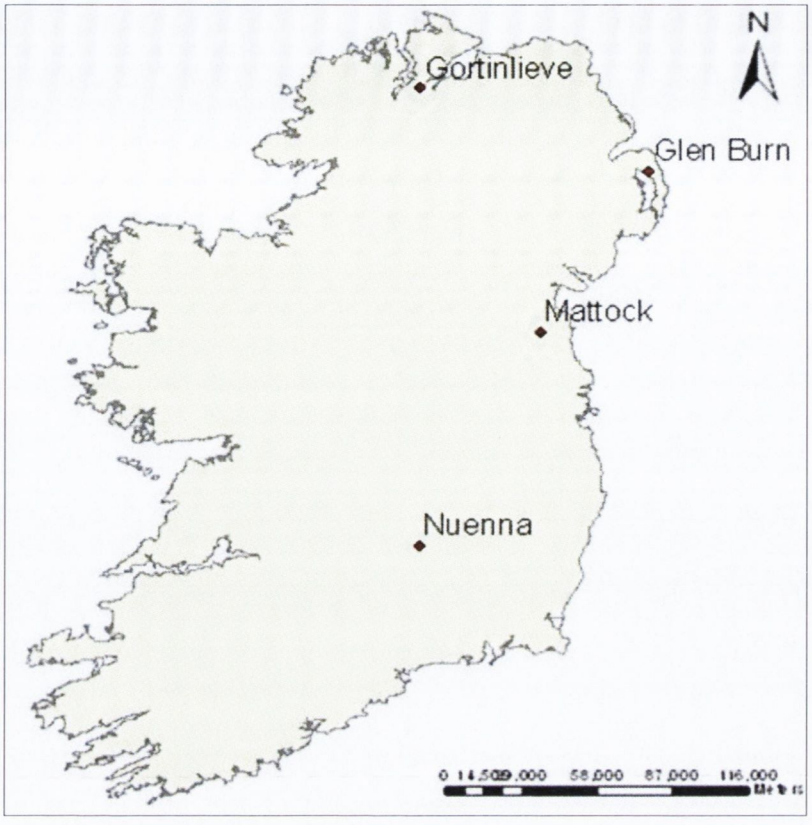

Figure 4-1. Study catchment locations.

4.2 Carrigan's Catchment, Gortinlieve

The Gortinlieve study catchment, a tributary of the River Foyle, is located in Donegal, approximately 5 km southeast of Newtown Cunningham. The catchment is approximately 4.3 km^2 from the catchment outlet, known as the Outlet, to the headwaters. Upstream from the Outlet, the catchment is further divided into a subcatchment, EPA Weir (0.94 km^2). The main channel measures approximately 2.9 km from the headwaters to the catchment outlet. At this point the catchment is at a height approximately 17 mOD and rises to a height of 234 mOD in the northeast of the catchment.

4.2.1 Instrumentation

The catchment has been instrumented to monitor stage height in the rivers, rainfall, groundwater levels, river and groundwater temperature and a selection of river quality parameters (as detailed in Chapter 5). The locations of the two hydrometric stations (Outlet and EPA Weir) are identified in Figure 4-2. Also in Figure 4-2 are the locations of the two rainfall gauges at the EPA Weir and near the headwaters, and the three clusters of boreholes that were drilled as part of the part of the EPA's longer term monitoring of groundwater bodies programme (EPA, 2006). The upland cluster (GO1) monitors temperature and groundwater levels for deep groundwater, shallow groundwater and transition zone. GO2 records deep groundwater, shallow groundwater and transition zone water levels, while at GO3, deep and shallow groundwater, transition zone and subsoil water levels are measured. Temperature data were also obtained in the river at the Outlet, as well as in the instrumented boreholes. Electric conductivity and other river water quality data was recorded within the catchment. The rating curve developed for the Outlet hydrometric station had not sufficiently covered high levels of discharge, resulting in large uncertainty in any discharges calculated from the recorded river stages. Consequently the EPA Weir subcatchment is the only catchment discussed quantitatively in this report.

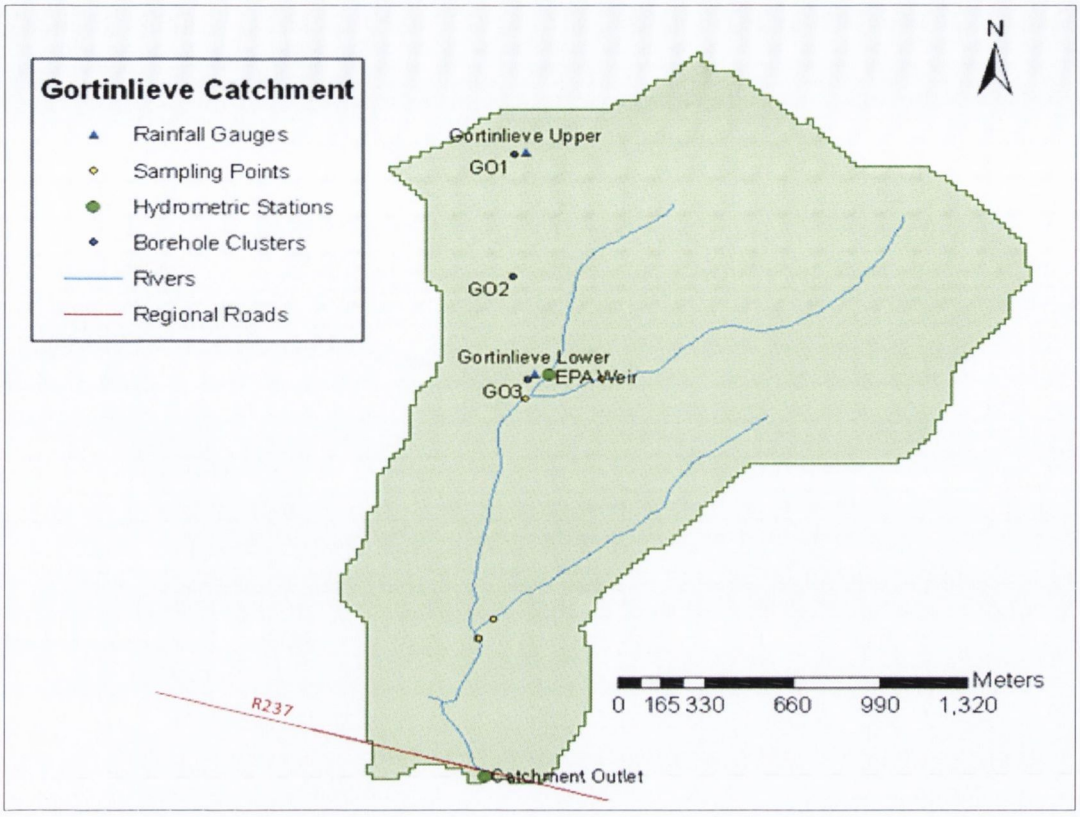

Figure 4-2. Catchment map showing location of river, catchment boundary, EPA boreholes, monitoring infrastructure and sampling points (Archbold and Deakin, 2011).

4.2.2 Land-use and Geology

Land-use in the area is estimated at 53% pasture (dairy and sheep), 43% arable for cereals and <2% forestry (Archbold and Deakin, 2011). Soils within the Gortinlieve are mostly poorly drained with areas of shallow soils in the higher ground and near the catchment outlet, as illustrated in Figure 4-3(a). Near the shallow soil areas in the higher ground there are some poorly draining sections of peat. The majority of subsoils in the Gortinlieve area are poorly draining metamorphic tills with rock outcrop in the higher ground, as can be seen in Figure 4-3(b). The aquifer underlying the Gortinlieve catchment is formed of quartzites, gneisses and schists (Figure 4-4) that are part of the Lough Foyle Succession that are classified as a poor aquifer (Figure 4-5(a)) with bedrock which is generally unproductive, except for local zones (Pl). Figure 4-5(b) shows vulnerability classification ranges from Extreme, where there is rock outcrop in the higher parts of the catchment, to Moderate where the depth to bedrock is greater

under the poorly draining till subsoils. In Figure 4-6 a cross-section schematic illustrates the geological setting along the borehole cluster transection.

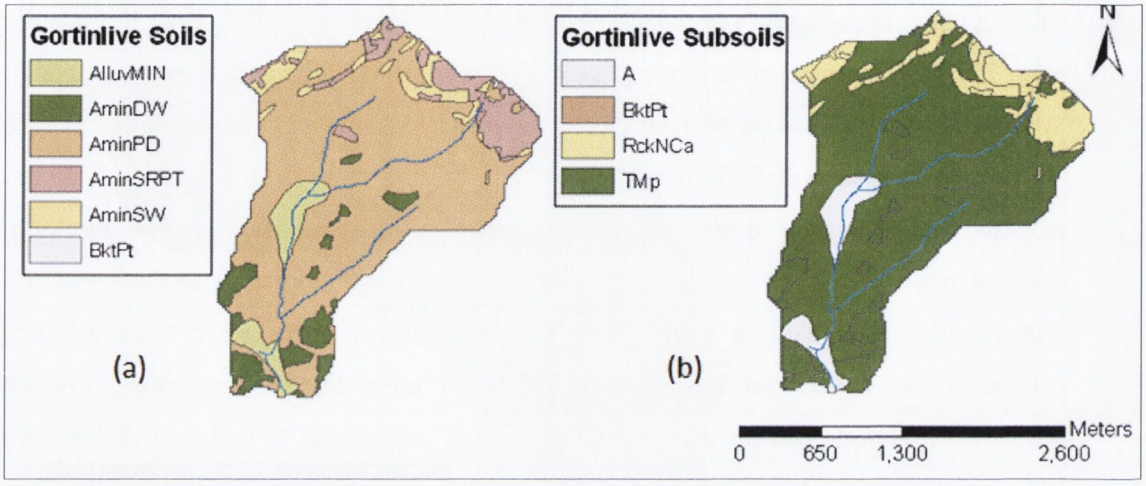

Figure 4-3. (a) Soils and (b) subsoils within the Gortinlieve catchment.

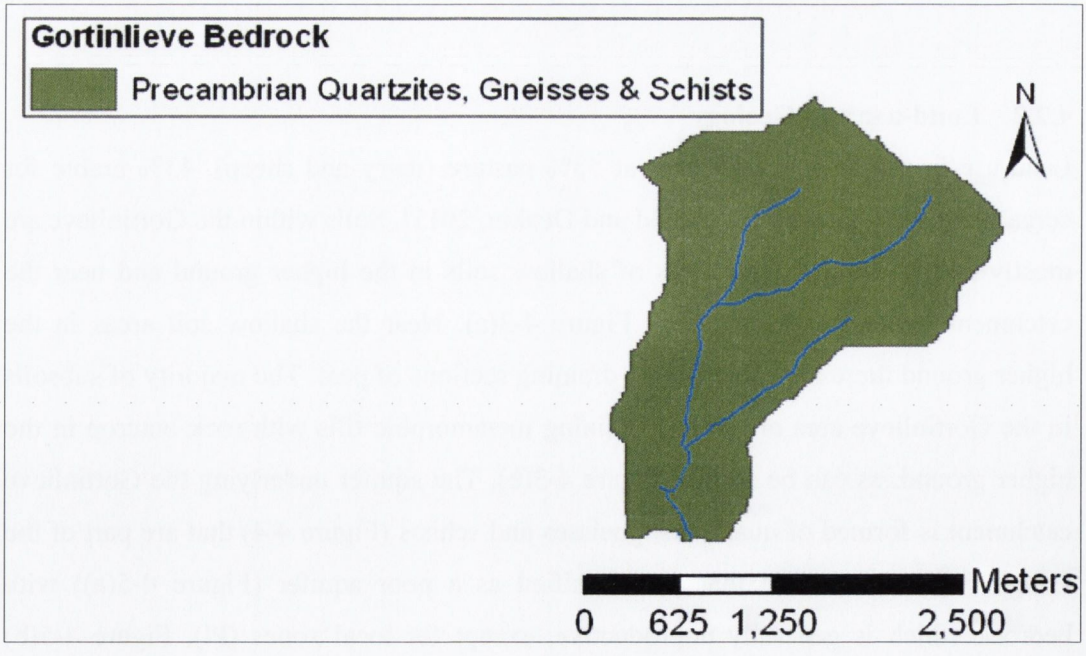

Figure 4-4. Gortinlieve Bedrock.

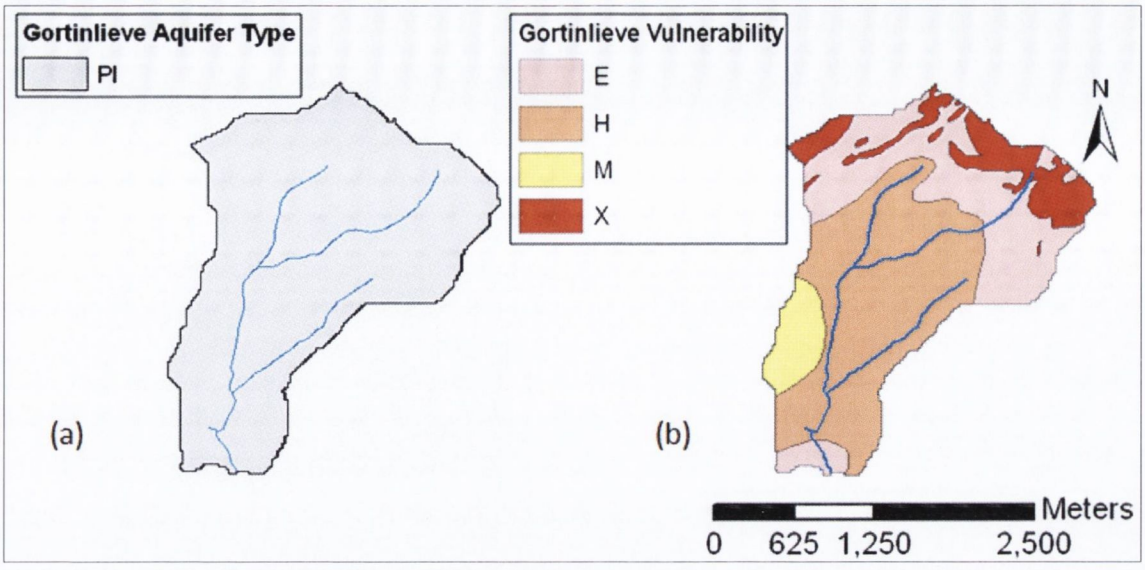

Figure 4-5. (a) Aquifer type and (b) vulnerability mapping in the Gortinlieve catchment.

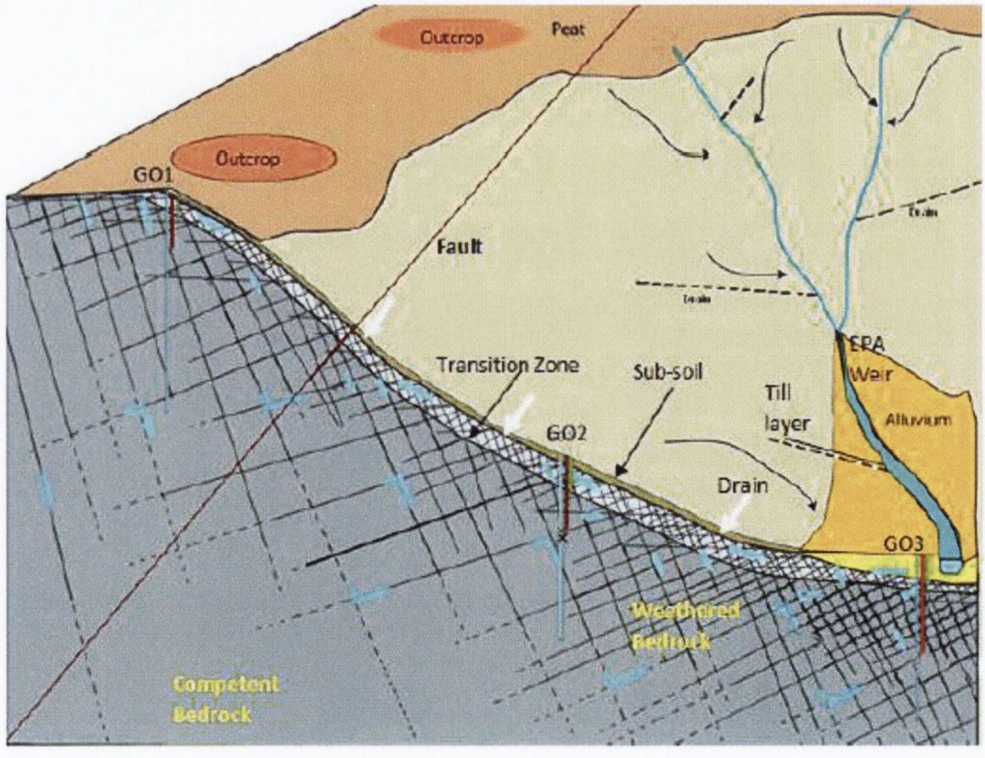

Figure 4-6. Cross-section schematic along EPA borehole transection (Archbold and Deakin, 2011).

4.2.3 Hydrology

The mean annual rainfall in the catchment (1981-2010) is estimated to be 1000-1200 mm, with average annual potential evapotranspiration for the region (1961-1990) estimated to be approximately 452 mm (Met Éireann, 2011). This is further investigated in Chapter 5 utilising data collected from the catchment during this research.

The Gortinlieve catchment responds very quickly to rainfall, with discharge in the river rising sharply before receding back to low flows following the rainfall event (Figure 4-7). This is typical behaviour of a 'flashy' catchment where most water falling on the land enters the river by means of quick responding pathways rather than recharging into the groundwater pathways. The discharge, calculated from stages recorded at the EPA Weir range from 0.001 m^3/s to greater than 0.75 m^3/s. The mean recorded discharge was 0.021 m^3/s in the period May 2010 to June 2012, while the median discharge was significantly lower at 0.011 m^3/s, a difference of greater than 47%. These recorded indices of discharge are typical of the behaviour of a 'flashy' catchment.

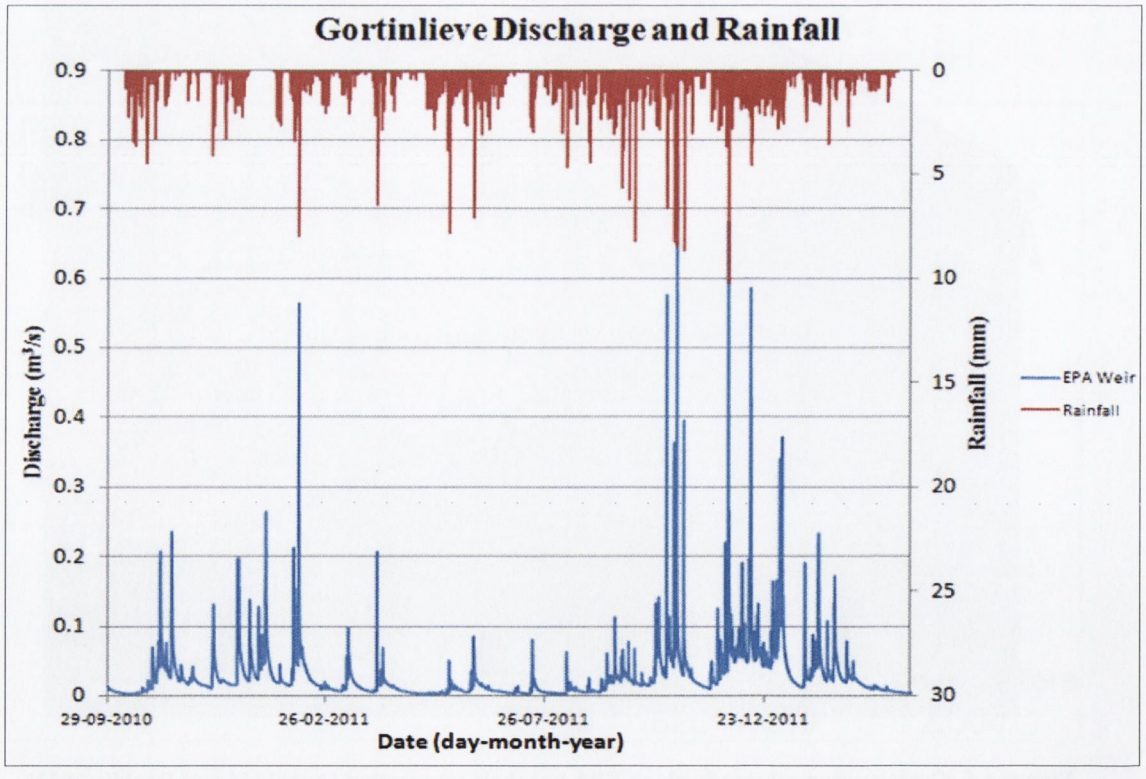

Figure 4-7. Gortinlieve discharge at the EPA Weir and catchment rainfall (Sept 2010 to March 2012).

Monitoring at the EPA Weir is affected by silt at low flows maintaining the head of the water in the stilling well at a higher stage that is present in river. This has the effect of a horizontal recession being recorded by the logger when a further recession should be observed (Chapter 6, Figure 6-10). This problem is only at very low discharges and is being addressed by the EPA hydrometrics team monitoring the weir. During periods of low discharges the hydrograph becomes approximately horizontal for extended periods.

4.2.4 Hydrogeology

As previously stated in Section 4.2.2, the Gortinlieve bedrocks are classified as poorly productive with aquifer type Pl covering the entire catchment. Transmissivities, hydraulic conductivities and specific storage values of the bedrock surrounding the borehole clusters are plotted in Figure 4-8. In this figure, the shallow groundwater (shallow bedrock and transition zone) and the deep groundwater have a comparable potential to deliver similar quantities of water based on their tranmissivity values, though specific storage in the deep groundwater is low compared to the higher (though more variable) shallow bedrock. The contribution of these pathways to discharge in the river will also be dependent on availability of more permeable routes through the low permeable till overburden.

The water levels in the borehole clusters are shown in Figure 4-9. These levels indicate a downward gradient from GO1 shallow and transition boreholes to the deep borehole. At GO3, which is adjacent to the river, it is observed that there is an upward gradient from the deep groundwater through the shallow groundwater and transition zones to the subsoil. This indicates that, if the groundwater pathways are not confined by the tills from the river, the deep and shallow groundwater pathways are contributing to discharge in the river at this point in the catchment.

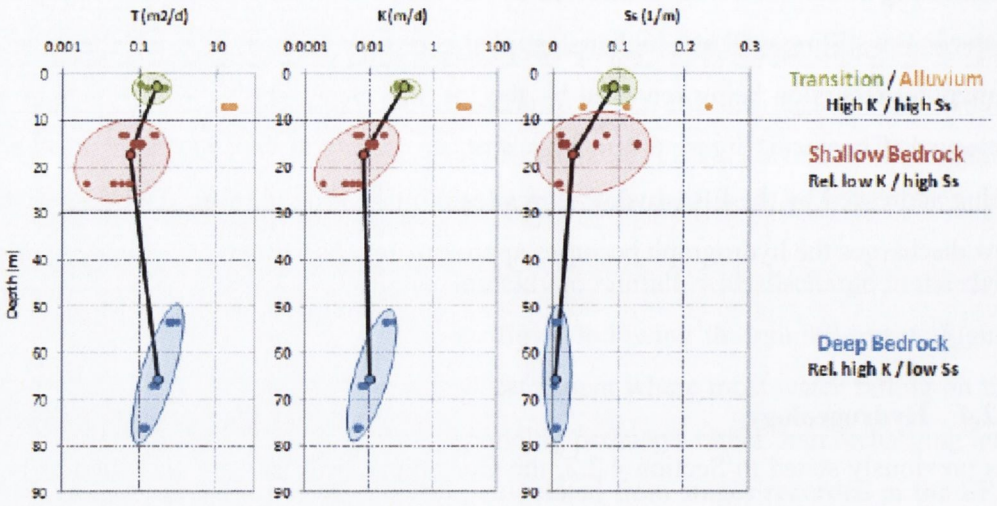

Figure 4-8. Comparison of transmissivity (T), hydraulic conductivity (K) and specific storage (Ss) in the transition/alluvium, shallow bedrock and deep bedrock in GO1, GO2 and GO3 (Nitsche, 2009; Cassidy et al., 2010).

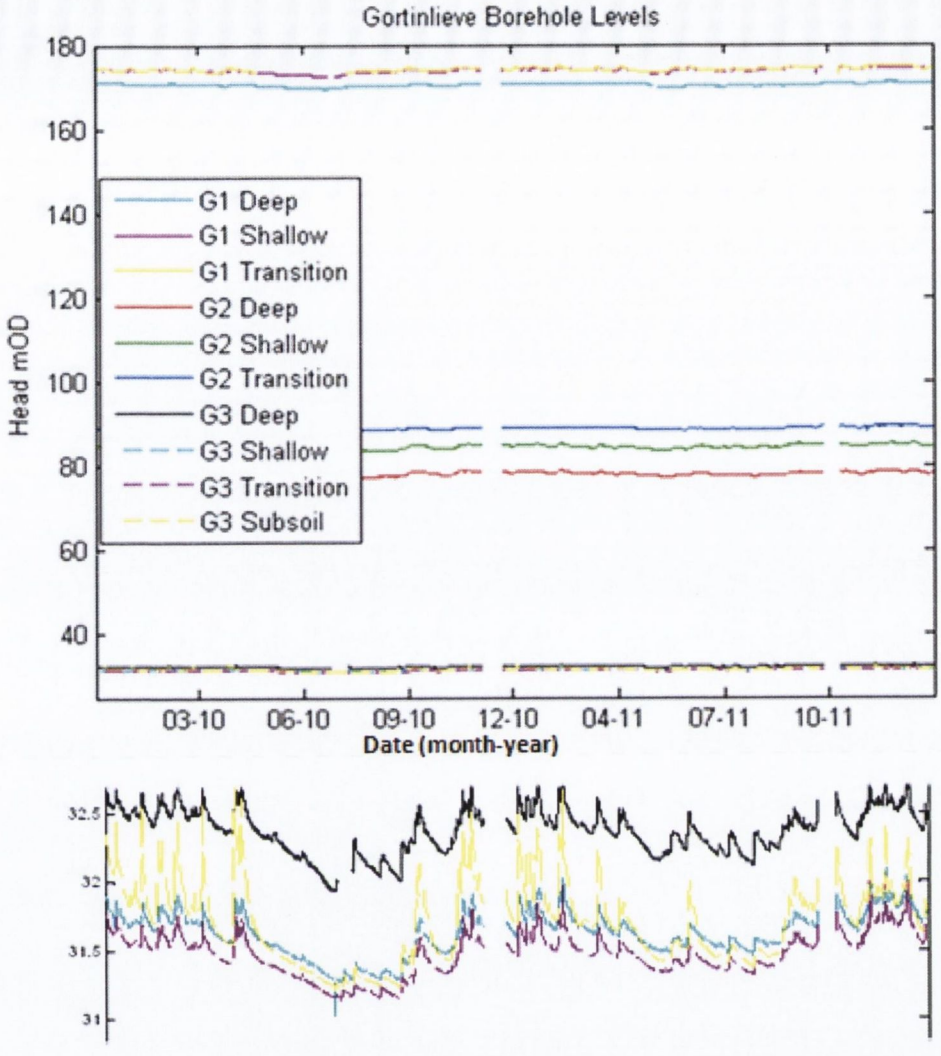

Figure 4-9. Gortinlieve borehole levels from clusters GO1, GO2 and GO3.

4.3 Glen Burn (Mount Stewart) Catchment

The Glen Burn river flows directly into Strangford Lough. Its catchment is located in county Down, approximately 7 km southeast from Newtownards on the Ards Penninsula. The catchment area is approximately 5 km^2 from the catchment outlet, known as the Outlet, to the headwaters. Upstream from the Outlet, the catchment is further divided into another subcatchment, referred to as Subcatchment (4.8 km^2). The main channel measures approximately 4.6 km from the headwaters to the outlet. At the outlet, the catchment is at a height of approximately 5 mOD and rises to a height of 44

m OD to the west of the catchment. Permission was granted by both the Geological Society of Northern Ireland (GSNI) and National Trust to access the boreholes and install temporary hydrometric monitoring points in Mount Stewart Estate.

4.3.1 Instrumentation

The catchment was instrumented to record stage height in the rivers, rainfall, potential evapotranspiration, groundwater levels, river and groundwater temperature and a selection of river quality parameters (see Chapter 5). The locations of the two hydrometric stations (Outlet and Subcatchment) can be identified in Figure 4-10. Also in Figure 4-10 are the locations of the rainfall gauge and meteorological station in the centre of the catchment, and the clusters of boreholes which were installed as part of the Geological Survey of Northern Ireland/Northern Ireland Environment Agency monitoring programme. There are a total of 16 boreholes within Mount Stewart Estate that are located in the Glen Burn catchment. There are nine open uncased boreholes and seven screened piezometers covering an area of approximate 2 km^2. Each cluster contains three boreholes with one borehole in the transition (more transmissive shallow groundwater) zone, one in the transition and shallow groundwater zone and the final borehole intersecting the transition, shallow and deep groundwater zones. Electric conductivity and other river water quality data were also sampled within the catchment.

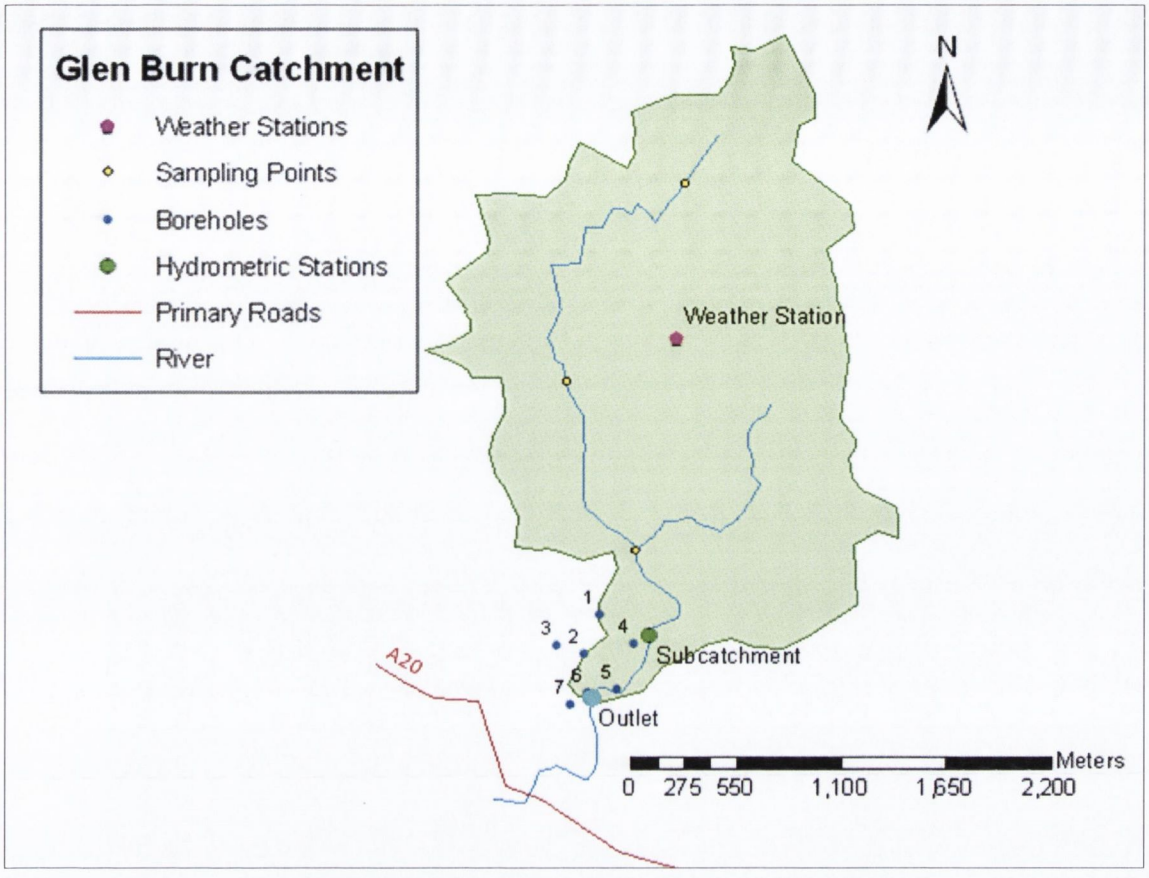

Figure 4-10. Catchment map showing location of river, boreholes and monitoring infrastructure (Archbold and Deakin, 2011).

4.3.2 Land-use and Geology

Catchment land-use is mainly intensive pasture (82%) with some areas of tillage (10%) and small areas of woodland (5%), with the remaining area comprising diffuse rural settlement and roads (Archbold and Deakin, 2011). The dominant soils within the Glen Burn are poorly drained gleys with areas of alluvium and peat located by the river in the north of the catchment (Figure 4-11 (a)). The majority of subsoils in the higher areas of the Glen Burn are dominated by deep till drumlins with the lower areas having thin subsoils and numerous outcrops of rock, as shown in Figure 4-11 (b). The aquifer underlying the Glen Burn is classified as a poor aquifer with greywacke bedrock which is generally unproductive, except in local zones (Pl), as can be seen in Figure 4-11(d). Vulnerability in the Glen Burn is Extreme E in general due to thin covering of the bedrock and the numerous outcrops in the catchment. Under the drumlins vulnerability

is much reduced due to the depth of the subsoils. Values range from Extreme to Low (Figure 4-11(c)). A schematic cross-section illustrates the geological setting of the catchment as viewed upstream from the Outlet, as illustrated in Figure 4-12. Greywacke (coloured green) underlies the catchment with alluvium being present underneath the river at the Outlet and upstream of the major tributary (Orange and yellow). The outcrop of rock throughout the catchment is illustrated by the multiple light green sections on the schematic, while the poor draining drumlins (red) are straddling the catchment boundary by the boreholes. The influence of these poorly drained soils and the poorly productive aquifer induces the quick responding nature of the Glen Burn.

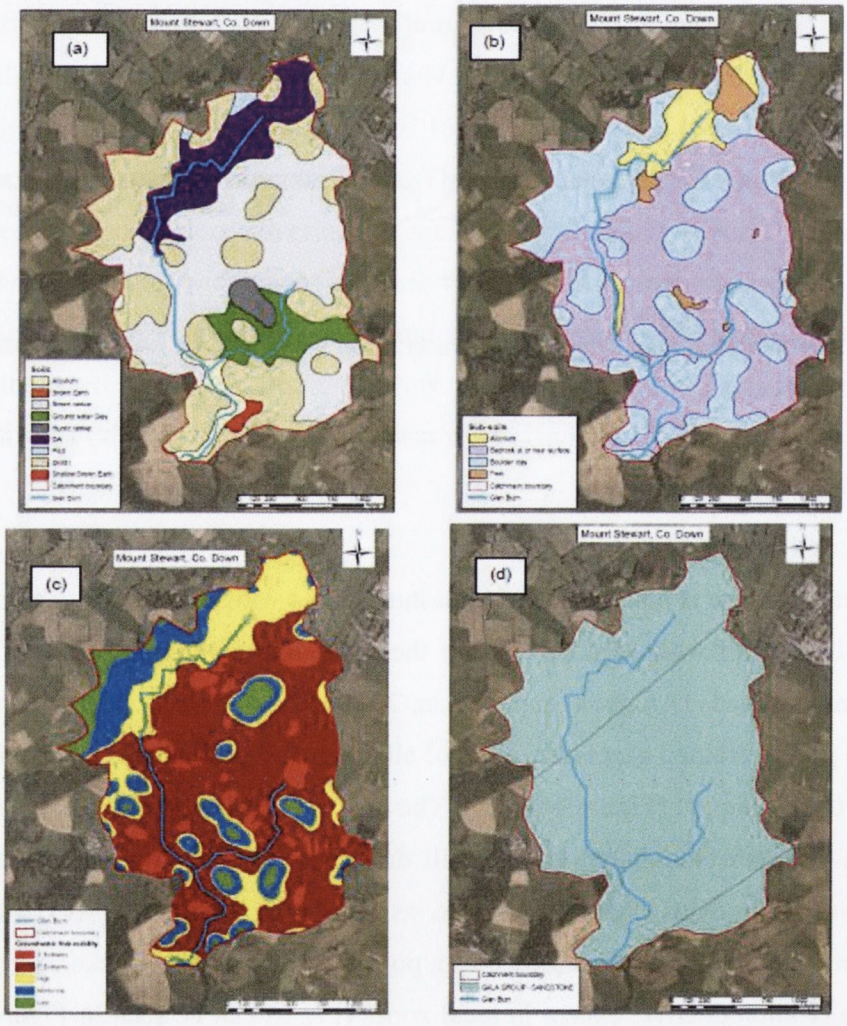

Figure 4-11 (a-d). shows soil, sub-soil, groundwater vulnerability and bedrock maps.

(Source: Map a,b,d OSNI base maps, GSNI Map; (c) OSNI base map, (Meredith, 2010)).

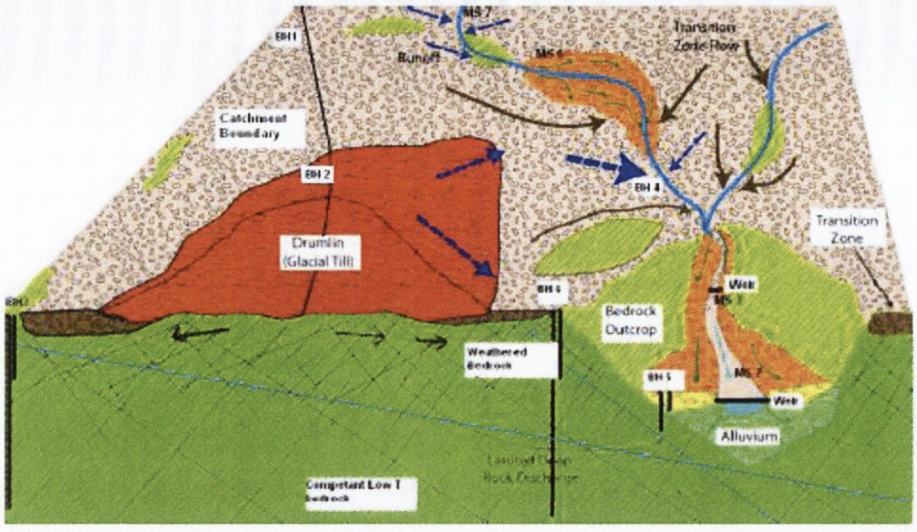

Figure 2.5: Cross section schematic of BHs and catchment boundary in Mount Stewart Estate

Figure 4-12. Cross-section schematic of BHs and catchment boundary in Mount Stewart Estate (Archbold and Deakin, 2011).

4.3.3 Hydrology

The total rainfall for 2011 was 843 mm (recorded by a Campbell Scientific meteorological station location in the middle of the catchment (Figure 4-10). Average annual rainfall for the Ards Peninsula is reported to be approximately 800 mm with the largest proportion falling between August and January. PE for 2011 was 497 mm and this was also calculated using data from the meteorological station.

The Glen Burn, much like the Gortinlieve catchment, responds very quickly to rainfall, with discharge in the river rising sharply before receding back to low flows following the rainfall event, as shown in Figure 4-13. The low permeability soils in the drumlins and the limited ability of the aquifer to accept recharge generates the quick responding pathways as rainfall occurs in the catchment. This again is the behaviour of a 'flashy' catchment where most water falling on the land enters the river by means of the quick responding pathways rather than recharging into the groundwater pathways. The discharge, calculated from the river stage recorded at Outlet, ranges from less than 0.001 m^3/s to greater than 1.11 m^3/s in the period October 2010 to March 2012. The mean recorded discharge was 0.07 m^3/s, while the median discharge was significantly

lower at 0.037 m^3/s, a difference of greater than 47%. These recorded indices of discharge are again characteristic of the behaviour of a 'flashy' catchment.

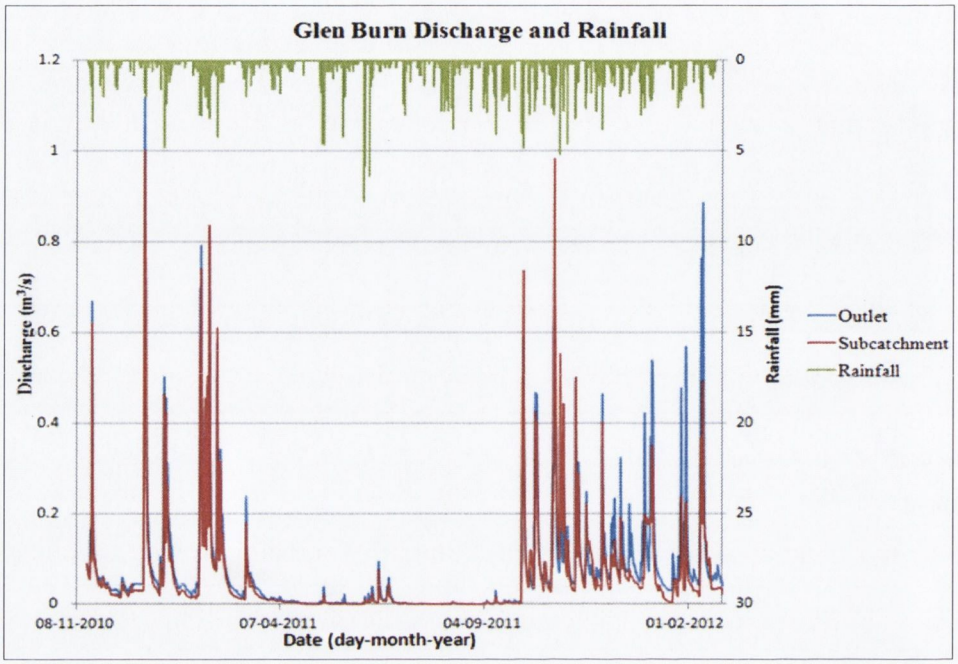

Figure 4-13. Glen Burn discharge at catchment the Outlet and Subcatchment hydrometric stations, and catchment rainfall (Aug 2010 to Feb 2012).

4.3.4 Hydrogeology

As determined in Section 4.3.2, the Glen Burn bedrocks are classified as poorly productive with aquifer type Pl covering nearly 100% of the catchment. Transmissivities of the bedrock are estimated to be $1.7x10^{-1}$ m^2/d for shallow groundwater (weathered bedrock) and $7x10^{-2}$ m^2/d for deep groundwater (bedrock). However, these calculations are based on the boreholes concentrated in one area of the catchment and may not be representative of the entire catchment as bedrock thickness will vary spatially (Archbold and Deakin, 2011).

Glen Burn was instrumented with 16 boreholes, covering an area of 2 km^2 and varying subsoil and shallow groundwater conditions. The water levels in three of these boreholes, along with rainfall and the water level at the Outlet (MS2), are shown in Figure 4-14. Boreholes 6-2 (deep groundwater) and 6-1 (shallow groundwater) indicate

an upward gradient contributing to river discharge, as can be seen in Figure 4-14(a and b). The levels indicate a downward gradient from the river to borehole 5-1 during low flows suggesting that the river may be losing flow to the alluvium during these periods (Figure 4-14(c)). All three boreholes demonstrate a direct response to rainfall and river discharge, with large rises in groundwater level during high rainfall and river discharge.

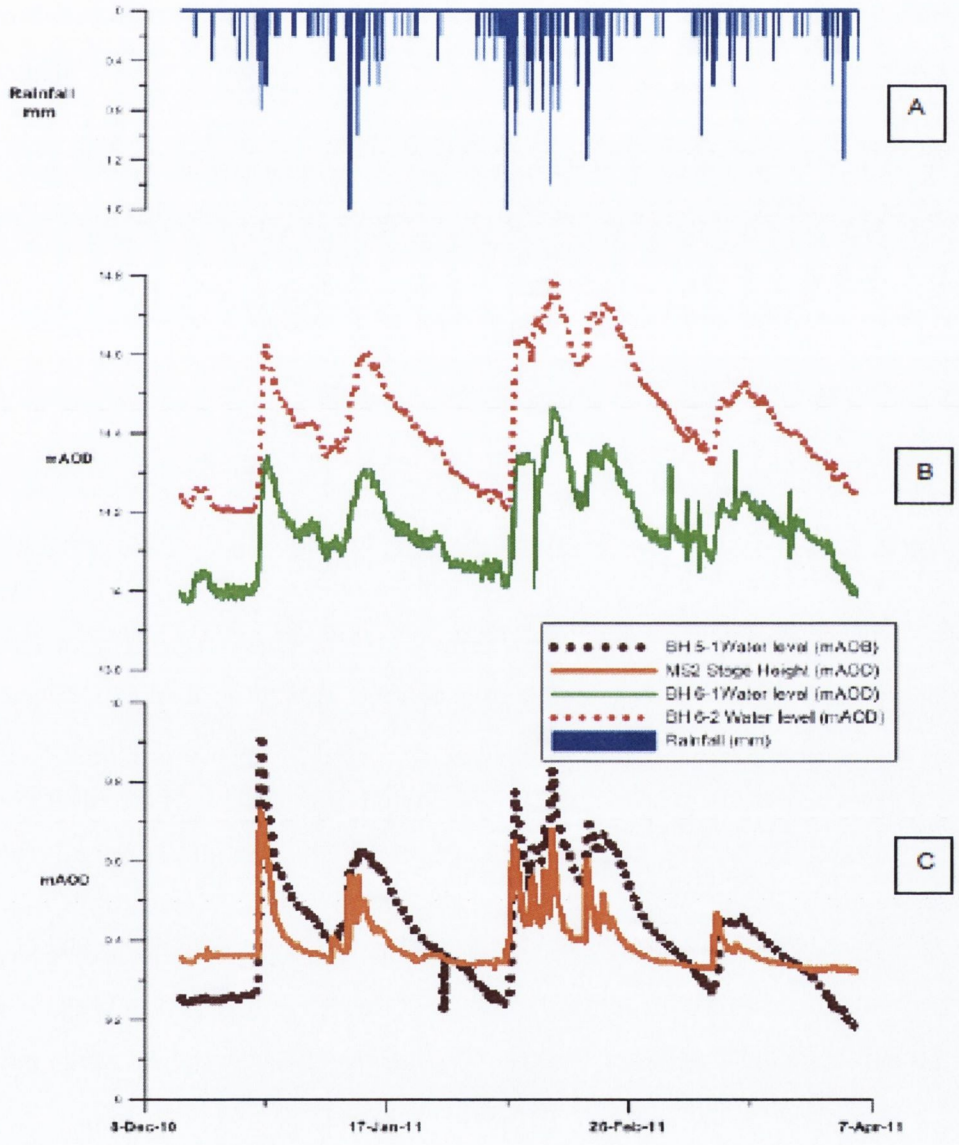

Figure 4-14. Glen Burn: (a) rainfall; (b) groundwater levels in boreholes 6-1, 6-2; (c) groundwater levels in borehole 5-1 and river stage at the Outlet (MS2) (Archbold and Deakin, 2011).

4.4 Mattock catchment, Co. Louth/Meath

The Mattock study catchment, a tributary of the River Boyne, straddles the Louth and Meath border. The catchment area is approximately 16.8 km^2 from the catchment outlet, known as Berril's, to the headwaters. Upstream from Berril's, the catchment is further divided into two subcatchments, Collon Weir (11.6 km^2) and Diversion Weir (7 km^2). The Diversion Weir subcatchment is contained within the Collon Weir subcatchment and is located just downstream of off-take from the river for Drogheda's public water supply. This off-take was instrumented with a stage level logger to estimate the flow that is taken from the catchment. The main channel measures approximately 8.8 km from the headwaters to the outlet at Berril's. At this point the catchment is at an elevation of approximately 77 mOD and rises to a height of 250 in the north of the catchment.

4.4.1 Instrumentation

The catchment was instrumented to monitor stage height in the rivers, rainfall, groundwater levels, river and groundwater temperature and a selection of river quality parameters. The locations of the four hydrometric stations (Berril's, Collon Weir, Diversion Weir and Diversion Off-take) can be seen in Figure 4-15. Figure 4-15 also displays the locations of the two rainfall gauges at the WWTP in Collon and near the headwaters, and the three clusters of boreholes that were drilled as part of the part of the EPA's longer term monitoring programme of groundwater bodies. The upland cluster (MK1) monitors temperature and groundwater levels for deep groundwater, shallow groundwater and subsoil. MK2 monitors deep and shallow groundwater, while at MK3, deep and shallow groundwater, and subsoil at two different levels are recorded. Temperature data were also obtained in the river at Berril's and at Collon Weir, as well as in the instrumented boreholes. Electric conductivity and other river water quality data were also sampled within the catchment.

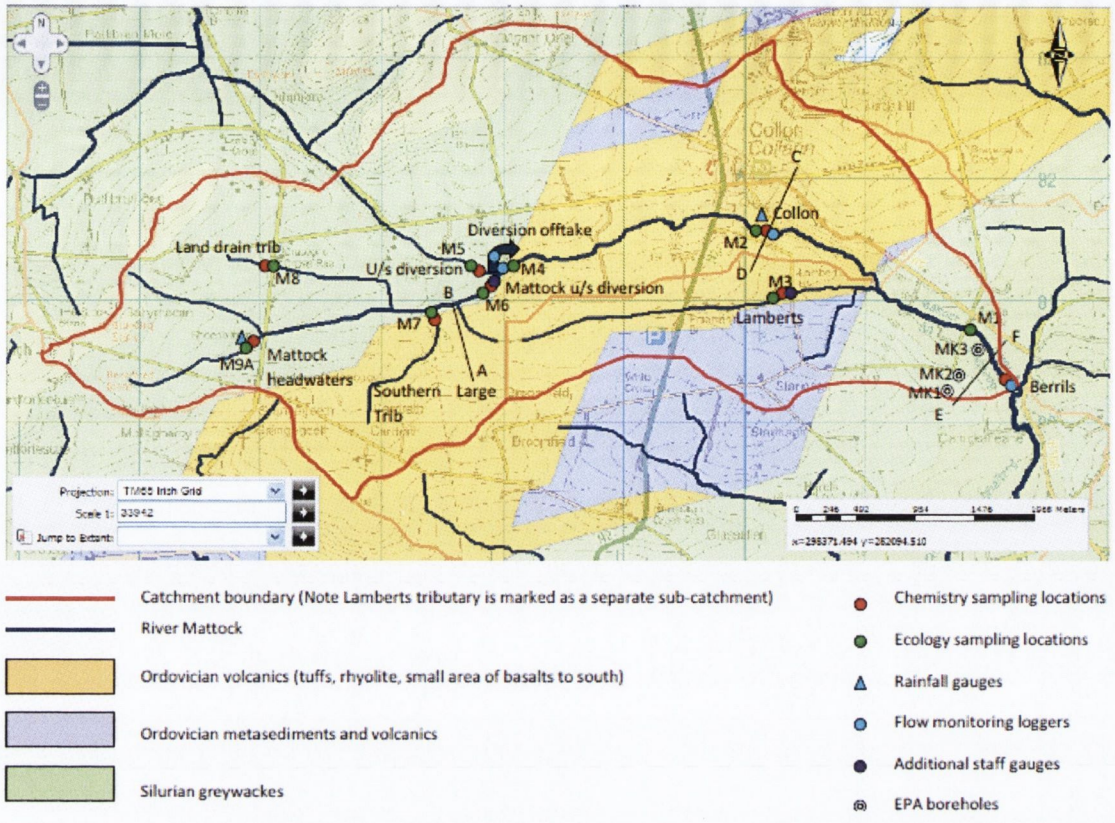

Figure 4-15. Location map showing geology with catchment boundary (Archbold and Deakin, 2011).

4.4.2 Land-use and Geology

A detailed land-use survey was carried out within the catchment which found that there is approximately 83% pasture (dairy, cattle, sheep, with some limited horses) and 7% arable for cereals and maize, with the remainder a mixture of woodland, scrub, urban and other categories (Archbold and Deakin, 2011) . Soils within the Mattock catchment are mostly poorly drained with areas of well drained soils in the higher ground and overlying the sands and gravels located near the Collon Weir and Diversion, as shown in Figure 4-16(a). The majority of subsoils in the Mattock are poorly draining tills with rock outcrop in the higher ground and well draining sands and gravels located at Collon Weir and the Diversion (Figure 4-16(b)). The bedrock geology of the Mattock is composed of metasediments and volcanic as illustrated in Figure 4-17. These bedrock aquifers underlying the Mattock are mainly classified as a poor aquifer with bedrock

which is generally unproductive, except for local zones (Pl). In the south east of the catchment, the metasediment bedrock is classified as a poor aquifer with bedrock which is generally unproductive (Pu), as can be seen in Figure 4-18(a). Vulnerability ranges from Extreme, where there is rock outcrop in the higher parts of the catchment, to Low by the river where the bedrock is overlain by poorly drained soils and deep till subsoils, as shown in Figure 4-18(b).

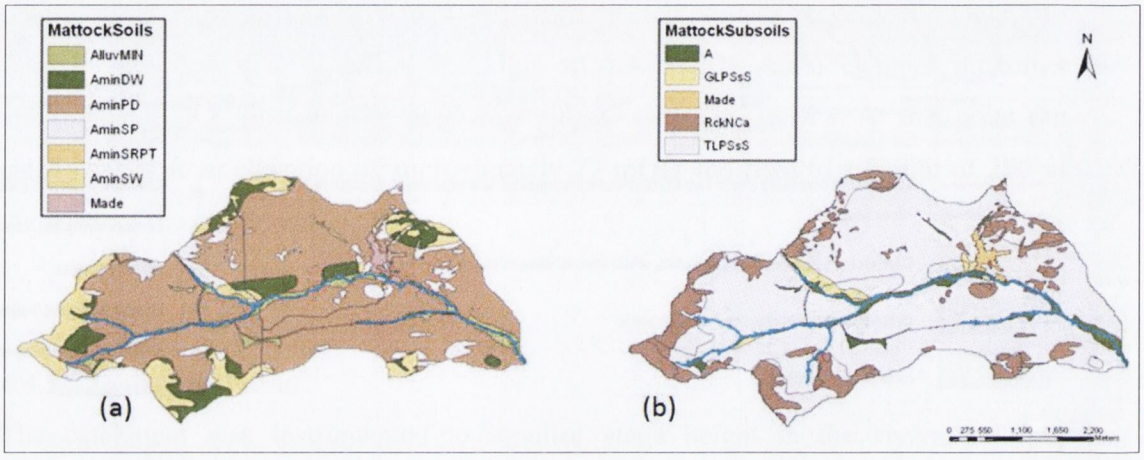

Figure 4-16. (a) Soils and (b) Subsoils within the Mattock catchment.

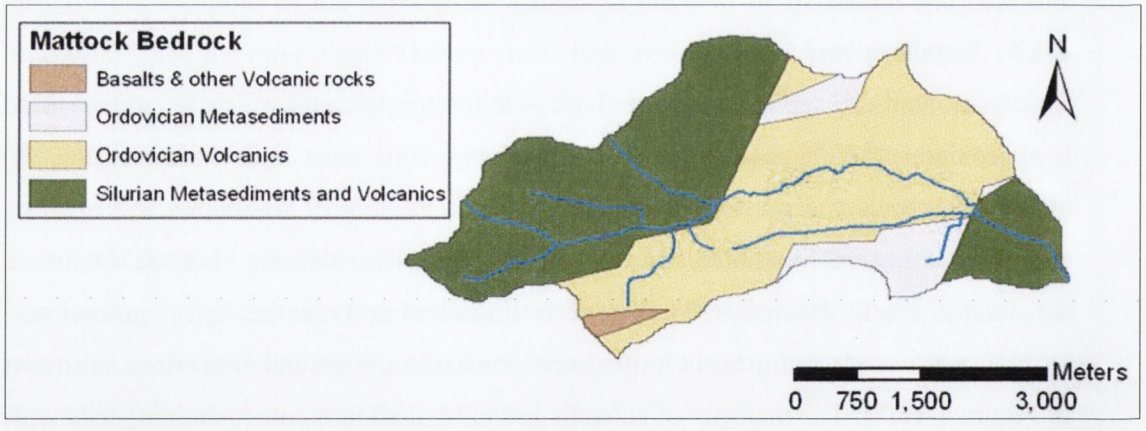

Figure 4-17. Mattock Bedrock.

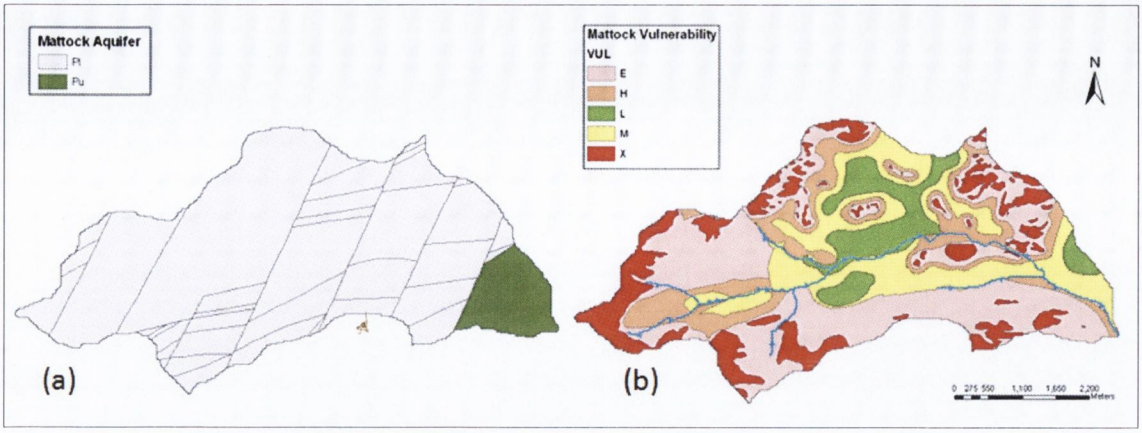

Figure 4-18. (a) Aquifer map and (b) Vulnerability map of Mattock catchment.

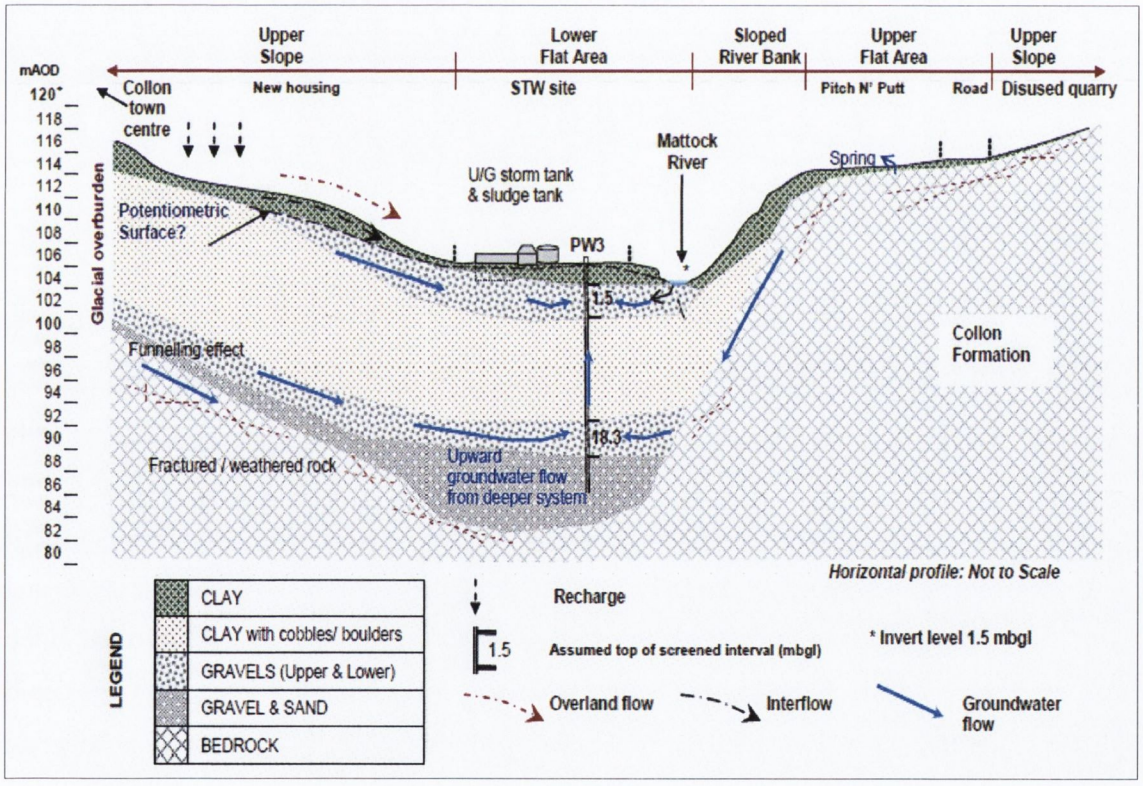

Figure 4-19. Cross-section through the gravels at the public at Collon Weir (Groves, 2010).

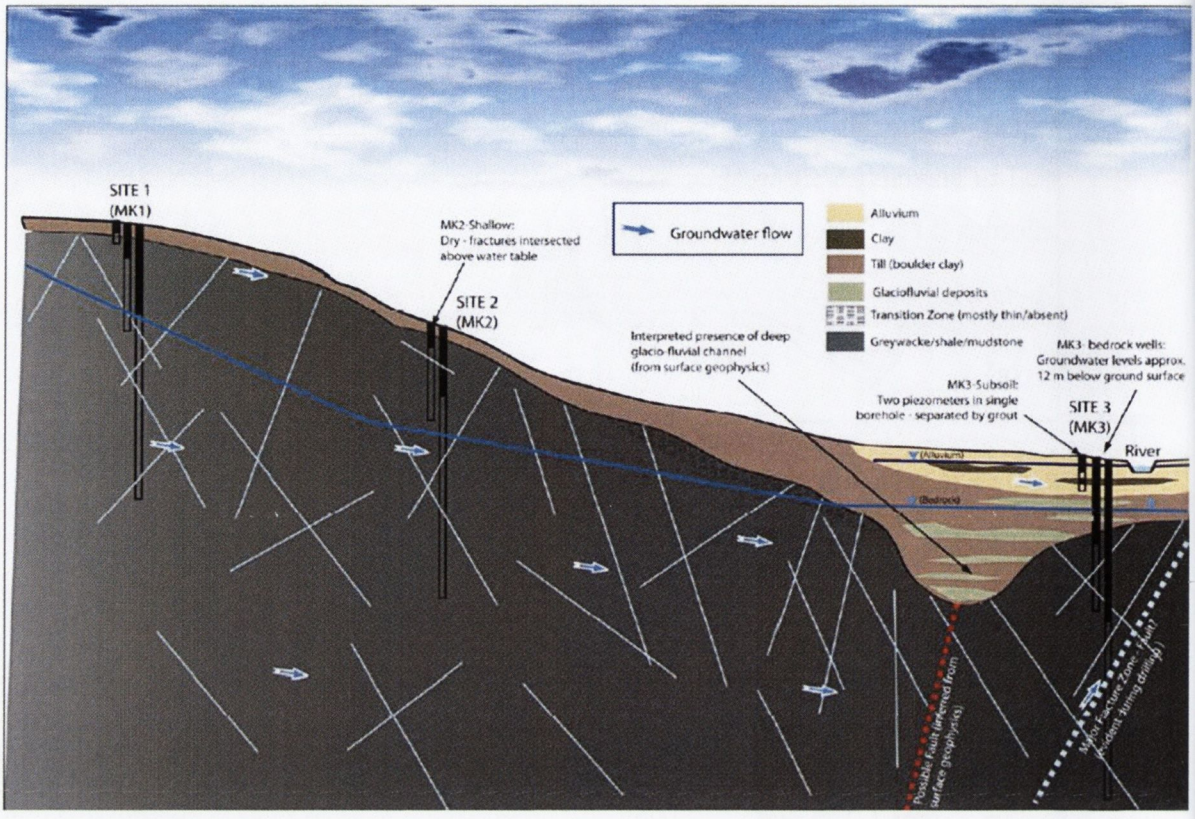

Figure 4-20. Cross-section through the EPA borehole transect (CDM/OCM, 2010).

Two cross-sections illustrate the geological setting at Collon Weir (Figure 4-19) and along the transect of the EPA borehole clusters (Figure 4-20). An extensive sand and gravel unit is observed in Figure 4-19. These sands and gravels are potentially contributing to the Mattock river at this point, maintaining higher discharges, during periods of low rainfall, than would be expected given the poorly productive nature of the bedrock in the catchment. There are also three boreholes located in these sands and gravels supplying the town of Collon with water. One of these boreholes, located in the wastewater treatment plant compound, is artesian; suggesting that water from this depth is contributing to the discharge in the river. The two other boreholes are abstracting water from shallower gravels than at the artesian borehole. The water levels in these boreholes are thought to be lower than that of the river and a study is currently being undertaken on behalf of Louth County Council to investigate this relationship while pumping is occurring in these boreholes.

The cross-section at the EPA boreholes (Figure 4-20) suggests that, at the catchment outlet at Berril's, the Mattock river is perched. The borehole and river water level data discussed in Section 4.4.4 confirms this. This implies that groundwater contribution in this area of the catchment is minimal and it will be expected that the percentage of the river hydrograph comprised of the groundwater pathways will be lower than at Collon Weir. This is further examined in Chapter 7.

4.4.3 Hydrology

The mean annual rainfall in the catchment (1961–1990) is of the order of 901 mm, with average annual potential evaporation for the region estimated to be approximately 481 mm (Met Éireann data). The meteorological data are examined in detail in Chapter 5.

The Mattock catchment responds very quickly to rainfall, with discharge in the river rising sharply before receding back to low flows following the rainfall event, as shown in Figure 4-21. Once more, this is usual of the type of behaviour expected of a 'flashy' catchment. The discharge, calculated from stages recorded at Berril's, ranges from less than 0.008 m^3/s to greater than 15 m^3/s. This maximum discharge was recorded during the large flooding event of 24th October 2011; the pipe storing the logger was actually damaged at this point and it is expected that a higher discharge occurred. The mean recorded discharge was 0.2 m^3/s, while the median discharge was significantly lower at 0.077 m^3/s. Once again these indices are typical of a 'flashy' catchment.

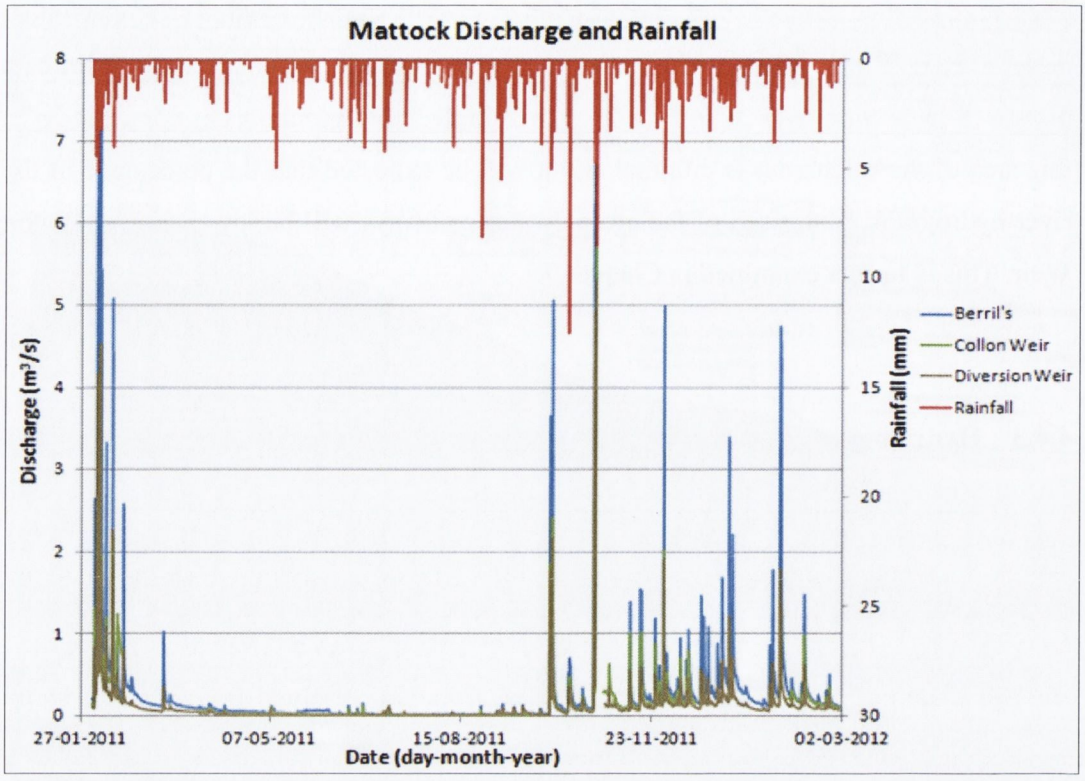

Figure 4-21. Mattock discharges plotted along with Mattock rainfall (Feb 2011 to Mar 2012).

The river flows at Berril's are impacted by the water diverted from the river at the Diversion. This is particularly true at low flows when a substantial percentage of water is removed. After February 2011, the diversion infrastructure was upgraded by Louth County Council. When the discharge of less than 0.008 m^3/s was recorded at Berril's, 0.0045 m^3/s was being diverted upstream, with 0.00016 m^3/s occurring at the Diversion Weir. Effectively, all the water of the upper subcatchment was being diverted during these periods of low flow. During the winter and periods of above-average flow, the effect of the diversion is much more muted. On the 18th October 2011, the discharge at Berril's was 0.241 m^3/s, while at the Diversion it was 0.009 m^3/s and at Diversion Weir it was 0.105 m^3/s, meaning that less than 8% of the discharge was being diverted to Drogheda. Following the high rainfall on the 24th October 2011, the diversion's efficacy for diverting water from the river was influenced due to the pipe diverting the flow being less effective at draining higher heads of water. This reduced the amount of water being diverted, as seen during the above average discharge recorded at Berril's on the 3rd February 2012 of 0.287 m^3/s, but only 0.0042 m^3/s at the Diversion and 0.11

m^3/s at the Diversion Weir. The discharges at the Diversion and recorded rainfall are illustrated in Figure 4-22.

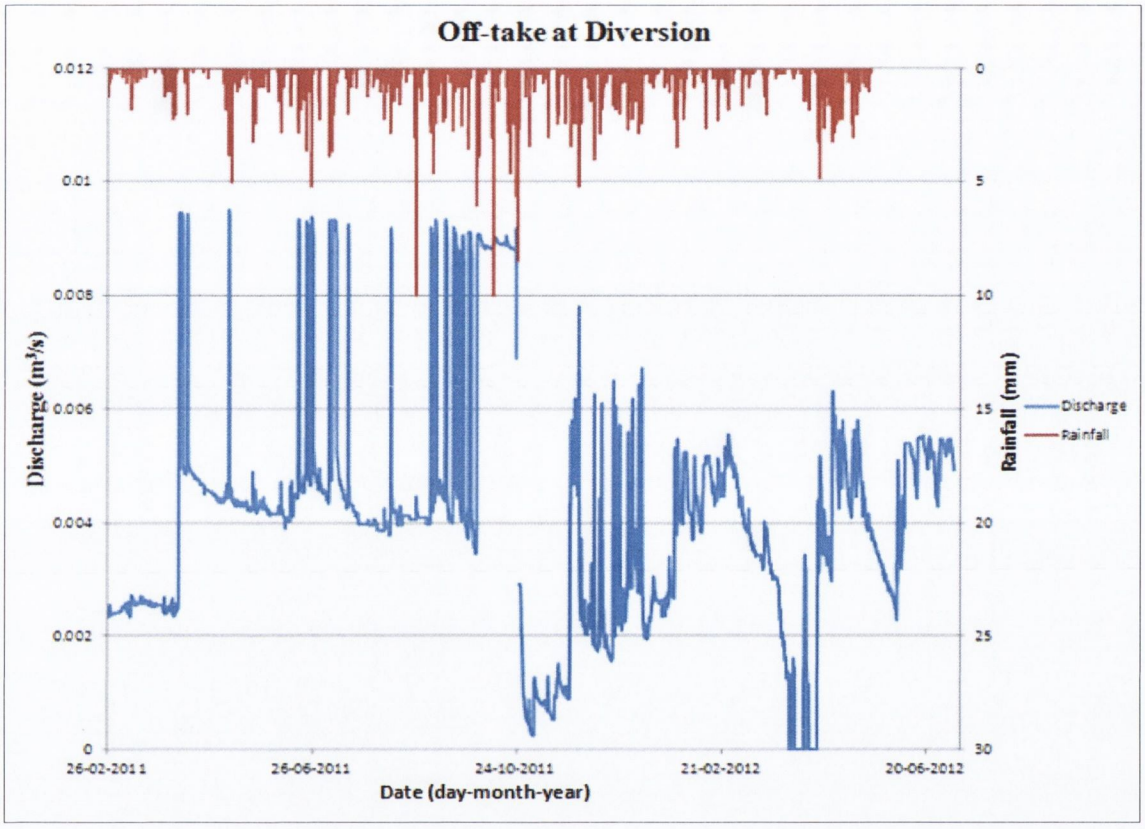

Figure 4-22. Off-take discharge at Diversion.

4.4.4 Hydrogeology

As previously stated in Section 4.4.2, the Mattock bedrocks are classified as poorly productive with aquifer type Pl covering approximately 92% of the catchment and Pu covering approximately 8%. Transmissivities of the bedrock surrounding the borehole clusters have been calculated as being less than 7 m^2/d (Nitsche, 2009). The water levels in these boreholes are shown in Figure 4-23. These levels indicate a downward gradient from MK1 subsoil, through the MK1 shallow borehole towards MK1 deep. At MK3, which is adjacent to the river, it is observed that the groundwater levels are at approximately 68 mOD, leaving the river perched by about 11 m above this. There is an upward gradient from the deep groundwater to the shallow groundwater zone, but as

can be seen from the subsoil water levels, water is being lost from the river down to this zone.

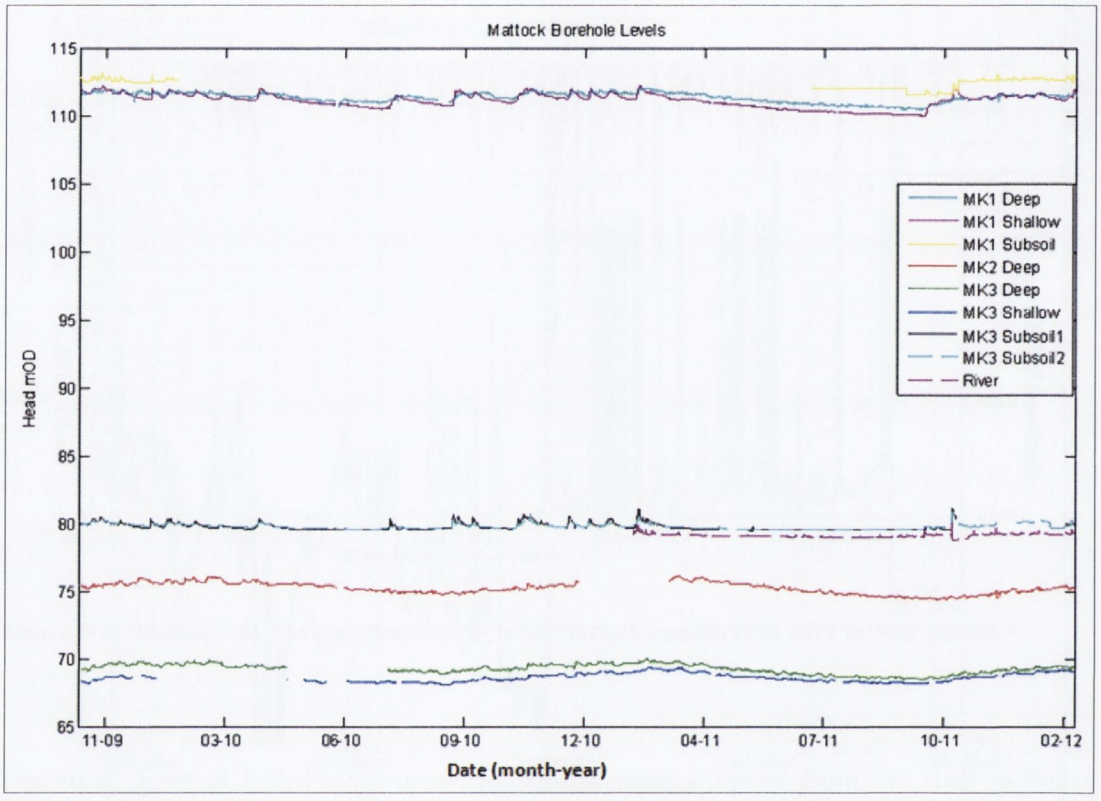

Figure 4-23. Water levels in Mattock boreholes. MK3 (next to the river), MK1 (up high in the catchment).

4.5 Nuenna catchment, Co. Kilkenny

The Nuenna study catchment, a tributary of the River Nore, is located in County Kilkenny, near the town of Freshford. The catchment area is approximately 35 km^2 from the catchment outlet, known as Monument, to the headwaters. Upstream from Monument, the catchment is further divided into two subcatchments, Rocky Weir (21.6 km^2) and Castle Weir (11.6 km^2). These catchment areas are based on topographic heights within the catchment and, as will be discussed later in Chapter 5, this may not be appropriate for catchments underlain by karst aquifers, which contain many large

springs contributing to the discharge in the river. This is particularly important as there is little variation in topography at the western boundary of the catchment. The main channel measures approximately 6.6 km from the headwaters to the outlet at Monument. At the outlet of the catchment the elevation is approximately 86 mOD and this rises to 343 mOD in the northwest of the catchment.

4.5.1 Instrumentation

The catchment was instrumented to record stage height in the rivers, rainfall, groundwater levels, river and groundwater temperature and a selection of river quality parameters. The locations of the three hydrometric stations (Monument, Rocky Weir and Castle Weir) are identified in Figure 4-24. Also shown in Figure 4-24 are the locations of the two rainfall gauges at the Clomantagh Castle and Kilrush house, and the two clusters of boreholes that were drilled as part of the EPA's longer term monitoring programme of groundwater bodies. The upland cluster (NU1) monitored temperature and groundwater levels of the deep groundwater. NU2 monitored deep and shallow groundwater, and subsoil water in the sands and gravel. Temperature data were also obtained in the river at Monument and Boiling Spring as well as in the instrumented boreholes. Electric conductivity and other river water quality data were also collected within the catchment.

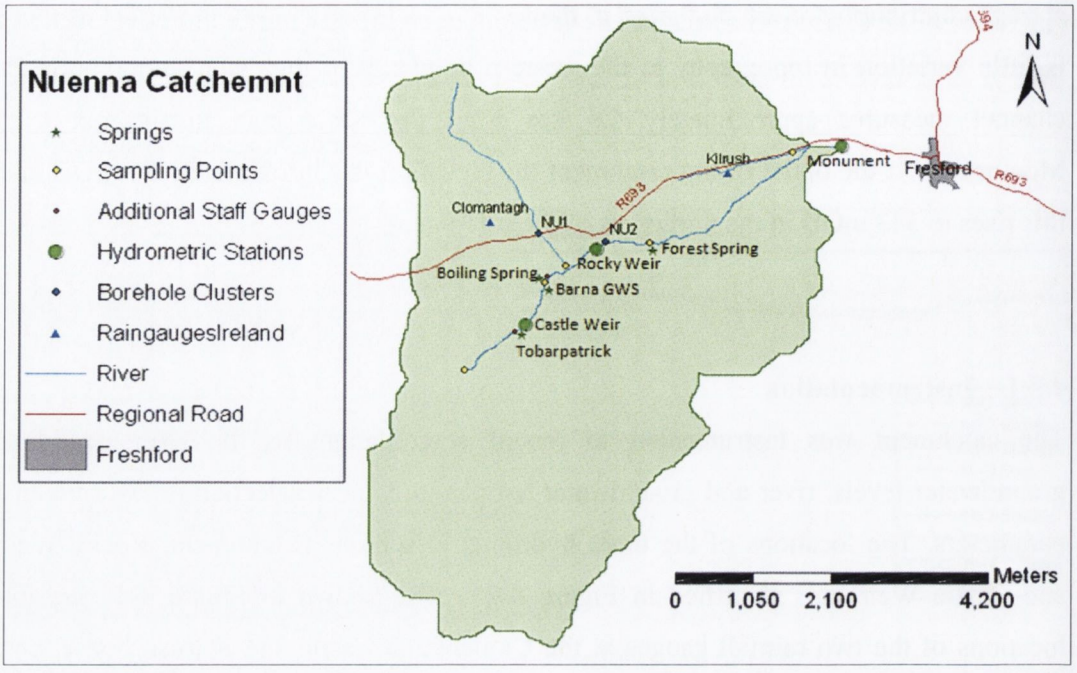

Figure 4-24 Nuenna catchment with hydrometric stations and monitoring sites.

4.5.2 Land-use and Geology

Land-use in the area is 73% pasture (dairy and sheep) and 19% arable for cereals (Archbold and Deakin, 2011). The dominant soils within the Nuenna are well drained with areas of poorly drained soils located in the higher ground (Figure 4-25(b)). The majority of subsoils in the Nuenna are permeable sands and gravels and moderately permeable tills, with rock outcrop in the higher ground (Figure 4-25(a)). The bedrock of the higher ground of the Nuenna catchment is dominated by Numurian shales, while the rest of the catchment is composed of Dinantian pure bedded limestone as seen in Figure 4-26. The main aquifer, corresponding to the pure bedded limestone, underlying the Nuenna is classified as a regionally important aquifer that is karstified with diffuse karst present (Rkd), while the shales are classified as a poor aquifer with bedrock which is generally unproductive, except for local zones (Pl) (Figure 4-27(a)). Vulnerability in the Nuenna is high due to highly permeable soils and subsoils, with rock being found at shallow depths in many places. Vulnerability classes ranges from Extreme to High, as illustrated in Figure 4-27(b). A cross-section illustrating the geological setting along the transect of the two borehole clusters is shown in Figure 4-28, while a more generic cross-section of the catchment is presented in Figure 4-29. The gravels (coloured green)

underlie the river towards the catchment outlet at Monument. These are fed by water from the karstified limestone (light blue) with moderately permeable tills (blue) present above the limestone away from the sands and gravels. The Pl aquifer lies in the high areas of the catchment with low permeability tills overlying the lower slopes of these hills. There is also a clay layer underlying the gravels beneath the river and clay way-boards present in the karstified limestone that may influence flow. Springs and swallow holes are common (Archbold and Deakin, 2011).

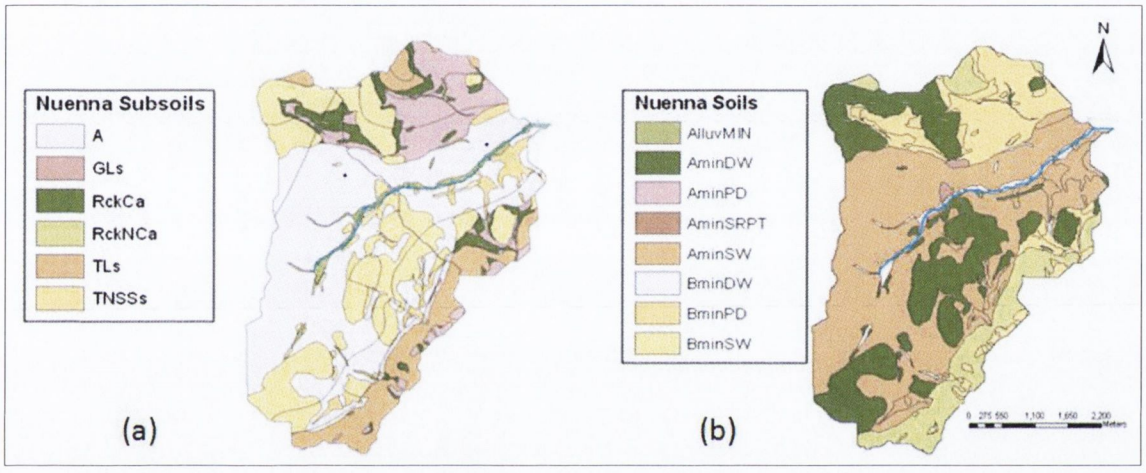

4-25. (a) Subsoils and (b) Soils within the Nuenna catchment.

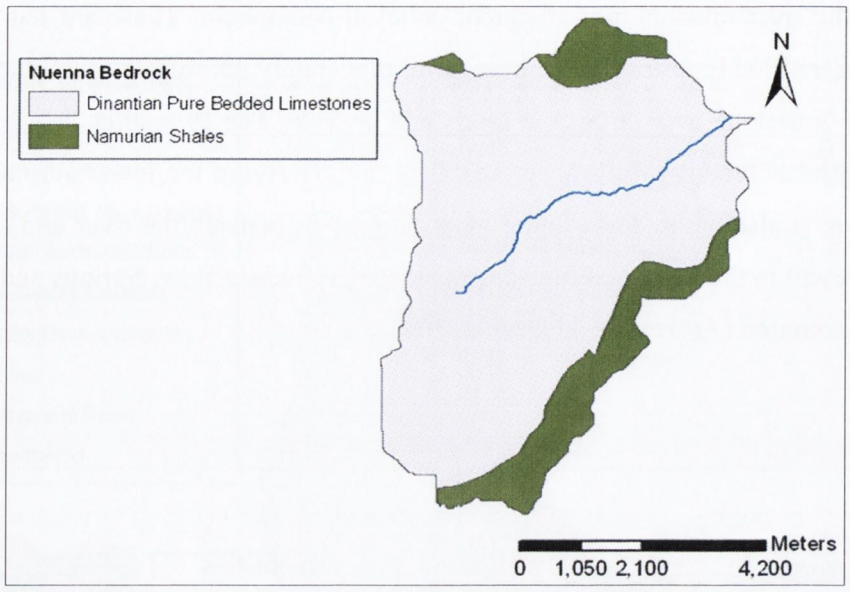

Figure 4-26. Nuenna bedrock.

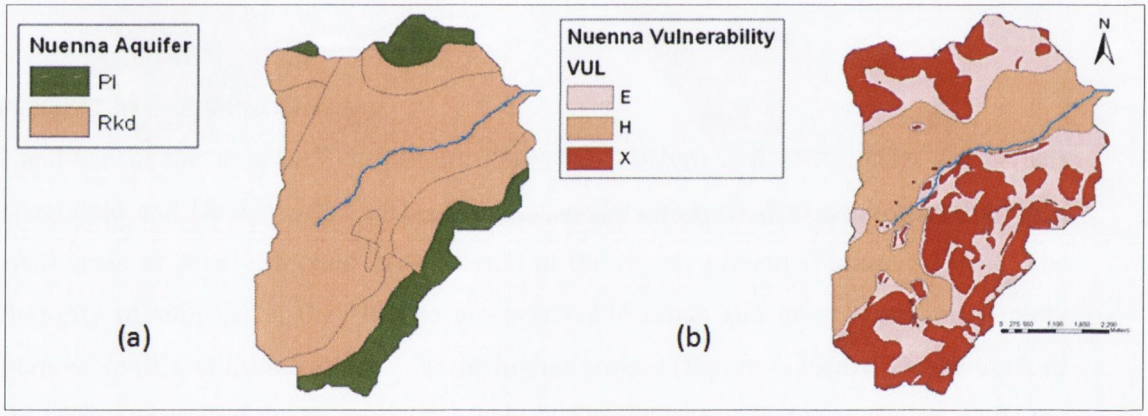

Figure 4-27. (a) Aquifer map and (b) Vulnerability map of the Nuenna catchment.

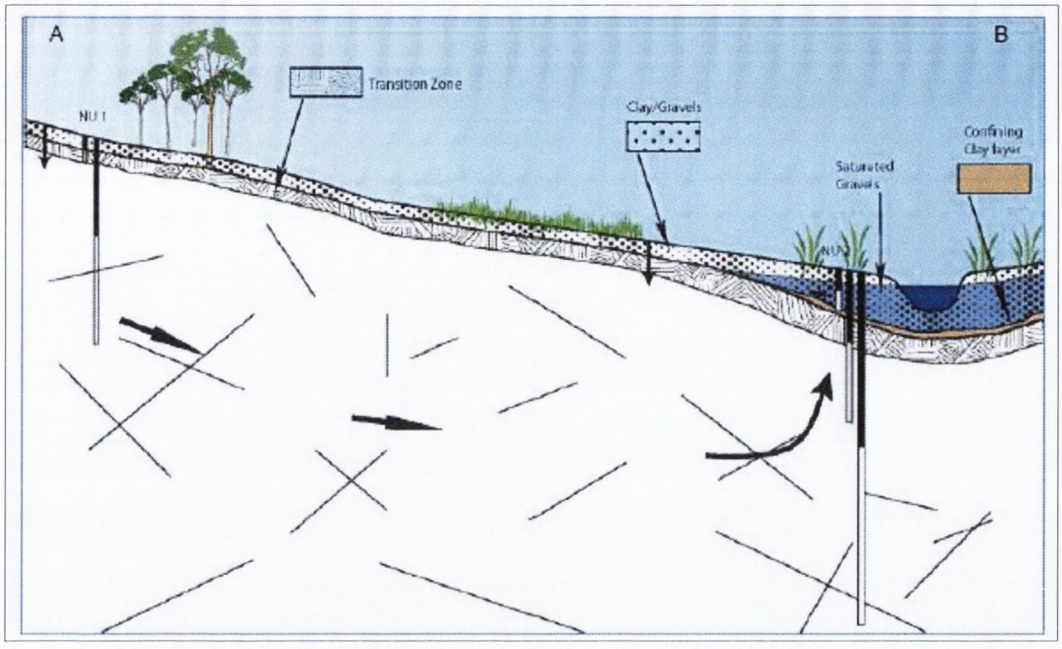

Figure 4-28. Cross-section through the EPA borehole transection from NU1 to NU2 (near the river) (CDM/OCM (2010).

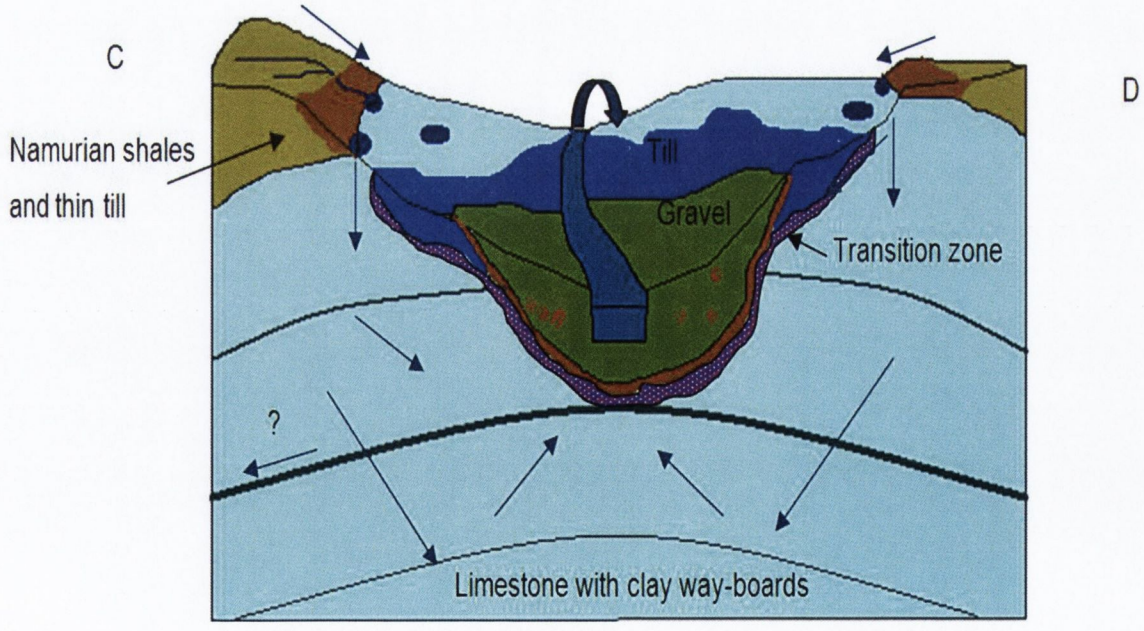

Figure 4-29. Schematic cross-section of the Nuenna, (Archbold and Deakin, 2011).

4.5.3 Hydrology

The average annual rainfall in the catchment (1961–1990) is 967 mm and average annual potential evapotranspiration (PE) is 527 mm. A preliminary soil moisture balance suggests that AE values range from 420 to 492 mm using the FAO Penman Montieth and Met Éireann Hybrid model, with varying assumptions on soil type and rooting depth etc (Kennedy, 2010; also, see Chapter 5).

The Nuenna river, unlike the rivers in the other three study catchments, responds slowly to rainfall in general but during a large rainfall event can respond quickly. During a rainfall event, discharge in the river typically rises gradually before receding very slowly. As a result of this slow recession, high baseflows are maintained throughout the winter months. This can be observed in Figure 4-30. This is the behaviour of a groundwater dominated catchment, characteristic of a catchment underlain by a regionally important aquifer. In the case of the Nuenna most of the water recharges the aquifer either by means of diffuse recharge percolating through the soils and subsoils or by point recharge entering the aquifer by means of swallow holes. Discharge, calculated from river stage recorded at the Monument site from October 2010 to May 2012, ranges from less than 0.08 m^3/s to more than 2.47 m^3/s. The mean recorded discharge was 0.57 m^3/s, while the median discharge was approximately 10% less than this at 0.51 m^3/s. The small variation between median and mean discharge is typical of a groundwater dominated catchment, where discharge rates vary more gradually than in a 'flashy', low permeability catchment.

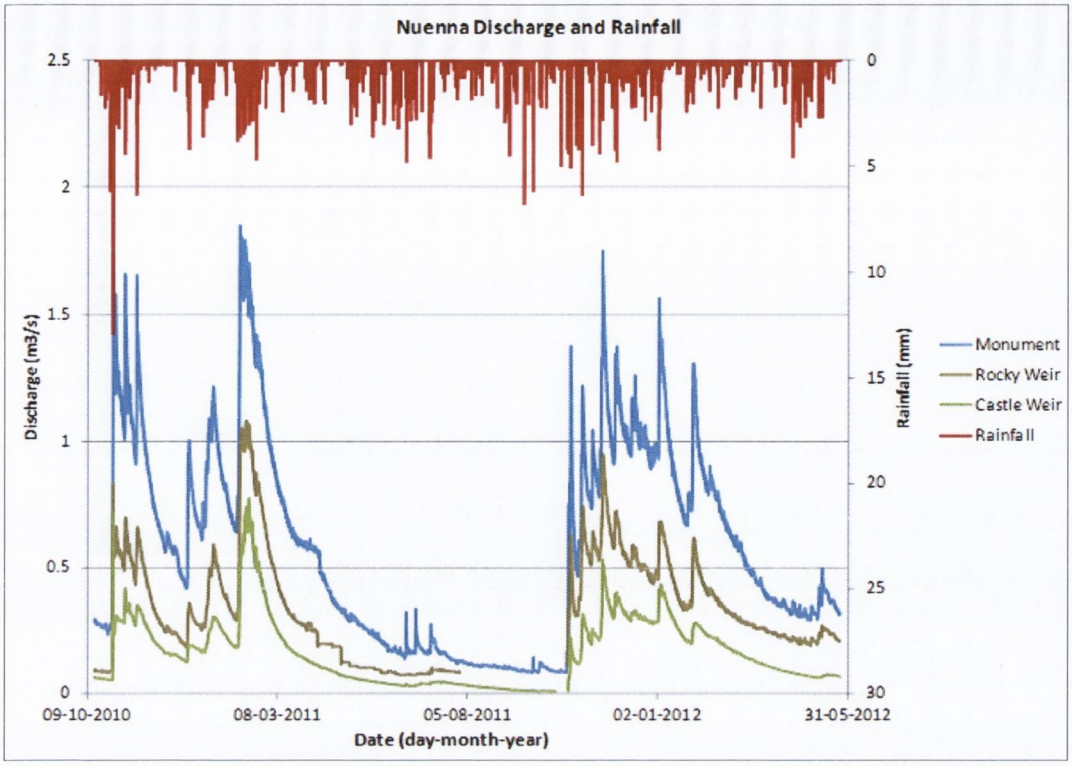

Figure 4-30. Nuenna discharges at the three catchment hydrometric stations with rainfall from Clomantagh Castle (October 2010 to May 2012).

Four large springs (Toberpatrick, Barna Group Water Scheme (GWS), Boiling Spring and Forest Spring, with their locations shown in Figure 4-24) provide a significant proportion of the discharge in the river at Monument, particularly during periods of low flow. During low flows on the 26th July 2011, it was estimated that approximately 92% of discharge was derived from these springs, while during higher 'winter' flows on 8th November 2011, it is estimated that 70% of discharge was derived from these springs.

4.5.4 Hydrogeology

The Nuenna bedrocks, as discussed in Section 4.5.2, are classified as regionally important karstified with aquifer type Rkd underlying approximately 81% of the catchment and poorly productive with aquifer type Pl in the higher areas of the catchment occupying approximately 19%. The gravels infilling the valley floor between Clomantagh and Freshford have been mapped by the GSI as a Locally Important

aquifer (Lg) (Archbold and Deakin, 2011). Transmissivities of the bedrock surrounding the borehole clusters have been calculated as being greater than 2.5 m^2/d, though it is especially difficult to find a representative T is karst due to large fracturing and the presence of conduits. The water levels in these boreholes are shown in Figure 4-31. These levels indicate a downward gradient from NU1 Shallow towards NU1 Deep borehole. At NU2, next to the river, deep groundwater levels are higher than the shallow groundwater levels, which in turn are higher than the subsoil levels This upward gradient from the deep groundwater to the shallow groundwater to the subsoil zone suggests that this river reach is gaining water from the groundwater pathways.

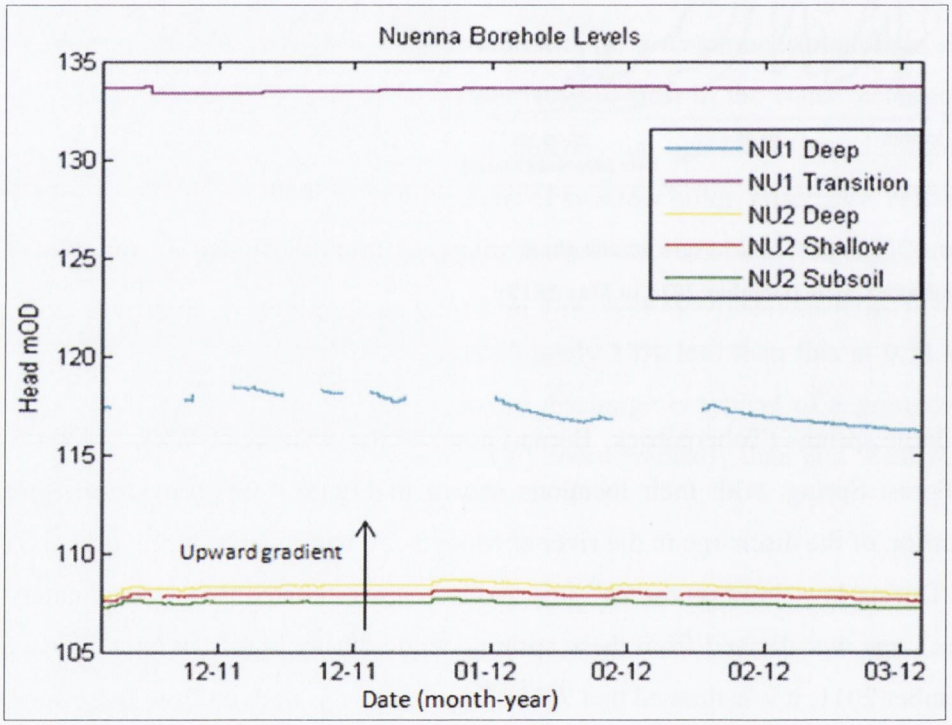

Figure 4-31. Water levels in Nuenna boreholes. NU2 (next to the river), NU1 (up high in the catchment).

There are two major swallow holes located to the south of the river that connect water draining from the Castle Weir subcatchment to the Rocky Weir and Monument subcatchment (Figure 4-24). This has implications on the assigned catchment areas for

both the Caste Weir subcatchment and the Rocky Weir subcatchment, which will be discussed further in Chapter 5.

5 Research Methodology

5.1 Introduction – Research Strategy

In this chapter the methodology employed for the separating of the hydrograph into its constituent pathways, the collection of data from the field and the evaluation of those data will be discussed.

The research strategy of this thesis has been developed following the outcomes of the literature reviews on hydrograph separations methods (Chapter 2) and hydrological models (Chapter 3). In order to simulate the four pathways of the conceptual model it was decided that the lumped, rainfall-runoff NAM model was the most appropriate model to use. NAM has few input requirements, only rainfall and potential evapotranspiration are necessary to run the model, and its lumped structure provides flexibility for adaptation in the variable geological settings encountered in Ireland.

As stated in Chapter 3, 'equifinality' is difficult to avoid when applying a hydrological model to a catchment and only one basis of constraining the model output is available. Typically, observed discharge in the river is used in this manner. In order to limit the potential for 'equifinality', hydrograph separation techniques are applied to provide limits within which the contribution of each pathway to the river is likely to be. These likely contributions, along with the observed discharge in the rivers, provide targets for the optimisation routine within NAM. Following the review of the hydrograph techniques in Chapter 2, Master Recession Curve (MRC) analysis, Irish recharge coefficient approach, digital signal filtering algorithms and temperature applied as a tracer were selected as techniques that could provide the constraints required for the hydrological modelling. While each of these methods has certain strengths and weaknesses, the application of these together provides separations of the pathways based on observed discharge, meteorological inputs (rainfall, potential evapotranspiration and temperature) and catchment geology. The application of these separation techniques, together with NAM, was unique to this research.

Some of these methods required modification (most notably the digital signal filtering algorithm) while others were applied in their current form. The Master Recession Curve analysis had the ability to identify the contribution of the four pathways, as well as the recession constants required to inform the digital signal filtering algorithm, but required the manual fitting of lines to the recessions, introducing subjectivity into the analysis (Section 6.3).

The recharge coefficient approach provided separations based on the geology of a catchment and the effective rainfall (rainfall minus potential evapotranspiration) falling on the catchment. While it was the only hydrograph separation method to directly account for the geology of the catchment, this approach could only distinguish between quick flow (overland flow and interflow) and groundwater flow (shallow and deep groundwater components). This method was modified during this research to account for point recharge occurring in karst catchments (Section 6.2).

The digital signal filtering algorithm applied in this thesis is a new algorithm based on a simple algorithm developed by Lyne and Hollick (Lyne and Hollick, 1979). The published algorithm can only separate the hydrograph into two pathways (quick flow and groundwater) and typically distributes the hydrograph equally between these two pathways. This algorithm was modified to provide separations for the four pathways of the conceptual model and to remove the subjective selection of parameters present in other modifications of the Lyne and Hollick algorithm (Section 6.4).

Finally temperature time series data available from boreholes in the catchment, the river itself and air temperature data from a nearby Met Éireann Synoptic station, were used in a simple mixing model to provide separations based on temperature rather than the response time of the pathways as with the other separation methods. All of these hydrograph separation methods and their application are described in detail in Chapter 6.

The NAM model, its application to the study catchments and the optimisation of its parameter sets taking the hydrograph separation results into account and the application of the model itself as a method of investigation, are described in Chapter 7. It was also decided after the literature review of hydrological models in Chapter 3 that MODFLOW should be implemented to further investigate the groundwater pathways

and the applicability of using a fully distributed modelling to investigate the pathway contributions in Irish catchments with scarce data describing the spatial variation of geological physical properties. In Chapter 8 the methodology of how MODFLOW was applied and the findings of this approach are detailed.

Once the hydrological modelling had been carried out, the process of relating the parameters of the NAM model to catchment characteristics is described in Chapter 9. This is achieved through the use the statistical method multiple linear regression. GIS data were utilised to weight the different catchment characteristics by their distance from the river. The relation of the NAM parameters to catchment characteristics using the regression equations ensures that the proportion of the river hydrograph derived from each of the pathways can be calculated in ungauged catchments. This provides the final approach necessary for the development of an integrated framework for determining the contributions of the pathways to rivers in Ireland. This framework is described in the discussion section at the end of Chapter 9. The regression equations also have error associated with them that is utilised for sensitivity analysis. The approach taken for this analysis is detailed in Chapter 10.

The following sections of this present chapter focus on the methodology of data collection from the study catchments and the assessment of these data. Although this thesis is primarily concerned with the computer simulation of the contributions of the different hydrological pathways to the river hydrograph, hydrological modelling involves more than generating pathway separations based on available datasets alone. Fieldwork was an integral part of this research for appreciation and conceptualisation of the different processes occurring in the study catchments and catchments in general. As such, a variety of different datasets were collected as part of this project. This involved the installation of hydrometric stations and screened boreholes within each of the four study catchments, continuous monitoring of river stage, groundwater and soil water levels, rainfall, electric conductivity in the rivers and springs, temperature in the rivers and springs, and turbidity at a selection of locations. Ambient temperature and potential evapotranspiration data were obtained directly from Met Éireann. River flow measurements were also taken periodically in order to help rate the different hydrometric stations and to provide longitudinal profiles of the rivers and streams within each study catchment. The author was responsible for collecting the rainfall and

river flow data in two of the study catchments (Mattock and Nuenna), as well as for quality assurance of the hydrometric data from the other two study catchments. The author was also responsible for the installation of rain gauges and river stage logging equipment in the Mattock and Nuenna (except for the EPA maintained hydrometric station at Collon Weir as discussed in Chapter 4), as well as staff gauges and controls at some of the flow gauging sites. Discrete sampling was also carried out for a suite of chemical parameters in the rivers, boreholes and where samples could be taken from ditches and overland. These were then analysed back in the college laboratory. This hydrochemical sampling was undertaken as part of the *Pathways Project*, but the collection and interpretation of these hydrochemical data was outside the scope of this thesis.

Once these data had been collected, it was necessary to evaluate the quality and consistency of these datasets, following which the datasets were ready to be utilised for the physical hydrograph separation approaches and the hydrological modelling. The methodology employed for this assessment of the data is outlined in Section 5.11 along with the results of the assessment.

5.2 River stage monitoring

River stage was continuously recorded at four locations in the Mattock (Berril's, Collon Weir, Diversion Weir and the Diversion Outlet), three locations in the Nuenna (Monument, Rocky Weir and Castle Weir), two locations in the Glen Burn (Outlet and Subcatchment) and two locations in Gortinlieve (Outlet and EPA Weir). These hydrometric stations are identified on the study catchment maps in Chapter 4. Three of these locations were managed by the EPA (Berril's, Collon Weir and EPA Weir), with supplementary flow measurements being provided to the EPA for rating purposes by this project.

Sites were selected for river stage monitoring with the assistance of the EPA hydrometric teams in the Mattock and Nuenna catchment. Appropriate site selection is vital to ensure that rating curves developed to convert river stage measurements river discharge remain stable. Over the course of the project measurements taken at similar

stages are be sensitive to any changes that may occur at a hydrometric station. Therefore, to ensure that a rating curve is stable, the hydrometric station should be located where the river banks are unlikely to change over time and a control, whether natural (steepening of gradient of the riverbed) or man-made (v-notch weir Figure 5-1), to ensure that increases in discharge are reflected by regular increases in river stage. Without a stable hydrometric station location, the rating curve will be sensitive to the time when the discharge measurement was taken. This will ultimately affect the discharge time series obtained from these locations and any conclusions drawn from the analysis of this data.

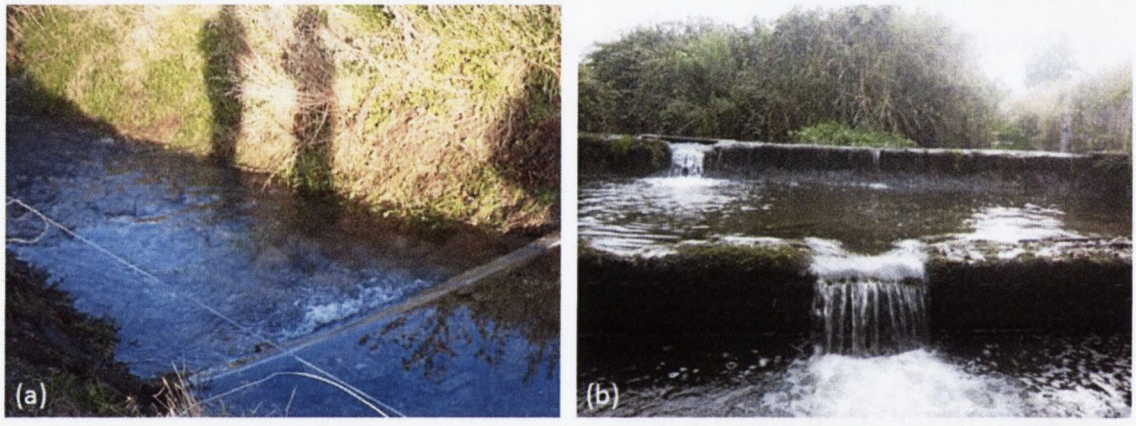

Figure 5-1 (a) V-notch weir in the Nuenna and (b) weir in the Mattock.

The installation of monitoring equipment varied from one gauging site to another gauging site. In general, a vertical 6" pipe was fixed to a wooded post or, if available, directly to a concrete wall (Figure 5-2). Vertical slits were cut on the downstream side of the pipe to create stilling wells. Where no natural control on the river was present, a control was created using a v-notch steel plate or a v-notch concrete slab. The stilling wells were fitted with OTT Thalimedes, float-operated shaft encoders with data loggers, as shown in Figure 5-3(a). As the float rises and falls, a pulley rotates, the change in electrical signal caused by this rotation is converted to a measure value and stored in the logger. According to manufacturer's specifications, the Thalimedes has a river stage range of $\pm$ 19.99 m (though this will be limited by the length of the stilling well, which is generally 2 m in length) with a resolution of 1 mm and accuracy of $\pm$ 2 mm. The

stilling wells at Berril's and Gortinlieve Outlet hydrometric stations were fitted with OTT Orpheus Minis, pressure transducers with data loggers (Figure 5-3(b)). The manufacturer reports that the Orpheus Mini has a river stage range of 0 – 10 m with a resolution of 1 mm and accuracy of ± 5 mm.

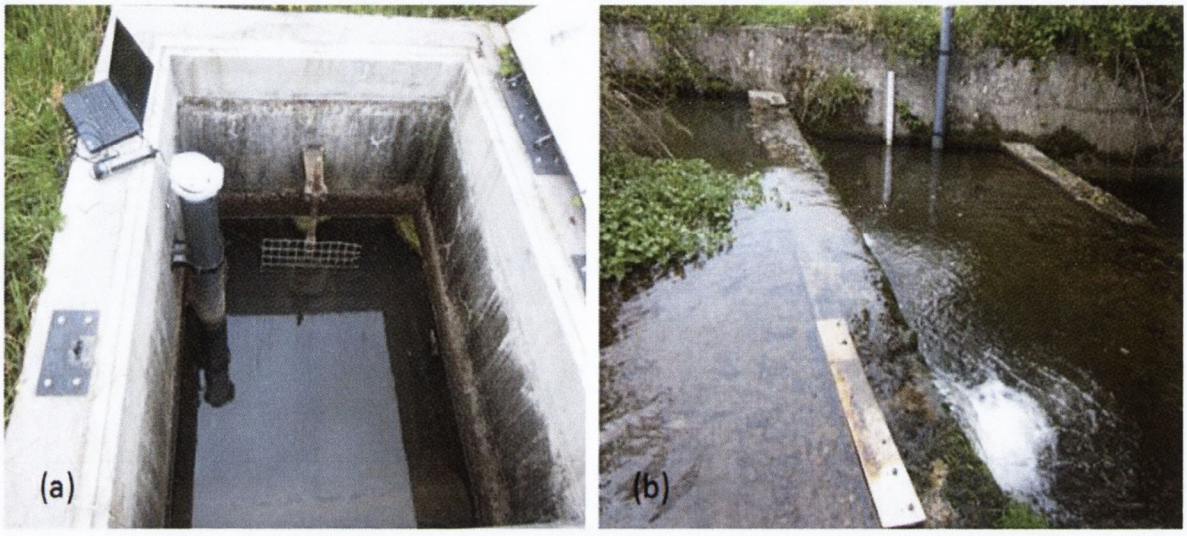

Figure 5-2. (a) Stilling well with top cap at the Diversion in the Mattock and (b) stilling well against far wall of Diversion Weir in the Mattock.

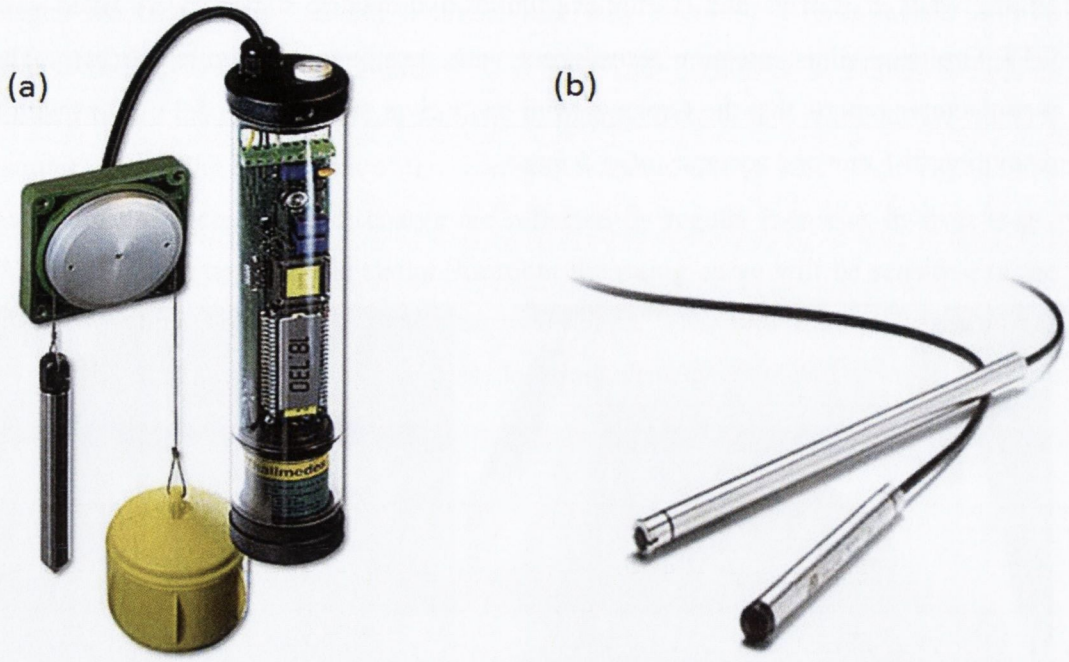

Figure 5-3. (a) Thalimedes float-operated shaft encoder with data logger (OTT, 2012b) and Orpheus Mini pressure transducer with data logger (OTT, 2012a).

Data from loggers were downloaded monthly using an OTT IrDa cable to connect to the infrared port on the data loggers. The floats and pressure transducers did not need to be removed from the water to download, therefore reducing the risk of affecting readings. Data were obtained monthly in order to assess the measurements for any gaps and instrument malfunction, and also to allow frequent inspection of the hydrometric station controls for debris and other obstructions to flow. This data were then imported into an Excel spreadsheet format.

5.3 Borehole level monitoring

As part of the Pathways Project, clusters of screened boreholes were installed in the Mattock, Nuenna and Gortinlieve. These clusters were located along transects from high up in the catchment, covering probable pathway flow directions, to near the river. These boreholes were drilled as part of the EPA's longer term monitoring programme

of groundwater bodies (EPA, 2006). The clusters were designed to provide improved understanding of catchments' hydrogeological characteristics.

In order to achieve this, clusters were developed firstly by carrying out geophysical surveys of the intended area of drilling in order to assess likely pathways present and the depth of drilling required to monitor these. Drilling of the boreholes followed these investigations, with samples of soils, subsoils and bedrock being taken periodically and logged. The construction of these boreholes was then completed with casing and screening being installed. Pumping tests were then carried out in order to estimate the hydrological characteristics of the aquifer at the different sites (CDM/OCM, 2010).

The screening of the wells, at the different depths required to observe the changes in head and chemistry of the particular pathways of interest, was an integral aspect of the clusters as this was required to ensure that there was no hydraulic interaction between the individual boreholes in the clusters. Orpheus Minis were installed to monitor the variations in water level inside each of the boreholes. These data were monitored and reviewed periodically by the EPA before being provided to the Pathways Project.

The clusters are divided into upper and lower clusters, with an intermediate cluster in the Mattock and Gortinlieve catchments. The distribution of monitoring boreholes among the clusters and the geological horizons that they targeted, are listed in Table 5-1, with finished boreholes shown in Figure 5-4.

Table 5-1 Borehole clusters and geological horizon interval distributions.

Gortinlieve	Mattock	Nuenna	Glen Burn
Upper Cluster Deep Shallow Transition	**Upper Cluster** Deep Shallow Subsoil 1 Subsoil 2	**Upper Cluster** Deep Transition	Three clusters with an open, uncased borehole with a depth to the start of the transition zone horizon, the start of the shallow groundwater horizon and one open borehole to the depth of deep groundwater horizon
Intermediate Cluster Deep Shallow Transition	**Intermediate Cluster** Deep Shallow		
Lower Cluster Deep Shallow Transition Subsoil	**Lower Cluster** Deep Shallow Subsoil 1 Subsoil 2	**Lower Cluster** Deep Shallow Subsoil	

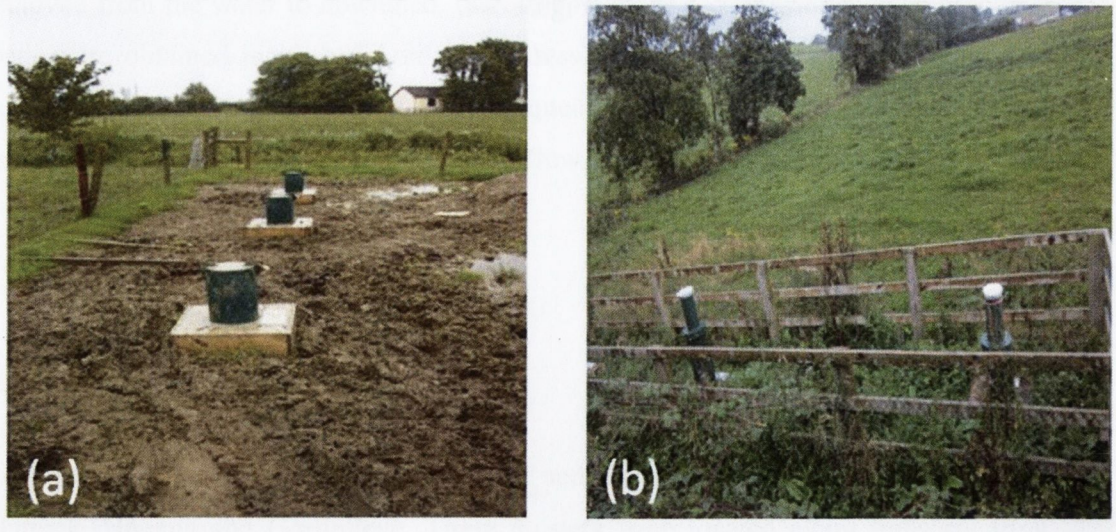

Figure 5-4. Borehole cluster in (a) Mattock at MK3 and (b) Nuenna at NU2.

5.4 Rainfall

Rainfall was measured in the four study catchments using ARG100 (Environmental Measurement Ltd.) tipping bucket rain gauges (Figure 5-5(a)) equipped with AR-DT2 data loggers (Figure 5-5(b)). The gauges were positioned level with the ground, ensuring they were a sufficient distance from any obstruction that would interfere with measurements (a maximum of 15° sight line to any trees or walls and equally not too over-exposed (Shaw, 1994).

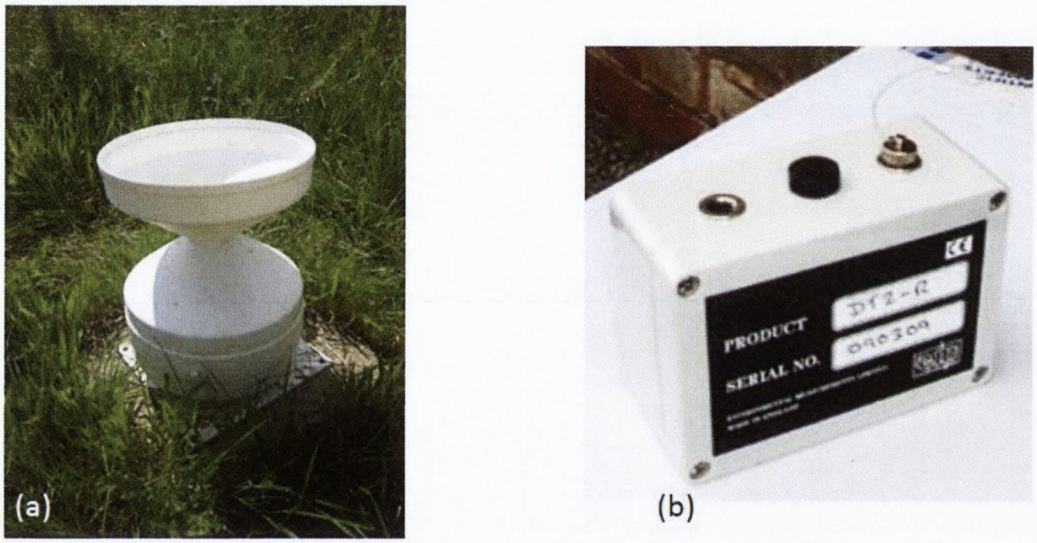

Figure 5-5. (a) ARG100 tipping bucket rain gauge and (b) AR-DT2 data logger.

Each gauge was sited and if necessary enclosed with a fence to protect it from livestock, surrounded by wooden posts in the case of horses (Figure 5-6(a)) and wire-fencing in the case of small animals, as seen in Figure 5-6(b).

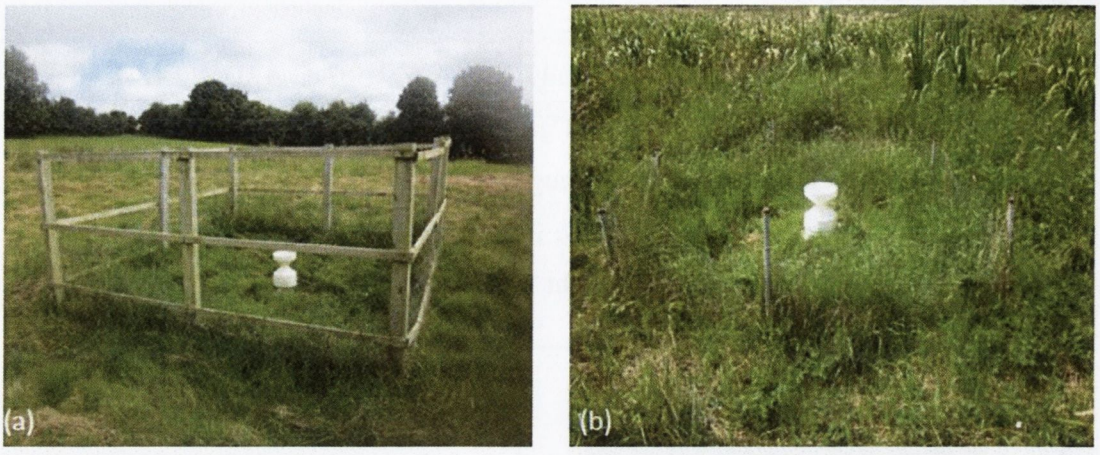

Figure 5-6. (a) Wooden fencing to protect from horses (Nuenna catchment) and (b) wire-fencing to protect rain gauge from small animals (Nuenna catchment).

The rain gauge loggers were downloaded once a month in order to check the working order of the rain gauge, clean the gauge, assess data regularly and clip back any grass and weeds that were growing next to the gauge.

5.5 River gauging

In addition to the continuous monitoring of stream stage at the 11 hydrometric stations in the study catchments, longitudinal profiles of the flows in the streams and rivers of the catchment were carried out. Staff gauges were installed at different locations to assist in measurements at these sites. These locations were selected based on natural local controls on flows (Figure 5-7(a)) or where simple control structures could be installed, as shown in Figure 5-7(b).These profiles informed the conceptual model as to how the rivers typically increased in discharge as measurements progressed from the headwaters to the catchment outlet. A gaining river generally increases in discharge regularly along its course, with steps in discharge typically occurring where tributaries join the main river. In a catchment such as the Nuenna, dominated by spring flow, flows increase in a step-like manner along the river corresponding to inputs from major springs. This is particularly noticeable at low flows. These longitudinal flow profiles

help identify these characteristics and also help with the rating curves for the continuous monitoring locations and staff gauges. In order to develop the rating curves (a discharge versus stage relationship) for each of the staff gauges and continuous monitoring stations, measurements of discharge were required at different stage levels. These relationships, outlined in Section 5.11.3, were then applied to convert observed stages on staff gauges and recorded stages at the hydrometric stations to discharge values.

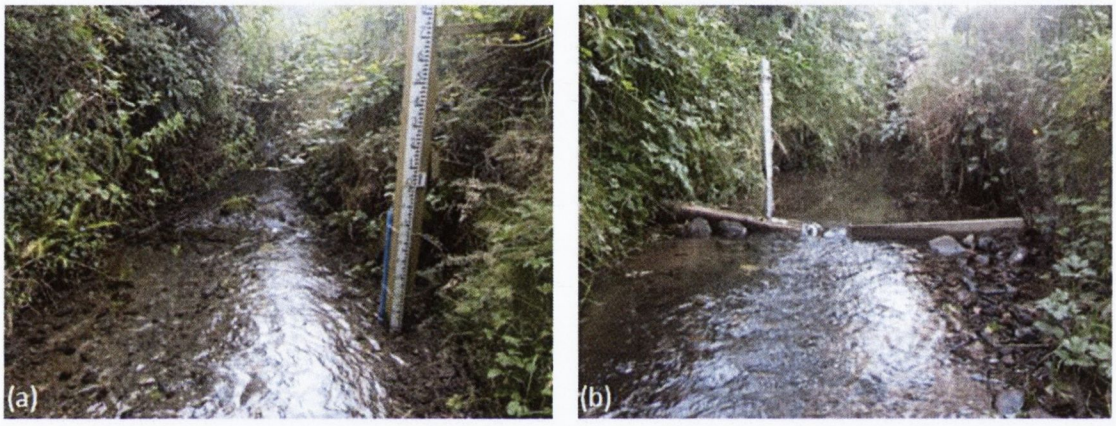

Figure 5-7. (a) Staff gauge with natural control on river and (b) where a simple control was erected.

5.5.1 Measurement of discharge

In order to develop a good rating curve, a wide distribution of discharges is required. A difficulty with this requirement is that different weather conditions are required to create the necessary flow regimes in the river. For this reason delays are inevitable when developing rating curves, but another problem is that the upper section of the curve may need to be based on extrapolation rather than direct measurement, since it may not be safe to enter a river and measure flows during flood events.

A site for discharge measurement is normally selected where the river channel is straight and of uniform cross-section and slope in order to minimise abnormal velocity distributions (EN ISO 748, 2007). Sections with stagnant water and eddy currents

should be avoided. In this research, once a site had been selected, the measurements were carried out in accordance with the ISO (the International Organization for Standardization) standards – measurement of liquid flow in open channels, Velocity-area methods (EN ISO 748, 2007). The method used from this standard is the mid-section method. This involves measuring the river velocity and depth at intervals along the cross-section of the river (Figure 5-8). Discharge was calculated as follows:

$$Q = \sum \bar{v}_i \, d_i \frac{b_i + b_{i+1}}{2} \qquad \text{5-1}$$

where $\bar{v}_i$ is the mean velocity [m/s], d_i is the depth [m/s] and b_i is the width [m], all for interval i. The mean velocity is calculated.

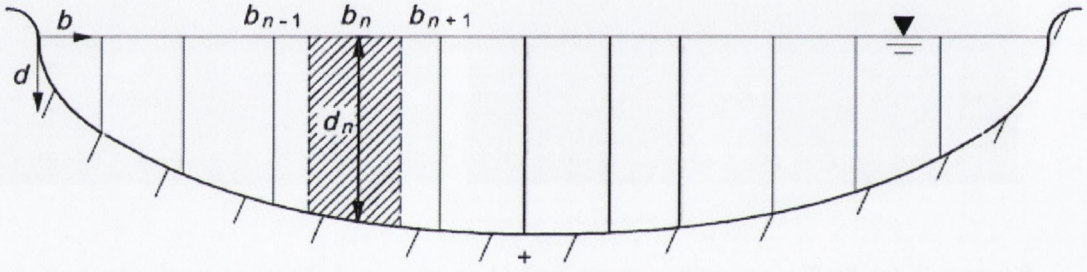

Figure 5-8 Mid-section method (EN ISO 748, 2007)

Two velocity meters were used to measure the mean velocity for each interval. An acoustic doppler current meter (OTT ADC) measured point velocities where these were less than 0.1 m/s, Figure 5-9(a), while an OTT Kemptem C2 current meter was used to measure flow velocities above this threshold, Figure 5-9(b). The manufacturer specifies that the velocity measuring range of the ADC was –0.2 to 2.5 m/s with a resolution of 0.001 m/s and accuracy of ±1%, while the velocity range of the C2 was 0.025 to 5m/s with a resolution of 0.001 m/s and accuracy of ±1%.

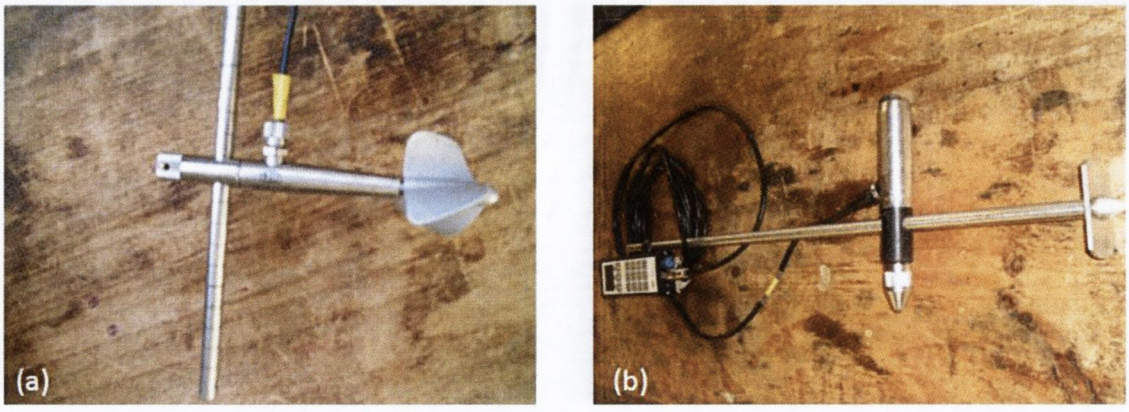

Figure 5-9. (a) OTT Kemptem C2 current meter and (b) OTT ADC current meter.

5.6 Electric conductivity

Electric conductivity was measured in the four study catchments using HOBO U24 Conductivity Loggers (Figure 5-10). The conductivity loggers were positioned in the river, ensuring they were always submerged in the flow to obtain representative values of the electric conductivity. The manufacturer reports that the measuring range was 0 to 10,000 µS/cm with a resolution of 1 µS/cm and an accuracy of ±1%. The electric conductivity data loggers were downloaded once a month in order to check the working order of the loggers, to assess data regularly and clear any debris that may have become entangled around the loggers and remove biological fouling.



Figure 5-10. HOBO U24 Conductivity Logger, (HOBO, 2012).

5.7 Temperature

Temperature was measured in boreholes and rivers in all four study catchments. The HOBO U24 Conductivity Loggers was utilised to measure river temperature, while the OTT Orpheus Mini® pressure transducers were used to measure temperature in the river in the Mattock and Gortinlieve, and in the boreholes. According to the manufacturer, the measuring range of the HOBO U24 Conductivity Loggers was – 2 to 35°C with a resolution of 0.01°C and an accuracy of ±0.01°C. The manufacturer reports that the measuring range of the OTT Orpheus Mini pressure transducers was – 25 to 70°C with a resolution of 0.1°C and an accuracy of ±0.5°C. The same approach to downloading and cleaning of the loggers applied as in the case of the electric conductivity loggers. Met Éireann data were also acquired to estimate the effect that ambient temperature has on the rivers during the year. Hourly air temperatures were obtained from the Dunsany Synoptic station, located approximately 25 km from the Mattock catchment.

5.8 Evapotranspiration

Evapotranspiration is the loss of water to the atmosphere by means of evaporation from water surfaces and transpiration from vegetation within the catchment. Potential evapotranspiration (PE) was computed from the relevant weather data: wind speed, relative humidity, net radiation and air (see Section 5.11.2). Once the PE had been calculated, the spatial distribution of soil, land-use and rainfall data within the study catchments was examined to calculate the actual evapotranspiration (AE). PE data were obtained from Met Éireann for the catchments in the Republic of Ireland and a weather station located in the Glen Burn catchment was used to calculate the PE data for this catchment. The weather station recorded air temperature, solar radiation, relative humidity and wind speed. Malin Head Synoptic station (approximately 40 km from Gortinlieve), Dunsany Synoptic station (approximately 25 km from the Mattock) and Oak Park Synoptic station (approximately 35 km from the Nuenna) provided the PE datasets for the study catchments.

5.9 Riverbed Surveying

The riverbed of the Mattock was surveyed during the summer of 2012. The survey was carried out using a Trimble 4700 GPS system with R6 Rover and Base Station and TSC2 Survey controllers, as shown in Figure 5-11. The base station was located in the middle of the area to be surveyed. This required four different base stations within the Mattock. The base station was levelled and the topographic location was obtained with a mobile phone connection with the Ordnance Survey Ireland's headquarters in Dublin. This established the base station's Eastings, Northings and elevation relative to Malin Ordnance Datum. The survey was then carried out using the rover to acquire the topographic points along the riverbed. The rover was connected to the base station by means of satellite communication. At each topographic point along the riverbed the data were stored by the controller and downloaded once the survey had been completed. This dataset helped constrain MODFLOW simulations in the Mattock (see Chapter 8 later) by providing a known head boundary for static simulations.



Figure 5-11. Trimble GPS equipment, (a) controller, (b) rover, (c) base station.

5.10 Visual Surveying

As discussed at the start of this chapter, fieldwork was an important part of this research for the observation and recognition of the different processes involved in generation river discharge in a catchment. This fieldwork provided the opportunity to visually survey the different aspects of a river throughout the year, such as the power of a river in flood. The variation of spring discharge in the Nuenna catchment throughout the year, and how certain drainage ditches only flowed during the winter, particularly in the Mattock, could also be witnessed in the field. During the summer the far bank is dry in Figure 5-12(a), but during winter time when the level of the water table is higher a close up of this bank shows an extra discharge pathway releasing the spring water, as seen in

Figure 5-12(b). These types of observations can help identify important pathways that are active in a catchment.



Figure 5-12. Spring discharge variation in the Nuenna catchment (a) during summer time, bank covered in green vegetation, (b) extra discharge visible during the winter.

Observing active pathways first hand is important for identifying if the contributions of pathways being simulated are feasible during the period for which they are being modelled (Figure 5-13).

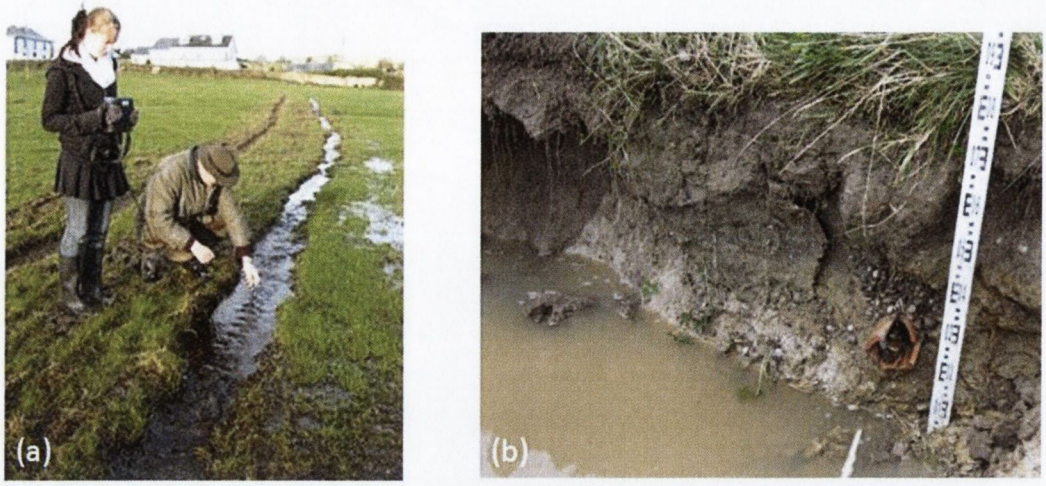

Figure 5-13. (a) Overland flow and (b) a land drain, a potential source of interflow (photos Jenny Deakin).

The temperature of the water when river gauging is taking place can help identify which pathways are dominating. The water in the Nuenna river is very cold all year round regardless of the weather. This assists in confirming that the groundwater spring discharges are dominating the flow regime as these cold temperatures are being maintained, even during rainfall events in warm periods of the summer when warmer quicker responding flows may be expected.

5.11 Raw data Analysis

Once data had been collected from each of the study catchments, they must be assessed for accuracy and periods of instrument malfunction, in order to utilise the data in hydrograph separation techniques and hydrological modelling with a higher degree of confidence. The datasets that are assessed in this section are rainfall, evapotranspiration and river discharge, as these allow a water balance approach to be applied to each study catchment to ascertain the overall confidence in the data collected. A water balance was calculated for each study catchment, as described in Section 5.11.4.

5.11.1 Rainfall

All rainfall is measured as the vertical depth of water that directly falls on a particular area of a catchment in an interval of time. The depth of water is calculated by dividing the volume of water measured by the aperture of the rain gauge used to collect the rainfall. As choosing an appropriate site is a key aspect of setting up a rain gauge, checks must be carried out to ensure that the values being recorded are indicative of the local rainfall and are not being affected by any local structures or vegetation. In order to assess this, a double mass curve approach was employed to compare the rain gauges within the study catchments and also to compare these rain gauges to nearby Met Éireann rainfall recording stations.

A rain gauge was compared to another by calculating the cumulative rainfall for selected intervals. These cumulative rainfall data points were then plotted against one another. Deviation from a straight line relationship indicates that error was present in the data. Data can be corrected by multiplying erroneous data by a correction factor. This method was applied to each of the catchments with the following results.

5.11.1.1 Gortinlieve

Gortinlieve exhibited a relatively linear relationship between the Upper and Lower rain gauges. Figure 5-14 illustrates this near linear relationship, particularly for the start of the curve until 1300 mm; after this, there is a slight dip in the curve that will require further monitoring to ensure that this was not just natural variation that can occur between rain gauges. For the data recorded, this was not a significant deviation.

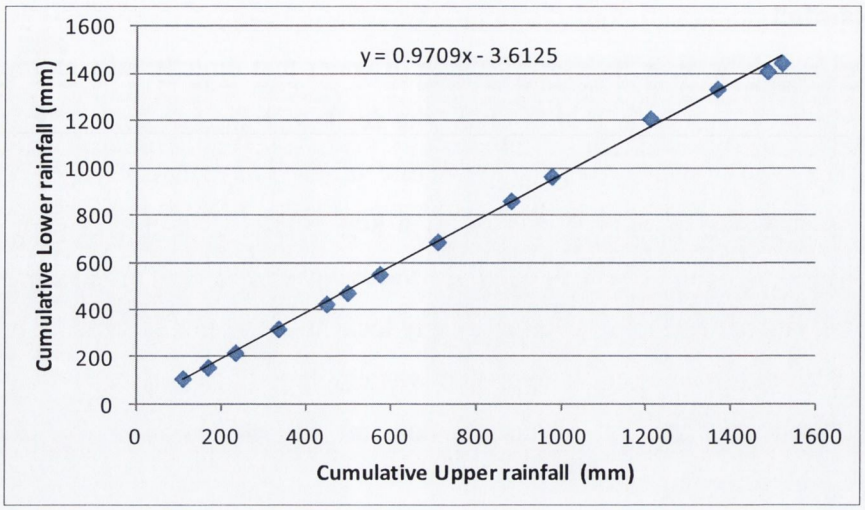

Figure 5-14. Gortinlieve double-mass curve for Upper and Lower rain gauges (for data collected from February 2011 to February 2012).

Figure 5-15 shows the near linear relationship between the Upper rain gauge in Gortinlieve and the nearby Met Éireann rain gauge at Carrigans.

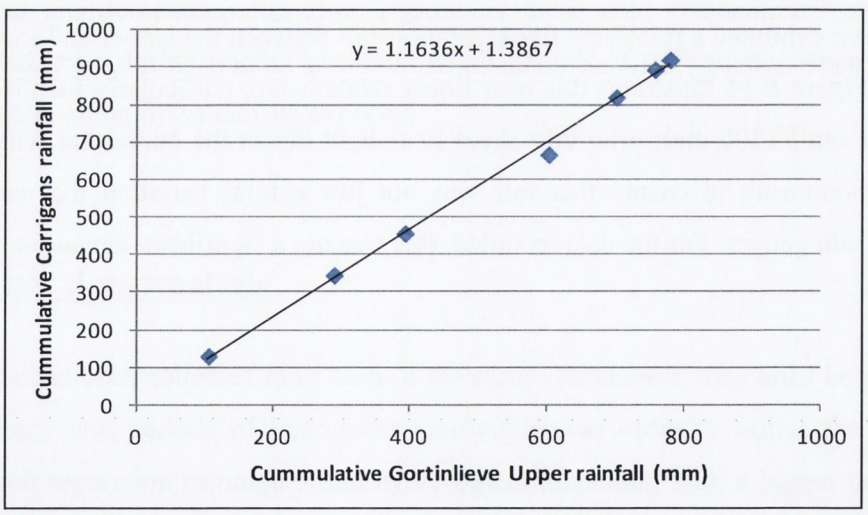

Figure 5-15 Gortinlieve double-mass curve for Upper and Carrigans rain gauges (Sept 2011 – Mar 2012).

5.11.1.2 Glen Burn

The Glen Burn only has one rain gauge located within the catchment as part of the weather station installation. No data could be obtained from a nearby rain gauge with which to develop a double-mass curve.

5.11.1.3 Mattock

The Mattock exhibits a good relationship between the Wastewater Treatment Plant and Headwaters rain gauges. Figure 5-16 illustrates this relationship as being linear without any significant deviations from the general trend. The Headwaters rain gauge was out of operation after May 2012 due to a malfunction in the equipment. These data were excluded from this comparison. The comparison of Mattock rainfall and a nearby Met Éireann rain gauge in Mellifont also displays a linear relationship in Figure 5-17.

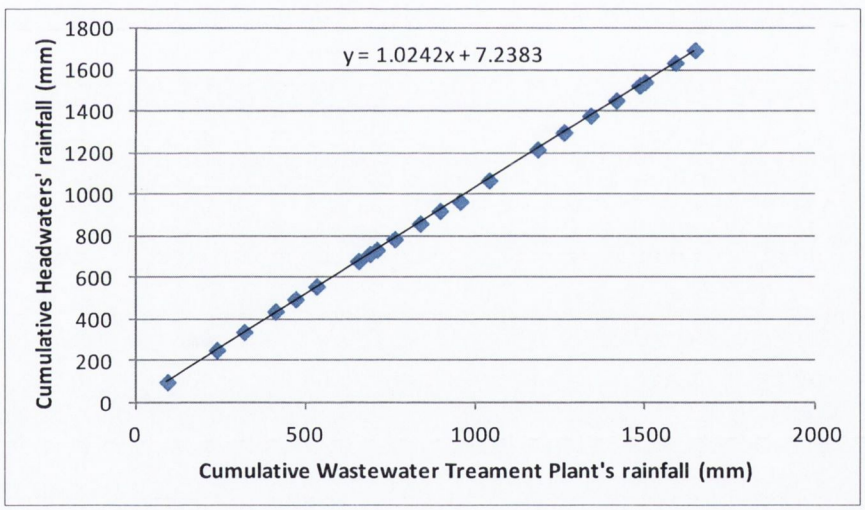

Figure 5-16. Mattock double-mass curve for Headwaters and Wastewater Treatment Plant rain gauges (Sept 2010 – Mar 2012).

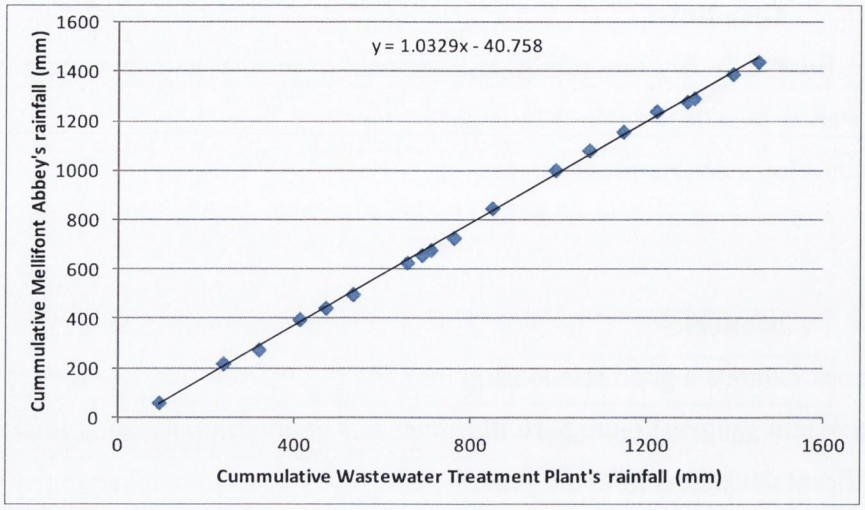

Figure 5-17. Mattock double-mass curve for Wastewater Treatment Plant and Mellifont Abbey rain gauges (Sept 2010 – May 2011, Sept 2011 – May 2012).

5.11.1.4 Nuenna

The Nuenna catchment's two rain gauges performed well throughout the duration of this research. The Kilrush and Clomantagh Castle rain gauges show a linear relationship without any departures from the linear trend, as illustrated in Figure 5-18, as does the Clomantagh Castle and nearby Met Éireann Lavistown rain gauge in Figure 5-19.

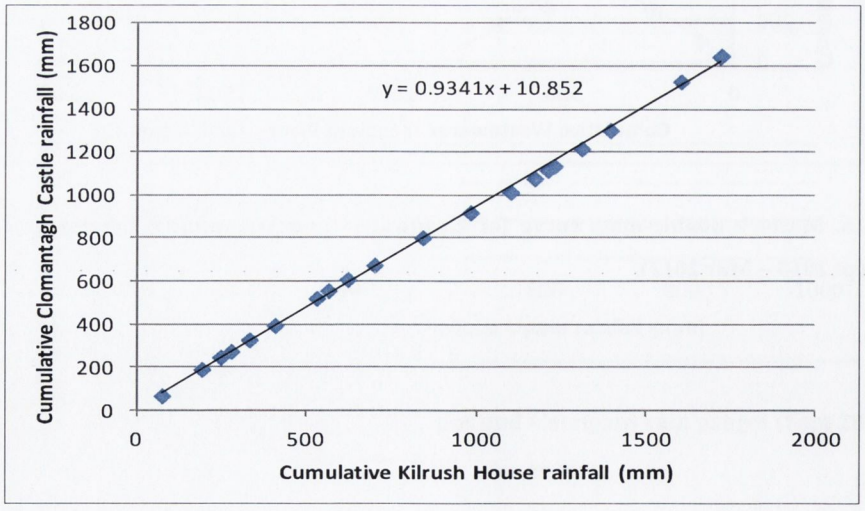

Figure 5-18. Nuenna double-mass curve for Kilrush House and Clomantagh Castle rain gauges (Nov 2010 – May 2012.

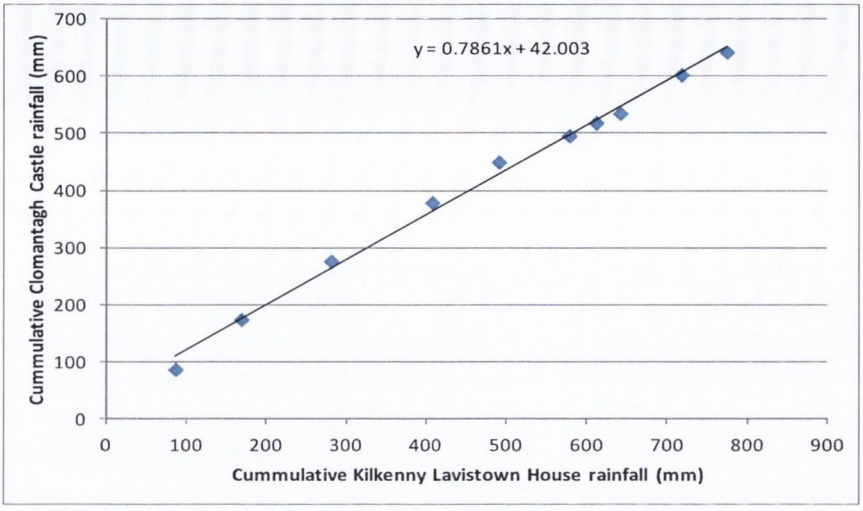

Figure 5-19. Nuenna double-mass curve for Clomantagh Castle and Kilkenny Lavistown House rain gauges (Aug 2011 – May 2012).

5.11.2 Evapotranspiration

Evapotranspiration, as referred to in Section 5.8, is the water that is lost from the catchment to the atmosphere by means of evaporation and transpiration. The potential evapotranspiration (PE) data were obtained from Met Éireann for Gortinlieve, Mattock and Nuenna, while data from a weather station in the Glen Burn catchment were used to calculate PE.

The Penman-Monteith equation is considered the most accurate method for calculating the potential evapotranspiration under most climatic conditions (Allen et al., 1994). PE is calculated using Equation 5-II:

$$PE = \frac{0.408\Delta(R_n - G) + \gamma \frac{900}{T + 273} U_2(e_s - e_a)}{\Delta + \gamma(1 + 0.34u_2)} \qquad \text{5-II}$$

where PE is the reference evapotranspiration [mm/day], R_n is net radiation at the crop surface [MJ/m^{2}day], G is soil heat flux density [MJ/m^{2}day], T is mean daily air temperature at 2 m height [°C], U_2 is wind speed at 2 m height [m/s], e_s is saturation vapour pressure [kPa], e_a is actual vapour pressure [kPa], $e_s - e_a$ is the saturation vapour pressure deficit [kPa], Δ is the slope of the vapour pressure curve [kPa/°C], and γ is the psychrometric constant [kPa/°C].

Once the PE value had been obtained, the actual evapotranspiration value was calculated using the FAO Penman-Monteith soil water budgeting approach (Allen et al., 1998). When there was no soil water deficit in the soil, actual evapotranspiration was assumed equal to potential evapotranspiration. This is taken as the starting point of the soil water budgeting carried out in this chapter. Calculations begin in the middle of winter for the first year when this assumption is reasonable. As the soil water deficit increases in the soil beyond a threshold known as the readily available water (RAW), actual evapotranspiration drops below the potential evapotranspiration linearly until no actual evapotranspiration occurs. The rate at which the actual evapotranspiration decreases is defined by the water stress coefficient K_s:

$$K_s = \frac{TAW - D_r}{TAW - RAW} \qquad \textbf{5-III}$$

where TAW is the amount of soil water that a crop can extract from its root zone before permanent wilting occurs [mm]. Dr is the soil water deficit calculated and RAW is the point at which if the soil water deficit is increased any further, actual evapotranspiration is no longer equal to potential evapotranspiration. Figure 5-20 describes these different points, where θ_{FC} is the water content at field capacity [m^3/m^3] and θ_{WP} is the water content at the wilting point [m^3/m^3].

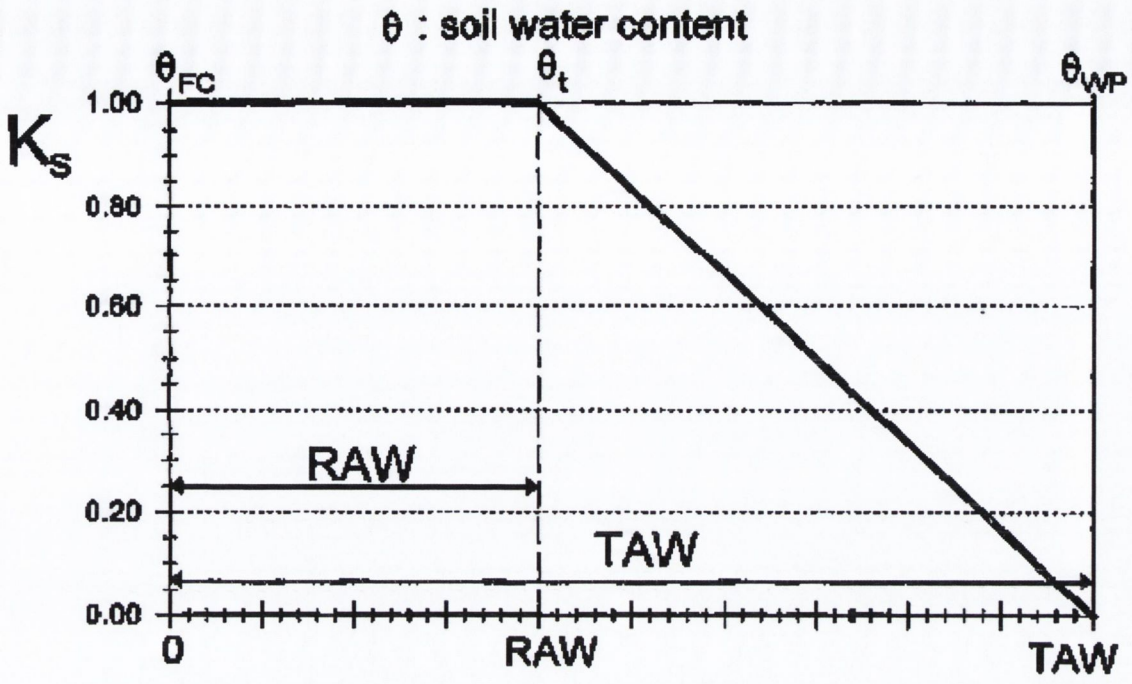

Figure 5-20. Dependency of K_s on soil water content (Allen et al., 1998).

Therefore once K_s is calculated, then

$$AE = PE \times K_s \qquad \text{5-IV}$$

Where possible, historical rainfall and PE data obtained from Met Éireann, were used to calculate an average AE value for the catchments with which data collected during the research project could be compared. This data was available for the Mattock and Nuenna catchments as there was a nearby rain gauge with a relatively uninterrupted historical rainfall time series. Ranges of AE were calculated using high, low and average *TAW* values based on the catchment characteristics. Average historical rainfall was also calculated while implementing this approach.

5.11.2.1 Mattock

In the Mattock catchment, average rainfall obtained from the nearby Met Éireann rainfall station at Mellifont was utilised. 40 years of rainfall data were available along with PE data from the Met Éireann Dublin Airport synoptic station. The soil type and land-use of the catchment were assessed and from this low, average and high values of

TAW were applied to the FAO method of calculating AE. The results of this approach are summarised in Table 5-2. This table displays minimal variation in the average AE/PE ratio over the 40 years. As such, a simple estimate of AE in this catchment can be obtained by taking the AE/PE ratio as being 0.90 – 0.91 on an annual basis, applying summation of the daily calculations of AE from each year as guidance.

Table 5-2. Calculated AE for Mattock using low, medium and high *TAW* values (mm).

TAW	60			
	Rainfall (mm)	PE (mm)	AE (mm)	AE/PE
Average	967.93	546.39	488.52	0.90
70s	938.90	544.35	466.28	0.86
80s	969.09	556.57	499.91	0.90
90s	979.70	537.63	475.99	0.89
00s	966.75	545.84	497.64	0.91
TAW	75			
	Rainfall (mm)	PE (mm)	AE (mm)	AE/PE
Average	967.93	546.39	494.51	0.91
70s	938.90	544.35	471.69	0.87
80s	969.09	556.57	505.93	0.91
90s	979.70	537.63	481.62	0.90
00s	966.75	545.84	504.14	0.92
TAW	85			
	Rainfall (mm)	PE (mm)	AE (mm)	AE/PE
Average	967.93	546.39	497.72	0.91
70s	938.90	544.35	474.97	0.87
80s	969.09	556.57	509.25	0.91
90s	970.95	542.95	496.70	0.91
00s	966.75	545.84	507.64	0.93

5.11.2.2 Nuenna

In the Nuenna catchment average rainfall data was used from the nearby Met Éireann rainfall station at Tullaroan. 30 years of rainfall data were available along with recorded PE data taken from the Met Éireann Kilkenny synoptic station that was closed in 2009. Oak Park synoptic station was used for obtaining PE values during this research. Once more, soil type and land-use were assessed. Low, average and high values of *TAW* were assigned to the FAO method of calculating AE. Table 5-3 outlines the results of this method with the table displaying relatively little variation in the average AE/PE ratio

over the 30 years. A simple approximation of AE from PE in this catchment would be to take the ratio as being 0.89 – 0.93 of PE on an annual basis, again applying the daily calculations of AE as guidance.

Table 5-3. Calculated AE for Nuenna using low, medium and high *TAW* values (mm).

TAW	52.50			
	Rainfall (mm)	PE (mm)	AE (mm)	AE/PE
Average	1079.37	533.32	472.21	0.89
80s	1020.16	529.81	478.34	0.91
90s	1100.88	535.80	467.26	0.88
00s	1086.72	532.65	473.94	0.89
TAW	67.50			
	Rainfall (mm)	PE (mm)	AE (mm)	AE/PE
Average	1079.37	533.32	486.22	0.91
80s	1020.16	529.81	489.64	0.93
90s	1100.88	535.80	482.24	0.90
00s	1086.72	532.65	488.30	0.92
TAW	82.50			
	Rainfall (mm)	PE (mm)	AE (mm)	AE/PE
Average	1079.37	533.32	496.26	0.93
80s	1020.16	529.81	496.50	0.94
90s	1100.88	535.80	492.69	0.92
00s	1086.72	532.65	499.40	0.94

5.11.3 River Discharge Rating Curves

As indicated in Section 5.5, rating curves were developed for the individual hydrometric stations within each of the study catchments. The EPA operates three of the stations: one in Gortinlieve, and two in the Mattock. Of the two stations in the Mattock the EPA solely managed the Collon Weir logging equipment while the EPA and this researcher developed a rating curve at Berril's in order to pool data to improve the rating. The rating curves and their ability to relate river stage to discharge are discussed in this section.

5.11.3.1 Gortinlieve

The EPA weir in Gortinlieve is operated by the EPA and as such, discharge data from this hydrometric station were provided to this project. The Outlet rating curve, however, was developed from data collected by Queens University Belfast as part of the *Pathways Project*. These data were used to develop the rating curve outlined in Figure 5-21. The fitted line presented here omits the highest discharge data point (marked by a red square). This data point is not a true measured point as it was estimated during a rainfall event standing out of the river due to difficulties in accessing the river. The rating curve is well developed at the lower discharges as can be observed in the figure but due to the uncertainty at the higher discharges, there is only limited confidence in the accuracy of this curve above discharge values of 0.165 m^3/s. The statistics to the right of the rating curve in Figure 5-21 show a good fit for the lower discharges with an R^2 value of 0.983 and a high significance for both coefficients *a* and *b*, higher than the *tcrit* value of 2.145 using the student t test.

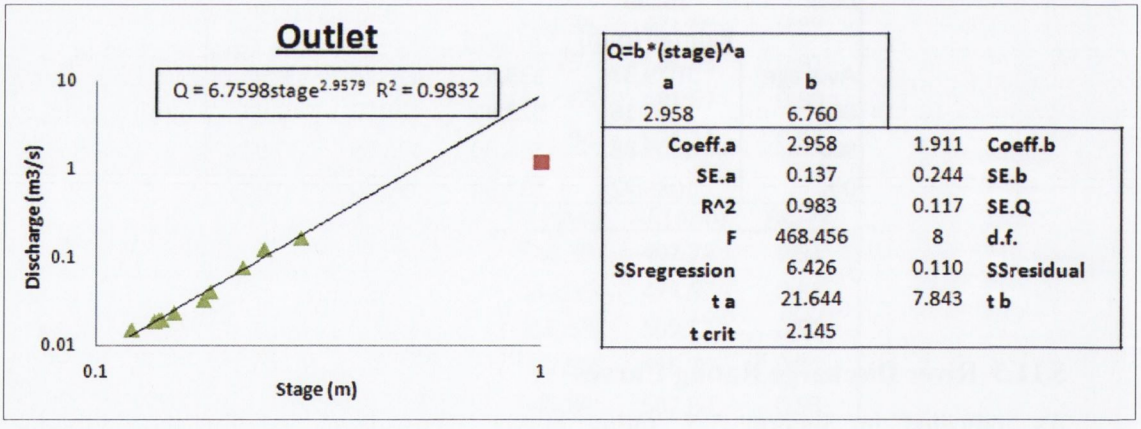

Q=b*(stage)^a			
a	b		
2.958	6.760		
Coeff.a	2.958	1.911	Coeff.b
SE.a	0.137	0.244	SE.b
R^2	0.983	0.117	SE.Q
F	468.456	8	d.f.
SSregression	6.426	0.110	SSresidual
t a	21.644	7.843	t b
t crit	2.145		

Figure 5-21. Outlet rating curve with associated power series fitting statistics.

5.11.3.2 Glen Burn

In the Glen Burn catchment rating curves were developed from river gauging data collected by Queens University as part of the *Pathways Project*. These datasets were applied to construct the rating curves shown in Figure 5-22 and Figure 5-23. The rating curves are well developed at the lower and higher discharges. In the case of the Outlet rating curve in Figure 5-23, two power series were required to fit the data at high and

low flows due to a break in the slope of the data as a result of the broad crested weir becoming drowned out at higher flows. The statistics to the right of the rating curve in Figure 5-22 and Figure 5-23 display a good fit for the discharges with an R^2 value of 0.982 for the Subcatchment station and R^2 values for the Outlet catchment of 0.983 and 0.967 for the higher and lower fits, respectively. There is high significance for all the *a* and *b* coefficients, all significantly higher than their associated *tcrit* values using the student t test.

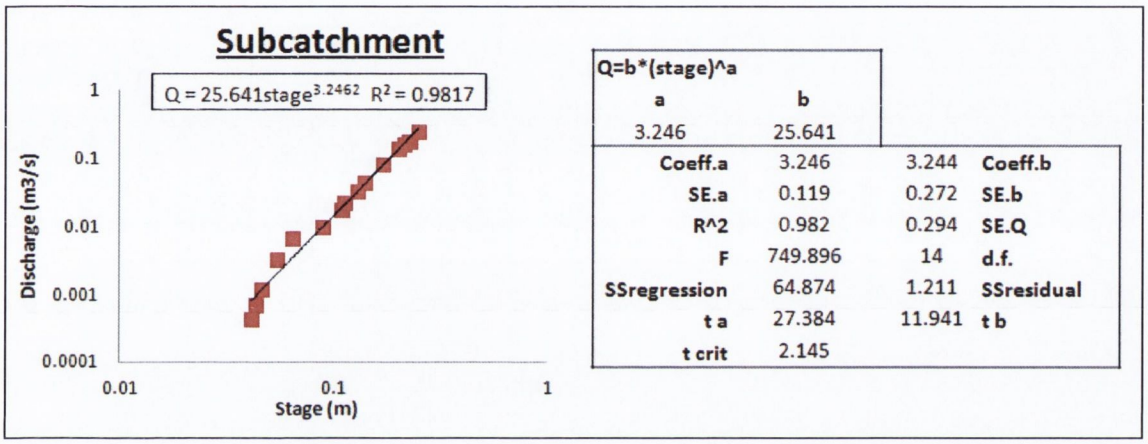

Q=b*(stage)^a			
a	b		
3.246	25.641		
Coeff.a	3.246	3.244	Coeff.b
SE.a	0.119	0.272	SE.b
R^2	0.982	0.294	SE.Q
F	749.896	14	d.f.
SSregression	64.874	1.211	SSresidual
t a	27.384	11.941	t b
t crit	2.145		

Figure 5-22. Subcatchment rating curve with associated power series fitting statistics.

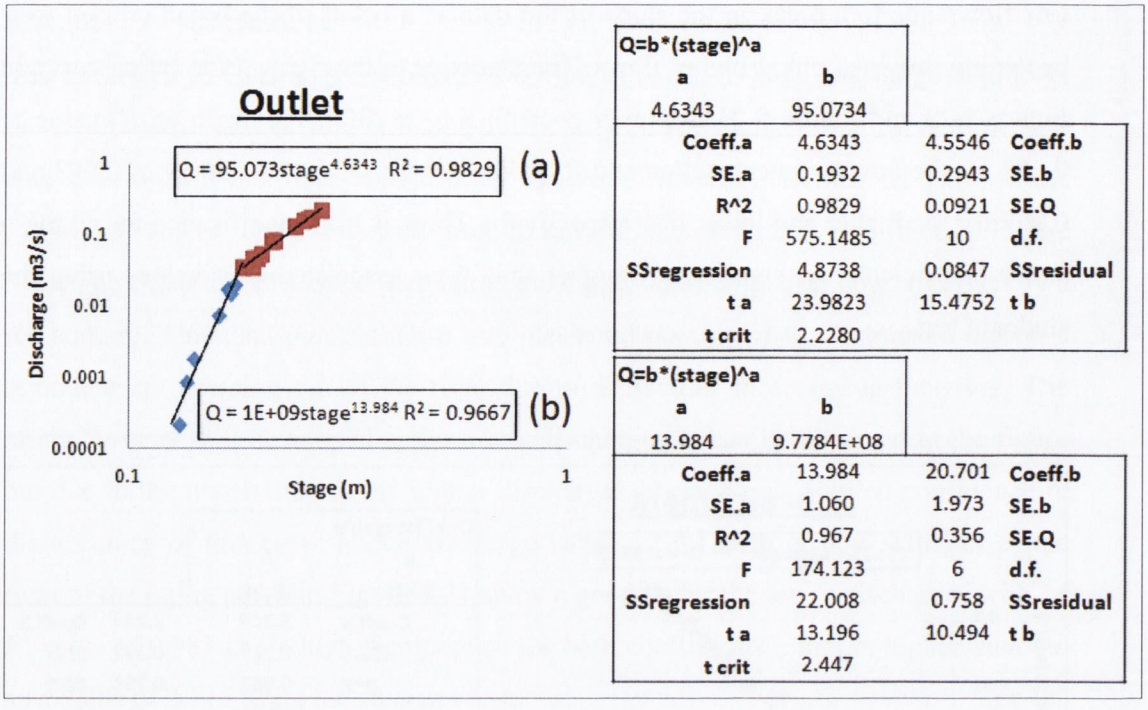

Q=b*(stage)^a			
a	b		
4.6343	95.0734		
Coeff.a	4.6343	4.5546	Coeff.b
SE.a	0.1932	0.2943	SE.b
R^2	0.9829	0.0921	SE.Q
F	575.1485	10	d.f.
SSregression	4.8738	0.0847	SSresidual
t a	23.9823	15.4752	t b
t crit	2.2280		

Q=b*(stage)^a			
a	b		
13.984	9.7784E+08		
Coeff.a	13.984	20.701	Coeff.b
SE.a	1.060	1.973	SE.b
R^2	0.967	0.356	SE.Q
F	174.123	6	d.f.
SSregression	22.008	0.758	SSresidual
t a	13.196	10.494	t b
t crit	2.447		

Figure 5-23. Outlet rating curve with power series fitting statistics for (a) higher flows and (b) lower flows.

5.11.3.3 Mattock

In the Mattock catchment, rating curves were developed for river gauging data collected as part of this thesis. These data were used to construct the rating curves, illustrated in Figure 5-24, Figure 5-25 and Figure 5-26. The Collon Weir hydrometric station is operated by the EPA and the rating curve for Berril's was developed using supplementary data obtained from the EPA. The rating curves are well developed at the lower and higher discharges for the Diversion Weir and for Berril's. The statistics to the right of the rating curve in Figure 5-24 and Figure 5-25 display a good fit for the discharges with an R^2 value of 0.993 for the Diversion Weir hydrometric station and an R^2 for Berril's station of 0.995. There is high significance for all the *a* and *b* coefficients, all significantly higher than their associated *tcrit* values using the student t test.

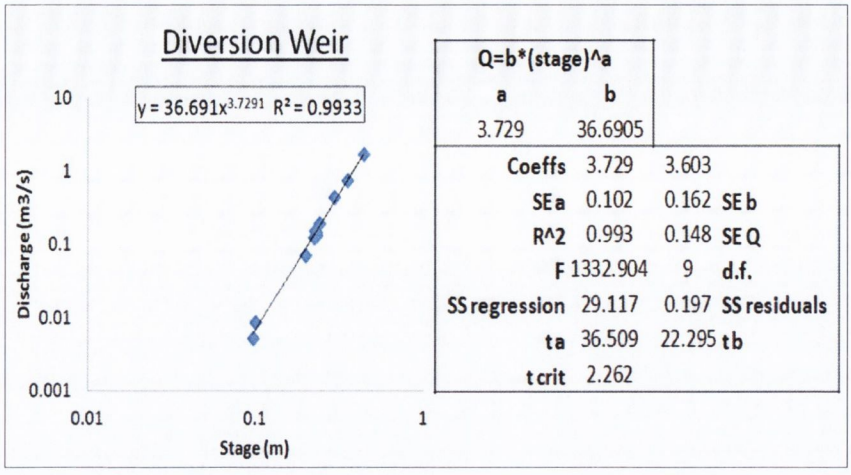

Figure 5-24. Diversion Weir rating curve with associated power series fitting statistics.

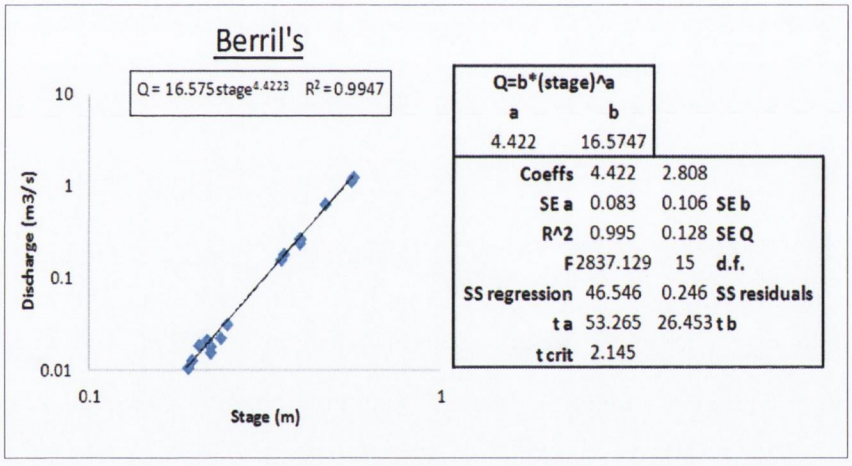

Figure 5-25. Berril's rating curve with associated power series fitting statistics.

Two rating curves were also produced for the Diversion that removes water from the catchment bringing it to the Drogheda public water supply reservoir approximately 10 km from the Mattock (see Chapter 4). The first rating curve (Figure 5-26(a)) was developed for the period after the Diversion infrastructure was renovated by Louth County Council in January 2011 until a particularly large rainfall event changed the dynamics of the pipe that drains the water from the Diversion in October 2011. Figure 5-26(b) is the rating curve that was developed from this point until the present. No statistics are supplied due to the small number of observations of discharge measured as

two curves have been prepared over a reasonably short period of time. Both rating curves have good fits with an R^2 value of 0.99 before the October 2011 flood event and an R^2 of 0.957 after this event.

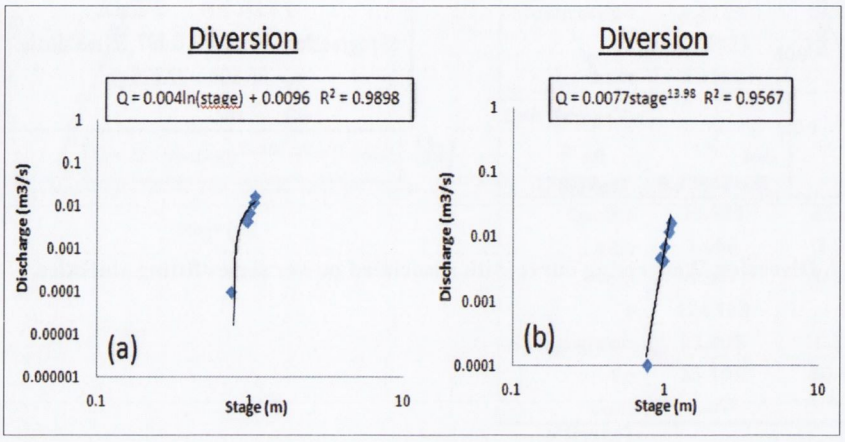

Figure 5-26. Diversion rating curve (a) before Oct 2012 event, (b) post Oct 2012 event.

5.11.3.4 Nuenna

In the Nuenna catchment, rating curves were produced for river gauging data collected as part of this doctoral thesis. These data were employed to construct the rating curves depicted in Figure 5-27, Figure 5-28 and Figure 5-29. The rating curves are well developed at the lower and higher discharges for the Castle Weir, Rocky Weir and Monument sites. The statistics to the right of these rating curves Figure 5-21exhibit a good fit for the discharges with an R^2 value of 0.991 for the Castle Weir hydrometric station, an R^2 for Rocky weir station of 0.963 and an R^2 value of 0.977 for Monument hydrometric station. There is high significance for all the a and b coefficients, all significantly higher than their associated *tcrit* values using the student t test.

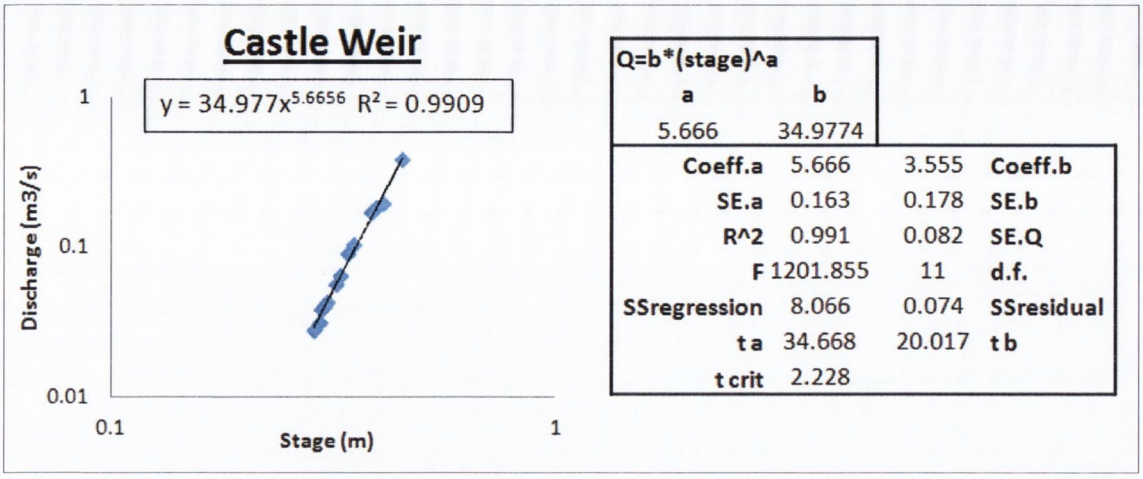

Q=b*(stage)^a			
a	b		
5.666	34.9774		
Coeff.a	5.666	3.555	Coeff.b
SE.a	0.163	0.178	SE.b
R^2	0.991	0.082	SE.Q
F	1201.855	11	d.f.
SSregression	8.066	0.074	SSresidual
t a	34.668	20.017	t b
t crit	2.228		

Figure 5-27. Castle Weir rating curve and associated power series fitting statistics.

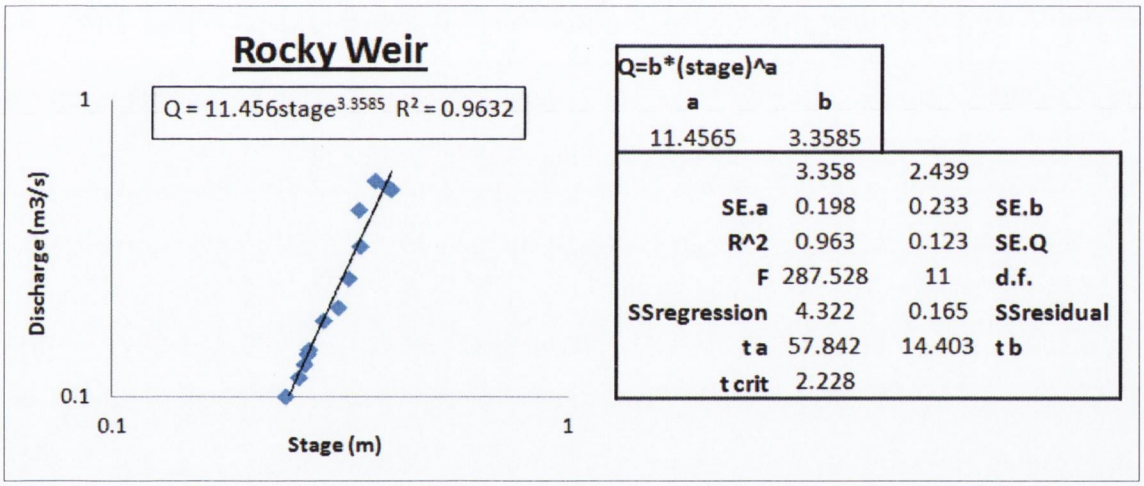

Q=b*(stage)^a			
a	b		
11.4565	3.3585		
	3.358	2.439	
SE.a	0.198	0.233	SE.b
R^2	0.963	0.123	SE.Q
F	287.528	11	d.f.
SSregression	4.322	0.165	SSresidual
t a	57.842	14.403	t b
t crit	2.228		

Figure 5-28. Rocky Weir rating Curve and associated power series fitting statistics.

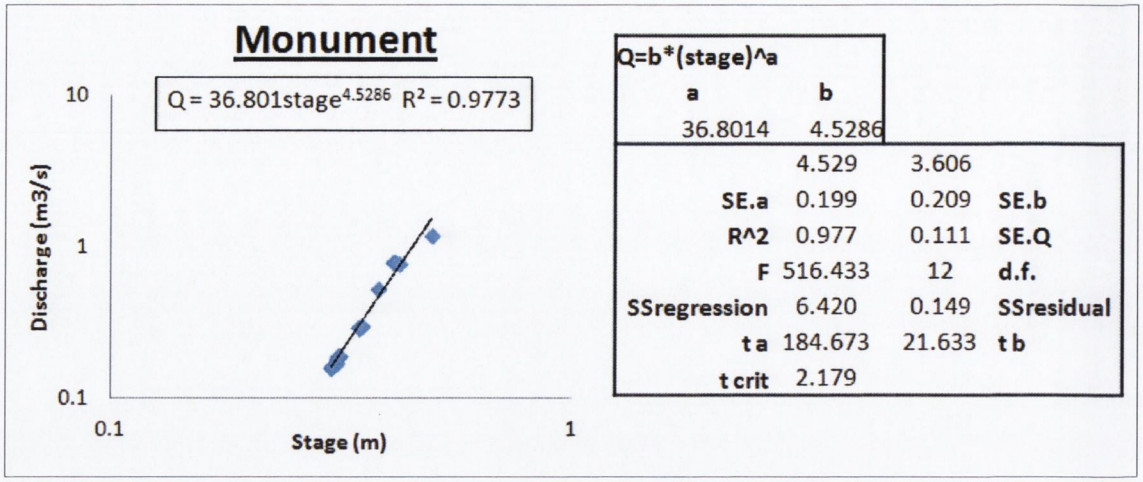

Figure 5-29. Monument rating curve and associated power series fitting statistics.

5.11.4 Water Balance

The water balance approach summarises the inputs and outputs of the study catchments, thereby allowing the consistency of the measured data to be assessed. Assuming that the storage within the soils, subsoils and bedrock does not significantly change from year to year, this method is very useful for assessing the accuracy of the rating curves of the different hydrometric stations within the catchments. Rainfall is the input that is measured in each of the catchments using at least one rain gauge. The outputs are then considered to be actual evapotranspiration (AE) and observed discharge in the river. This approach also assumes that there are no losses or gains from lateral groundwater flow out of or into the catchment. While this will be a reasonable assumption in some catchments, it may not be in others, particularly in the Nuenna (as is discussed at the end of this section). The AE was calculated, as outlined in Section 5.11.2, from the potential evapotranspiration (PE) data that were obtained from MET Éireann. The results of this approach for the four study catchments are summarised in Table 5-4.

Table 5-4. Water balances for the study catchments.

Gortinlieve								
	mm	mm	mm	mm	mm	mm	mm	
Year	Rain	PE	AE	AE/PE	Effective Rain	EPA Weir	Outlet	
2011[a]	1387.4	507.9	504.6	0.994	882.8	884.3		
2011 (6 months)	940.8	329.9	327.9	0.994	612.9		492.5	
Glen Burn								
	mm	mm	mm	mm	mm	mm	mm	
Year	Rain	PE	AE	AE/PE	Effective Rain	Outlet	Subcatchment	
2011	843.4	496.9	455.5	0.917	387.9	389.3	372	
Mattock								
	mm	mm	mm	mm	mm	mm	mm	mm
Year	Rain	PE	AE	AE/PE	Effective Rain	WWTP	DivWeir	Berrils
2010-11	884.9	501.9	467.4	0.931	417.4	430	401.3	406
Nuenna								
	mm	mm	mm	mm	mm	mm	mm	mm
Year	Rain	PE	AE	AE/PE	Effective Rain	Monument	Rocky	Castle
2011	944.4	498.3	489.3	0.982	455.1		418.5	337.3
2011	966.2	498.3	492.3	0.988	473.9	475.1		
				Topographic Area		35	21.6	13.8
				Calculated Area			19.9	10.2

[a]Estimated rainfall for the year 2011 as gaps were present in the rainfall record that could not be easily filled using a surrogate rain gauge. Rainfall was estimated by identifying periods of similar discharge and PE from which recorded rainfall was used to approximate overall quantity of rainfall that fell during this period.

Each catchment's data are summarised in terms of the calendar year of data utilised for the water balance, the rainfall for that year [mm], PE for the year [mm], AE [mm], the ratio of AE/PE and then the effective rain, calculated as rainfall less AE. This value was then cross-checked with the equivalent discharge observed during this year in

millimetres. There was reasonable agreement between the calculated effective rainfall and the observed river discharge for three of the four subcatchments. The exception to this was the Outlet catchment in Gortinlieve. Six months of rainfall data was available to calculate the effective rainfall for the same period as the discharge that was recorded at the Outlet. The rainfall time series used was for the first six months of 2011 as shown in Table 5-4. A difference of 120 mm was observed between the effective rainfall calculated and the discharge measured in the river. The water balance for same period at the EPA Weir subcatchment was evaluated in order to compare with the Outlet catchment. This was carried out to assess the likely difference between the effective rainfall and discharge that would be expected for six months as a year of data is generally required for the assumption of no change in storage to be valid (Section 5.11.2). For the same period the EPA catchment observed 591.7 mm of discharge leaving the subcatchment, 67% of the total effective rainfall for 2011. If the same relationship was applied to the Outlet catchment a total of 736 mm of discharge would be expected to leave the catchment at the Outlet in 2011. This would be approximately 155 mm less than the calculated effective rainfall for the year. This was too large a discrepancy for confidence to be held in these measurements. This large discrepancy was most likely due to the lack of high discharge observations measured in the rating curve as referred to in Section 5.11.3.1. Subsequently the rating curve was extrapolated using the stage-area/stage velocity method of extrapolation (Herschy, 1995), but this still resulted in large discrepancies comparable to the ones observed in Table 5-4.

These comparisons of water entering and leaving a catchment indicate the accuracy of measurements, provided that the assumption of no change in storage is appropriate. Another aspect of the water balance in the case of the Nuenna study catchment is the assumption of no inputs or outputs from the catchment in terms of groundwater contribution. Therefore, as well as providing a check on the degree of confidence in the rating curves for hydrometric points, rainfall and river stage monitoring, the water balance is an uncomplicated approach for assessing the areas that may be contributing to springs across surface water catchment divides in a groundwater-dominated river catchment such as the Nuenna. This was possible due to the tracer studies that have been carried out (Walsh, 2011) in the catchment showing connections between swallow holes in the upper Castle subcatchment that are connected to springs in the subcatchments with outlets at Rocky Weir and Monument (Figure 5-30). Therefore

water originating in the Castle subcatchment is bypassing the hydrometric gauging point at the outlet of this subcatchment to the Rocky Weir and Monument subcatchments. The areas of each subcatchment were calculated using topography and then adjusted to the area that would be required to achieve a balance with the rainfall falling on the catchment.

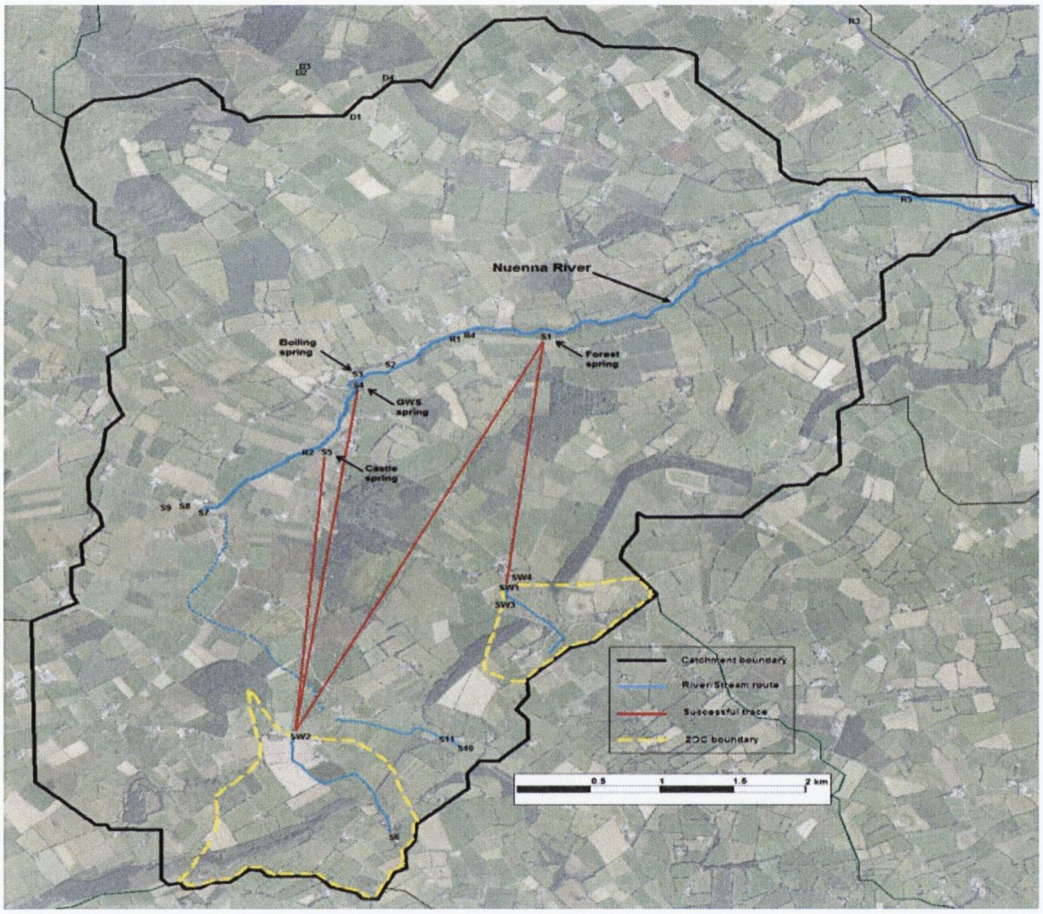

Figure 5-30. Tracer studies carried out in the Nuenna (Walsh, 2011).

5.11.5 Discussion of Data Analysis

Following on from the assessment of the consistency of the data using the water balance approach, it was decided to omit the Gortinlieve Outlet catchment from further discussion within this thesis due to the lack of confidence in the rating curve of the Outlet hydrometric station. The absence of higher discharge data will be addressed

within the *Pathways Project* in the future but due to the delay of this fieldwork in relation to this research, the catchment below the EPA Weir will remain outside the scope of this thesis.

The contributing catchment areas calculated from the water balance approach in the karst Nuenna catchment will be employed for physical separation approaches and lumped hydrological modelling (Chapters 6 and 7). These areas better reflect the processes that are generating the discharges in the Castle Weir and Rocky Weir catchments than the catchment area calculated using surface topography. The contributing areas are also more appropriate for hydrological modelling as the water removed from the upper Castle Weir subcatchment discharges into the Rocky Weir and Monument subcatchments via the swallow hole connections to springs in these subcatchments.

6 Physical River Hydrograph Separation

6.1 Introduction

Physical river hydrograph separation techniques, within the scope of this thesis, are those techniques that utilise data that are observable in the field and can be directly measured, i.e. rainfall, evapotranspiration, river discharge, water table levels and temperature. Essentially, these are techniques that do not require chemical analysis (see Chapter 2 for a brief account of chemical hydrograph separation methods). These graphical, digital filtering and other techniques are necessary to investigate the contribution of the different pathways to the river hydrograph. The basis of each method has been reviewed in Chapter 2. Each method was applied to constrain the contribution of the pathways as part of the hydrological modelling exercise that was carried out in the study catchments. The ability of these separation techniques and the hydrological modelling to provide physically realistic limits for the pathways is vital for any contaminant transport or attenuation models that may be applied to the work of this thesis.

Following on from the literature review, four approaches were employed in order to separate the hydrograph into its constituent pathways: recharge coefficients approach, recession analysis, digital filtering algorithms and tracer analysis. These methods, and any adaptations that have been applied to them, are outlined in the following sections. The physical separation approaches have been applied to the four study catchments as well as a number of supplementary catchments, that were subsequently utilised for the generalisation of the procedures developed within this thesis (see Chapter 9). An outline of these additional catchments, along with some characteristics of their geological setting, is provided in Appendix A.

6.2 Recharge Coefficients

As discussed in Chapter 2, the recharge coefficient approach determines the contribution of hydrologically effective rainfall (i.e. rainfall – actual evapotranspiration (AE)) to the groundwater pathways and subsequently the contribution of effective rainfall to the faster responding overland flow and interflow pathways. This is achieved by assessing the soil and subsoil cover within a catchment. Poorly draining soils and subsoils typically allow only limited amounts of infiltration of effective rainfall into the groundwater pathways and conversely well drained soils permit more infiltration and therefore more recharge into the aquifers. As a further constraint to this method, the type of aquifer underlying a catchment is also assessed. If an aquifer consists of a bedrock type with large storage capacity and high transmissivity (for example, a regionally important aquifer), it is likely to be able to accept all the potential recharge that infiltrates through the soils and subsoils, whereas if it is a poorly productive aquifer there is a limit to how much recharge it can receive; therefore, it is assumed that poorly productive aquifers can only accept 100 mm of recharge a year, while locally important aquifers can receive up to 200 mm (Working Group on Groundwater, 2005).

6.2.1 Implementation

The recharge to the groundwater pathways was calculated as a percentage of effective rainfall. This ensured that the recharge coefficients could be implemented directly as they are presented in Table 2-1. In order to apply the recharge caps for poorly productive and locally important aquifers, the effective rainfall would be required in order to convert the recharge caps to a percentage, as this percentage varies from catchment to catchment. The water balance calculated for each of the study catchments in Chapter 5 was utilised for this purpose as the FAO Penman-Monteith method (Penman and Long, 1960; Monteith, 1965; Allen et al., 1998) could be applied to estimate AE for the effective rainfall calculation. Once this had been determined the soil and subsoil conditions needed to be assessed. The catchments were delineated using DEM files obtained from the EPA. Teagasc soil and subsoil mapping were then interrogated for these delineated catchments. The area of each combination of soils overlying subsoils was calculated with GIS software and the appropriate recharge coefficient for each combination was applied, referring to Table 2-1 for guidance. If the

recharge coefficient selected was to produce a recharge value greater than that which the underlying aquifer would permit, the recharge coefficient was reduced to this cap. The overall catchment recharge coefficient was then computed applying a weighted mean approach, where area was selected as the weighting factor. The relevant soils, subsoils and aquifer classification mapping for each for study catchments that influence the recharge coefficient approach are illustrated in Section 6.2.3.

6.2.2 Modification of standard recharge coefficient approach

While the recharge coefficients approach is a useful method for calculating likely values of recharge for the groundwater pathways based on geology, it does this only by determining the diffuse recharge that occurs, i.e. the recharge that occurs by infiltration of the effective rainfall directly through the soils and subsoils. This method does not take into account the potential of any point recharges from surface runoff, i.e. recharge that occurs when water enters the aquifer at discrete points such as at a swallow hole. This type of recharge may occur in karst aquifers for example, such as the Nuenna. In order to take this process into account, surface water catchments draining to swallow holes were identified using the locations of swallow holes and DEM files. This process allowed the determination of the contributing areas of the swallow holes that were then assigned a recharge coefficient of 100%. This provided a more realistic value of groundwater recharge than the standard recharge coefficient approach would predict. Figure 6-1 illustrates two swallow hole subcatchments that were delineated within the Nuenna catchment with DEM data.

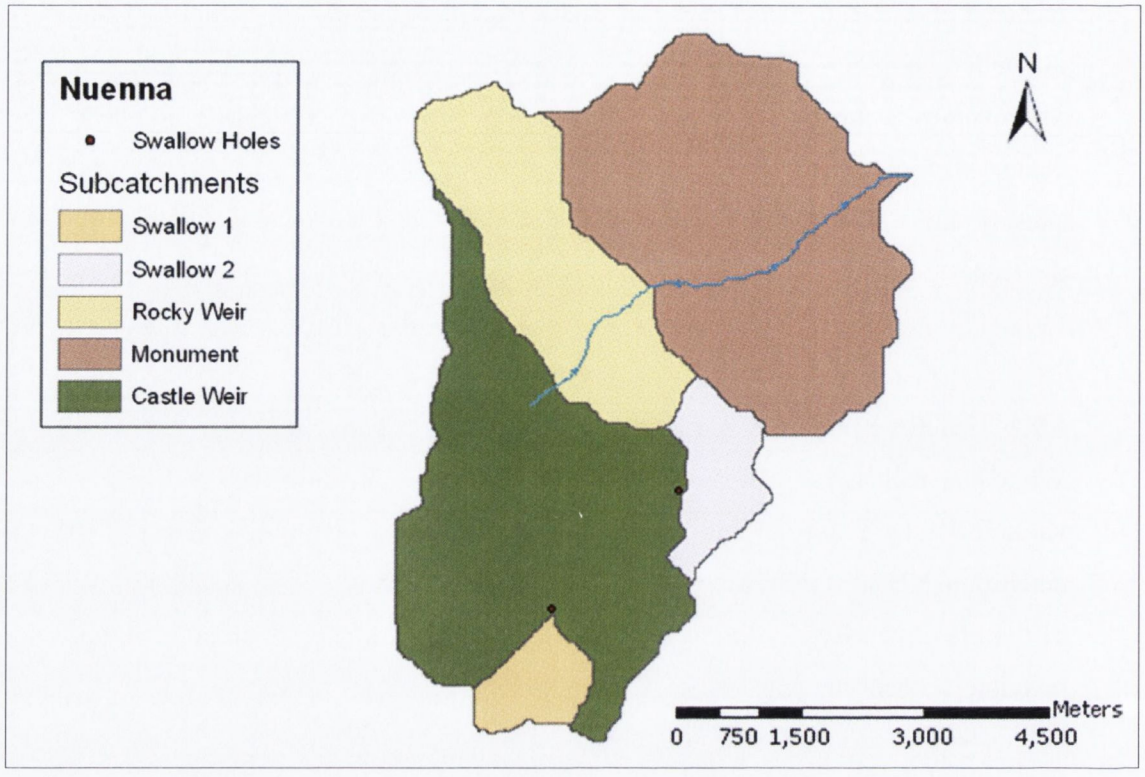

Figure 6-1. Swallow hole subcatchments within the subcatchment of Castle Weir in the Nuenna.

The recharge coefficient approach was applied to the four study catchments as well as to the supplementary catchments. The results of the study catchment recharge coefficients approach are discussed in Section 6.6, while the results of the supplementary catchments are included in Appendix B.

6.2.3 Results of recharge coefficient approach

The figures contained within each study catchment's subsections, present the mapping of the soil, subsoil and aquifer classification data for these catchments. These provide an indication of the percentage of effective rainfall that will expected to recharge the groundwater pathways in the catchment. Set alongside these are draft GIS data of the recharge coefficients calculated by the Geological Society of Ireland (GSI). These maps are still under review but provide an opportunity to cross-check the coefficients computed for each catchment in this thesis.

6.2.3.1 Gortinlieve

Gortinlieve, much like the Mattock and Glen Burn, was expected to have low recharge due to poorly draining soils and poorly draining till subsoils. This can be seen in Figure 6-2 with the dominance of the poorly draining soil (AminPD) and tills (TMp). The estimated average recharge coefficient here was 0.113. The recharge coefficient figure using the draft GSI recharge map was higher, computed at 0.146. This was higher than the 0.113 as a result of the mean annual effective rainfall applied in the mapping being 685 mm (again this would seem to be quite low as discussed in Chapter 4) compared with the mean annual effective rainfall of 883 mm computed in Chapter 5. This would result in the difference observed as the whole catchment is limited by the poorly productive aquifer underlying Gortinlieve, as shown in Figure 6-3(a). Therefore, the cap of 100mm, divided by the effective rainfall, resulted in the calculated recharge coefficient applying each approach.

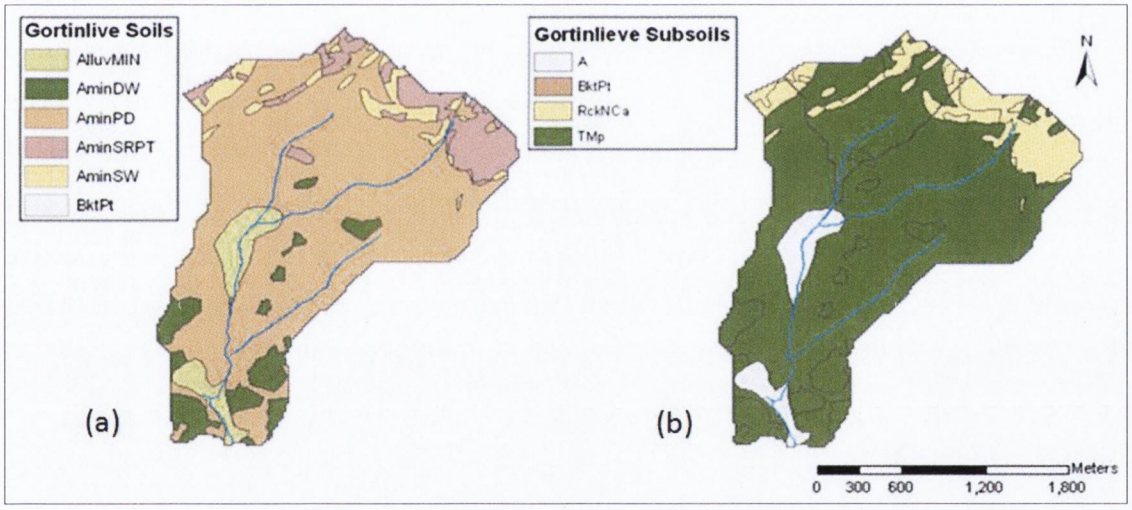

Figure 6-2. (a) Soils and (b) subsoils in Gortinlieve.

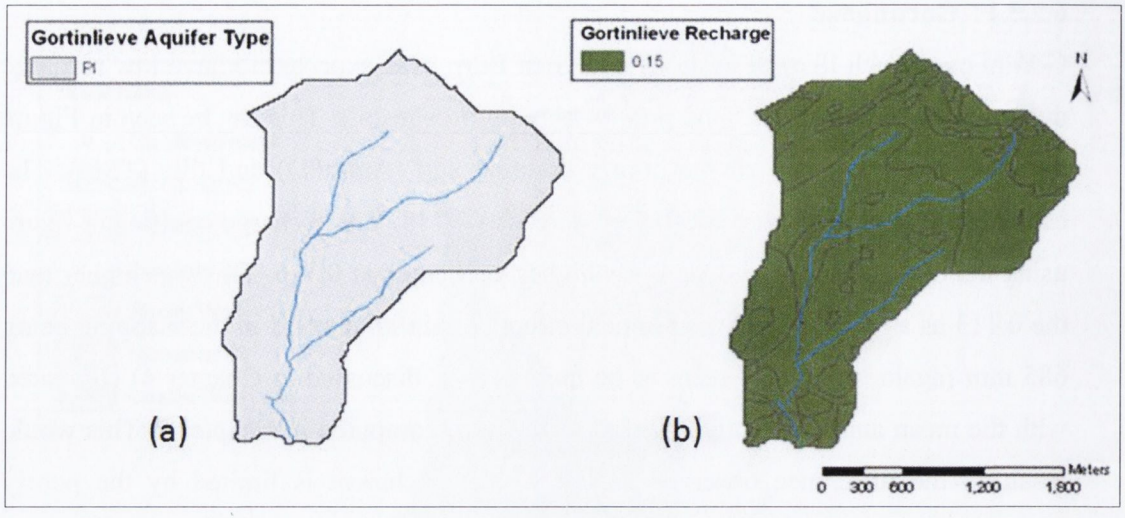

Figure 6-3. (a) Aquifer and (b) recharge mapping (GSI) in Gortinlieve.

6.2.3.2 Glen Burn

The Glen Burn catchment is predominately underlain by a poorly productive aquifer (Figure 6-5), which is overlain by poor draining soils and subsoils (Figure 6-4). In a similar manner to the Gortinlieve and the Mattock, low recharge was anticipated here. In this case the estimated recharge coefficient was 0.189, based upon a mean annual effective rainfall of 388 mm. There were no recharge figures from the draft GSI recharge map as it does not cover Northern Ireland. As a result of the low effective rainfall, the recharge cap of 100 mm did not significantly influence the recharge coefficient calculated, as the recharge cap was equivalent to 26% of effective rainfall.

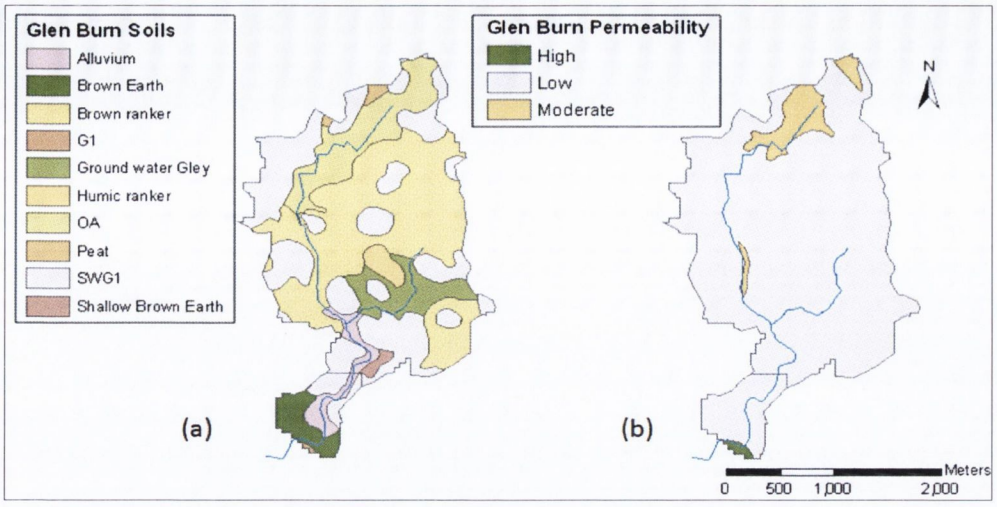

Figure 6-4. (a) Soils and (b) subsoil permeability in Glen Burn.

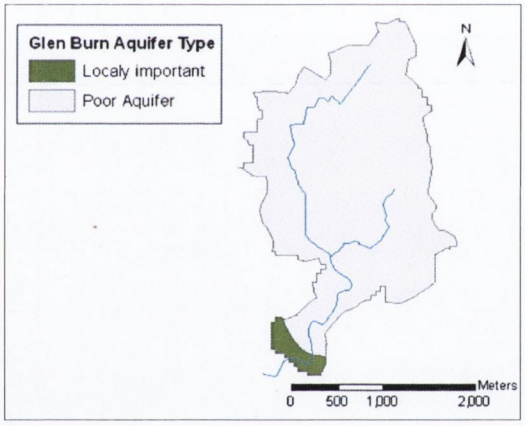

Figure 6-5. Aquifer Type in Glen Burn.

6.2.3.3 Mattock

As is suggested by Figure 6-6, the Mattock has a low recharge due to poorly drained soils (AminPD) overlying a poorly productive aquifers. The recharge coefficient was computed as 0.23, which compared with a recharge coefficient of 0.149 from the draft GSI recharge map. The mean annual effective rainfall using the recharge map was 623 mm, but assessing the data collected from the catchment for the year 2011 the annual effective rainfall was 417 mm and for 40 years of rainfall (1970-2009) for the area (as calculated in Chapter 5), the mean annual effective rainfall was 494 mm. This

discrepancy in rainfall would result in the differences observed as the 100 mm cap would be a lower recharge coefficient in the case of the higher effective rainfall utilising the recharge map.

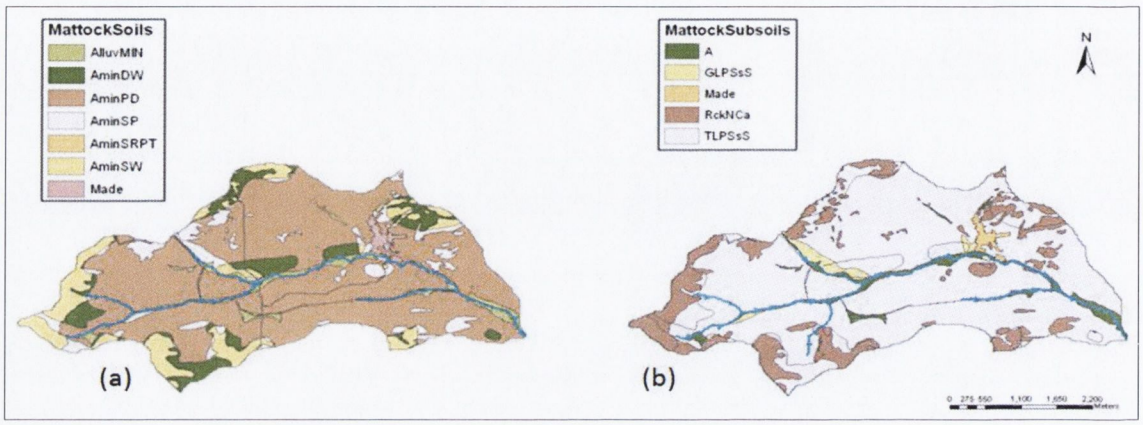

Figure 6-6. (a) Soils and (b) subsoils in the Mattock.

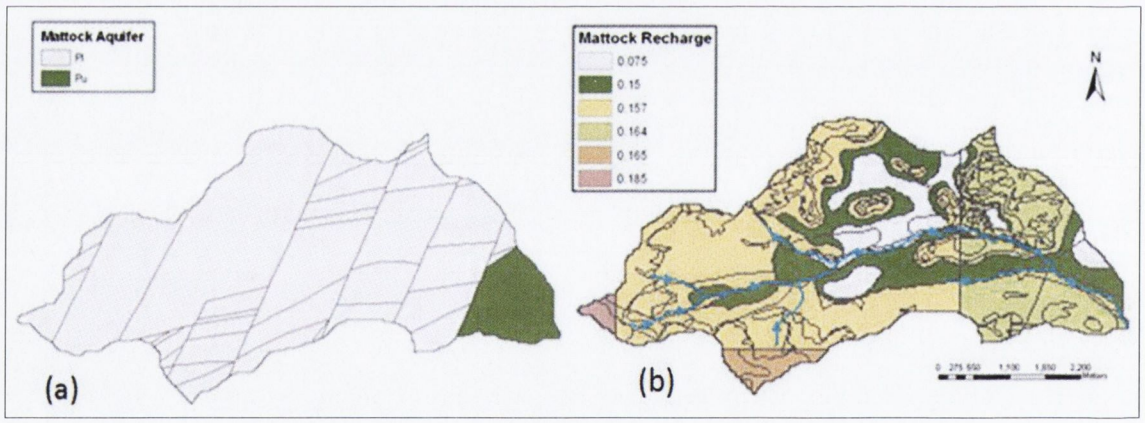

Figure 6-7. (a) Aquifer type and (b) Recharge Mapping (GSI) for Mattock.

6.2.3.4 Nuenna

The Nuenna, unlike the Mattock, has well drained subsoils (Figure 6-8(a)) and soils (Figure 6-8(b)) predominantly overlying a regionally important limestone aquifer (Figure 6-9(a)). High recharge was expected in this case. The calculated recharge coefficient value was 0.65 applying the recharge coefficient approach in its original

format which can be compared to a recharge coefficient of 0.535 computed from the draft GSI recharge map (Figure 6-9(b)). The estimated effective rainfall was again higher in the Nuenna using the recharge mapping with a mean of 664 mm compared with 464.5 mm for the rainfall collected in 2011 from the catchment and assessing 1980 to 2009 data (as described in Chapter 5). This would result in a greatly reduced recharge coefficient in areas where the 100mm cap was applied. The adapted approach, which takes into account the two swallow holes in the south west of the catchment (Figure 6-1) was applied and the recharge coefficient within the area draining to these swallow holes was set as 1. This approach calculated the recharge coefficient as 0.705.

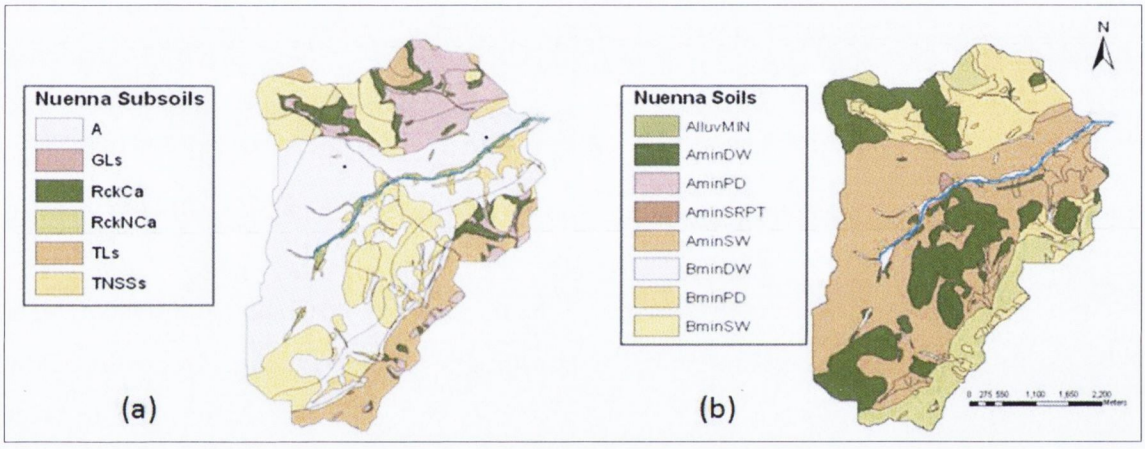

Figure 6-8. (a) Subsoils and (b) Soils within the Nuenna catchment.

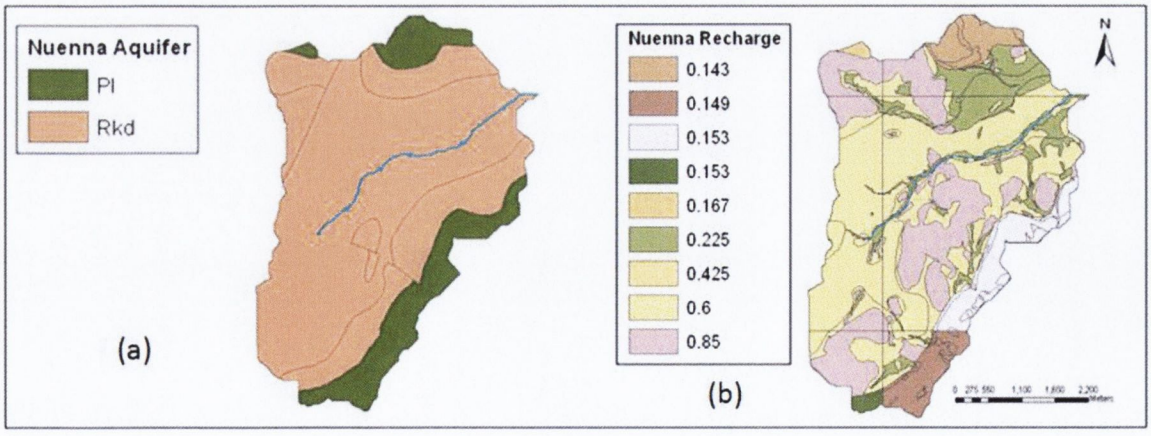

Figure 6-9. (a) Aquifer classification and (b) draft recharge map (GSI) within the Nuenna catchment.

These coefficients were utilised to estimate the percentage of effective rainfall that infiltrated into the groundwater system, while the remaining rainfall was assumed to contribute to discharge in the river by means of the quick responding pathways, overland flow and interflow. The subcatchment recharge coefficients are summarised in Table 6-1 at the end of the chapter, along with the results of the other hydrograph separation approaches discussed below.

6.3 Recession Analysis

As outlined in Chapter 2, recession analysis is the assessment of the hydrograph following a rainfall event. The analysis of the recession period after the hydrograph has peaked and no more rain is falling on the catchment provides an opportunity to observe the characteristic response of a catchment. A master recession curve (MRC) involves plotting many different recessions resulting from different magnitude rainfall events in order to better observe the catchment's response during different discharge conditions. Typically, the MRC is applied to identify the period when baseflow begins following a rainfall event so that a hydrograph may be split graphically into quick responding flow and baseflow. In this thesis, the MRC analysis was applied to identify the different recession constants of the different pathways for use in the recursive digital filter algorithms discussed in Section 6.4, and also to calculate the relative storages of the different responses, allowing the estimation of each pathway's contribution to the hydrograph. Following the literature review two methods of MRC analysis were applied to the study catchments: the Matching Strip method and the Tabulation method. While both methods can be applied to identify the recession constants of each pathway, the Tabulation method was implemented to estimate the contribution of each pathway to the hydrograph.

6.3.1 Implementation

The first step of MRC analysis is to identify the individual recessions that are plotted together to form the MRC. An algorithm was written in MATLAB that selected these recessions from the discharge datasets available. The algorithm identified periods in

which recessions were located, i.e. periods of time greater than two days with mean daily rainfall less than 0.2 mm to approximate drought conditions as per Chapter 2. Next the discharge time series during this period was interrogated to extract recessions of a length that allowed pathways to be identified using the MRC analysis, two days was chosen as the minimum length. The longer the available time series of discharge was, the more accurate the inferences from a MRC would be, as a greater variation of discharge levels observed and provides a more complete overview of how the catchment would respond to different rainfall events. This was a limitation of applying this method as the longest time series available to the project was just over two years. Therefore, in order to increase the recessions that could be identified implementing this algorithm, three of the parameters were relaxed: the volume of rainfall permitted for periods in which recessions could be identified (mean of 2 mm per day), the length a recession required for analysis (greater than two days), and an allowance for small increases in discharge that may be due to turbulence in the stage recorder so that recessions that displayed marginal increases in discharge were not excluded. These relaxations, whilst introducing errors in the analysis, allow inferences to be made for short time series that may not be possible otherwise.

6.3.1.1 Tabulation method

The tabulation method involves plotting recessions sequentially in order of descending initial discharge. This approach focuses on identifying initial recessions of the faster responding pathways with greater accuracy, which will help in recognising the temporal resolution of input data required to drive the hydrological modelling. If overland flow responds with a time constant of less than twenty four hours, and especially if less than twelve hours, daily rainfall data will not be sufficient to model peaks in the hydrograph. This is considered in more detail in Chapter 7. As this method tends not to overestimate the groundwater responses due to the focus on the faster responding pathways, the calculation of the relative storages will provide useful indications of pathway contributions.

6.3.1.2 Matching strip method

The matching strip method, unlike the tabulation method, places emphasis on the slower responding pathways. Recessions are plotted sequentially in order of descending final discharge. Utilising this approach together with the tabulation approach, physically appropriate values can be identified for the two groundwater time constant parameters (i.e. the deep and shallow groundwater pathways) in the NAM model. It should be noted, however, that this method is not suitable for calculating the relative storages of each pathway as the emphasis placed on the groundwater pathways, though helping to identify response time constants, results in the wintertime high groundwater flows dominating the response equation. Consequently, when the integration of each pathways corresponding equation is carried out, the winter high response will skew the average well above what is a feasible contribution for the groundwater pathways in the catchment.

6.3.2 Calculation of relative storages

The Tabulation method and the Matching Strip method typically assigned comparable values of the recession parameter k to the groundwater pathways but the Tabulation method provided more plausible k values for the faster responding pathways due to the extra emphasis placed on identifying these pathways with this method. In order to avoid the bias that would be introduced to the slower responding pathways implementing the Matching Strip method, relative storages were only determined for the pathways using the Tabulation method.

The relative storage approach involves the integration of the area below the MRC relating to the active pathways. The equation for each pathway was calculated by assessing the superposition of responses as the basis for separating each pathway response. In the case of the interflow equation (the second of the recession equations) in Figure 6-10, the equation of interflow response is as follows:

$$Q_{0I}e^{-t/\tau_I} = Q_{0*}e^{-t/\tau^*} - Q_{0S}e^{-t/\tau_S} - Q_{0D}e^{-t/\tau_D} \qquad \text{6-I}$$

where $_I$, *, $_S$ and $_D$ and refer to interflow, combined, shallow and deep groundwater storages respectively. The combined response equation is the line that was fitted to the data for that pathway, interflow in this case. The deep groundwater response equation

can be read directly from the graph, while the shallow groundwater response equation has to be calculated applying the same approach as above given that the observed shallow groundwater response in this situation is actually the combined response of shallow and the deep groundwater. Once all the pathway response equations have been calculated, the area below these curves attributable to each pathway is calculated over the period during which these pathways are active.

These relative storages were calculated for the study catchments and the supplementary catchments. The values were then utilised to estimate the average contribution of these pathways. This approach will typically slightly overestimate the groundwater input as this generally recedes for a period following the beginning of a rainfall event. Nonetheless, this method further provided a useful technique for estimating average responses of catchments based on observed discharge. The results of these MRC analyses are assessed in the next section with discussion at the end of this chapter. The results of the supplementary catchments are presented in Appendix B.

6.3.3 Results of recession analysis

It was observed that typically higher values were predicted for the faster responding pathways implementing the Tabulation method, but there was a reasonable correlation with the Matching Strip method for the groundwater pathways. Additionally, the τ values obtained, allowed the recession constant k to be calculated for the modified Lyne and Hollick algorithm. The results from each of the study catchments are described in this section, with Table 6-1 summarising the results of the hydrograph separations.

6.3.3.1 Gortinlieve

Due to the omission of the Outlet subcatchment in Gortinlieve (see Chapter 4), the MRC analysis was only carried out for the upper catchment with discharge measured at the EPA weir. This weir has silting issues during low discharges which can be identified during the low flow periods in Figure 6-10. As the water level in the weir dropped the silt tended to deposit which had the effect of maintaining the river stage at an artificially high level. This resulted in the horizontal recessions at the end of the lower discharges. Four pathways were identified using both MRC methods with the

slope of the slowest pathway at higher flows being used as a surrogate for the slowest pathway's slope when silting had become an issue. Comparable τ values for the groundwater pathways are observed in Figure 6-11 to those obtained applying the tabulation method.

EPA Weir

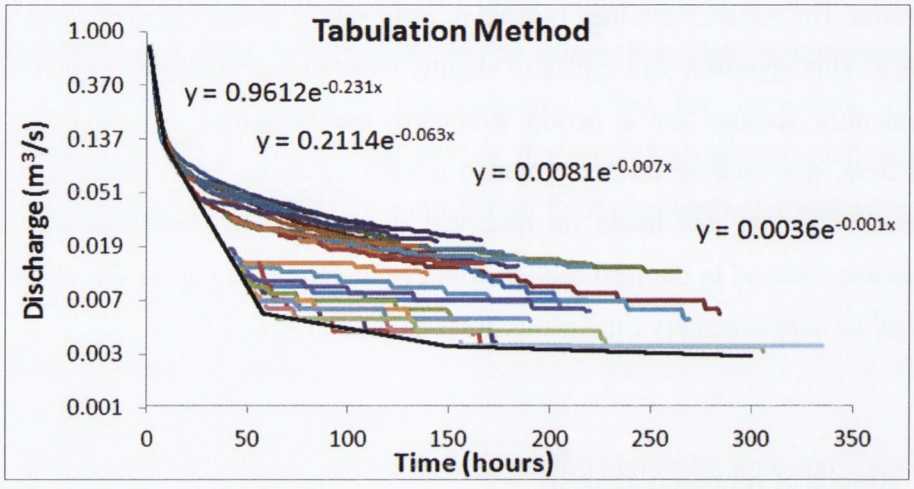

Figure 6-10. Gortinlieve EPA Weir subcatchment Tabulation method.

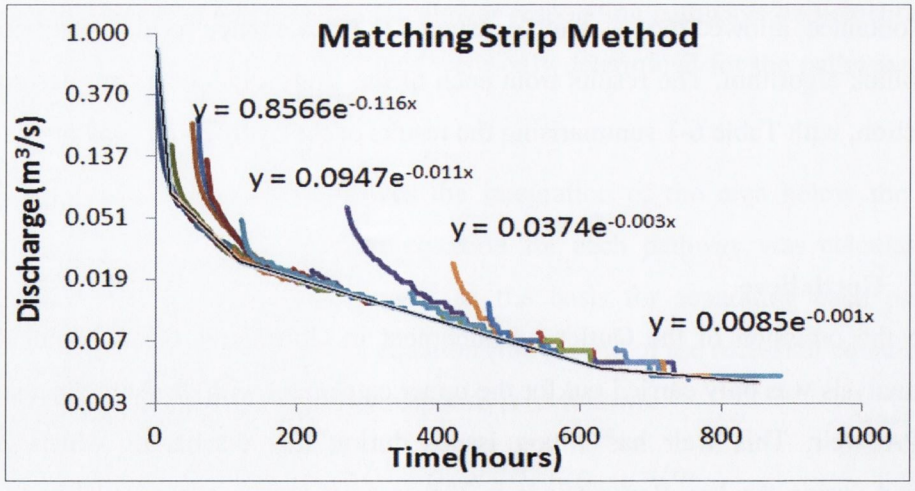

Figure 6-11. Gortinlieve EPA Weir subcatchment Matching Strip method.

6.3.3.2 Glen Burn (Mount Stewart)

In the Glen Burn, the four pathways could be identified implementing both the Tabulation and the Matching Strip methods. Both the Subcatchment and Outlet subcatchments displayed similar responses, most likely due to their proximity to one another (as stated in Chapter 4). The groundwater pathways once more had comparable τ values applying both methods (as seen in Figure 6-12, Figure 6-13, Figure 6-14 and Figure 6-15), with the rate of response of the quick pathways being more rapid in the case of the Tabulation method. The marginally faster τ values of the Subcatchment, compared to the Outlet, are most likely due to the effects of the alluvium and locally important aquifer at the Outlet catchment, as shown in Figure 6-4 and Figure 6-5.

Subcatchment

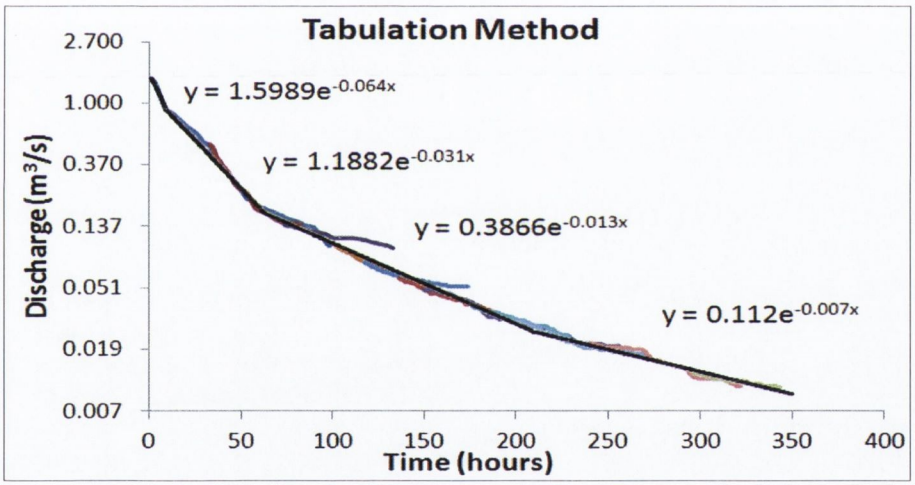

Figure 6-12. Glen Burn subcatchment Tabulation method.

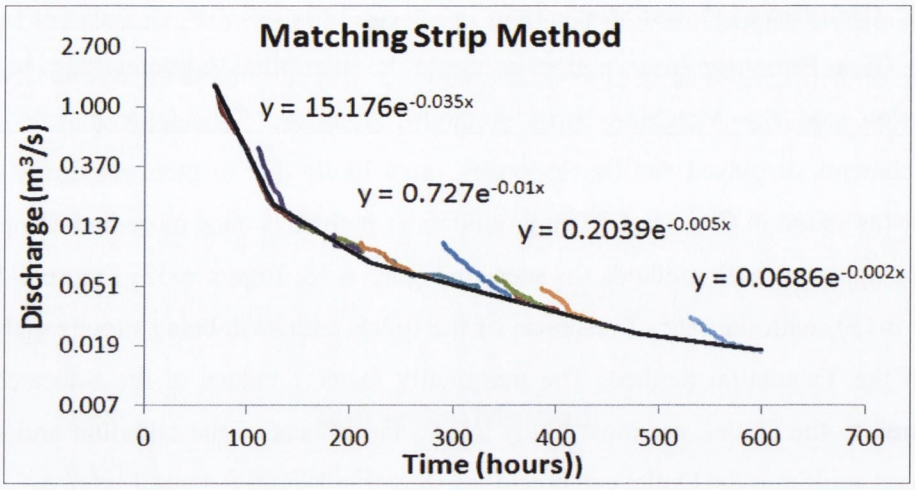

Figure 6-13. Glen Burn subcatchment Matching Strip Method.

Outlet

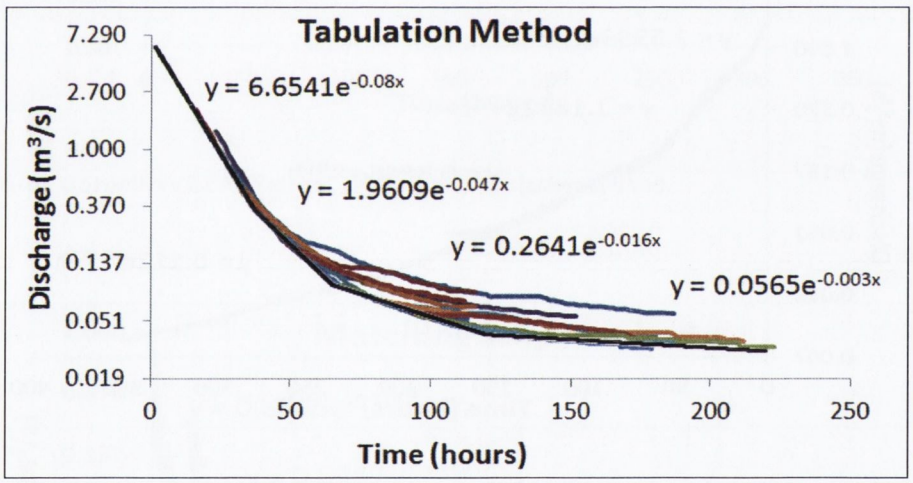

Figure 6-14. Glen Burn catchment Tabulation method.

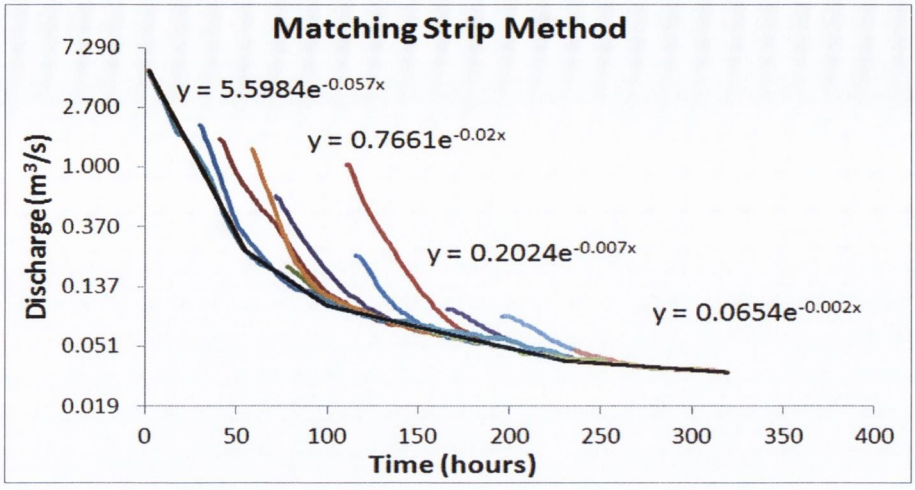

Figure 6-15. Glen Burn catchment Matching Strip method.

6.3.3.3 Mattock

Diversion Weir

At the Diversion Weir only three pathways could be identified. If a longer time series were available over wide ranging flow conditions, a fourth pathway might have been distinguished, but with the current data only three could be determined. The groundwater τ values were comparable for both methods, with the τ for the Tabulation Method being greater for the fast responding pathways, as shown in Figure 6-16 and Figure 6-17.

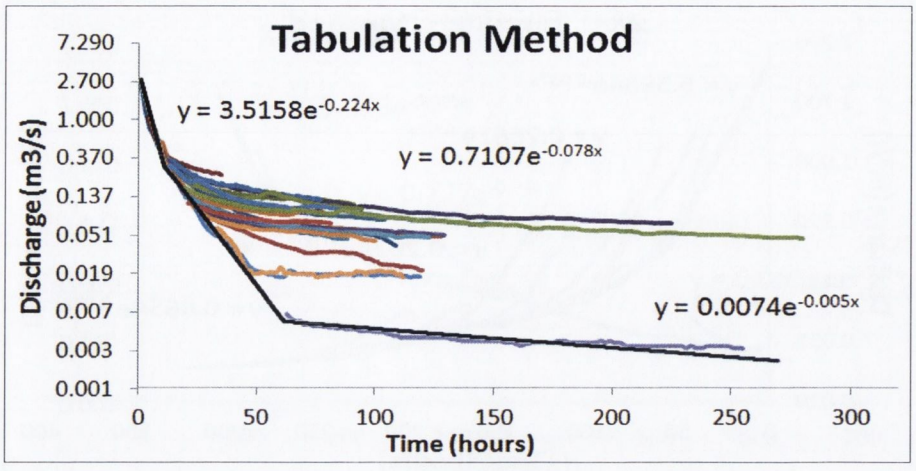

Figure 6-16. Mattock Diversion Weir subcatchment Tabulation method.

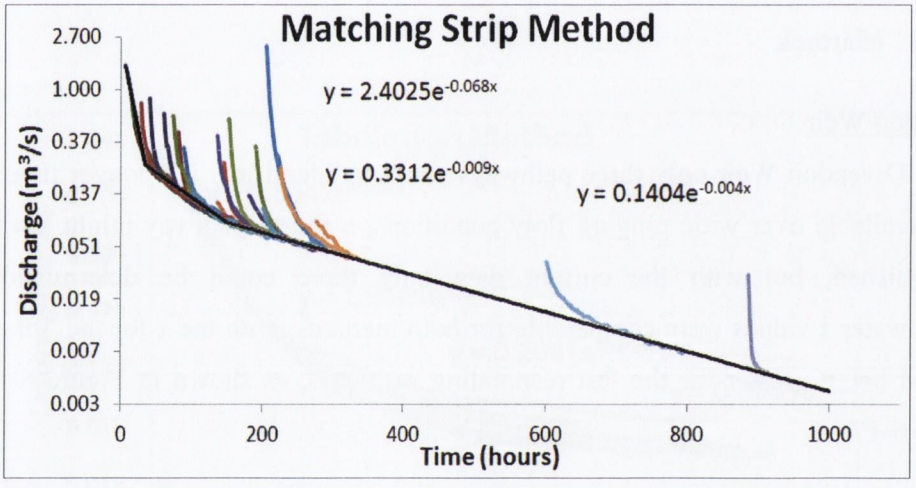

Figure 6-17. Mattock Diversion Weir subcatchment Matching Strip method.

Collon Weir

Applying the two MRC methods, four pathways were identified at this hydrometric station. As with the EPA Weir in Gortinlieve, there was a problem with silting up of the intake pipe for the stilling well at this site. The EPA hydrometric team clear this silt out each time they download. This has had the effect of maintaining stage readings at higher levels than were actually occurring. This issue does not have a large effect on the MRC analysis as more accurate readings will compensate, but it will have had an effect on the hydrological model with which the simulated pathways are constrained by these

observed discharges (see Chapter 7). Hence, groundwater contributions were likely to have been over-estimated as a result of this, if observed discharge was considered alone to constrain the hydrological modelling. Once more, as can be seen in Figure 6-18 and Figure 6-19, the slower responding pathways have similar τ values, with the tabulation method computing higher τ values for the faster responding pathways.

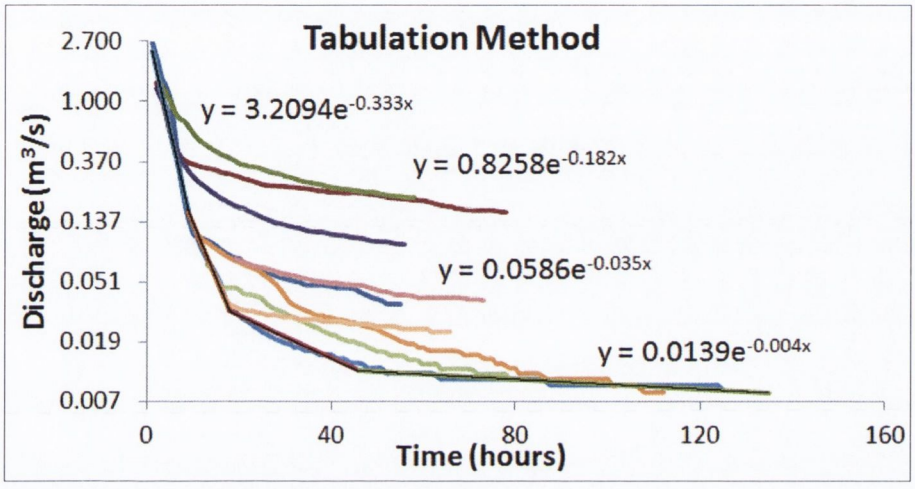

Figure 6-18. Mattock Collon Weir subcatchment Tabulation method.

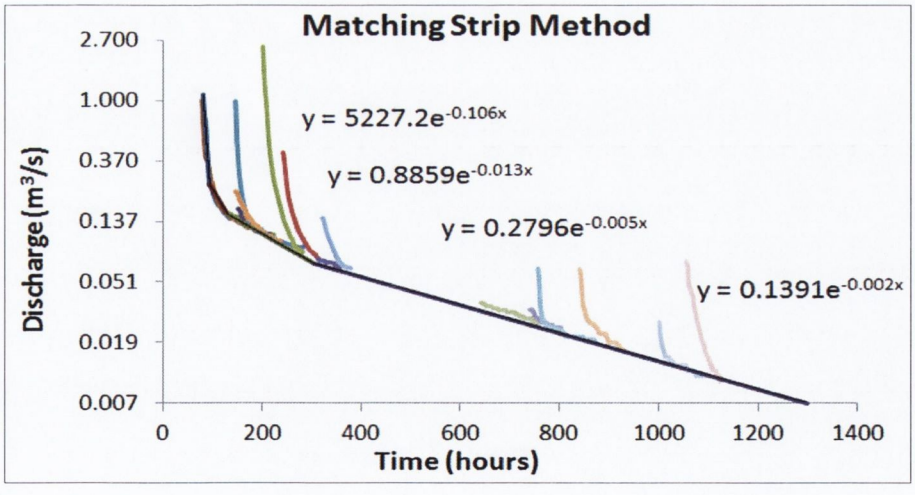

Figure 6-19. Mattock Collon Weir subcatchment Matching Strip method.

Berril's

Four pathways were again identified in Figure 6-20 with the difference in winter and summer baseflow levels observed when the higher recessions are ceasing around a discharge of 0.1 m^3/s and the lower recessions at 0.015 m^3/s. The groundwater τ values were again similar (Figure 6-20 and Figure 6-21) but the τ value for overland flow was less here than at the Collon Weir, indicating a slower response in this fast responding flow pathway, possibly due to steeper topographic slopes in the upper catchments.

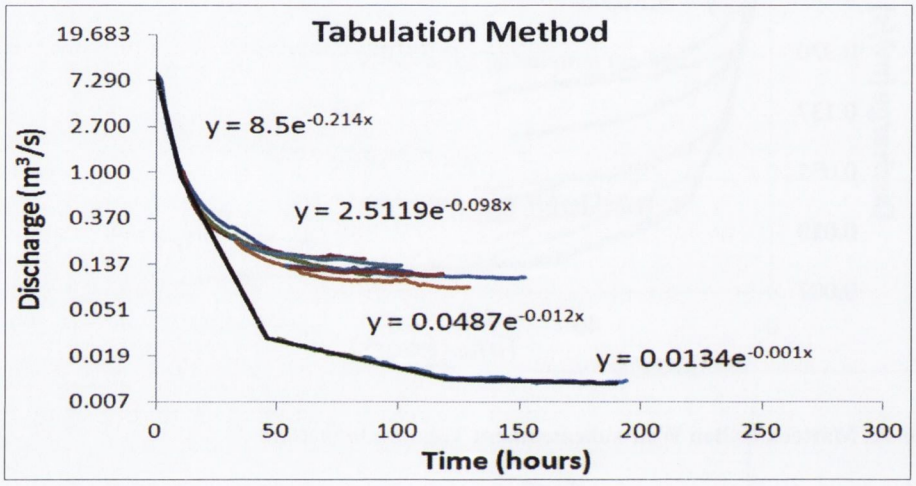

Figure 6-20. Mattock Berril's catchment Tabulation method.

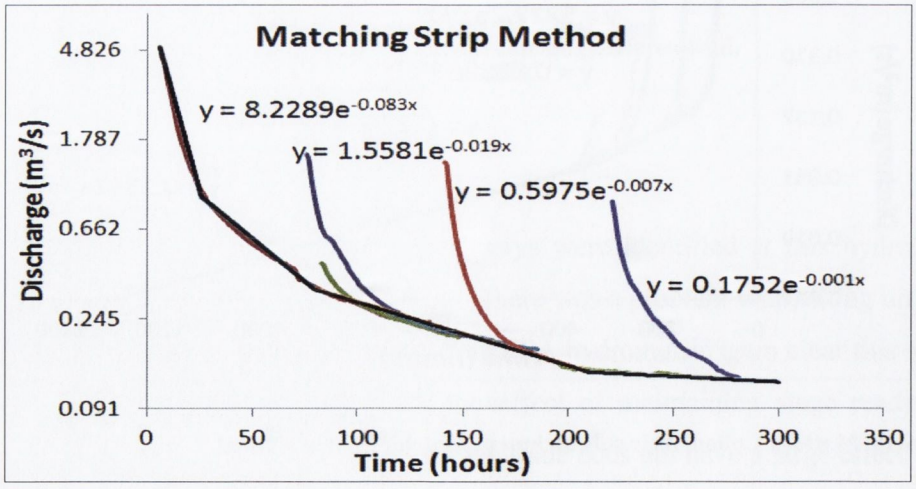

Figure 6-21. Mattock Berril's catchment Matching Strip method.

Examining the τ values from the three subcatchments, it is observed that the response time of the catchment increases from the Diversion Weir to the Collon Weir subcatchment and then has a small decrease in response time at Berril's at the catchment outlet. A significant tributary enters the river downstream of the Collon Weir and it was observed that the river becomes perched at the outlet (see Chapter 4). This will have a bearing on the response of the catchment to rainfall and was the probable reason for the observed decrease in τ for the faster responding pathways. The discharge record was longer at the Collon Weir which will also have had an effect on the fastest responding pathway, as higher observed discharges (than those which had already been recorded) will have altered the τ value computed, particularly by the Tabulation method.

6.3.3.4 Nuenna

The Nuenna, being the only study catchment underlain by a regionally important aquifer, behaves significantly differently to the other three catchments. This was observed in the MRC analysis as the Tabulation method and the Matching strip method were effectively equivalent to one another. This was a result of the slow responding nature of the catchment which requires pathways to become active sequentially before receding in the same manner each time. It can be seen in Figure 6-22, Figure 6-23 and Figure 6-24, that the faster responding pathways increased in the speed of their response to rainfall going from the upper Castle subcatchment to the catchment outlet at Monument. The groundwater pathways, however, remained consistent throughout the three subcatchments.

Castle Weir

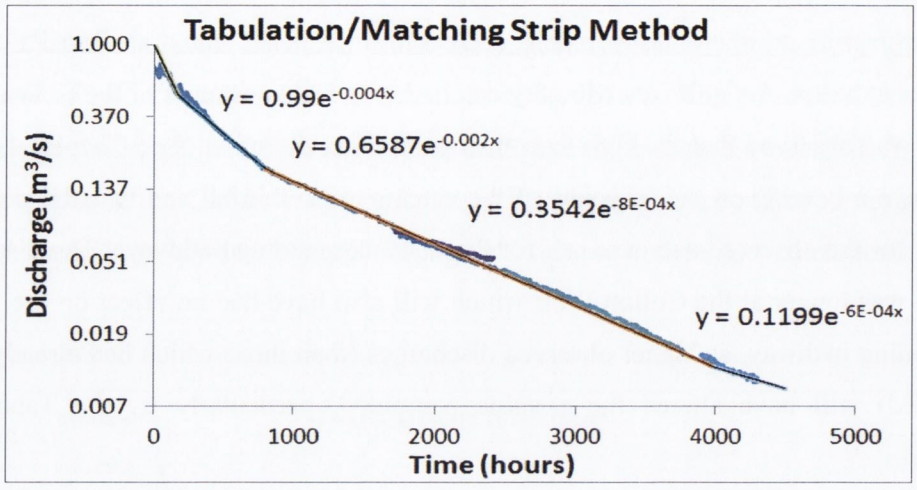

Figure 6-22. Nuenna Castle Weir subcatchment MRC analysis.

Rocky

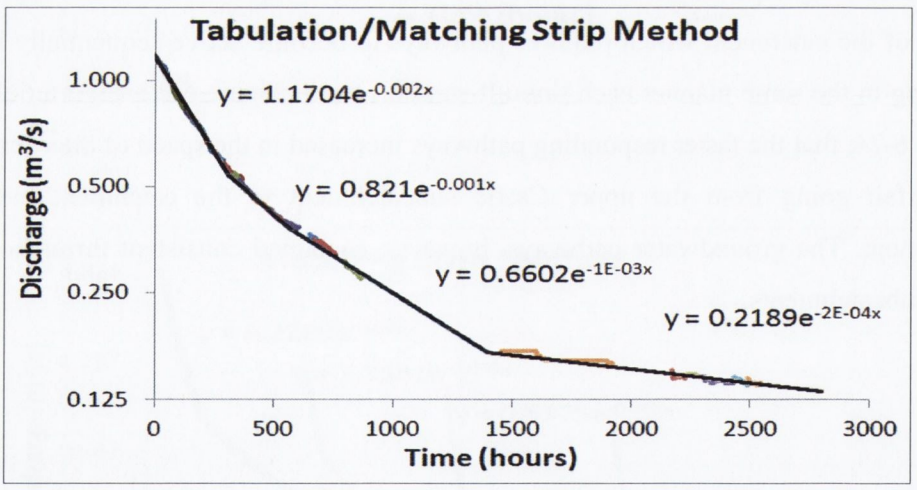

Figure 6-23. Nuenna Rocky Weir subcatchment MRC analysis.

Monument

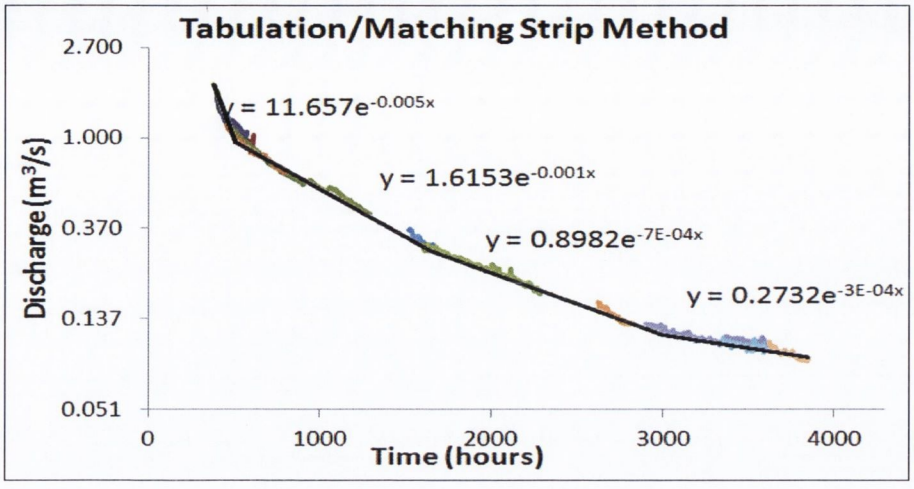

Figure 6-24. Nuenna Monument catchment MRC analysis.

Examining these MRCs it was observed that although there was some variation between the methods, similar responses were identified for the two slowest responding pathways in each catchment. This was encouraging as it is these pathways that are of most importance in predicting the *k* values for the modified Lyne and Hollick recursive digital algorithm.

6.4 Digital Filtering Algorithm

Digital filters are commonly utilised in signal analysis and processing. This method allows the filtering out of different frequency signals, with the higher frequency signals conceptually being a proxy for overland flow and interflow, and the lower frequency signals being a proxy for shallow and deep groundwater. The Lyne and Hollick 'one-parameter' algorithm (Lyne and Hollick, 1979), the Boughton 'two-parameter' algorithm (Boughton, 1993), the Eckhardt 'two-parameter' algorithm (Eckhardt, 2005) and the IHACRES 'three-parameter' algorithm (Jakeman and Hornberger, 1993) were all reviewed in Chapter 2. The application of these algorithms, while useful for providing a method for obtaining time series of baseflow, requires an *a priori* knowledge of the catchment, as subjective decisions are necessary to determine the

different parameters included in the algorithms. As such, while these approaches have value for assisting in understanding the baseflow distribution for the hydrograph, they do not provide an objective means of identifying the baseflow contribution. Moreover, their applications are normally restricted to identifying only two main pathways: baseflow and quick responding flow. To be applicable in this research, it was therefore necessary to modify one of these algorithms, so that it could represent the four pathways of the conceptual model underpinning the catchment studies in this research. The 'one-parameter' algorithm was the method selected for modification, due to its lack of subjectivity in parameter selection.

6.4.1 Adapted Lyne and Hollick filtering algorithm

The algorithm presented here is one based on the principles of the 'one-parameter' algorithm (Lyne and Hollick, 1979), but modified to separate the hydrograph into four, rather than two constituent pathways. Lyne and Hollick's 'one-parameter' algorithm, has been updated (Chapman and Maxwell, 1996) to a form that represents the groundwater flow being a simple weighted average of the quick response flow and the slow response flow at the previous time interval. Equation 6-II calculates baseflow at any time step, as being the baseflow from the previous time step, receding at a rate k, while quick flow (discharge minus baseflow at that time step) contributes 1-k times its value, an approximation of the supplementary discharge increasing river flow that is derived from baseflow.

$$Q_{Bt} = kQ_{Bt-1} + (1-k)Q_{Qt} \qquad \textbf{6-II}$$

Using the continuity of discharge, this is rearranged to:

$$Q_{Bt} = \frac{k}{2-k}Q_{Bt-1} + \frac{1-k}{2-k}Q_t \qquad \textbf{6-III}$$

subject to the condition that

$$Q_{Bt} \leq Q_t \qquad \textbf{6-IV}$$

where Q_{Bt} is baseflow [m^3/s], Q_{Qt} is quick flow, Q_t is stream discharge [m^3/s], all at time t, and k is the recession constant. This essentially divides the equation into two parts: the recession component to the left and a baseflow component. In this equation, k

can be calculated from the MRC analysis. Utilising this equation in practice tends to estimate baseflow as being close to fifty percent of the total hydrograph, since quick flow maintains the same percentage of itself in time step *t* as baseflow does, resulting in a baseflow contribution close to fifty percent. The 'two-parameter' algorithm avoids this problem by replacing *1-k* by a free variable that is not based on direct analysis but on achieving an *a priori* estimated baseflow contribution, or equally chosen from 'experience'.

In order to address this issue and thus implement the recursive filter approach as a means of investigation, as well as a method of obtaining a time series of separations, the additional two pathways of the conceptual model were included and Equation 6-III was modified to accommodate them. Discharge is considered to consist of overland flow, interflow, shallow and deep groundwater flow, as shown in Equation 6-V:

$$Q = Q_O + Q_I + Q_S + Q_D \qquad \textbf{6-V}$$

where Q_O, Q_I, Q_S and Q_D are overland flow, interflow shallow, and deep groundwater flow respectively [m^3/s]. In Equation 6-VI, quick flow is now redefined as overland flow for the supplementary component of Equation 6-II, and with further modification of the algorithm, thus the equation to calculate interflow becomes:

$$Q_{It} = k_I Q_{It-1} + (k_S + k_D - 1)(3 - k_I - k_S - k_D)(Q_t - Q_{It} - Q_{St} - Q_{Dt}) \qquad \textbf{6-VI}$$

where k_I, k_S and k_D refer to the recession constants associated with interflow, shallow and deep groundwater respectively. This equation is analogous to Equation 6-II with baseflow being replaced by interflow and quick flow being replaced by overland flow. The second factor, $(3\text{-}k_I\text{-}k_S\text{-}k_D)$, preceding the overland flow value, relates to the total amount of water available to replenish the subsurface pathways. It is proposed that the amount of water available is controlled by the rates at which the different pathways can accept water. The recession constant is an approximation of the rate at which a pathway releases water from storage and therefore is related to the transmissivity of that pathway. This suggests that the recession constant may be used as an approximation of the rate at which the pathways may also accept available water. It is proposed that this water would infiltrate into the interflow pathway would also include the shallow and deep recharge represented by $1\text{-}k_S$ and $1\text{-}k_D$ respectively. This is represented by the summation of the 1-*k* terms of each of the pathways, $(3\text{-}k_I\text{-}k_S\text{-}k_D)$, in Equation 6-VI. The

recharge for the groundwater pathways would further infiltrate and in so doing reduce the contribution to interflow. The (k_S+k_D-1) factor before the overland flow calculation addresses this issue. The recharge that each of the groundwater pathways can accept is defined by the *1-k* relating to each pathway. Therefore, as described in Equation 6-VII, the recharge to each groundwater pathway from the total available recharge is computed as follows:

$$Groundwater\ Recharge = (1-k)(3-k_I-k_S-k_D)(Q_t - Q_{It} - Q_{St} - Q_{Dt}) \quad \textbf{6-VII}$$

where k here is either k_S or k_D depending on whether the shallow or deep groundwater pathways is being addressed. This water is then removed from the total subsurface replenishment and is represented by the first factor before the overland flow calculation in Equation 6-VI as shown in Equation 6-VIII and Equation 6-IX:

$$(1-(1-k_s)-(1-k_D)) * Total\ \ subsurface\ replenishment \quad \textbf{6-VIII}$$

or

$$(k_S + k_D - 1) * Total\ \ subsurface\ replenishment \quad \textbf{6-IX}$$

Shallow groundwater flow is determined in much the same manner in Equation 6-VI. The first part of the equation is set up as before with the discharge of the previous time step's receding according to the associated recession constant with the supplementary component taken from Equation 6-VI, as shown in Equation 6-X:

$$Q_{St} = k_S Q_{St-1} + (1-k_S)(3-k_I-k_S-k_D)(Q_t - Q_{It} - Q_{St} - Q_{Dt}) \quad \textbf{6-X}$$

Deep groundwater is handled in the same manner as shallow groundwater with *1-*k_D coefficients used in Equation 6-XI:

$$Q_{Dt} = k_D Q_{Dt-1} + (1-k_D)(3-k_I-k_S-k_D)(Q_t - Q_{It} - Q_{St} - Q_{Dt}) \quad \textbf{6-XI}$$

These equations are reliant upon each other with dependencies on values from other equations as well as the discharges being sought appearing on both sides of the equation. As such it was necessary to solve them in parallel. Therefore an iterative approach was taken, with each equation solved in turn on a spreadsheet model until the discharges converged towards the solution. The results of this hydrograph separation method are covered in the next section, with discussion in Section 6.6.

6.4.2 Results of recursive digital filter algorithm

Due to the linear nature of this algorithm, it was more effective at identifying the groundwater pathways than the faster responding surface pathways. Nevertheless, the slower response of interflows to rainfall than overland flow ensured that the algorithm provided a contribution that was indicative of the type of response expected.

6.4.2.1 Gortinlieve

The 'flashy' catchment in Gortinlieve, which is underlain by a poorly productive aquifer, has a small groundwater contribution that increased slightly during rainfall events. Figure 6-25 shows how interflow and overland flow dominates as per the recharge coefficients approach and MRC analysis.

EPA Weir

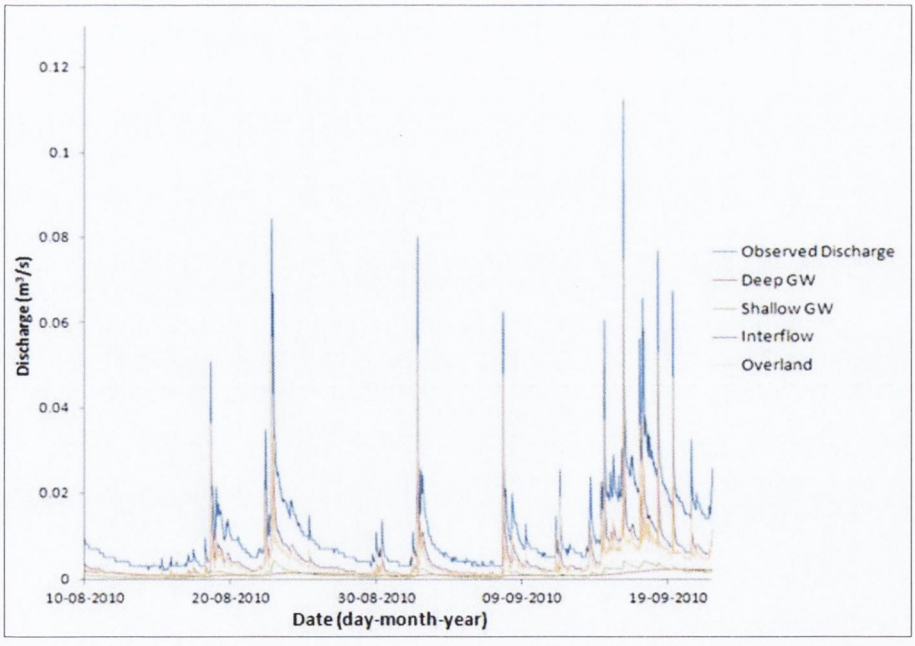

Figure 6-25. Gortinlieve EPA Weir subcatchment modified Lyne and Hollick algorithm separations (Aug 2010 – Sept 2010).

6.4.2.2 Glen Burn

The 'flashy' nature of the Glen Burn was again observed by applying the digital filter algorithm, with a relatively small groundwater pathway contribution to the river hydrograph. The groundwater pathways displayed a marginal response to rainfall events, with overland flow and interflow having the largest flow contribution to the hydrograph. The Subcatchment and Outlet subcatchments also appear quite similar in Figure 6-26 and Figure 6-27. This was expected due to the close proximity of both hydrometric stations (less than 1 km apart).

Subcatchment

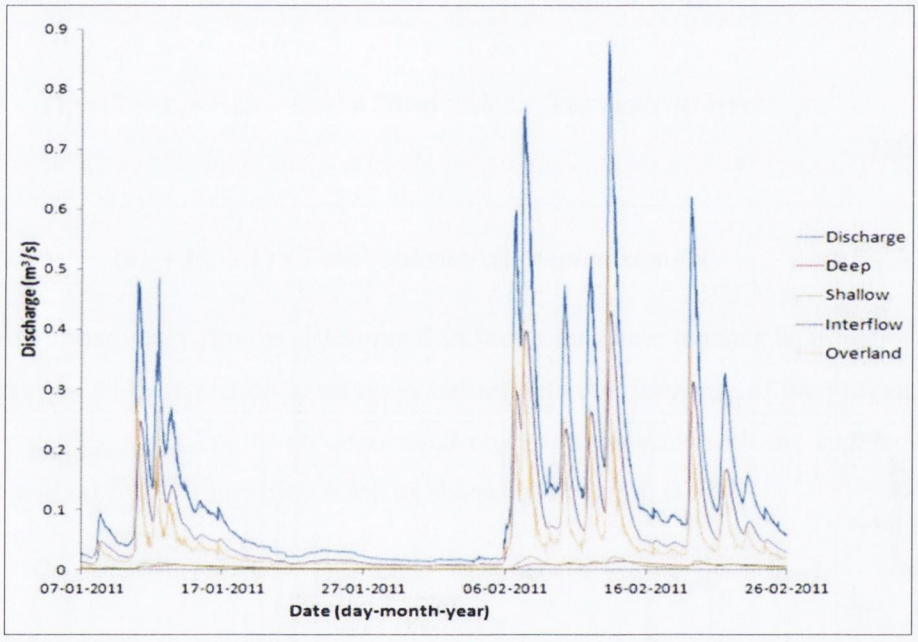

Figure 6-26. Glen Burn Subcatchment modified Lyne and Hollick algorithm separations (Jan 2011 – Feb 2011).

Outlet

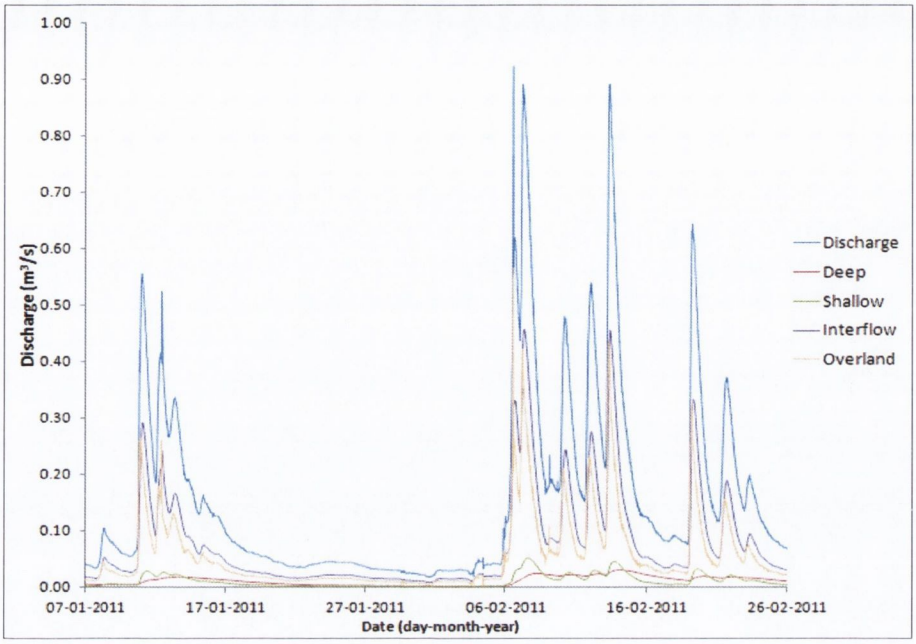

Figure 6-27. Glen Burn Outlet catchment modified Lyne and Hollick algorithm separations (Jan 2011 – Feb 2011).

6.4.2.3 Mattock

Diversion Weir

Figure 6-28 depicts groundwater as a minor contributor to the river hydrograph but one that does respond to large storm events. Overland and interflow were responsible for the majority of river flow.

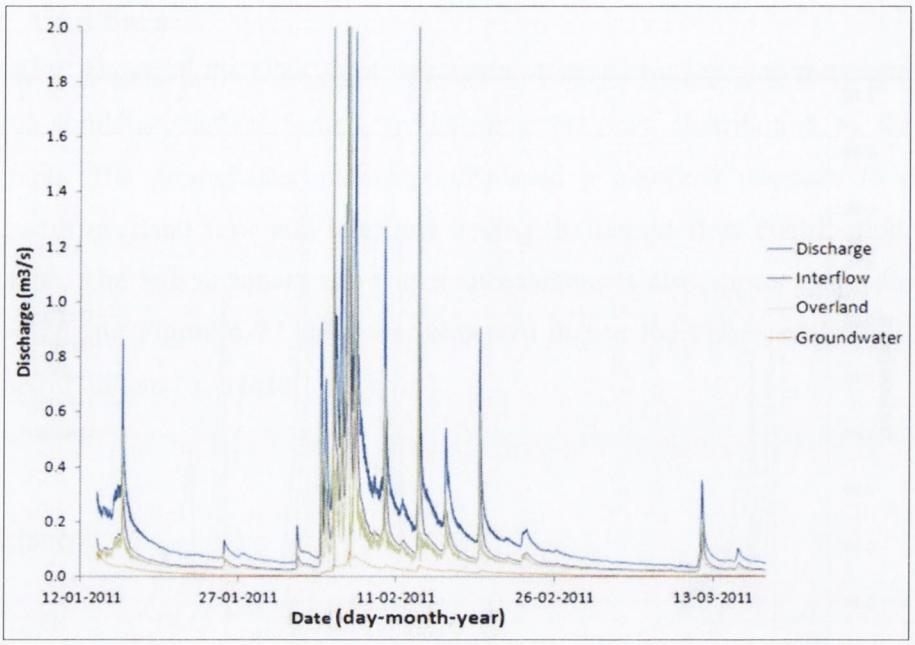

Figure 6-28. Mattock Diversion Weir subcatchment modified Lyne and Hollick algorithm separations (July 2011 – Aug 2011).

Collon Weir

At the Collon Weir, groundwater played a more important role than at the Diversion, as shown on Figure 6-29. In this case shallow groundwater was of particular importance during large events. It is probable that this is the influence of the sands and gravels that are present at Collon, near the vicinity of Collon Weir, as discussed in Chapter 4.

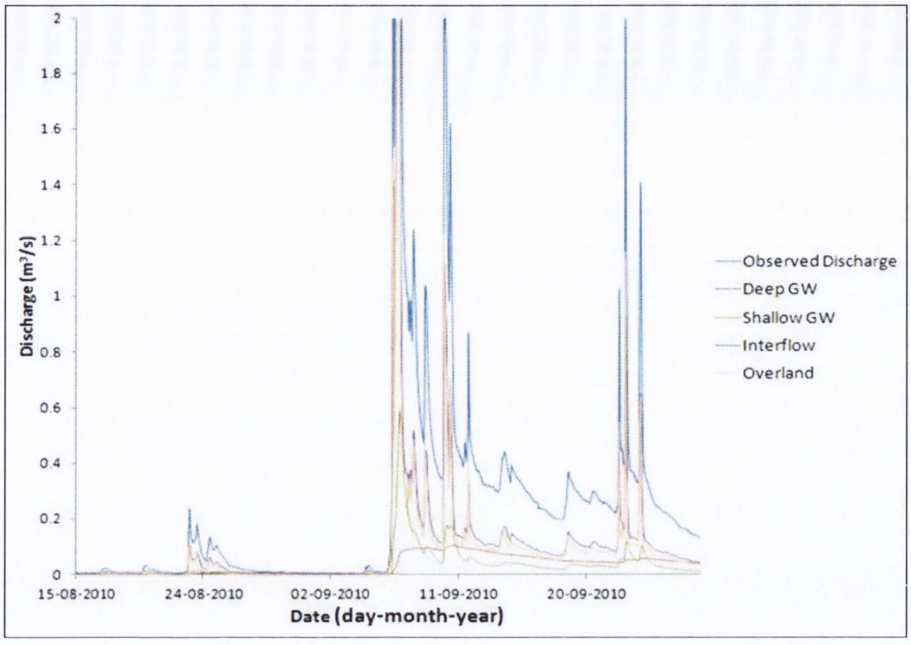

Figure 6-29. Mattock Collon Weir subcatchment modified Lyne and Hollick algorithm separations (Aug 2010 – Sept 2010).

Berril's

At Berril's groundwater is represented as having a very small contribution during events and high flows (Figure 6-30), consistent with the perched nature of the river at this point in the Mattock catchment (see Chapter 4). This area of the catchment is also underlain by the Pu aquifer (Figure 6-7) that would support the suggestion that there is smaller contribution of groundwater at Berril's compared with the Collon Weir and Diversion Weir subcatchments.

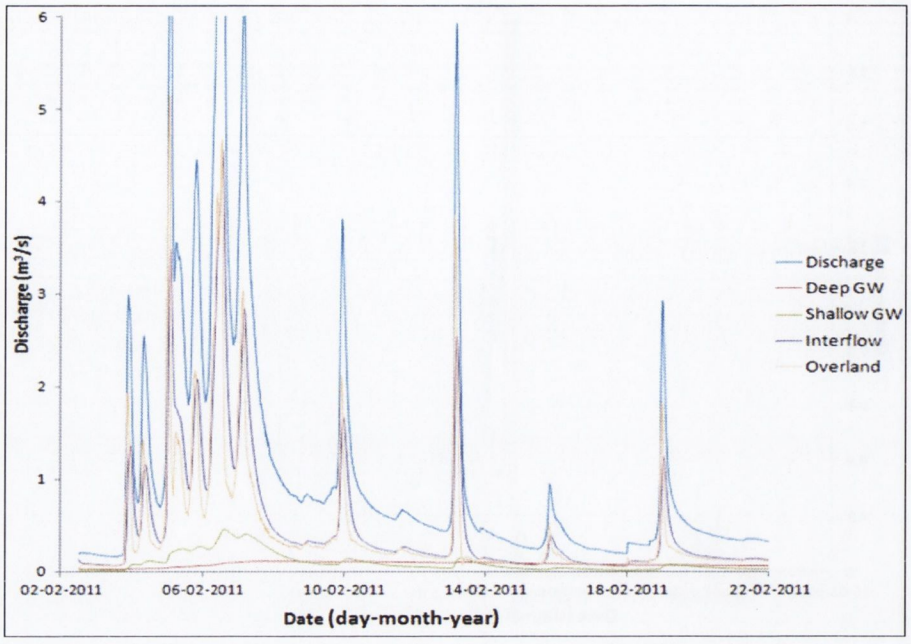

Figure 6-30. Mattock Berril's catchment modified Lyne and Hollick algorithm separations (Feb 2011 – Feb 2011).

6.4.2.4 Nuenna

The Nuenna, due to the karst nature of the regionally important aquifer, was not a suitable catchment for applying the modified Lyne and Hollick algorithm. The point recharge that directly enters the aquifer system through swallow holes in the catchment results in a much higher contribution of the groundwater pathways than was evident from the digital filtering approach. A modification would be required to the recharging structure of the algorithm in order to address this issue. As an example, Figure 6-31 was plotted to illustrate the underestimation of the groundwater contribution to the river at the Monument site. Conduit flow (applied here as an equivalent to shallow groundwater) is chosen as having faster response than diffuse discharge (equivalent to deep groundwater). These pathways are typically present in karst limestone catchments such as the Nuenna and behave quite differently to the matrix flow generally present in poorly productive aquifers in Ireland.

Monument

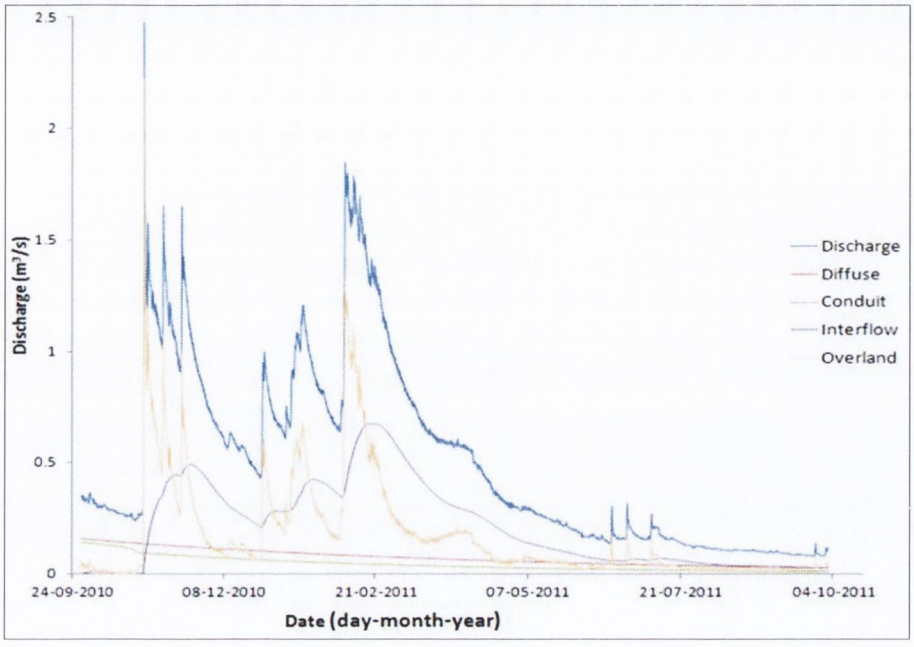

Figure 6-31. Nuenna Monument catchment modified Lyne and Hollick algorithm separations (Sept 2010 – Sept 2011).

6.5 Hydrograph Separation using Temperature Data

Within the Mattock, Nuenna and Gortinlieve catchments, temperature is being measured in the river and in the subsoil and groundwater within the clusters of boreholes. Each borehole is screened in order to sample water from each of the different active horizons within the geology of the catchment. This provides an opportunity to utilise the signature of the temperature time series of each pathway as a means of separating the hydrograph using temperature as a tracer in a simple mixing model. The application of geochemical tracers was discussed in Chapter 2 and while temperature would not be considered a geochemical, it provides a method of assessing the signatures of the pathways and not just their response times to rainfall in the same manner.

A river's temperature time series is conceptually described in this section as being comprised of different temperature signatures with relatively consistent frequencies. These are the annual mean, seasonal, diurnal and evaporation effects. These are separated by applying a time series signal analysis approach. An application of spectral

analysis to a data series enables the frequencies distinct from 'white' noise to be identified. 'White' noise is the data within a time series that is considered to have no systematic relationship to the data being measured and is representative of random error present in monitoring. Although there is an *a priori* understanding of the frequencies of the responses, Fourier analysis provides a means of verifying these assumptions.

6.5.1 Fourier analysis

Fourier analysis is applied to identify the frequencies of the signals that combine to form the original analysed time series. The *fft* (Fast Fourier Transform) function is used within a routine in MATLAB to identify these frequencies. The function `Y=fft(x)` implements the transform given for vectors of length N by:

$$X(k) = \sum_{j=1}^{N} x(j)\omega_N{}^{(j-1)(k-1)} \qquad \textbf{6-XII}$$

$$x(j) = \frac{1}{N}\sum_{k=1}^{N} X(k)\omega_N{}^{-(j-1)(k-1)} \qquad \textbf{6-XIII}$$

where

$\omega_N = e^{(-2\pi i)/N}$ is an Nth root of unity.

The 'spikes' in the output allow the frequencies of importance to be identified.

6.5.2 Temperature mixing model

Once the frequencies influencing the temperature had been identified in the temperature series, these were utilised to fit series to the signals in order to filter out noise present in the data. This assisted in reducing the effect of data gaps and periods of logger malfunction. These fitted signals were then utilised to provide the time series in a simple mixing model to identify the contribution of each pathway to the observed river hydrograph.

The mixing model applied was a simple conservative mass balance approach. River discharge, Q, is conceptually comprised of overland flow, interflow, shallow groundwater and deep groundwater, Q_O, Q_I, Q_S and Q_D respectively, Equation 6-V. This approach was implemented in conjunction with the simple mixing equation, with temperature being the tracer being mixed.

$$Q(T - T_W') = Q_O T_O + Q_I T_I + Q_S T_S + Q_D T_D \qquad \textbf{6-XIV}$$

where T, T_W', T_O, T_I, T_S, T_D are the temperature time series associated with river discharge, effect of the weather, overland flow, interflow, shallow groundwater and deep groundwater respectively.

6.5.3 Signal Identification

The analysis of each pathway's time series displayed distinct differences in the pattern of the time series. For example, there was little or no variation in the time series of the groundwater in the boreholes. Groundwater tends to have a long residence time and the aquifer is generally covered by an overburden of soil and subsoil that provides insulation from the effects of seasonal and diurnal temperature effects. These time series were characterised as having a mean value with little or no variation about this mean throughout the year. Interflow – considered here to be water originating from the subsoil – consists of a mean value, like the groundwater pathways, but with an associated seasonal variation about this mean. There were little or no diurnal or evaporation effects, but this water was reasonably 'new' and therefore still retains the seasonal variation associated with surface water. Discharge on the other hand, as it was influenced by all the pathways as well as ambient temperature effects and solar radiation was a composition of all the signals, namely the mean, seasonal, diurnal and evaporation effects. Therefore, this signal was not useful for spectral analysis as it was a composite of non-stationary signals that are not present all year round, particularly the more complex overland flow and interflow. It was assumed, however, that the pathway signals themselves maintain stationary signals of varying amplitudes that can be identified and approximated. These signals, once identified, can be applied to estimate the quantity of overland flow and interflow being contributed to the hydrograph.

Groundwater

The time series for groundwater, sampled from MK3 Deep, is displayed in Figure 6-32. Here, groundwater was considered to be a combination of shallow and deep groundwater as their temperature signature differed by less than 0.1°C on average. It was observed in Figure 6-32 that a single mean value will suitably describe this time series as there was little or no variation about a mean value of 10.6°C.

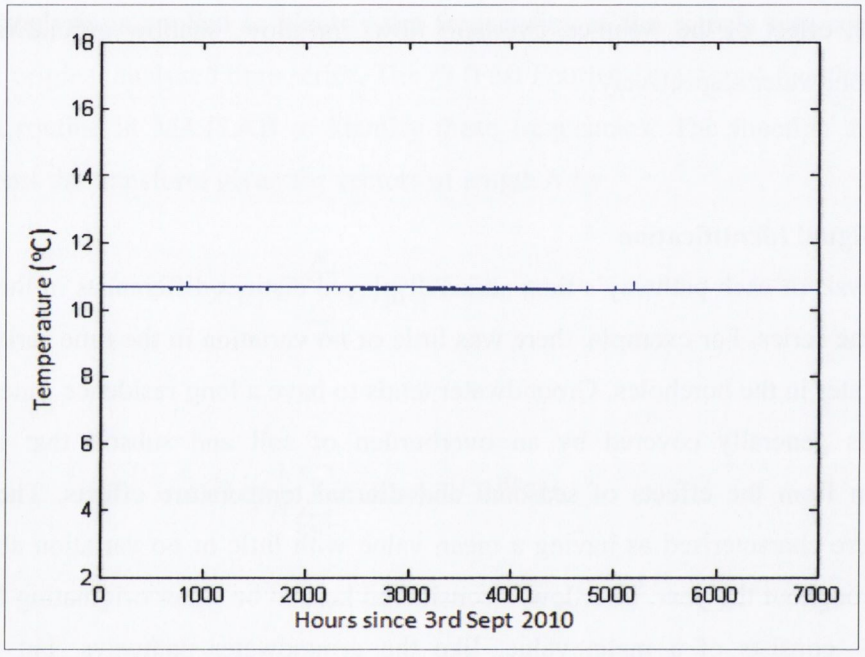

Figure 6-32. Mattock groundwater temperature time series from MK3 Deep.

Interflow

The interflow time series, sampled from MK3 Subsoil 1, was more typical of a time series consisting of a mean effect and the seasonal effects of winter and summer. This can be observed in Figure 6-33, where the temperature falls during winter and early spring, then rises to peak in late summer and early autumn before falling back again. The proximity of the water in the subsoil to the surface ensures that the water retained the seasonal effect but was generally insulated from the diurnal and evaporation effects of the ambient temperature that affected the river discharge.

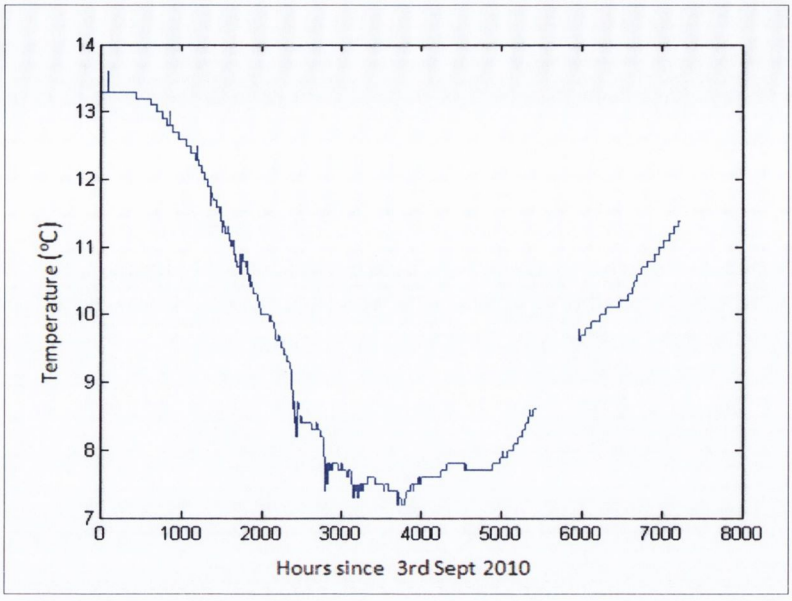

Figure 6-33. Mattock interflow temperature time series from MK3 Subsoil 1.

River

The river temperature time series at Berril's (Figure 6-34) contains the effects of the groundwater and interflow pathways, but also diurnal temperature and evaporation effects. This was a much more complicated signal than the other signals, with the Fourier analysis confirming the presence of the diurnal and 12 hour frequencies in the temperature time series. In Figure 6-35, we see the spikes in energy, highlighted by the red circles, occurring at approximately 0.041 and 0.08 cycles per hour corresponding to diurnal temperature and 12 hour evaporation frequencies, respectively.

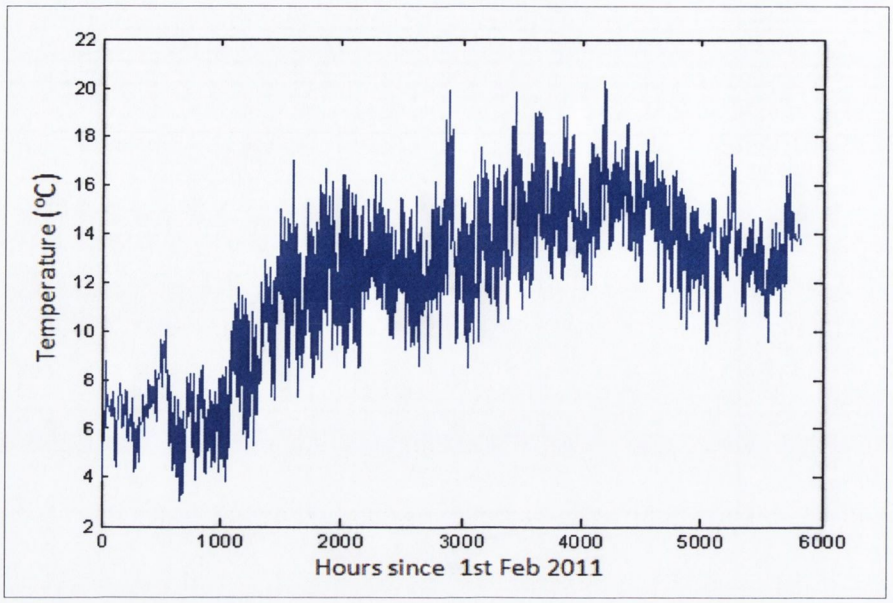

Figure 6-34. Mattock river temperature time series at Berril's.

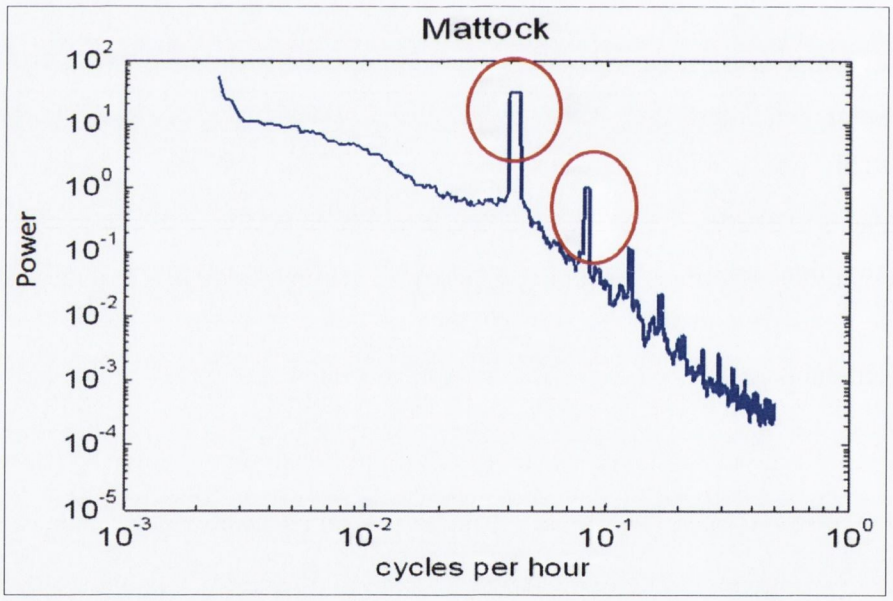

Figure 6-35. Fourier analysis of the Mattock river time series.

Weather

Figure 6-36 contains the weather time series obtained from Met Éireann for the Dunsany automatic recording station in Meath. These data (Figure 6-36) are measured hourly air temperatures.

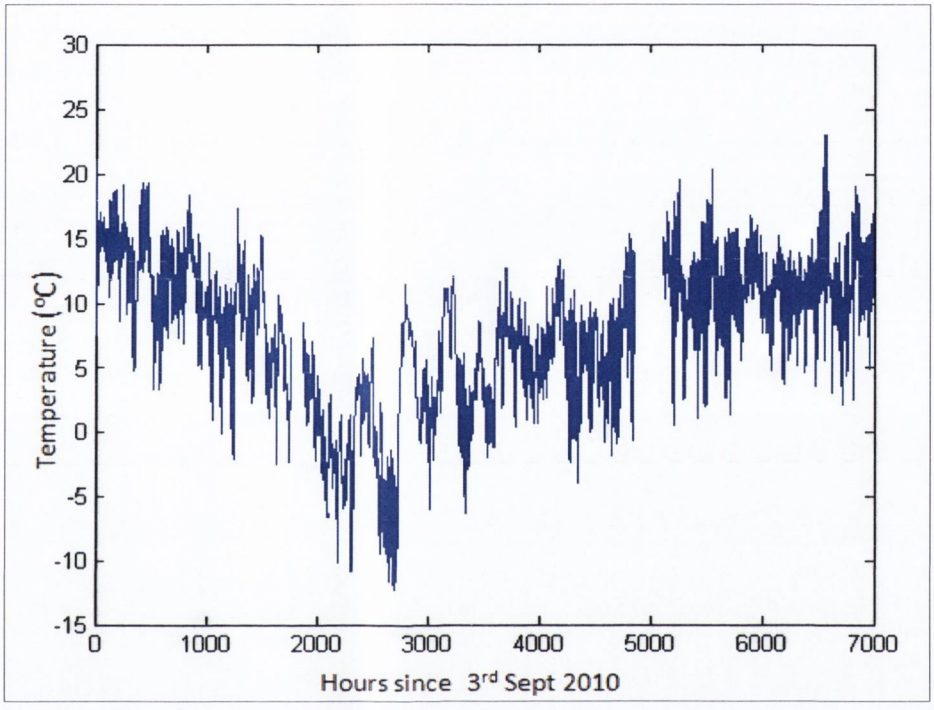

Figure 6-36. Dunsany ambient temperature time series.

Overland flow temperature time series

Once these signals had been identified in order to remove interference or 'white' noise, the pathways' time series were applied to represent the overland flow time series. This was achieved by approximating the effect that the weather time series has on the river temperature during baseflow conditions. Baseflow conditions were described as the periods of low rainfall where interflow and the shallow and deep groundwater pathways are maintaining the low flows of the river. The effect that the weather time series has on the river was considered to be analogous to the overland flow time series. Rearranging Equation 6-XIV, Equation 6-XV was utilised to calculate this effect, with the discharge of the groundwater pathways being used from analyses carried out in the catchment to

make this equation determinate, as the temperature time series of weather, interflow and shallow and deep groundwater had been measured in the field.

$$T_W' = (QT - Q_I T_I - Q_S T_S - Q_D T_D)/Q \quad \textbf{6-XV}$$

$$T_W{}' \approx T_O \quad \textbf{6-XVI}$$

This time series was related back to the original weather time series to represent the transfer function between the different components of the signals applying the *fmincon* optimisation routine programmed in MATLAB. In this way the overland flow time series and weather effect time series may be approximated from the weather time series outside of the baseflow periods. Figure 6-37 displays an example of the type of output obtained using this approach for the overland flow equation.

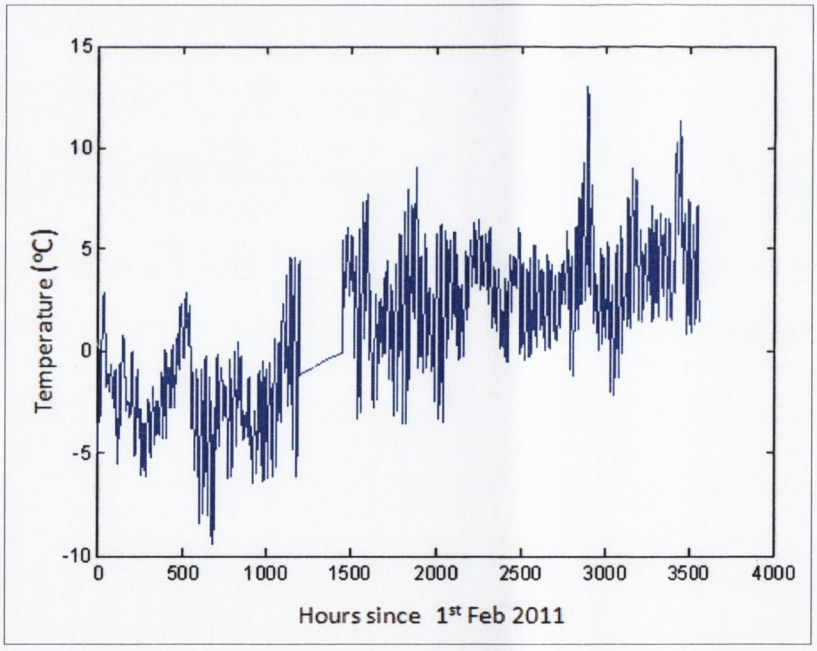

Figure 6-37. Mattock calculated overland flow temperature time series.

This temperature time series then was provided as input into Equation 6-XIV to calculate the proportion of the remaining hydrograph derived from overland flow and interflow. In this manner, provided that the contribution of groundwater was reasonably

constrained, the proportion of the quick flow response of a catchment may be apportioned between interflow and overland flow implementing temperature as a geochemical tracer. The temperature signature of the pathways can therefore be applied to separate interflow and overland flow responding at similar rates, such as may be the case when fields contain drainage in the soils and subsoils.

6.5.4 Results of hydrograph separation using temperature data

Applying temperature data as a physical tracer the hydrograph was separated into the different pathways contributing to the river discharge. A temperature separation algorithm was implemented in MATLAB to provide a means of determining the contributions of the different pathways to the hydrograph with temperature as the tracer. Implementing the separation approach on the Mattock catchment yielded the separations presented in Figure 6-38. This analysis suggests that interflow was the main flow pathway for the period February 2011 – June 2011 with overland flow only present during sharp rises in the hydrograph and rapidly receding thereafter.

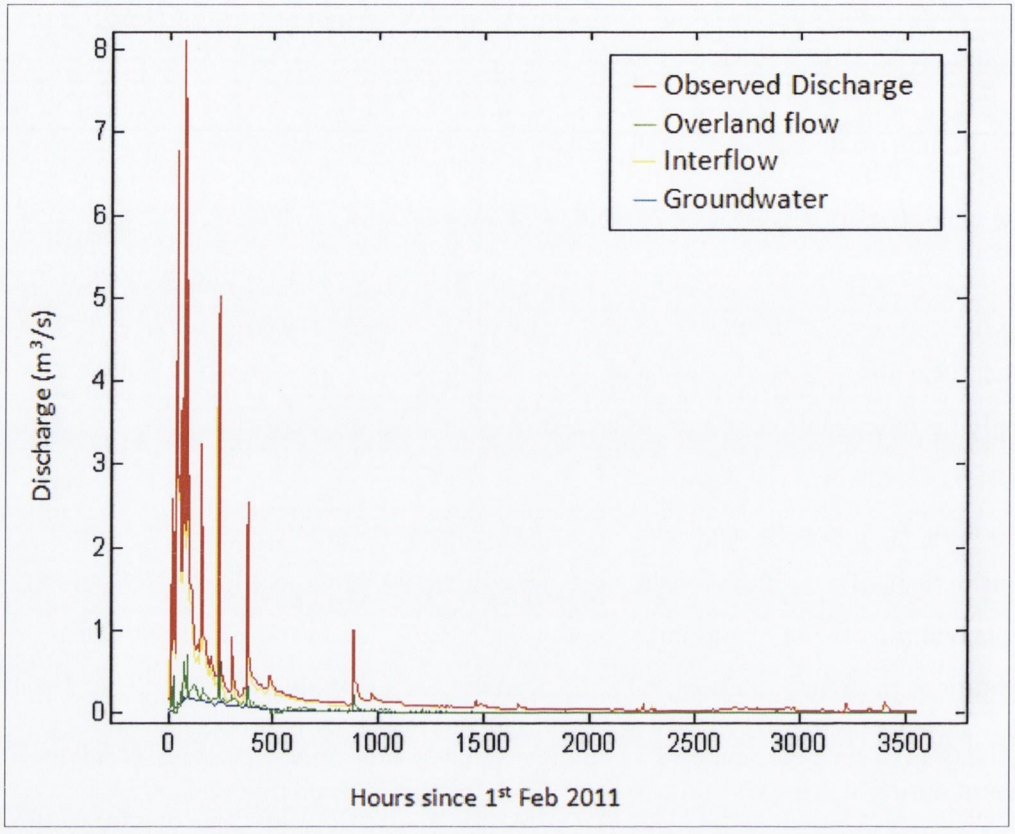

Figure 6-38. Mattock catchment temperature separations (Feb 2011 – June 2011).

The dominant interflow contribution to the hydrograph would suggest that there was a proportion of interflow that responded comparatively quickly to overland flow, as the other separation methods would suggest, but that it retains the temperature signature of subsoil water. The discharge in Figure 6-38 comprises of 68.3% interflow, a higher proportion than was computed using any of the other separation methods. This may be indicative of tile drainage in the soils and subsoils that was delivering water quickly to the river due to an increase in pressure gradients within the saturated zones near rivers when there was rainfall, or due to uncertainties present in the overland flow temperature time series as the temperature time series in this pathway was not measured.

6.6 Discussion

The different separation methods (recharge coefficient approach, master recession curve analysis, the modified Lyne and Hollick algorithm and the temperature separation technique) have been applied to the study catchments to ascertain the contribution of each pathway to the rivers' hydrographs. These separations are important as they provide constraints for the calibration of the hydrological modelling, as discussed in the following chapters. The overall performance of each approach is summarised in Table 6-1.

Table 6-1. Summary of the results of physical hydrograph separation approaches.

Catchment	Area (km^2)	Deep Groundwater		Shallow Groundwater		Groundwater	Interflow		Overland		Quick Flow
		MRC	Mod Lyne	MRC	Mod Lyne	Recharge Coeff[a]	MRC	Mod Lyne	MRC	Mod Lyne	Recharge Coeff[a]
		%	%	%	%	%	%	%	%	%	%
Gortinlieve	0.94	14.6	6	5.3	5.9	11.3	51.6	50	28.5	38.1	88.7
Glen Burn (Sub)	4.79	11.7	2.4	11.1	2.4	18.4	34.3	56.7	42.9	38.5	81.6
Glen Burn (Outlet)	5	11.7	3.4	10.4	3.5	18.9	43.8	62.8	34.2	30.3	81.1
Mattock (Div Weir)	6.99	8.5	8.8			23.1	49.6	52.2	41.9	39	76.9
Mattock (Collon)	11.61	12.9	7.4	15.8	7.6	23.1	33.7	45.8	37.7	39.2	76.9
Mattock (Berril's)	16.88	5.6	5	3.5	5.1	23	50.3	53.8	40.6	36.2	77
Nuenna (Castle)	10.24[b]	48.5		36		70.5	10.3		5.2		29.5
Nuenna (Rocky)	19.89[b]	51.4		40.3		82.2	6.5		1.8		17.8
Nuenna (Mon)	34.99	44.1		35.7		71.3	14.2		6		28.7

[a] Recharge coefficient approach used to separate into quick (interflow and overland flow) and slow (deep and shallow groundwater) pathways, they are placed under deep groundwater and Interflow, respectively, for convenience.

[b] Refers to equivalent catchment areas calculated using the Water Balance.

6.6.1 Recharge coefficient approach

Applying the approach outlined in Section 6.2, recharge coefficients were classified for each of the four catchments for each soil, subsoil and aquifer combination. The effective rainfall for the year was calculated from the water balances, and verified using observed discharges. The recharge cap limits of 200 mm and 100 mm per annum were placed on the local and poorly productive aquifers, respectively, in line with previous practice. Using this information, the total recharge expected (and conversely, the quick

flow contribution), was calculated for the four catchments. This method provided initial estimates for the combined shallow and deep groundwater flow pathways, and combined interflow and overland flow pathways. The three 'flashy' catchments were predicted as having a much lower groundwater input compared with the quick flow pathways. In the Nuenna catchment, however, while predicting a large groundwater input, the standard approach was inclined to underestimate the recharge that will occur. This was due to point recharge not being accounted for, and therefore invalidates this approach for catchments in which a considerable proportion of the recharge occurs as point recharge. When the adapted method was applied, with the surface catchments draining to swallow holes assigned a recharge coefficient of 1, the recharge coefficient of the catchment increased towards a more realistic value. The area to the north of the river has a lack of surface water channels much like the area to the south, and it is likely that there may be more swallow holes in this region, which is supported by anecdotal evidence from local landowners, but as yet these have not been mapped. Should these be identified in the future, it would be likely that these would bring estimates of groundwater contribution to the river in line with the MRC results in Table 6-1.

The results of Gortinlieve, Mattock and Nuenna as a whole were compared with those computed using the draft recharge map provided by the GSI. There were comparable recharge coefficients calculated for areas of land within each catchment not constrained by a recharge cap due to a poorly productive aquifer underlying the area. When a recharge cap was required there were discrepancies due to different calculations of effective rainfall that directly influence the recharge coefficient due to the contribution to the groundwater pathways being calculated as percentages of hydraulically effective rainfall. These differences in effective rainfall were as a result of the methods applied to calculate the annual rainfall and the AE. In this thesis, rainfall data were collected from the catchment over the period of the research and AE was calculated using the FAO Penman-Monteith outlined in Chapter 5. The recharge map bases the annual recharge on 30-year average Met Éireann data from the nearest station and takes AE as a fixed percentage of PE. While this is a useful approach to obtain a quick estimate of AE, yearly fluctuations of rainfall, differences between locations of rain gauges and variation in AE annually should be taken into account if possible.

6.6.2 Master recession curve analysis

The MRC analysis was able to identify the four pathways in every catchment and subcatchment except for the Diversion weir subcatchment in the Mattock. As previously discussed this was probably due to the similarity of the response times of both groundwater pathways (or the possibility that only one pathway was present) and the length of discharge time series available. The results for the three 'flashy' catchments were generally the same, with overland flow and interflow being responsible for the majority of the discharge observed in the river. The opposite was true for the Nuenna, where groundwater dominates, and as such, the majority of the river discharge was calculated to be from slow and fast diffuse groundwater pathways in all three subcatchments. The Tabulation method and the Matching Strip method assigned comparable values of k to the groundwater pathways but the Tabulation method provided more plausible k values for the faster responding pathways due to the extra emphasis this method places on identifying these pathways. Due to the Tabulation method providing more physically feasible values of k, the Tabulation k values were then used for the modified Lyne and Hollick algorithm. This method was also used for calculating the relative contributions of each pathway, with the results of this approach summarised in Table 6-1.

6.6.3 Modified Lyne and Hollick algorithm

The modified Lyne and Hollick algorithm was applied to all the catchments and subcatchments, except for the outlet at Gortinlieve. As previously mentioned, this algorithm was based on the assumption of discharge receding for interflow and shallow and deep groundwater as if discharged from a linear reservoir. This assumption was most applicable to the groundwater pathways and hence, it is considered that this method has most merit in estimating the groundwater pathways contributions. This algorithm was conservative in nature as any type of recharge bypassing the interflow soil and subsoil horizons was omitted. Therefore, estimations from this algorithm are best considered as an indication of a lower limit on the shallow and deep groundwater pathway flows. The focus of this algorithm was on the groundwater pathways, with indicative contributions of the quick flow pathways to the river hydrograph being provided. However, it is observed in Table 6-1 that the interflow and overland flow,

calculated using this method, are similar to the values from the MRC separations. The three 'flashy' catchments were observed to be dominated by the quick flow pathways using this method. Disappointingly, the dominant groundwater contribution in the Nuenna catchment was not reflected by the algorithm which was again attributed to the point recharge that occurs via swallow holes located in the Castle subcatchment that drain mini-catchments. This point recharge was unaccounted for in the algorithm. This approach is therefore not applicable in catchments where significant point recharge occurs.

6.6.4 Temperature separation

The temperature separation results imply that interflow is the most important contributing pathway in the Mattock catchment. While the groundwater contribution was based on the other separation methods, the interflow and overland flow pathways were apportioned according to their temperature time series. There were uncertainties associated with the overland flow temperature time series, potentially resulting in an overestimation of interflow due to the lack of temperature data for the overland pathway. The striking dominance of interflow in this analysis though, would suggest that interflow was being underrepresented by the physical hydrograph separation methods which base their separations on response times of the pathways, rather than using tracers along those pathways. This result would suggest that part of the interflow was responding as quickly as overland flow during events. This may be due to the effect of land drains that are prevalent throughout the Mattock which have been installed by landowners over numerous generations owing to the poorly draining nature of the soils and subsoils. Therefore, while parts of interflow and overland flow seem to show similar response times, making them indistinguishable using the physical separation methods, they have very different temperature signatures and most likely, chemical signatures. This suggests that in order to further separate the 'perceived' overland flow, based on the observed response times, into overland flow and interflow, tracer or chemical analysis will be required in catchments like the Mattock. It should be noted that end member mixing analysis using chemical tracer data is currently being undertaken as part of the overall *Pathways Project* and the results will later be used to refine the flow separations based on the physical methods described in this thesis.

6.6.5 Conclusion of physical hydrograph separations

The separation of the river hydrograph into the contributing pathways using the physical separation techniques was based on the response times of these contributing pathways, with the exception of the temperature separation approach. If two pathways or portions of pathways are responding similarly as the temperature separation approach suggests, post processing of these results is required for attenuation modelling. This must be directed by either chemical or attenuation analysis as hydrological modelling, particularly lumped modelling, is based on response times to identify different contributions.

After individually assessing the results of each of the separation techniques, they were evaluated as a whole. Reviewing the separations in Table 6-1, it can be seen that there is a general agreement in the separations for the groundwater pathways applying the different physical separation techniques. There was good agreement between the combined interflow and overland flow pathway contributions for the different methods. It was also observed that in a karst environment, the modified Lyne and Hollick algorithm was not applicable in its current form. Therefore, the separations in the Nuenna were reliant on the MRC analysis and the recharge coefficient approach, which appear to perform well and their separations were in close agreement once the modified recharge coefficient approach had been adapted to allow for point recharge. This table is reappraised later in Chapter 7 following the outcomes of the hydrological modelling which will provide more insight into the contributions of the pathways to the river hydrograph.

7 Lumped Hydrological Modelling

7.1 Introduction

This chapter examines the application of the hydrological model NAM, a lumped model that averages the spatial variability of a catchment and treats it as a single equivalent unit. As such, all of the lumped model's parameters are reflective of an average characteristic behaviour of the catchment. Typically, for each time step one rainfall and one evapotranspiration value is all that is required for the model to function. NAM is described in detail here as are the preprocessing methods required for the input data and the steps involved in simulating the separated discharges, with the results of this modelling presented in Section 7.5 and Section 7.6 and discussed in Section 7.7.

NAM was applied to the four study catchments, with observed discharge and the overall water balance of the catchment being utilised to calibrate the model parameters implementing the auto-calibration routine. At least one year of data was provided for the calibration period as this would be necessary for the assumption of negligible storage change to be valid for the water balance objective function. Simulations were carried out with the smallest time step of rainfall data available. This allowed for improved simulation of peaks in quickly responding catchments, as considered in Section 7.4.2, particularly in the fast responding catchments of Gortinlieve, Glen Burn and the Mattock. The results of NAM modelling calibration are summarised in Table 7-2, with a validation of its ability to predict total discharge summarised in Table 7-3.

Different objective functions were utilised in order to assess the ability of NAM to simulate the observed discharges in a catchment. The Nash–Sutcliffe R^2 value (Nash and Sutcliffe, 1970), calculated with Equation 7-I, was applied to assess the goodness of fit for the simulated against the observed discharge:

$$R^2 = 1 - \frac{\Sigma(Q_{obs} - Q_{sim})^2}{\Sigma(Q_{obs} - Q_{mean})^2} \qquad \textbf{7-I}$$

where Q_{obs} is the observed discharge recorded in the river [m^3/s], Q_{sim} is the simulated discharge from NAM [m^3/s] and Q_{mean} the mean of all the observed discharges [m^3/s].

This allows the variance of the difference between the observed and simulated discharges to be compared with the variance of the observed discharge. A value of 1 is a perfect fit while a value of zero suggests the model values would perform as well as the mean of the observed discharges. A value of less than zero suggests the mean of the observed discharges would actually do better.

The assessment of fit, applying the Nash-Sutcliffe approach, is more weighted towards the higher discharges that the lower discharges. In order to address this, the square-root of each term in Equation 7-I provides an objective function that is weighted towards the low discharge conditions. Equation 7-I is altered as follows:

$$\sqrt{R^2} = 1 - \frac{\Sigma(\sqrt{Q_{obs}} - \sqrt{Q_{sim}})^2}{\Sigma(\sqrt{Q_{obs}} - \sqrt{Q_{mean}})^2} \qquad \textbf{7-II}$$

Bias was also assessed to evaluate the overall balance between the observed and simulated discharges:

$$Bias = \frac{\Sigma(Q_{obs} - Q_{sim})}{n} \qquad \textbf{7-III}$$

where n is the number of observations of discharge. Here a value of zero is the optimum with values less than and greater than this signifying a difference between the total observed and total simulated discharge for the simulation period.

While a good fit between the observed and simulated discharge was an important objective of the modelling, applying the physical river hydrograph separation method results of Chapter 6 to guide the optimisation of the parameters was vital to ensure the separations were consistent with the catchment setting. This will typically affect the R^2 values negatively but was a necessary compromise. Examples of the observed discharge versus simulated discharge, the simulated separated pathways and the subsurface pathways are presented for each catchment in Section 7.4. The subsurface pathways are displayed separately in order to view their responses that are difficult to observe at the scale when all the pathways are included.

7.2 NAM

The Danish 'Nedbør-Afstrømnings-Model' was developed by the Department of Hydrodynamics and Water Resources at the Technical University of Denmark (Nielsen and Hansen, 1973). It is a deterministic, lumped, conceptual rainfall–runoff model used to simulate the hydrological cycle. Due to the versatility of its structure it has the capacity to simulate the four pathways required by the conceptual model employed in this research (see Chapter 1). NAM has been applied in Ireland previously in several catchments as part of a study concerned with groundwater-surface water interactions (RPS, 2008). The conceptual model followed in that earlier study was a simpler three-pathway (overland, intermediate flow and groundwater) model compared with the four-pathway conceptual model of this research. NAM is considered to be a very useful tool in catchment modelling in the Irish setting as it can simulate the four separate flow pathways, while the model's lumped approach does not require the same degree of data required by a distributed model. As will be seen in Chapter 8, this level of data is not generally available either at the required temporal or spatial resolution for Irish catchments and so this lumped approach is considered appropriate. The NAM model also has the flexibility to be adapted to the variable geological settings encountered in Ireland. The NAM structure is presented in Figure 3-4, while a simplified schematic of the NAM is displayed in Figure 7-1.

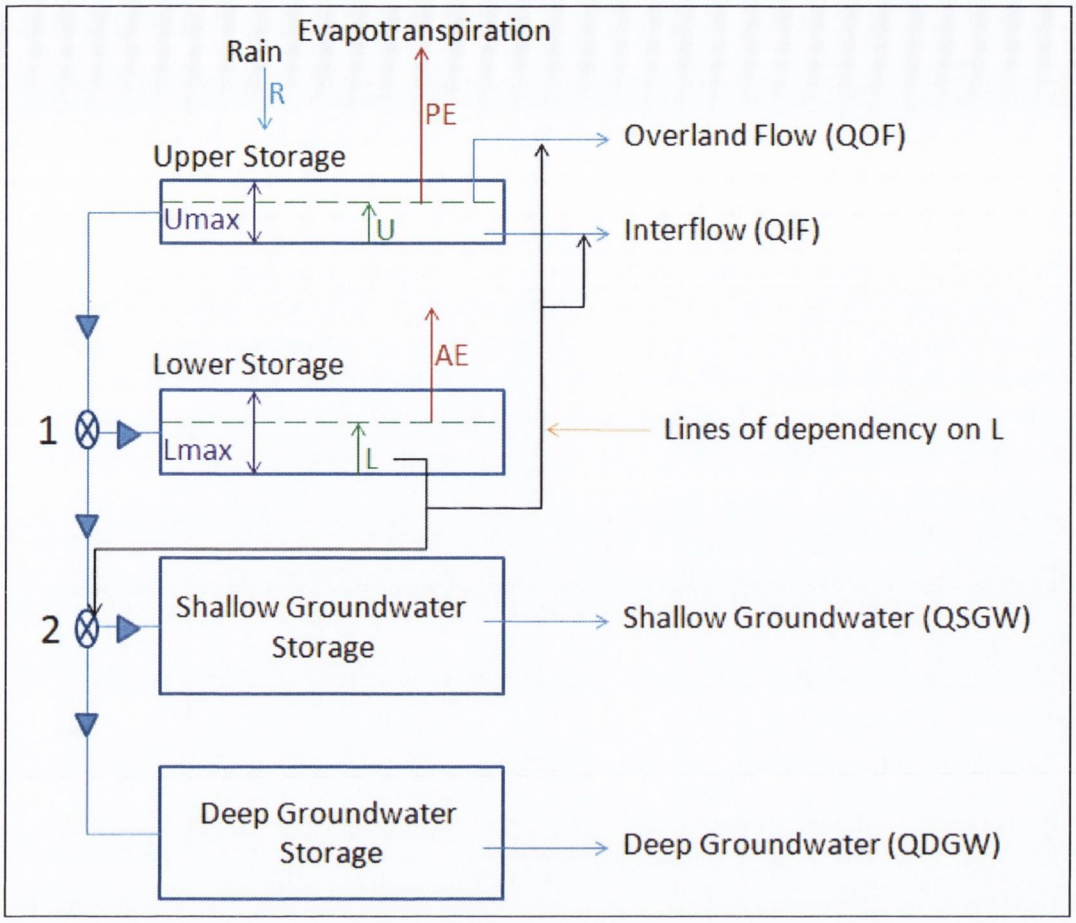

Figure 7-1. Simplified NAM structure schematic.

NAM simulates flow using rainfall and potential evapotranspiration (PE) as inputs to the model, with observed discharge being utilised to calibrate the flows generated. The temperate climate of Ireland permits the snow module option to be omitted from the model structure for these modelling studies, as shown in Figure 7-1.

Overland and interflow pathways

As rainfall occurs (*R* in Figure 7-1), water enters into the upper storage reservoir. From this reservoir, water is discharged as interflow (*QIF*) once the proportion of the lower storage (*L*) is above the interflow threshold, which is then routed through two linear reservoirs. Overland flow (*QOF*) occurs when the upper storage fills to its capacity (*Umax*) and L is above the overland flow threshold. This is also routed through a linear reservoir, but unlike interflow, this reservoir has a variable time constant, *CK*, value.

Excess water from the overflowing of the upper storage that is not released as overland flow, infiltrates into lower storage and groundwater storages. The amount of excess water recharging these storages is dependent upon the proportion of the lower zone storage that is filled ($L/Lmax$). The excess water that does not recharge the groundwater storages or is lost as overland flow enters into the lower zone storage where it can only be lost by evapotranspiration. This calculation occurs at valve 1 in Figure 7-1.

Evapotranspiration occurs at the potential rate from the upper storage, as water is readily available here, and at an actual rate, related to the proportion of the lower storage that is filled, from the lower storage according to Equation 7-IV:

$$AE = (PE - U)\frac{L}{L_{max}} \qquad \textbf{7-IV}$$

This is analogous to the approach used in Chapter 5 to calculate AE where AE is less than PE when PE is greater than U, i.e. when there is not enough easily-available soil moisture.

Shallow and deep groundwater pathways

In order to simulate the shallow and deep groundwater pathways of the conceptual model, the groundwater storage can be split into two separate storages, shown in the NAM schematic in Figure 7-1. This facility is contained within the NAM structure. Recharge is then apportioned between the two storages by the parameter CQ_{Low} (schematically shown as valve 2 in Figure 7-1) with each having a different τ value (time constant that defines the rate of discharge from a linear reservoir, see Chapter 2) to represent the different response times of each pathway.

There are 11 empirical parameters associated with these storages and outflows. The sizes of the upper storage and the lower storage are U and L respectively, measured in millimetres. $CQOF$ is the parameter that calculates the percentage of available excess water which runs off as overland flow. This has a value between 0 and 1. $CKIF$ is the parameter that calculates the amount of interflow that is released from the surface storage which is related to the interflow time constant value. Both of the groundwater storages have τ values that define the rate of release of groundwater from the deep and shallow groundwater storages, $CKBF$ and CK_{Low} respectively. The distribution of recharge to each of the groundwater storages is also defined by CQ_{Low}. Three

parameters *TOF*, *TIF* and *TG* all define thresholds that must be surpassed by the proportion of the lower zone storage that is filled in order for overland flow, interflow and recharge, respectively, to occur. These have a value of between 0 and 1.

As there are 11 parameters within the model that can be calibrated, there is a danger of equifinality of optimised solutions during the calibration process. Equifinality is the risk of there being many very different sets of solutions that give 'nearly' as good fits for the simulated and the observed flows. This is where the value of the hydrograph separation techniques described in Chapter 6 is apparent as they provide further means of constraining the calibration of the NAM model simulations. In addition to using the hydrograph separations to guide the selection of these parameters, the more parameters that can be based on observable data from the field, the lower the risk of equifinality distorting inferences made for generalisations of catchments. For example, *CQOF*, in conjunction with the *TO* and *TG* parameter values, will have a relationship with the recharge coefficient as these parameters affect recharge to the groundwater storages. The MRC analysis will also assist in determining the time constants *CK*, *CKBF* and CK_{Low} as these are related to the reciprocal of the retention time τ value in the fitted equations to the recessions of the pathways.

7.3 Preprocessing Data

The input data necessary for a hydrological model to function usually require a degree of preprocessing. This can take many forms such as calculating composite values from multiple observation points; removing suspect data due to instrument malfunction; filling of data gaps using surrogate data from elsewhere and computation of catchment size from available GIS data.

7.3.1 Rainfall

The NAM model requires a rainfall value, composed of the averaged rainfall from rain gauges located in and around a catchment being modelled, for each time step of the model. This is generally calculated using three different approaches. There is the simple arithmetic mean of the rain gauges where all the data from each rain gauge for the

required interval are summed and then divided by the mean to produce the rainfall value, Equation 7-V:

$$\frac{1}{n}\sum_{i=1}^{n} R_i \qquad \text{7-V}$$

where R is the rainfall value [mm], i is the rain gauge being assessed, and n is the total number of rain gauges being assessed.

The next approach is the widely implemented Thiessen polygon method, which was adopted for this research. In this method rainfall gauge locations were connected by lines to form polygons. Perpendiculars were then drawn at the midpoint of each of the rain gauge connecting lines, and the intersection of these perpendicular lines then formed areas around each of the rain gauges, as shown in Figure 7-2. The rainfall value in the model was then calculated according to Equation 7-VI:

$$\frac{\sum_{i=1}^{n} R_i A_i}{\sum_{i=1}^{n} A_i} \qquad \text{7-VI}$$

where A_i is the area [km^2] related to the rain gauge R_i. This method was implemented using a simple routine in ArcGIS.

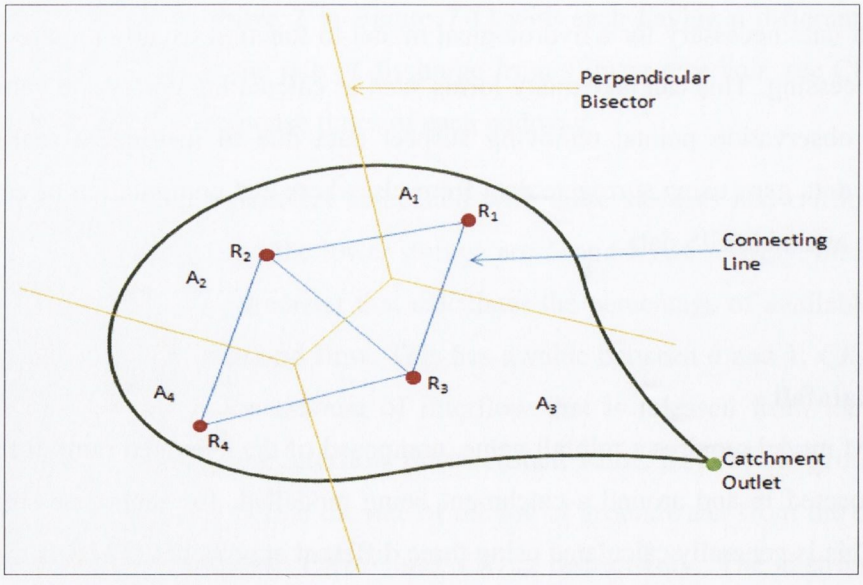

Figure 7-2. Thiessen polygons.

The final method is the isohyetal method. Unlike the standard Thiessen polygon approach, which is purely objective, this method could account for the effects that elevation and other location factors have on rainfall by interpolating rainfall amounts between rain gauges at selected intervals. Equal rainfall values were then connected to form lines of equal rainfall, isohyets, as illustrated in Figure 7-3. The rainfall to be used in the model was then computed according to Equation 7-VII:

$$\frac{\sum_{i=1}^{n} A_i P_i}{\sum_{i=1}^{n} A_i} \qquad \text{7-VII}$$

where P_i is the rainfall related to A_i.

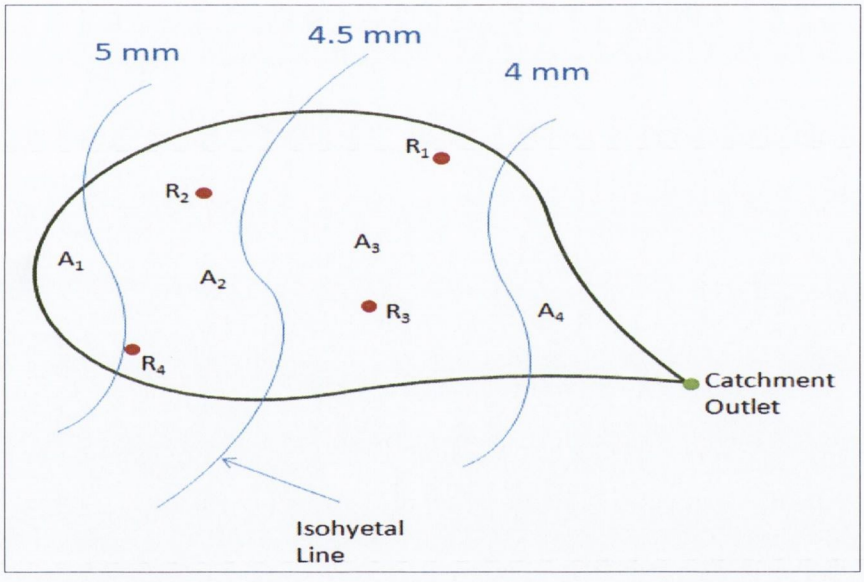

Figure 7-3. Isohyetal method.

This method can be subjective in the manner by which the isohyets are drawn. It generally requires many nearby rain gauges to construct the isohyets even subjectively. The relationship may not be static either between the rain gauges and may require the development of a new isohyetal map for different rainfall time steps. As there were generally two rain gauges available for each catchment, at most, the Thiessen polygon method was applied to all four catchments.

7.3.2 Potential Evapotranspiration

Ideally, the distribution of PE would have been processed in the same manner as the rainfall data but due to the limitations on the availability of PE instrumentation – only one value of PE was available for each catchment – no averaging technique was required. The PE value was taken from the nearest Met Éireann synoptic station or, in the case of the Glen Burn catchment, from the weather station located within the catchment. The data available from the Met Éireann synoptic stations only had a temporal resolution of 1 day, which introduced a substantial error in the estimation of effective rainfall when 15 minute rainfall data were being utilised. The daily value, when inputted into NAM, could be distributed evenly across the 96 time steps to form a 15 minute dataset across each day. However, data applied in this manner give the same PE values at night as in the daytime, a very unlikely situation in reality. In order to address this issue, the Gaussian function (Equation 7-VIII) was applied to the data to distribute these normally over the day with the peak occurring at 13:00, the estimated time of the PE peak during the day (Ben-Gal et al., 2010). Ireland's average daylight hours during June are 16.7 hours and 7.4 hours during December (Met Éireann). Using these values to estimate a mean of 12 hours for the year, the standard deviation of the distribution for Equation 7-VIII required was 2 hours as three standard deviations encompass approximately 99.7% of the Gaussian probability density function (i.e. 99.7% of the time when PE will be occurring):

$$f(x) = \frac{e^{-\frac{1}{2}\left(\frac{x-\mu}{\sigma}\right)^2}}{\sigma\sqrt{2\pi}} \qquad \text{7-VIII}$$

where x is the hour of the day for which the probability is being computed, μ is the hour of the day at which the peak is said to occur [13:00] and σ is the standard deviation of the function [2 hours]. The recorded daily PE data apply to the time period from 9am the previous morning to 9am of the morning of the day the data are associated, and so the distribution of PE for these daily values matched this time frame. An example of Equation 7-VIII applied to a daily value of PE is illustrated in Figure 7-4. As can be observed, the peak value at 1 pm was 0.2 of the PE value for that day compared with a value of 0.042 if the data had been simply averaged equally across the 24-hour period. Once the daily data had been transformed to hourly values, these were inputted into NAM, where the soil moisture budgeting routine, outlined in Section 7.2, calculated the AE.

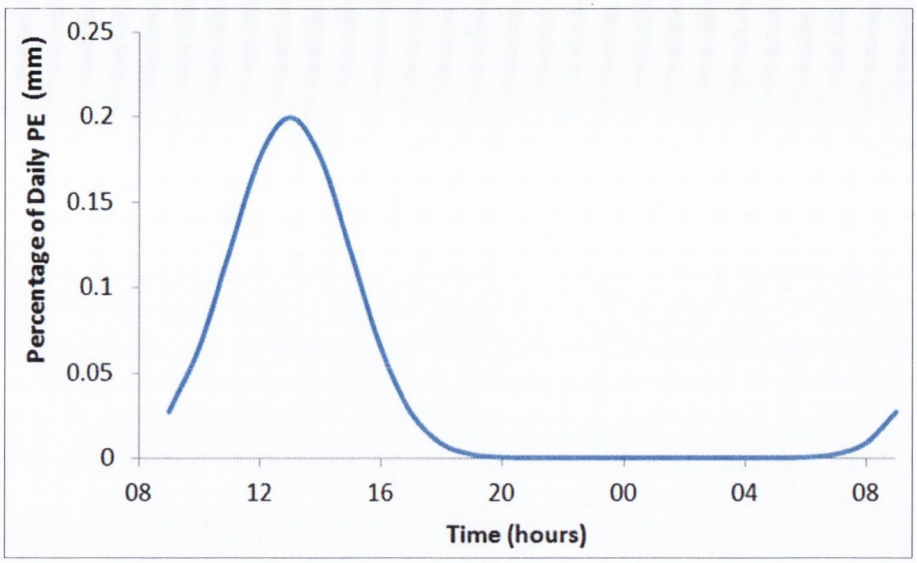

Figure 7-4. Distribution of PE throughout a day.

7.3.3 River discharge

The preprocessing required for the river discharge data in the study catchments was minimal once the water balance had assessed that the rating curves for the different hydrometric stations were reliable. This work is outlined in Chapter 5. Before inputting discharge data into the model, suspect data that had been identified using field data measurements at staff gauges, during flow gauging and logger downloads, were removed. Examples of this from the Collon Weir in the Mattock is shown in Figure 7-5. Here the unusual step up and then subsequently down on the February 8th 2011, and the vertical step in discharge on February 15th, suggest the stage was being incorrectly monitored. Data after February 17th February were actually removed by the EPA hydrometric team as a result of silting at the stilling well. The data marked in black were removed based on the discharge data from the corresponding period at Berril's and Diversion weir hydrometric stations indicating inaccuracies in the data.

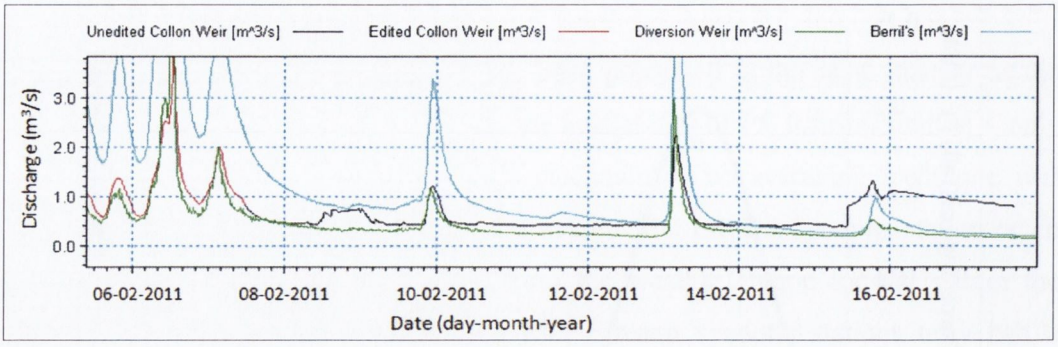

Figure 7-5. Mattock hydrometric discharges from February 2011. Edited discharge at Collon Weir shown in red, having removed suspect discharge data, shown in black. Diversion Weir and Berril's hydrometric station discharge data used as guidance.

7.3.4 Catchment Area

The size of catchment must be specified within the NAM model in order to provide the equivalent volume of the water that the catchment receives as rainfall and loses as evapotranspiration. This is an important parameter that is necessary to achieve an accurate water balance and satisfactory simulations of discharge. Within NAM there are essentially two catchment area constants; the first constant, *model area*, that corresponds to the topography of the catchment and generally is of most consequence to the overland flow and interflow pathways; the second constant, C_{area}, is related to the groundwater pathways. C_{area} relates the groundwater catchment area to the topographical area as a ratio. A value of unity sets the two areas as equivalent, whereas a value greater than 1 implies a groundwater catchment that is C_{area} times larger than the topographical catchment.

The topographical area was calculated using DEM data to delineate the different cells that contribute water to the catchment outlet based on the slope of the land. The DEM datasets contained elevation values for each 20 by 20 m cell. The processing of these data involved calculating the slope between a cell and the eight neighbouring cells, as depicted schematically in Figure 7-6. The cell being examined is highlighted in blue with an elevation value of 93 m above datum. The eight neighbouring cells are assessed, with 75 m above the same datum being the cell with the lowest value, highlighted in orange. Therefore, on the basis of slope, water will flow from the middle blue cell to the orange cell as illustrated by the red arrow. The chains of cells that contribute to the outlet of a catchment or subcatchment were identified in this manner

and hence the area occupied by these cells was defined by the topographical catchment area.

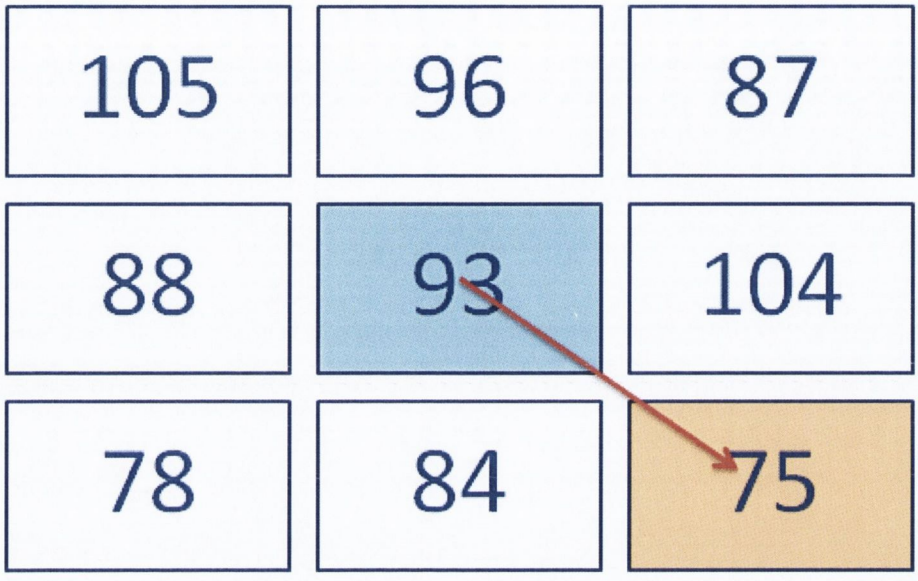

Figure 7-6. DEM cell with neighbouring cells.

In most instances the groundwater catchment area was assumed to be coincident with the topographic area. While this was unlikely to be the case at every point around the perimeter of the topographical catchment, it was deemed to be satisfactory as an overall assumption. Previous studies in catchments or distributed modelling, such as the MODFLOW modelling described in Chapter 8, can help to determine a more accurate groundwater catchment area to inform C_{area}. The water balances carried out in Chapter 5 also assisted in determining the appropriate area for the catchment. In the case of the Nuenna catchment, the catchment area was approximated utilising the water balance due to the influence of the swallow holes in the upper area of the Castle Weir subcatchment.

7.4 Model Execution

Once the rainfall, PE, discharge and catchment area had been inputted into the model, it was ready to be initialised and run. This was all carried out through a graphical user interface (GUI) whereas the sensitivity analysis applied to the catchments, (implemented in Chapter 10) was undertaken through MS-DOS command lines.

7.4.1 Parameters

The 11 parameters outlined in Section 7.2 were assigned initial values based on observations taken from the physical separation approaches, the NAM user guide and decision tables outlined in the Groundwater-Surface Water Interaction report by RPS (2008). While these provided a useful starting point, the values suggested in the user guide and interaction report were based on simpler conceptual models and tended not to be entirely consistent with the one employed in this thesis. A value for CQ_{Low} was also selected when a deep groundwater pathway was identified from the physical hydrograph separation work carried out in Chapter 6, otherwise it was left inactive with a value of zero. Some parameter values could be inferred from analysis, such as time constants within NAM being informed by the MRC analyses. Even if, hypothetically, all parameters could be measured, it has generally found elsewhere that the results have not been entirely satisfactory, even when using an intensive series of measurements of parameter values (Beven, 2001). As such, sensible initial values were based on physical hydrograph separations, the model structure itself and, where possible, the user guide and RPS report. These initial values were applied, though calibration was still required to improve simulated results.

7.4.2 Preliminary modelling

The study catchments were instrumented over a period of time beginning during the summer of 2010. While sufficient data were not available initially in the study areas to apply the physical hydrograph separation methods outlined in Chapter 6 and the modelling described in this chapter, a number of other catchments were analysed. Four of these catchments, Balycahalan, Owneshree, Owendullalagh and Bawn (details of which are summarised in Appendix A), were of particular interest. Fifteen minute

rainfall and observed discharge data were available for the Balycahalan, Owenshree and Owendullalagh catchments, while hourly data were available for the Bawn catchment. These high resolution temporal data allowed the ability of NAM to simulate peak flows to be evaluated in quick-responding catchments such as these (their 'flashy' behaviour is due to their mainly poorly draining soils and subsoils). This was achieved by applying different temporal resolution rainfall data. NAM was implemented for each of these catchments using 15 minute, hourly and daily rainfall data, with the exception the Bawn where hourly rainfall was the minimum time step. These catchments were all under 100 km^2 in area (the Bawn catchment was the smallest at 5 km^2).

An example of the performance of NAM in simulating observed flow peaks using different frequency rainfall input data is illustrated in Figure 7-7 for the Owendullalagh catchment. For this rainfall event the effectiveness of the three different rainfall temporal resolutions is evident. Daily rainfall is unable to simulate the quick responding nature of the peak, with three different points defining the event: one before the discharge rises; one point at the peak and another when the discharge has receded back to low flow conditions. The hourly and 15 minute rainfall input data, however, allow NAM to perform much better at simulating the peak flow. This is due to the rainfall being recorded as occurring when the hydrograph is rising and not just providing an average hourly value as before. The hourly simulation rises quickly but still not quick enough to match the observed discharge, suggesting that even hourly averaged rainfall does not allow NAM to simulate the quick response of the hydrograph. Unsurprisingly, the 15-minute data simulate this peak the most accurately of the three resolutions, in which the simulated increase in discharge and subsequent recession are in reasonable agreement with that observed data. In this case, rainfall is being recorded before the hydrograph rises, allowing NAM to simulate the quick responding nature of the event. Also of interest in Figure 7-7, is the dip in the simulated discharge at the peak for both hourly and 15 minute rainfall. This suggests that the rainfall measured in the catchment did not record further rainfall, causing the observed peaks to further increase. This highlights the need for accurate input data in order for the model to satisfactorily simulate discharge.

These different simulations were then assessed applying the R^2 objective function outlined in Section 7.1. The results of this are summarised in Table 7-1 along with

preliminary modelling results from the Nuenna (a slow responding catchment) for comparison. There was a marked increase in the model performance when implementing NAM with hourly rainfall data compared with when daily data was applied. There is another increase in performance when using 15 minute data compared with hourly data, but not as significant as the increase in R^2 when moving from daily to 15 minutes. The Bawn does not have any result for 15 minute rainfall data as this was not available for the catchment. The Nuenna however, behaves very differently, there is no marked increase in R^2 from daily to 15 minute data. This is as a result of the Nuenna being dominated by groundwater, which generally takes longer than 24 hours to respond. This is discussed further in Section 7.7.

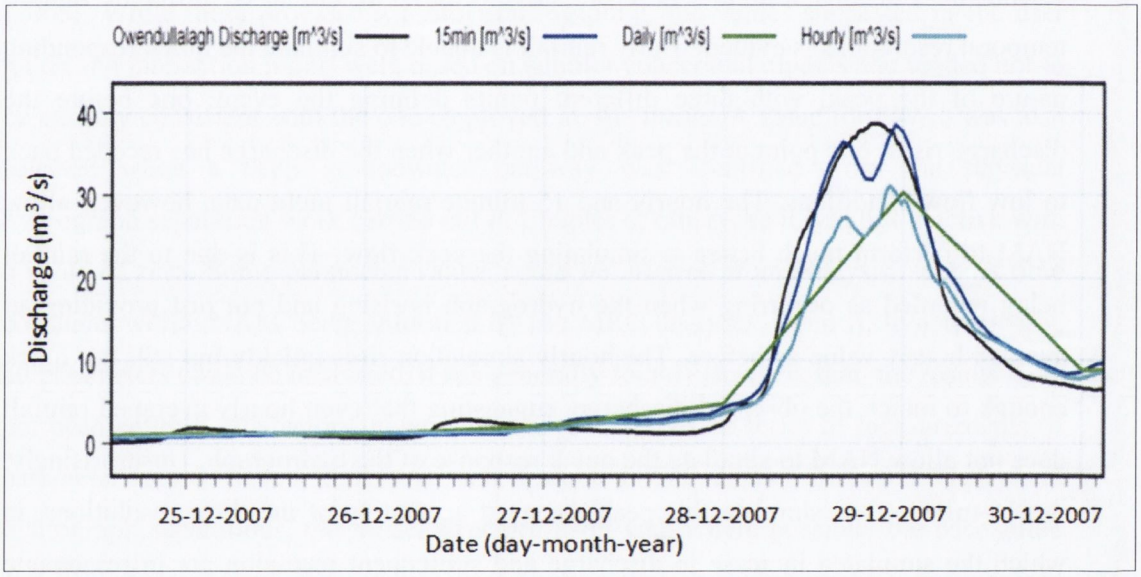

Figure 7-7. Simulated discharges in the Owendullalagh catchment for 15 minute, hourly and daily rainfall input, (December 2007).

Table 7-1. Summary of variation in R^2 obtained applying different temporal resolution rainfall data as input to NAM.

Catchment Name	Area (km^2)	Daily R^2	Hourly R^2	15min R^2
Balycahalan	48	0.33	0.79	0.85
Owenshree	35	0.61	0.8	0.89
Owendullalagh	89	0.45	0.79	0.9
Bawn	5	0.35	0.75	
Nuenna (Monument)	36	0.907	0.918	0.958

7.5 Calibration

Once the NAM model had been run with the initial parameter settings, the results were compared with the water balance results from Chapter 5, the physical hydrograph separation results from Chapter 6 and the overall discharge observed from the fieldwork. Assessing these comparisons as objective functions of the model, the boundaries within which the optimum parameters were likely to lie were set and an auto-calibration routine provided with the NAM software assisted in identifying an optimum parameter set. The auto-calibration was based on an optimisation technique known as the shuffle complex evolution algorithm (Madsen, 2000). This was an iterative process, as the auto-calibration routine was affected by the initial set of parameter values.

One thing to bear in mind was that the observed data, against which the simulated data were being calibrated, were not without error. All measurements have a degree of error associated with them. Therefore, the optimum parameter set cannot be taken as being necessarily correct. This was why more than one objective function was used in an attempt to satisfy all the functions which might have restricted the effect of the error

associated with observed measurements. The calibration routine required an upper and lower boundary to be set for each parameter. Once set, the routine then required the objective functions to test the simulated results against. The options were water balance, Nash-Sutcliffe coefficient (Equation 7-I) and then the Nash-Sutcliffe coefficient weighted for either high or low discharge values by assessing only values above a threshold discharge for high discharge scenarios and below another threshold discharge for low discharge situations. The iterations of the routine were then selected based on the time that would be allocated to running the routine. Between 2000 and 5000 iterations were generally acceptable with run time dependent on the length of the simulation and the length of each time step. The routine would then try to optimise each of the objective functions, with a selection of parameter sets outputted to a text file.

7.5.1 Calibration Results

7.5.1.1 Gortinlieve

Overall NAM performed well in terms of the simulated discharge closely matching the observed discharge, as shown in Figure 7-8(a). The R^2 value was 0.9, $\sqrt{R^2}$ value of 0.89, with a bias of 0.0011; this bias represents a difference of 4% when compared with mean discharge. Interflow dominates throughout the different discharge levels, with overland flow becoming an important contributing pathway during rainfall events when discharge was peaking, as can be seen in Figure 7-8(b). In Figure 7-8(c) we observe that interflow responded faster than the two groundwater pathways with shallow groundwater responding faster than deep groundwater. This dominance of interflow is most likely a result of the land drainage installed in the fields as a result of the poor draining nature of the catchment. These land drains encourage subsurface flow that produces the interflow dominance in this, and the other 'flashy' study catchments, as seen in Table 7-2. The deep and shallow groundwater contributions maintain the river discharge during periods of low flow.

EPA Weir

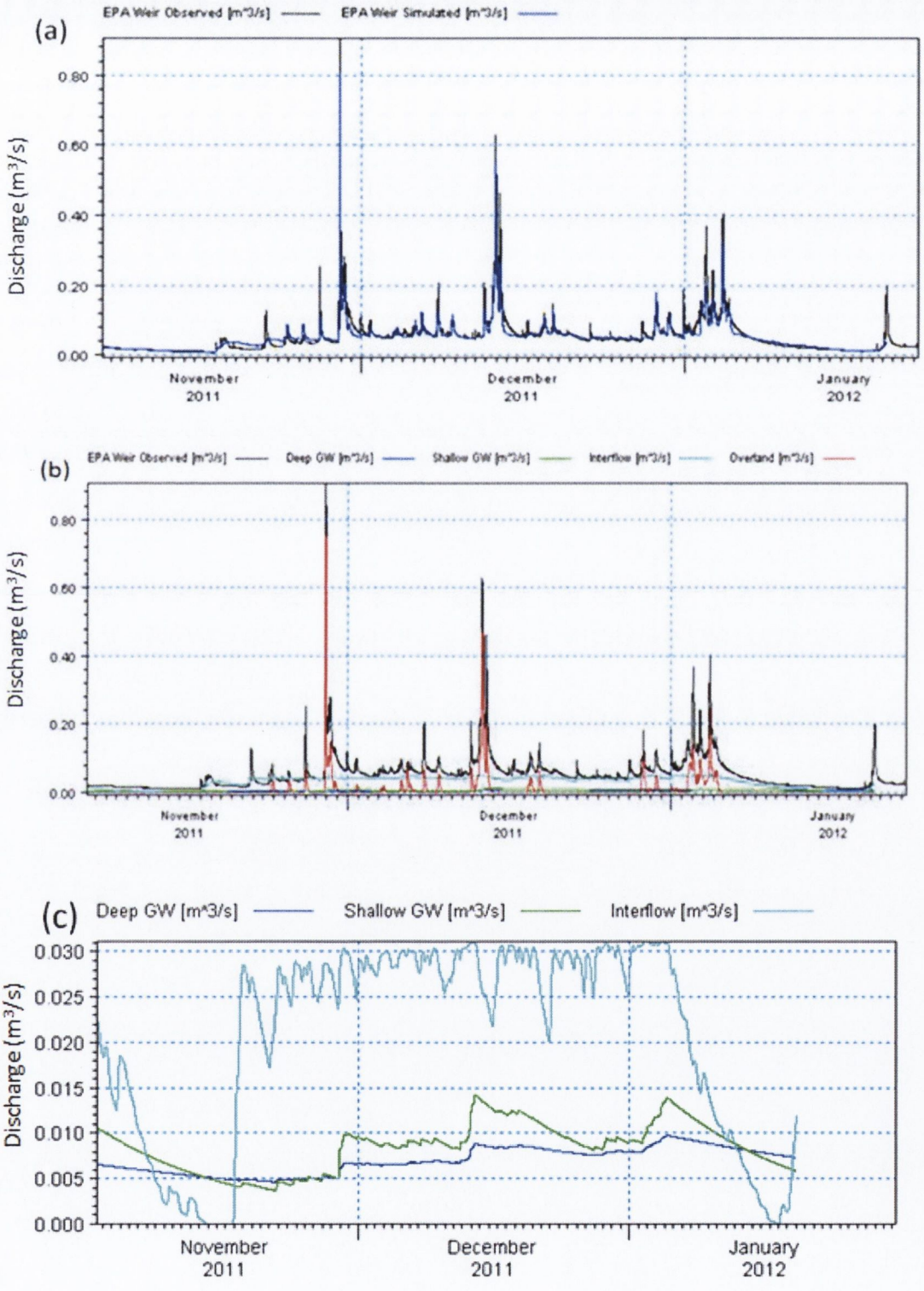

Figure 7-8. Gortinlieve EPA Weir subcatchment showing a) observed discharge compared with simulated discharge, b) simulated pathways and observed discharge and c) simulated subsurface pathways .

7.5.2 Glen Burn

NAM provided good matches between simulated discharge and observed discharge for the Subcatchment and the Outlet catchments within the Glen Burn, as can be seen in Figure 7-9(a) and Figure 7-10(a) respectively. The R^2 value for the Subcatchment was 0.91, the $\sqrt{R^2}$ value was 0.94, with a bias of – 0.0022, while the R^2 for the Outlet catchment was 0.95, the $\sqrt{R^2}$ was 0.93, while the bias was 0.0036. The biases indicate differences of 4.2% and 5.1% for the Subcatchment and Outlet catchments, respectively. In the Subcatchment and the Outlet catchment, interflow was observed to contribute most of the discharge with overland flow dominating during rainfall events, when discharge started to increase, as shown in Figure 7-9(b) and Figure 7-10(b). As referred to in Section 7.5.1.1, this interflow dominance is most probably due to land drainage within the catchment. In Figure 7-9(c) and Figure 7-10(c) we can see that interflow responded faster than the two groundwater pathways, with shallow groundwater responding faster than deep groundwater. The shallow groundwater in the Outlet catchment was observed to contribute a greater percentage of the discharge to the river than in the Subcatchment; this may be related to the alluvium present near the Outlet hydrometric station (as discussed in Chapter 6) or could be an artefact of the calibration process. The deep and shallow groundwater contributions are primarily responsible for sustaining the river discharge during periods of low flow.

Subcatchment

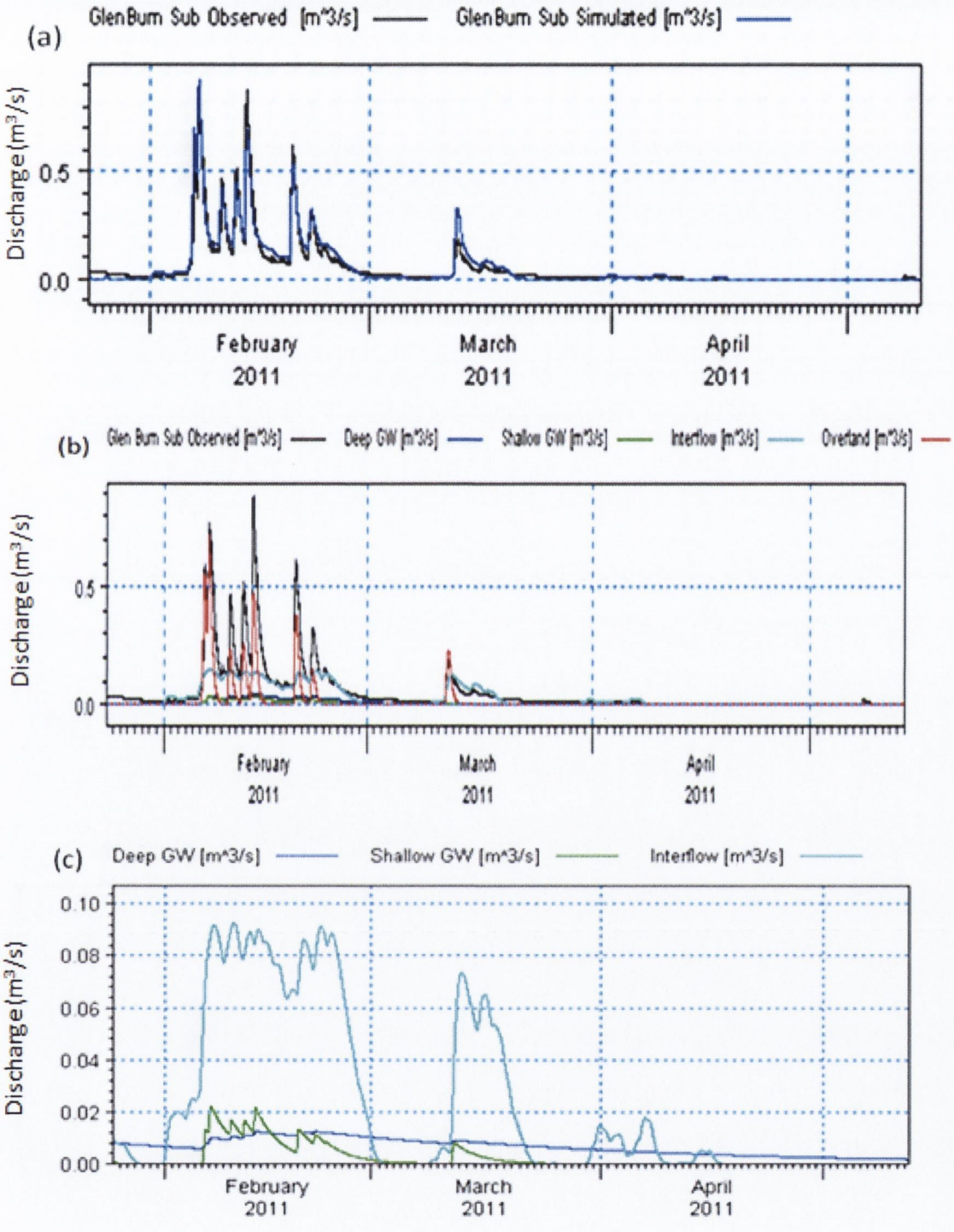

Figure 7-9. Glen Burn subcatchment showing a) observed discharge with simulated discharge, b) simulated pathway flows with observed discharge and c) simulated subsurface pathway flows.

Outlet

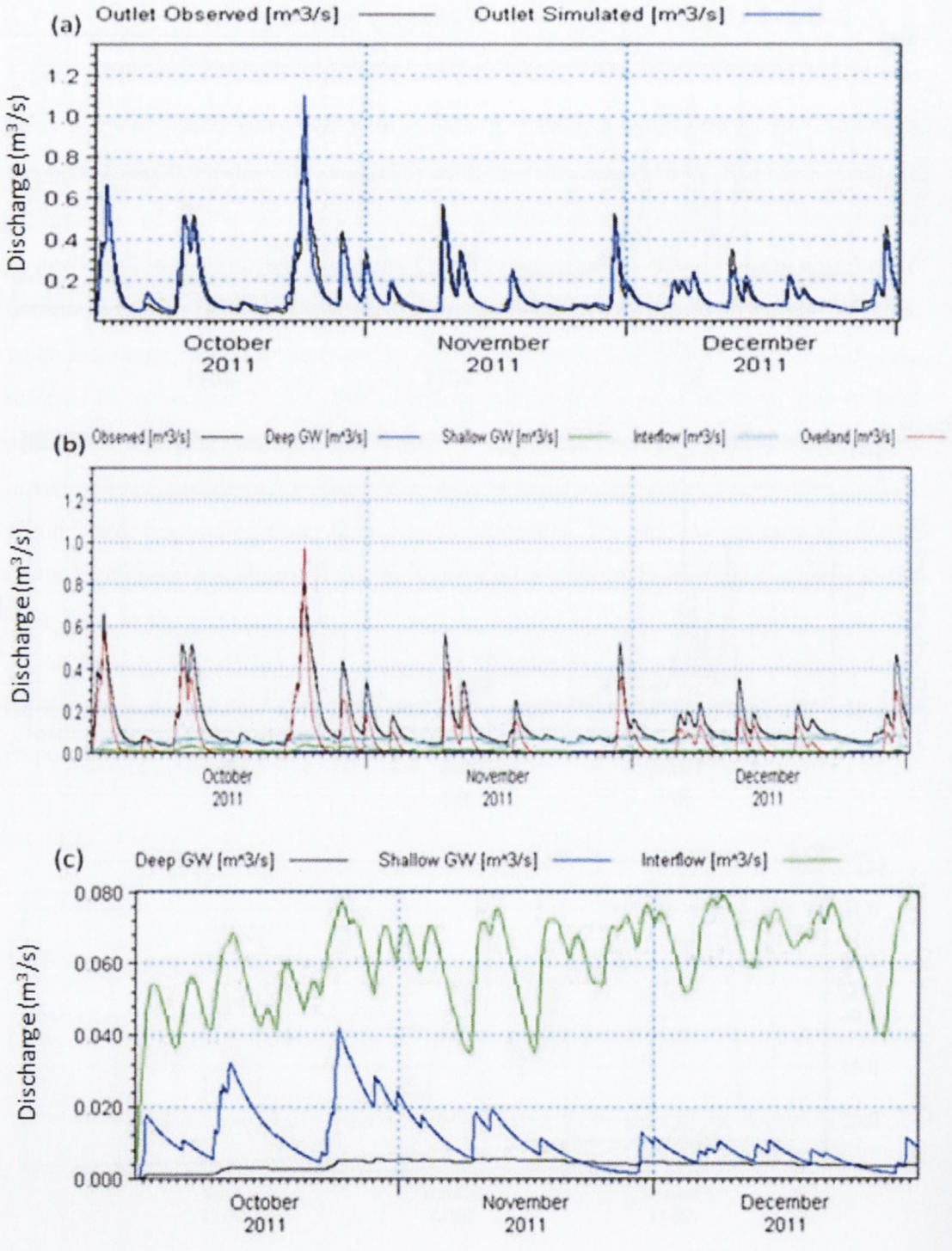

Figure 7-10. Glen Burn catchment showing a) observed discharge with simulated discharge, b) simulated pathway flows with observed discharge and c) simulated subsurface pathways.

7.5.3 Mattock

The comparison of the simulated and observed flows in the Mattock catchment gave the lowest R^2, mixed $\sqrt{R^2}$ and highest bias. This was a reflection of the complexity of the catchment, which included the off-take from the catchment at the Diversion (the abstraction near Diversion Weir), and the perching of the river at Berril's. Figure 7-11(a), Figure 7-12(a) and Figure 7-13(a) show the observed and simulated discharge for the Diversion Weir, Collon Weir and Berril's, respectively. The overestimation of discharge at the lower flows at Collon Weir may be related to the abstraction of water taken from the gravels at this location, estimated to be approximately 1300 m^3/day (Groves, 2010). The R^2 value for the Diversion Weir catchment was 0.87, with an $\sqrt{R^2}$ of 0.96 and a bias of – 0.0028; the R^2 for the Collon Weir catchment was 0.84, an $\sqrt{R^2}$ value of 0.86, with a bias of – 0.0153; while the R^2 at Berril's was 0.87, the $\sqrt{R^2}$ was 0.86, and the bias was – 0.0139. These biases represent differences of 3.1%, 17.9% and 11.2% for the Diversion Weir, Collon Weir and Berril's catchments, respectively. The large biases at Collon Weir were most likely due to the abstractions. An abstraction of 1300 m^3/day is equivalent to approximately 0.015 m^3/s, which, if added to each observed discharge, would reduce the bias to 0.3%. This abstraction and the perched nature of the river at Berril's would also explain the 11.2% difference.

At the Diversion Weir only three pathways could be identified using the physical hydrograph separation approaches – groundwater, interflow and overland flow. With a longer observed discharge time series the groundwater may have been able to be split further into shallow and deep groundwater, but for now they are modelled as combined contributing pathways. In each of the subcatchments, interflow was observed to be the dominant pathway (again most like a result of land drains) with overland flow coming to prominence during rainfall events when the discharge increases rapidly, as illustrated in Figure 7-11(b), Figure 7-12(b) and Figure 7-13(b). In Figure 7-11(c) and Figure 7-12(c) it is observed that interflow was the faster responding groundwater pathway. In Figure 7-12(c) groundwater receded slower than at the Diversion or at Berril's (Figure 7-13(c)). This was most likely a result of the sands and gravels adjacent to the river at Collon providing a more consistent discharge than in the other two catchments. The full year of data is displayed at Berril's (Figure 7-13(c)) as it can be difficult to observe the different response times of the two groundwater pathways at smaller time scales.

Diversion Weir

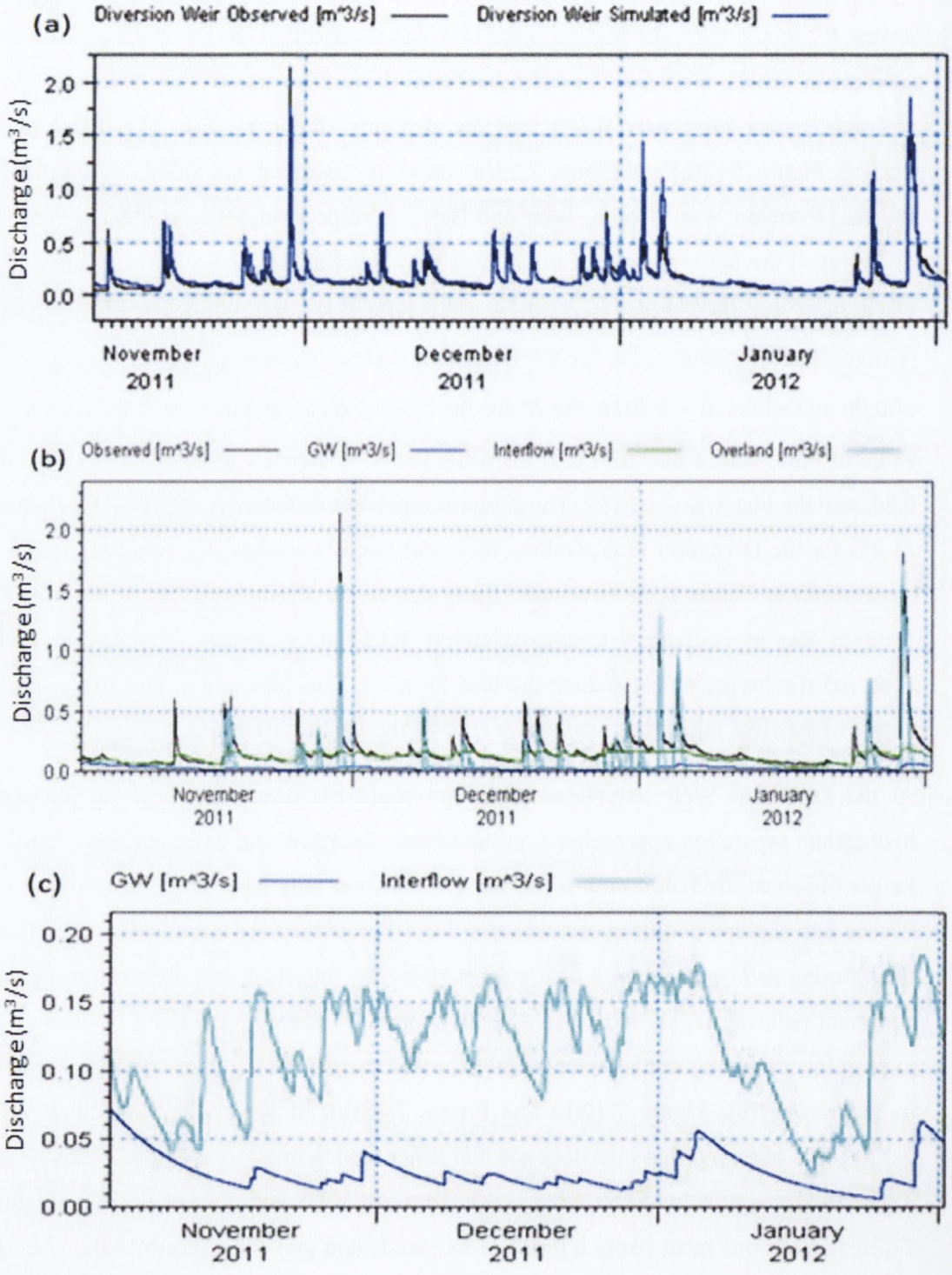

Figure 7-11. Mattock Diversion Weir subcatchment showing a) observed discharge with simulated discharge b) simulated pathway flows with observed discharge and c) simulated subsurface pathway flows.

Collon Weir

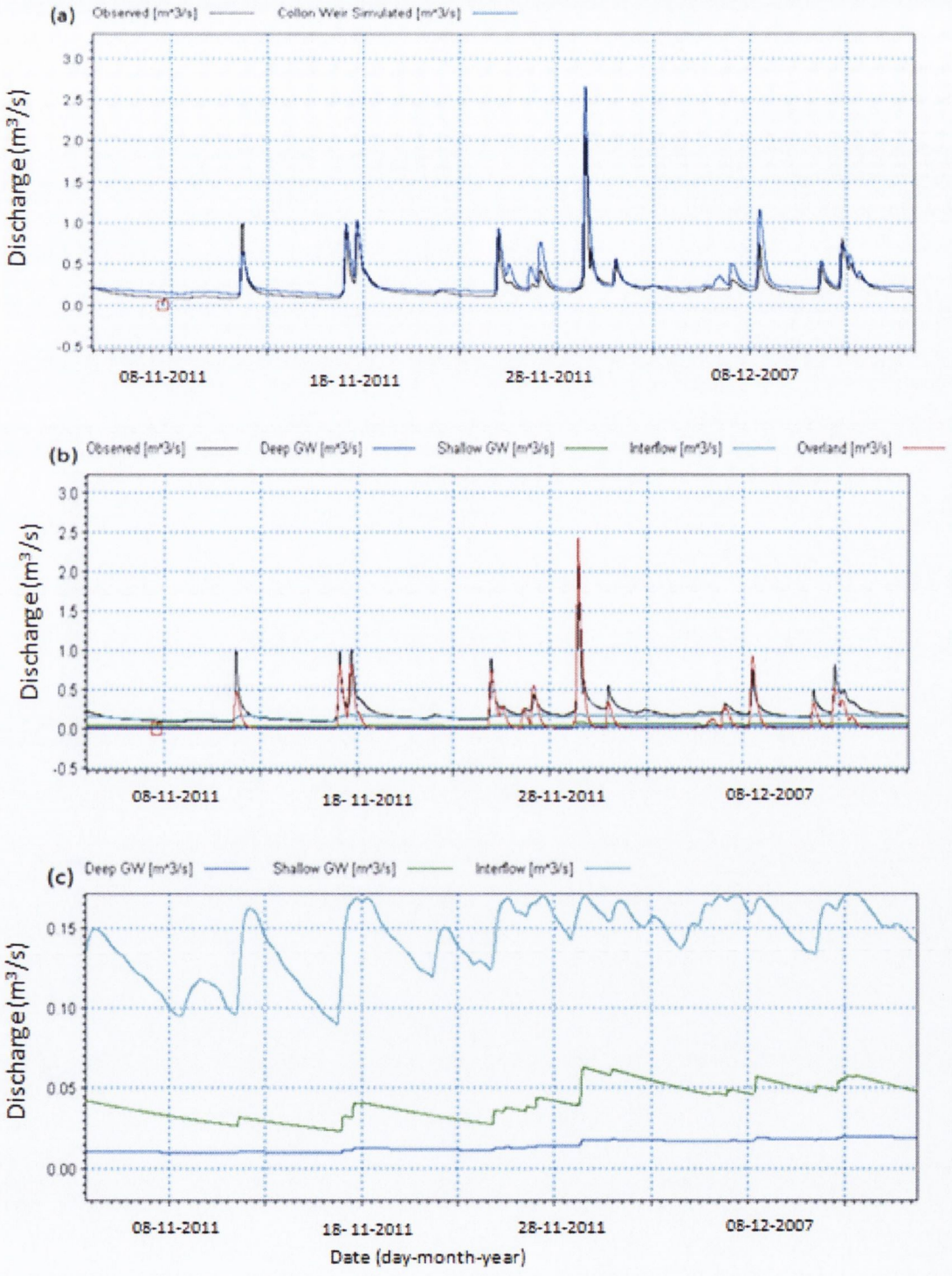

Figure 7-12. Mattock Collon Weir subcatchment showing a) observed discharge with simulated discharge, b) simulated pathway flows with observed discharge and c) simulated subsurface pathway flows.

Berril's

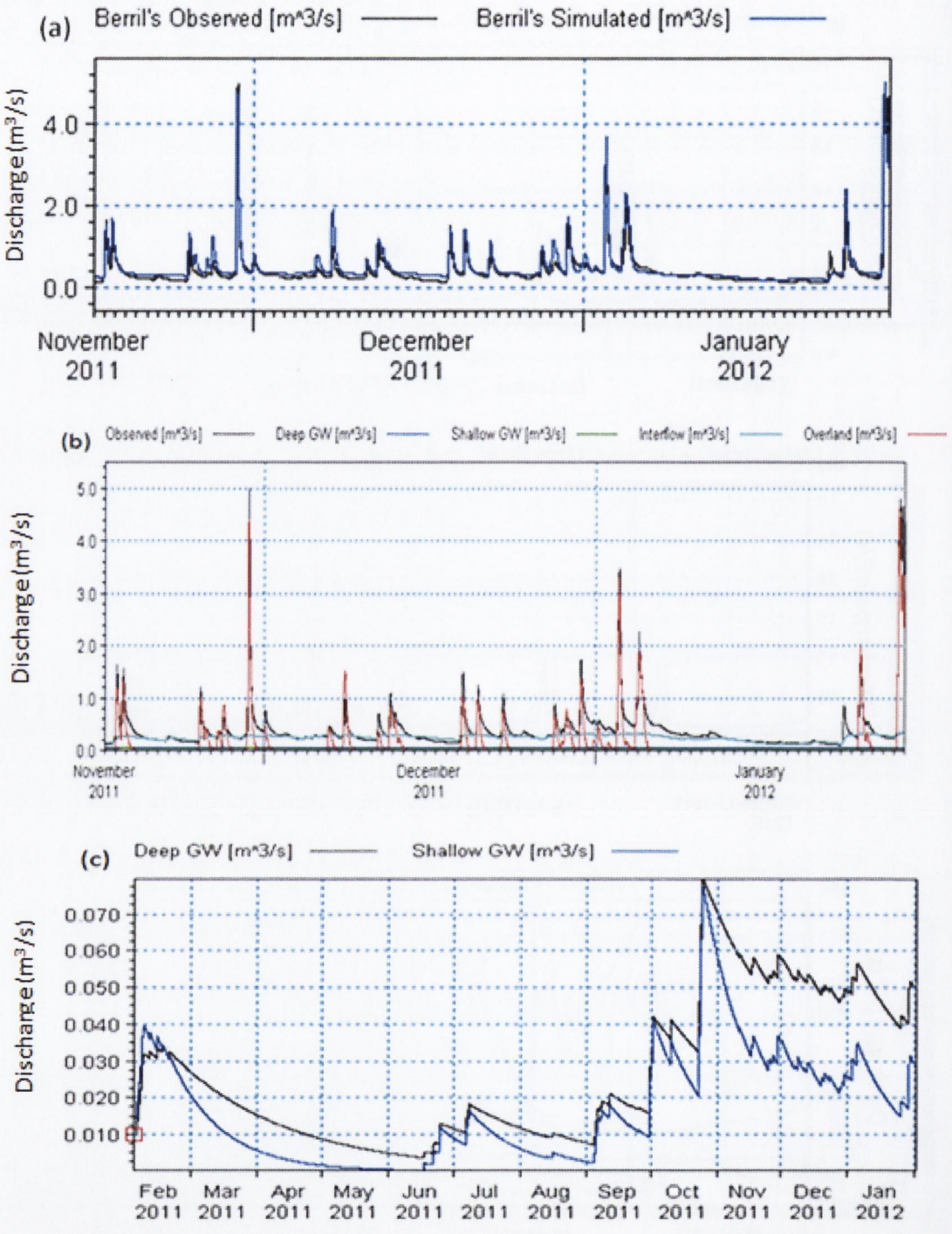

Figure 7-13. Mattock catchment showing a) observed discharge with simulated discharge, b) simulated pathway flows with observed discharge and c) simulated groundwater pathway flows.

7.5.4 Nuenna

NAM performed well during the calibration stage for the Nuenna catchment with a good fit between the simulated and observed discharges in the subcatchments, as can be seen in Figure 7-14(a), Figure 7-15(a) and Figure 7-16(a). Approximate values for catchment area were applied, as outlined in Chapter 5 and Chapter 8, to Castle Weir and Rocky Weir due to the presence of swallow holes removing water from the contributing areas to these catchments. The R^2 value for the Castle Weir subcatchment was 0.97, the $\sqrt{R^2}$ value was 0.95, with a bias of – 0.0003; the Rocky Weir catchment had an R^2 value of 0.96, $\sqrt{R^2}$ was 0.9, with a bias of – 0.0077; while the R^2 for the Monument catchment was 0.97, an $\sqrt{R^2}$ of 0.98 and a bias of 0.0046. The biases represent differences of 0.04%, 1.5% and 0.8% for the Castle Weir, Rocky Weir and Monument catchments, respectively.

In the these catchments, unlike Gortinlieve, Glen Burn and Mattock, the groundwater pathways dominant flows due to the presence of karst in the catchment, with the presence of long recessions in the hydrograph as a result, as shown in Figure 7-14(a), Figure 7-15(a) and Figure 7-16(a). These karst features made it appropriate to rename the shallow and deep groundwater pathways as conduit flow and diffuse groundwater flow respectively. The Conduit flow term was applied to reflect the connections identified between swallow holes and springs identified in a tracer study (Walsh, 2011), as discussed in Chapter 5. The influence of these karst pathways can be observed in Figure 7-14(b), Figure 7-15(b) and Figure 7-16(b) for the Castle Weir, Rocky Weir and Monument catchments, respectively. It is also evident in these figures that overland flow, although a small contributor to discharge in general, was important for generating the observed peaks in discharge.

Castle

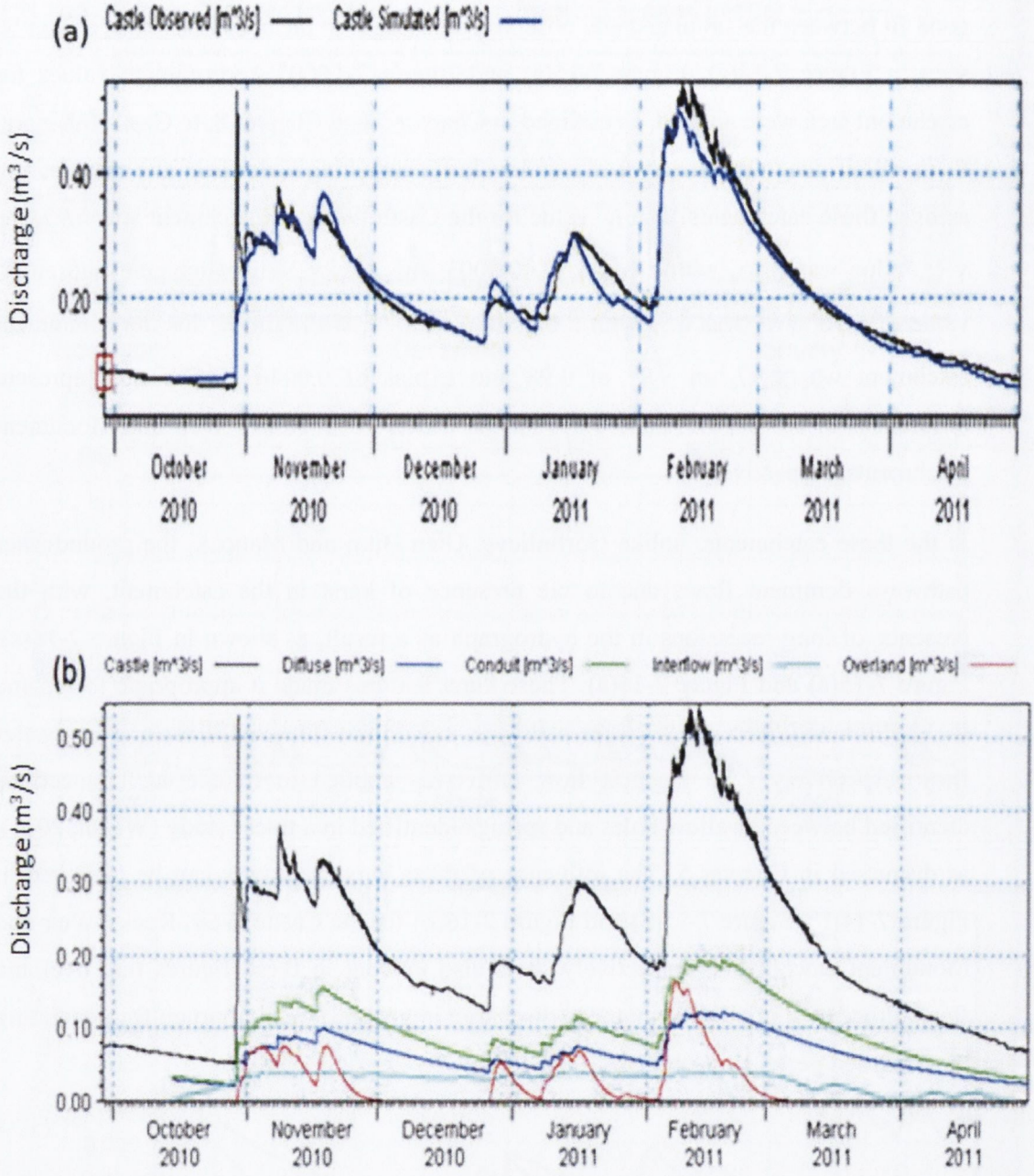

Figure 7-14. Nuenna Castle subcatchment showing a) observed discharge with simulated discharge, and b) simulated pathway flows with observed discharge.

Rocky Weir

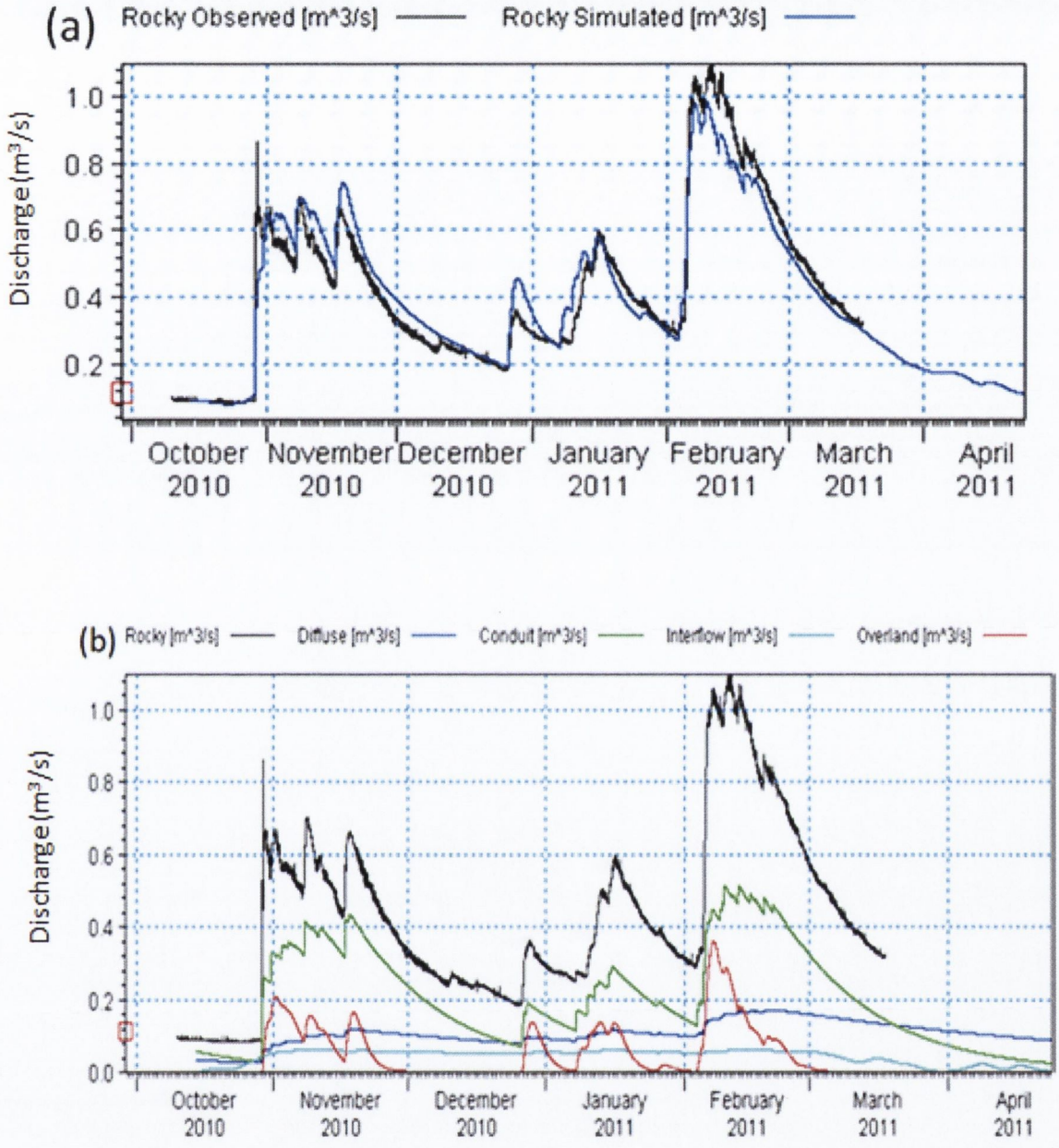

Figure 7-15. Nuenna Rocky subcatchment showing a) observed discharge with simulated discharge, and b) simulated pathway flows with observed discharge.

Monument

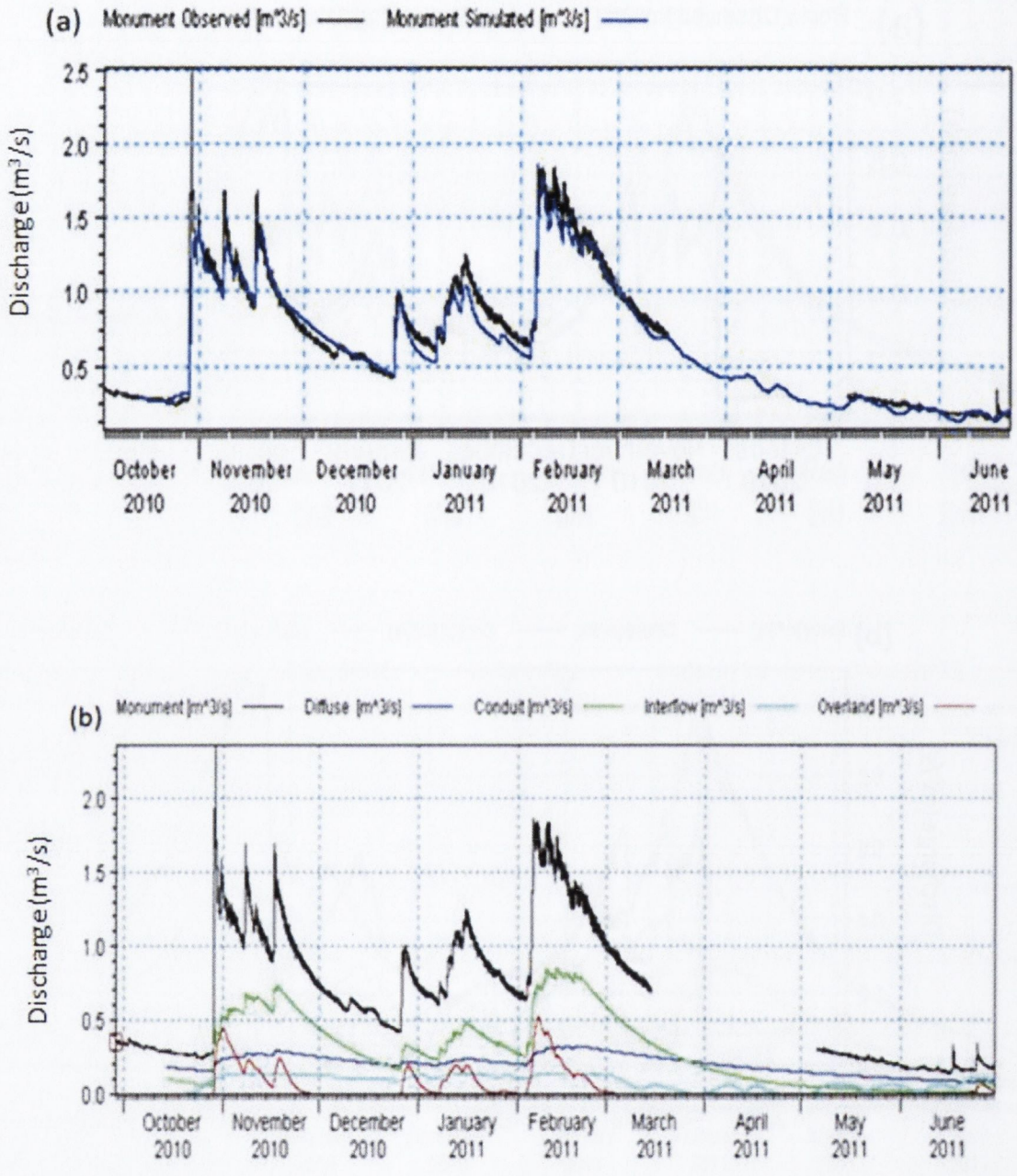

Figure 7-16. Nuenna catchment showing a) observed discharge with simulated discharge and b) simulated pathway flows with observed discharge.

The overall results of the NAM calibration simulations for each catchment are presented in Table 7-2.

Table 7-2. Results of NAM modelling after calibration.

Catchment	Area (km^2)	Deep Groundwater	Shallow Groundwater	Interflow	Overland	R^2	$\sqrt{R^2}$	Bias
		%	%	%	%			
Gortinlieve	0.9	12.9	14.5	50.8	21.8	0.9	0.89	0.0011
Glen Burn (Sub)	4.8	12.2	6.1	39.9	41.8	0.91	0.94	-0.0022
Glen Burn (Outlet)	5	4.9	7.8	43.6	43.7	0.95	0.93	0.0036
Mattock (Div Weir)	7	16.1		51.2	32.7	0.84	0.96	-0.0028
Mattock (Collon)	11.6	6.2	11.8	48.3	33.7	0.88	0.86	-0.0153
Mattock (Berril's)	16.9	9.9	6.8	45.7	37.6	0.89	0.86	-0.0139
Nuenna (Castle)	10.2	30.6	44.6	15.4	9.4	0.97	0.95	-0.0003
Nuenna (Rocky)	19.9	31.9	47.8	13.2	12.1	0.96	0.9	-0.0077
Nuenna (Mon)	35	31.7	45.3	13.4	9.7	0.97	0.98	0.0046

7.6 Validation

Model validation is a difficult process to implement properly. Generally this process involves the comparison of data from a period of simulation that was not utilised in the calibration process. One limitation is that, as with the calibration process, the observed data used for comparison with the simulated data are not without error. Therefore, discrepancies between simulated values and observed values may be less or even greater than those predicted. Validation in itself is a term often misapplied: in fact, Bredehoeft and Konikow (2012) suggest that scientific theory cannot be validated, only invalidated. As we only have one data type that can be measured directly and compared with model output (i.e. observed discharge), this is the only data employed for the purpose of validation. As such, only the total discharge simulated for a period after the calibration period can be evaluated, with the caveat that this observed discharge set also contains errors and thus cannot provide an absolute validation. Validation of each catchment was carried out implementing the parameter values identified by calibration. As previously outlined, validation of the simulated pathways was performed for data outside of those employed during calibration. A period of six months was used for each catchment as this was generally the extent of data available after at least one year of

data had been utilised for model calibration. The results of simulations are summarised in Table 7-3. The validation statistics applied were the R^2, $\sqrt{R^2}$ and bias as per the calibration, with the separations of the pathways included as a comparison with the calibration separations. These results are discussed in detail in Section 7.7.3.

Table 7-3. Validation results for study catchments.

Catchment	Area (km^2)	Deep Groundwater		Shallow Groundwater		Interflow		Overland		R^2		$\sqrt{R^2}$		Bias	
		Cal %	Val %	Cal %	Val %	Cal %	Val %	Cal %	Val %	Cal	Val	Cal	Val	Cal	Val
Gortinlieve	**0.94**	12.9	19.6	14.5	12.1	50.8	56.1	21.8	12.1	0.9	0.85	0.89	0.84	0.0011	0.0011
Glen Burn (Sub)	**4.79**	12.2	7.8	6.1	3.4	39.9	53.5	41.8	35.3	0.91	-0.67	0.94	0.17	-0.0022	0.0280
Glen Burn (Outlet)	**5**	4.9	3.9	7.8	6	43.6	48.8	43.7	41.3	0.95	0.95	0.93	0.94	0.0036	0.0006
Mattock (Div Weir)	**6.99**	16.1	16.6			51.2	46.1	32.7	37.3	0.84	0.74	0.96	0.92	-0.0028	-0.0135
Mattock (Collon)	**11.61**	6.2	9.4	11.8	14.6	48.3	42.6	33.7	33.3	0.88	0.54	0.86	0.45	-0.0153	-0.0573
Mattock (Berril's)	**16.88**	9.9	13	6.8	7.2	45.7	46.4	37.6	33.4	0.89	0.68	0.86	0.76	-0.0139	-0.0268
Nuenna (Castle)	**10.24**	30.6	29.3	44.6	44.4	15.4	15.9	9.4	10.4	0.97	0.92	0.95	0.9	-0.0003	-0.0010
Nuenna (Rocky)	**19.89**	31.9	27.1	47.8	49.4	13.2	12.6	12.1	10.9	0.96	0.8	0.9	0.81	-0.0077	0.0012
Nuenna (Mon)	**34.99**	31.7	21.7	45.3	53.6	13.4	13.5	9.7	11.2	0.97	0.88	0.98	0.93	0.0046	-0.0041

7.7 Discussion

NAM has been applied to the same catchments as the other physical hydrograph separation methods (Chapter 6). The results have been presented within this chapter for the calibration (Section 7.5) and the validation (Section 7.6) stages of the NAM modelling. In comparison to the approaches applied in Chapter 6, NAM is more adept at representing the quick responding pathways, due to the non-linear nature of the discharges from the storages within the NAM structure (Section 7.2). This supports the use of NAM as an investigative approach for separating the hydrograph as well as a validation tool for comparing simulated and observed discharge.

7.7.1 Preliminary modelling

Section 7.4.2 describes how the temporal resolution of the input rainfall data for the NAM model impacts the ability of NAM to simulate peaks, particularly in 'flashy' catchments. Figure 7-7 illustrates this with the simulated peak approaching the shape of

the observed discharge as the rainfall data time steps decrease from one day to 15 minutes. As the rising and falling limbs of the rainfall event are both contained within a period of just over 24 hours, daily time steps cannot adequately represent the shape of the hydrograph. The hourly data provided a marked improvement, with 15 minute data simulating the best approximation of the hydrograph.

This suggests that in smaller catchments (less than 100 km^2 in the example of the catchments assessed here), higher temporal resolution rainfall data will be required in order to simulate the rainfall events acceptably. To evaluate this proposition a small, 'non-flashy' catchment was investigated to see if the same relationship applied. The Nuenna catchment, as discussed in Chapters 4, 6 and within this chapter, is a groundwater-dominated catchment that responds slowly to rainfall, with a long recession following events. Whereas the Balycahalan, Owenshree, Owendullalagh and Bawn catchments are 'flashy' catchments, with typically poorly draining soils and subsoils. The 'flashy' catchments exhibit a similar trend of increasing R^2 values as the temporal resolution of the rainfall data increases (Table 7-1), implying that the time step of the rainfall is crucial for simulating peaks in the hydrograph. The Nuenna, however, does not display this same behaviour with R^2 increasing only modestly from 0.907 to 0.958 as the time step for rainfall input decreases. This compares with the significant increase in R^2 of 0.33 to 0.85 for the Balycahalan catchment. The Bawn also shows a large increase from 0.35 to 0.89 for the rainfall time step reducing from daily to hourly, with another increase in R^2 expected had 15 minute rainfall data been available. This suggests that the size of the catchment alone is not enough to determine whether high temporal resolution data are required, and that the responsiveness of the catchment also needs to be taken into account. One approach to investigating the catchment response is to assess the master recession curve output of Chapter 6. The tabulation method MRC is presented for the Bawn and for the Nuenna Monument catchments in Figure 7-17 and Figure 7-18. The fastest responding pathway (conceptually overland flow) has a τ value of 0.258 for the Bawn catchment and 0.005 for the Nuenna Monument catchment. These correspond to response times of 3.87 hours and 200 hours, respectively. These are the fastest responding pathways according to the MRC approach. This would be the minimum time step of rainfall required to simulate these responses and so provides an indication of the acceptable time step of rainfall required for modelling. Also, the recession from a peak on a hydrograph is typically slower than the rise in the

hydrograph to the peak, therefore an even shorter time step for rainfall data would be required than the one suggested by the MRC analysis.

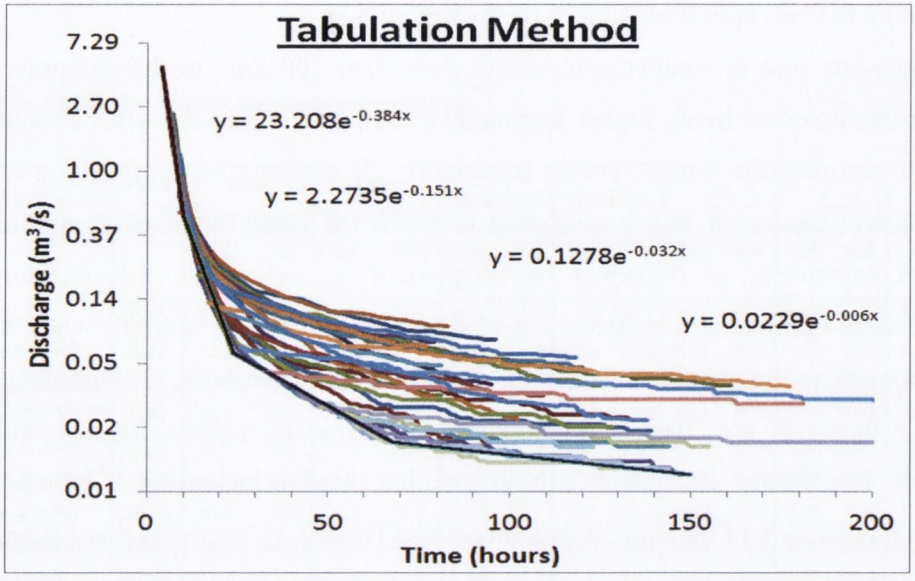

Figure 7-17. Tabulation MRC from the Bawn catchment.

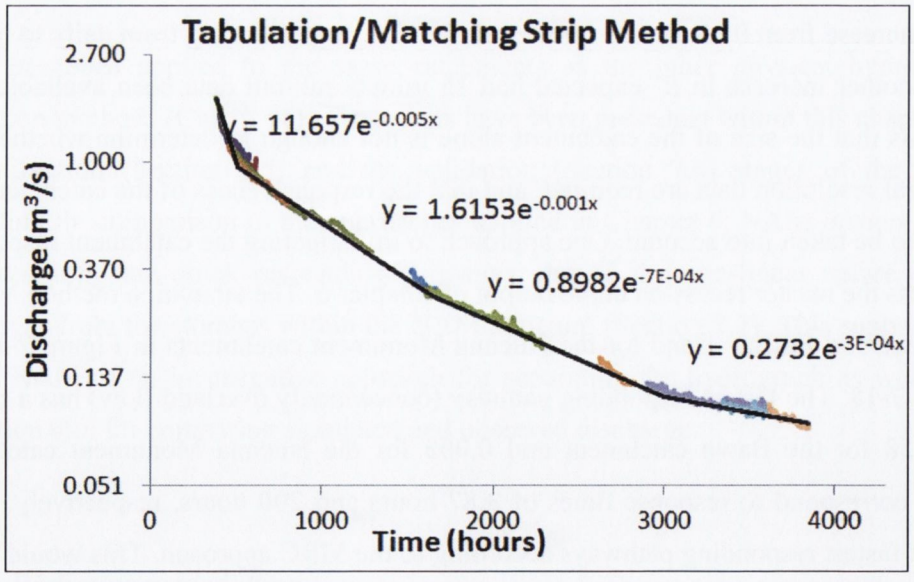

Figure 7-18. Tabulation MRC from the Nuenna Monument catchment.

One other notable observation from the initial modelling is the dip in the hydrograph of the hourly and 15 minute simulated discharges in Figure 7-7. The observed discharge shows no such dip, suggesting that rain fell on the catchment during this period to sustain this flow peak but was not recorded by the rain gauge. This will always be an issue with catchment scale modelling due to the variations inherent in rainfall distribution and intensity. This was part of the reasoning of locating two rain gauges in the study catchments, even though the catchments are relatively small in size.

7.7.2 Calibration

The calibration process involved the implementation of an auto-calibration routine built into the NAM program, evaluating simulations based on their water balance achieved, the R^2 value and by a weighted R^2 value that only considers high or low discharges as described in Section 7.5. The physical hydrograph separations of Chapter 6 provided realistic ranges for the percentage of river discharge derived from each of the pathways, and could thus be used to inform the range of NAM parameter values employed in the calibration process. This helped to address the issue of equifinality, as discussed in Chapter 3 and Section 7.2, whereby many different parameter sets could be implemented in NAM that would generate an overall discharge that would be as good (assessed using the objective functions) or nearly as good as the best parameter set identified applying the auto-calibration routine. As such, the model was not free to choose parameter values from any range and in this way accounted for the pathway separations predicted in Chapter 6. The NAM model itself, however, was also employed as an investigative tool. Furthermore, when the calibration process implied that a certain pathway may be more or less prominent than the physical hydrograph separations suggested, this was also taken into account when setting the limits of a parameter value in the auto-calibration routine, provided that a physically plausible separation was still being obtained. This approach typically has the effect of reducing the performance of the objective functions, as restrictions on the parameter values that can be implemented may prevent NAM from achieving the optimum calibration. The pathway contributions, simulated using the optimum parameter set, may be unrealistic (for example, a large contribution of groundwater in a 'flashy' catchment underlain by a poorly productive aquifer). In this manner, calibration of each of the study catchments

was an iterative process, culminating in the results summarised in Table 7-2; these are now compared with the physical separation results in Table 7-4.

As can be seen in Table 7-4, there are general trends evident among the four study catchments, particularly between the Gortinlieve, Glen Burn and Mattock catchments. This is to be expected as all three of these catchments, and their subcatchments, have generally poorly draining soils and subsoils, underlain by poorly productive aquifers, as outlined in Chapter 4. Typically, the combined groundwater contribution (deep and shallow groundwater) to the river is less than 20%, with the exception of the Gortinlieve EPA Weir catchment where the "baseflow" is somewhat above this (27.4%). Reviewing the results of Chapter 6, this is consistent with the range of contributions predicted by the MRC analysis, the digital filtering algorithms and the recharge coefficient approach, again with the exception of Gortinlieve. The recharge coefficients suggest that only 11.3% of river discharge in Gortinlieve would be derived from the groundwater pathways due to the Pl aquifer in the catchment, while the MRC suggests 19.9%. Applying NAM, the model was predicting a high contribution from the groundwater pathways (greater than 30%). Taking the physical separations into account, this contribution was refined back to 27.4%, while maintaining the performance of the objective functions. This still appears to unrealistically high, taking the recharge coefficients approach into account which is a good indicator of the upper limit of the groundwater contribution as discussed in Chapter 6. This would suggest that NAM is predicting a groundwater response closer to that of the MRC analysis than that suggested by the recharge coefficients approach. As discussed in Chapters 4, 5 and 6, the hydrometric station in Gortinlieve for the EPA Weir subcatchment experiences issues with silt during low flow conditions that maintains the level recorded by the stage logger higher than the equivalent discharge in the river. These periods can be difficult to identify and will have the effect of skewing the groundwater discharge predicted by NAM upwards, which may have influenced the results of Table 7-2. Also the major controlling factor for the recharge coefficients in poorly productive aquifers is the recharge cap applied. As discussed in Chapter 6, a recharge cap of 100 mm per annum is applied to Gortinlieve as a Pl aquifer underlies the whole catchment. The difference in classification between a Pl aquifer and Ll aquifer can be small, yet results in an increase of the assigned recharge cap from 100 mm to 200 mm. If the catchments aquifer classification was upgraded to a Ll aquifer, this would bring the recharge

coefficients more in line with what NAM and the MRC analyses are predicting here, taking into account that the NAM predictions are probably over-estimated due to the effects of the silting at the hydrometric station.

The interflow contributions computed by NAM are generally within the range of those calculated in Chapter 6. There are some discrepancies: the Nuenna Rocky subcatchment is one example where interflow is more than would be expected applying the separations obtained in Chapter 6. Taking into account that only the MRC analysis could be applied to calculate interflow for this catchment, and that when the combined interflow and overland flow contribution as determined applying the modified recharge coefficient approach, the separation appears reasonable. As considered within Section 7.5, the dominance of the interflow pathway as a contributor to river discharge is most likely a result of the prevalence of field drains within the poorly draining soils of the fast responding catchments (Gortinlieve, Glen Burn and Mattock). Therefore, this drainage is augmenting the contribution of interflow by providing a path of less resistance for the water to flow along quickly when compared with the surrounding soils. The simulated overland flow behaves much like the interflow contributions with most of the catchment's overland flow output from NAM lying within the ranges calculated in Chapter 6.

Table 7-4. Calculated catchment pathway separations.

Catchment	Area (km^2)	Deep Groundwater			Shallow Groundwater			Groundwater	Interflow			Overland			Quick Flow
		MRC	Mod Lyne	NAM	MRC	Mod Lyne	NAM	Recharge Coeff[a]	MRC	Mod Lyne	NAM	MRC	Mod Lyne	NAM	Recharge Coeff[a]
		%	%	%	%	%	%	%	%	%	%	%	%	%	%
Gortinlieve	0.94	14.6	6	12.9	5.3	5.9	14.5	11.3	51.6	50	50.8	28.5	38.1	21.8	88.7
Glen Burn (Sub)	4.79	11.7	2.4	12.2	11.1	2.4	6.1	18.4	34.3	56.7	39.9	42.9	38.5	41.8	81.6
Glen Burn (Outlet)	5	11.7	3.4	4.9	10.4	3.5	7.8	18.9	43.8	62.8	43.6	34.2	30.3	43.7	81.1
Mattock (Div Weir)	6.99	8.5	8.8					23.1	49.6	52.2	51.2	41.9	39	32.7	76.9
Mattock (Collon)	11.61	12.9	7.4	6.2	15.8	7.6	11.8	23.1	33.7	45.8	48.3	37.7	39.2	33.7	76.9
Mattock (Berril's)	16.88	4.5	2.9	9.9	6.5	2.8	6.8	23	30.1	59.2	45.7	58.9	30.13	37.6	77
Nuenna (Castle)	10.24[b]	48.5		30.6	36		44.6	70.5	10.3		15.4	5.2		9.4	29.5
Nuenna (Rocky)	19.89[b]	51.4		31.9	40.3		47.8	82.2	6.5		13.2	1.8		12.1	17.8
Nuenna (Mon)	34.99	44.1		31.7	35.7		45.3	71.3	14.2		13.4	6		9.7	28.7

[a] Recharge coefficient approach used to separate into quick (interflow and overland flow) and slow (deep and shallow groundwater) pathways, they are placed under deep groundwater and Interflow, respectively, for convenience.

The objective functions in Table 7-2, provide a means of assessing the efficiency of the NAM model at simulating the overall observed discharge in the river. The R^2, $\sqrt{R^2}$ and bias values indicate the success of the calibration, illustrated in the plotted simulated and observed discharge series in Section 7.5.1. R^2 provides an assessment of the overall fit of the simulated discharge with the observed discharge. As this function contains squared values it will tend to weight the higher discharges more heavily than the lower discharges. In order to obtain an assessment of the fit of the lower simulated discharges, the $\sqrt{R^2}$ parameter is employed. The bias is then an assessment of the overall average sum of all the observed discharges less the simulated discharges. Provided the bias is only a small proportion of the average discharge, the model performance is deemed satisfactory due to the error inherent in measurement devices as described in Chapter 5. As all three objective functions measure the efficiency of the simulated discharges, there is a general correlation between the three. It is observed in Table 7-2 that the overall performance of NAM in the study catchments is generally good, with most R^2 values greater than 0.9 or just below this. The same comment applies to the $\sqrt{R^2}$ values, with biases being typically small – being both positive and negative percentages indicating that NAM is not consistently over- or underestimating discharge.

The worst performing catchment in terms of the objective functions is the Mattock. This is a reflection of many complexities in the catchment that are difficult to quantify. These issues have already been outlined in Chapter 4. The Mattock has water diverted from the catchment upstream at the Diversion Weir hydrometric station. This water is removed to the nearby town of Drogheda outside of the catchment. There is a river stage logger, monitoring water leaving the catchment, but this water is removed by a pipe from a reservoir that has had its efficiency at removing water changed by a large storm in October 2011. This has complicated the rating curve at this point, adding further uncertainty to recorded discharges. At Collon Weir there is an issue with silting of an intake pipe to the stilling well at this point; this affects low flow conditions, but has also led to gaps in the data set at higher flow conditions as discussed in Section 7.3.3, and which will be further addressed in Section 7.7.3. Also described in Chapter 4 is the irregular pumping of water for supply in the town of Collon from sands and gravels located near the river at this point. It is thought that this may have an effect on the river discharge and this issue is being investigated by Louth County Council, with no findings available as yet. One final known complication in the catchment, as outlined in Chapter 4 also, is that the Mattock river becomes perched near the catchment outlet, with the bedrock groundwater level being 11 m below the river. These complexities are difficult to

fully represent in a lumped model such as NAM. The bias in Table 7-2 for Collon Weir and Berril's is reduced substantially when the water being pumped at Collon Weir is accounted for. These complexities are further investigated in Chapter 8 when a fully distributed model is applied to the Mattock catchment.

7.7.3 Validation

Validation, as discussed in Section 7.7.3, was carried out to assess the closeness of fit between the simulated and observed discharge for the six month period directly after the calibration period. The pathway contributions for these periods are also presented for this period Table 7-3, but should not be viewed as part of the validation process.

In general, there is a decrease in the performance of the objective functions, which is to be expected as there are new data to model situations that have not been calibrated for. The trends for the validation are somewhat similar to those of the calibration discussed in Section 7.7.2, with the catchments performing well in general with the exception of the Mattock, where the model performs less well due to the same complexities outlined in Section 7.7.2. The bias again varies between positive and negative values, with some improvements on the bias encountered in the calibration process. Omitting the two worst performing subcatchments (Mattock Collon Weir and Glen Burn Subcatchment), the validation is on average 90% of the calibrated value for R^2 and 93% for $\sqrt{R^2}$. These validations are for a period of six months after the calibration period; it is assumed that the objective function performances would decrease for longer timeframes as the simulations move further and further from the conditions under which they were calibrated.

The Mattock Collon Weir and Glen Burn Subcatchment were omitted due to issues arising from the observed discharges for these two subcatchments. In the Glen Burn subcatchment, the performance of the R^2 was -0.67, a value representing a worse fit with the observed discharge than obtained from modelling this observed discharge using a straight line through the data with the value of the mean discharge. On closer inspection of the simulated and observed discharges, it was evident that the measured discharges for the subcatchment appeared to be offset above what would seem feasible (Figure 7-19). These two hydrometric stations are located less than a kilometre apart with no tributaries located between them, therefore, the Subcatchment discharge is typically similar to the Outlet discharge, generally marginally less. In February there was an issue with the logger and it was reset, but it appears

to have been set too high (as shown from April to August 2012). If the Outlet discharge is used as an approximate for the subcatchment data, an R^2 of 0.93, an $\sqrt{R^2}$ of 0.9 and a bias of 0.007, providing a good match with the data (Figure 7-20). Unfortunately the Collon Weir discharge errors are more subtle and not as readily remedied. It can be seen in Figure 7-21 that the discharge at Collon Weir typically exceeds the discharge at the Diversion Weir by approximately 0.1 m^3/s. However in Figure 7-22, the discharge at Collon Weir is approximately the same as at the Diversion Weir during the validation period for March and April but continues to decrease until it is less than the Diversion Weir discharge in June. At the end of Figure 7-21 it can be seen that there is a break in the discharge recorded at Collon Weir; when this time series resumes in 2012, it starts above the Diversion Weir discharge but the difference slowly decreases until the Collon Weir discharge is actually less than the Diversion Weir discharge (Figure 7-22). As this is a gradual and non regular decay of the difference of the two discharges it is very difficult to obtain an accurate time series with which to validate the predicted discharges.

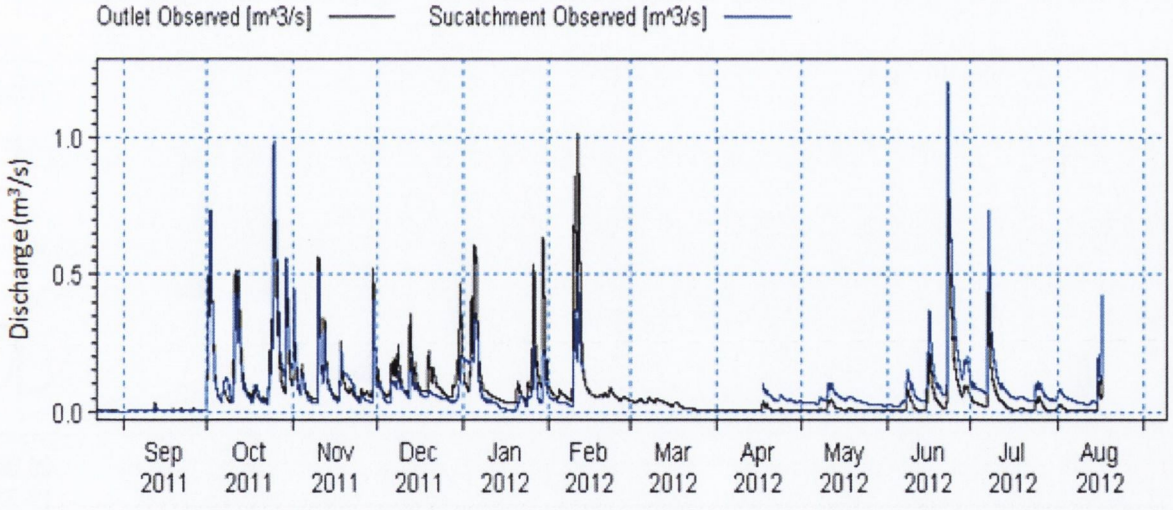

Figure 7-19. Comparison of Glen Burn Outlet and Subcatchment observed discharges (Sept 20122 – Aug 2012).

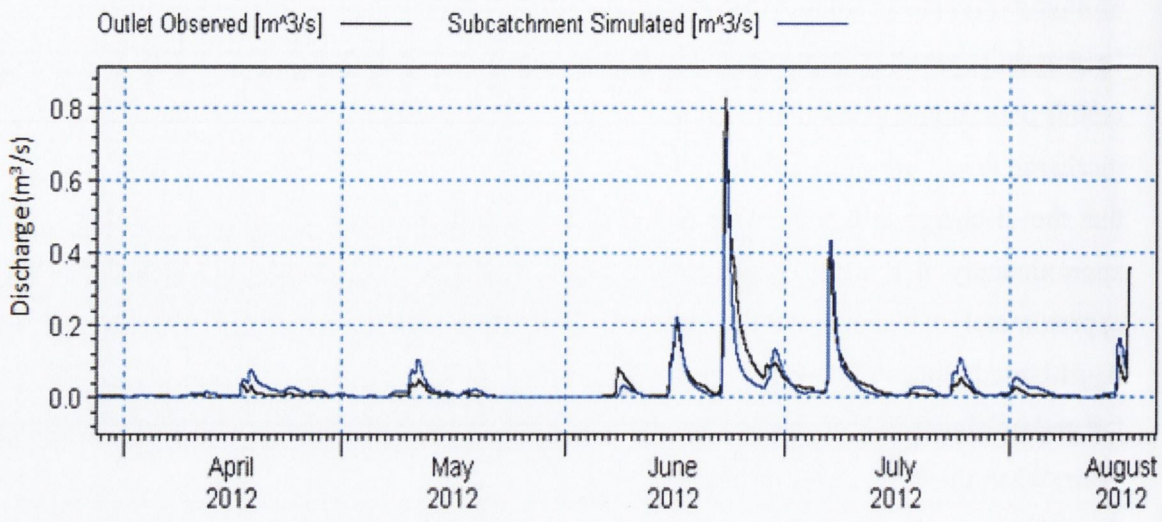

Figure 7-20. Comparison of Glen Burn observed Outlet discharge and simulated Subcatchment discharge (Apr 2012 – Aug 2012).

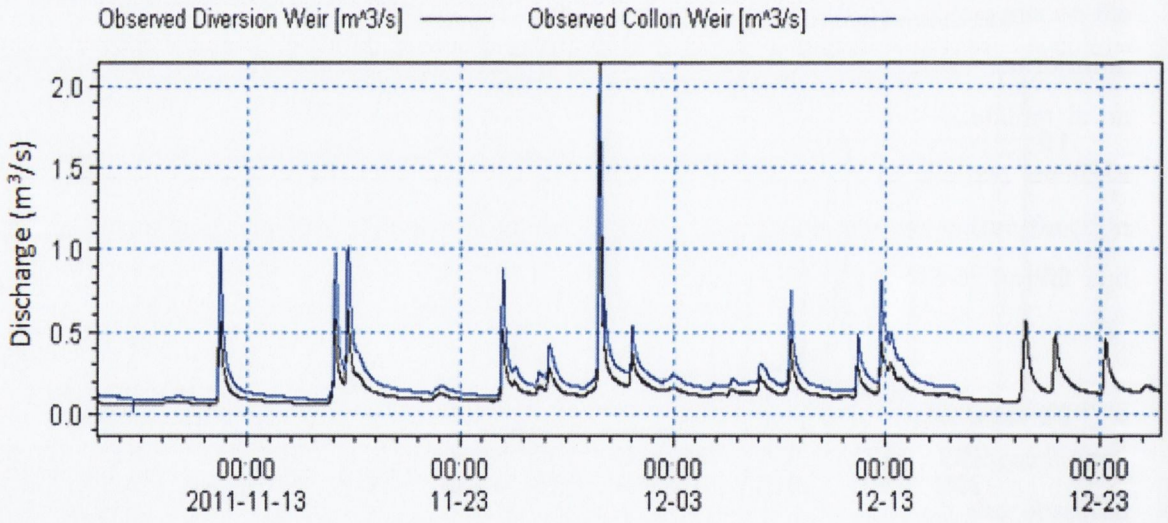

Figure 7-21. Observed discharge in the Mattock for the Diversion Weir and Collon Weir (Nov – Dec 2011).

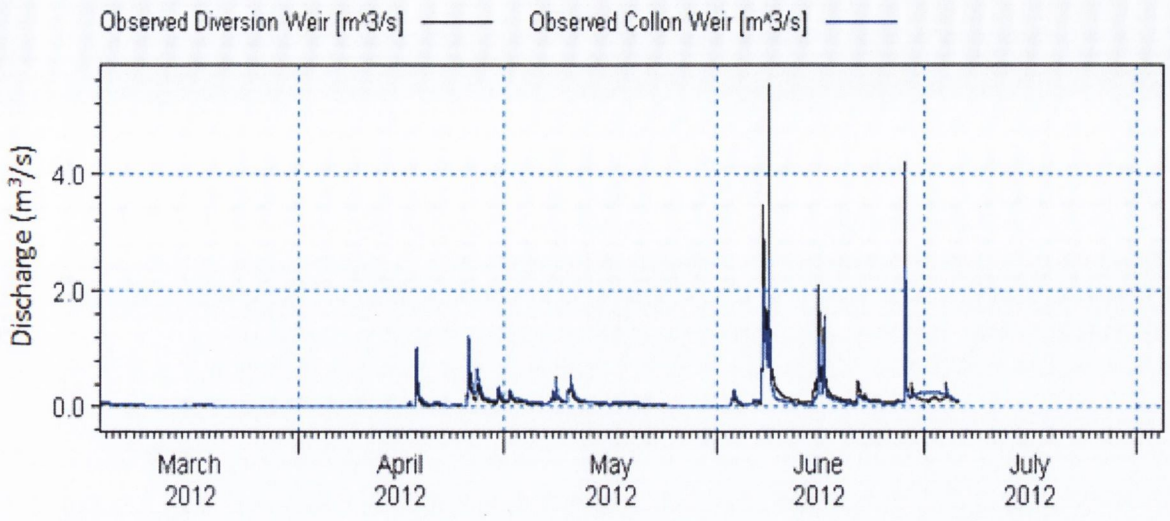

Figure 7-22. Observed discharge in the Mattock for the Diversion Weir and Collon Weir (Mar – July 2012).

Overall NAM performs well at reproducing the observed discharges for the calibration period, with a decrease in the performance of the simulations in the validation period, though not a substantial one. The separations obtained from the calibration period are in general agreement with those of the physical hydrograph separations in Chapter 6. The validation separations in Table 7-3 are broadly similar to those of the calibration process, but as these are not actually observed separations, they do not represent a proper validation of the simulated separations and as such are of less importance than the overall discharge for the validation process.

8 Catchment Modelling: Finite Difference Modelling

8.1 Introduction

The Mattock catchment has been assessed applying physical hydrograph separation and temperature tracer methods (Chapter 6) and semi-distributed lumped modelling (Chapter 7). In this chapter, the groundwater system will be further investigated implementing a fully distributed finite-difference model. The objective is to obtain further insight into the groundwater surface-water interactions and to evaluate the applicability of a distributed modelling approach given that limited data are available, though more information is available for the Mattock than most catchments in general. The Mattock is shown in Figure 8-1.

The amount of data required to populate a finite difference model and calibrate it is an important aspect of applying a distributed model to a catchment such as the Mattock. These types of models required a spatial distribution of hydraulic conductivity and storage properties as well as the location of the water table at certain points in order to calibrate the model. These data can be difficult to acquire in a catchment that does not have a long history of detailed field studies or where a national database of this information does not exist. The approach of this chapter will further highlight this.

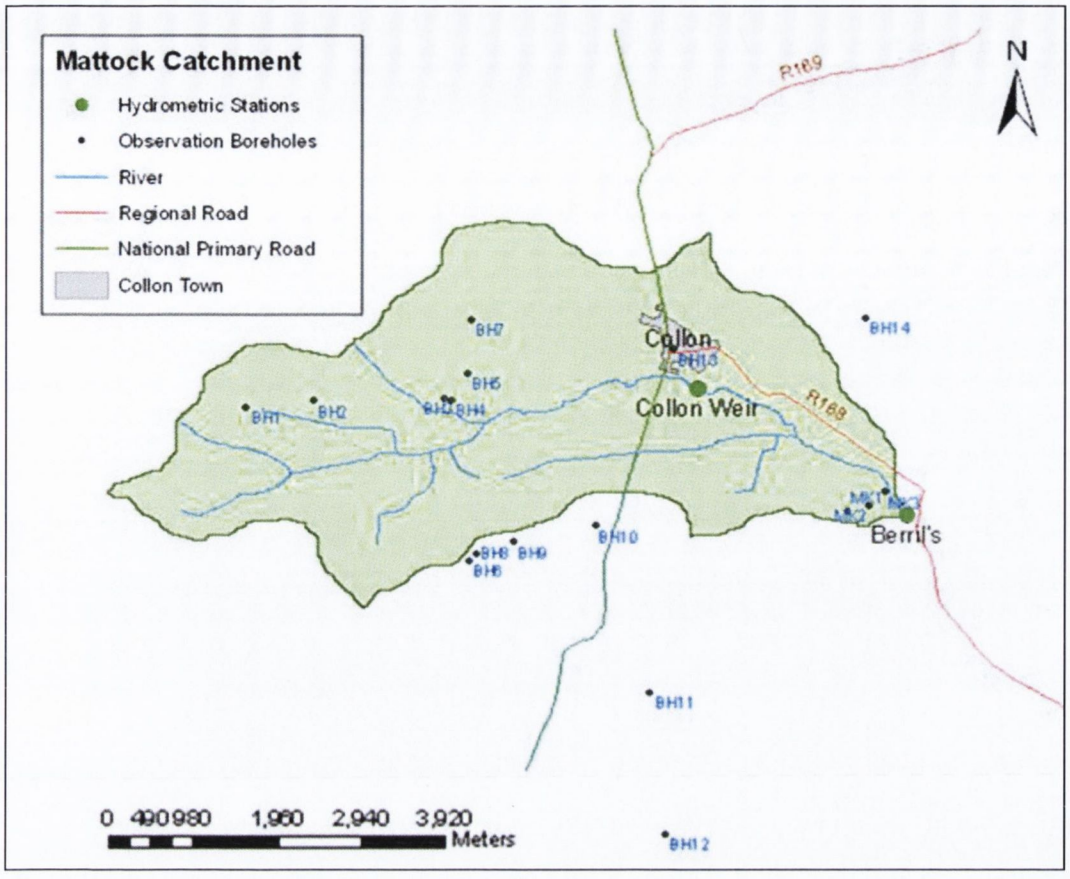

Figure 8-1. Mattock catchment with borehole locations.

8.2 MODFLOW

As reviewed in Chapter 3, MODFLOW is a finite difference groundwater flow model developed by the United States Geological Survey (McDonald and Harbaugh, 1984). Its modular structure allows the insertion of necessary programs into the model only when required, such as the well package when assessing pumping well effects, and facilitates the easy implementation of any newly developed packages for the model. As a result of this, there are a lot of file management requirements so that MODFLOW is generally implemented using a graphical user interface (GUI) as the front end of the model. This research utilizes Ground Water Vistas to implement MODFLOW in the Mattock catchment to further investigate the groundwater-surface water interactions in this catchment. A sample screenshot of the program can be seen in Figure 8-2.

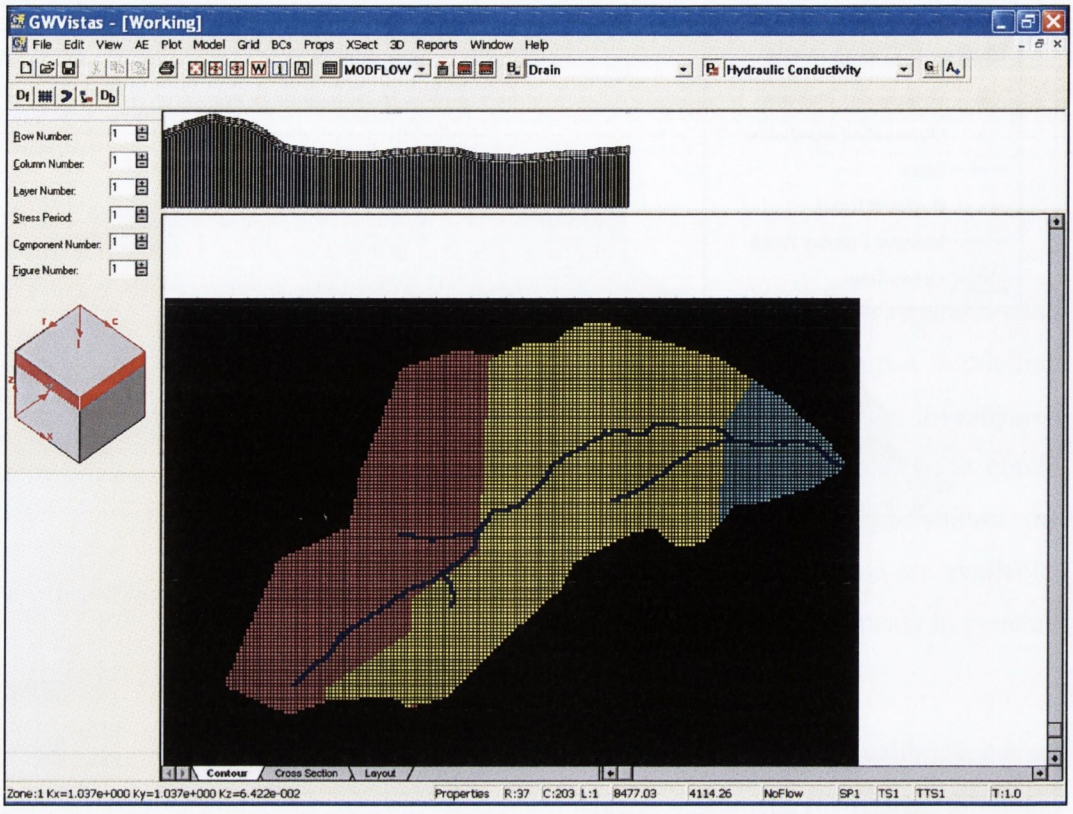

Figure 8-2. Screenshot of Ground Water Vistas showing different bedrock units and the catchment orientated to align with major faulting in the bedrock.

MODFLOW computes the head within the cells of the model in order to calculate the three-dimensional groundwater flow in the catchment. This is achieved by the finite-difference solution to Equation 3-I that describes flow of water through a porous material with the water having constant density.

$$\frac{\delta}{\delta x}\left(K_{xx}\frac{\delta h}{\delta x}\right)+\frac{\delta}{\delta y}\left(K_{yy}\frac{\delta h}{\delta y}\right)+\frac{\delta}{\delta z}\left(K_{zz}\frac{\delta h}{\delta z}\right)+W=S_s\frac{\delta h}{\delta t} \qquad \text{8-I}$$

where K is hydraulic conductivity in the axis direction [m/day], xx, yy and zz are the axis directions, h is hydraulic head [m], x, y and z, are the dimensions of the cells in the corresponding directions [m], W is change in water flux [day^{-1}], S_s is specific storage of the aquifer material [m^{-1}], and t is time [day]. From the finite-difference solution, a contoured groundwater table can be determined along with the flows in each cell and

subsequently discharges to the river, as well as discharges from the river to the groundwater.

The solution of Equation 3-I requires values of hydraulic conductivity in each direction, the specific storage of the bedrock along with recharge and abstraction data for the catchment. These data requirements are challenging to satisfy spatially and temporally within the Mattock catchment. The methods of approximating each of these are discussed in Section 8.3. The importance of boundary conditions is also considered in Section 8.3 as these will greatly influence the flow conditions in an aquifer and therefore the interactions between the surface water and the groundwater. These will include defining the extent of the groundwater catchment, the location of rivers and the outlet point of the catchment. Once the catchment has been set up within MODFLOW, the model requires daily recharge to provide the water that will affect the flow within the aquifer and a time series of the boundary conditions, such as river head, that affects the constraints on the groundwater flow. These are also examined in Section 8.3. The automated calibration software PEST (Doherty et al., 1994) was applied to calibrate data within the model, with this software contained within Ground Water Vistas.

8.3 Conceptual model and model design

Applying a numerical model to a catchment requires a simplification of the physical processes occurring within the catchment. The different hydrostratigraphic units and boundary conditions must be identified. Elements of the model such as abstraction wells, drains and rivers, need to be identified. The conceptual model is a pictorial representation of the groundwater flow system, frequently in the form of a block diagram or a cross-section (Anderson and Woessner, 1992). Applying this approach we can see in Figure 4-20 and Figure 4-19, a representation of the catchment at Berril's and at Collon. In these figures an estimation of the depth to bedrock and the type of subsoil overlying this bedrock can be obtained for these locations. Mapping, carried out by the Geological Society of Ireland (GSI), of depth to bedrock and permeability of the overburden, provides a useful starting point for conceptualisation of the catchment. A

selection of the types of data that can be acquired from these sources is presented in Figure 8-3 and Figure 8-4.

The model is bounded by the topographical highs to the north, south and east. The conceptual model of the groundwater flow is that it originates from more permeable bedrock (shallow groundwater) and less permeable bedrock (deep groundwater). The shallow and deep groundwater are divided into layers based on reducing hydraulic conductivity with depth, taking discrete intervals of depth and applying the hydraulic conductivity related to that depth to the layer (as will be discussed further in Section 8.3.3). The bedrock within the catchment can be classified between volcanic bedrock (basalt and rhyolite as shown in Figure 8-6(a)) and metasediment bedrock (Ordivician-Silurian greywacke and turbidite as shown in Figure 8-6(a)). The metasediment bedrock to the east of the catchment is classified as a Pu aquifer, with the volcanic and metasediment bedrock to the west of this classified as Pl (Figure 8-6(b)). Pu aquifers are poorly productive aquifers (i.e. small storage and low transmissivity), while the Pl aquifer typically have higher storage and transmissivity values, but still exhibit the characteristics of a poorly productive aquifer. The river at Berril's is above the bedrock water levels in the MK3 boreholes adjacent to the river (Figure 8-1), suggesting that the river is perched at this location (as discussed in Chapter 4). The elevation of the river is approximately 11 m above the groundwater table in the boreholes. This was shown in Chapter 4 in Figure 4-20.

Along with the bedrock aquifers in the catchment, there are two sand and gravel aquifers, one located at Collon and the other along the tributary by borehole 3 and 4 (BH3 and BH4) in Figure 8-1. An indication of their extent can be inferred from the High (H) permeability subsoil mapped in Figure 8-4 and from the cross-section at Collon (Figure 4-19). The extent of the different bedrock and sand and gravels modelled are presented in Figure 8-9. There is a confining layer of clay present in the sands and gravels at Collon. This requires a layer with low hydraulic conductivity to be inserted in this area between the upper and lower sand and gravel units. The upper unit is conceptually less connected to the lower sands and gravels and therefore will most likely be comprised of water flowing into it laterally from surrounding bedrock and recharge infiltrating from the surface. In contrast the lower sand and gravel unit will contain water flowing from the bedrock underlying it as well as lateral inflow. These

sands and gravels also supply three boreholes located there, abstracting approximately 1300 m^3/day of water. This abstraction rate along with an estimated of the hydraulic conductivity of these sands and gravels are taken from a groundwater protection study undertaken by CDM (2010).

The subsoils, as can be seen in Figure 8-4, have generally Low (L) draining potential, the term N/A in the legend refers to subsoil less than three metres in depth that are generally poorly draining soils and subsoils (as described in Chapter 4). As such, most recharge to the bedrock layers will occur near the catchment divide where soils are shallower and at the locations of High (H) and Medium (M) permeability subsoils in Figure 8-4.

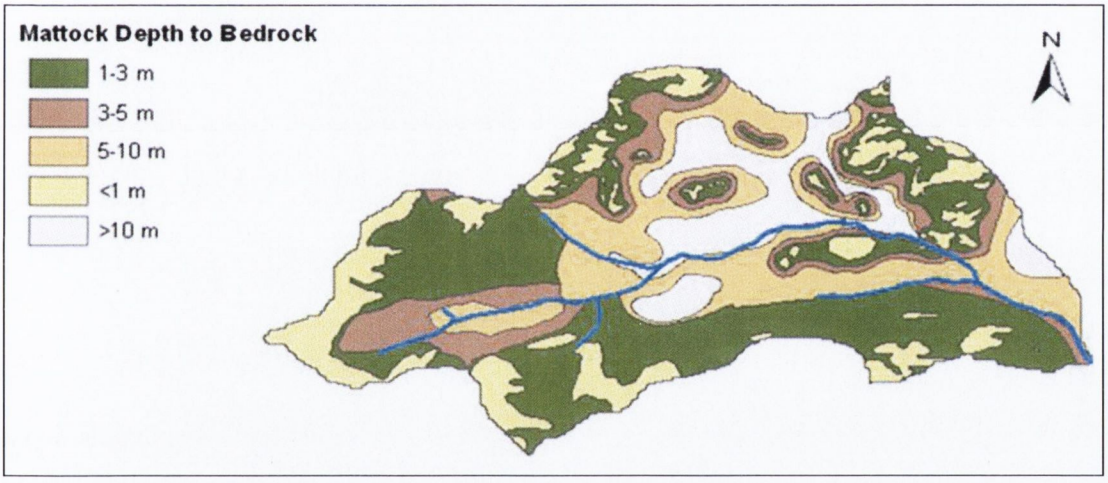

Figure 8-3. Depth to bedrock mapping in the Mattock.

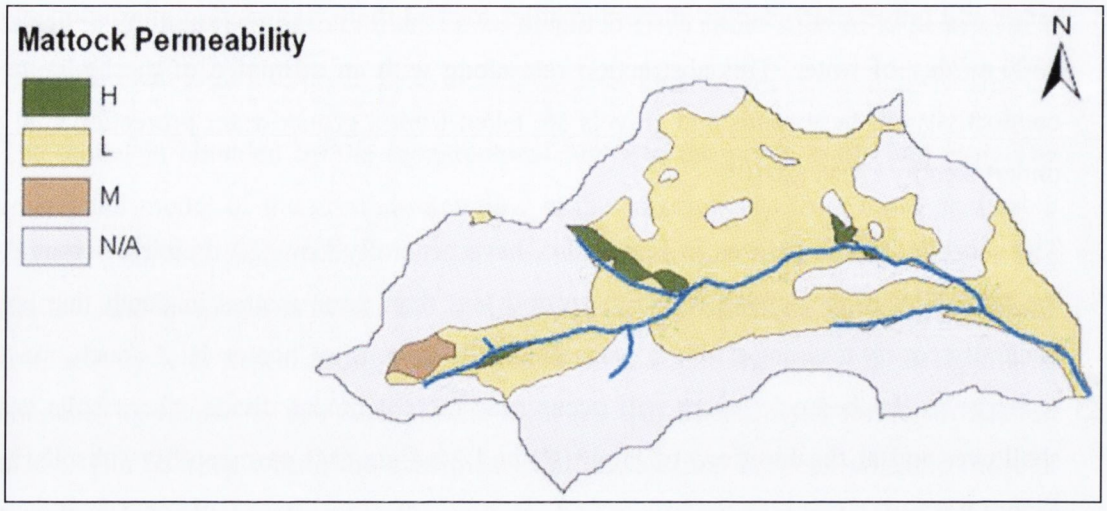

Figure 8-4. Subsoil permeability in the Mattock.

The topographical catchment drains an area of 16.9 km^2, with the neighbouring catchments modelled in order to compute the groundwater catchment to the outlet point at Berril's (see Section 8.4.1). The Mattock and the surrounding catchments drain an area of 120.4 km^2.

8.3.1 Modelling the continuous surface

The grid of numerical models used for groundwater flow simulations requires the input parameters to be represented at each cell location. These parameters are often only sampled at discrete locations sparsely distributed throughout the study area. In order to obtain values for all the cells located between measured points, interpolation that reflects the actual field conditions is required to estimate these input parameters. Kriging interpolation (Krige, 1951) was applied to estimate these surfaces due to its ability to maintain the observed values at their locations in the continuous surface space unlike other interpolation methods. 20 m Digital Elevation Model (DEM) data, that provide elevation points of the land surface, were processed and then inputted into the contouring software SURFER in order to create a three-dimensional representation of the conceptual model. A survey of the river bed was carried out using the Trimble 4700 GPS system. This provided an accurate elevation of the riverbed that updated the DEM

files for the channels topography. The topology of the catchment was then determined using Surfer, as shown in Figure 8-5.

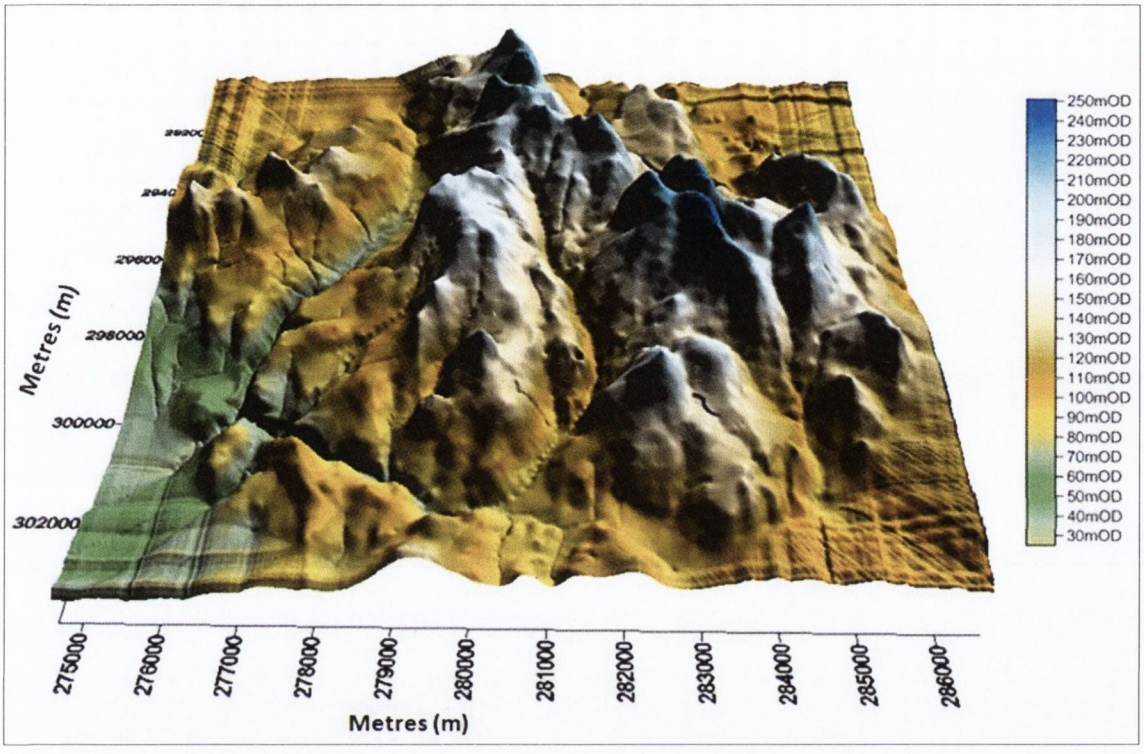

Figure 8-5. Three dimensional rendering of Mattock surface (note, vertical scale exaggerated).

8.3.2 Layer elevations

Utilising the depth to bedrock mapping (Figure 8-3), the depth from the surface to bedrock was calculated with SURFER to create a continuous surface of the top of the bedrock. Cross-sections at Collon (Figure 4-19) and at Berril's (Figure 4-20), combined with observations from borehole logs from the drilling of the MK1, MK2 and MK3 borehole clusters and other boreholes that have been located within and surrounding the catchment, shown in Figure 8-1, helped to refine the depth to bedrock mapping.

Applying the borehole logs from the MK clusters, an average shallow groundwater layer depth was defined as an offset from the base of the subsoil layer. Conceptually, this shallow groundwater layer is most permeable at the top of the layer where the highly weathered rock is in contact with the overlying subsoil. The permeability is

represented as decreasing with depth (see Section 8.3.3) due to decreasing exposure to weathering effects and less chance of fracturing due to the bedrock becoming more competent. The shallow groundwater layer was further subdivided into 4 m intervals to accommodate these increments in permeability.

The deep groundwater layer was defined as a further offset from the overlying shallow groundwater layer. This deeper, less fractured bedrock was subdivided into two zones to reflect the assumed reduction in permeability with depth. These subdivisions were relatively large (10 m) due to the small changes in permeability that were expected.

8.3.3 Hydraulic conductivity

Hydraulic conductivity ranges were calculated based on the bedrock type and aquifer classification in the catchment. The changes in bedrock type were identified with GSI mapping, Figure 8-6. The turbidite bedrock, identified as the Pu aquifer type, has been related to turbidite bedrock that has been studied in the Glen Burn catchment for initial estimates of hydraulic conductivity. Hydraulic conductivity of this type of bedrock has been observed to be inversely proportional to the depth below the surface of the bedrock by Equation 8-II (Comte et al., 2012).

$$K = 1.01d^{-1.57} \qquad \textbf{8-II}$$

where K is the hydraulic conductivity [m/day] at depth d [m]. Equation 8-II was used to assign hydraulic conductivity values to the shallow and deep groundwater layers in the turbidite bedrock. The bedrock and aquifer type mapping in combination with a table provided by the GSI to relate these two maps to transmissivities formed the basis of transferring the hydraulic conductivity in the turbidite to the other volcanic and metasediment bedrock types. The transmissivity of the turbidite was thus related to the other bedrocks with the Equation 8-II relationship applied to transform the hydraulic conductivities. The relationship between depth and hydraulic conductivity is illustrated for turbidite in Figure 8-7 with a schematic of decreasing weathering and fracturing with depth and a graph of decreasing hydraulic conductivity with depth based on Equation 8-II. Data were also provided by Janka Nitsche (Queens University Belfast) from pumping tests carried out in the MK boreholes, which were also utilised to help

constrain the hydraulic conductivity at the catchment outlet; these are presented in Table 8-1. The sands and gravels located at Collon are of particular interest as discussed in Chapter 4 and a cross-section of this area is illustrated in Figure 4-19. As discussed in Section 8.3, the groundwater protection study carried out by CDM (2010) provided the initial estimations of hydraulic conductivity in these sands. These sands and gravels are represented within the model as areas of higher hydraulic conductivity that are located in the upper layers of the model, with a lower hydraulic conductivity layer located in the middle of the sand and gravel layers to represent the clay layer in Figure 4-19. This is then underlain by bedrock. The final ranges of the hydraulic conductivities implemented in the model are shown in Table 8-4.

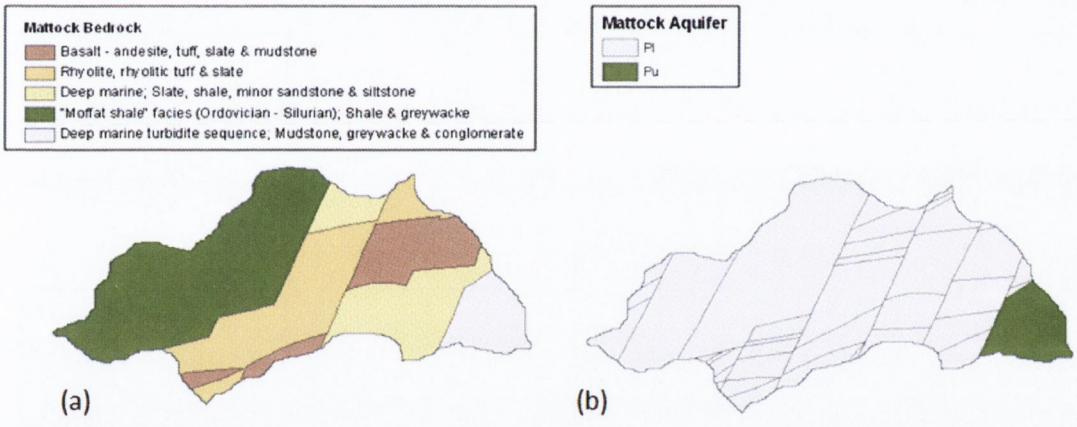

Figure 8-6. (a) Bedrock in the Mattock and (b) aquifer type.

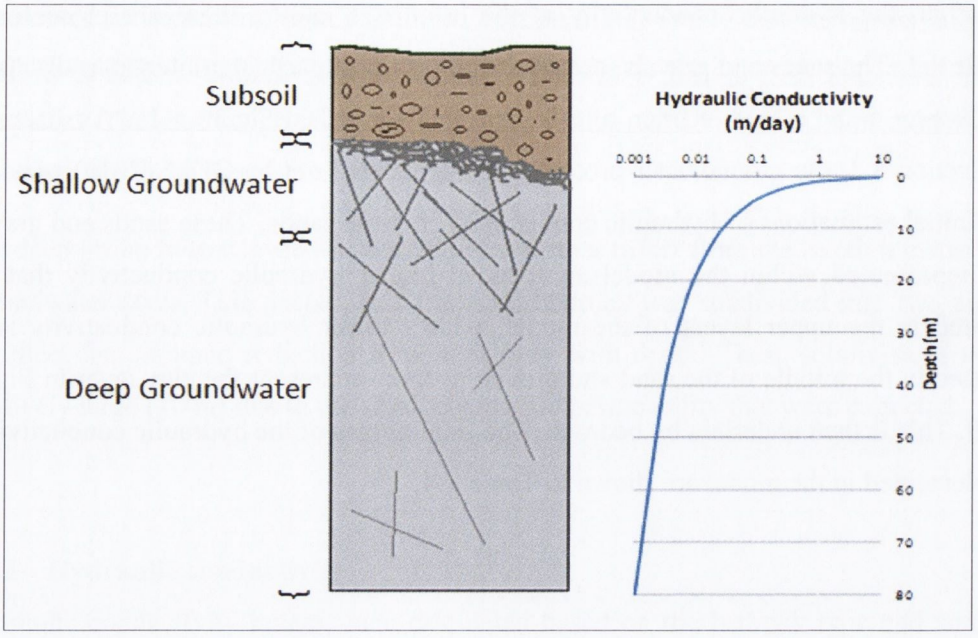

Figure 8-7. Decreasing hydraulic conductivity with depth and fracturing/weathering for turbidite.

Table 8-1. Hydraulic conductivity and storativity data from the MK boreholes (data provided by Janka Ntsche, QUB).

		Saturated thickness (m)	Storativity	Hydraulic Conductivity (m/d)
MK1	Deep	39.9	0.0017	0.003
	Shallow	16.2	0.398	0.004
MK2	Deep	33.6	0.584	0.461
MK3	Deep	21.3	0.0466	0.220
	Shallow	6.1	0.152	0.004

8.3.4 Storage characteristics

The shallow groundwater layers were simulated as containing the groundwater table at different locations throughout the catchment (Section 8.4.2) and as such are modelled as being unconfined aquifers with specific yields varying according to bedrock type. Specific yields were obtained using values from Morris and Johnson (1967), as shown in Table 8-2. Specific yield has a relatively small range, varying by an order of

magnitude as opposed to many orders of magnitude when compared to the ranges of hydraulic conductivity and specific storage (see Table 8-3). As the lower layers of the deep groundwater layer remained confined throughout the simulation, they only required the specific storage parameter. The remaining layers required both specific yield and specific storage parameters depending on whether they were confined or not by the layer overlying them. The sands and gravels within the model, as per their hydraulic conductivity in Section 8.3.3, were assigned initial values of specific storage and specific yield higher than that of the bedrock. Estimates of storativity outlined in Table 8-1 also assisted in constraining the specific storage and specific yield values, but as can be seen from the unrealistically high values storativity for MK1 Shallow, MK2 Deep and MK3 Deep, the error that can be involved in field sampling of these values can lead to misguiding values being obtained. The final calibrated ranges of specific storage and specific yield are presented in Table 8-5.

Table 8-2.Specific Yield ranges (Morris and Johnson, 1967).

Material	No. of analyses	Range	Arithmetic mean
Sedimenary materials			
Sandstone (fine)	47	0.02-0.40	0.21
Sandstone (medium)	10	0.12-0.41	0.27
Siltstone	13	0.01-0.33	0.12
Sand (fine)	287	0.01-0.46	0.33
Sand (medium)	297	0.16-0.46	0.32
Sand (coarse)	143	0.18-0.43	0.3
Gravel (fine)	33	0.13-0.40	0.28
Gravel (medium)	13	0.17-0.44	0.24
Gravel (coarse)	9	0.13-0.25	0.21
Siltstone	299	0.01-0.39	0.2
Clay	27	0.01-0.18	0.06
Limestone	32	0-0.36	0.14
Wind-laid materials			
Loess	5	0.14-0.22	0.18
Eolian sand	14	0.32-0.47	0.38
Rock			
Schist	11	0.22-0.33	0.26
Tuff	90	0.02-0.47	0.21

Table 8-3. Specific Storage ranges, adapted from Domenico (1972).

Material	Specific storage (S_s) (m^{-1})
Plastic clay	2.0×10^{-2} - 2.6×10^{-3}
Stiff clay	2.6×10^{-3} - 1.3×10^{-3}
Medium-hard clay	1.3×10^{-3} - 9.2×10^{-4}
Loose sand	1.0×10^{-3} - 4.9×10^{-4}
Dense sand	2.0×10^{-4} - 1.3×10^{-4}
Dense sandy gravel	1.0×10^{-4} - 4.9×10^{-5}
Rock, fissured, jointed	6.9×10^{-5} - 3.3×10^{-6}
Rock,sound	Less than 3.3×10^{-6}

8.3.5 Boundary conditions

Applying the correct boundary conditions to a groundwater model is a critical part of simulating the groundwater flow. The setting of boundary conditions is the step in model design that is most subject to serious error (Franke et al., 1987). There are three types of mathematical conditions that can represent a boundary:

1. Dirichlet condition (Dirichlet, 1839), where a head value is assigned to a cell in the model. This is also known as specified head boundary.
2. Neumann condition (Neumann and Witherspoon, 1970), where the flux across the boundary is assigned. This is also known as a specified flow boundary. This would include the no-flow boundary condition of zero flux.
3. Head-dependent flow boundary. This boundary condition defines the flux across a boundary based on head. This is also known as a mixed boundary.

These boundary conditions are defined within the model to constrain the flow pattern within the aquifer being modelled. The Dirichlet boundary is usually selected for the catchment outlet position to provide a sink for water within the catchment to drain to. The Neumann boundary is typically applied as a no-flow condition to define the groundwater catchment divide, where no groundwater flow can leave or enter the modelled area laterally. The head-dependent flow boundary is applied for rivers where the flow entering or leaving the river is determined by the head in the river and the head in the aquifer. These three boundary types are employed in the Mattock model and can

be seen in Figure 8-2, with the black cells representing the no-flow boundary, the blue lines representing the head dependent flow boundaries for the rivers in the catchment and the constant head located under the furthest river cell to the right of the figure.

8.3.6 Recharge

Recharge to the aquifer was calculated by implementing the FAO soil moisture accounting method (Allen et al., 1998) outlined in Chapter 4, with the amount of excess water infiltrating into the groundwater determined by the recharge coefficients approach outlined in Chapter 5. This recharge was then apportioned across the catchment in proportion to the percentage recharge expected based on the soils and subsoils, also calculated by the recharge coefficient approach. The time step of transient model (see Section 8.4.3) was one day. Therefore, recharge calculated in this manner was assumed to occur on the day of the rainfall. This assumption was made due to the limited options in MODFLOW to simulate flow in the unsaturated zone, discussed in Section 8.7.5.5.

8.3.7 Target heads

In order to calibrate MODFLOW, known head values located around the Mattock catchment and neighbouring catchments were required. Twelve target values were identified utilising datasets from the MK borehole clusters in the catchment, available data from private wells (Crockford, 2010; Quigley, 2011) and data from drilling of private wells carried out in the catchment with data records that were held by the GSI. These target heads provided calibration targets for the steady-state simulations. Some of these wells were pumped irregularly, and the variation in water level was not recorded throughout the day. Consequently, these target values were assigned a lower weighting than those that were not pumped and continuously monitored in the calibration of the model. The MK boreholes had loggers installed to monitor the water levels in these boreholes resulting in a continuous time series that were utilised for target data for transient simulations.

8.4 Model Design

In order to investigate the impact groundwater flow has on discharge in the Mattock river, three model set-ups were implemented:

1. Steady-state simulation that included the Mattock catchment and eight neighbouring catchments.
2. Steady-state simulation of the delineated Mattock groundwater catchment.
3. Transient simulation of the delineated Mattock groundwater catchment.

Each of these simulations is outlined in the following subsections, with the results assessed in Section 8.5.

8.4.1 Model set-up 1

This was a coarse model that used large cell sizes (150 m x 150 m) and just three layers to represent shallow and deep groundwater pathways in the aquifer. The cells were refined to a minimum of 75 m x 75 m near the Mattock to facilitate a more detailed delineation of the contributing catchment utilising eight neighbouring catchments (Figure 8-8). This was carried out in order to compute the contributing groundwater catchment to the outlet in the Mattock. DEM data were assessed inside ArcGIS to delineate each catchment's contributing area based on topography. The heads of the river were defined utilising the DEM elevation data and the river survey data from the Mattock (Chapter 5). The mean difference between the heads surveyed and the DEM data corresponding to the same locations were subtracted from the DEM elevations in the surrounding catchments to define the river heads. This approach was also employed when defining the constant heads at the outlet point of each catchment. Recharge was calculated using the discharge records in the Mattock to calculate the recharge required to sustain the discharge measured on the day the river survey was carried out in June 2012, for above baseflow conditions. The recharge was then apportioned across the catchment as described in Section 8.3.6. Twelve head targets were utilised for the calibration of the model for this steady state period as per Section 8.3.7. The model was then run as a steady-state simulation with the MODPATH model add-in being utilised

to carry out particle tracking in order to define the contributing groundwater catchment of the Mattock.

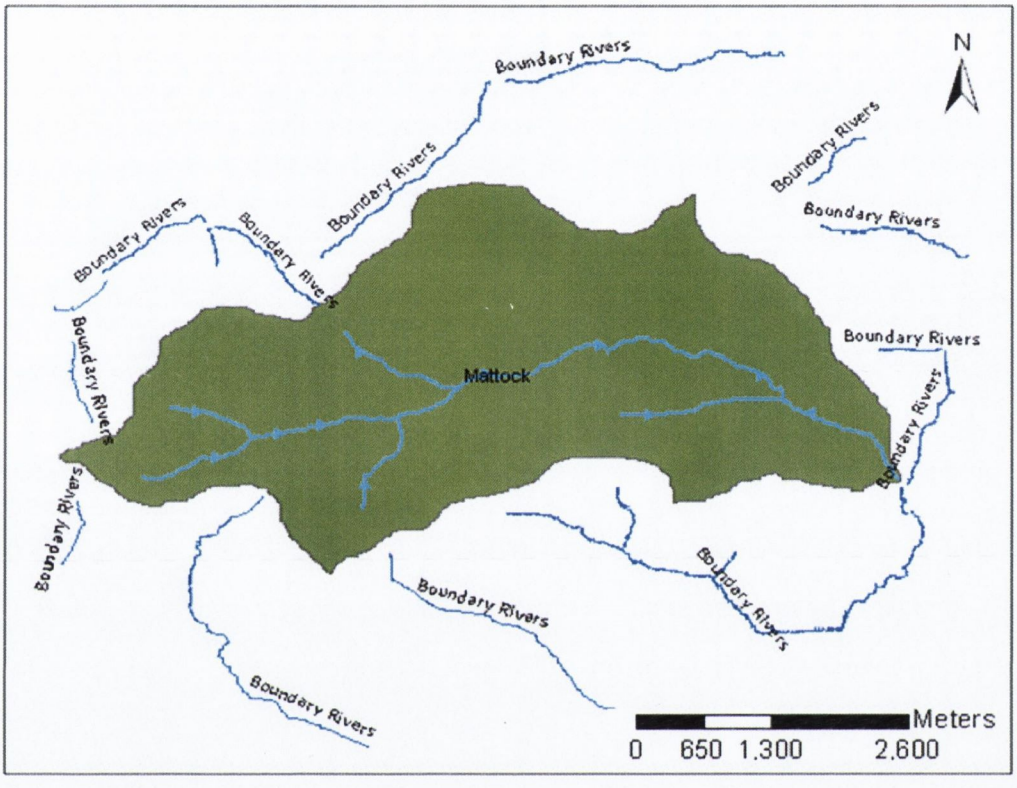

Figure 8-8. Mattock catchment with surrounding rivers in neighbouring catchments acting as boundary conditions.

8.4.2 Model set-up 2

After determining the contributing groundwater catchment for the Mattock in Model set-up 1, a more refined model was designed with just the Mattock considered. Cell sizes employed were 40 m x 40 m to provide enough cells to account for variation between different hydraulic conductivities within the model as recommended in (Haitjema et al., 2001). This also provided more detail on the contouring of the water table in the catchment. Five layers were used this time to further investigate the effect of decreasing hydraulic conductivity with depth, as described in Section 8.3.3. The heads of the Mattock river and its tributaries were defined using the river survey data, with the constant head at the outlet selected using borehole data from the MK1

boreholes near the catchment outlet. The public water supply located in the sands and gravels at Collon was set with a pumping rate of 1300 m^3/day, as per Section 8.3.3. Recharge was calculated according to model set-up 1. Nine target groundwater heads were used for the calibration of this model set-up, with three being omitted from model set-up 1 as they lay outside the groundwater catchment. The model was run for steady-state conditions. This simulation encountered difficulties in modelling the perched conditions of the Mattock river at the MK3 borehole cluster next to the river, as outlined in Section 8.3. As a result, hydraulic conductivity was increased approaching the river from the catchment divide in this area to provide the necessary transmissivity required to reproduce the perch conditions. The variations of hydraulic conductivity zones are shown in Figure 8-9.

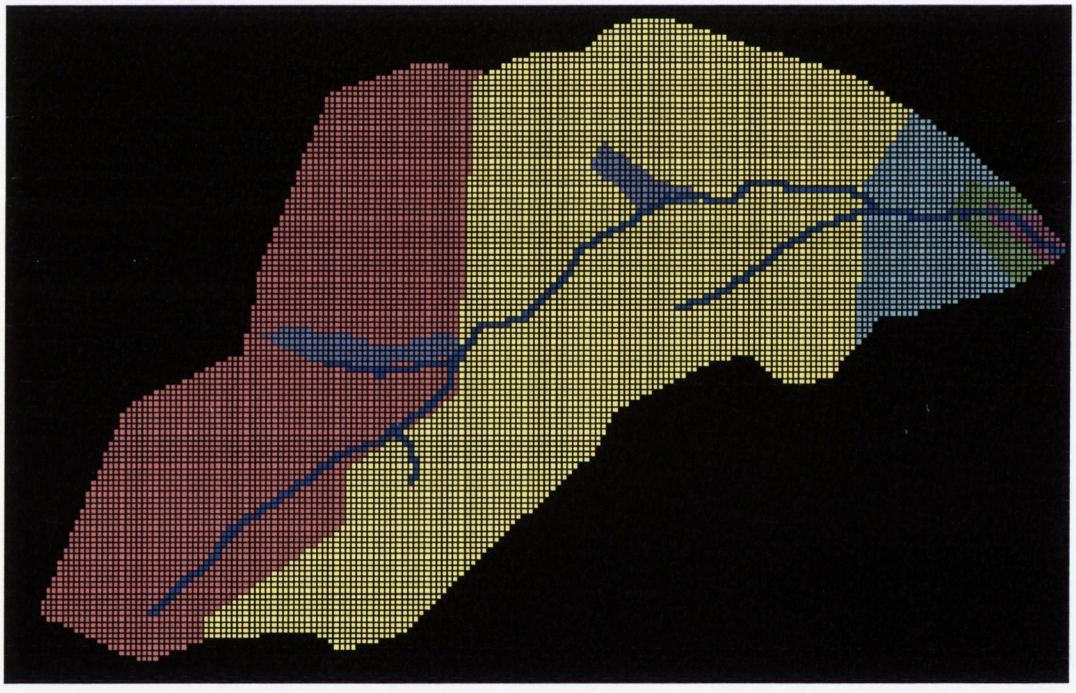

Figure 8-9. Hydraulic conductivity zones in the Mattock. Red and light blue zones are the metasediment bedrock with yellow the volcanic bedrocks. The green and pink zones are the increased hydraulic conductivity zones required to simulate the perched river conditions at the catchment outlet. The purple zones are the areas of sands and gravels in the catchment.

8.4.3 Model set-up 3

Following on from the calibration process, the water table heads and the target heads in model set-up 2, together with the model boundary conditions, were all modified for a transient simulation of the groundwater and surface water interactions for the same period as was modelled with NAM in Chapter 7 (February 2011 to February 2012). The time step for the transient model was one day to reflect the slow moving nature of groundwater. This can be observed by evaluating the time constants of 38 hours and 83 hours for the shallow groundwater pathway of Collon Weir and Berril's respectively, taken from the master recession curve analysis in Chapter 6. It was necessary to select the boundary conditions for the simulation period: river heads, the constant head boundary at the outlet and the recharge boundary conditions needed to be defined. The river heads were estimated using the daily recorded stages at Berril's, Collon Weir and the Diversion Weir to approximate changes in head across the catchment. This was achieved by relating the percentage change in head from the surveyed head at each hydrometric station to the next station linearly. The calculated percentage change along the course of the river was then applied to the surveyed river heads. This was computed for each time step of a day. Recharge was calculated applying the approach outlined in Section 8.3.6. The constant head at the outlet was varied proportionately to the change in head of the shallow and deep groundwater at MK1. As this was a transient simulation, storage characteristics were required to run the model. Storage values were applied as described in Section 8.3.4. The model was first run as a steady-state simulation to define initial heads across the catchment, and then in transient mode at daily time steps.

8.5 Results

8.5.1 Model set-up 1

Employing the coarse model set up and utilising MODPATH, the catchment area along the edges of the Mattock catchment was defined. The outline of the Mattock catchment computed using DEM data along with a selection of particle traces are shown in Figure 8-10 to demonstrate how the groundwater catchment was delineated, the extent of which was presented previously in Figure 8-9. As can be seen from Figure 8-10, the particle trace shows water moving from inside the topographical catchment (defined by

the green line) to neighbouring topographical catchments indicating that the surface water catchment and groundwater catchment are not coincident. In other sections of the catchment the opposite was true with water from outside the surface water catchment being computed as part of the Mattock groundwater catchment according to the set-up of the model.

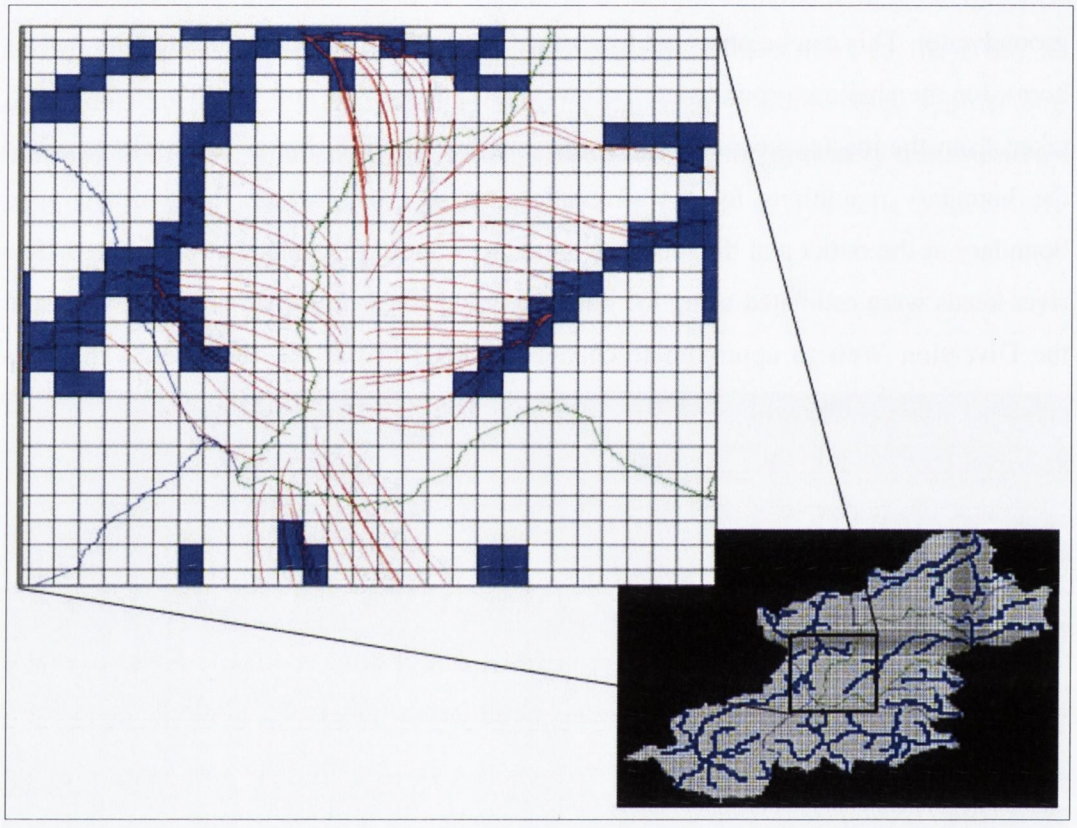

Figure 8-10. Selected particle traces carried out in model set-up 1.

Once this had been completed for the entire Mattock catchment, this approach was applied internally to the catchment to compute the groundwater contributing area for each of the three subcatchments. These calculated areas of the Mattock catchment and subcatchments are summarised in Table 8-6, with the groundwater catchment area of Mattock computed as being 16.7 km^2, compared with 16.9 km^2 as determined using the topography of the catchment.

8.5.2 Model set-up 2

Implementing the refined model and PEST as the calibration tool to minimise the difference between observed heads and simulated heads by varying the hydraulic conductivities of the different layers, the water table within the calculated groundwater catchment of the Mattock was computed as shown in Figure 8-11. In this simulation the cells that are contributing flow to the river can be determined by examining whether the water table head is located in the cell. Figure 8-12 displays the top layer of the model (conceptually the most fractured upper part of the shallow groundwater pathway). As can be seen from this figure, the active cells are those next to the river. There is generally a trend of increasing number of active cells with depth as would be expected. Shallow groundwater is conceptualised as being the upper three layers as these have the highest hydraulic conductivity. The two bottom layers are conceptually the deep groundwater pathways. The mass balance of this simulation has an error of 0.04% difference between inflows and outflows, with 57% of groundwater discharge to the river originating from deep groundwater pathways and 43% being contributed by shallow groundwater pathways. The RMS difference between observed and simulated heads for the nine target heads was 3.03 with a plot of observed versus computed heads presented in Figure 8-13.

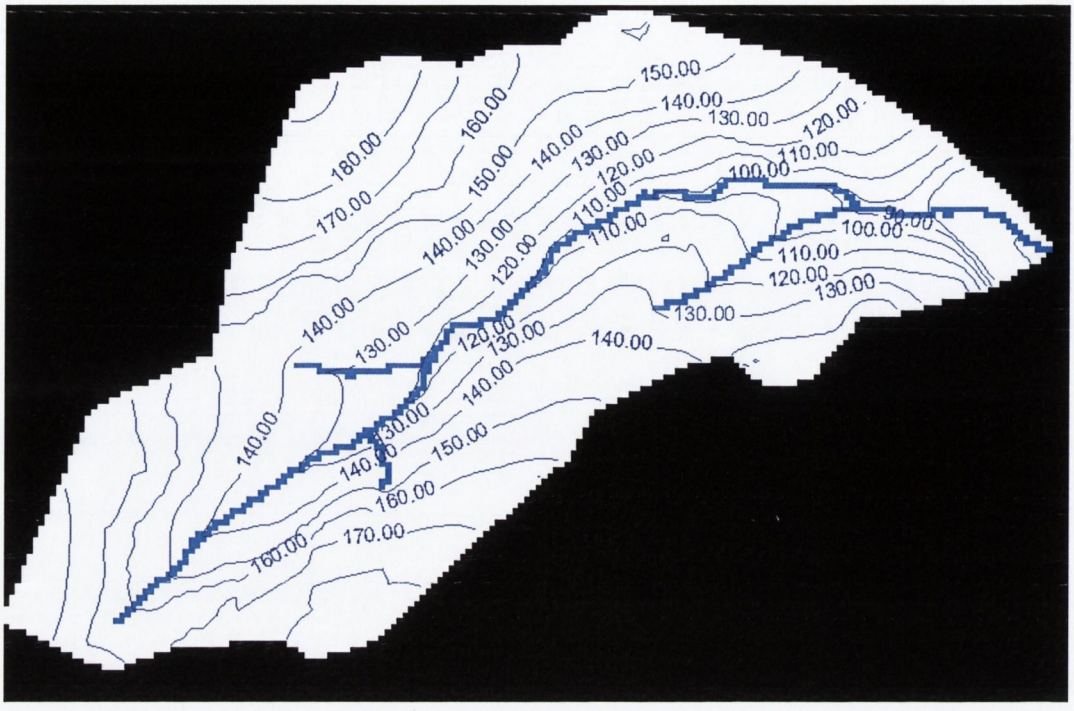

Figure 8-11. Model set-up 2 water table contours in metres above Datum.

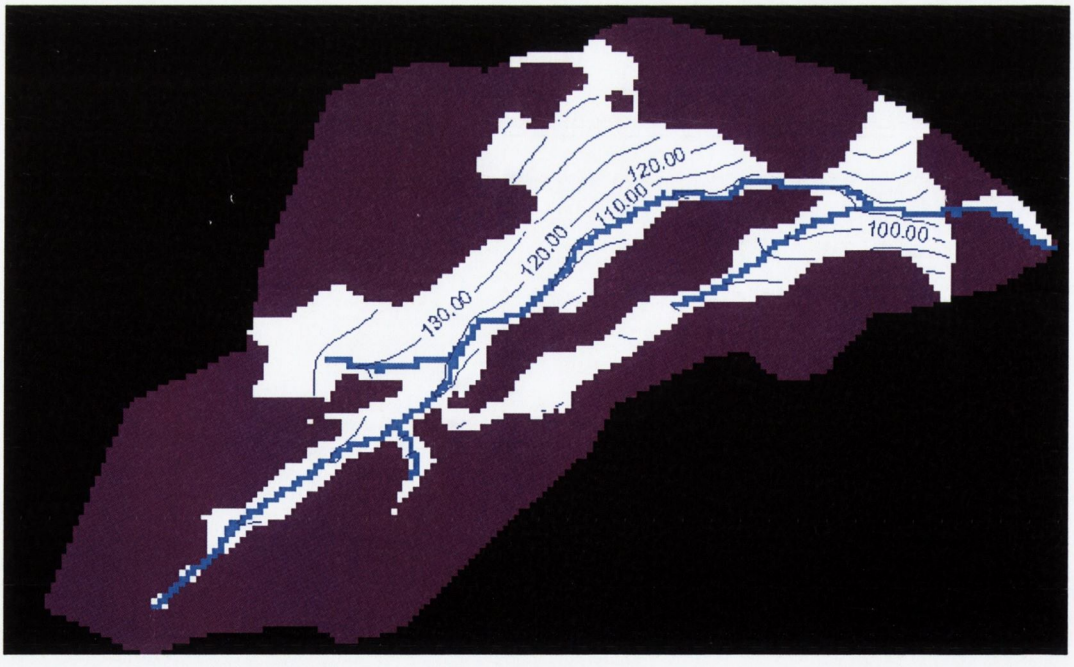

Figure 8-12. Model set-up 2 simulation of contributing cells to the river in upper layer. Purple cells are dry cells with white cells being cells that have water contributing to discharge in the river. The head contour lines are metres above Datum.

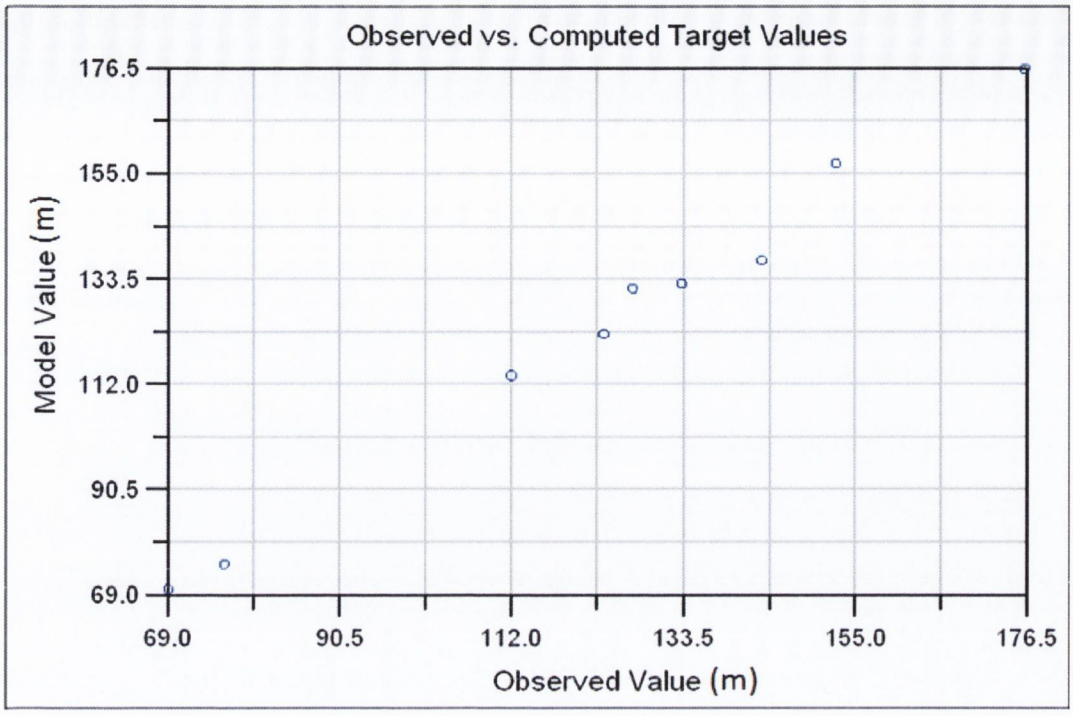

Figure 8-13. Observed versus computed heads for target values.

8.5.3 Model set-up 3

Once the model had been calibrated in model set-up 2, a transient simulation was required to calculate the contribution of the groundwater pathways to the river over time. As described in Section 8.4.3, the simulation was for the same period as the NAM simulation for the Mattock (see Chapter 7). The contribution of each pathway was computed along with the percentage error between inflows and outflows in the mass balance. The mean difference computed in the mass balance was 0.15% with a maximum difference of 7.1% observed. Time series of the shallow and deep groundwater pathways generated are plotted in Figure 8-14, Figure 8-16 and Figure 8-18, along with the NAM shallow and deep groundwater simulations for each of the three subcatchments, Diversion Weir, Collon Weir and Berril's, respectively. Comparisons of the combined groundwater pathways obtained from MODFLOW and NAM are also included in Figure 8-15, Figure 8-17 and Figure 8-19.

As can be seen in these figures, there is a considerable difference between the groundwater time series computed with NAM and those simulated using MODFLOW, particularly during baseflow conditions. In general, NAM generates higher groundwater

discharges during the winter periods but recedes to very low contributions during the summer period. The MODFLOW groundwater contributions do not display the same range of discharges as the NAM pathways, with spikes in discharges noticed (particularly for the MODFLOW and NAM shallow groundwater pathway) during periods of recharge as marked by sharp rises in the hydrographs containing all the pathways.

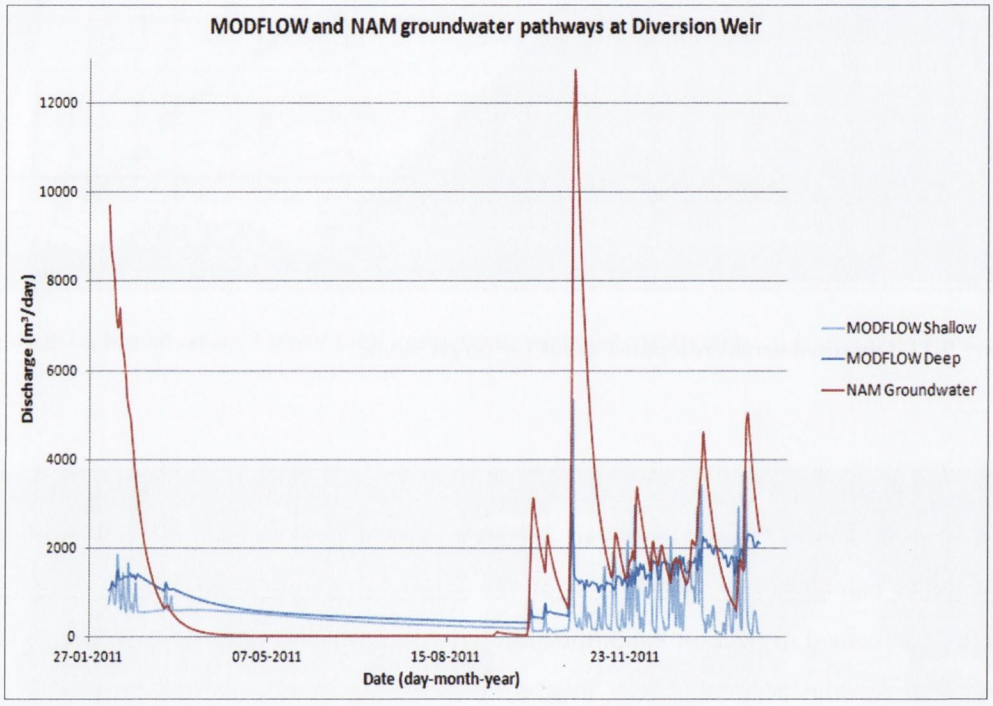

Figure 8-14. Deep and shallow groundwater pathways simulated by MODFLOW and groundwater simulated by NAM in the Mattock at Diversion Weir (Feb 2011 – Feb 2012).

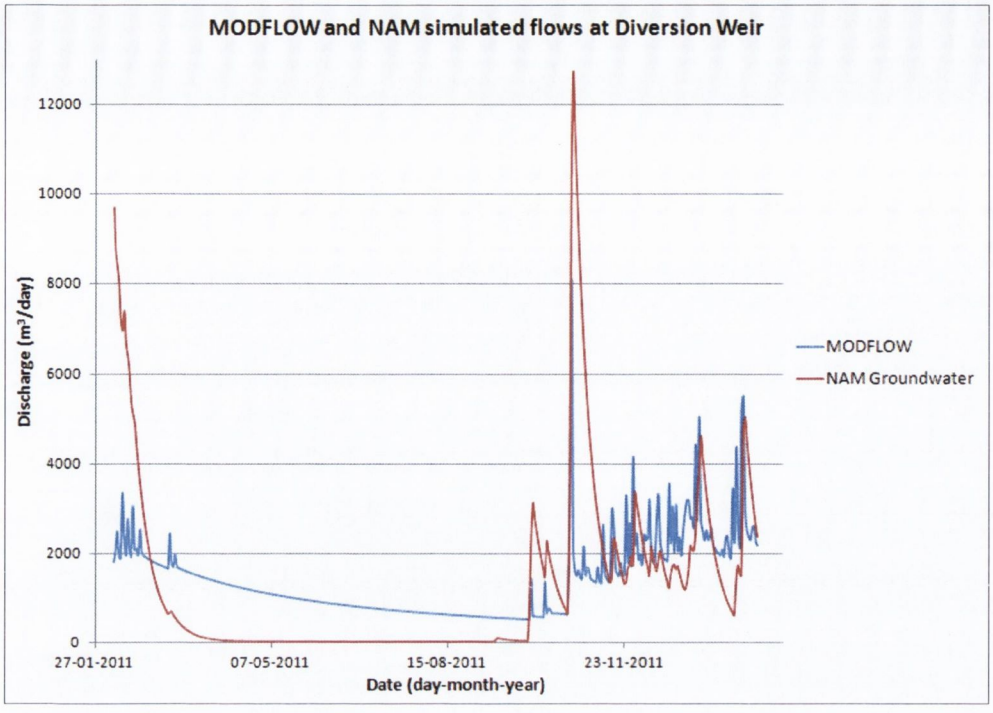

Figure 8-15. NAM and MODFLOW groundwater contributions to discharge in the Mattock at Diversion Weir (Feb 2011 – Feb 2012).

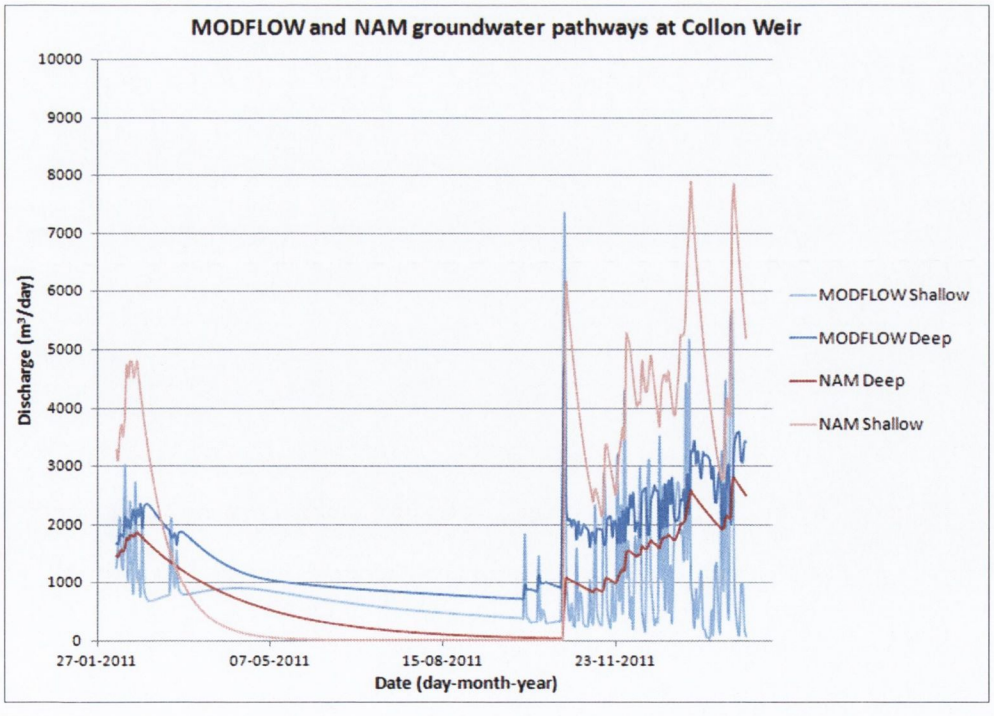

Figure 8-16. Deep and shallow groundwater pathways simulated by MODFLOW and NAM at Collon Weir (Feb 2011 – Feb 2012).

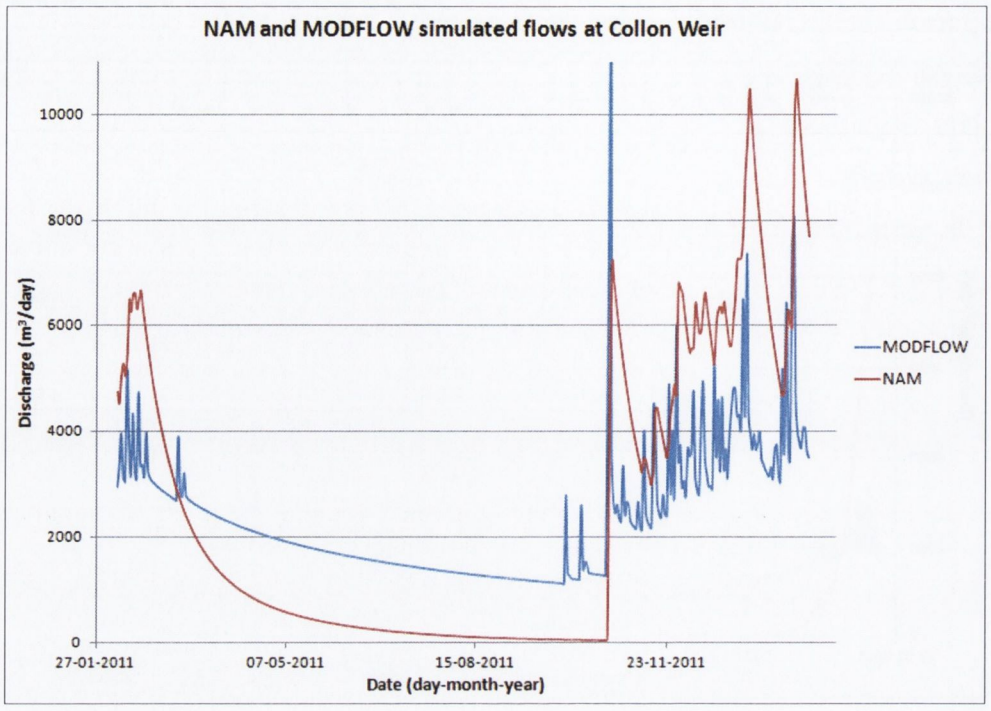

Figure 8-17. NAM and MODFLOW groundwater contributions to discharge at Collon Weir (Feb 2011 – Feb 2012).

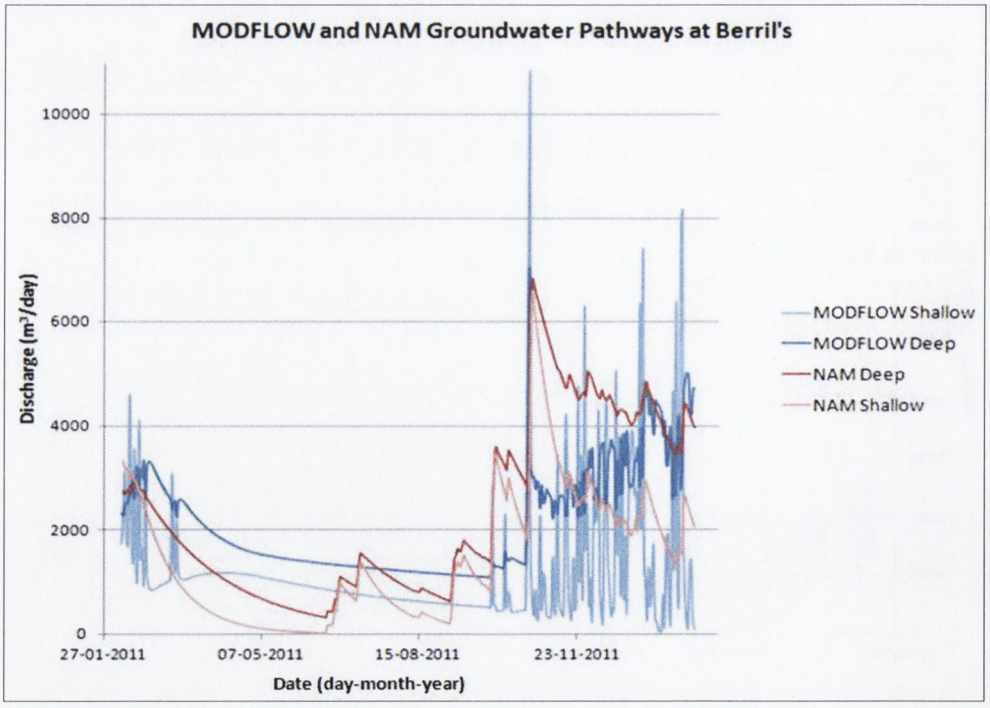

Figure 8-18. Deep and shallow groundwater pathways simulated by MODFLOW and NAM the catchment outlet at Berril's (Feb 2011 – Feb 2012).

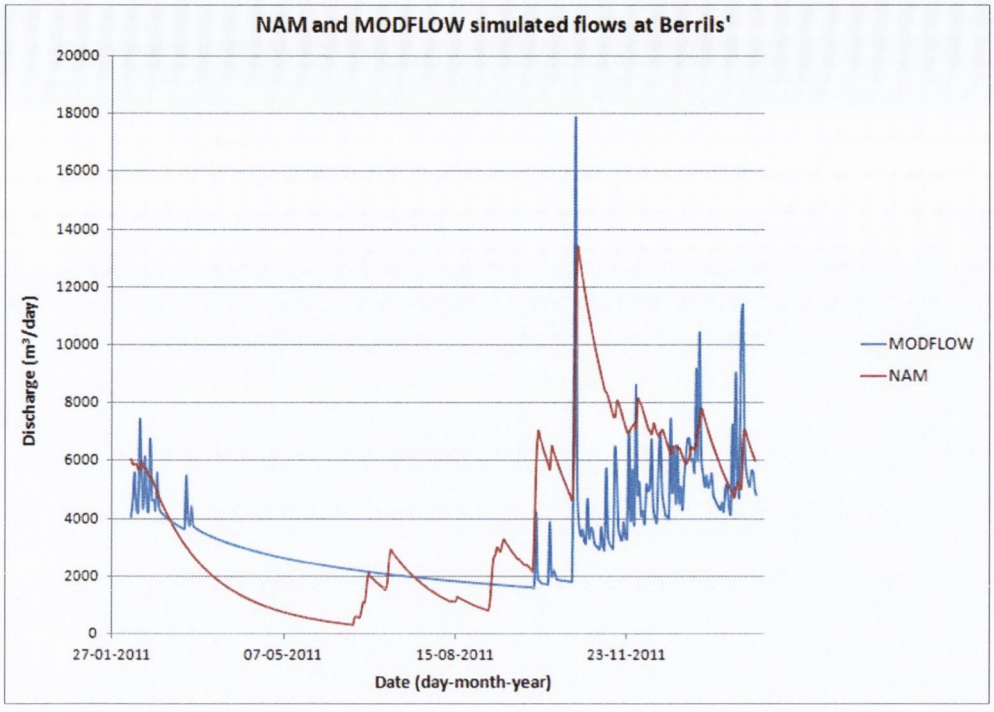

Figure 8-19. NAM and MODFLOW groundwater contributions to discharge at Berril's (Feb 2011 – Feb 2012).

The transient simulation was calibrated by varying the specific storage and specific yield values utilising the data from the MK boreholes near the catchment outlet, as these were the only data available to constrain the storage parameters of the model. As shown in Figure 8-1, these boreholes are only representative of the bedrock near the catchment outlet. As noted in Section 8.5.2, the bedrock in this area was assumed to be more transmissive than in the rest of the catchment in order to achieve the perched river conditions. A comparison of the simulated heads at a borehole of each cluster is presented in Figure 8-20.

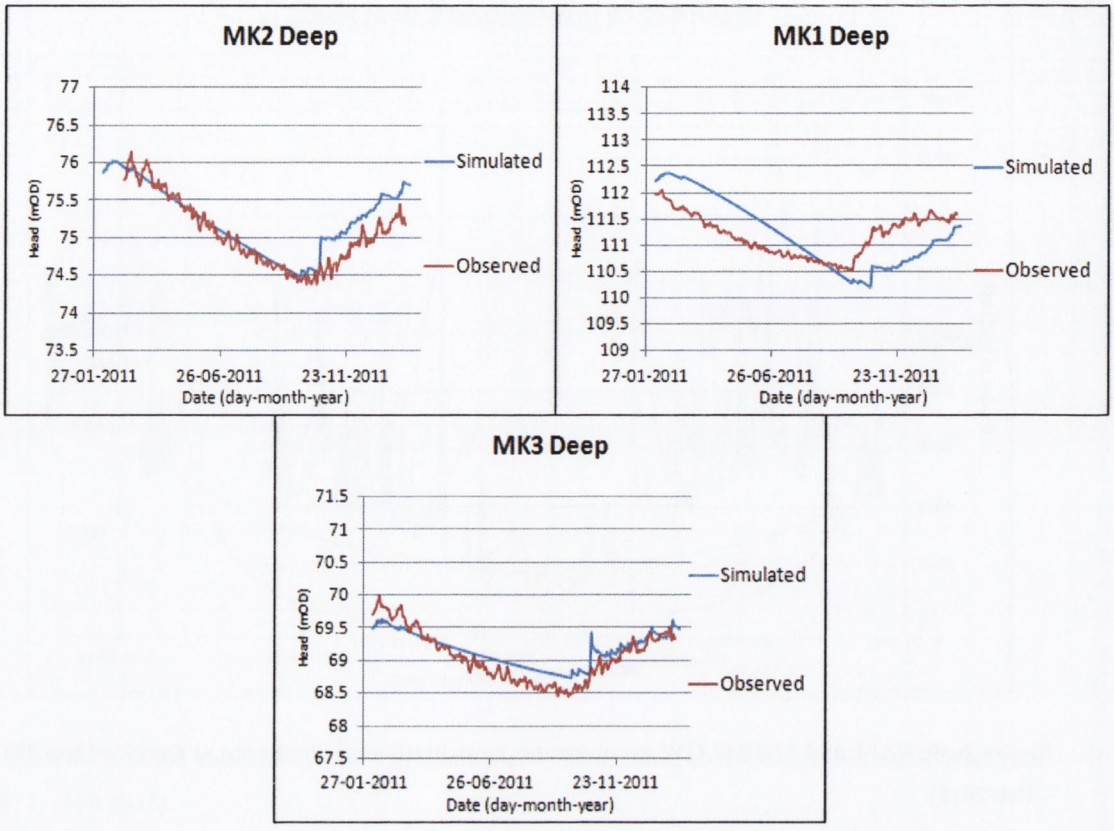

Figure 8-20. Simulated and modelled heads in the MK1, MK2 and MK3 Deep boreholes.

The comparison between observed and simulated water levels in the MK boreholes shown in Figure 8-20, suggest a reasonable comparison was obtained between the simulated levels at MK2 and MK3. MK2 largely matches the recession of the observed data, with the shape of the rise in the groundwater levels for the second half of the graph similar to the simulated rise, but offset higher. This is most likely related to the recharge during large rainfall events during this period, with recharge being over-estimated. There are small oscillations in all three of the borehole's observed groundwater levels that may be linked to tidal effects on the ground. These rises and falls in the observed data match local tidal data (Jenny Deakin, personal communication, 2010) which would account for the inability of MODFLOW to simulate these oscillations not derived from recharge. The rate recession of MK3 is generally well matched by the simulated groundwater levels, though a rate slightly less than what is observed. The comparison of the observed and simulated groundwater levels at MK1 is of most concern, with the rate of recession and rise of the simulated

levels slow than that of the observed data. This was the best calibration that could be obtained taking all three boreholes into account, the effects of varying parameter values around the ones utilised in Table 8-4 and Table 8-5, to simulate the groundwater levels in Figure 8-20 are examined in Section 8.6. The higher end of the hydraulic conductivity ranges are taken from the shallow groundwater layers, while the lower ranges are taken from deep groundwater layers.

Table 8-4. Summary of the range of hydraulic conductivity values applied in shallow and deep groundwater bedrock units.

Hydraulic Conductivity	Kx (m/d)		Kz (m/d)	
	Upper	Lower	Upper	Lower
Pl Metasediments	1.53	0.021	0.08	0.007
Pu Metasediments	0.21	0.002	0.04	0.003
Adjusted Pu	17.60	0.037	1.86	0.013
Volcanics	1.54	0.02	0.11	0.006
Sands and gravels	14.40	1.542	1.02	0.114
Clay confining layer in sands and gravels	1.70E-03		4.10E-04	

Table 8-5. Summary of storage values implemented for the different bedrock units.

Storage	Pl and Pu Metasediments		Volcanics		Adjusted Pu		Sands and gravels	
	Ss (m^{-1})	Sy	Ss (m^{-1})	Sy	Ss (m^{-1})	Sy	Ss (m^{-1})	Sy
More fractured shallow groundwater	1.76E-05	0.012	3.20E-05	0.024	4.80E-04	0.1108	6.00E-04	0.168
Less fractured shallow groundwater	4.15E-06	0.01	5.40E-06	0.012	4.80E-04	0.1108	Clay layer	
Deep groundwater	3.61E-06	0.008	5.00E-06	0.006	3.12E-05	0.015	5.00E-03	0.01

The comparison of catchment area calculated by MODFLOW and computed with DEM GIS data, the comparison of the contribution yearly of each pathway, the change in groundwater storage and the average percentage error between inflows and outflows of the MODFLOW model are presented in Table 8-6, with the discussion of these results in Section 8.7.3.

Table 8-6. Results of MODFLOW modelling in the Mattock

	MODFLOW Catchment Area km2	DEM Catchment Area km2	MODFLOW Deep GW mm/year	MODFLOW Shallow GW mm/year	NAM Deep GW mm/year	NAM Shallow GW mm/year	ΔS mm/year	Average Error %
Diversion Weir	6.6	7	49.57	31.82	71.75		1.23	0.11
Collon Weir	11.8	11.6	36.39	39.42	26.09	50.71	1.98	0.15
Berril's	16.7	16.9	46.70	27.63	50.65	31.72	2.35	0.15

8.6 Sensitivity analysis of transient simulation

In order to assess the effect that increasing and decreasing parameter values had on the results of the transient modelling in Section 8.5.3, the model was rerun with storage values increased by 20% and decreased by 20% and then separately rerun with hydraulic conductivity values increased by 20% and then decreased by 20%. The effect that these simulations had on the transient calibration plots in Figure 8-20 and the overall discharge simulated in the catchment are presented in this section (Figure 8-21 to Figure 8-24) and discussed in Section 8.7.4.

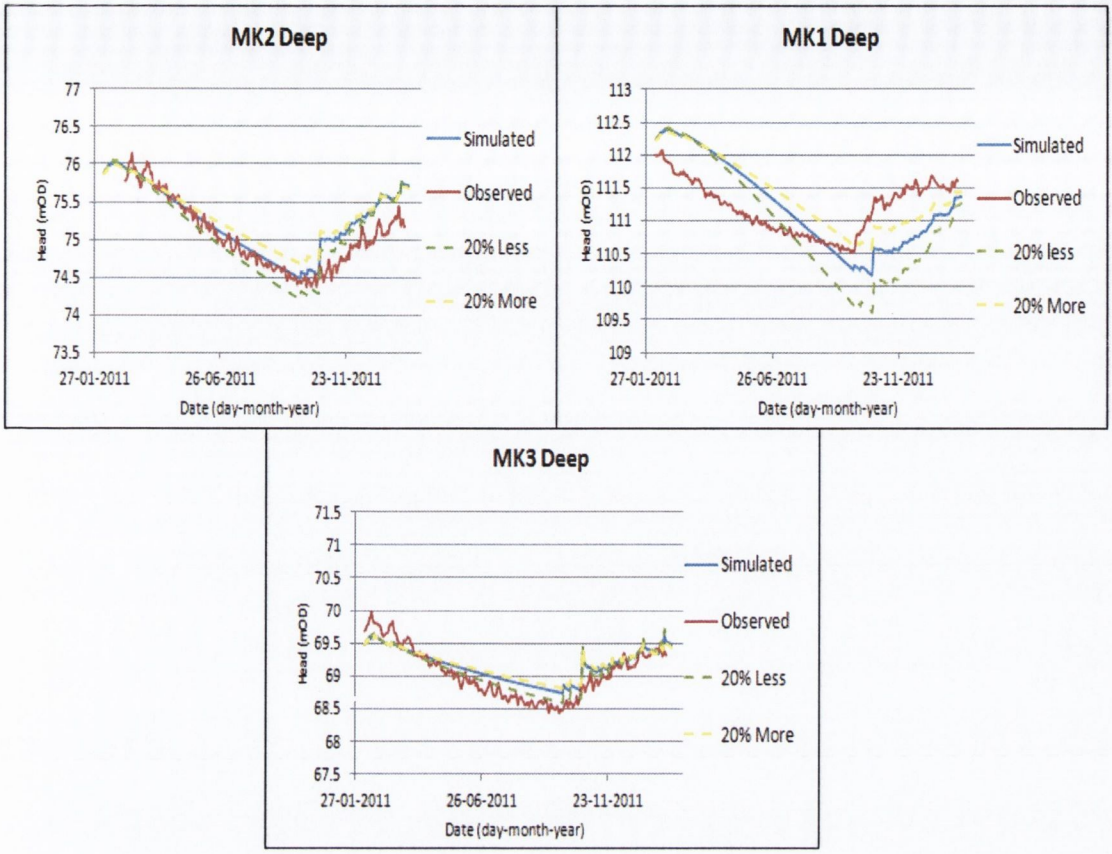

Figure 8-21. Comparison of simulated and observed groundwater levels in MK boreholes with the effects of increasing and decreasing the values of specific storage and specific yield by 20% of their calibrated value.

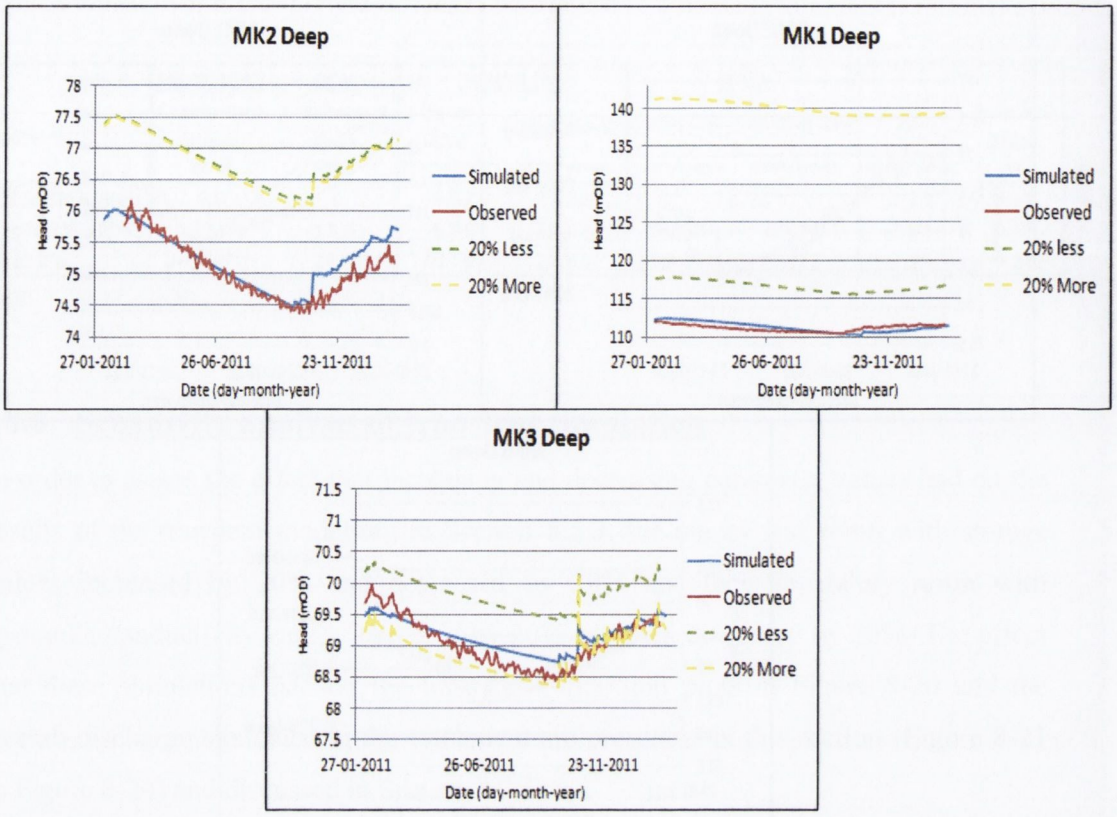

Figure 8-22 Comparison of simulated and observed groundwater levels in MK boreholes with the effects of increasing and decreasing the values of hydraulic conductivity by 20% of their calibrated value.

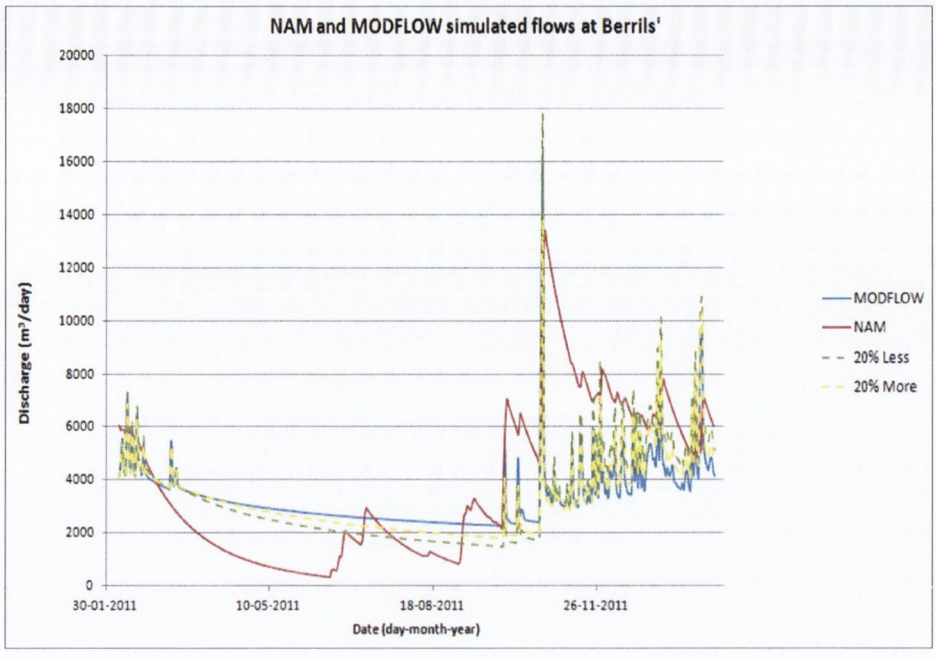

Figure 8-23 Comparison of MODFLOW and NAM discharges at Berril's with the effects of increasing and decreasing the values of specific storage and specific yield by 20% of their calibrated value for the MODFLOW simulations.

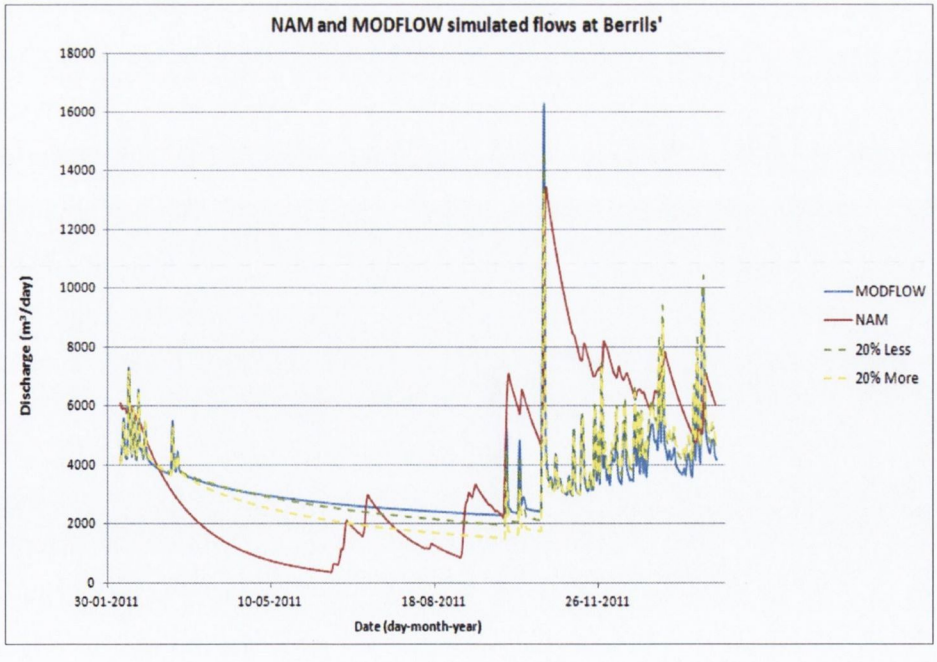

Figure 8-24. Comparison of MODFLOW and NAM discharges at Berril's with the effects of increasing and decreasing the values of hydraulic conductivity by 20% of their calibrated value for the MODFLOW simulations.

8.7 Discussion

The three model designs employed for the simulations in this chapter provide learning outcomes that could not be determined from a lumped modelling approach as described in Chapter 7. Nonetheless, there are many assumptions involved in implementing a distributed modelling approach that must be appreciated when considering the results.

8.7.1 Model set-up 1

The objective of the first model set-up was to identify the contributing area to each of the hydrometric stations in the catchment. This was important as the general assumption applying NAM was that the surface catchment area and groundwater catchment area were coincident. In Table 8-6 it is shown that while there were differences in the areas calculated, there was close agreement between the areas of the overall catchment to the outlet at Berril's and between the subcatchments.

Utilising the neighbouring catchments and the estimations of the elevations of the river heads from DEM data and the river survey (as described in Section 8.4.1), the contributing areas were computed. This method of calculating the contributing area is advantageous when compared to assuming a catchment divide based on topography or geology or a combination of both. This approach takes into account both topography and geology, but also the boundary conditions of the rivers that the catchment divide separates. Consequently, more confidence can be associated with the groundwater catchment areas applying this approach. While this is a particular case involving one catchment, and therefore is difficult to generalise from, it is reassuring that the two different methods of calculating the groundwater catchment area provide comparable results.

There are a number of ways that this approach could be improved upon. An accurate survey of the river heads would provide more certainty in the delineations determined. The current grid of 20 m x 20 m DEM available does not have a sufficiently high spatial resolution to obtain this, which subsequently requires the estimations of head in the river, outside of the river survey completed for the Mattock. A better understanding of the distribution of hydraulic conductivity from boreholes providing known values of head in the catchments would also improve the accuracy of results. The demand for

accurate data with improved spatial distribution will always be a requirement of a distributed model, as will be observed when discussing the model set-up 2 and 3.

8.7.2 Model set-up 2

The objective of the second model set-up was to simulate the heads within the layers of the computed groundwater catchment of the Mattock. The finer grid utilised in this model allowed a more detailed surface of heads to be calculated in each layer than was achieved in the model set-up 1. The addition of two more aquifer layers also allowed the declining hydraulic conductivity with depth relationship (as considered in Section 8.3.3) to be more effectively approximated.

Once more, the target heads from boreholes in the catchment were used, though some of these were private wells that were pumped irregularly (as discussed in Section 8.3.7) and so were assigned less weight in the calibration than non-pumped borehole target heads. Despite the inclusion of these pumped boreholes, target data for calibration within the catchment were scarce, with only 9 borehole locations providing target head values for a 16.7 km^2 catchment. As such, while the heads in these locations were in agreement with simulated values, outside of the surrounding areas of these target boreholes, much more uncertainty is present, particularly to the north and south of the catchment.

The river elevation survey in June 2012 provided mid-range levels of discharge; generally, flows would be expected to be lower for this time of the year, but due to high rainfall in the Mattock in summer 2012 (184 mm of rainfall for June), heads elevations could not be obtained for low flow conditions. If data were not available for a transient simulation, such as distributed recharge and change in river head estimations, the approach of model set-up 2 for high flow and low flow conditions would help approximate the contribution of groundwater to the river for summer and winter conditions and hence provide an estimation of river discharge derived from groundwater annually.

Improvements in DEM data spatial resolution would help better define topography and hence the surface of the aquifer that is calculated from this, utilising depth to bedrock GIS information (Section 8.3.2). As with model set-up 1, a higher quality of hydraulic

conductivity and borehole target data would help improve the accuracy of model outputs.

8.7.3 Model set-up 3

The objective of model set-up 3 was to identify how the contribution of the groundwater pathways to the river varied throughout the year starting February 7th 2011 and ending February 7th 2012. The initial heads of the simulation were calculated from approximating the river heads using the times series of river stages from the hydrometric stations as per Section 8.4.3. The model was initialized utilising the steady-state simulation (i.e. model set-up 2) to match these head values. The grid layout and layers of the model were the same as in the model set-up 2. Recharge was calculated for each daily time step of the model following the approach outlined in Section 8.3.6.

Applying this approach, the time series of the deep and shallow groundwater pathways were computed and these were compared with those computed in Chapter 7 from the NAM modelling (Figure 8-14 to Figure 8-19). It is observed that while the overall contributions of combined groundwater for the year were similar (Table 8-6), the temporal distribution of these pathways displayed greater variation. In the combined groundwater contribution plots for both MODFLOW and NAM (Figure 8-15, Figure 8-17 and Figure 8-19), the MODFLOW contributions to the river discharge, during low flow periods, are too large to be discharged into the river as the flow at the hydrometric stations confirms in Figure 8-25. This figure indicates that the contribution of groundwater being predicted during this month was higher than can be accounted for in the river, except for periods when rainfall causes the river discharge to increase sharply. This increase in flow and subsequent fast recession implies that this increase was as a result of quicker responding pathways that are most likely not groundwater. As such, the temporal distribution of groundwater discharges being predicted by MODFLOW would suggest errors during these periods

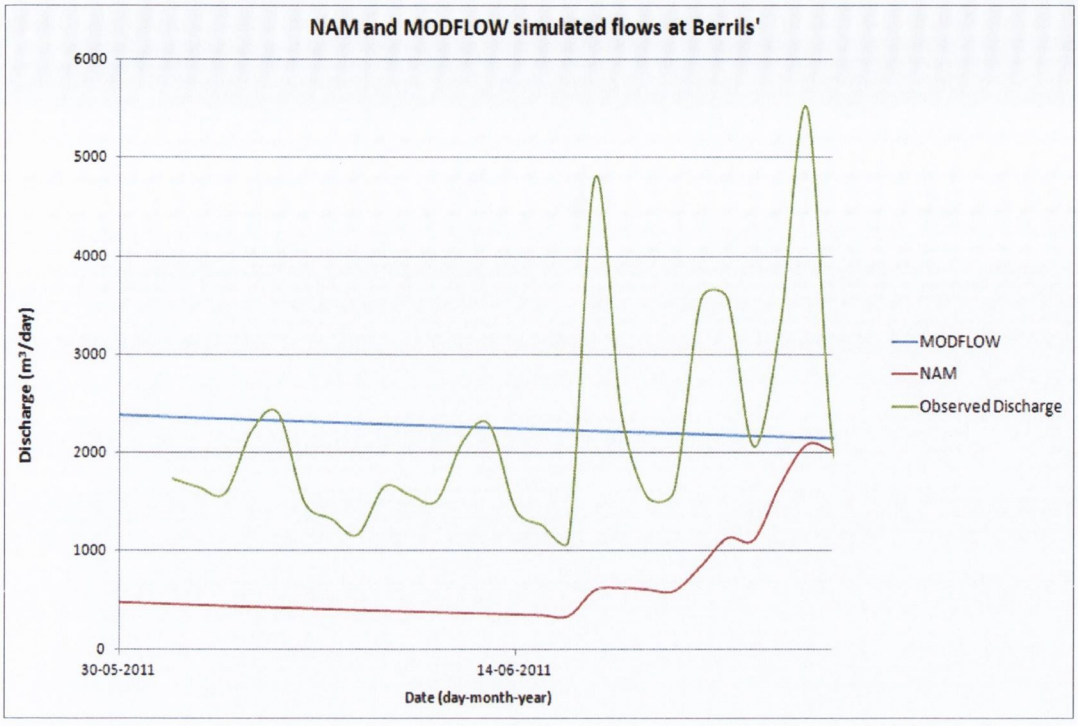

Figure 8-25. MODFLOW and NAM groundwater contributions along with total river discharge measure at Berril's (June 1st – June 30th 2011).

One likely source of error that would account for these differences would be the storage parameters used in the simulation. Initial values of these were taken from literature and pumping test data (Section 8.3.4) with calibration carried out with the continuous monitoring of the borehole levels in the MK1, MK3 and MK3 boreholes. Though, as considered in Section 8.3.4, some of these storage values from the pumping tests appear unrepresentative and as such, were not included when estimating initial values of storage. The continuous monitoring provided a time series that could be utilised for predicting the storage values appropriate for the Mattock. These boreholes though, are not very representative of the catchment bedrock as a whole as they are located near the catchment outlet – and are only representative of one rock type. Also they are located where the river is perched and as such may represent a situation of disconnect between the river and the aquifer that is limited to this location in the catchment. It was therefore difficult to implement a calibration that would be representative of the catchment even though comparable heads were obtained at the borehole clusters, as shown in Figure 8-20.

Also of note are the changes in storage for the annual period. One assumption from Chapter 4 is that when assessing the annual water balances of the catchment, the change in storage of the catchment was negligible over the period of a year, provided that similar hydrological conditions were present for the start and the end of the year. Table 8-6 presents these data as calculated by MODFLOW, and the results are consistent with the assumption of negligible storage change, being approximately 0.35% of effective rainfall for the catchment for 2011 as calculated in Chapter 4. This small change must be viewed cautiously, though, due to the large discrepancies between the simulated contribution of groundwater to the river and the actual discharge observed in the river. Since the overall change in storage was very low and the recharge coefficients approach of Chapter 4 was applied to obtain the recharge to the groundwater pathways, it is reassuring that the annual MODFLOW groundwater contributions to the river are comparable to the NAM annual groundwater pathways contributions.

As with the other two model set-ups there are many ways in which this model set-up would have benefited from more accurate and spatially distributed data. In addition, as this model was set up as a transient simulation, an improvement of the temporal distribution of data would have assisted in providing more confidence in the results obtained. An accurate time series of the variations of the river heads throughout the year would facilitate improved boundary conditions to be applied throughout the simulation. Increased numbers of target heads from a well distributed selection of boreholes in the catchment with daily measurements of head would also assist in improving the calibration of the storage coefficients. The limitations of the model due to the availability of data are considered in more detail in the next subsection.

8.7.4 Sensitivity Analysis

In order to further investigate the effects that these storage values (and the hydraulic conductivities) were having on both the simulated groundwater levels and discharge to the river, a sensitivity analysis was carried out. Four additional simulations were run of this model set-up, two with storage values increased and decreased by 20% respectively and two with hydraulic conductivity values increased and decreased by 20% respectively. The work, presented in Section 8.6, indicates that with the current model set-up, any marginal improvements in simulating groundwater levels in one borehole

will result in a decrease in the accuracy at which the groundwater levels are simulated in another borehole as can be seen in Figure 8-21 when storage is varied. When comparing these results with those of Figure 8-22 for the variation in hydraulic conductivity values, it is evident that these values are important for the initial starting point of the groundwater level in the simulation but after that the shape of the change in groundwater level for the three simulations are comparable. This suggests that the hydraulic conductivities are of most importance for the starting values of the groundwater levels (particularly in the case of MK3 in Figure 8-22), with the shape of the variation of the groundwater levels more dependent on the storage coefficients.

Figure 8-23 and Figure 8-24 indicate that by increasing or decreasing the parameters, a noticeable improvement in the simulation of the low flow conditions can be obtained, though still unrealistically high. This suggests that with the current model, that an improvement in the simulated discharges can be acquired by varying the storage and hydraulic conductivity parameters, but that this will come at the expense of the accuracy with which the groundwater levels are simulated (particularly when varying the hydraulic conductivity). It is therefore important to assess what is of most value, with regards to the outcome of the model results, when applying a model such as this. As MODFLOW is being implemented as a tool of investigation in this chapter, the matching of the simulated and observed groundwater levels were of more importance than the comparison of simulated discharges with simulated NAM discharges, as this provides the simulated discharges predicted when the best calibration of simulated groundwater levels were achieved. The difference between the observed and simulated groundwater levels are a concern (most notably MK1 in Figure 8-20), as is the higher than observed discharge in the river (highlighted in Figure 8-25). This would suggest that that a different method of distributing the different storage and hydraulic conductivity values throughout the catchment, other than by bedrock type, may be appropriate. Without further information on variation of these parameters within the bedrock units, such an approach would not be based on available data.

8.7.5 Limitations of distributed modelling

A distributed model can provide many informative learning outcomes when applied as an investigative tool, as it has been in this chapter. Nevertheless, one must be aware of

the many assumptions made when implementing a model such as MODFLOW and the assumptions made when computing values to be used as input data to the model. The Mattock is a well instrumented catchment by Irish standards, but throughout this chapter it is evident that there are many instances where improved data quality would have benefited the conclusions drawn from simulation results. The effects of the different parameters required to run MODFLOW on these limitations are discussed now. Bedrock topography, hydraulic conductivity, storage parameters, river heads and recharge are considered here.

8.7.5.1 Bedrock topography

The bedrock topography is an important input to the model as this defines the model extent. This dataset is informed by two spatially distributed GIS databases: depth to bedrock and DEM. A poorly defined topography will result in an inaccurate development of hydraulic gradients, with aquifers becoming unconfined when they should be confined and other such storage issues. DEM datasets available to this research were at 20 m x 20 m grid resolution and depth to bedrock mapping is available for Ireland, though this only provides bands of possible depth, for example greater than 10 m to bedrock from the surface.

8.7.5.2 Hydraulic conductivity

Hydraulic conductivity is one of the most important parameters in the model as the values define how water flows through the aquifer by itself in the steady-state simulation and, along with the storage parameters, in the transient simulation. These data are generally difficult to obtain with accuracy across a catchment as pumping tests are typically only reflective of a small area around the borehole in which the test takes place. General relationships between bedrock type and hydraulic conductivity do exist, but these provide wide ranges of values (Section 8.3.3). This relationship of decreasing hydraulic conductivity with depth is with the more fractured shallow groundwater layers of the model providing the higher values in Table 8-4, with the lower values from the deep groundwater layers

8.7.5.3 Storage

Storage parameters consist of specific storage for confined aquifers and specific yield for unconfined aquifers. Specific yield is generally orders of magnitude larger than specific storage as shown in Table 8-5. These values will have an important effect on

water taken into and released from storage during transient simulations and therefore accurate values are vital for prediction of groundwater contribution to the river, as can be seen from the sensitivity analysis in Section 8.7.4. As discussed in Section 8.5.3, storage values calculated from the MK boreholes were most likely not representative of the catchment as a whole and provide a significant source of the differences between computed groundwater contribution to the river and the discharge observed in the river, though as suggested, the changing of the model structure may assist in reducing these differences. Unfortunately due to the scarcity of storage data in the Mattock, basing the structure, other than on bedrock type, is difficult.

8.7.5.4 River heads

Boundary conditions have a significant role within MODFLOW for the constraining of simulations. It is therefore important to set these as correctly as possible. River heads will affect the hydraulic gradient between water in the aquifer and water in the river. Where inaccuracies are present, MODFLOW will simulate inaccurate contributions of water to or from the river. The river heads used in this model were based on a river survey carried out in the catchment (see Chapter 5), with the approach taken to estimate the variations in river head described in Section 8.3.5. As the temporal distribution of these heads required estimation due to a lack of information, this would have influenced the calculated contributions of groundwater to the river.

8.7.5.5 Recharge

The calculation of recharge was considered in Section 8.3.6. This involved a soil moisture budgeting approach combined with the recharge coefficient approach calculating the recharge the aquifer received each day. This simplistic approach assumed that the recharge infiltrated through the soil and subsoil to the aquifer on the day it occurred. This assumed that the recharge that entered the soil and subsoil displaced the same quantity of water at the base of this layer into the aquifer. A better approach would be to investigate the vertical infiltration of this water through the unsaturated zone towards the saturated groundwater. However, if this method of calculating the recharge was implemented it would include all the uncertainty outlined in this section in this one aspect of the model, as the soil and subsoil topography would need to be defined, as would hydraulic conductivity, storage and again the river heads would influence water infiltrating into this zone. Extra parameters for the calculation of

the recharge, such as moisture content of the subsoil, would also be required. It was due to the added uncertainty that such an approach would provide, that the soil moisture budgeting and recharge coefficient approach was adopted. Applying a distributed approach would result in a large amount of uncertainty that would not be warranted even though this type of calculation would provide a better approximation of the physical processes involved. Again, this highlights the limitations of a distributed approach when the necessary data required to populate the model are not available at the scale of catchment that is being investigated.

9 Generalisation of NAM Parameters

9.1 Introduction

The general purpose of an investigation of a system is to understand the controlling factors that most influence the output of that system. Consequently, it is necessary that the insights obtained from the hydrograph separation techniques, recharge coefficients, temperature data and hydrological modelling, can be assessed and related back to specific characteristics of the geology and land-use within a catchment. The flow pathway separation results are summarised for the study catchments at the end of Chapter 7 and for the supplementary catchments in Appendix C. These separations are considered reasonable based on the assessment of the data available and from a qualitative understanding of the geological setting of the catchments. The parameters implemented in NAM to generate these separations, require relationships to be developed between the parameters and characteristics of the catchments, by applying the different GIS layers available. These relationships will provide NAM with likely values for each of the parameters allowing the model to predict separations in ungauged catchments of comparable geological settings, once the meteorological data to run NAM are available for those areas. As such, the NAM parameters for the study catchments, and the supplementary catchments of Appendix A, were utilised to develop the relationships in this chapter. With these equations it is therefore possible to simulate the pathway separations in ungauged catchments. This is the last necessary step in developing a framework for separating the hydrograph into the pathways of the conceptual model in Chapter 1. This framework is outlined in Section 9.6.2. The uncertainty associated with these relationships and the effect that this uncertainty will have on model outputs will be further investigated in Chapter 10.

9.2 NAM Modelling

The objective of the modelling, carried out by NAM, was to separate the hydrograph into the different pathway time series within feasible limits based on the different

separation methods and knowledge of the catchment in question. Once NAM had been applied to simulate these pathways, the NAM parameters applied in the model must be related back to catchment descriptors available in GIS format. When these relations are established, NAM can be applied to ungauged catchments, provided that rainfall and evapotranspiration data are available to simulate the likely discharges.

9.2.1 NAM parameters

The following is a list of the NAM parameters required for a simulation of the four pathway conceptual model employed in this research:

Umax – volume of upper storage in the catchment.

Lmax – volume of lower storage in the catchment.

CQOF – percentage of excess water that is released as overland flow.

CKIF – constant that controls the release of interflow from storage.

CK – time constant for overland flow.

CKBF – time constant for shallow groundwater.

CKLow – time constant for deep groundwater.

CQLow – separating value of shallow and deep groundwater.

TO – threshold needed to be surpassed in the lower storage for overland flow to occur.

TI – threshold needed to be surpassed in the lower storage for interflow to occur.

TG – threshold needed to be surpassed in the lower storage for recharge to occur.

Table 9-1 contains the parameter values for the study catchments based on the hydrograph separation work as discussed in Chapters 6 and 7.

Table 9-1. NAM parameters of the study catchments.

	Umax	Lmax	CQOF	CKIF	CK	TOF	TIF	TG	CKBF	CKLow	CQLow
Gortinlieve	11.971	92.475	0.485	99.957	1.995	0.695	0.355	0.502	406.811	50.104	1233.815
Glen Burn (Sub)	9.229	179.617	0.897	109.686	8.491	0.765	0.759	0.82	85.017	64.366	915.904
Glen Burn (Outlet)	10.59	197.469	0.868	166.104	8.885	0.791	0.792	0.87	126.52	33.43	1005.6
Mattock (Div Weir)	11.369	124.728	0.69	110.472	2.987	0.446	0.678	0.71	222.581		
Mattock (Collon)	13.632	159.61	0.496	255.309	2.989	0.486	0.14	0.904	404.551	37.052	1460.933
Mattock (Berril's)	14.585	189.112	0.964	135.029	3	0.525	0.563	0.401	571.182	64.668	1300.21
Nuenna (Castle)	20.198	182	0.206	984.3	43.065	0.876	0.811	0.879	741	52.578	1913.34
Nuenna (Rocky)	14.742	170	0.161	1363.22	39.295	0.97	0.14	0.9	528.8	42.9	2570.342
Nuenna (Mon)	10.142	172.54	0.104	697.89	39.904	0.953	0.537	0.948	619.835	37.465	2120.348

The groundwater-surface water interaction study (RPS, 2008), which implemented NAM to simulate flows, related the *Umax*, *CQOF* *CKIF* and *CKBF* parameters to catchment parameters. This was achieved by providing broad ranges of values for these parameters that were dictated by decision tables directing the user. There are certain incompatibilities with the ranges of the RPS report and this research as a result of different conceptual models being employed. In the case of *Umax* and *CKIF*, for example, this research found that the parameters given in Table 9-2 and Table 9-3 are located within lower ranges than those of this research. This is a consequence of the interflow and shallow groundwater flow being combined into an 'intermediate flow' pathway in the RPS study. Larger discharges with slower response times were therefore required of this pathway than in the present research, where these pathways have been separated. In order to obtain the larger discharges with slower response times, the RPS report required higher *Umax* and higher *CKIF* parameters. The *CQOF* parameters were similarly affected due to the *Umax* being smaller, with less rainfall was required to saturate this reservoir, therefore more water will tend to overflow from this surface storage, resulting in more water being available for recharging the groundwater reservoirs and also generating overland flow. The *CKBF* parameter from the RPS report was more comparable with the *CQLow* parameter in this thesis, as both of these control the rate of discharge from the deep groundwater reservoir. These parameters were in close agreement due to the similarity in the conceptual model for deep groundwater utilised in this research and the RPS report.

Table 9-2. Surface water-Groundwater approach to determining *Umax* (RPS, 2008).

NAM Parameter	Corine	Broad range of NAM parameter value	Slope	Lakes	Poorly drained soils	Urban	Pilot catchment
U_{MAX} (mm)	>5% Forestry & Semi-natural areas	15 -25	Steep slope (>5%): lower end of limit	Lakes > 1%: 15 – 20	High percentage of poorly drained soils (>50%): upper end of limit	If >2% urban areas: upper end of limit	Boro / Bride
	Forestry 0 – 5% & Pastures > 40%	10 – 20	Relatively flat slope (<5%): upper end of limit		Low percentage of poorly drained soils (<20%): lower end of limit		Suck / Deel / Ryewater / Shournagh
	Forestry 0%, Pastures <40% and Bare rock >20%	8 - 15					Owenduff

Table 9-3. Surface water-Groundwater approach to calculating *CKIF* (RPS, 2008).

NAM Parameter	Slope / Bedrock aquifer	Refinement of NAM parameter value and subsoils			Pilot catchment
CK_{IF} (hours)	Slope >0.07	~ 200			Owenduff
	Slope 0.03 – 0.07	~ 400	Low permeability subsoils > 40%	400 - 800	Boro
			Low permeability subsoils 20% - 40%	300 - 600	
			Low permeability subsoils < 20%	200 – 300	Shournagh / Bride
			Peat > 20%	> 600	
	Slope <0.03	> 600			Deel / Ryewater
	Karst or productive fissured bedrock aquifer	< 400	If > 50% peat: > 600		Suck

9.3 Catchment Characteristics

In order to relate the parameters of NAM to catchment characteristics, GIS datasets were interrogated. There were many GIS datasets available from a multitude of public and private organisations in Ireland. The datasets utilised here were soils, subsoils, aquifer classification, vulnerability, bedrock type, Corine land-use, DEM files and River Basin District river and stream mapping. All of these were available from the Geological Survey of Ireland (GSI) and the Environmental Protection Agency (EPA).

9.3.1 GIS database

Due to the variety of classifications within each dataset, a simplification of each data type was made to enable a statistical analysis of significant catchment characteristics. The main datasets and their subsets are illustrated in Figure 9-1.

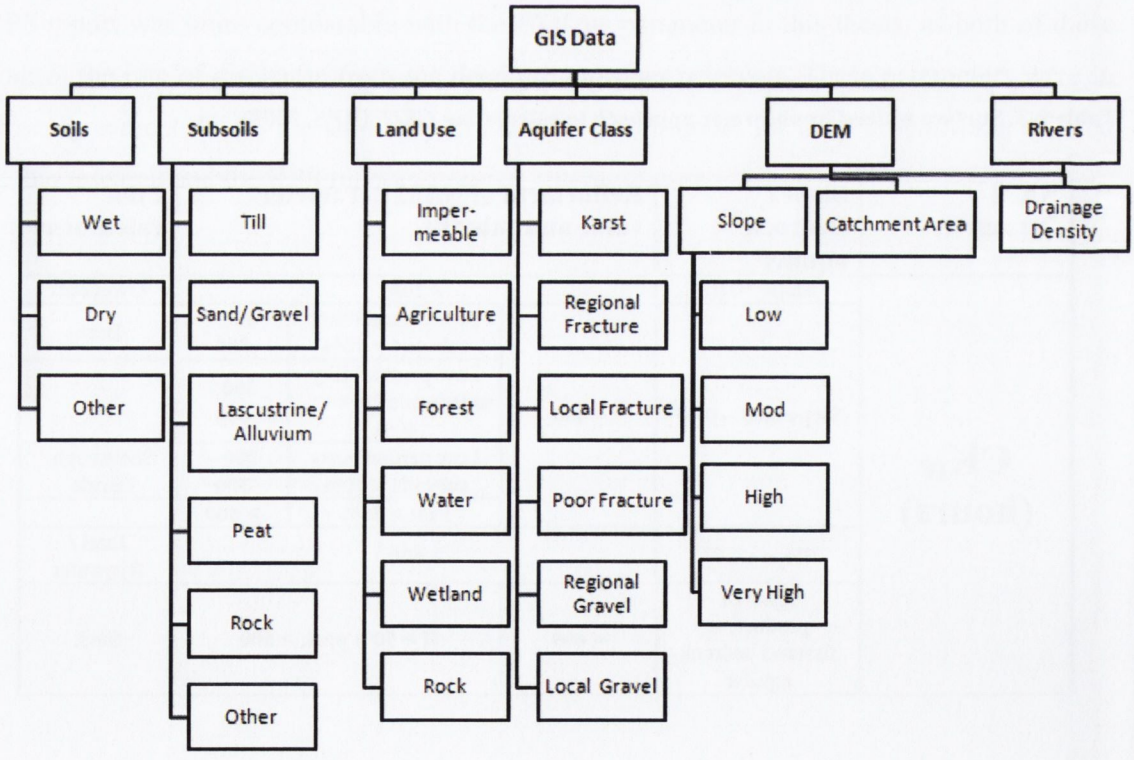

Figure 9-1. Classification of catchment descriptors.

Some subgroups had the potential to be represented as continuums which would help reduce the complexity of this set up, but may reduce the ability to assess regressions intuitively and to identify 'lurking' variables (see Section 9.6.1). An obvious example would be slope that could be redefined as an average slope that is present in the catchment, with each slope weighted to maintain the importance of proximity of the river. Another example would be to apply approximate permeability values to reduce the number of types of soil and subsoil subgroups.

The different classification of each dataset was based on combining soils of similar characteristics into the same subgroup for the statistical analysis. The group and subgroup composition of the datasets are outlined in Table 9-4.

Table 9-4. Catchment descriptors group (red), subgroups (blue) and subgroup breakdown (black).

Soils				Subsoil					
Wet	Dry	Water	Other	Tills	Sands/Gravels	Lascustrine/ Alluvium	Peat	Rock	Other
Poorly drained	Well drained	Lakes	Miscella-neous	Till deposits	Glaciofluvial deposits	Glacious-lacustrine deposits	Peat	Rock	Marine deposits
Poorly drained with peat topsoils						Alluvial deposits			Aeolian deposits
Alluvium									
Peat									

Land Use							Catchment Area	Drainage Density
Impermeable	Agriculture	Forest	Water	Wetland	Rock	Other		
Urban	Pasture	Broad leaved	Water bodies	Moors	Bare rocks	miscella-neous	DEM files used to calculate area	DEM and RBD stream dataset
Roads	Arable	Mixed	Sea and ocean	Marshes				
Industrial Areas	Natural grassland	Coniferous	Streams	Peat bogs				
			Coastal lagoons					

Aquifer Type						Slope			
Karst	Regional Fractured	Regional Gravel	Local Fractured	Local Gravel	Poor	Low	Moderate	High	Very High
Regionally important - Karst	Regionally important - fractured	Regionally important gravel	moderately productive	locally productive	unproductive	0-3.583°	3.584-10.507°	10.508-34.233°	34.234-90°
Regionally important - Karst (conduit)	Regionally important - Karst (diffuse)		lmoderately productive in local zones		unproductive, except in local zones				
			Karstified						

These classifications were based on a conceptual understanding of the general properties of each dataset and not on rigorous quantification of fundamental parameters such as permeability and storativity. The slope intervals were calculated in order to identify four different slope types: waxing, waning, free face and constant slope (Wood, 1942; Kent, 2011). The catchment area was defined as the surface area draining to the point at which discharge was measured in the river, with the drainage density being the total length of rivers and streams in the catchment divided by the catchment area.

In order to reclassify each dataset and calculate the areas of each classification in a catchment, several routines were written in ArcGIS. These essentially cut out the area of a catchment, added a new field in the attribute table for the new classification type, then recalculated the area of each classification. This was carried out for soils, subsoils, land-use and aquifer classification. The slope calculation required a raster DEM file to be masked by the catchment area, followed by the slope calculation tool being applied, the slope intervals being defined and then converted to a new dataset for the area of each slope classification to be calculated.

Once the areas of each new classification of the different datasets had been calculated, another routine converted each polygon in the file to a point in order to identify the centroid of each polygon. This was then utilised to calculate a distance to the nearest stream within the catchment. This was carried out in order to ensure that a polygon located near the catchment boundary was not ranked the same as one intersecting a river. The attribute tables were then exported to excel. Each polygon area was weighted by dividing by the distance it was from a stream and then these products were normalised by dividing the summation of each classification by the catchment area. This process is presented schematically in Figure 9-2, with input data highlighted in green, routines in blue with a hammer symbol, yellow circles signify output from one routine that is required in another routine and the red circle is the final weighted and normalised data output of the process.

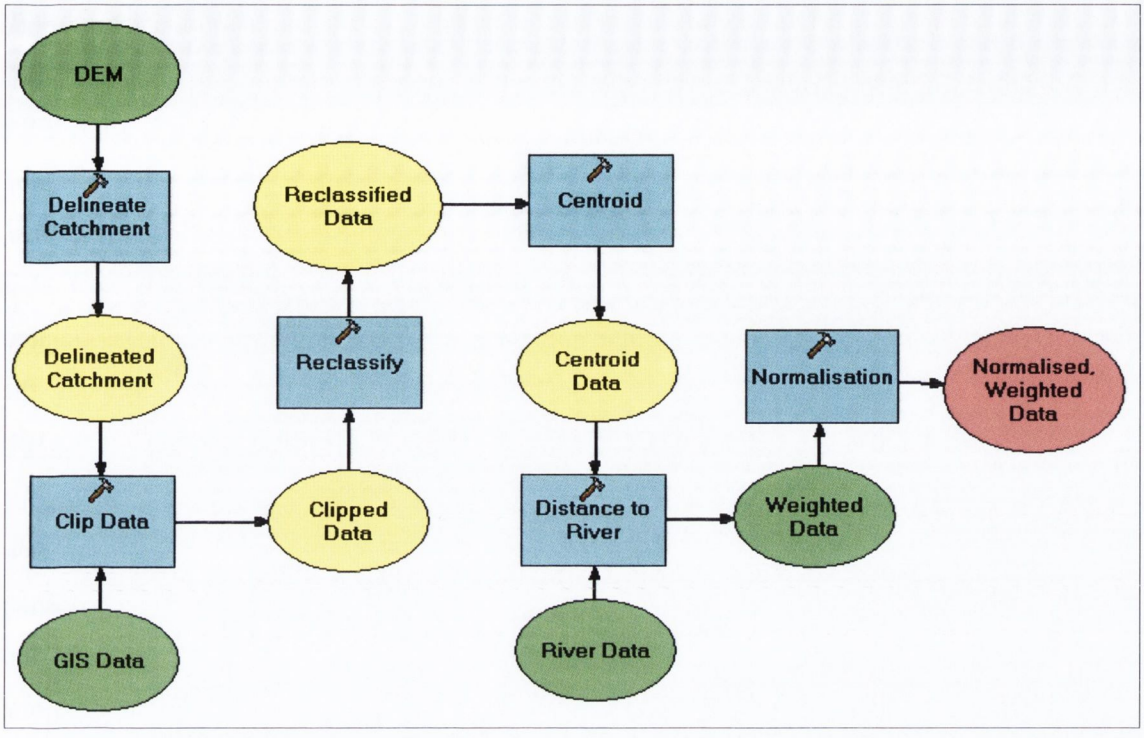

Figure 9-2. Schematic of normalisation and weighted process carried out in ArcGIS.

9.4 Multiple Linear Regression

Regression is one of the most useful statistical techniques available. It allows the fitting of equations to data in order to predict a response of interest (Mullins, 2003). In this case the response required was each of the parameters of NAM and the data used to predict this were the different catchment descriptors. In the case of linear regression the relationship between the predictor and the response is assumed to be linear, i.e. that as the area of a certain catchment predictor increased the NAM parameter would respond proportionally to this change. It is not assumed that one catchment descriptor will be a perfect predictor of a NAM parameter, as there will always be known (systematic) and random variation present in the application of statistical analysis. By utilising multiple predictors, and hence multiple linear regression, it was attempted to reduce these random variations to within ranges that provide feasible answers when NAM was applied to simulate the flow pathway separations. Each parameter will have an error associated with it that will introduce uncertainty as to what the actual value of that parameter is. This error allows confidence intervals to be calculated around a predicted NAM parameter, as calculated for *Umax* in Figure 9-3. Simple linear

regressions including only one predictor to calculate the response have smooth confidence intervals that increase as predictions move further away from the mean predictor, thus increasing associated error. Multiple linear regressions have more complex confidence intervals. At each response the combination of predictors will result in some predictors being near their mean while others will be far from it. This will change at each predicted response, producing the jagged complex confidence intervals observed in Figure 9-3. This interval is the range within which a parameter is likely to lie when predicting it using the associated catchment descriptors. Probability distribution functions were then computed utilising the associated error at these points for sensitivity analysis which will be discussed in Chapter 10.

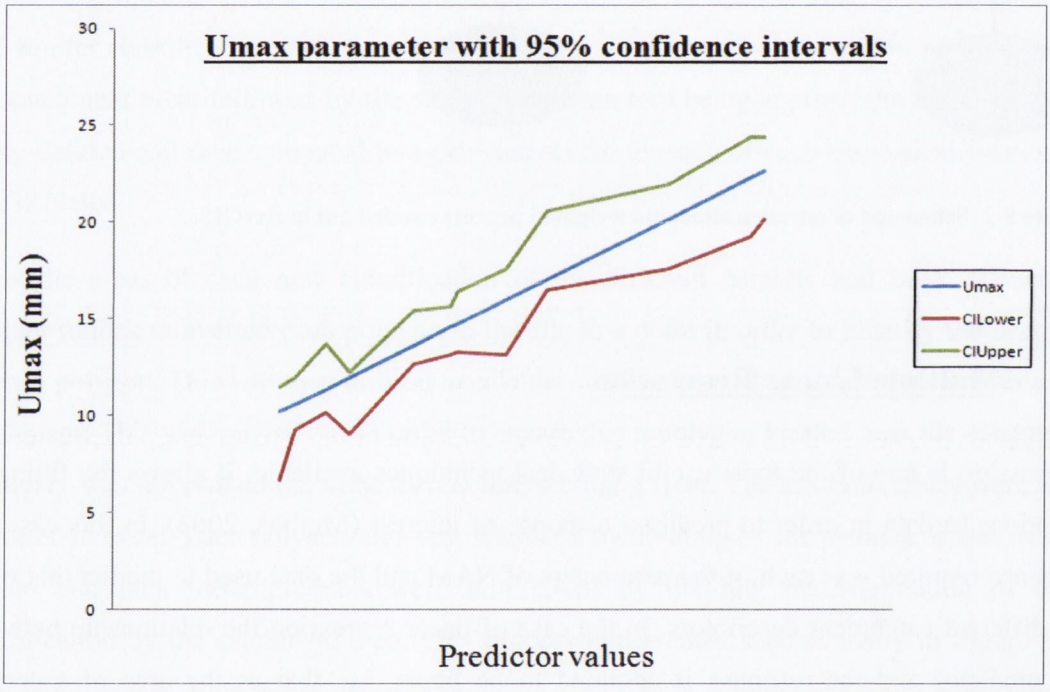

Figure 9-3. *Umax* relationship with predictors along with associated 95% confidence intervals.

9.4.1 Statistical model

As outlined in the introduction to Section 9.4, multiple linear regression (MLR) involves the estimation of a response calculated by the linear combination of predictor variables:

$$Response = Coeff_1 x Predictor_1 + Coeff_2 x Predictor_2 + Coeff_3 x Predictor_3 + \ldots \quad \textbf{9-I}$$

In order to take account of the effect of statistical variation on estimations of the response, the NAM parameter in this case, an underlying statistical model was required for the data that were handled here. Mullins (2003) defines the statistical model that underlies the regression analysis as follows:

- Independent observations
- Normal distribution of a response at any single predictor
- Means of responses can be joined by a straight line

These underlying assumptions were required to be satisfied or closely approximated in order for useful regressions to be obtained from this analysis. The independence of observations was satisfied to an extent as each NAM parameter was calculated based on data for each particular catchment. Study catchments with smaller study subcatchments within them were only partially independent as even though parameters were based on that catchment's data and not surrogated from the subcatchment, the selection of these parameters are affected by the subcatchment. This may skew regressions, but is unavoidable due to the limitation on the number of study catchments. The normal distribution of a response due to any single predictor was calculated within Minitab software. This was achieved by carrying out the Anderson-Darling test (Anderson and Darling, 1954) that evaluates the null hypothesis that the data were normally distributed. The final assumption of the mean of the responses being located on a straight line will underpin the success of the regression. If the means cannot be connected by straight line, as they are in Figure 9-3, a satisfactory relationship between the predictors and responses cannot be developed.

9.4.2 Assessing the regression analysis

Once the MLR approach has been applied to the data, it must be assessed to determine whether or not the equations developed were useful or not. The underlying assumptions must be investigated also in order to validate any inferences made on relationships developed. The analysis of variance approach assists in identifying whether the predictors used in the MLR are significant predictors of the response, while the sample test deviation (s), the coefficient of determination (r^2) – not to be confused with the Nash-Sutcliffe coefficient (R^2) – and the adjusted coefficient of determination (r^2_{adj}) objective functions were utilised to check the

quality of the regression. Residual analysis was then applied to appraise the normal distribution underlying assumption.

9.4.2.1 Analysis of Variance

Statistically, the NAM response parameters are viewed as a combination of systematic and chance components. The systematic component is the part of the response that can be calculated with the catchment predictors. The chance component is the difference between the observed NAM parameter and the predicted value. The objective of the MLR was to maximise the systematic component and simultaneously minimise the chance component. Minitab produces an ANOVA (ANalysis Of VAriance) table as an output after each regression calculation, an example of which is included in Figure 9-4. The coefficient of the regression equation and the standard error associated with each predictor are displayed, along with the T-value and P-value. A P-value of less than 0.05 and, depending on the degrees of freedom available, a T-value greater than 2 was generally considered significant (Holder, 1985; Brezonik and Stadelmann, 2002; Interlandi and Crockett, 2003). This was taking significance as occurring once the mean for a test hypothesis lies outside 95% of the null hypothesis mean. The P-value does not depend on degrees of freedom and therefore significance can be read straight from the ANOVA table. Once the P-value was less than 0.05 it was considered significant, again taking significance as occurring once a test hypothesis mean lies outside 95% of the null hypothesis mean. The example shown in Figure 9-4 illustrates that the each of the predictor variables were highly significant, as T-values and P-values were much greater than 2 and less than 0.05, respectively.

Regression Analysis: Umax versus Wet, Dry, ...

The regression equation is

Umax = 26.7 - 0.000323 Wet + 0.00482 Dry - 0.0212 Sand/gravels - 0.0130 Regional
+ 0.00637 Local - 0.0149 Urbanish - 12.4 Drainage Density

Predictor	Coef	SE Coef	T	P
Constant	26.724	1.845	14.48	0.000
Wet	-0.00032294	0.00005048	-6.40	0.000
Dry	0.0048188	0.0003728	12.93	0.000
Sand/gravels	-0.021250	0.003649	-5.82	0.001
Regional	-0.012967	0.001438	-9.02	0.000
Local	0.006371	0.001010	6.31	0.000
Urbanish	-0.014937	0.002472	-6.04	0.001
Drainage Density	-12.401	1.529	-8.11	0.000

S = 1.16528 R-Sq = 96.4% R-Sq(adj) = 92.9%

Analysis of Variance

Source	DF	SS	MS	F	P
Regression	7	257.189	36.741	27.06	0.000
Residual Error	7	9.505	1.358		
Total	14	266.695			

Figure 9-4. Example of ANOVA table output from the *Umax* MLR.

9.4.2.2 Objective functions

In Figure 9-4 there are three outputs of the regression that provide a measure of the performance of the MLR analysis. S is a measure of the standard deviation for the sample of observations. It is computed from the standard deviations of each of the predictors as shown in Equation 9-II. This provided an estimation of the variability of predicted responses. A low value of S would suggest that variations associated with chance variation are small.

$$S = \sqrt{\frac{s_1^2 + s_2^2 + s_3^2 + \ldots}{n_p}} \qquad \text{9-II}$$

where S is the estimate of the response standard deviation, $s_{1,2,3}$ are estimates of the predictor standard deviations and n_p is the number of predictors used to calculate the response in the regression.

R-Sq (in Figure 9-4) is the coefficient of determination r^2. This coefficient is a measure of the 'goodness of fit' of the regression equation with the observed data. The maximum value this can have is 1. This is calculated using sums of squares regression (*SSR*), which is associated with the systematic component of the observed data (the differences between the response data and the mean of the calculated response data squared) and the sums of squares error (*SSE*), associated with the chance variation component (the difference between the observed response data and the predicted response data squared):

$$r^2 = \frac{SSR}{SS} = 1 - \frac{SSE}{SS} \qquad \textbf{9-III}$$

where *SS* is the total sums of squares, *SSR* + *SSE*.

R-Sq (adj) (Figure 9-4) is the adjusted coefficient of determination r^2_{adj}. The weakness of the standard r^2 is that as extra predictors are added to the regression model, r^2 must decrease as *SSE* decreases. This occurs regardless of the increase in r^2, though S can increase if the extra variable is a particularly poor predictor. This will result in a MLR relationship that may be accurate within the set of observations it is based on, but outside of this its prediction of the NAM parameters would be very poor due to the effects of over-parameterisation. To address this issue r^2_{adj} was calculated to take into account the loss in degrees of freedom:

$$r^2_{adj} = 1 - \frac{(n-1)}{n-n_p}\frac{SSE}{SS} \qquad \textbf{9-IV}$$

where n is the number of observations.

9.4.3 Residual Analysis

In order for a regression relationship to have the potential of being successfully applied outside of the range within which it was developed, the underlying assumptions must be adhered to. Residual analysis permits the assessment of the independence of observations, normality of the distribution and also that the means being connected by a straight line are

accounting for the systematic variation. Residuals are the deviations of the observed data from the fitted regression equation:

$$Residual_i = Observation_i - Predicted\ Response_i \quad \text{9-V}$$

These residuals, if the underlying assumptions are observed, are an estimate of the chance variation not explained by the systematic regression Equation, 9-I. As such they should also obey the underlying assumptions. Figure 9-5 illustrates different types of residual plots that may be obtained. Figure 9-5A portrays a plot of residuals in which the assumptions are obeyed, there is approximately as much data above the line as below, there are no clear trends and no large outlier residuals. Figure 9-5B to Figure 9-5F are very different, with the normality assumption being violated. In B and C, the residuals are changing depending on the value of the fitted value, which implies a lack of independence. In D, there is a non-linear aspect to the residuals, suggesting that the ability of a straight line to fit the data does not hold true. E implies a time-dependent aspect to the data, again showing a lack of independence, with F also having this problem due to a relationship with another predictor variable. In this research, the residuals should follow the distribution shown in Figure 9-5A if the regression equations are to be of a quality that renders them useful outside of the range of observations they were developed from.

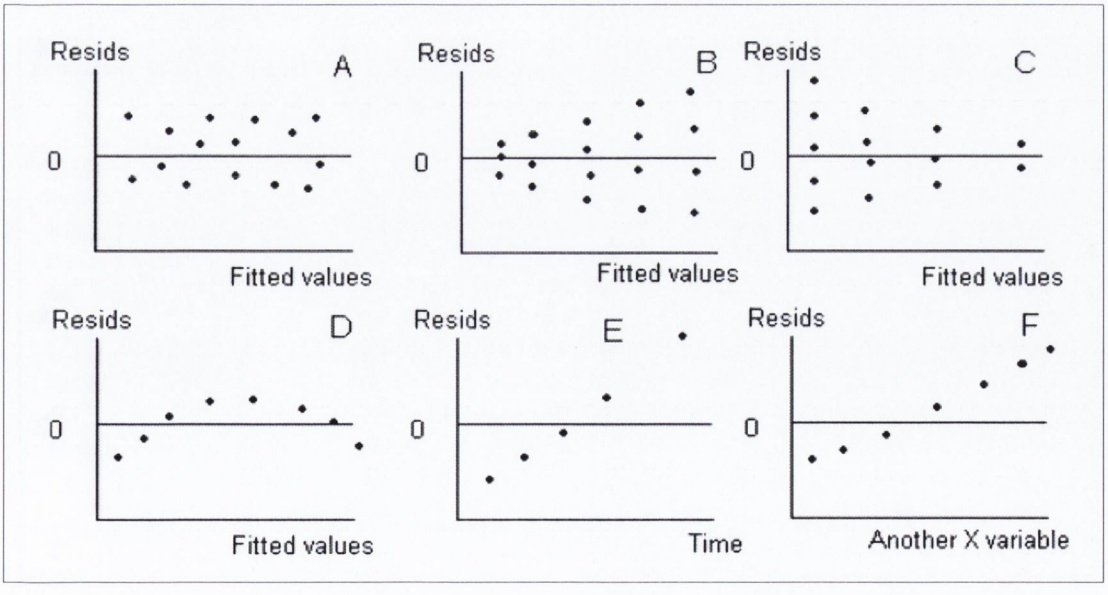

Figure 9-5. Residual plots (Mullins, 2003).

9.5 Catchment descriptor and NAM parameter relationships

Applying the classifications from Section 9.3.1 as predictors for a statistical multiple linear regression, each of the parameters was predicted using catchment characteristics. The equations of each parameter were calculated from the study catchment data as well as by using the supplementary catchments, as listed in Appendix A, in order to generalise the equations to other settings in Ireland.

9.5.1 Relationships

The equations fitted to the NAM parameter data, along with the calculated S, r^2 and r^2_{adj} indices associated with each, are presented in this section. The standardised residual versus the fitted value was plotted for each predicted parameter. This provided an overview of the normality of the distribution of the residuals. This was an important assessment as the normal distribution was an underlying assumption of this type of statistical analysis. Each Minitab output is discussed and the applicability of predictors assessed. Each of the plots of residuals are also presented. The residuals adhere to the assumptions made for each regression with no obvious trends or distributions evident, suggesting that the underlying statistical model outlined in Section 9.4.1 was valid for the regressions.

Umax *– the volume of upper storage in the catchment*

```
Umax = 26.7 - 0.000323 Wet + 0.00482 Dry - 0.0212 Sand/gravels - 0.0130 Regional
       + 0.00637 Local - 0.0149 Urbanish - 12.4 Drainage Density


Predictor              Coef     SE Coef      T      P
Constant             26.724       1.845  14.48  0.000
Wet              -0.00032294  0.00005048  -6.40  0.000
Dry                0.0048188   0.0003728  12.93  0.000
Sand/gravels       -0.021250    0.003649  -5.82  0.001
Regional           -0.012967    0.001438  -9.02  0.000
Local               0.006371    0.001010   6.31  0.000
Urbanish           -0.014937    0.002472  -6.04  0.001
Drainage Density     -12.401       1.529  -8.11  0.000


S = 1.16528   R-Sq = 96.4%   R-Sq(adj) = 92.9%
```

Figure 9-6. Minitab output of *Umax* regression.

In Figure 9-6, it is shown that for the Umax parameter, soils (Wet and Dry) are important, along with aquifer type and drainage density. This is intuitive as these parameters have an influence on recharge and overland flow generation.

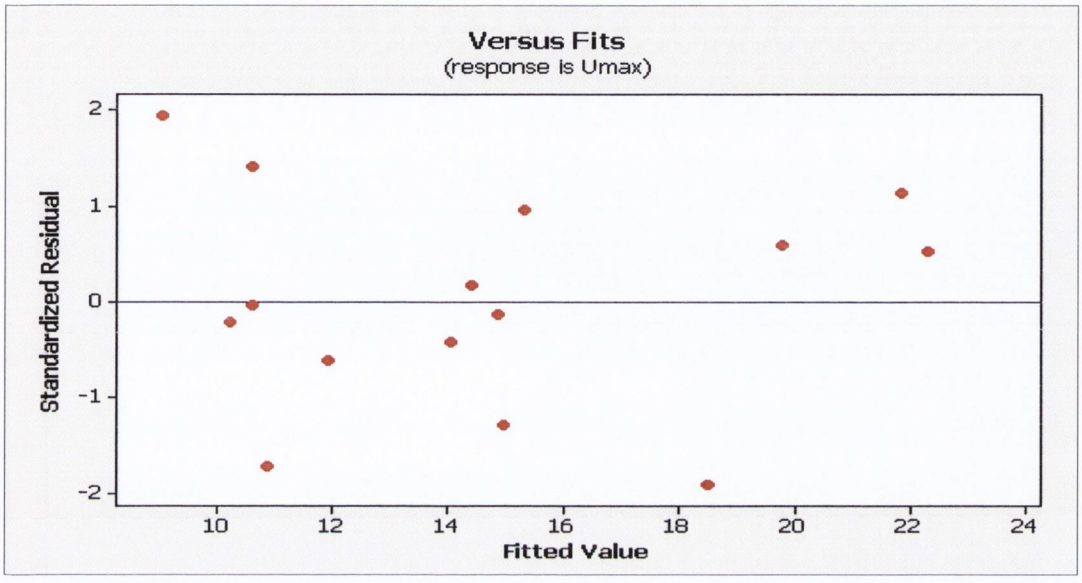

Figure 9-7. Residuals of *Umax*.

Lmax *– the volume of lower storage in the catchment*

```
Lmax = 178 - 0.0745 Sand/gravels + 0.0221 Forest - 0.0238 Wetland + 0.00395 Peat
       + 0.000586 Low - 0.00137 Poor + 0.000958 Agri - 0.0714 Area


Predictor          Coef    SE Coef      T      P
Constant         177.737      4.316  41.18  0.000
Sand/gravels    -0.07451    0.01997  -3.73  0.010
Forest          0.022111   0.003295   6.71  0.001
Wetland        -0.023839   0.002662  -8.95  0.000
Peat           0.0039537  0.0007514   5.26  0.002
Low            0.0005860  0.0002034   2.88  0.028
Poor          -0.0013678  0.0005001  -2.73  0.034
Agri           0.0009576  0.0002710   3.53  0.012
Area            -0.07140    0.01810  -3.95  0.008


S = 9.04512   R-Sq = 97.8%   R-Sq(adj) = 94.8%
```

Figure 9-8. Minitab output of *Lmax* regression.

Figure 9-8 outlines land-use (Wetland, Agriculture and Forest) and subsoils (Sands and Gravels and Peat) as the most important predictors of the lower storage reservoir in NAM. This reservoir reflects field capacity to an extent of which land-use will partly reflect field capacity and soils are typically derived from subsoils. Area is a surprising predictor but this may be related to the response time of the catchment, as larger catchments typically respond more slowly, with the ability to store more water in the soils and subsoils a factor in how quickly a catchment can respond.

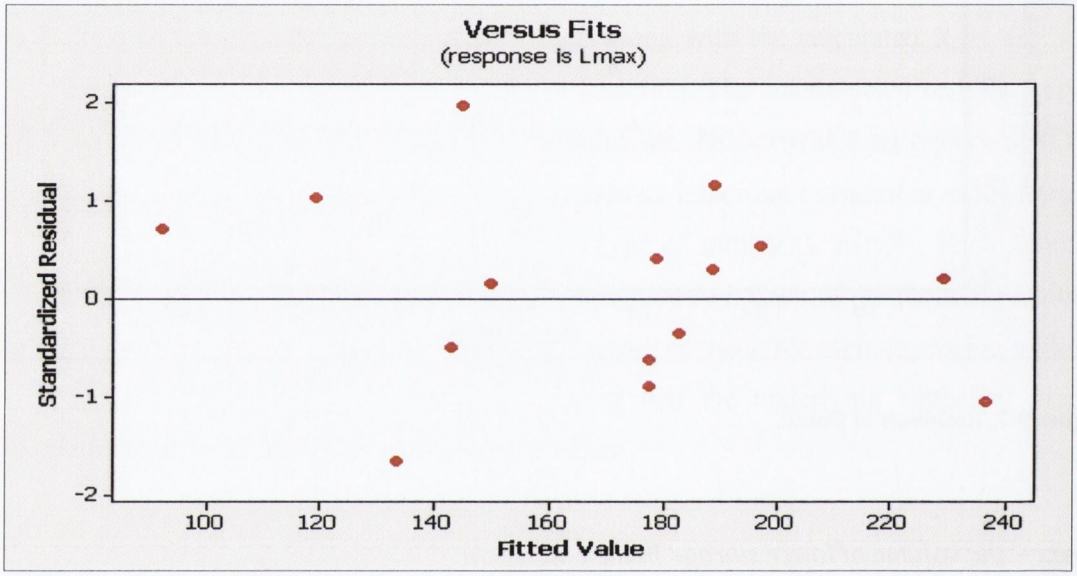

Figure 9-9. Residuals of *Lmax*.

CQOF *– the percentage of excess water that is released as overland flow*

```
CQOF = 0.126 + 0.000098 Wet + 0.000800 Sand/gravels - 0.000095 Las/Alluvium
       - 0.000119 Peat + 0.000012 Agri - 0.000123 Wetland


Predictor            Coef     SE Coef      T      P
Constant          0.12589     0.04763   2.64  0.030
Wet            0.00009827  0.00001109   8.86  0.000
Sand/gravels    0.0007995   0.0001327   6.03  0.000
Las/Alluvium  -0.00009548  0.00001131  -8.44  0.000
Peat          -0.00011922  0.00001489  -8.01  0.000
Agri           0.00001194  0.00000197   6.05  0.000
Wetland       -0.00012301  0.00002100  -5.86  0.000


S = 0.0803405   R-Sq = 94.9%   R-Sq(adj) = 91.1%
```

Figure 9-10. Minitab output of *CQOF* regression.

In Figure 9-10, it is observed that soils and subsoils are important for generating overland flow and recharge as controlled by *CQOF*. This is analogous to the controlling factors in the recharge coefficient approach outlined in Chapters 2 and 6.

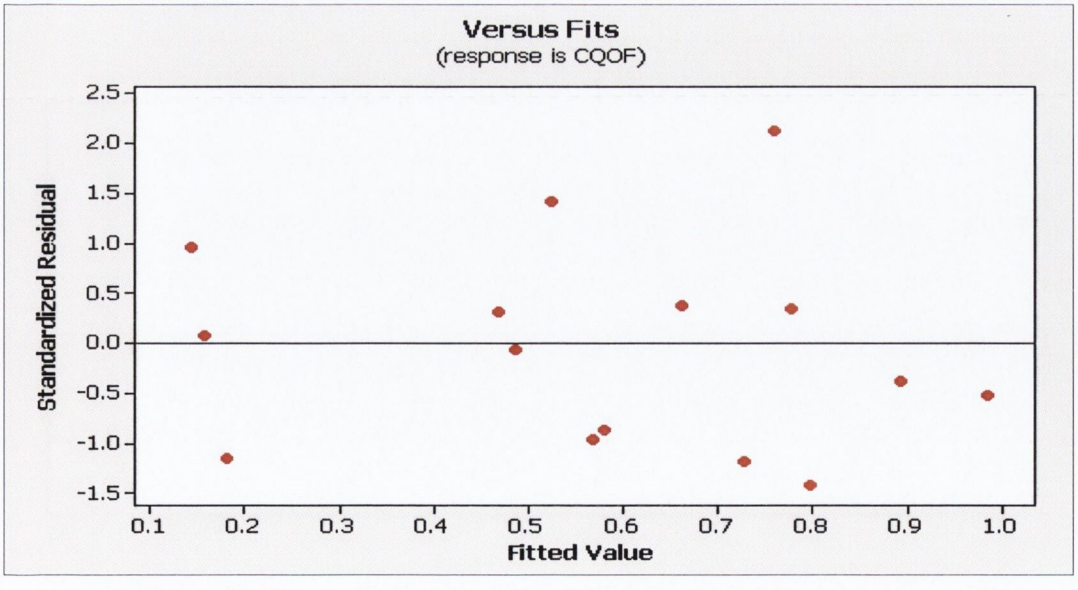

Figure 9-11 Residuals of *CQOF*.

CKIF *– the constant that controls the release of interflow from storage*

```
CKIF = 4274 + 0.231 Dry + 213 Water - 1.15 Las/Alluvium + 0.0774 Moderate
       + 599 Very High + 0.0593 Poor + 1.40 Urbanish + 0.162 Forest
       - 3781 Drainage Density - 8.82 Area


Predictor             Coef   SE Coef       T      P
Constant           4274.05     74.90   57.07  0.000
Dry                0.230925  0.007000   32.99  0.000
Water               213.199     6.598   32.31  0.000
Las/Alluvium       -1.14725   0.02629  -43.64  0.000
Moderate           0.077435  0.002326   33.29  0.000
Very High            599.46     13.78   43.50  0.000
Poor               0.059340  0.002013   29.49  0.000
Urbanish            1.39885   0.02730   51.23  0.000
Forest             0.161672  0.004860   33.27  0.000
Drainage Density  -3781.13     73.45  -51.48  0.000
Area                -8.8157    0.2808  -31.40  0.000


S = 11.5858   R-Sq = 100.0%   R-Sq(adj) = 99.9%
```

Figure 9-12. Minitab output of *CKIF* regression.

Soils, slopes and drainage density are determined as being important for *CKIF*, the main control on interflow, as shown in Figure 9-12. This would suggest that the drainage density and the soils and slopes surrounding them greatly influence interflow, which is to be expected.

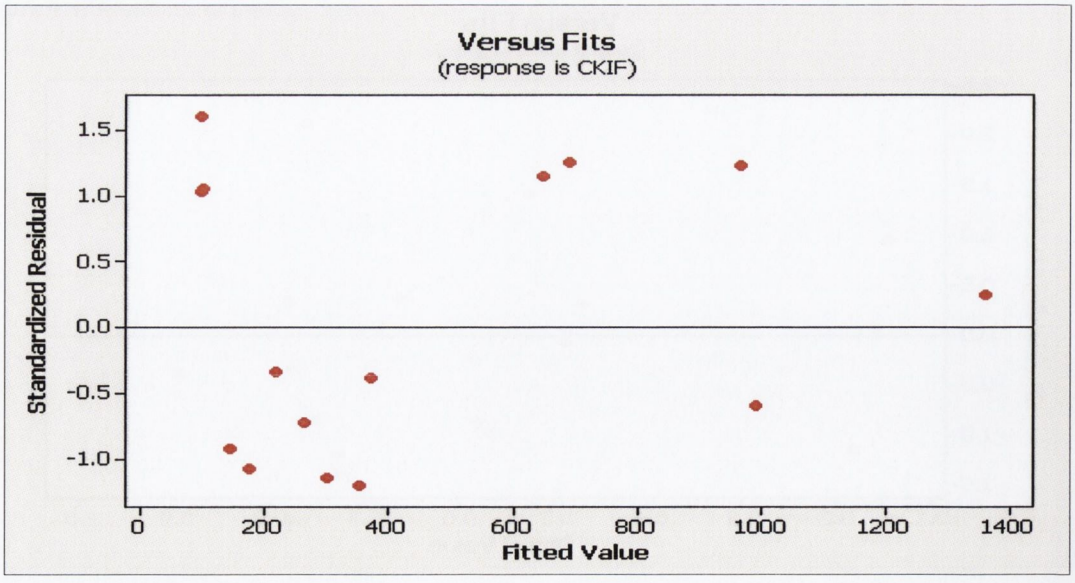

Figure 9-13. Residuals of *CKIF*.

CK *– the time constant for overland flow*

```
CK = 24.0 - 0.000694 Wet + 1.38 Water + 0.00832 Till + 0.0824 Rock
     - 0.000693 Low + 0.0119 Local - 0.00153 Poor - 71.3 Drainage Density


Predictor                Coef     SE Coef       T      P
Constant               24.010       2.236   10.74  0.000
Wet                -0.00069372  0.00004342  -15.98  0.000
Water                  1.37862     0.07872   17.51  0.000
Till                 0.0083164   0.0006509   12.78  0.000
Rock                  0.082374    0.007999   10.30  0.000
Low                -0.00069328  0.00007298   -9.50  0.000
Local                 0.0119237   0.0009347   12.76  0.000
Poor                 -0.0015337   0.0001328  -11.55  0.000
Drainage Density       -71.311       4.422  -16.13  0.000


S = 1.95521   R-Sq = 99.7%   R-Sq(adj) = 99.3%
```

Figure 9-14. Minitab output of *CK* regression.

Figure 9-14 highlights wet soils and poorly productive aquifers as being the best predictors of the overland flow response. These predictors, like the *CQOF* predictors, would be comparable to those of the recharge coefficient approach as the controlling factors of runoff generation.

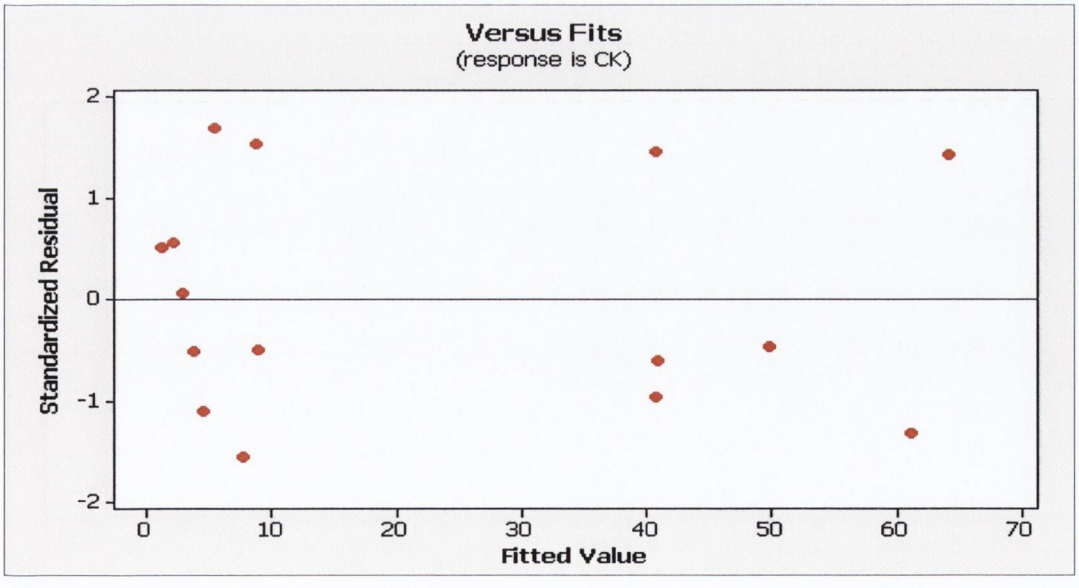

Figure 9-15. Residuals of *CK*.

CKBF *– the time constant for shallow groundwater*

```
CKBF = 590 + 0.0988 Wet - 18.1 Water - 0.904 Rock - 0.0334 Moderate
       - 59.4 Very High


Predictor       Coef   SE Coef       T      P
Constant       589.87     44.05   13.39  0.000
Wet          0.098827  0.002485   39.77  0.000
Water         -18.070     1.421  -12.72  0.000
Rock          -0.90357   0.09354   -9.66  0.000
Moderate    -0.033356  0.004044   -8.25  0.000
Very High     -59.379     1.304  -45.55  0.000


S = 48.6473   R-Sq = 99.6%   R-Sq(adj) = 99.4%
```

Figure 9-16. Minitab output of *CKBF* regression.

Slope and soil type are the most important predictors of shallow groundwater response according to Figure 9-16. Water is surprisingly included but this may be the influence of water features in the Blackwater catchments that are not reflected elsewhere. The inclusion of further catchments containing lakes would assist in determining the actual impact of water on *CKBF*.

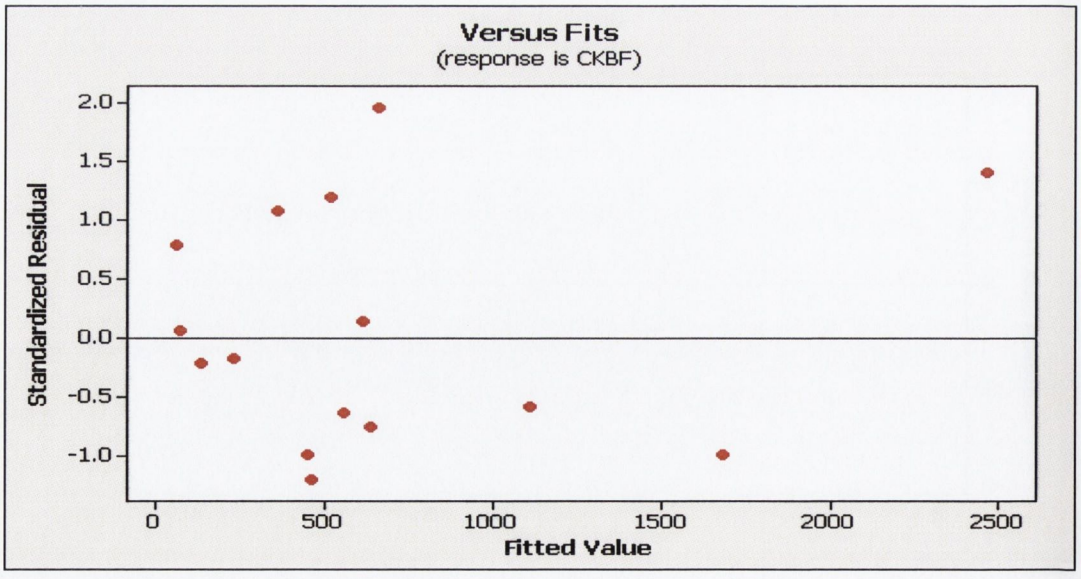

Figure 9-17. Residuals of *CKBF*.

CK_{Low} *– the time constant for deep groundwater*

```
CKLow = 4472 - 1.02 Wet + 0.138 Moderate + 543 Very High + 0.474 Local
        + 2.55 Forest + 75.7 Water_1 + 911 Drainage Density


12 cases used, 3 cases contain missing values


Predictor             Coef  SE Coef       T      P
Constant            4472.1    211.1   21.18  0.000
Wet                -1.02148  0.09810  -10.41  0.000
Moderate            0.13841  0.01616    8.56  0.001
Very High            542.65    53.33   10.18  0.001
Local               0.47403  0.03481   13.62  0.000
Forest               2.5543   0.2806    9.10  0.001
Water_1              75.713    6.578   11.51  0.000
Drainage Density      911.2    185.1    4.92  0.008


S = 56.4245   R-Sq = 99.7%   R-Sq(adj) = 99.2%
```

Figure 9-18. Minitab output of *CKLow* regression.

Again, soil type and slope are important for this groundwater response constant as they were for the shallow groundwater response, as indicated in Figure 9-18. This factor is one of the less sensitive parameters, as will be discussed in Chapter 10, so it is difficult to assess some of the other predictors included here without further catchments being included in the regression.

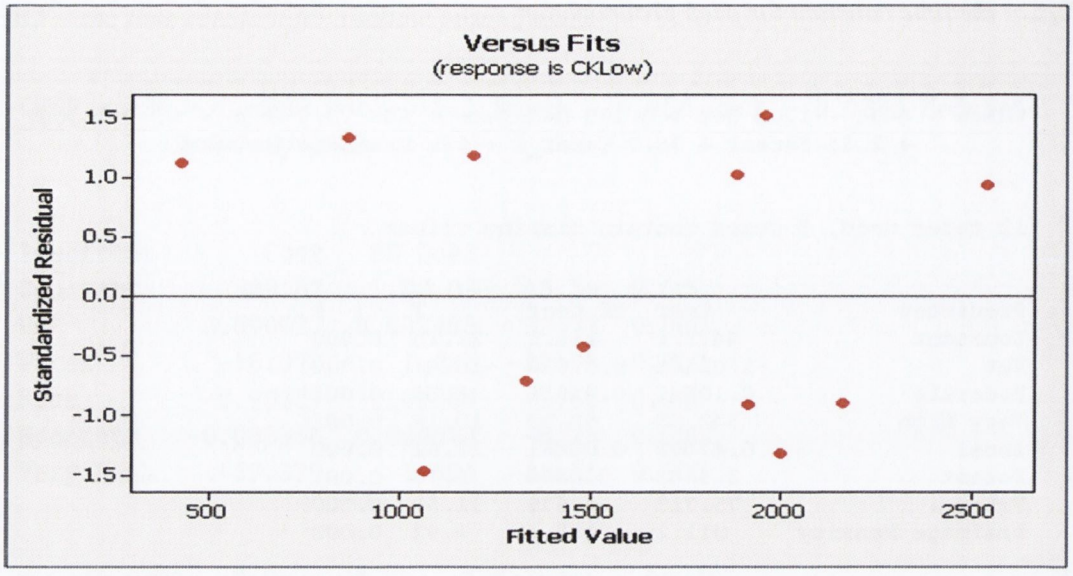

Figure 9-19. Residuals of *CKLow*.

TO *– the threshold value for overland flow*

```
TO = 0.845 - 0.000022 Poor - 0.000045 Forest - 0.000005 Wet - 0.00586 Water
     + 0.000086 Regional + 0.000048 Local


Predictor         Coef     SE Coef      T      P
Constant       0.84496     0.02704  31.25  0.000
Poor       -0.00002218  0.00000238  -9.31  0.000
Forest     -0.00004496  0.00001035  -4.34  0.002
Wet        -0.00000479  0.00000079  -6.05  0.000
Water        -0.005863    0.001374  -4.27  0.003
Regional    0.00008559  0.00002673   3.20  0.013
Local       0.00004848  0.00001530   3.17  0.013


S = 0.0379347   R-Sq = 97.7%   R-Sq(adj) = 96.0%
```

Figure 9-20. Minitab output of *TO* regression.

TO affects when overland flow occurs, as such, it is reasonable that influences on the 'flashiness' are the most important predictors. In Figure 9-20 aquifer classification is important (poorly and locally productive and regionally important) with wet soil and forested

land-use also playing a role. Water is also identified as an important predictor. This, as was the case with the *CKBF* parameter, may be related to high runoff in the supplementary catchments presented in Appendix A, such as Blackwater catchments.

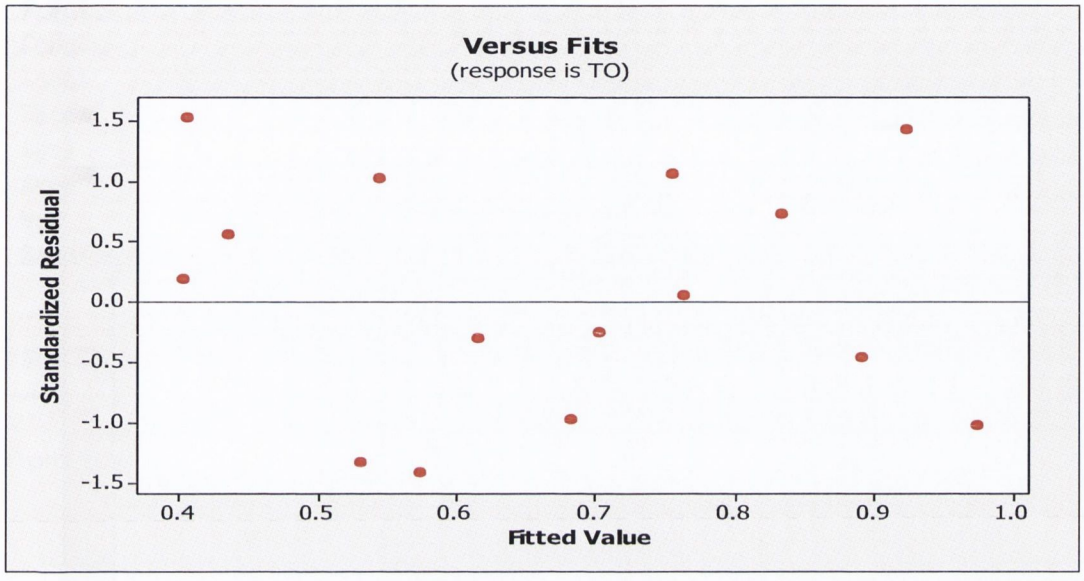

Figure 9-21. Residuals for *TO*.

TI *– the threshold value for interflow*

```
TI = 0.298 + 0.000077 Local - 0.000046 Peat + 0.000187 Forest + 0.000454 Rock


Predictor         Coef     SE Coef      T      P
Constant        0.2977      0.1894   1.57  0.147
Local       0.00007687  0.00005763   1.33  0.212
Peat       -0.00004618  0.00001690  -2.73  0.021
Forest      0.00018665  0.00007368   2.53  0.030
Rock         0.0004536   0.0003475   1.31  0.221


S = 0.225916   R-Sq = 52.0%   R-Sq(adj) = 32.8%
```

Figure 9-22. Minitab output of *TI* regression.

The MLR could not relate the catchment predictors to the *TI* parameter successfully. A low r^2_{adj} value of 32.8% was obtained, with two of the four predictors (locally productive aquifers and rock outcrop) deemed not significant in Figure 9-22. This is most likely a result of the insensitivity of the *TI* parameter as will be discussed in Chapter 10. As a result of this insensitivity, many values of *TI* would produce similar outcomes and so a consistent relationship between the predictors and *TI* is difficult to establish.

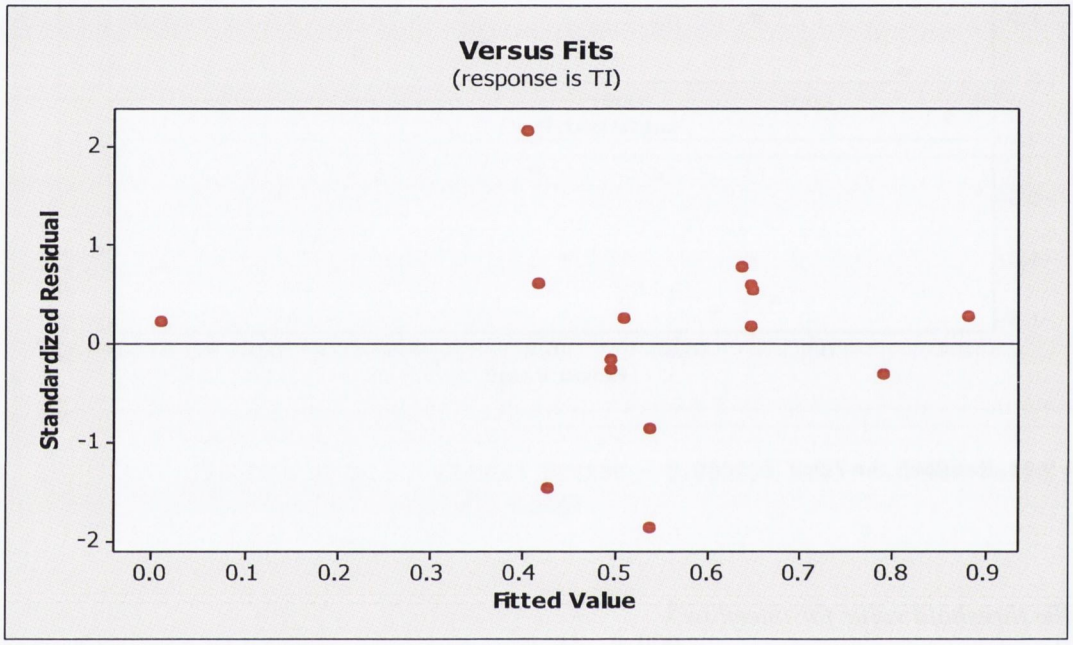

Figure 9-23. Residuals for *TI*.

***TG** – the threshold value for groundwater recharge*

```
TG = 0.939 + 0.000097 Local - 0.0241 Water - 0.000011 Agri + 0.000613 Area
     - 0.000004 Wet - 0.000344 Sand/gravels


Predictor            Coef     SE Coef      T      P
Constant          0.93855     0.02705  34.69  0.000
Local          0.00009729  0.00002341   4.16  0.003
Water           -0.024110    0.004632  -5.20  0.001
Agri          -0.00001080  0.00000113  -9.57  0.000
Area            0.0006126   0.0002219   2.76  0.025
Wet           -0.00000369  0.00000130  -2.84  0.022
Sand/gravels   -0.0003440   0.0001424  -2.42  0.042


S = 0.0540409   R-Sq = 96.4%   R-Sq(adj) = 93.7%
```

Figure 9-24. Minitab output of TG regression.

Figure 9-24 indicates that there are a number of important predictors of *TG*. Aquifer type (locally productive), soils (wet) and subsoils (sands and gravels) are logical inclusions, as is agriculture land-use as this reflects the soil type which impacts the recharge to groundwater like the other predictors mentioned. Water and area are surprising inclusions, area may be a reflection of the relatively small sizes of the study catchments as most of these are 'flashy' in nature, but again water is more difficult to explain. Again, like *TO* and *CKBF*, this may be the effect of the Blackwater catchments and the till soil coverage. This would require further catchments for the MLR analysis to assess if the regressions are being skewed by the presence of the Blackwater catchments.

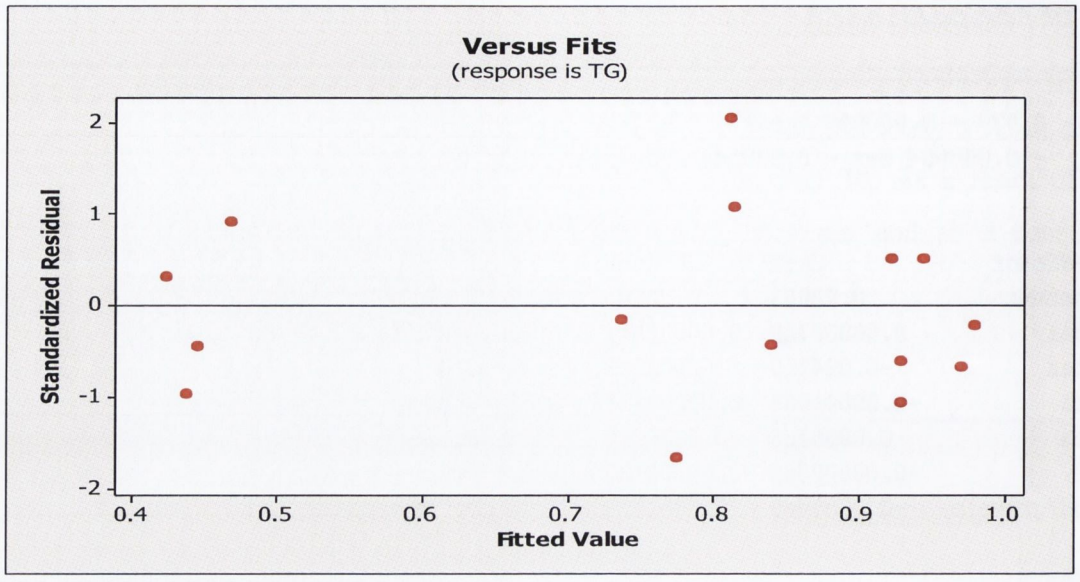

Figure 9-25. Residuals for *TG*.

The MLR was successfully applied for the different NAM Parameters, with the exception of *TI*. Omitting *TI*, the lowest r^2_{adj}, the most important when fit was being assessed, was 91.1% for the *CQOF* parameter. While this was the lowest r^2_{adj}, this may not be the regression that will have the most variation associated with it during simulations of flow separations. Small changes in a parameter with a very good regression fit, such as *CKBF*, may have a large effect on separations predicted. The uncertainty involved in a simulation, due to the sensitivity of parameters, particularly *TI*, is investigated in Chapter 10.

In order to assess the performance of the regression equations, two catchments were selected to populate the NAM parameters by implementing these regression equations. NAM was applied with these parameters for the same periods as calibration and validation in Chapter 7. The catchments selected were Mount Stewart Outlet, a 'flashy' catchment reflecting the majority of the observed data, upon which the regression equations were based, and Mattock Diversion Weir as the only "three-pathway" catchment amongst the study catchments. The contribution of each pathway, the Nash-Sutcliffe coefficient (R^2), the root Nash-Sutcliffe coefficient ($\sqrt{R^2}$) and the bias were compared in Table 9-5. The regression equations selection of parameters compare well with the calibration and validation period, though this would be expected as these catchments were utilised to develop the regression equations.

Table 9-5. Results of application of generalised parameters in Glen Burn Outlet and Mattock Diversion Weir catchments.

	Calibration Period	Validation Period	Generalised Calibration Period	Generalised Validation Period
Glen Burn Outlet 5 km²				
Pathway				
Deep GW	4.9%	3.9%	3.8%	3.0%
Shallow GW	7.8%	6.0%	5.2%	4.8%
Interflow	43.6%	48.8%	49.0%	51.2%
Overland	43.7%	41.3%	42.0%	41.0%
Objective Function				
R^2	0.95	0.95	0.94	0.92
$\sqrt{R^2}$	0.94	0.94	0.90	0.90
Bias	0.0036	0.0066	0.0080	0.0110
Mattock Diversion Weir 6.99 km²				
Pathway				
Groundwater	16.1%	16.6%	12.3%	11.9%
Interflow	51.2%	46.1%	66.4%	59.8%
Overland	32.7%	37.3%	21.3%	28.0%
Objective Function				
R^2	0.84	0.74	0.80	0.75
$\sqrt{R^2}$	0.96	0.92	0.86	0.90
Bias	-0.0028	-0.0145	-0.0053	-0.0098

9.6 Discussion

In Chapter 7, the pathway separations were assessed. Following on from this, this chapter related the parameters required for the NAM modelling of each of the catchments to the different catchment descriptors available in GIS format. Soils, subsoils, land-use, aquifer classification, DEM and river datasets were utilised to define all the descriptors. These data were then employed to create predictor characteristics for each study and supplementary catchment, with multiple linear regression equations relating these descriptors to the NAM parameters of the catchments.

In a previous study, NAM was applied to model a multitude of catchments in Ireland in the RPS groundwater-surface water interaction report (2008). In the RPS report, key physical characteristics of the selected catchments were utilised to derive guiding values for the NAM parameters assigned to the simulation of these catchments. Decision tables were developed in that study to guide the selection of parameters, but this resulted in tables that had a large range of suggested values rather than providing equations to calculate a suitable value for a parameter as is achieved in this chapter. Certain land-use types were also omitted from the list of predictors considered for catchment characteristics, with classification of datasets being rudimentary, rather than the more comprehensive classification employed in this chapter. The RPS study also lumped interflow and shallow groundwater flow together, which affected the selection of parameters for simulations and also resulted in underestimates of the groundwater contribution to river discharge. A crucial difference between the predictors utilised here and in that earlier study is the weighting given here to the datasets based on the distance from the nearest stream or river. This assisted in differentiating between land located at the catchment boundary that is most likely to affect recharge, compared with land located at the stream's edge and thus more likely to have a significant influence on the fast-responding overland and interflow pathways.

Multiple linear regression was used to define the relationships between catchment characteristics, based on the predictors outlined in Section 9.3, and NAM parameters. The regression equations were then applied for the same calibration and validation periods as in Chapter 7 for Glen Burn Outlet and Mattock Diversion Weir catchments. As can be observed in Table 9-5, there was good agreement for both catchments for the calibration period and validation period using the auto-calibration approach (informed by the separation techniques of Chapter 6), and the regression equations developed from these simulations. This is particularly true of the Outlet catchment, with more variation present in the Diversion Weir as interflow is calculated as being higher from the regression equations approach, with overland flow consequently having a smaller contribution. It was anticipated that there would typically be good agreement, as both of these catchments were among a limited number of catchments involved in the development of the regression equations, but as the number of catchments increases, assessments such as this will become more and more indicative of the success of the generalisation. These equations can then be applied to ungauged catchments with more confidence. Currently, the numbers of predictors are quite large compared to the number of calculated values of each NAM parameter. Therefore further catchments would be

required to improve the generality and the validity of these equations and provide validation opportunities.

9.6.1 Limitations of regression

While the results of the regression equations outlined in this chapter were successful, with most r^2_{adj} values greater than 90%, these must be viewed with a caveat in mind. These equations were fitted to values that were observed to provide reasonable separations in the catchments in question, taking the different separation methods into account. The parameters utilised for these catchments may be close to the 'best' combination but there is no certainty about this. As such, the regression equations in this study were for the set of parameters that were implemented, not necessarily the optimum and also these regression equations will be less applicable outside the ranges within which they were developed. This is of particular importance in catchments with unusual features that were not covered by the catchments that were employed to develop these equations. Catchments with large karst conduit systems are an example of situations that these equations may not be able to represent adequately.

Another limitation of regression is the lack of connection between correlation and causality. A predictor may have a statistical relationship with a response but this may be a result of coincidence and not due to any systematic relationship between two variables. Predictor values have been divided by catchment area in this study to help avoid such spurious relationships being developed, as the actual difference in descriptors between catchments can be more readily observed once the data have been normalised by catchment area. Applying available scientific knowledge to avoid non-causal relationships will also help. For example, that the type of soil in a catchment influences the surface storage is intuitive as soil type will have a bearing on how much water can infiltrate and hence how much storage there is on the surface. 'Lurking' variables, as referred to by Box (1966), are of concern for the issue of correlation and causality. This is when a non-related predictor reacts similarly to another important predictor and masks the importance of that predictor. An example would be pasture land for cattle being generally well drained. If cattle stocking density in the field were applied as a predictor of drainage ability of the land, this may perform well if cattle were counted during the summer in one catchment but poorly if they were counted during the winter in another catchment after they have been taken indoors. As such, the land-use is the important predictor not the cattle stocking density, which is behaving in this example as a lurking

variable. When using regression it is always important to assess developed relationships with these limitations in mind.

Overall the regression equations successfully predict the NAM parameters employed for the modelling in Chapter 7 and Appendix C. The exception to this is the regression equation developed for the *TI* parameter. The r^2_{adj} for this regression was low (32.8%). However, it is suggested in the NAM user manual that this parameter may be relatively insensitive compared to the other parameters in the model in temperate climates. This would account for the difficulty in determining a MLR equation to predict this parameter, as a wide range of values may produce comparable outcomes from the modelling. It is therefore unreasonable to expect an equation to be able to predict these parameter values for many catchments if *TI* is indeed quite insensitive. The sensitivity of *TI* and the other parameters are considered in detail in Chapter 10.

9.6.2 Framework for determining pathway contributions to Irish rivers.

The developed regression equations provide the final piece of the framework required for separating the hydrograph into its constituent pathways, as outlined in Chapter 5. This framework is illustrated in the flow chart in Figure 9-26.

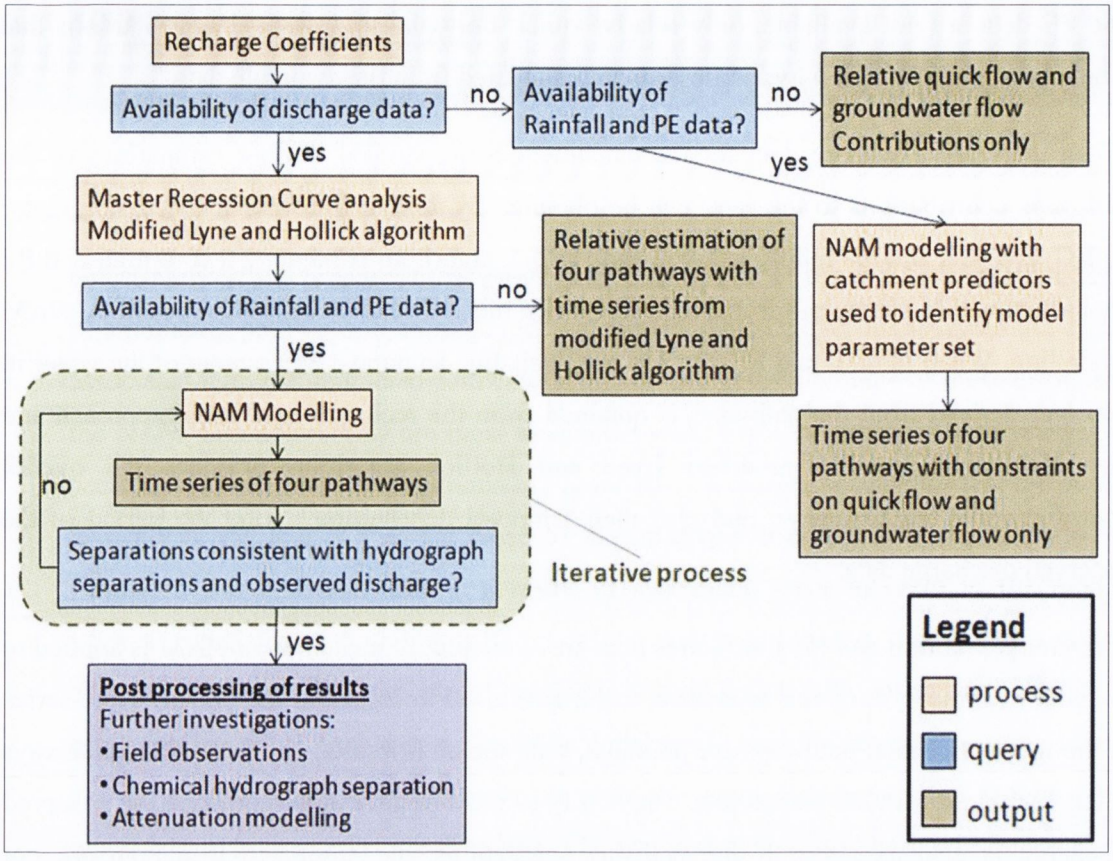

Figure 9-26. Framework for hydrograph separation in Ireland.

For all studies in Ireland, the Recharge coefficient approach (Chapter 6) will be applicable as GIS data can be obtained for the whole of the country. After this it is necessary to check if discharge data for the catchment being studied are available. If discharge data are not available, it is necessary to examine if there is access to rainfall and potential evapotranspiration (PE) data. If these data are accessible, the recession equations of this chapter can be utilised to carry out NAM modelling that will provide separations based on the study catchments and supplementary catchments. Although the four pathways will be modelled, the only actual constraints on these pathways, based on information from the catchment being studied, will be from the recharge coefficient approach. Therefore, only assessments of quick flow (overland flow and interflow) and combined groundwater flow (deep and shallow groundwater flow) can be used for adjustments of the NAM parameters. The effects of adjusting the parameters are discussed in more detail in Chapter 10. If rainfall

and PE data are not available, only relative quick flow and groundwater contributions that would be appropriate for a hydraulic year are calculated from the available data.

When there are discharge data for the catchment being studied, further estimations of the pathways contributions to the river can be obtained by applying the master recession curve (MRC) analysis and the modified Lyne and Hollick algorithm (Chapter 5). If rainfall and PE data are available, the output from these separation methods can be utilised to constrain NAM modelling. When rainfall and PE data are not available, an annual assessment of the water in the river derived from the pathways is obtained from the recharge coefficient approach and the MRC analysis. The modified Lyne and Hollick algorithm provides the overall contribution of the pathways, and also their temporal distribution during the period of the observed discharge data.

If discharge, rainfall and PE time series data are available for a catchment NAM is applied to the data with the hydrograph separation techniques used to constrain the output. Time series of the four conceptual pathways are obtained, with the contributions of each of the pathways being compared with the constraints. The ability of these pathways to reproduce the observed discharge is also assessed. If the pathway separations and simulated discharge are not consistent with the available data the modelling process is implemented until a suitable simulation is achieved. This is the iterative process highlighted in the green box in Figure 9-26. As discussed in Chapter 7, the frequency of the input data will affect the ability of the model to simulate the quicker responding pathways present, particularly in smaller 'flashy' catchments.

Once this process has been carried out, the outputs should be further assessed through the collection of more detailed data that will most likely require field investigations. This will include observations made in the field (such as when certain pathways are active), chemical hydrograph separation and attenuation modelling (both of which will require sampling of the river and pathways where possible) that will provide information on the pathways not based on the response time of the pathways. Attenuation modelling provides further insight into the movement of pollutants, such as phosphorus or nitrogen, can help indicate if pathways associated with these pollutants are contributing significantly to the river.

10 Uncertainty Analysis

10.1 Introduction

Uncertainty of the predictions made in modelling is one of the most important aspects of simulating pathways in an ungauged catchment. This chapter investigates the errors associated with the simulated pathway flows and evaluates the range of these errors and the NAM parameters they are most associated with. Error is generally associated with accuracy and precision as illustrated in Figure 10-1. Accuracy is the ability of the model to generate discharges that are close to the observed discharges. The error between simulated and observed data is a result of systematic error inherent in the model, whereas, precision is the ability of a model to generate discharges that are consistently close to one another. In the case of precision, a good match with observed values is not necessary but all generated data should be consistently near the same value. Precision is not an issue as a model will always simulate the same discharge value provided the input data and parameters are the same. The uncertainty assessed here will be based on the change in accuracy caused by a change in the NAM parameters.

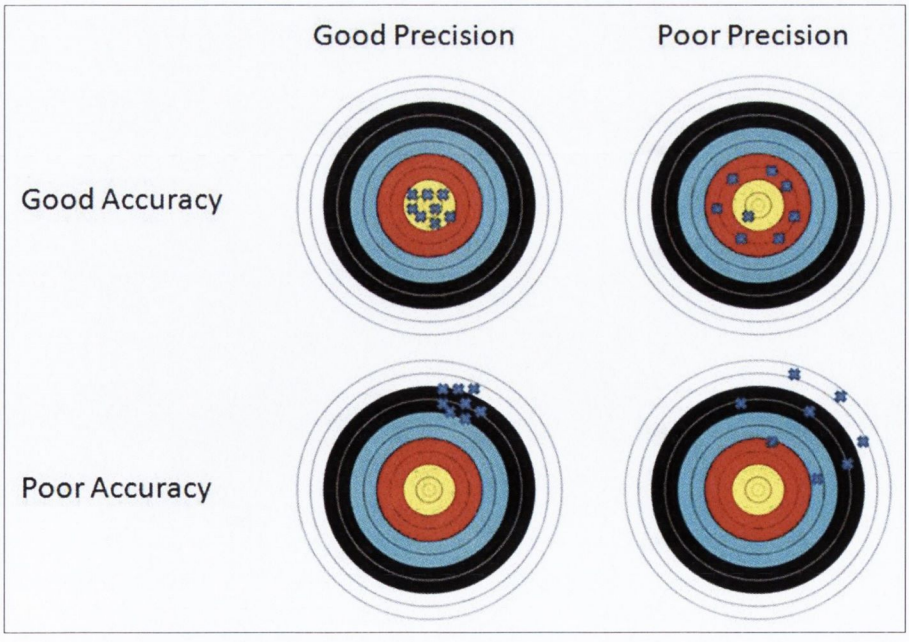

Figure 10-1. The effects of accuracy and precision on errors.

10.2 Regression Equation Error

In Chapter 9, a relationship between the NAM parameters and the characteristic catchment descriptors was developed using multiple linear regression. The error associated with these regression relationships provides a means of examining the effect these parameters have on the accuracy of NAM when generating the discharges of the different pathways. Each regression equation has an associated calculated standard deviation that is a combination of the error associated with each of the predictors implemented in the regression equation, as outlined in Chapter 9. Utilising these calculated standard deviations associated with each of the parameters, confidence intervals were calculated within which the value of the NAM parameter, representative of the catchment in question, was expected to be located. Confidence was set at 95%; i.e. it was expected that 95% of the time the representative value of the NAM parameter, applying the regression equation, would be located within the confidence intervals. These confidence intervals, with the mean predicted value of each NAM parameter, defined the distributions of the representative value of each NAM parameter based on the multiple linear regression equations. For example, Figure 10-2 depicts the distribution obtained for the *Umax* NAM parameter for the Glen Burn catchment applying this approach. Here the distribution is normal about a mean of 19.75 mm.

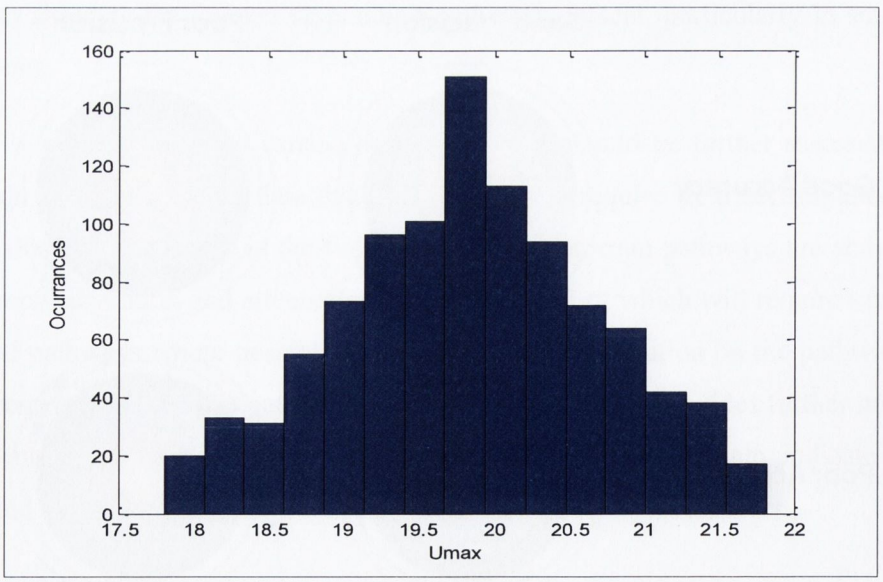

Figure 10-2. Distribution of *Umax* parameter for Glen Burn Outlet catchment using regression equation.

10.3 Sensitivity Analysis

Identifying the parameters that have the most effect on model output is important for calibration but also for assessing the performance of the regression equation at predicting parameter values. When the regression equations were defined in Chapter 9, the associated performance function of r^2_{adj} was evaluated as the best means of determining the overall performance of the regression. This performance function, while assessing the effectiveness of the regression, does not reflect the importance of the parameter on the overall performance of NAM. For example, an r^2_{adj} of 0.9 could be obtained for a parameter that is relatively insensitive, i.e. does not affect model results to a great extent, and so this relatively poor fit for a regression could perform acceptably well in the model. Alternatively, an r^2_{adj} of 0.96 could be computed for a parameter that is very sensitive, so even small deviations from the target parameter value could have large effects on model output. Consequently, a sensitivity analysis is an important aspect of assessing the uncertainty in the NAM model, when applying the regression equations.

10.3.1 One at a time sensitivity analysis

One at a time (OAT) sensitivity analysis (Hamby, 1994) involves evaluating the change in output of a model by incrementing one parameter of the model's set up per run of the model. This approach allows the effect of a single parameter to be assessed each time the model is run. In the case of NAM, the effect of changing each parameter will be determined by selecting a single value from a distribution of the parameter values each time and then evaluating the simulated discharges and pathway separations. A Monte-Carlo simulation was set up, utilising MATLAB to define the distributions and then call the NAM model through command line prompts (see Section 10.3.4). The output was assessed with the Nash-Sutcliffe coefficient (R^2) (Nash and Sutcliffe, 1970), the square-root R^2 coefficient ($\sqrt{R^2}$) and bias, with the contribution of each pathway to river discharge also evaluated. These were then compared with the calibration results from Chapter 7.

10.3.2 Evaluation of sensitivity

In order to compare sensitivities of each parameter between catchments and with other parameters a method for normalising the results of the analyses was required. The method implemented was that of McCuen (1973) in which the changes in the objective functions applied, R^2, $\sqrt{R^2}$ and bias, per run, were normalised by the calibrated objective function value divided by the calibrated parameter value as in Equation 10-I:

$$S_i = \frac{\Delta PF / \Delta p_i}{PF / p_i} \qquad \textbf{10-I}$$

where S_i is the sensitivity of parameter p_i for the ith NAM parameter, PF is the performance function being evaluated.

10.3.3 Parameter prediction distributions

95% confidence intervals were selected as the bounds to the mean predicted values from the regression equations. 95% was chosen as the confidence level based on previous statistical studies in hydrology (Binley et al., 1991; Moradkhani et al., 2005; Wentz et al., 2007), with the confidence intervals and parameter predicted means obtained utilising the statistical software *Minitab* when developing the regression equations. Applying these values, distributions were then developed for the Monte-Carlo simulations. A routine was written in MATLAB that implemented the *normrnd* function to compute a normally distributed probability density function, with a defined mean and standard deviation based on the difference between the mean and the confidence intervals. The standard deviation was defined as a quarter of the difference between the two confidence intervals (as the 95% confidence interval is generally located two standard deviations from the mean). Because the confidence intervals were set as boundaries within which all parameter values were likely to be situated, the 5% of values predicted outside of these boundaries were reset as the mean of all values that had occurred before this in the distribution. This also allowed for distributions that were slightly skewed, a situation when one confidence interval was further from the mean than the other, to be approximated as close to normality as possible. Parameters with means near a limit of feasibility such as 0 or 1 in the case of *CQOF*, had the confidence interval reset to these limits after the calculation of the standard deviation to avoid values that would cause NAM to crash.

10.3.4 MATLAB/NAM syncing

Batch runs of NAM were implemented with the routine programmed in MATLAB. This was carried out with the distributions of each parameter that were computed as per Section 10.2, by selecting a value at random and assigning this to the model parameter. The other parameters were set as predicted by the regression equations determined in Chapter 9. This was achieved by rewriting the input files for each iteration of the model. The model was then run with these parameter settings by calling the model from MATLAB with command line prompts. The output of each simulation was stored and assessed, implementing the objective functions that were selected in Section 10.3.2. The outputs of these functions were then utilised to determine the sensitivity of each parameter for the catchment applications. The results of these sensitivity runs are outlined in the following Section 10.4 and in Appendix D for the supplementary catchments. Each simulation required approximately 12 seconds to run. Ten parameters were evaluated for their sensitivity in each catchment with four hydrological pathways identified and nine in catchments with three pathways. 1000 iterations were used for the Monte-Carlo simulations for each parameter, with the exception of *TO*, *TI* and *TG* where only 500 iterations were applied per parameter. This was as a result of the apparent insensitivity of *TI*, as discussed in Chapter 9. In order to fully evaluate this insensitivity, the maximum upper and lower boundaries were implemented as the confidence intervals for these three parameters, i.e. from zero to one. As *TO* and *TG* function in the same manner as *TI*, this approach was applied to these parameters also. In total, the simulations required a net computation time of approximately 420 hours for the 15 catchments.

10.4 Results

Once the simulations had been completed the data were processed in MATLAB in order to assess the performance of each simulation, applying the three objective functions discussed in Section 10.3.1 as well as evaluating the contributions to discharge from each of the hydrological pathways. The sensitivity of each NAM parameter was determined by applying Equation 10-I. The sensitivity of each parameter, with reference to the objective functions and each of the pathway contributions, is summarised in Table 10-1. The values for sensitivity provided within

this table have no units and provide a relative scale of sensitivity within each column. The highest value indicates the most sensitive parameter (marked in red), followed by the second most sensitive (orange) and the third most sensitive (green), with sensitivity of parameters decreasing with decreasing values in the column. The magnitudes of values between columns are not comparable due to different variations associated with each column, such as a variation of 0.0004 about 0.96 for *Umax* in Figure 10-3 with 0.02 about 0.29 for *Umax* in Figure 10-4. Within each of the objective function columns and pathway contribution columns, a value greater than one is of importance, as this indicates that the output of the Monte-Carlo simulations has more variation than the inputted parameter values. This highlights parameters that have a substantial impact on results obtained from simulations, as is the case with *CQOF* for shallow groundwater, (although it should be noted that it also has a value just less than one with respect to its influence on the deep groundwater pathway (see Table 10-1)).

Table 10-1. Summary of sensitivity analysis. The most influential parameter is indicated in red, with the second and third most influential indicated in orange and green respectively.

	R^2	$\sqrt{R^2}$	Bias	Deep	Shallow	Interflow	Overland
Umax	0.0444	0.0233	0.1667	0.3025	0.3956	0.8912	0.4342
Lmax	0.0263	0.0227	0.3283	0.0979	0.1362	0.4653	0.0578
CQOF	0.1265	0.0505	1.2979	0.9209	1.3028	0.1768	0.8307
CKIF	0.0137	0.0144	0.0421	0.2329	0.2617	0.6687	0.3211
CK	0.3533	0.0809	0.0258	0.0040	0.0040	0.0045	0.0041
CKBF	0.0126	0.0133	0.5816	0.0140	0.0869	0.0149	0.0204
CKLow	0.0047	0.0180	0.0541	0.0304	0.0033	0.0033	0.0033
TO	0.0969	0.0505	0.2268	0.3469	0.5144	0.1073	0.3287
TI	0.0161	0.0178	0.0739	0.0650	0.0705	0.1044	0.1041
TG	0.0670	0.0580	0.0484	0.7242	0.8478	0.2887	0.3448

Table 10-2 presents an example of a detailed breakdown of the output computed from the Monte-Carlo simulations, here the output from the Monument catchment in Nuenna is examined. Each one of the NAM parameters is listed along the left-hand side of the table, with the mean value of that parameter and an upper and lower boundary, upon which the distribution of the Monte-Carlo simulation was based. The ranges of contributions of each of the pathways are presented in the next four sets of columns. As

explained in Chapter 7, the deep and shallow groundwater labels have been replaced by 'diffuse' and 'conduit' to represent the slower and quicker responding groundwater karst pathways. The performance of the objective functions are then outlined in the final three sets of columns, with R^2, $\sqrt{R^2}$ and bias being assessed. The R^2 and 'diffuse' ranges are graphically presented in Figure 10-3 and Figure 10-4, respectively. These plots, for each of the NAM parameters, provide a better indication of the distribution of the output from the simulations between the upper and lower bounds for R^2 and the 'diffuse' contributions. As can been seen from these plots, the majority of the output is close to 0.96 for R^2 and 29% for the 'diffuse' contribution. The parameters that provide the output with the greatest variation are *CQOF* and *TG* for R^2 and *CQOF* and *TG* for the 'diffuse' contribution. As is evident from Table 10-1, *CQOF* is an important parameter for achieving a high R^2, whereas *TG* is fourth in the sensitivity ranking. However, due to relatively large range of values utilised for *TG*. *TG* values are between 0 and 1 varying around a mean of 0.5. This would provide a normalised range of 2, calculated by dividing the range by the mean. If the same calculation was computed for *CQOF*, with values between 0.08 and 0.283 around a mean of 0.182, a normalised range of 0.36 is obtained, much less than the *TG* normalised range. This is why *TG* appears to have the most variability, but this is a reflection of the variability of the inputted *TG* values as well variability of the output, the advantage of applying Equation 10-I to assess the sensitivity. In addition, it should be noted that both *CQOF* and *TG* rank highly for deep/'diffuse' groundwater in Table 10-1.

Table 10-2. Summary of the variation of the Nam parameters and the range of results obtained implementing them into a Monte-Carlo simulation for the Nuenna Monument subcatchment.

	NAM Parameters			'Slow Diffuse'		'Quick Diffuse'		Interflow		Overland		R^2		$\sqrt{R^2}$		Bias	
				%	%	%	%	%	%	%	%					%	%
	mean	min	max	min	max	min	max	min	max	min	max	min	max	min	max	min	max
Umax	10.2	7.9	12.6	27.8	29.6	46.2	49.9	10.8	17.0	9.0	9.8	0.960	0.960	0.970	0.971	1.1	1.1
Lmax	177.6	167.7	187.4	28.7	28.7	48.0	48.1	13.8	13.9	9.4	9.4	0.960	0.961	0.971	0.972	0.8	1.2
COF	0.2	0.1	0.3	23.6	29.4	38.0	49.5	13.5	13.9	7.3	24.9	0.880	0.960	0.932	0.972	0.6	5.0
CKIF	689.6	663.2	715.9	28.5	28.8	47.7	48.3	13.5	14.4	9.3	9.4	0.960	0.960	0.971	0.972	1.1	1.2
CKIF	40.9	38.1	43.6	28.7	28.7	48.1	48.1	13.8	13.8	9.4	9.4	0.958	0.961	0.970	0.972	1.1	1.1
CKBF	613.9	560.3	667.6	28.6	28.8	47.9	48.3	13.8	13.9	9.4	9.4	0.958	0.961	0.969	0.973	0.6	1.9
CKLow	2163.2	2080.6	2245.8	28.5	28.7	47.1	48.1	13.6	13.8	91.1	9.4	0.958	0.961	0.969	0.972	1.0	1.1
TO	0.5	0.0	1.0	28.1	28.6	46.9	48.0	13.7	13.8	9.6	11.3	0.960	0.962	0.966	0.971	1.1	1.3
TI	0.5	0.0	1.0	28.5	29.1	47.7	49.0	12.3	14.4	9.3	9.6	0.953	0.962	0.959	0.972	1.0	1.2
TG	0.5	0.0	1.0	28.6	32.4	47.9	55.1	10.9	13.9	1.6	9.7	0.905	0.960	0.893	0.971	1.1	3.1

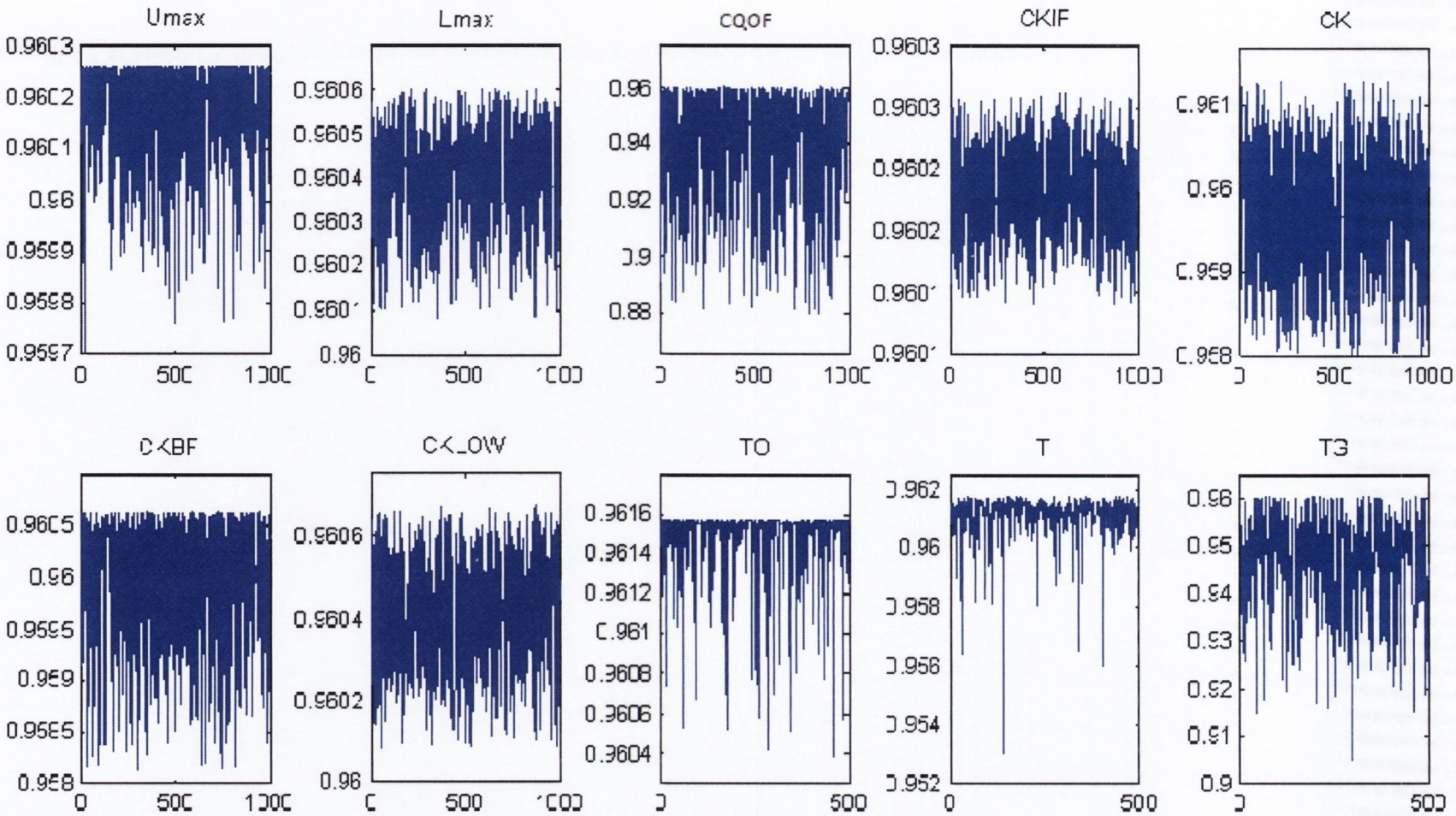

Figure 10-3. R^2 variation for each NAM parameter for Monte-Carlo simulations in Nuenna Monument subcatchment.

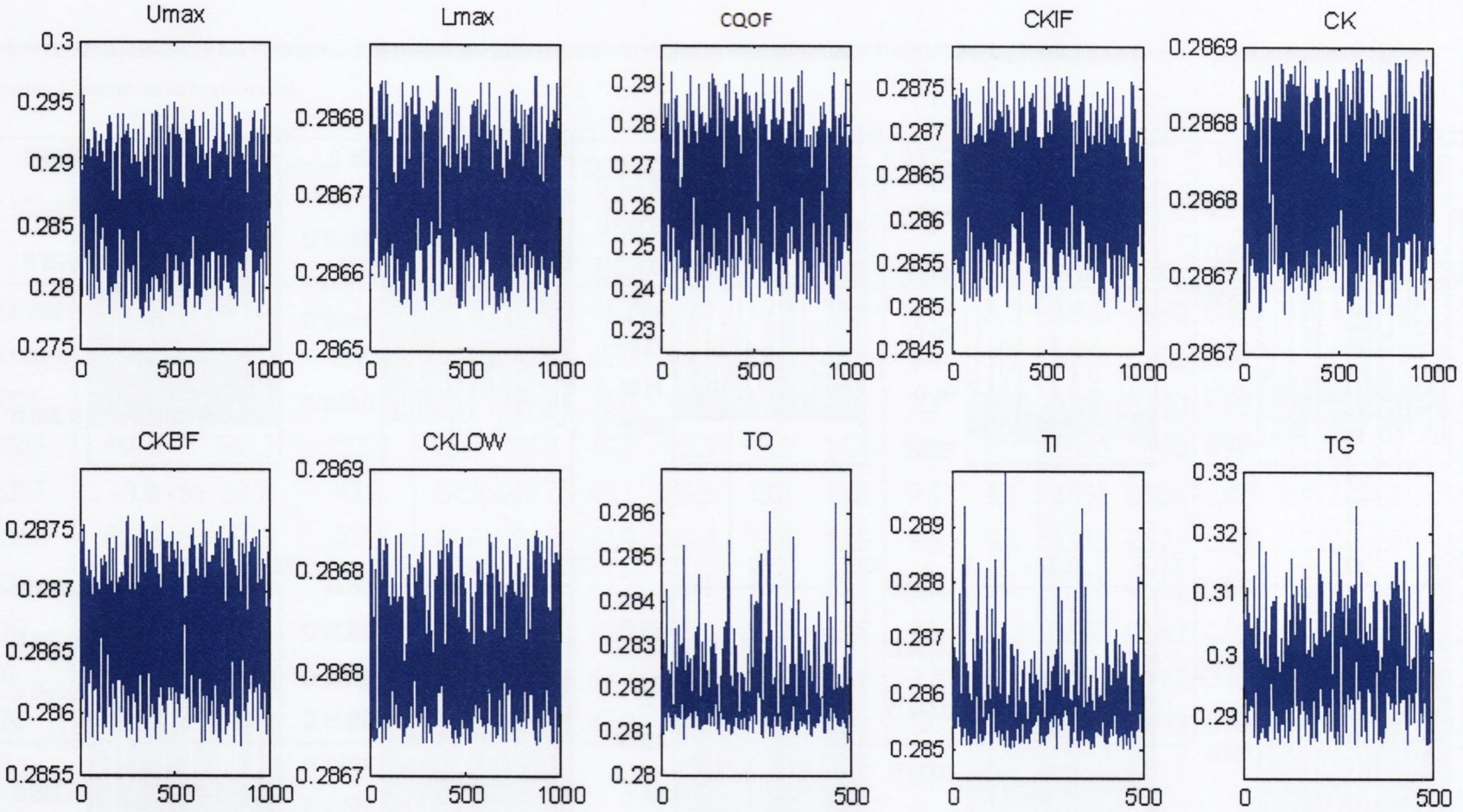

Figure 10-4. Variation of 'diffuse' pathway annual contribution to river discharge in the Nuenna Monument catchment.

In order to assess the impact that the variation of the NAM parameters has on the simulated discharges, the Gortinlieve EPA Weir subcatchment is further assessed. Analysing a rainfall event that takes place at the end of October 2011 (Figure 10-5), the blue line is the observed discharge at the weir, while the red line is the maximum simulated discharge and the green line is the minimum simulated discharge. By varying the model parameters, it is not just the relative contribution of each pathway that is altered but the overall discharge simulated (both the shape of the hydrograph and the quantity of discharge being simulated). This reflects the variation of parameters, such as Umax and Lmax, as these affect the storage available within the soils, resulting in the model being able to hold more water in these storages, thus reducing simulated discharge. It is for this reason that the objective functions values vary within this chapter. The maximum and minimum simulated discharges were chosen from all 8,500 simulations carried out for the sensitivity analysis of this subcatchment. The maximum was taken from the Monte-Carlo simulations of the *CK* parameter, while the minimum was taken from the *CQOF*, these were both highlighted in Table 10-1, as being among the three most sensitive parameters for R^2, a good indication of the ability of simulated discharges to match observed discharges (as discussed in Chapter 7).

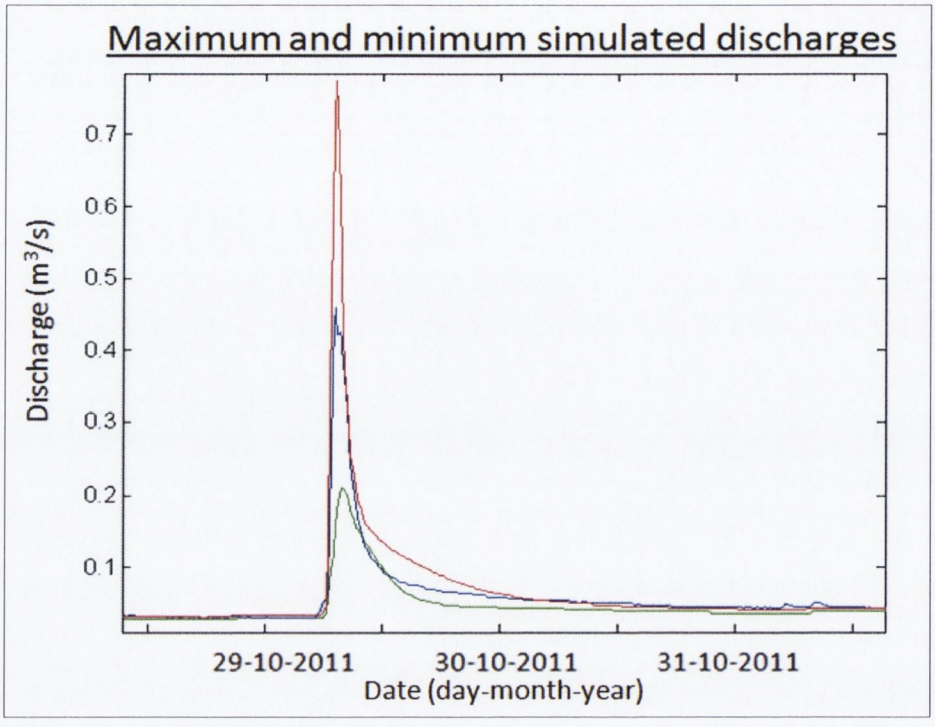

Figure 10-5. Maximum and minimum simulated discharges for rainfall event in Gortinlieve at the EPA Weir subcatchment (October 2011). Blue is observed discharge, red is maximum simulated discharge and green is minimum simulated discharge.

Along with the maximum and minimum overall discharges, the individual variations of the simulated pathways are plotted in Figure 10-6 to Figure 10-9. The variation observed between the minimum and maximum discharges reflects the percentage of the overall discharge that is derived from that pathway for the simulation, i.e. pathways that contribute most to the river are most affected by changes in the parameters relating to them. In Figure 10-6, the maximum deep groundwater contribution was obtained from the *TO* parameter, while the minimum deep groundwater contribution was obtained from the *CQOF* parameter again. Both of these parameters are listed as being in the top three most sensitive parameters for the deep groundwater pathway.

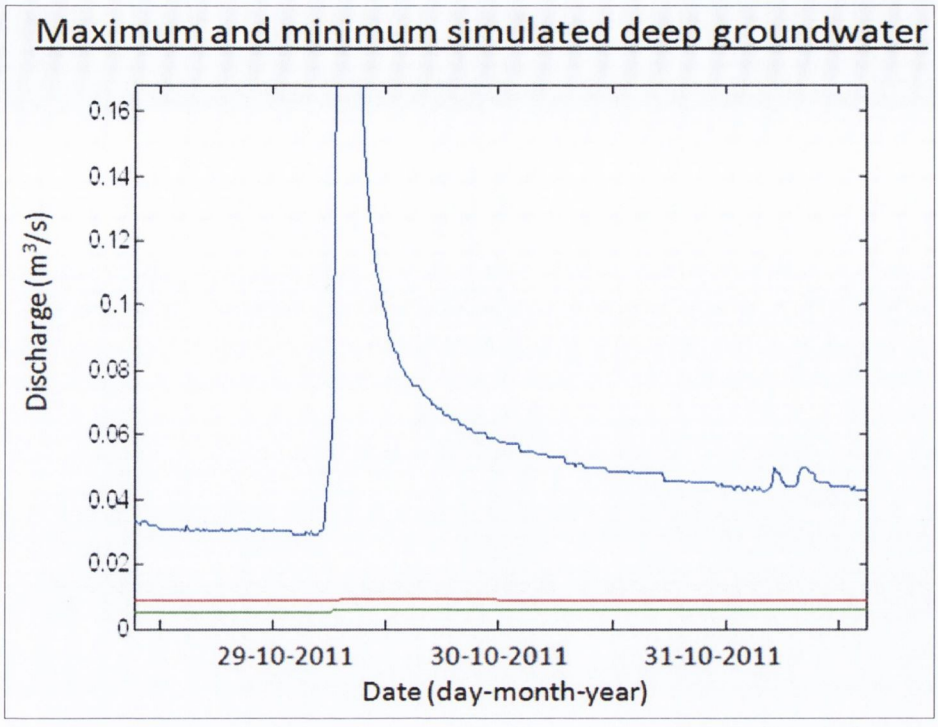

Figure 10-6. Maximum and minimum simulated deep groundwater at the EPA Weir subcatchment (October 2011). Blue is observed discharge; red is maximum simulated deep groundwater and green is minimum simulated deep groundwater.

Figure 10-7 illustrates the variation between the maximum and minimum discharges from shallow groundwater for this event. The contribution of this pathway is larger than in the case of the deep groundwater, but overall makes up only a small proportion of the observed discharge (as is expected in this 'flashy' catchment). The *TO* parameter is once more the parameter responsible for the maximum shallow groundwater contribution, while the *CQOF* parameter is again the dominant parameter for the minimum discharges.

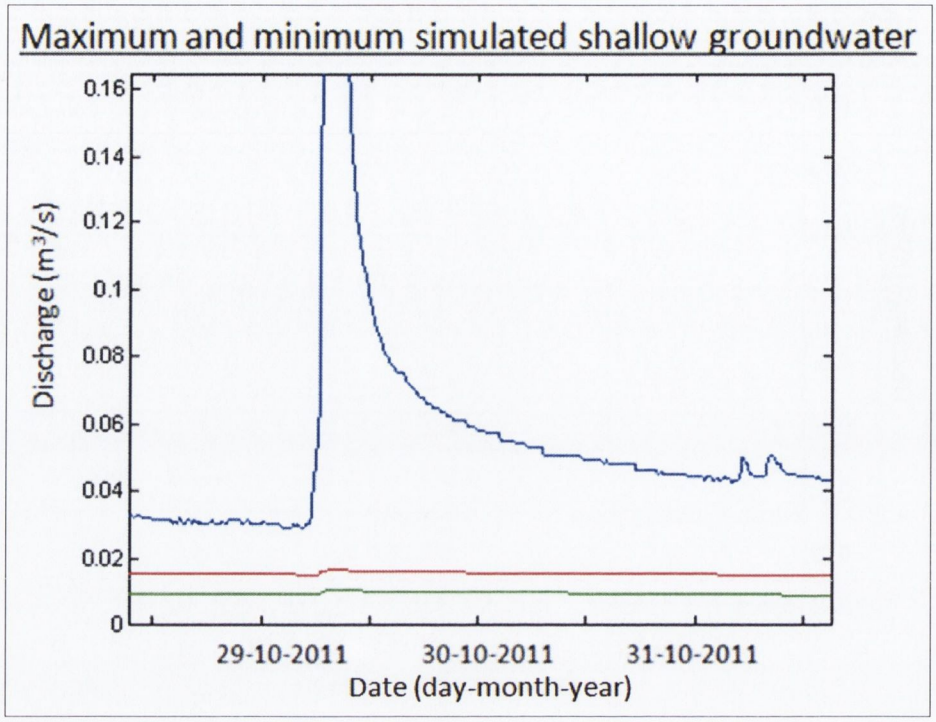

Figure 10-7. Maximum and minimum simulated shallow groundwater at the EPA Weir subcatchment (October 2011). Blue is observed discharge; red is the maximum and green is the minimum simulated shallow groundwater.

Interflow has been calculated as having the biggest contribution to discharge in the river in Gortinlieve (as discussed in Chapters 6 and 7). This is reflected by the larger contribution to the event discharge than from either of the groundwater pathways, and by the larger variation between the simulated maximum and minimum interflows in Figure 10-8. The *CKIF* and *Umax* parameters were responsible for the maximum and minimum interflow contributions respectively. This again is to be expected as both of these parameters have been highlighted in Table 10-1.

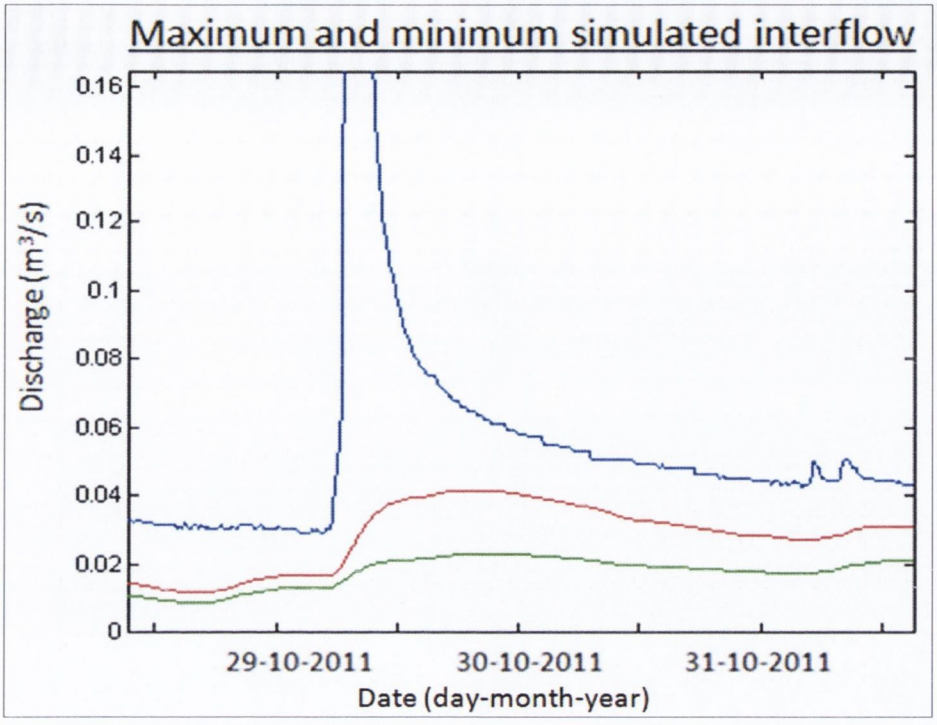

Figure 10-8. Maximum and minimum simulated interflow at the EPA Weir subcatchment (October 2011). Blue is observed discharge; red is maximum simulated interflow and green is minimum simulated interflow.

As can be seen in Figure 10-9, overland flow has the ability to dominate the contribution of flow to the river during an event, particularly at its maximum, as this is actually greater than the observed discharge for the period. The maximum and minimum overland flows are both taken from the *CQOF* Monte-Carlo simulation, highlighting the importance of this parameter for overland flow generation. Once again, as with interflow, the higher proportion of river discharge derived from overland flow results in a large variation between the maximum and minimum values.

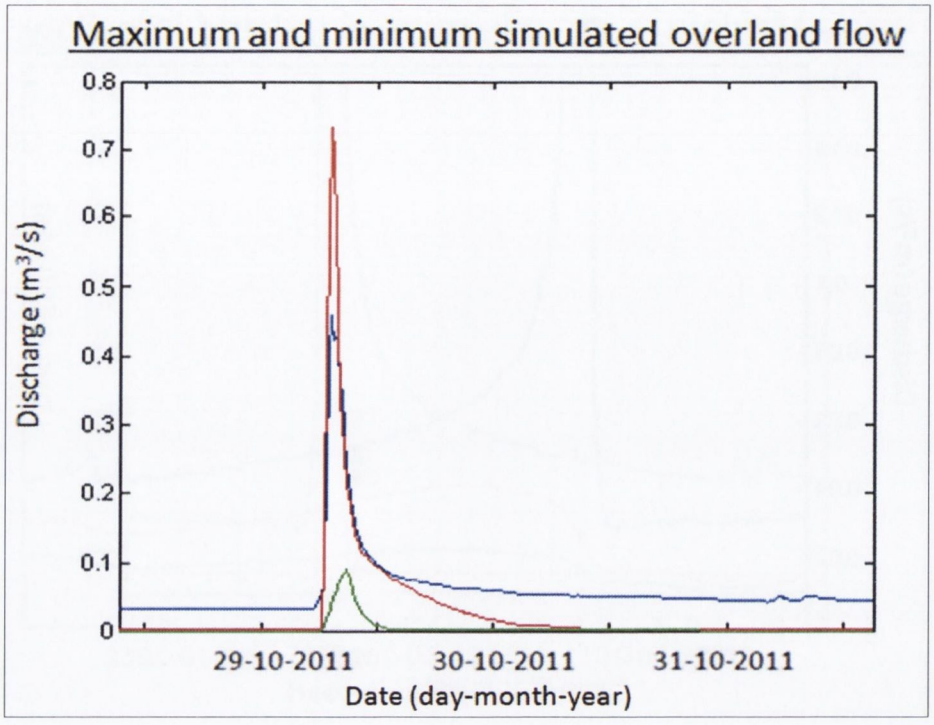

Figure 10-9. Maximum and minimum simulated overland flow at the EPA Weir subcatchment (October 2011). The blue line is observed discharge; red is maximum simulated interflow and green is minimum simulated interflow.

The mean contribution of the different pathways and the mean performance of the objective functions in each of the catchments from all the Monte-Carlo simulations are summarised in Table 10-3. This table also presents the calibrated results of the hydrological modelling carried out in the same catchments for the same periods using NAM for comparison. In this way the average responses expected from a representative value taken from the distribution of the parameters based on the different regression equations are computed.

Table 10-3. Summary of average response for the percentage of the river hydrograph derived from each pathway and the performance of the simulations for R^2, $\sqrt{R^2}$ and bias, of all the Monte-Carlo simulations in each catchment using the predicted NAM parameter sets. These results are compared with the calibrated results of the 'best' separations obtained in Chapter 8.

Catchment	Area (km^2)	Deep Groundwater		Shallow Groundwater		Interflow		Overland Flow		R^2		$\sqrt{R^2}$		Bias	
		Calibrated %	Predicted %	Calibrated %	Predicted %	Calibrated %	Predicted %	Calibrated %	Predicted %	Calibrated	Predicted	Calibrated	Predicted	Calibrated	Predicted
Gortinlieve	0.9	12.9	11.8	14.5	14.3	50.8	50.4	21.8	22.3	0.9	0.88	0.89	0.87	0.0011	0.0010
Glen Burn (Sub)	4.8	12.2	9.1	6.1	7.6	39.9	40.3	41.8	41.7	0.91	0.82	0.94	0.88	-0.0022	-0.0020
Glen Burn (Outlet)	5	4.9	6.8	7.8	9.4	43.6	41.3	43.7	42.5	0.95	0.84	0.93	0.86	0.0036	-0.0072
Mattock (Div Weir)	7	16.1	18.7			51.2	48.5	32.7	31.6	0.84	0.8	0.96	0.84	-0.0028	0.0002
Mattock (Collon)	11.6	6.2	7.5	11.8	11.6	48.3	45.2	33.7	35.6	0.88	0.81	0.86	0.85	-0.0153	-0.0095
Mattock (Berril's)	16.9	9.9	11.5	6.8	7.3	45.7	42.1	37.6	38.8	0.89	0.81	0.86	0.84	-0.0139	-0.0125
Nuenna (Castle)	10.2	30.6	31.5	44.6	38.1	15.4	18.8	9.4	11.6	0.97	0.93	0.95	0.94	-0.0003	0.0026
Nuenna (Rocky)	19.9	31.9	27.8	47.8	44.6	13.2	12.4	12.1	14	0.96	0.93	0.9	0.94	-0.0077	-0.0043
Nuenna (Mon)	35	31.7	28.1	45.3	47.1	13.4	13.6	9.7	9.9	0.97	0.95	0.98	0.96	0.0046	-0.0082

10.5 Discussion

The Monte-Carlo simulation technique, in conjunction with the NAM parameter regression equations and associated error, provided a suitable means of assessing the sensitivity of the NAM pathway simulations to its different parameters. This is discussed in terms of the performance of the regression equations and the sensitivity observed in the NAM parameters for each objective function and pathway contribution to river discharge.

10.5.1 Performance of predictors equations

The assessment of the associated variation of results, obtained when implementing the regression equations, assisted in highlighting the parameters that have the most effect on each of the criteria applied. Once all the Monte-Carlo simulations had been carried out, the data were evaluated using the R^2, $\sqrt{R^2}$ and bias objective functions as outlined in Chapter 7. The percentage of the river discharge was also assessed. An example of the output obtained for each of the parameters in the Nuenna Monument catchment can be seen in Table 10-2, with the variation in R^2 and the 'diffuse' groundwater contribution to river discharge for the catchment illustrated in Figure 10-3 and Figure 10-4 respectively.

As previously mentioned, the regression equations provided values for each of the NAM parameters, which were then applied as the initial parameters. As such, it was important that these predicted parameters provided similar outputs to the calibrated parameters, upon which they were based. Table 10-3 summarises the comparison of the averaged output from all the Monte-Carlo simulations with the output obtained from the hydrological modelling in Chapter 7. The comparison of the data reflects the generally well-correlated regression equations with the data from Chapter 9, in that the calibrated and predicted values in Table 10-3 are in moderate agreement. There is a general trend of increased groundwater contribution in the 'flashy' catchments (Gortinlieve, Glen Burn and the Mattock), when compared to the calibrated results, with the groundwater contribution in the groundwater-dominated Nuenna decreasing. The R^2 and $\sqrt{R^2}$ typically decrease, with the performance of bias varying. The decrease in the performance parameters is reasonable as calibrated solutions would be expected to be

the optimum balance between the parameters to match the observed flows (as well as indicative pathway splits) compared to the artificially varied parameter sets used for the sensitivity analyses. The increase in groundwater contribution is most likely a reflection of the physical hydrograph separation approaches applied to assess limits to the pathway contributions in catchments. Groundwater contributions would have been limited in the 'flashy' catchments generally as a result of the recharge coefficient approach, the master recession curves and the digital filtering algorithms as discussed in Chapter 6 and this will have influenced the calibration in Chapter 7.

10.5.2 Sensitivity of discharges to NAM parameters

The sensitivity of the NAM parameters has also been assessed in relation to the effect the parameters have on the contribution of each of the pathways to the river. This is summarised in Table 10-1, with the three most influential parameters highlighted in each situation. This is a significant table that identifies the parameters that are most likely to influence simulations and help to identify those that should be altered when model results are not in agreement with observations from the field. In addition, it assists in identifying the parameters that have a significant impact on simulations. This is important in ungauged catchments where qualitative information may be available, such as which pathway is likely to be most dominant. In such a scenario, the parameters to be changed manually can be identified. These parameters will be altered to reflect the qualitative data while maintaining the general catchment response as would be predicted by the regression equations. Table 10-1 will assist in this process as it lists *CK*, *CQOF* and *TO* as the most important parameters that affect R^2, if this is the objective function that is required to be maintained, manual adjustments of pathway contributions should avoid these parameters. *TI* is identified by the analysis as a parameter that is particularly insensitive to the value that is implemented in the model. This reinforces the argument made in Chapter 9 that the poor fit of the regression for TI may be related to its insensitivity. Alternatively to changing parameters manually, in catchments where observed data are available, a calibration can be carried out, whereby the insensitive parameters can be held constant, thus providing more emphasis on the important, sensitive parameters.

Each of the column headings of Table 10-1 are discussed in turn in the next subsections, with consideration given to the NAM structure (as outlined in Chapter 7).

10.5.2.1 Nash-Sutcliffe Coefficient (R^2)

The R^2 coefficient is most affected by the *CK* parameter, then the *CQOF* parameter, followed by the *TO* parameter. *CK* is an important parameter as this is responsible for the rate at which overland flow is discharged into the river. The shape of peaks is greatly influenced by this and as such this has a large impact on R^2 as higher flows are more heavily weighted than lower flows. *CQOF* also has a substantial influence on R^2, due to the partitioning of excess water, from the upper soil storage of NAM by this coefficient, between infiltrating water and overland flow. Therefore, this parameter will have a large effect on peaks as well as groundwater discharge, thus impacting the R^2 value. The third most significant parameter is *TO*, the parameter controlling the threshold point at which overland flow occurs in a catchment. This parameter again will have a noticeable effect on simulated peak discharges.

10.5.2.2 Square-root Nash-Sutcliffe coefficient ($\sqrt{R^2}$)

The $\sqrt{R^2}$ coefficient is most affected by *CK*, *TG*, *CQOF* and *TO* jointly. These are similar to the situation for R^2 due to the similar objective function format. The $\sqrt{R^2}$ coefficient tends to place more emphasis on the goodness-of-fit to the lower discharges (compared to the R^2 coefficient), resulting in the *TG* parameter being of more importance than the *CQOF* and *TO* parameters. *TG* affects the water that recharges the groundwater, as if the *TG* threshold in the lower storage is not surpassed, no recharge can occur and all infiltrating water enters the lower storage zone.

10.5.2.3 Bias

The bias accounts for the general water balance between the observed and simulated discharges. If there is a negative value, there is more observed discharge than simulated discharge and *vice-versa* in the case of a positive value. This may be a result of too much storage in a catchment or that the groundwater pathways are responding too

slowly to release the water that is recharging them. As such, *CQOF*, *CKBF* and *Lmax* are shown to be the most important parameters for this objective function. *CQOF* will affect the amount of water infiltrating, while *CKBF* will affect the rate at which discharge will leave the groundwater storages and *Lmax* will define the size of storage in the lower storage zone. Therefore, each of these parameters will have a significant bearing on the bias of a simulation.

10.5.2.4 Deep and Shallow Groundwater

Deep and shallow groundwater have similar generation mechanisms (as outlined in Chapter 8) that rely on the quantity of groundwater recharging their storages and the rate at which this groundwater is released. Of most importance to the contribution of discharge is the water recharging the storages, as confirmed in Table 10-1, where *CQOF*, *TG* and *TO* are the most significant parameters affecting these groundwater pathways. As with R^2 and $\sqrt{R^2}$, these parameters affect how much excess water from the upper storage (*COF* and *TO*) infiltrates into the ground, followed by how much of this infiltrated water enters the lower storage or recharges the groundwater pathways (*TG*). The *CQOF* value in Table 10-1 is close to one for the deep groundwater pathway and actually greater than 1 for the shallow groundwater. This suggests that the influence of *CQOF* is substantial in the model, as the variation of the output of the model is greater than the variation of the input, (i.e., the measure of sensitivity in Equation 10-I). Therefore, this parameter requires special attention, especially as it is present in all columns in Table 10-1except for interflow.

10.5.2.5 Interflow

Interflow is most influenced by *Umax*, *CKIF* and *Lmax* parameters. As explained in Chapter 7, interflow is discharged from the upper storage. The size of this storage is affected by *Umax* and the rate of discharge is affected by *CKIF*. Therefore, both of these parameters exert a substantial influence over the generation of Interflow. The threshold for Interflow to occur is controlled by the percentage of the lower storage that is filled; as such, *Lmax* (defining the size of the lower storage) is the third most influential parameter for interflow.

10.5.2.6 Overland flow

Overland flow is generated by excess water from the upper storage zone being partitioned between overland flow and infiltrating water and then being routed to the river. The most influential parameters, as indicated in Table 10-1, are *CQOF*, *Umax* and *TG*. *CQOF*, as stated for the other objective functions and contributing pathways (except interflow), partitions excess water from the upper storage zone. *Umax* defines the size of this upper storage zone and therefore the amount of water that is stored during a rainfall event before excess water is produced. The *TG* parameter has more of an indirect effect on overland flow that emphasises the importance of carrying out such a sensitivity analysis as this. *TG* affects the recharge entering into the groundwater storages and subsequently the infiltrating water that enters into the lower storage. Similar to interflow, the threshold for overland flow to occur is controlled by the percentage of the lower storage that is filled. Therefore, as *TG* affects the filling of the lower storage, it is the third most important parameter for overland flow generation from the results of the sensitivity analysis.

10.5.3 Identifying upper and lower bounds to pathway contributions

The sensitivity analysis carried out in this chapter also provides the opportunity to assess the range of pathway contributions to rivers and the performance of objective functions implementing the parameter sets obtained from the multiple linear regression in Chapter 9. The maximum and minimum contribution of each pathway to river discharge was stored for each iteration of the Monte-Carlo simulation for each parameter, as was the maximum and minimum discharge series for each parameter. In Table 10-2, the ranges of contributions and objective function performances are presented for the groundwater-dominated Nuenna Monument catchment, while in Figure 10-5 – Figure 10-9, the upper and lower discharges for the overall discharge and each individual pathway are presented for an event in the more 'flashy' Gortinlieve EPA Weir subcatchment.

It can be seen in Figure 10-5 that the upper and lower discharges almost entirely envelope the observed discharge. The start of the event is well defined by both boundaries until the rising limb of the event; at this point the higher boundary follows the observed discharge with the greater accuracy until the observed peak occurs. At this

point, however, the higher boundary continues rising and then peaks at almost twice the observed peak. Meanwhile, the lower boundary peaks at almost half the observed peak. As the higher boundary recedes to below the observed peak discharge, it corresponds to the observed recession until it starts to flatten out too early. This is when the lower simulated discharge starts to approximate the observed discharge accurately until it continues receding as the observed discharge levels out. Both the upper and lower boundaries converge once more at approximately a day and a half after the peak. The simulated discharge obtained from the modelling carried out in Chapter 7 is presented alongside the upper and lower boundaries in Figure 10-10. The calibrated solution in Figure 10-10(a) falls in between the upper and lower boundaries, with the peak being underrepresented by the simulated discharge and the recession being quicker than that observed. For this single event, this would suggest that a change in the *CK* parameter would assist in improving the accuracy of the simulation, but it is likely that this would adversely affect the accuracy of other rainfall events. Figure 10-6 – Figure 10-9 present the individual pathway simulations, with the upper and lower boundaries shown. These boundaries again define the possible discharges applying the range of parameter values from the Monte-Carlo simulation and provide an indication of the type of separations that may be generated using the multiple linear regression equations for the Gortinlieve EPA Weir subcatchment. It is also noted that the difference between the upper and lower ranges increases as the contribution to the river discharge increases.

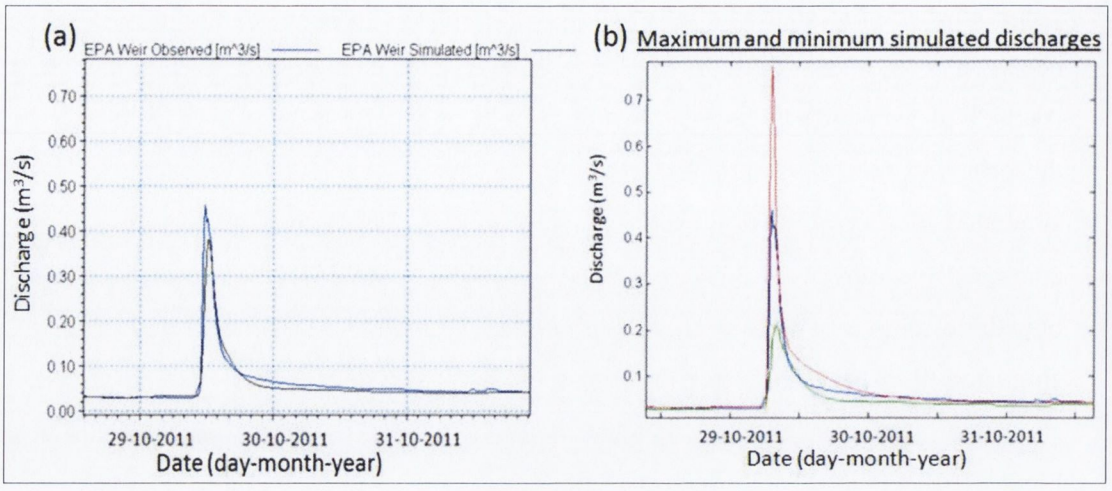

Figure 10-10. (a) Observed and simulated discharges for the Gortinlieve EPA Weir subcatchment and (b) the upper and lower boundaries of discharge obtained from the Monte-Carlo simulation for the same period (Oct 2011).

This sensitivity analysis overall provides a framework within which the uncertainty associated with the prediction of NAM parameter sets using the multiple linear equations from Chapter 9 can be assessed. The potential ability of NAM, utilising these parameter sets, to simulate the discharges in a catchment can be evaluated, as well as which parameters are having the most influence on the generated simulations. The analyses have shown that the *CQOF* parameter appears as one of the top three most sensitive parameters in six of the seven columns in Table 10-1 and therefore, the regression equation describing this parameter would be of most importance to the simulations, as discussed in Section 10.3.

11 Conclusions

11.1 Introduction

This thesis has proposed a framework for quantifying the proportion of the hydrograph derived from deep and shallow groundwater, interflow and overland flow components, as shown in Figure 9-26. This has been developed through the use of physical hydrograph separation techniques, recharge coefficients, temperature data and the implementation of hydrological models, which have enabled the separations to be consistent with the geological setting of the catchment in question and the responses observed in the river. These separations have been based largely on generating separations that designate the fastest responding pathway as overland flow, with interflow, shallow groundwater and deep groundwater then identified in turn as the next fastest responding pathways. The semi-distributed and lumped conceptual rainfall-runoff model NAM was effective at separating the hydrograph into its constituent pathways, reflecting the results of the separation techniques and, in general, maintaining a satisfactory correlation between simulated and observed river discharge, the assessment of which was carried out applying the data monitored in the study catchments during the course of this thesis. The comparison between observed and simulated flows was evaluated utilising the Nash-Sutcliffe coefficient R^2, $\sqrt{R^2}$ and bias.

Groundwater pathways' contributions to river discharge were further investigated applying the fully distributed MODFLOW groundwater model. This finite difference model simulated the contributing catchment in the NAM catchment, utilising the neighbouring catchments. It also provided a hydrograph of the contribution of the pathways for the same time period as the NAM simulation for this catchment. The comparison of the two hydrological models highlighted the large demand for high spatial resolution data from such a model as MODFLOW. The results obtained suggested that in a complex catchment like the Mattock, the data available were not sufficient for achieving a good fit between simulated and observed discharge in the river, particularly during low flows when it is likely that groundwater was the only pathway present. This reinforces the approach of applying NAM in Irish catchments as

though data was not sufficiently available across the Mattock catchment; it would be considered a well instrumented catchment by Irish standards.

Once these separations had been determined from the hydrological modelling, the parameters implemented in NAM were related to the different catchment characteristics, i.e. soil, subsoil, slope, aquifer type etc. This was accomplished utilising multiple linear regression that related each parameter to a selection of catchment descriptors, enabling NAM to be implemented in ungauged catchments of similar type to the study catchments and supplementary catchments of this thesis. Applying the uncertainty associated with these regressions, a sensitivity analysis was carried out to assess the importance of the NAM parameters. This sensitivity analysis provided a ranking of the parameters that are of most importance, with regard to the separations and objective function, when implementing the model, particularly when calibrating it.

The conclusions from each of the separation, modelling, generalisation and uncertainty analysis chapters, highlighting modifications and novel contribution to knowledge, are discussed in the following sections, with recommendations for further research outlined in Section 11.7.

11.2 Physical Separation Methods

11.2.1 Recharge coefficient approach

This approach provided an estimation of the effective rainfall (rainfall less actual evapotranspiration) that infiltrated into the groundwater pathways. The method takes into account the soil type, subsoil and aquifer classification, providing a combined estimation of groundwater pathways, and subsequently a combined estimation of the interflow and overland flow, contributing to the river. However, the method does not allow for indirect (point) recharge). This approach was therefore modified during the current research to include the scenario where surface water recharges the groundwater in karst catchments through swallow holes (see Chapter 6). This has improved upon the established approach in Ireland (Misstear et al., 2009a), by availing of digital elevation model files to delineate surface catchments to swallow holes and define recharge in these areas as 100% of effective rainfall, resulting in an improved estimation of recharge within the Nuenna study catchment.

11.2.2 Master recession curve analysis

This analysis provided an estimation of the response time associated with the pathways by examining the characteristic behaviour of observed discharge during periods of recession. An assessment of the average contribution of the pathways could be calculated utilising the fitted equations to the different segments of the master recession curve. Overland flow was assigned the fastest recession equation, with deep groundwater being assigned the slowest. This method was improved upon from a previous study (RPS, 2008), by identifying that the fitted equation relating to a pathway, is the superimposed combination of that pathway being assessed and any slower responding pathway that is present. For example, the fitted interflow equation would be a summation of the actual interflow equation, the shallow groundwater equation and the deep groundwater equation. Applying this approach, responses were identified for all of the pathways in all of the catchments with the exception of the Diversion Weir in Mattock (see Chapter 6), where the groundwater response could not be split between shallow and deep groundwater. This was most likely the result of the limited recessions that were observed during the period of this research; if more data were available, then it is likely that these groundwater pathways could be split. Another novel aspect of this method was the linking of the responses of the shallow and deep groundwater and interflow with a digital filtering algorithm, developed by this research, in the next section.

11.2.3 Modified Lyne and Hollick algorithm

This digital filtering algorithm was based on the simple 'one-parameter' algorithm developed by Lyne and Hollick (1979). This algorithm relies on a recession constant as an input that can be calculated from analysis such as described in Section 11.2.2. The 'one-parameter' algorithm, however, typically predicts the same contribution of groundwater to the river in the region of 50%. As a result of this there have been many variations of this algorithm (Boughton, 1993; Eckhardt, 2005), but these generally add a subjective coefficient that can be adjusted until a satisfactory separation is obtained, the selection of which is based on other investigative studies or sometimes just experience. This removes the investigative potential of this method. Therefore, utilising only the recession constants obtained from the master recession analysis of Section 11.2.2, the

Lyne and Hollick algorithm was modified to predict separations of the catchments studied within this thesis. This algorithm predicts conservative groundwater contributions, as it does not consider any type of preferential recharge. As such, this method provided useful lower bounds to the groundwater contribution that may be expected in a catchment and the results were in general agreement with those from the other separation methods. Disappointingly, it did not perform adequately in the Nuenna catchment. This is related to the omission of any type of preferential flow, which is certainly present in a catchment with swallow holes.

11.2.4 Temperature separation

This method employed temperature as a tracer in a simple mixing model approximation of the pathways combining in the river. This is analogous to the geochemical analysis proposed by Pinder and Jones (1969) or End Member Mixing Analysis (Hooper et al., 1990). While temperature is not a chemical, the process is the same – a signature concentration (in this case temperature) is identified for each pathway and, by knowing the temperature in the river and the river discharge, the pathways can be separated. The novel aspect of this is that time series analysis was applied to the temperature time series available in the catchment from the boreholes and the river to decompose the temperature time series into its constituent signals. This provided a means of identifying the temperature at each time step of the measured discharge, as the temperature values vary throughout the day rather than remaining a stationary value. The results of this analysis indicated that interflow may be responding as quickly as overland flow during rainfall events, suggesting that the quickest responding pathway being modelled conceptually as overland flow may be comprised of a quicker responding element of interflow (Chapter 6).

11.3 Lumped Hydrological Modelling

NAM provided the means of simulating each of the pathways, utilising rainfall and potential evapotranspiration data as the model inputs. This approach to modelling the pathway contributions to river discharge was effective at generating simulated discharge which, when assessed using objective functions, provided a good match with

observed discharge (as shown in Chapter 7). The Mattock catchment, though, performed the least satisfactorily out of the study catchments with regards to the match between observed and simulated discharge. This was most likely due to the complexities of the Diversion in the upper catchment, the difficulties with the EPA hydrometric station at Collon, as well as the abstractions from sands and gravels adjacent to the river at Collon and the river becoming perched at the outlet. Nonetheless, the calculated contribution of each pathway to the river was in general agreement with the results of separation methods, outlined in Section 11.2, that were also used to constrain the auto-calibration routine embedded in NAM. This approach improves upon the work of Madsen (Madsen, 2000), which only employs R^2 and catchment water balance as the means of assessing the effectiveness of the calibrations. Following this, the parameters implemented in NAM to produce these results allowed the development of a relationship between individual NAM parameters and catchment characteristics as discussed in Section 11.5

NAM also provided a means of assessing the improvement of simulations with increasing temporal resolution of input data. This research showed that when rainfall data were provided at smaller time intervals in 'flashy' catchments the Nash-Sutcliffe coefficient (R^2) increased substantially. It was subsequently demonstrated that the same substantial increase in R^2 was not observed in slow responding catchments such as the Nuenna. This helped develop the novel link between the time constant of quickest responding pathway of the Master Recession Curve analysis indicating the maximum time interval for input rainfall data that would produce adequate R^2 values. The inverse of the τ (time constant, see Chapter 6) value of the fastest responding pathway of the Master Recession Curve would provide the characteristic response time of this pathway. In this way, the minimum temporal resolution of rainfall data required to accurately simulate this pathway could be predicted. This expands upon the observation of simulations with increased temporal resolution of data improving the performance of objective functions (Littlewood et al., 2011), by also linking the required time step for accurate simulation of hydrograph peaks with analysis of recorded discharge data. This can therefore inform the appropriate frequency at which to record rainfall prior to the installation of rain gauges in study catchments, if discharge data are available.

Another useful contribution to knowledge was the distributing of the daily potential evapotranspiration (PE) data over the day, avoiding the situation where the same rate of PE is occurring during the night as during the day. This approach, involved in the preprocessing of PE data for NAM, provides a more realistic representation of PE when only daily data are available.

11.4 Distributed Modelling

MODFLOW was applied to the Mattock catchment to assess if a distributed groundwater model would provide greater insight into the conceptual model, taking into account the limited data generally available for this and other catchments in Ireland. While this model produced annual contributions in agreement with those computed with the separation methods and lumped modelling, the temporal distribution of these contributions resulted in overestimations of groundwater discharge during periods of low flow. Sensitivity analysis suggested that a change in conceptual model structure may address this issue as varying the parameters improved discharge simulations marginally but lead to a decline in the goodness of fit between simulated and observed groundwater levels. Currently the parameters are assigned according to bedrock and aquifer type. A change from this approach would be difficult to implement due to a lack of data in the catchment to suggest otherwise.

The model does, however, provide a means of calculating the contributing area of the groundwater catchment, which is directly applicable to the NAM modelling. Utilising neighbouring catchments and the rivers within them, MODFLOW computed a groundwater catchment area of 16.7 km^2 compared with 16.9 km^2 when calculated with the topography of the catchment. Without further information the groundwater catchment area is considered coincident with the catchment area calculated with topography. This is an encouraging result for the lumped modelling approach.

Of importance is that the change in storage for the period of one year was negligible (0.35%). This is a typical assumption when assessing catchment water balances (Scanlon et al., 2002); another approach that is utilised in this thesis to assess the size of the groundwater catchment. While this result must be viewed cautiously, it is encouraging that the yearly contribution of the groundwater pathways generated by

MODFLOW was comparable to that simulated by NAM and predicted by the recharge coefficient approach.

11.5 Generalisation of NAM Parameters

Using the parameters sets for NAM that were applied in each catchment for the simulation the pathways, multiple linear regression was used to develop relationships between the parameters and catchment descriptors. This is an important contribution to knowledge, as the development of these predictive equations allow NAM to be applied to ungauged catchments, provided that rainfall and potential evapotranspiration data are available and also that the required catchment descriptor data are available as GIS layers. This approach had been attempted before, but not for each NAM parameter, nor utilising the comprehensive list of catchment descriptors to produce values of NAM parameters. Equations successfully related the ten NAM parameters to catchment descriptors, with the exception of the threshold for interflow (*TI*) parameter (as outlined in Chapter 9). These regression equations were based upon a limited set of catchments. This will affect their performance in catchments that significantly differ from the geology of the catchments that the equations were developed for. These different regressions had errors associated with them that enabled the derivation of probability distribution functions within which the appropriate value for each NAM parameter (as deemed by the approach taken in this thesis) was likely to be found. This provided a distribution of the *TI* parameter values that allowed a Monte-Carlo simulation to assess their sensitivity to be carried out as discussed in Section 11.6. Following on from this sensitivity analysis, it was concluded that this parameter was insensitive in the Irish catchment settings investigated within this research and therefore a good regression fit was not necessary.

11.6 Uncertainty Analysis

Finally, the uncertainty analysis carried out gave an overview of the range of outputs expected from the pathway contributions to the river discharge, the performance of the objective functions, and an overview of the sensitivity of these to the NAM parameters.

This analysis provided an assessment of the effectiveness of the predicted parameter sets applying the derived regression equations, referred to in Section 11.5. Importantly, with respect to contribution to knowledge, the sensitivity analysis provided a ranking of the most important parameters relative to the contribution of each of the pathways and the performance of the objective functions. This provides the user of NAM with a set of likely parameters to vary should further information on pathway separations become available. The parameter of most importance to three of the four pathways (excluding interflow) and all three of the objective functions was *CQOF*, the partitioning parameter of excess water from the upper storage between overland flow and infiltrating water.

11.7 Further Research Recommendations

1. Modified Lyne and Hollick algorithm: This algorithm in its current form is unable to represent point recharge occurring through swallow holes in the Nuenna and other such catchments. Therefore, further modification of this technique to incorporate this preferential flow through the soils and subsoils is required.

2. Temperature separation approach: This approach has only been applied in the Mattock catchment thus far. In catchments where the necessary temperature time series are available, it is recommended that this approach be applied with the results compared with those of the Mattock to further investigate if there are other catchments where a proportion of interflow is responding analogous to overland flow. In implementing this recommendation, temporally distributed temperature measurements of overland flow would assist in evaluating the accuracy of the determined overland flow temperature time series.

3. Chemical separation and attenuation modelling: The results of chemical analysis currently being undertaken within the *Pathways Project* will require integration with the results of the pathway separation work carried out within this thesis. The robustness of the predictions would be enhanced if the chemical separations can improve the constraints on the pathways currently being provided by the physical separations and hydrological modelling.

4. Improved of hydrometric stations: The improvement in the accuracy of recorded data will assist in providing more confidence in physical separation methods and assist in further understanding of the complexities present in catchments, particularly in the Mattock as outlined in Section 11.3. These improvements would include remediation work at the EPA Weir in the Mattock at Collon and development of an enhanced rating curve at the outlet of Gortinlieve to ensure that data from this catchment may be utilised.

5. Improved temporal and spatial resolution of data: An improvement in the availability of data is recommended, as a better representation of the variation in rainfall and PE data, hydraulic conductivity and storage, spatially and temporally (in the case of rainfall and PE) will assist future hydrological modelling in these catchments. As discussed in Chapter 7, for future implementation of hydrological models, it would be appropriate to use at least hourly rainfall in the case of the 'flashy' catchments, such as the Bawn, with daily data being adequate for slow responding catchments, such as the Nuenna.

6. Number of catchments modelled: An increase in the number of catchments modelled, applying the framework developed by this thesis, will help enhance the effectiveness of the regression equations developed in Chapter 9. An increase in the number of catchments modelled will assist this, but it is necessary to include catchments that are not well represented by the study catchments and supplementary catchments of this thesis, such as catchments dominated by karst conduit flow.

7. Application of research methodology outside Ireland: Finally, the methodology applied within this research to separate the hydrograph into its constituent pathways is applicable to catchments outside of Ireland, provided the necessary data are available and the conceptual model is consistent with the catchment being assessed. If this expansion of the research methodology internationally is successful, it can provide further robustness to the regression equations of Chapter 9.

References

Abbott, M., Bathurst, J., Cunge, J., O'connell, P., Rasmussen, J., 1986a. An introduction to the European Hydrological System—Systeme Hydrologique Europeen,"SHE", 2: Structure of a physically-based, distributed modelling system. Journal of Hydrology, 87(1): 61-77.

Abbott, M.B., Bathurst, J.C., Cunge, J.A., O'Connell, P.E., Rasmussen, J., 1986b. An introduction to the European Hydrological System—Systeme Hydrologique Europeen,"SHE", 1: History and philosophy of a physically-based, distributed modelling system. Journal of Hydrology, 87(1): 45-59.

Albek, M., Bakır Öğütveren, Ü., Albek, E., 2004. Hydrological modeling of Seydi Suyu watershed (Turkey) with HSPF. Journal of Hydrology, 285(1): 260-271.

Allen, R., Pereira, L., Raes, D., Smith, M., 1998. Crop evapotranspiration-Guidelines for computing crop water requirements-FAO Irrigation and drainage paper 56. FAO, Rome, 300.

Allen, R., Smith, M., Pereira, L., Perrier, A., 1994. An update for the calculation of reference evapotranspiration. ICID bulletin, 43(2): 35-92.

Allik, H., Hughes, T.J.R., 1970. Finite element method for piezoelectric vibration. International Journal for Numerical Methods in Engineering, 2(2): 151-157.

Anderson, M., Burt, T., 1980. Interpretation of recession flow. Journal of Hydrology, 46(1): 89-101.

Anderson, M., Woessner, W., 1992. Applied groundwater modeling: simulation of flow and advective transport. Academic Press San Diego.

Anderson, M.P., 2005. Heat as a ground water tracer. Ground Water, 43(6): 951-968.

Anderson, T., Darling, D.A., 1954. A test of goodness of fit. Journal of the American Statistical Association: 765-769.

Archbold, M., Bruen, M., Deakin, J., Doody, D., Flynn, R., Kelly-Quinn, M., Misstear, B., Ofterdinger, U., 2010. Contaminant Movement and Attenuation along Pathways from the Land Surface to Aquatic Receptors–A Review. Environmental Protection Agency, Wexford Ireland, 978: 1-84095.

Archbold, M., Deakin, J., 2011. Current Conceptual Understanding of Study Catchments, unpublished report to the Steering Committee of the STRIVE funded *Pathways Project*.

Arnold, J., Srinivasan, R., Muttiah, R., Williams, J., 1998. Large area hydrologic modeling and assessment, Part I: model development, Journal of the American Water Resources Association, 34, pp. 73- 89.

Ashraf, A., Ahmad, Z., 2008. Regional groundwater flow modelling of Upper Chaj Doab of Indus Basin, Pakistan using finite element model (Feflow) and geoinformatics. Geophysical Journal International, 173(1): 17-24.

Banks, D., 2009. Thermogeological assessment of open-loop well-doublet schemes: a review and synthesis of analytical approaches. Hydrogeology Journal, 17(5): 1149-1155.

Barnes, B., 1939. The structure of discharge recession curves. Transsactions American Geophysical Union, 20(4): 721-725.

Bathurst, J., Kilsby, C., White, S., Brandt, C., Thornes, J., 1996. Modelling the impacts of climate and land-use change on basin hydrology and soil erosion in Mediterranean Europe. Mediterranean desertification and land use.: 355-387.

Ben-Gal, A., Kool, D., Agam, N., van Halsema, G.E., Yermiyahu, U., Yafe, A., Presnov, E., Erel, R., Majdop, A., Zipori, I., Segal, E., Rüger, S., Zimmermann, U., Cohen, Y., Alchanatis, V., Dag, A., 2010. Whole-tree water balance and indicators for short-term drought stress in non-bearing 'Barnea' olives. Agricultural Water Management, 98(1): 124-133.

Bergstrom, S., 1976. Development and application of a conceptual runoff model for Scandinavian catchments.

Beven, K., 1977. TOPMODEL: A physically-based variable contributing area hydrological model program, Working Paper 183, School of Geography, University of Leeds, UK.

Beven, K., 1993. Prophecy, reality and uncertainty in distributed hydrological modelling. Advances in water resources, 16(1): 41-51.

Beven, K., 1997. TOPMODEL: a critique. Hydrological Processes, 11(9): 1069-1085.

Beven, K.J., 2001. Rainfall-runoff modelling, The Primer. John Wiley&Sons Ltd.

Bicknell, B., Imhoff, J., Kittle Jr, J., Jobes, T., Donigian Jr, A., Johanson, R., 2001. Hydrological Simulation Program–Fortran: HSPF, Version 12 User's Manual. AQUA TERRA Consultants, Mountain View, California.

Binley, A.M., Beven, K.J., Calver, A., Watts, L., 1991. Changing responses in hydrology: assessing the uncertainty in physically based model predictions. Water Resources Research, 27(6): 1253-1261.

Birkinshaw, S.J., Webb, B., 2010. Flow pathways in the Slapton Wood catchment using temperature as a tracer. Journal of Hydrology, 383(3–4): 269-279.

Black, A., Lewis, R., Grout, M., Witterick, W., 2012. Crossing boundaries, the influence of groundwater model boundaries and a method to join and split MODFLOW models. Geological Society, London, Special Publications, 364(1): 155-172.

Blazkov, S., Beven, K., 1997. Flood frequency prediction for data limited catchments in the Czech Republic using a stochastic rainfall model and TOPMODEL. Journal of Hydrology, 195(1): 256-278.

Boughton, W., 1993. A hydrograph-based model for estimating the water yield of ungauged catchments. Institution of Engineers, Australia, pp. 317-317.

Box, G.E.P., 1966. Use and abuse of regression. Technometrics, 8(4): 625-629.

Bredehoeft, J., Konikow, L., 2012. Ground-Water Models: Validate or Invalidate. Ground Water, 50(4): 493-495.

Brezonik, P.L., Stadelmann, T.H., 2002. Analysis and predictive models of stormwater runoff volumes, loads, and pollutant concentrations from watersheds in the Twin Cities metropolitan area, Minnesota, USA. Water research, 36(7): 1743-1757.

Brodie, R., Hostetler, J., 2005. A review of techniques for analysing baseflow from stream hydrographs.

Burns, D.A., McDonnell, J.J., Hooper, R.P., Peters, N.E., Freer, J.E., Kendall, C., Beven, K., 2001. Quantifying contributions to storm runoff through end-member mixing analysis and hydrologic measurements at the Panola Mountain Research Watershed (Georgia, USA). Hydrological Processes, 15(10): 1903-1924.

Cassidy, R., Comte, J.C., Flynn, R., Nitsche, J., Ofterdinger, U., Pilatova, K., 2010. Hydrogeological characterisation of Irish poorly productive aquifers: a multidisciplinary research methodology, LoPro: The value of low yield aquifers, Edinburgh, 6th September 2010.

CDM/OCM, 2010. Groundwater Works Programme. Well Completion Report, Mattock Catchment, Co. Meath. Report to EPA and Carlow Carlow County Council.

Chapman, T., 1999. A comparison of algorithms for stream flow recession and baseflow separation. Hydrological Processes, 13(5): 701-714.

Chapman, T., Maxwell, A., 1996. Baseflow separation-comparison of numerical methods with tracer experiments. Institution of Engineers, Australia, pp. 539.

Chen, X., Chen, D.Y., Chen, X., 2006. Simulation of baseflow accounting for the effect of bank storage and its implication in baseflow separation. Journal of Hydrology, 327(3/4): 539-549.

Chezy, A., 1769. Canal de l'Yvette.

Chow, V.T., 1964. Statistical and probability analysis of hydrologic data. Handbook of applied hydrology: A compendium of water resources technology: 8.1-8.90.

Clarke, R.T., 1973. A review of some mathematical models used in hydrology, with observations on their calibration and use. Journal of Hydrology, 19(1): 1-20.

Coffey, R., Cummins, E., Bhreathnach, N., Flaherty, V., Cormican, M., 2010. Development of a pathogen transport model for Irish catchments using SWAT. Agricultural Water Management, 97(1): 101-111.

Comte, J.C., Cassidy, R., Nitsche, J., Ofterdinger, U., Pilatova, K., Flynn, R., 2012. The typology of Irish hard-rock aquifers based on an integrated hydrogeological and geophysical approach. Hydrogeology Journal: 1-20.

Coutagne, A., 1948. Etude générale des variations de débits en fonction des facteurs qui les conditionnent, 2ème partie: Les variations de débit en période non influencée par les precipitations. La Houille Blanche: 416-436.

Crockford, L., 2010. Conceptual Model of the River Mattock Catchment, Unpublished MSc Thesis. School of Planning, Architecture and Civil Engineering, Queen's University Belfast, UK.

Diersch, H., 1980. Finite-Element-Programmsystem FEFLOW. Program Description. Institut fur Mechanik der AdW DDR, Berlin (In German).

Diersch, H., 2002. FEFLOW reference manual. WASY Ltd.

Dirichlet, P.G.L., 1839. Recherches sur diverses applications de l'analyse infinitésimale à la thëorie des nombres: première partie.

Doherty, J., Brebber, L., Whyte, P., 1994. PEST: Model-independent parameter estimation. Watermark Computing, Corinda, Australia, 122.

Doherty, R., Kalin, R., Ofterdinger, U., Yang, Y., Dickson, K., 2002. 15. Observed and modelled hydraulic aquifer response to slurry wall installation at the former gasworks site, Portadown, Northern Ireland, UK. Advanced groundwater remediation: active and passive technologies: 239.

Domenico, P.A., 1972. Concepts and models in groundwater hydrology, 405. McGraw-Hill New York,, USA.

Eckhardt, K., 2005. How to construct recursive digital filters for baseflow separation. Hydrological Processes, 19(2): 507-515.

Eckhardt, K., 2008. A comparison of baseflow indices, which were calculated with seven different baseflow separation methods. Journal of Hydrology, 352(1): 168-173.

EN ISO 748, 2007. Hydrometry - Measurement of liquid flow in open channels using current meters and floats. International Organisation for Standardization, Geneva.

Engeland, K., Hisdal, H., 2009. A comparison of low flow estimates in ungauged catchments using regional regression and the HBV-model. Water Resources Management, 23(12): 2567-2586.

EPA, 2006. Water Framework Directive, Monitoring Programme prepared to meet the requirements of the EU Water Framework Directive (2000/60/EC) and National

Regulations implementing the Water Framework Directive (S.I. No. 722 of 2003) and National Regulations implementing the Nitrates Directive (S.I. No. 788 of 2005), Environmental Protection Agency, Co. Wexford, Wexford, Ireland.

Faust, C., Mercer, J., 1980. Ground-water modelling: numerical models. Ground Water, 18(4): 395-409.

Fenicia, F., Savenije, H.H.G., Matgen, P., Pfister, L., 2006. Is the groundwater reservoir linear? Learning from data in hydrological modelling. Hydrology and Earth System Sciences, 10(1): 139-150.

Franchini, M., Wendling, J., Obled, C., Todini, E., 1996. Physical interpretation and sensitivity analysis of the TOPMODEL. Journal of Hydrology, 175(1): 293-338.

Franke, O.L., Reilly, T.E., Bennett, G.D., 1987. Definition of Boundary and Initial Conditions in the Analysis of Saturated Ground-water Flow Systems: An Introduction. Department of the Interior, US Geological Survey.

Gassman, P., Reyes, M., Green, C., Arnold, J., 2007. The soil and water assessment tool: historical development, applications, and future research directions. Transactions of the ASABE, 50(4): 1211-1250.

Githui, F., Thayalakumaran, T., 2011. Calibration of SWAT model using remotely-sensed evapotranspiration for an irrigated catchment in southeastern Australia. Engineers Australia, pp. 1387.

Govender, M., Everson, C.S., 2005. Modelling streamflow from two small South African experimental catchments using the SWAT model. Hydrological Processes, 19(Copyright 2005, IEE): 683-92.

Gray, D., 1973. Handbook on the Principles of Hydrology. Water Information Center Port Washington, New York.

Green, W.H., Ampt, G., 1911. Studies on soil physics. Journal of Agricultural Sciences, 4(1): 1-24.

Grossmann, A., Morlet, J., 2006. Decomposition of Hardy functions into square integrable wavelets of constant shape. Fundamental papers in wavelet theory.

Groves, P., 2010. Collon Public Water Supply Scheme - Groundwater Source Protection Zones. Draft report. Geological Survey of Ireland.

Güntner, A., Uhlenbrook, S., Seibert, J., Leibundgut, C., 1999. Multi-criterial validation of TOPMODEL in a mountainous catchment. Hydrological Processes, 13(11): 1603-1620.

Haitjema, H., Kelson, V., Lange, W., 2001. Selecting MODFLOW cell sizes for accurate flow fields. Ground Water, 39(6): 931-938.

Hamby, D., 1994. A review of techniques for parameter sensitivity analysis of environmental models. Environmental Monitoring and Assessment, 32(2): 135-154.

Harbaugh, A., 2005. MODFLOW-2005, the US Geological Survey modular ground-water model—the ground-water flow process. US Geological Survey Techniques and Methods, 6.

Herschy, R.W., 1995. Streamflow measurement. Taylor & Francis.

Hewlett, J.D., Hibbert, A.R., 1967. Factors affecting the response of small watersheds to precipitation in humid areas. Forest hydrology: 275-290.

HOBO, 2012. HOBO U24 Conductivity Logger. Retrieved July 28, 2012, from <http://www.onsetcomp.com/products/data-loggers/u24-001>

Hoeg, S., Uhlenbrook, S., Leibundgut, C., 2000. Hydrograph separation in a mountainous catchment - combining hydrochemical and isotopic tracers. Hydrological Processes, 14(7): 1199-1216.

Holder, R., 1985. Multiple regression in hydrology. Institute of hydrology.

Hooper, R., Christophersen, N., Peters, N., 1990. Modelling streamwater chemistry as a mixture of soilwater end-members--An application to the Panola Mountain catchment, Georgia, USA. Journal of Hydrology, 116(1-4): 321-343.

Hooper, R., Shoemaker, C., 1986. A comparison of chemical and isotopic hydrograph separation. Water Resources Research, 22(10).

Horton, R., 1933. The role of infiltration in the hydrologic cycle. Trans. Am. Geophys. Union, 14: 446-460.

Hunter Williams, N.H., Misstear, B.D.R., Daly, D., (In Press). Development of a national groundwater recharge map for the Republic of Ireland. Quarterly Journal of Engineering geology and Hydrogeology.

Institute of Hydrology, 1980. Low Flow Studies Report, Resources Report 1, Oxon, Wallingford, U.K.

Interlandi, S.J., Crockett, C.S., 2003. Recent water quality trends in the Schuylkill River, Pennsylvania, USA: a preliminary assessment of the relative influences of climate, river discharge and suburban development. Water research, 37(8): 1737-1748.

Jakeman, A., Hornberger, G., 1993. How much complexity is warranted in a rainfall-runoff model? Water Resources Research, 29(8): 2637-2650.

Johanson, R.C., Davis, H.H., 1980. Users manual for hydrological simulation program-Fortran (HSPF), 80. Environmental Research Laboratory, Office of Research and Development, US Environmental Protection Agency.

Johnson, E.A., Dils, R.E., Station, S.F.E., 1956. Outline for Compiling Precipitation, Runoff and Ground Water Data from Small Watersheds. Southeastern Forest Experiment Station, US Dept. of Agriculture, Forest Service.

Johnson, M.S., Coon, W.F., Mehta, V.K., Steenhuis, T.S., Brooks, E.S., Boll, J., 2003. Application of two hydrologic models with different runoff mechanisms to a hillslope dominated watershed in the northeastern US: a comparison of HSPF and SMR. Journal of Hydrology, 284(1): 57-76.

Kent, T., 2011. Evaluating if it is Possible to Determine a Methodology, using GIS, to Develop a Surface Water Run-Off Map Using Data that is Currently Available. Unpulished Master's Thesis, University College Cork.

Krige, D.G., 1951. A statistical approach to some mine valuation and allied problems on the Witwatersrand. University of the Witwatersrand.

Lamb, R., Beven, K., 1997. Using interactive recession curve analysis to specify a general catchment storage model. Hydrology and Earth System Sciences, 1(1): 101-113.

Lautz, L.K., Siegel, D.I., 2006. Modeling surface and ground water mixing in the hyporheic zone using MODFLOW and MT3D. Advances in water resources, 29(11): 1618-1633.

Lindström, G., Johansson, B., Persson, M., Gardelin, M., Bergström, S., 1997. Development and test of the distributed HBV-96 hydrological model. Journal of Hydrology, 201(1-4): 272-288.

Linsley, K., 1958. Paulhus,'Hydrology for Engineers'. McGraw-Hill.

Littlewood, I.G., Croke, B.F.W., Young, P.C., 2011. Discussion of "Effects of temporal resolution on hydrological model parameters and its impact on prediction of

river discharge". Hydrological Sciences Journal–Journal des Sciences Hydrologiques, 56(3): 521-524.

Lukey, B., Sheffield, J., Bathurst, J., Hiley, R., Mathys, N., 2000. Test of the SHETRAN technology for modelling the impact of reforestation on badlands runoff and sediment yield at Draix, France. Journal of Hydrology, 235(1): 44-62.

Lyne, V., Hollick, M., 1979. Stochastic time-variable rainfall-runoff modelling, Hydro. and Water Resour. Symp. Institution of Engineers Australia. 89-92, Perth, Australia.

Madsen, H., 2000. Automatic calibration of a conceptual rainfall-runoff model using multiple objectives. Journal of Hydrology, 235(3-4): 276-288.

Maillet, E.T., 1905. Essais d'hydraulique souterraine & fluviale. A. Hermann.

Manning, R., 1889. On the flow of water in open channels and popes. *Trans. Inst. Civ. Eng. Ireland, 20,* 161-207.

McCuen, R.H., 1973. The role of sensitivity analysis in hydrologic modeling. Journal of Hydrology, 18(1): 37-53.

McDonald, M.G., Harbaugh, A.W., 1984. A modular three-dimensional finite-difference ground-water flow model. US Geological Survey Open-File Report 83-875, 528 pp.

Mellor, D., Sheffield, J., O'Connell, P., Metcalfe, A., 2000. A stochastic space-time rainfall forecasting system for real time flow forecasting II: Application of SHETRAN and ARNO rainfall runoff models to the Brue catchment. Hydrology and Earth System Sciences, 4: 617-626.

Meredith, S., 2010. Groundwater vulnerability mapping of Mount Stewart Catchment, Unpublished MSc Environmental Engineering thesis, QUB.

Merz, S.K., Murphy, R., Graszkiewicz, Z., Hill, P., Neal, B., Nathan, R., 2009. Australian Rainfall and Runoff Revision Project 7: Baseflow for Catchment Simulation. P7/S1/004.

Misstear, B., Brown, L., Daly, D., 2009a. A methodology for making initial estimates of groundwater recharge from groundwater vulnerability mapping. Hydrogeology Journal, 17(2): 275-285.

Misstear, B., Fitzsimons, V., 2007. Estimating groundwater recharge in fractured bedrock aquifers in Ireland. Chapt. 16. In: Krasny J, Sharp J (eds) Groundwater in fractured rocks. IAH Spec. Publ. 9, IAH Kenilworth, UK, pp 243–257.

Misstear, B.D.R., Brown, L., Johnston, P., 2009b. Estimation of groundwater recharge in a major sand and gravel aquifer in Ireland using multiple approaches. Hydrogeology Journal, 17(3): 693-706.

Monninkhoff, B.L., Li, Z., 2009. Coupling FEFLOW and MIKE11 to optimise the flooding system of the Lower Havel polders in Germany. International Journal of Water, 5(2): 163-180.

Monteith, J., 1965. Evaporation and environment, Symposia of the Society for Experimental Biology, pp. 4.

Moradkhani, H., Hsu, K.L., Gupta, H., Sorooshian, S., 2005. Uncertainty assessment of hydrologic model states and parameters: Sequential data assimilation using the particle filter. Water Resources Research, 41(5): W05012.

Morlet, J., Arens, G., Fourgeau, E., Glard, D., 1982. Wave propagation and sampling theory—Part I: Complex signal and scattering in multilayered media. Geophysics, 47: 203.

Morris, D., Johnson, A., 1967. Summary of hydrologic and physical properties of rock and soil materials as analyzed by the Hydrologic Laboratory of the U.S.

Geological Survey 1948–1960. U.S. Geological Survey Water Supply Paper 1839-D. Denver, CO: U.S. Geological Survey.

Mugo, J.M., Sharma, T.C., 1999. Application of a conceptual method for separating runoff components in daily hydrographs in Kimakia forest catchments, Kenya. Hydrological Processes, 13(17): 2931-2989.

Mullins, E., 2003. Statistics for the quality control chemistry laboratory. Springer Verlag.

Nash, J., Sutcliffe, J., 1970. River flow forecasting through conceptual models part I--A discussion of principles. Journal of Hydrology, 10(3): 282-290.

Nasr, A., Bruen, M., Jordan, P., Moles, R., Kiely, G., Byrne, P., 2007. A comparison of SWAT, HSPF and SHETRAN/GOPC for modelling phosphorus export from three catchments in Ireland. Water research, 41(5): 1065-1073.

Nasr, A., Bruen, M., Parkin, G., Brinkshaw, S., Moles, R., 2003. Modelling phosphorus loss from agriculture catchments: a comparison of the performance of SWAT, HSPF and SHETRAN for the Clarianna catchment.

Nathan, R., McMahon, T., 1990. Evaluation of Automated Techniques for Baseflow and Recession Analysis. Water Resources Research, 26(7): 1465-1473.

Nawarathna, N., Ao, T., Kazama, S., Sawamoto, M., Takeuchi, K., 2001. Influence of human activities on the BTOPMC model runoff simulations in large-scale watersheds, pp. 93-99.

Ndomba, P.M., Mtalo, F.W., Killingtveit, A., 2008. A Guided SWAT Model Application on Sediment Yield Modeling in Pangani River Basin: Lessons Learnt. Journal of Urban and Environmental Engineering, 2(2): 53-62.

Neitsch, S., Arnold, J., Kiniry, J., Williams, J., 2005. Soil and water assessment tool theoretical documentation, version 2005. Agricultural Research Service, Grassland, Soil and Water Research Laboratory and Texas Agricultural Experiment Station, Blackland Research Center, Temple, TX.

Neumann, S.P., Witherspoon, P.A., 1970. Finite element method of analyzing steady seepage with a free surface. Water Resources Research, 6(3): 889-897.

Newland, D., 1996. An introduction to random vibrations, spectral and wavelet analysis. Longman UK.

Nielsen, S.A., Hansen, E., 1973. Numerical simulation of the rainfall-runoff process on a daily basis. Nordic Hydrology, 4(3): 171–190.

Nitsche, J., 2009. Physical Hydrologeology of a Fractured Metamorphic Bedrock Aquifer in Gortinlieve, Co. Donegal Unpublished MSc Environmental Engineering Thesis, Queens University Belfast.

Niu, G.Y., Yang, Z.L., Dickinson, R.E., Gulden, L.E., 2005. A simple TOPMODEL-based runoff parameterization (SIMTOP) for use in global climate models. Journal of Geophysical Research, 110: D21106.

Osman, Y.Z., Bruen, M.P., 2002. Modelling stream–aquifer seepage in an alluvial aquifer: an improved loosing-stream package for MODFLOW. Journal of Hydrology, 264(1): 69-86.

OTT, 2012a. Orpheus Mini. Retreived on July 27, 2012, from <http://www.ott.com/web/ott_de.nsf/id/pa_orpheusmini_e.html>.

OTT, 2012b. Thalimedes. Retrieved July 27, 2012, from <http://www.ott.com/web/ott_de.nsf/id/pa_thalimedesog_e.html>.

Parkin, G., 1995. SHETRAN Water Flow Component, WRSRU/TR/9510/61.0. Water Resource Systems Research Unit, Department of Civil Engineering, University of Newcastle upon Tyne.

Parsons, J., Sabbagh, G., Heatwole, C., Evans, R., 1998. Evaluation Criteria for Water Quality Models1. Editors: John E. Parsons, Daniel L. Thomas, Rodney L. Huffman: 23.

Penman, H., 1948. Natural evaporation from open water, bare soil and grass. Proceedings of the Royal Society of London. Series A, Mathematical and Physical Sciences, 193(1032): 120-145.

Penman, H., Long, I., 1960. Weather in wheat: An essay in micro-meteorology. Quarterly Journal of the Royal Meteorological Society, 86(367): 16-50.

Pettyjohn, W.A., Henning, R.J., 1979. Preliminary estimate of regional effective groundwater recharge rates in Ohio.

Pinder, G., Jones, J., 1969. Determination of the ground-water component of peak discharge from the chemistry of total runoff.

Quigley, M., 2011. The Importance of Groundwater in the Mattock Catchment, Co. Louth. Unpublished MEng Civil Engineering Thesis, School of Planning, Architecture and Civil Engineering.

Refsgaard, J.C., Knudsen, J., 1996. Operational validation and intercomparison of different types of hydrological models. Water Resources Research, 32(7): 2189-2202.

Restrepo, J.I., Montoya, A.M., Obeysekera, J., 1998. A wetland simulation module for the MODFLOW ground water model. Ground Water, 36(5): 764-770.

Rohan, P.K., 1975. The Climate of Ireland. The Stationery Office, Dublin, 112pp.

RPS, 2008. Further Characterisation Study: An Integrated Approach to Quantifying Groundwater and Surface Water Contributions of Stream Flow.

Saint-Venant, A., 1843. Notea joindre au Mémoire sur la dynamique des fluides. CR Acad. Sci, 17: 1240-1243.

Scanlon, B.R., Healy, R.W., Cook, P.G., 2002. Choosing appropriate techniques for quantifying groundwater recharge. Hydrogeology Journal, 10(1): 18-39.

Scanlon, T.M., Kiely, G., Amboldi, R., 2005. Model determination of non-point source phosphorus transport pathways in a fertilized grassland catchment. Hydrological Processes, 19(14): 2801-2814.

Schöniger, M., Sommerhäuser, M., Herrmann, A., 1997. Modelling flow and transport processes in fractured rock groundwater systems on a small basin scale. International Association of Hydrological Sciences Publication(241): 143-149.

Searcy, J.K., 1959. Flow-Duration Curves. US Government Printing Office.

Shanley, J.B., Peters, N.E., 1988. Preliminary observations of streamflow generation during storms in a forested Piedmont watershed using temperature as a tracer. Journal of contaminant hydrology, 3(2-4): 349-365.

Shaw, E., 1994. Hydrology in Practice. Spon Press.

Singh, J., Knapp, H.V., Arnold, J., Demissie, M., 2005. Hydrological Modeling of the Iroquois River Watershed using HSPF and SWAT. Journal of the American Water Resources Association, 41(2): 343-360.

Sklash, M., Farvolden, R., 1979. The role of groundwater in storm runoff. Contemporary hydrogeology: the George Burke Maxey memorial volume.

Sloto, R.A., Crouse, M.Y., 1996. HYSEP: A computer program for streamflow hydrograph separation and analysis. USGS Branch of Information Services, Box 25286, Denver Federal Center, Denver, CO 80225(USA).[nd].

SMHI, 2008. Integrated Hydrological Modelling System Manual

Srikanthan, R., Elliott, J., Adams, G., 1994. A review of real-time flood forecasting methods. Cooperative Research Center for Catchment Hydrology Tech. Rep, 94(2): 120.

Stonestrom, D.A., Constantz, J., 2003. Heat as a tool for studying the movement of ground water near streams. US Dept. of the Interior, US Geological Survey.

Subramanya, K., 1994. Engineering hydrology. Tata McGraw-Hill.

Sujono, J., Shikasho, S., Hiramatsu, K., 2001. Hydrograph recession analysis using wavelet transforms. Journal of the Faculty of Agriculture Kyushu University, 45(2): 557-564.

Sujono, J., Shikasho, S., Hiramatsu, K., 2004. A comparison of techniques for hydrograph recession analysis. Hydrological Processes, 18: 403-13.

Tallaksen, L.M., 1995. A review of baseflow recession analysis. Journal of Hydrology, 165(1-4): 349-370.

Taylor, A., Martin, N., Everard, E., Kelly, T., 2012. Modelling the Vale of St Albans: parameter estimation and dual storage. Geological Society, London, Special Publications, 364(1): 193-204.

Tingsanchali, T., Gautam, M.R., 2000. Application of tank, NAM, ARMA and neural network models to flood forecasting. Hydrological Processes, 14(14): 2473-2487.

Toebes, C., Strang, D., 1964. On recession curves. J. Hydrol.(NZ), 3: 2-14.

Trefry, M.G., Muffels, C., 2007. FEFLOW: A Finite-Element Ground Water Flow and Transport Modeling Tool. Ground Water, 45(5): 525-528.

Uhlenbrook, S., Hoeg, S., 2003. Quantifying uncertainties in tracer-based hydrograph separations: a case study for two-, three- and five-component hydrograph separations in a mountainous catchment. Hydrological Processes, 17(2): 431-453.

Walsh, P., 2011. Investigation of point recharge, flow and nutrient levels in a lowland karst system in the South-East of Ireland. Unpublished MSc Environmental Engineering Thesis, Trinity College Dublin.

Wentz, F.J., Ricciardulli, L., Hilburn, K., Mears, C., 2007. How much more rain will global warming bring? Science, 317(5835): 233-235.

WFD, 2000. Directive 2000/60. EC of the European Parliament and of the Council of, 23: 1.

Wicks, J., Bathurst, J., Johnson, C., 1992. Calibrating SHE soil-erosion model for different land covers. Journal of irrigation and drainage engineering, 118(5): 708-723.

WMO, 1992. Simulated real-time intercomparison of hydrological models. Operational Hydrology Report 38, World Meteorological Organization, Geneva.

Wood, A., 1942. The development of hillside slopes. Proceedings of the Geologists' Association, 53(3-4): 128-140, IN1-IN3.

Working Group on Groundwater, 2005. The characterisation and analysis of Ireland's river basin districts in accordance with section 7 (2&3) of the European communities (water policy) regulations 2003 (SI 722 of 2003).

Xiuwan, C.J.C., 2004. Water Balance of the SWAT Model and Its Application in the Suomo Basin [J]. Acta Scicentiarum Naturalum Universitis Pekinesis, 2: 015.

Yang, Y., McGeough, K., Kalin, R., Dickson, K., 2003. Numerical modeling for remediation of contaminated land and groundwater. Bulletin of Environmental Contamination and Toxicology, 71(4): 729-736.

Youhao, E., Zhaodong, F., Jihe, W., Yaolin, W., Zihui, Y., 2004. GIS-assisted FEFLOW modeling of groundwater moving processes within the Minqin Oasis

in the lower reach of the Shiyang River, Northwest China, Geoscience and Remote Sensing Symposium, pp. 4614-4617.

Zhang, X., Lindström, G., 1997. Development of an automatic calibration scheme for the HBV hydrological model. Hydrological Processes, 11(12): 1671-1682.

APPENDIX A – Supplementary Catchments

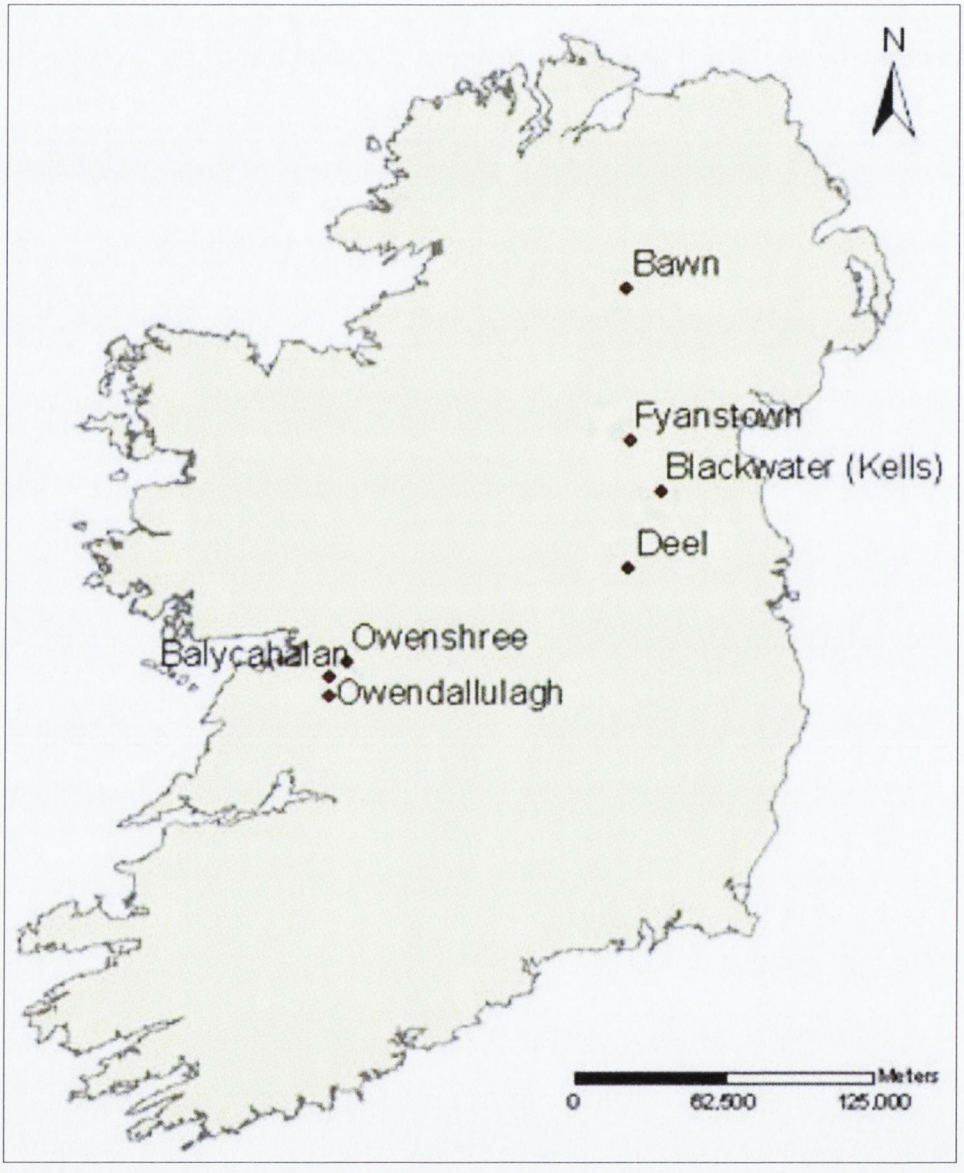

Figure A-1. Locations of supplementary catchments.

Table A.1. Supplementary catchment characteristics.

	Catchment Descriptors					
	Area	Land-use	Aquifer Classification	Annual Rainfall	Actual Evapotranspiration	Net Rainfall
	km^2	Type (%)	Type (%)	mm	mm	mm
Bawn	4.9	Pasture (100)	Pl (100)	1039	447	592
Owenshree	34.5	Pasture (41.1) Peat (27.9)	Pl (75.7)	1528	524	1004
Ballycahalan	47.7	Forest (37.5) Peat (31.6)	Pl (85)	1542	531	1011
Owendallulagh	89.3	Pasture (49.6) Forest (31.1)	Pl (92.3)	1568	540	1028
Fyanstown	187.6	Pasture (86.5)	Ll (34.7) Pl (59.7)	1020	476	544
Deel	283.1	Pasture (78.6)	Ll (88.1)	973	481	492
Blackwater (Kells)	699	Pasture (80.1)	Pl (74.1)	1026	491	535

APPENDIX B – Supplementary Physical Separations

Table B.1. Summary of the results of physical hydrograph separation approaches.

Catchment	Area (km^2)	Deep Groundwater		Shallow Groundwater		Groundwater	Interflow		Overland		Quick Flow
		MRC %	Mod Lyne %	MRC %	Mod Lyne %	Recharge Coeff %	MRC %	Mod Lyne %	MRC %	Mod Lyne %	Recharge Coeff %
Bawn	**4.9**	12.7	7.8	11	7.3		36.3	46.6	40	38.3	
Owenshree	**34.5**	12.3	7	8.3	6.8	14.2	42.1	48.9	37.3	37.3	85.8
Ballycahalan	**47.7**	10.3	5.4	7.1	5.6	11.7	33.9	42.7	48.7	46.3	88.3
Owendullalagh	**89.3**	16.1	8.1			8.1	27.4	50.2	56.5	41.7	91.9
Fyanstown	**187.6**	15.3	7.6	4.9	7	21.5	42.3	48.1	37.5	37.3	78.5
Deel	**283.1**	28.9	6	12.1	6.2	28.7	32.9	53.1	26.1	34.7	71.3
Blackwater (Kells)	**699**	18.2	8	10.5	7.3	19.7	42.5	48	28.8	36.7	80.3

Recharge Coefficients Approach

Bawn

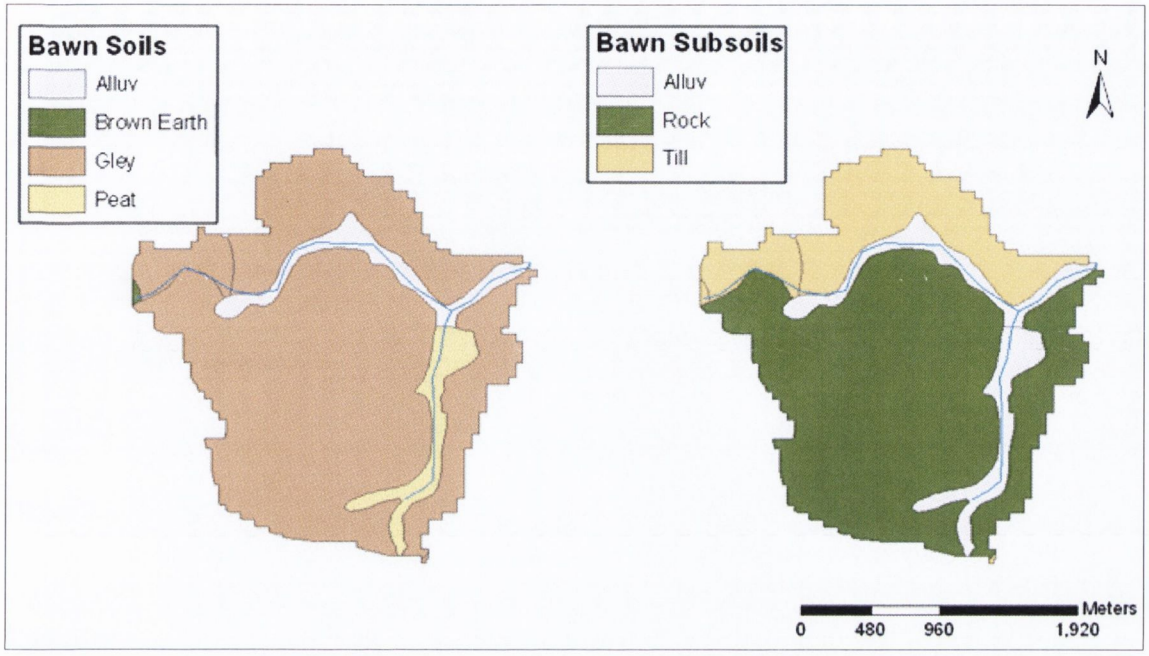

Figure B.1. Bawn soils and subsoils mapping.

Owenshree

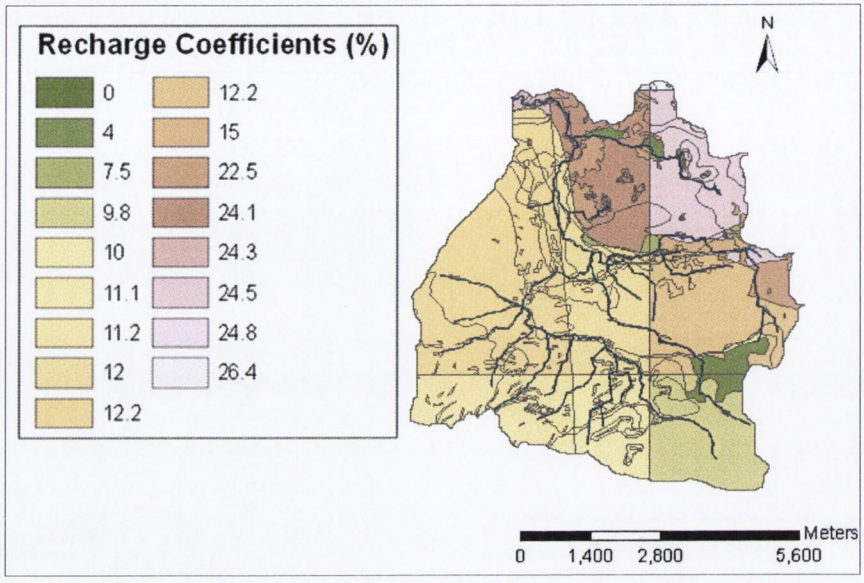

Figure B.2. Owenshree recharge coefficient mapping.

Ballycahalan

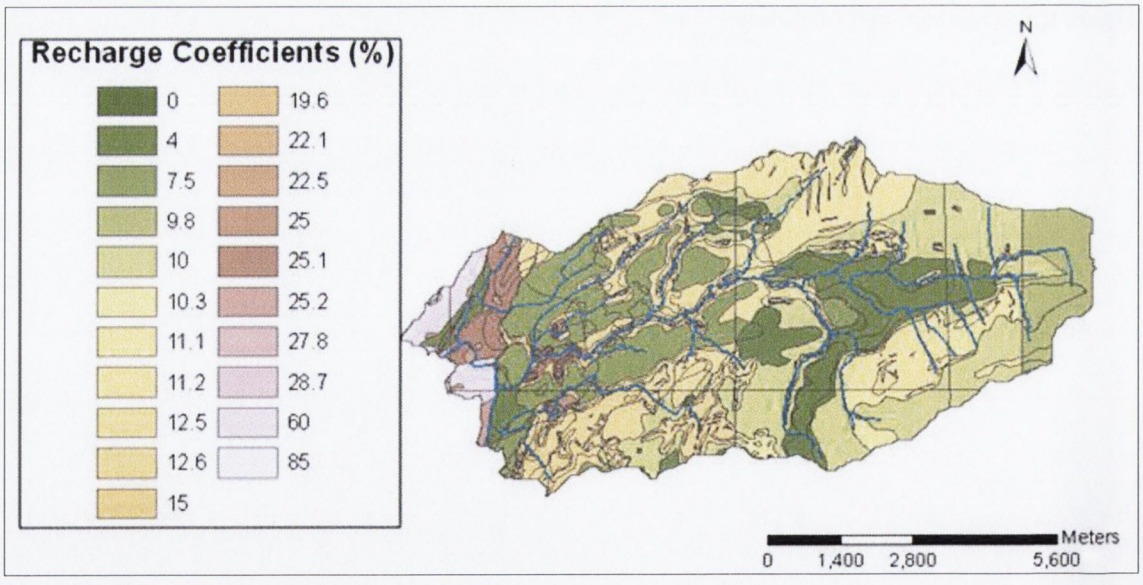

Figure B.3. Ballycahalan recharge coefficient mapping.

Owendullalagh

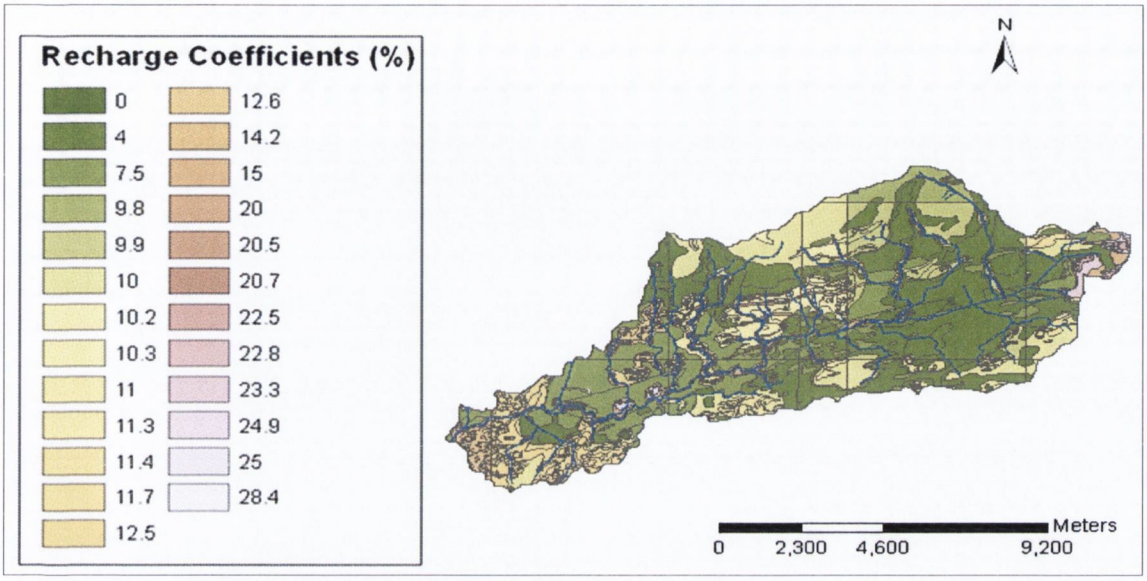

Figure B.4. Owendullalagh recharge coefficient mapping.

Fyanstown

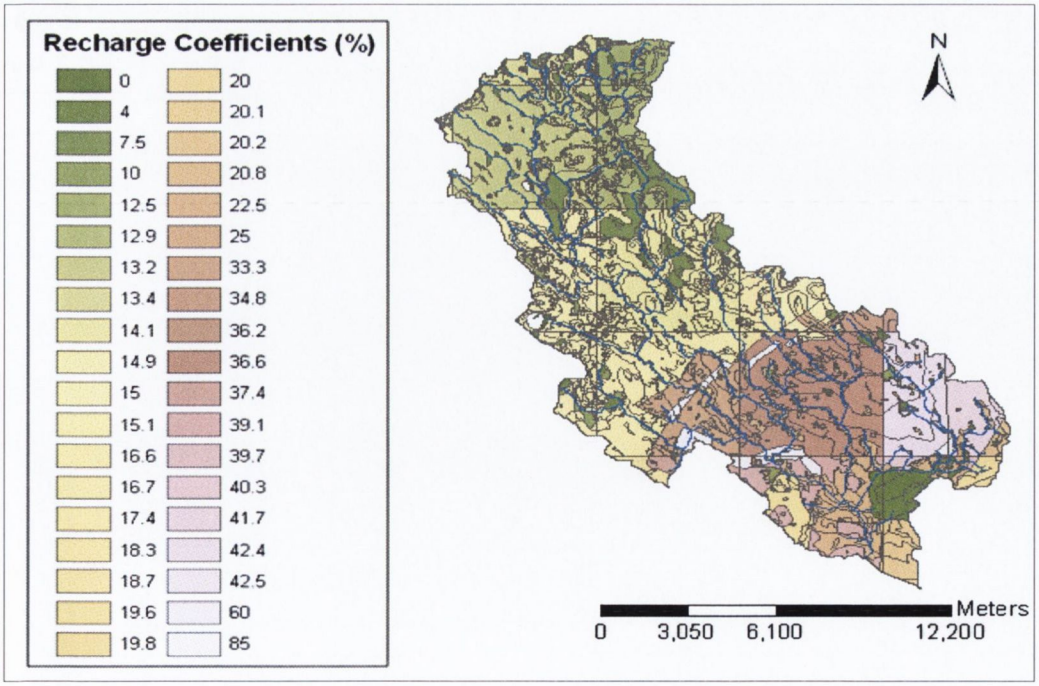

Figure B.5. Fyanstown recharge coefficient mapping.

Deel

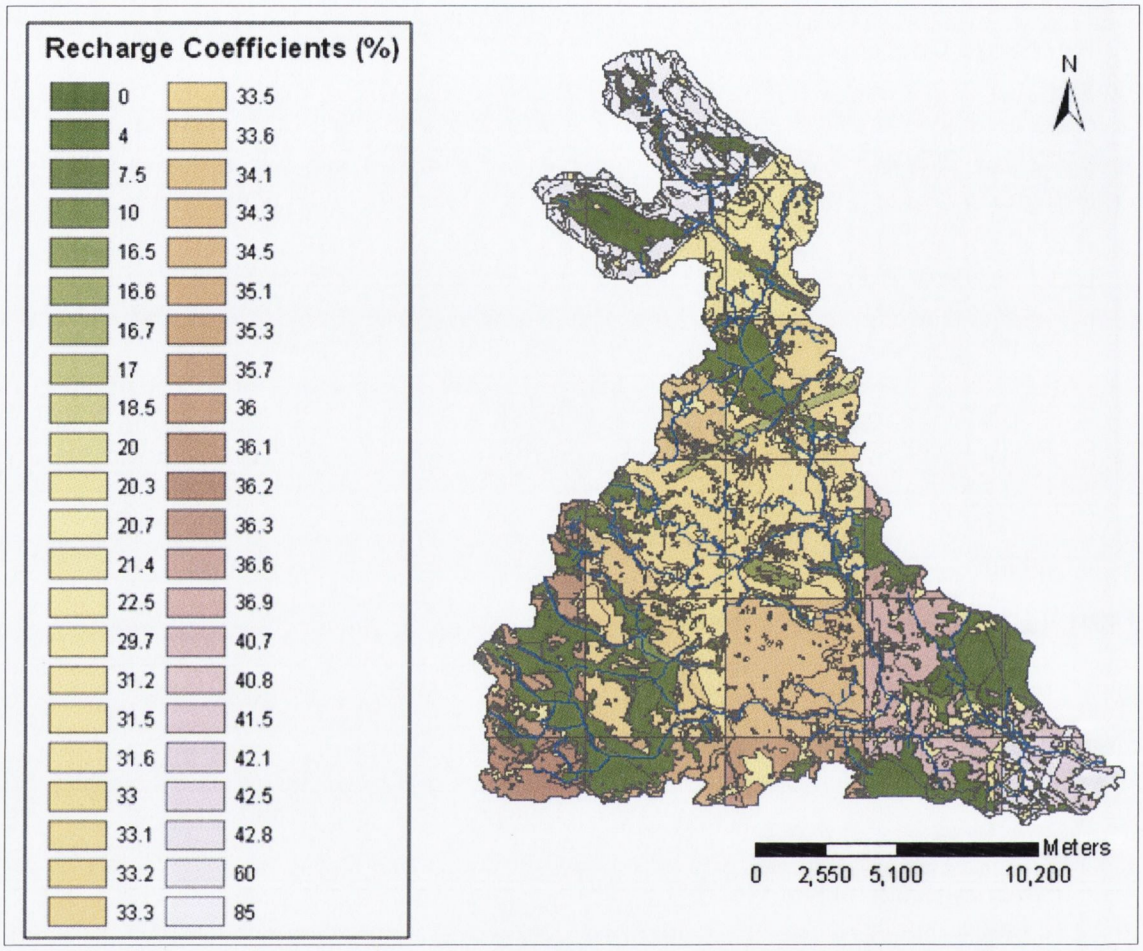

Figure B.6. Deel recharge coefficient mapping.

Blackwater

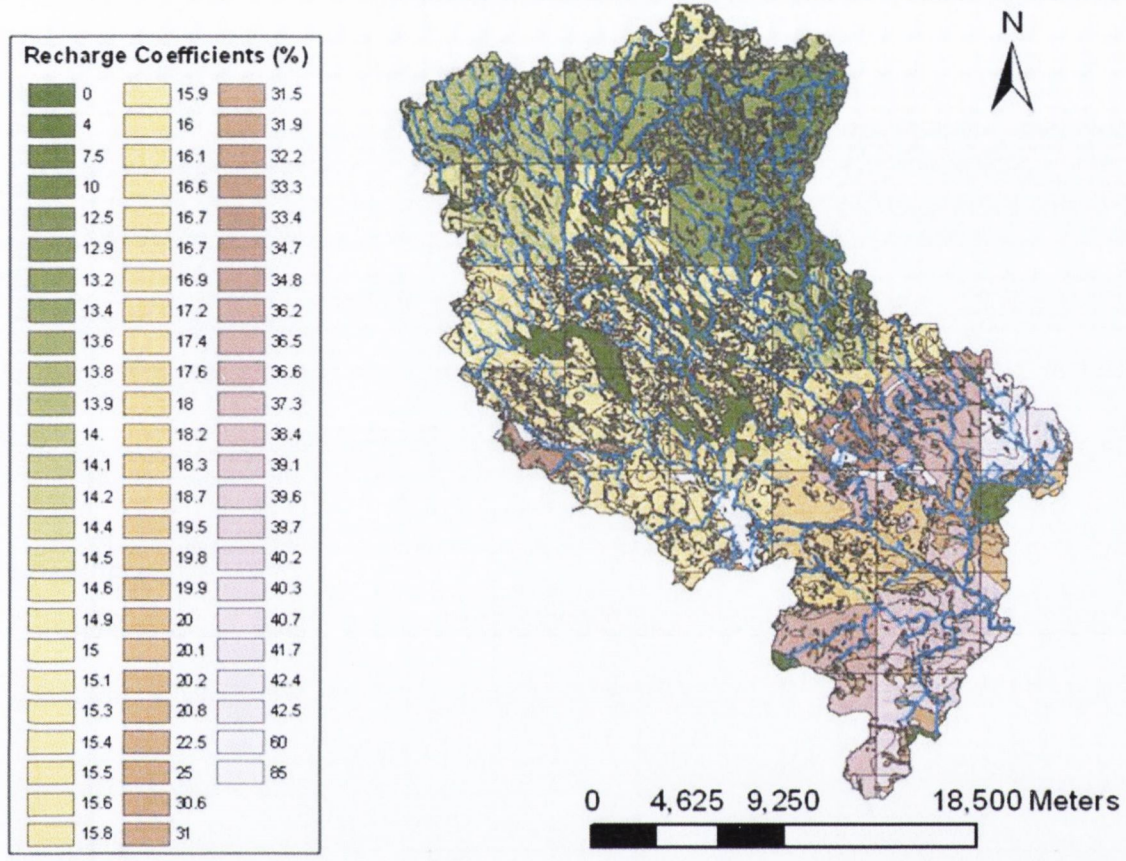

Figure B.7. Blackwater (Kells) recharge coefficient mapping.

Master Recession Curve Analysis

Bawn

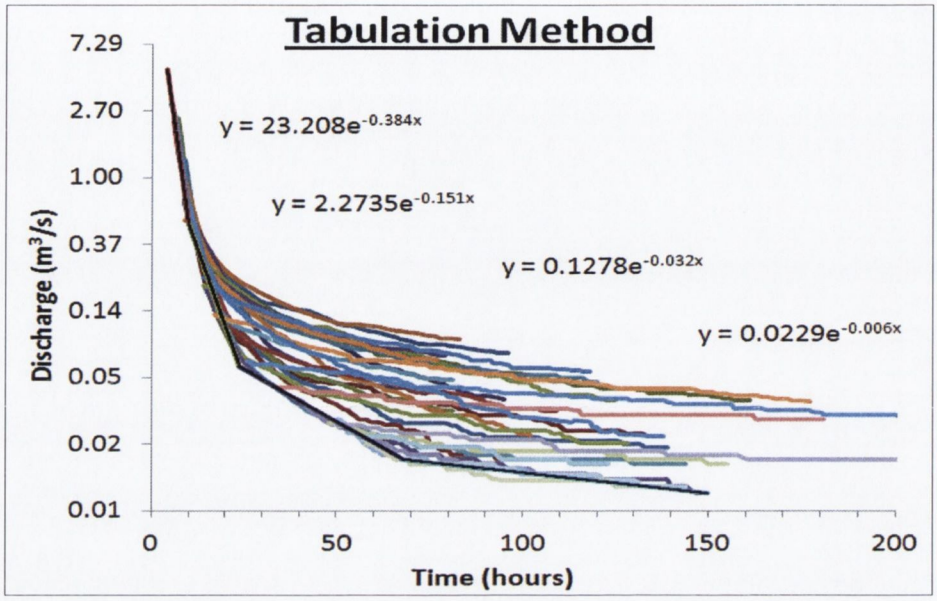

Figure B.8. Bawn master recession curve, tabulation method.

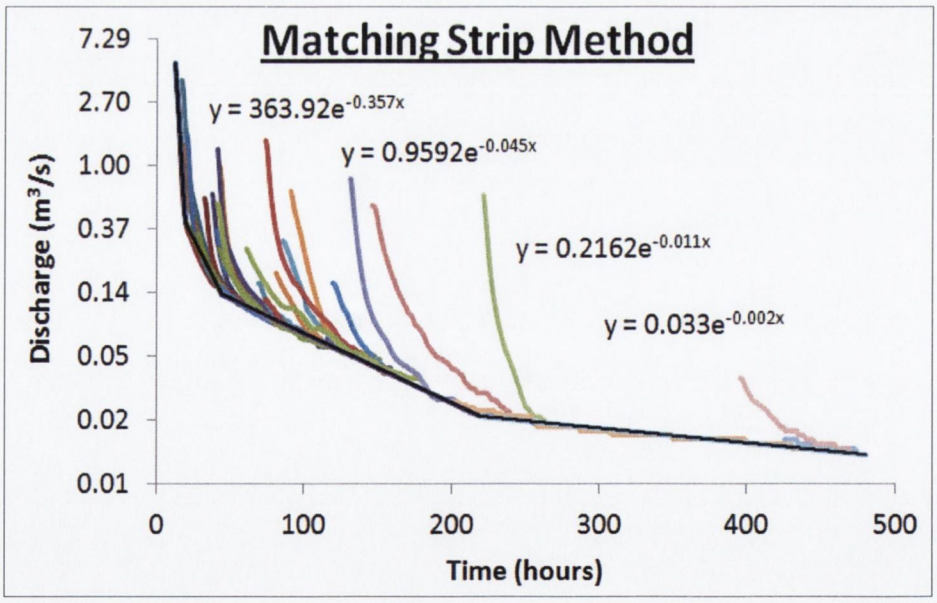

Figure B.9. Bawn master recession curve, matching strip method.

Owenshree

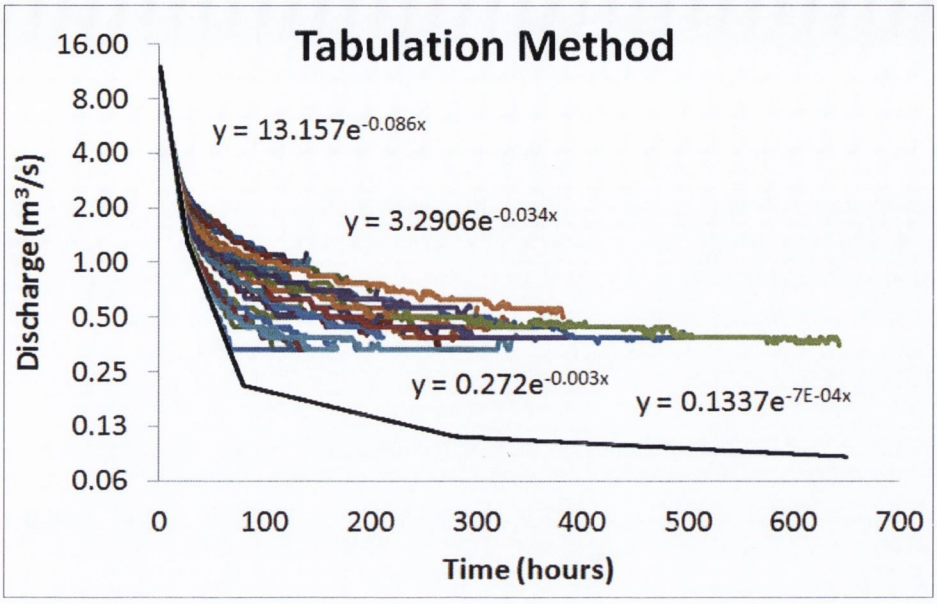

Figure B.10. Owenshree master recession curve, tabulation method.

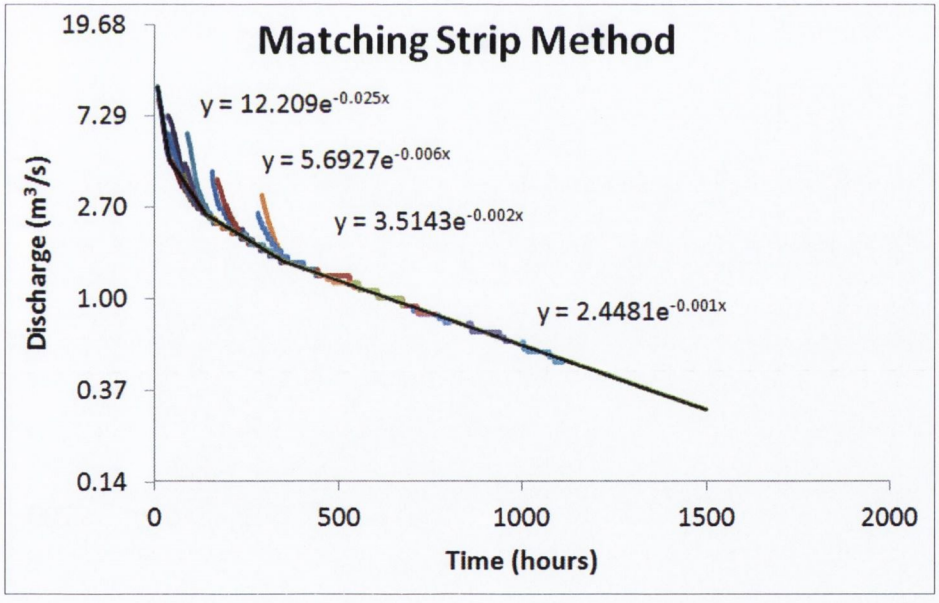

Figure B.11. Owenshree master recession curve, matching strip method.

Ballycahalan

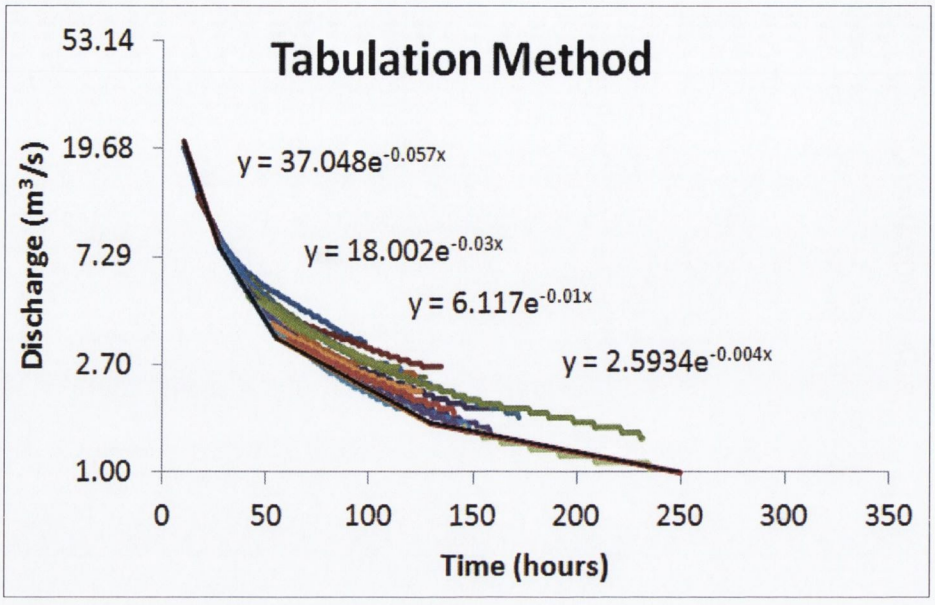

Figure B.12. Ballycahalan master recession curve, tabulation method.

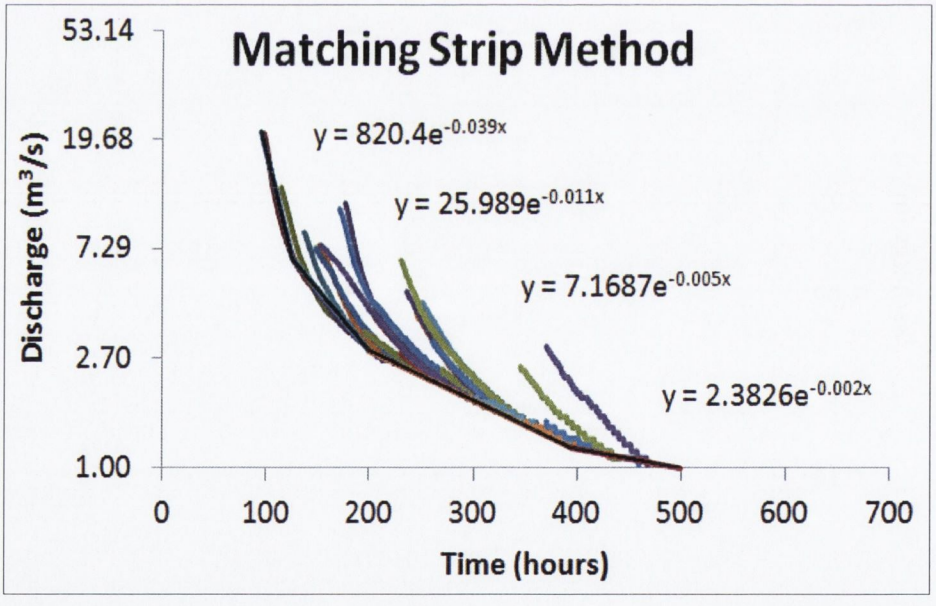

Figure B.13. Ballycahalan master recession curve, matching strip method.

Owendullalagh

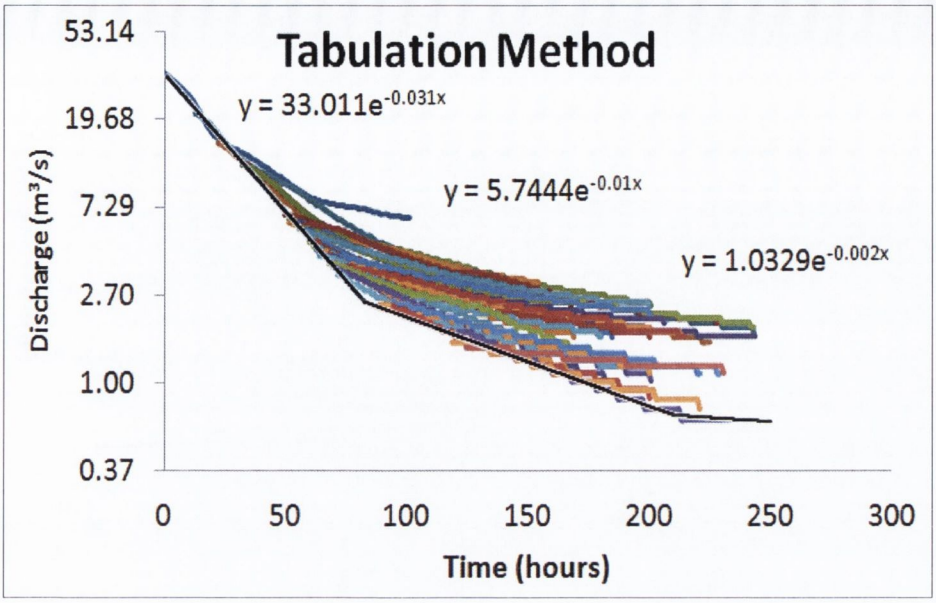

Figure B.14. Owendullalagh master recession curve, tabulation method.

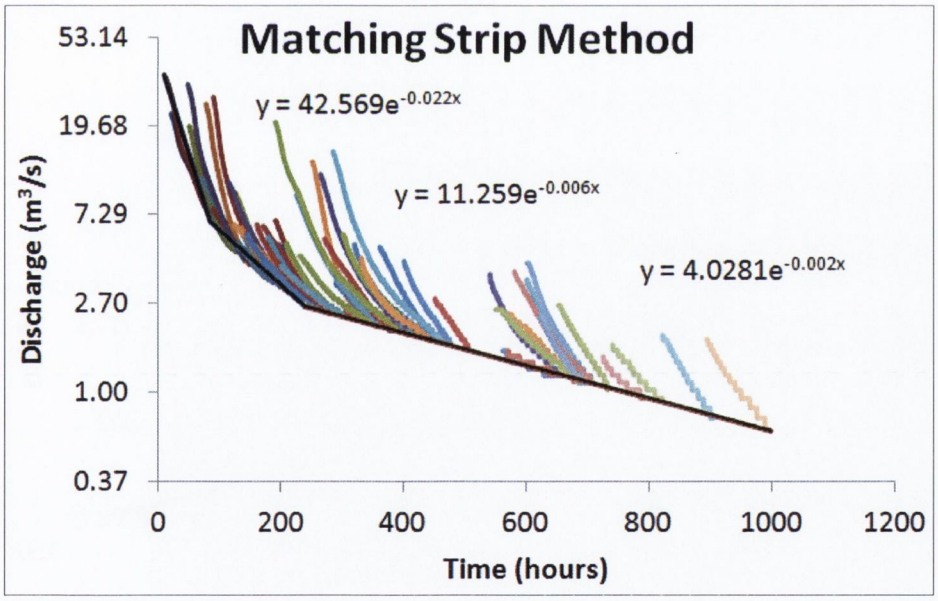

Figure B.15. Owendullalagh master recession curve, matching strip method.

Fyanstown

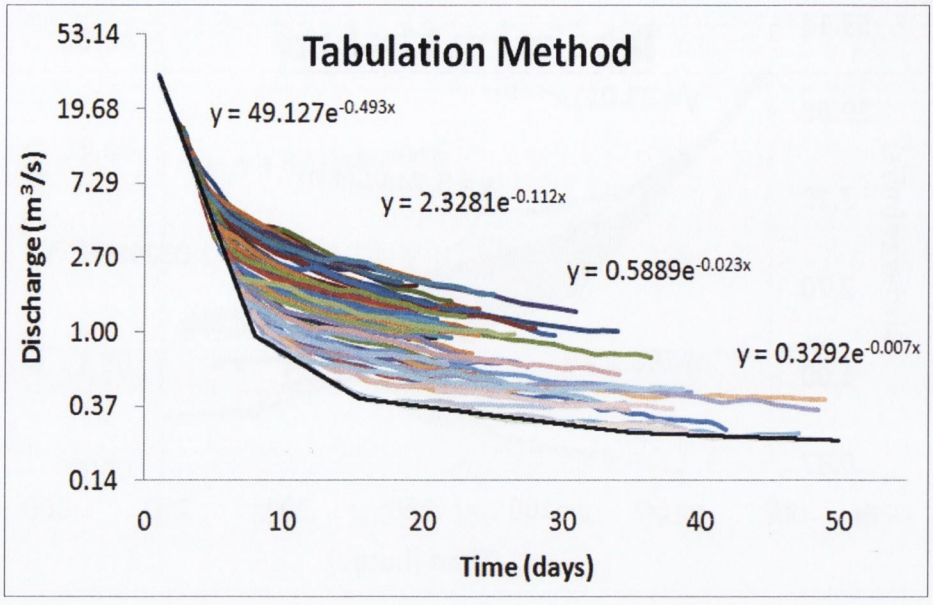

Figure B.16.Fyanstown master recession curve, tabulation method.

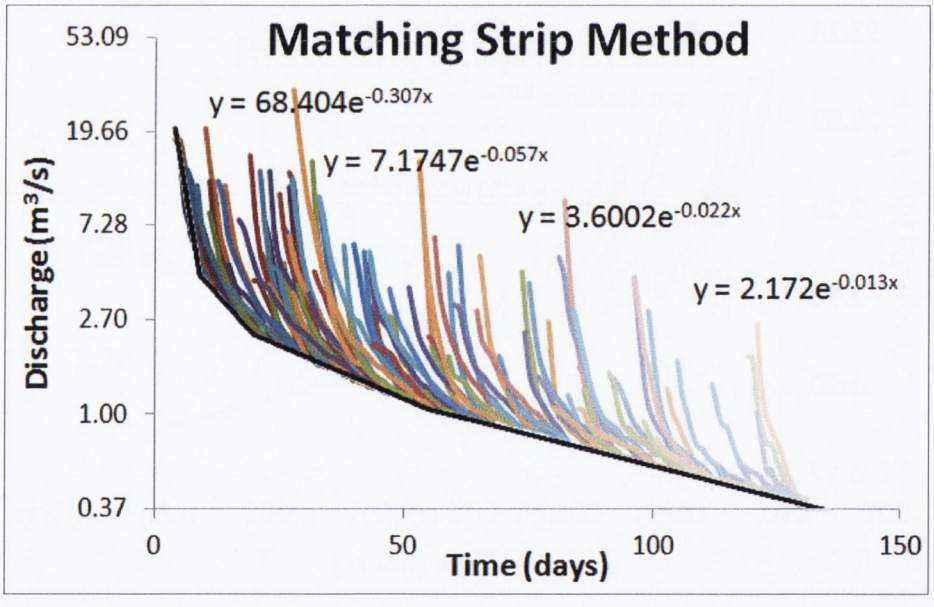

Figure B.17. Fyanstown master recession curve, matching strip method.

Deel

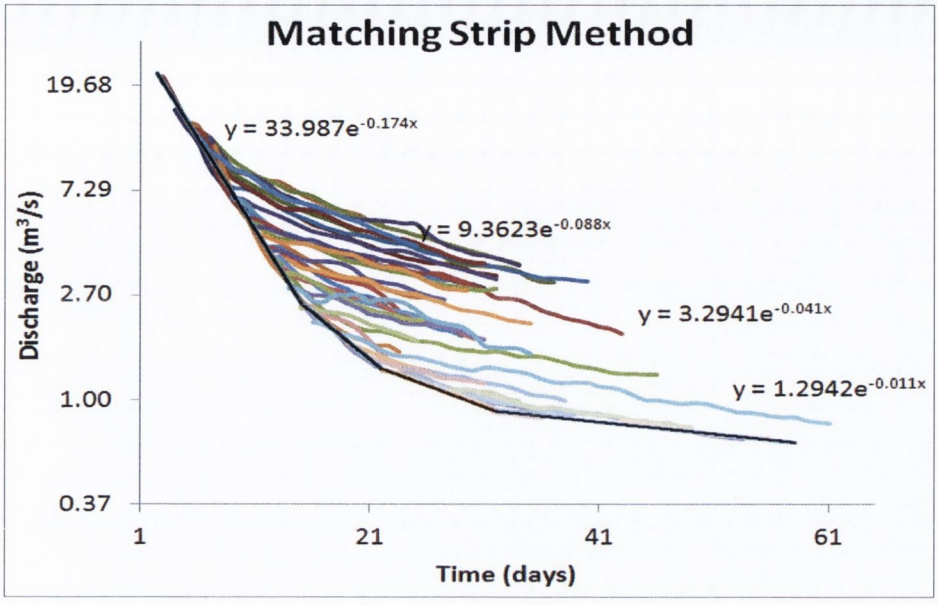

Figure B.18. Deel master recession curve, tabulation method.

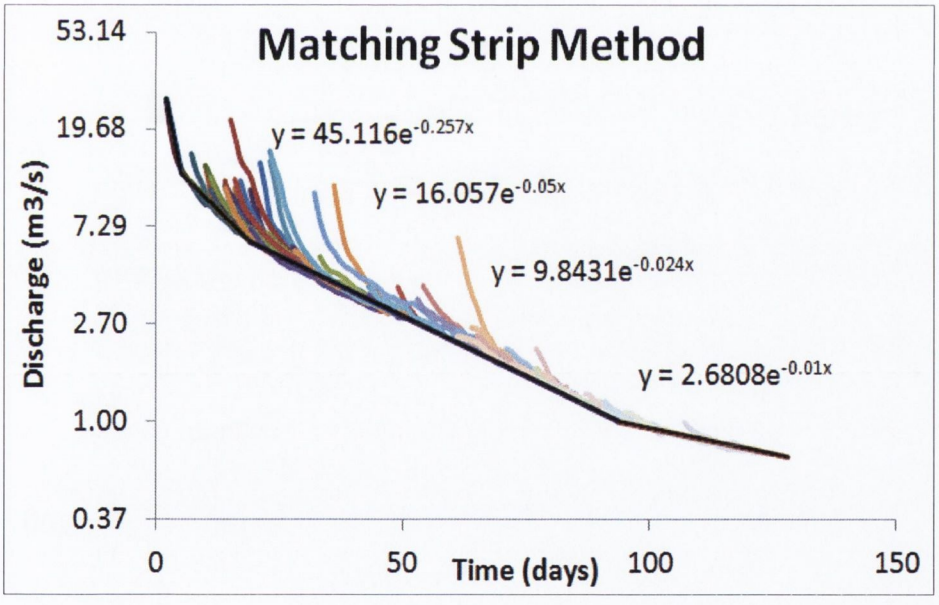

Figure B.19. Deel master recession curve, matching strip method.

Blackwater (Kells)

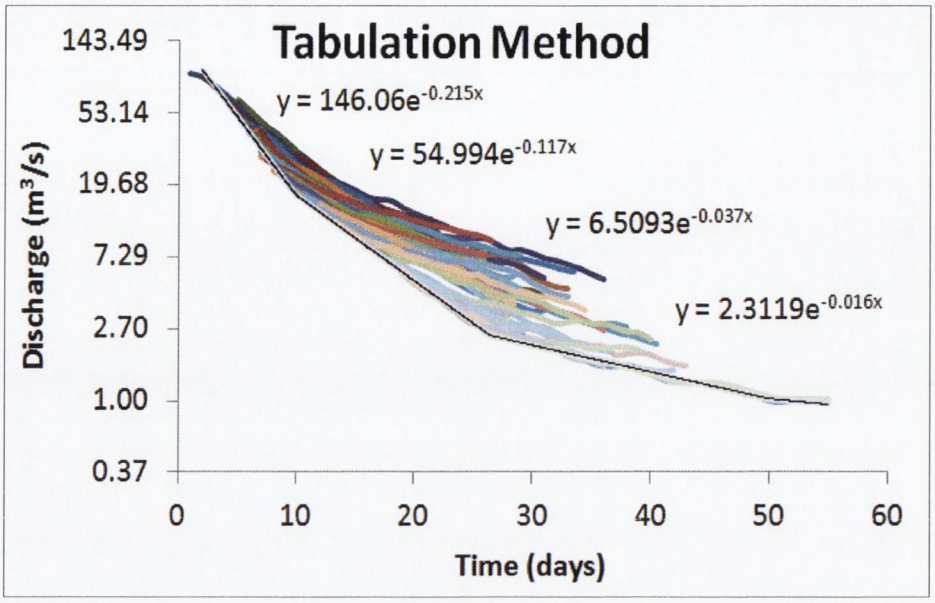

Figure B.20. Blackwater (Kells) master recession curve, tabulation method.

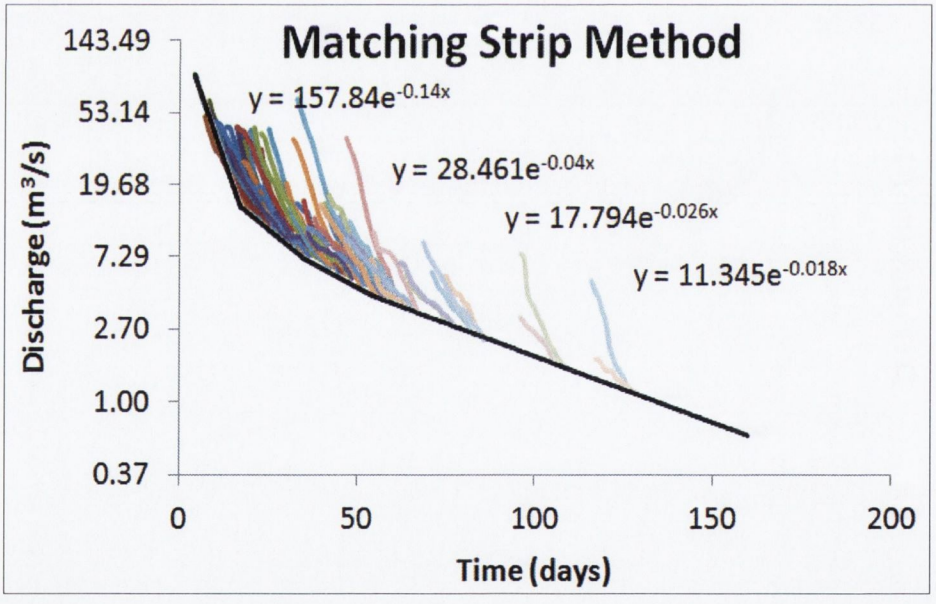

Figure B.21. Blackwater (Kells) master recession curve, matching strip method.

Modified Digital Filter Algorithm

Bawn

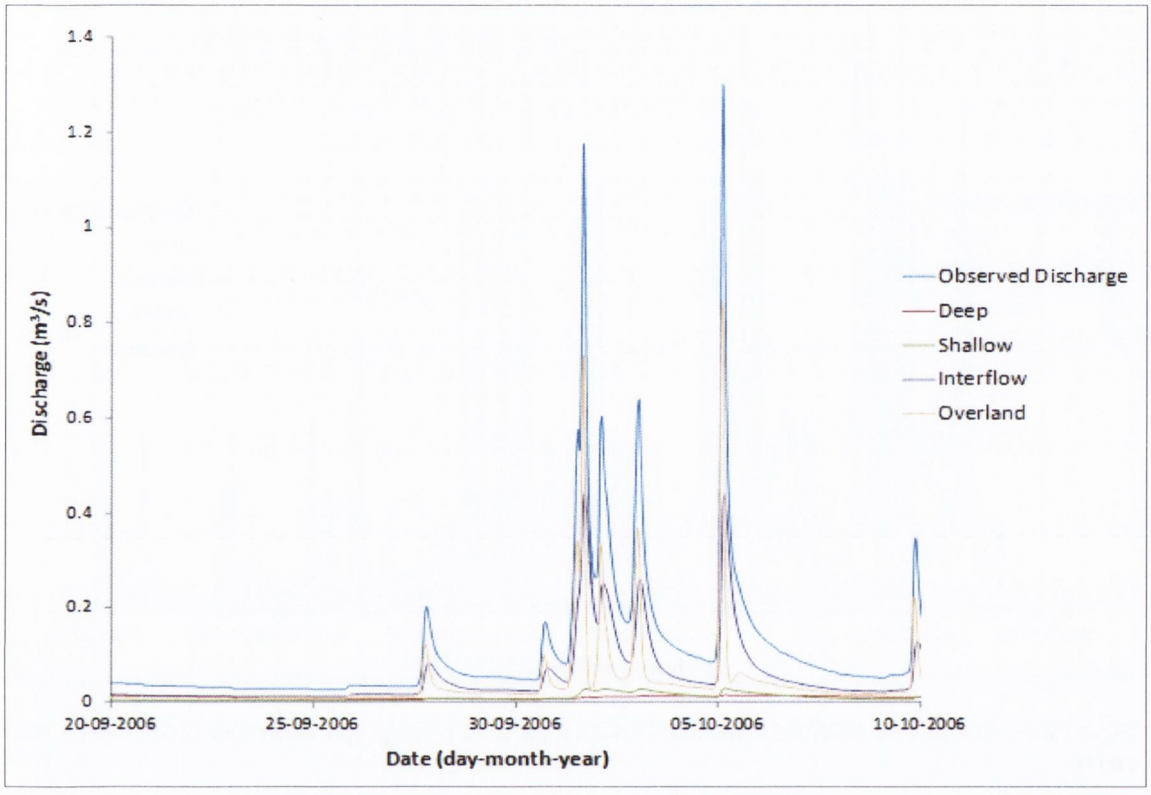

Figure B.22. Bawn modified Lyne and Hollick algorithm hydrograph separations (Sept 2006 – Oct 2006).

Owendullalagh

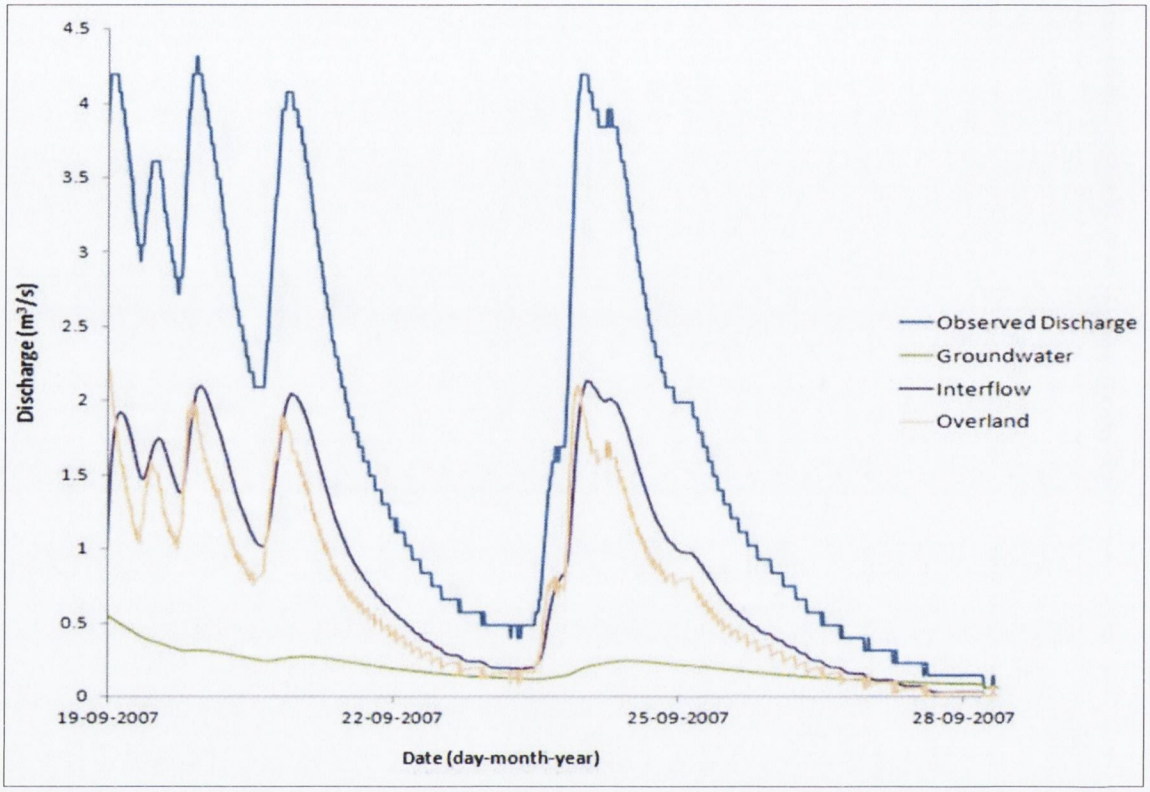

Figure B.25. Owendullalagh modified Lyne and Hollick algorithm hydrograph separations (Sept 2007 – Sept 2007).

Fyanstown

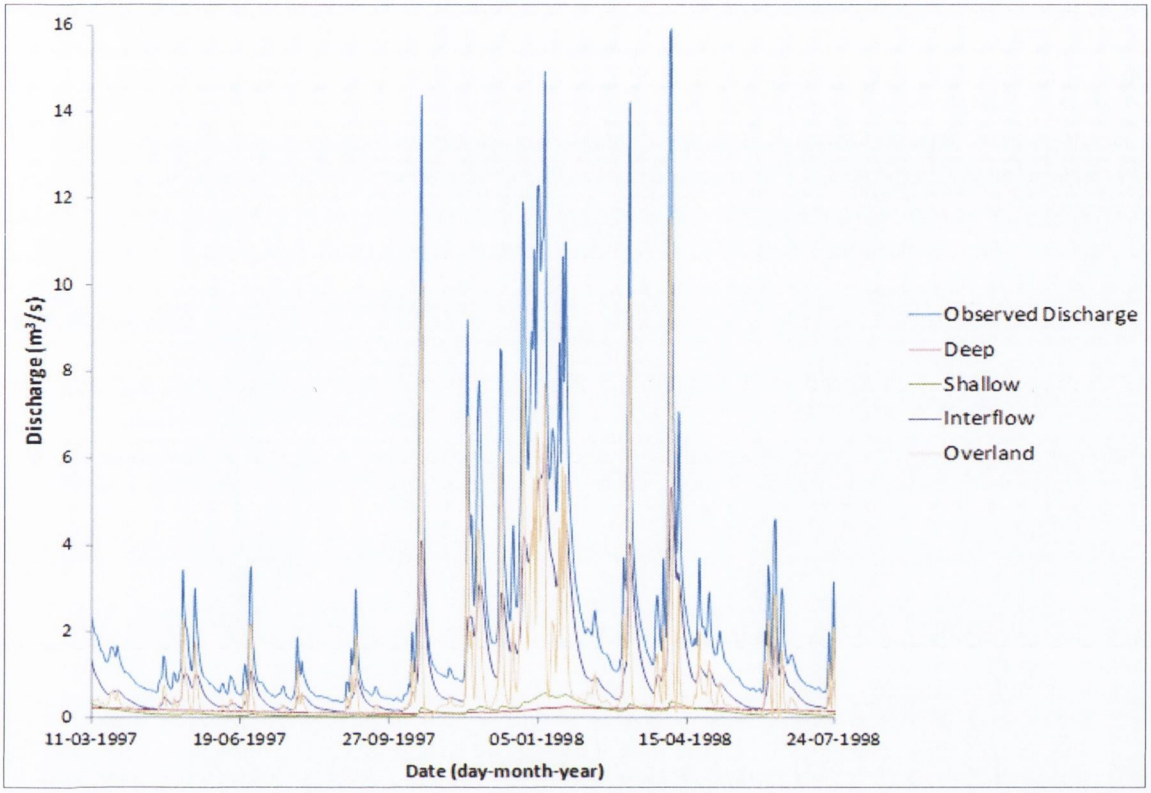

Figure B.26. Fyanstown modified Lyne and Hollick algorithm hydrograph separations (Mar 1997 – July 1998).

Deel

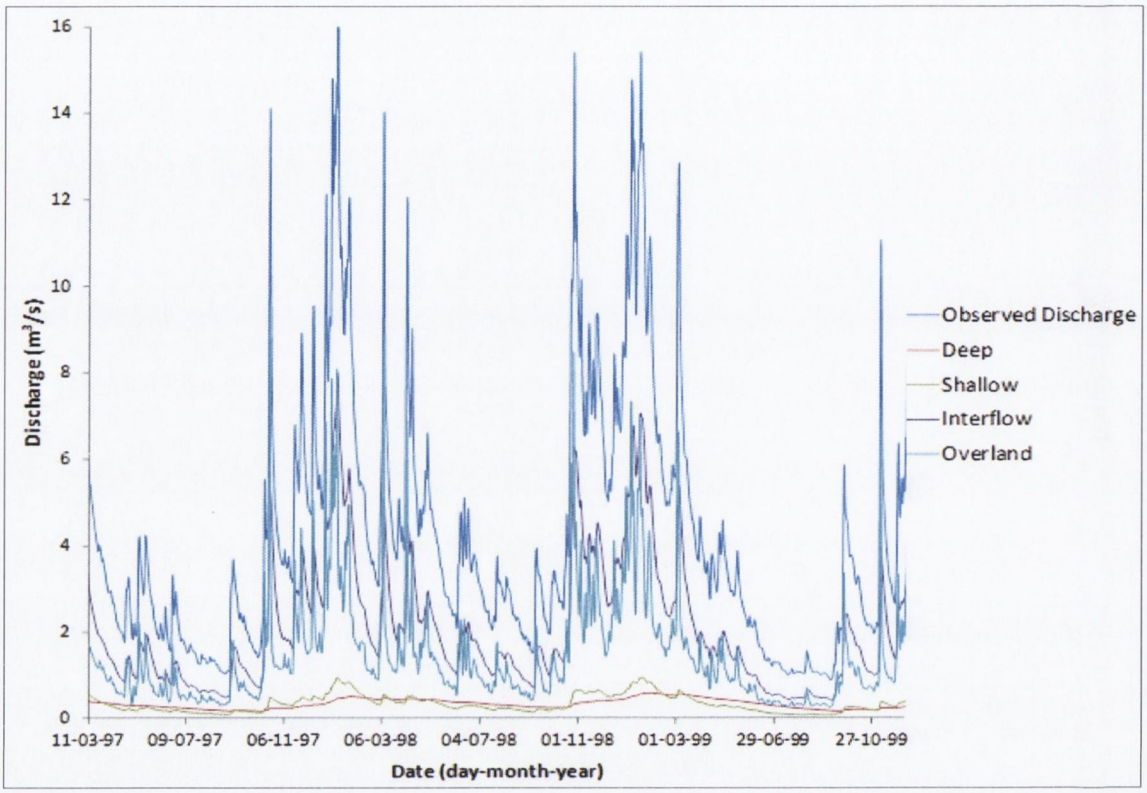

Figure B.27. Deel modified Lyne and Hollick algorithm hydrograph separations (Mar 1997 – Oct 1999).

Blackwater (Kells)

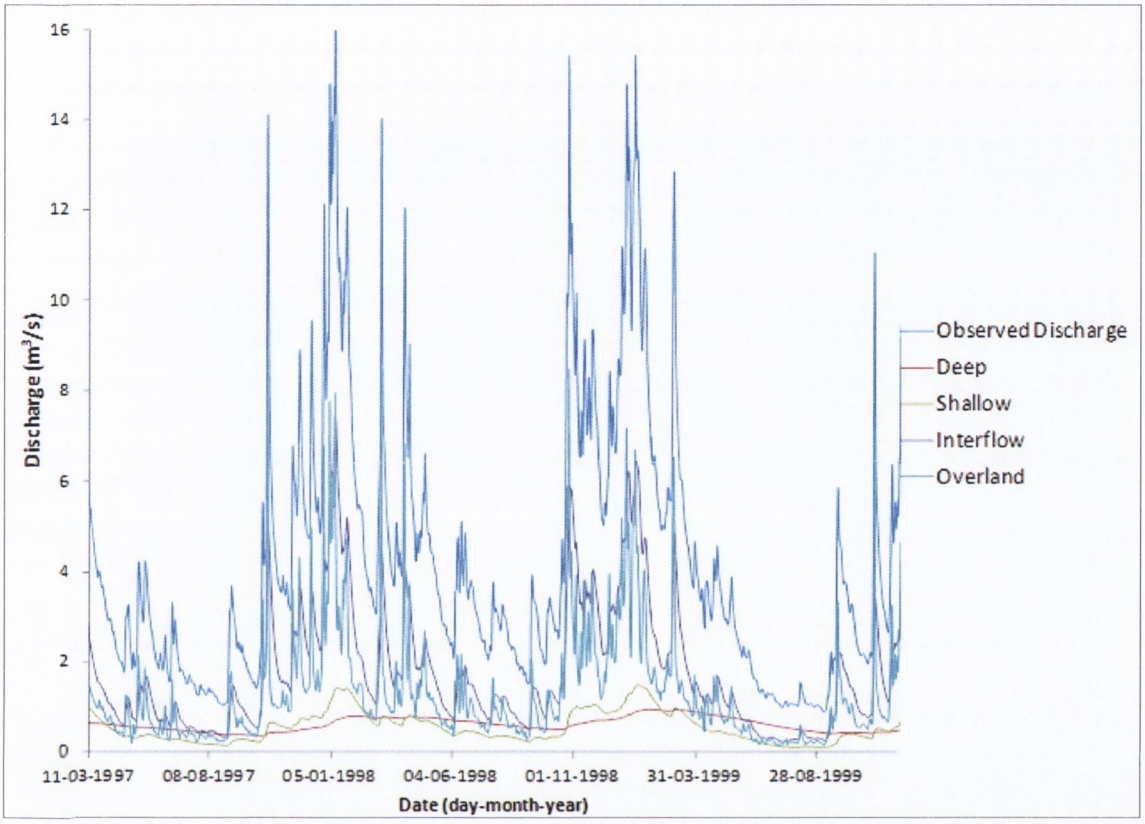

Figure B.28. Blackwater (Kells) modified Lyne and Hollick algorithm hydrograph separations (Mar 1997 – Apr 2001).

APPENDIX C – Supplementary NAM Modelling

Table C.1. Results of NAM modelling for supplementary catchments.

Catchment	Area (km^2)	Deep Groundwater	Shallow Groundwater	Interflow	Overland	R^2	$\sqrt{R^2}$	Bias
		%	%	%	%			
Bawn	4.9	6	2.7	36.3	55	0.87	0.89	0.0430
Owenshree	34.5	13.6		42.7	43.7	0.85	0.83	0.0250
Ballycahalan	47.7	7.1		24.6	68.3	0.9	0.91	-0.0600
Owendullalagh	89.3	9.9		28.2	61.9	0.89	0.86	-0.3400
Fyanstown	187.6	15.6	5.1	43.9	35.4	0.83	0.87	-0.2700
Deel	283.1	29.7	14.7	26.8	28.7	0.9	0.94	0.3500
Blackwater (Kells)	699	8.6	6.7	50.8	33.8	0.92	0.91	-0.5000

Bawn

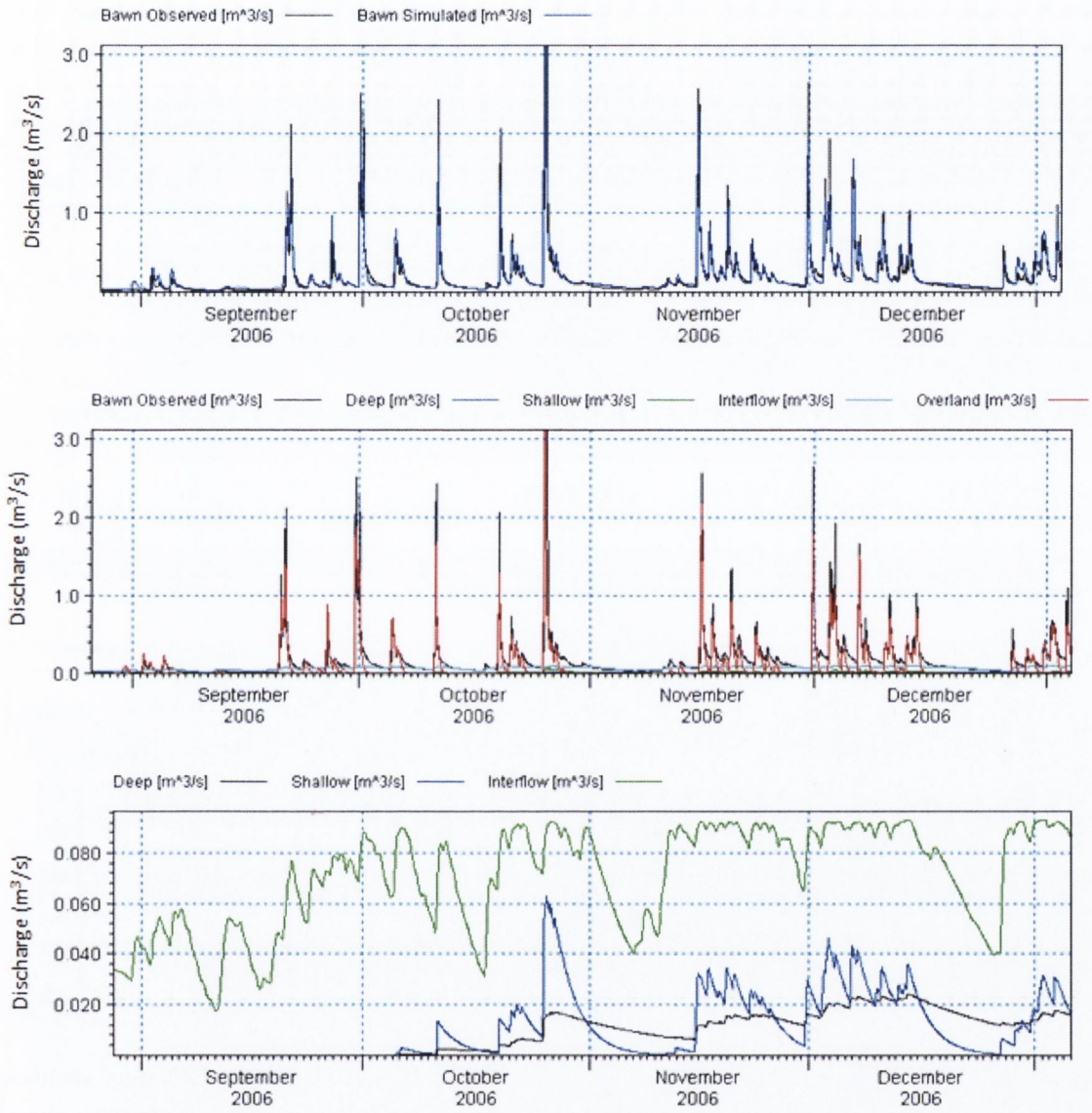

Figure C.1 Bawn catchment showing observed discharge with simulated discharge; simulated pathway flows with observed discharge; and simulated subsurface pathway flows (Aug 2006 – Jan 2007).

Owenshree

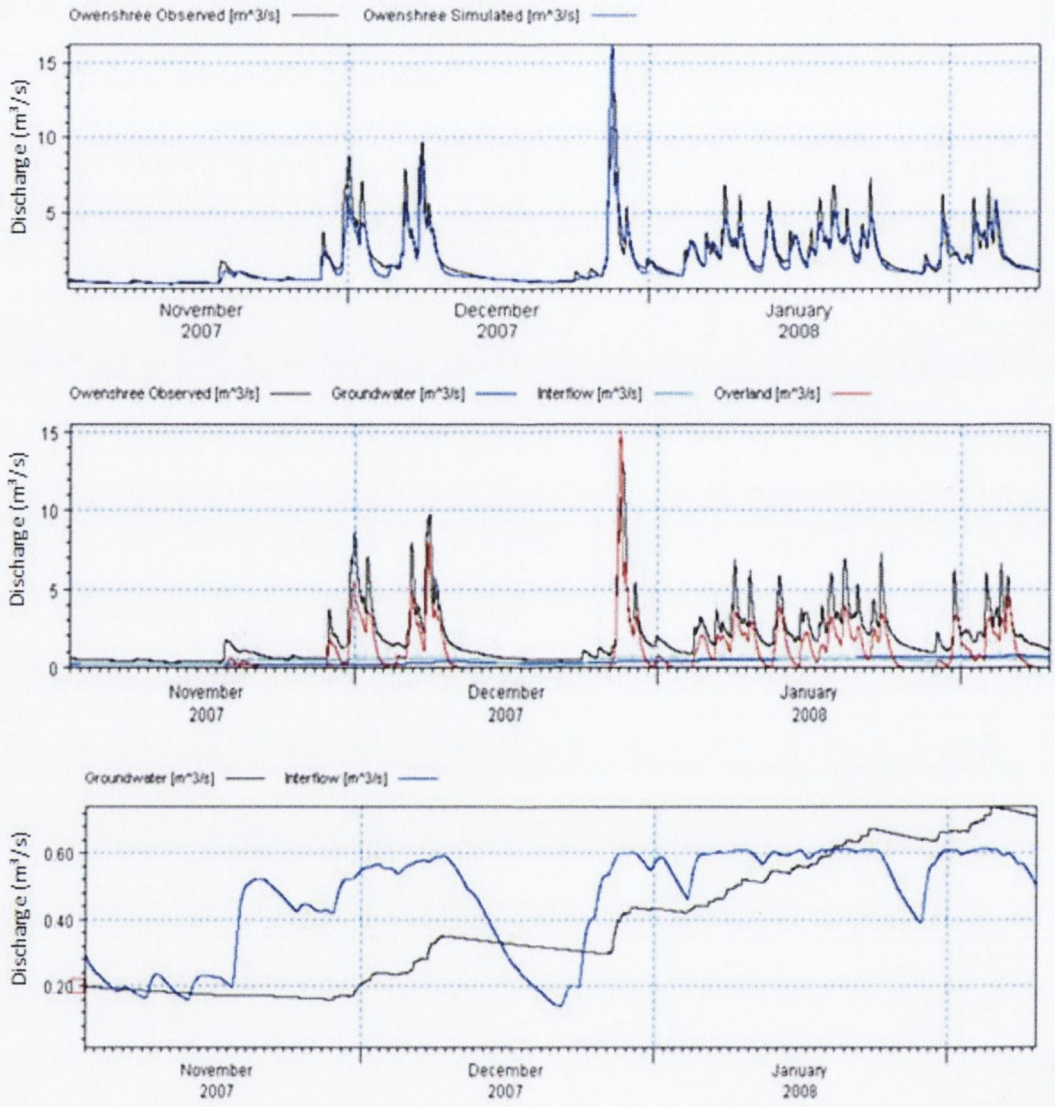

Figure C.2 Owenshree catchment showing observed discharge with simulated discharge; simulated pathway flows with observed discharge; and simulated subsurface pathway flows (Nov 2007 – Feb 2008).

Ballycahalan

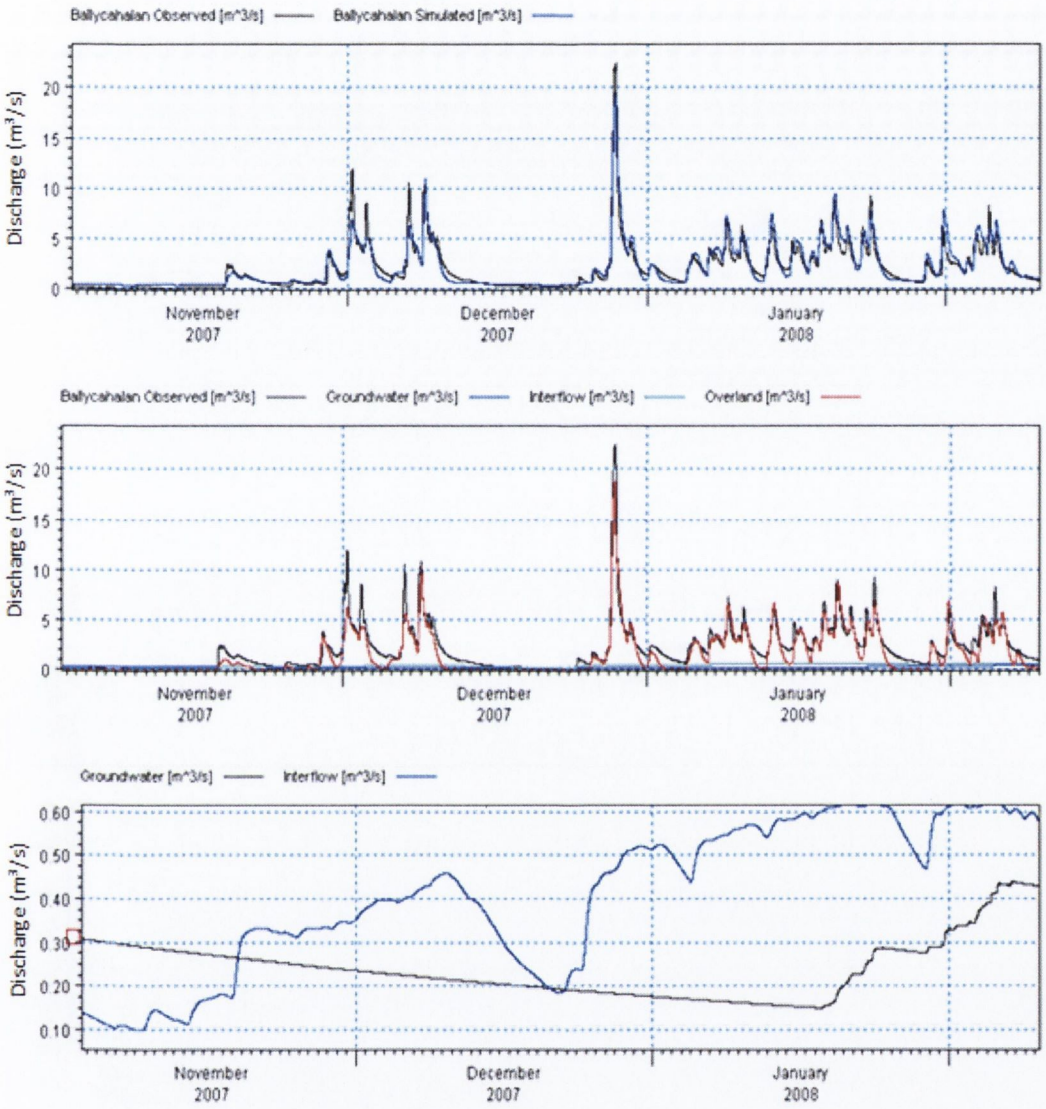

Figure C.3 Ballycahalan catchment showing observed discharge with simulated discharge; simulated pathway flows with observed discharge; and simulated subsurface pathway flows (Nov 2007 – Feb 2008).

Owendullalagh

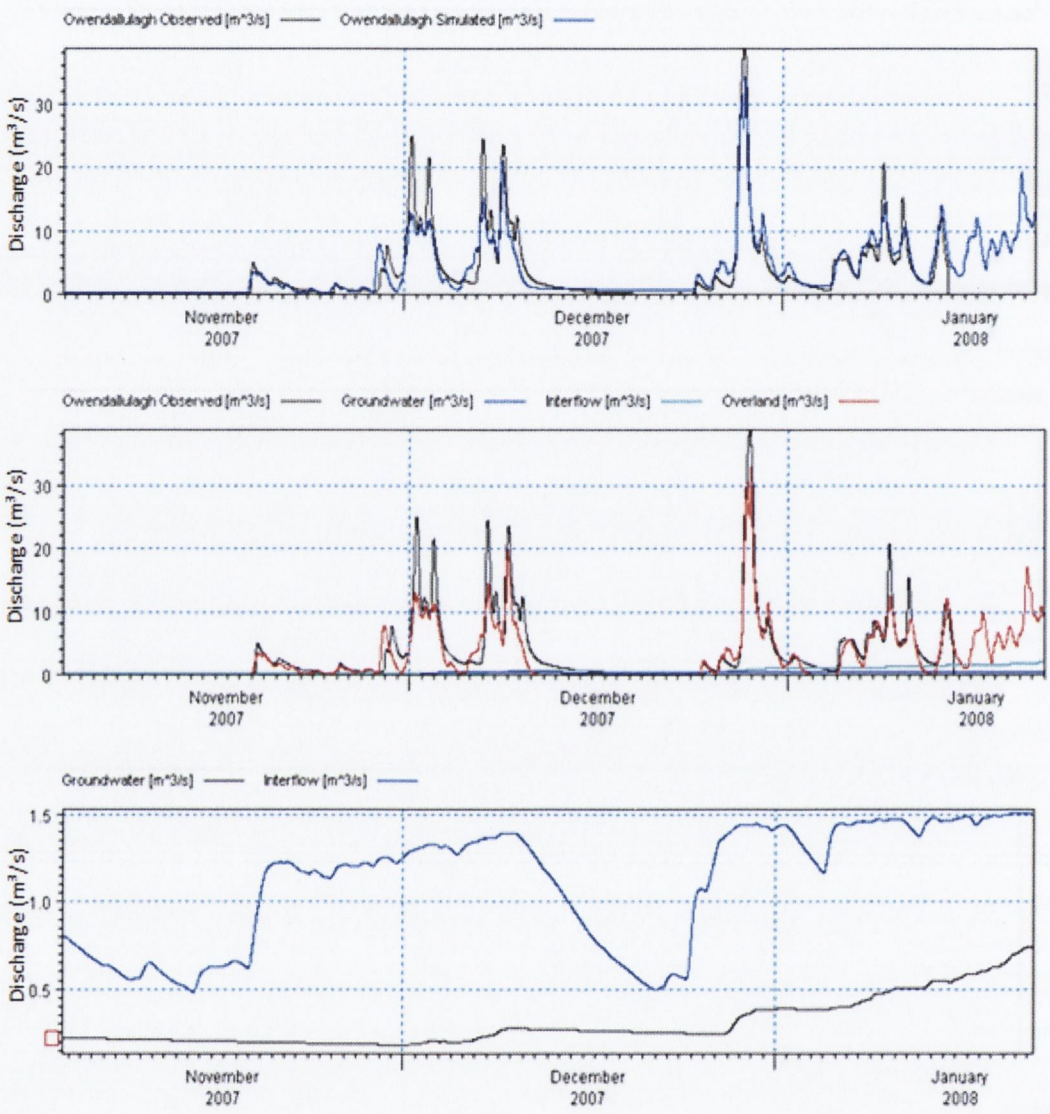

Figure C.4 Owendullalagh catchment showing observed discharge with simulated discharge; simulated pathway flows with observed discharge; and simulated subsurface pathway flows (Nov 2007 – Jan 2008).

Fyanstown

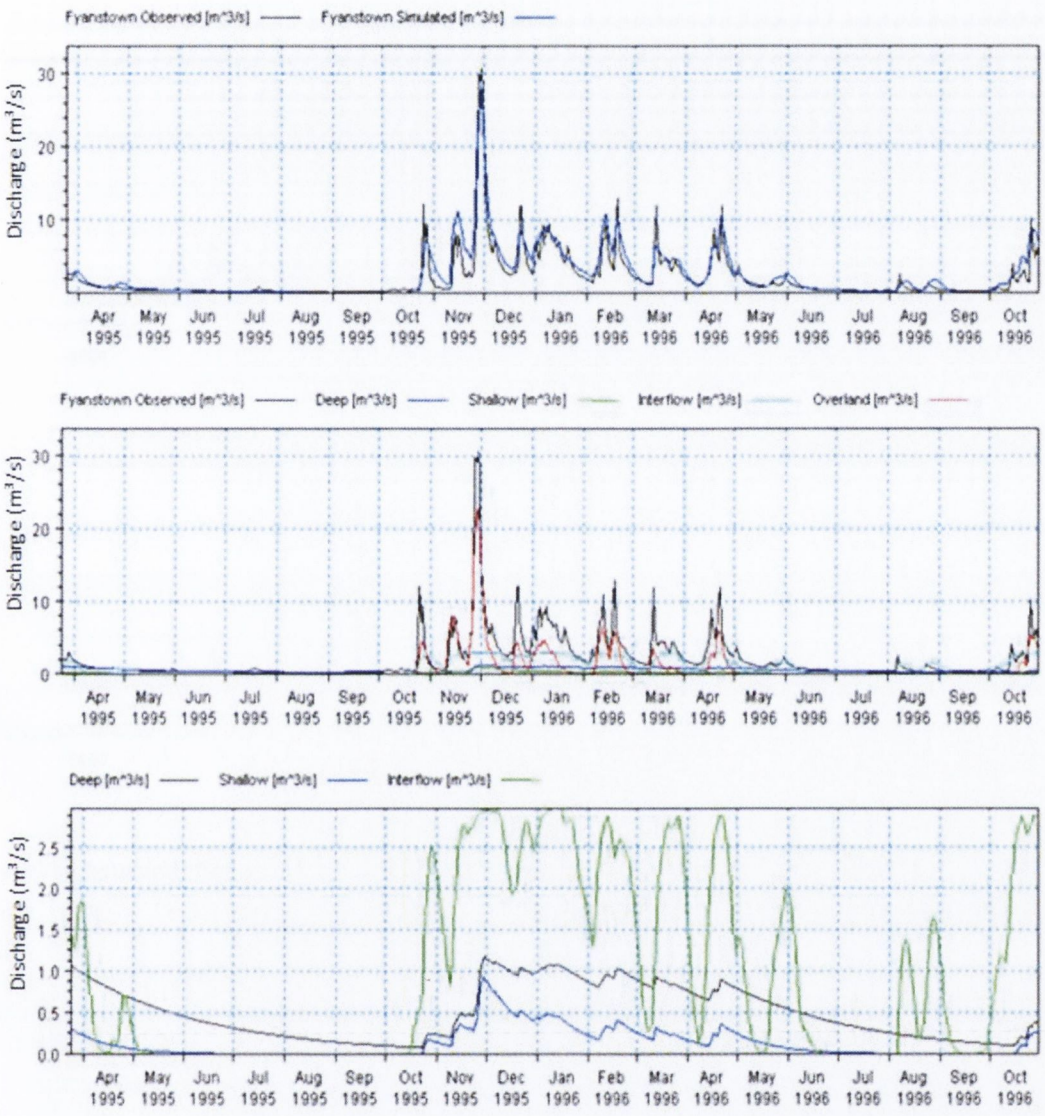

Figure C.5 Fyanstown catchment showing observed discharge with simulated discharge; simulated pathway flows with observed discharge; and simulated subsurface pathway flows (Mar 1995 – Oct 1996).

Deel

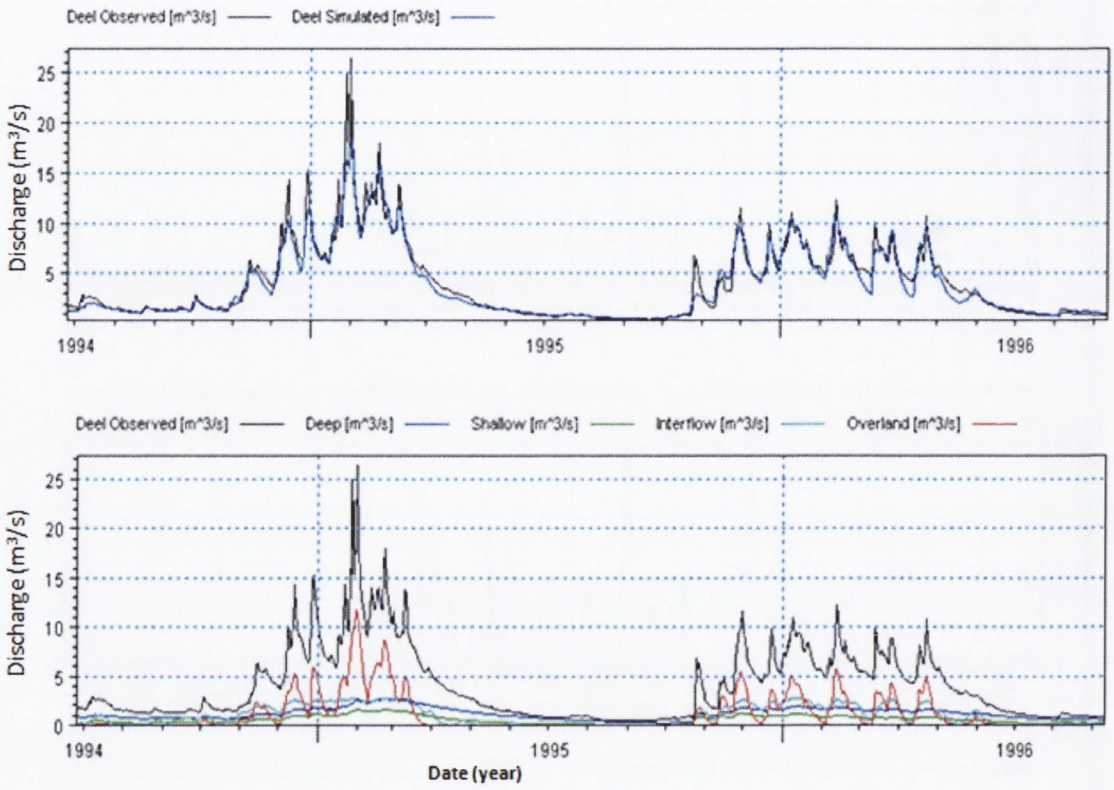

Figure C.6 Deel catchment showing observed discharge with simulated discharge and simulated pathway flows with observed discharge (June 1994 – Sept 1996).

Blackwater (Kells)

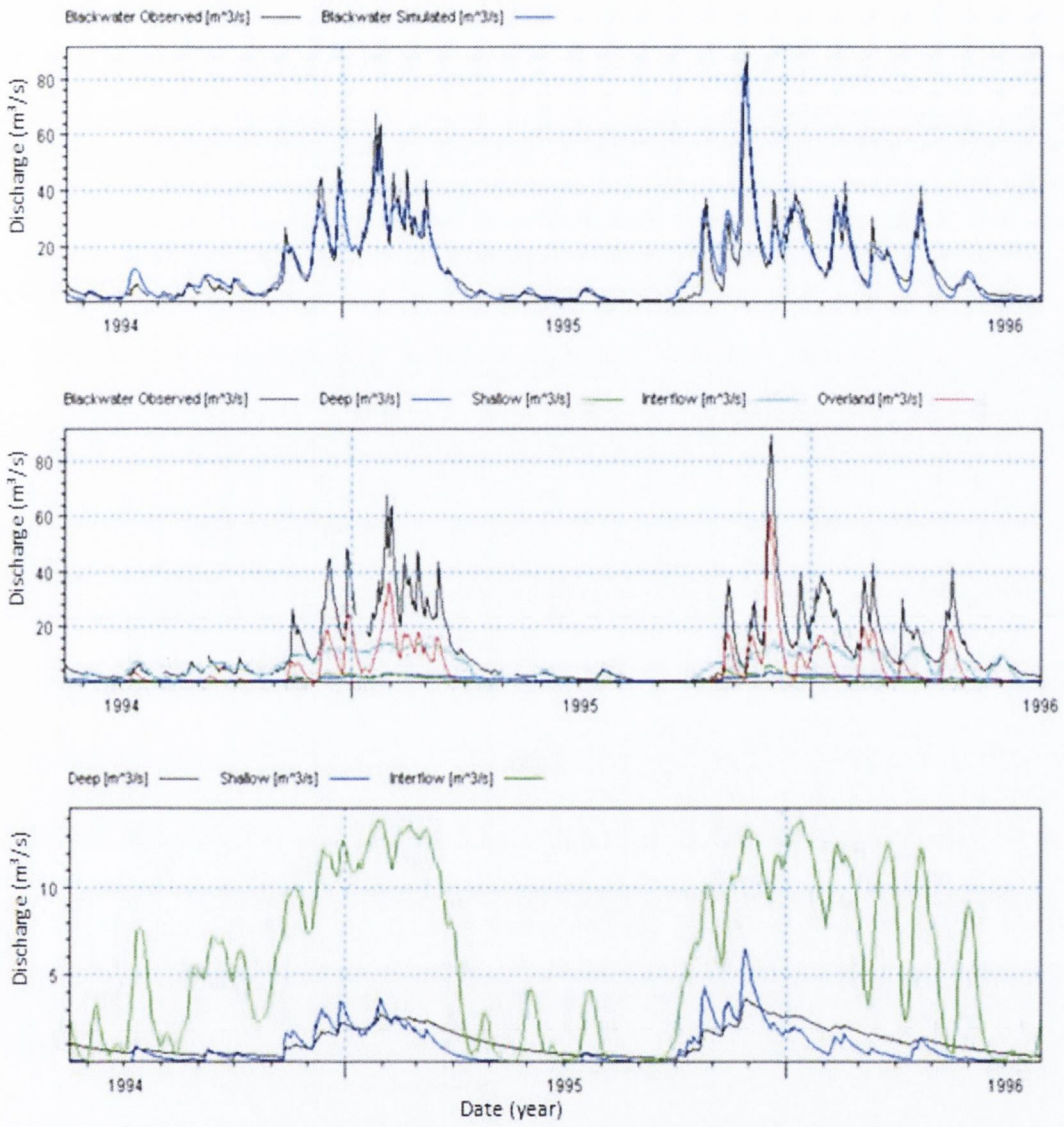

Figure C.6 Blackwater (Kells) catchment showing observed discharge with simulated discharge; simulated pathway flows with observed discharge; and simulated subsurface pathway flows (May 1994 – July 1996).

APPENDIX D – Supplementary Catchments' Regression Performance

Table D.1. Summary of average response for the percentage of the river hydrograph derived from each pathway and the performance of the simulations for R^2, $\sqrt{R^2}$ and bias, of all the Monte-Carlo simulations in each supplementary catchment using the predicted NAM parameter sets. These results are compared with the calibrated results of the 'best' separations presented in Appendix C.

Catchment	Area (km^2)	Deep Groundwater		Shallow Groundwater		Interflow		Overland Flow		R^2		$\sqrt{R^2}$		Bias	
		Calibrated	Predicted	Calibrated	Predicted	Calibrated	Predicted	Calibrated	Predicted	Calibrated	Predicted	Calibrated	Predicted	Calibrated	Predicted
		%	%	%	%	%	%	%	%						
Bawn	4.9	6	5.1	2.7	4.5	36.3	41.6	55	48.8	0.87	0.87	0.89	0.9	0.0430	0.0450
Owenshree	34.5	13.6	18.1			42.7	39.1	43.7	42.8	0.85	0.82	0.83	0.93	0.0250	0.0340
Owendullalagh	89.3	9.9	11.3			28.2	20.9	61.9	67.8	0.89	0.87	0.86	0.87	-0.3400	-0.1140
Fyanstown	187.6	15.6	11.6	5.1	3.8	43.9	48.1	35.4	36.5	0.83	0.8	0.87	0.79	-0.2700	-0.3290
Deel	283.1	29.7	35.5	14.7	16	26.8	18.3	28.7	33.2	0.9	0.9	0.94	0.92	0.3500	0.3390
Blackwater (Kells)	699	8.5	13.4	6.7	9.1	50.8	47.4	33.8	30.1	0.92	0.93	0.91	0.86	-0.5000	-0.1170